Alma Mater Studiorum - Università di Bologna

DOTTORATO DI RICERCA IN

SCIENZE DELLA TERRA, DELLA VITA E DELL'AMBIENTE

Ciclo 34

Settore Concorsuale: 05/A1 - BOTANICA

Settore Scientifico Disciplinare: BIO/01 - BOTANICA GENERALE

RELATIONSHIPS BETWEEN AIRBORNE POLLEN ALLERGENS AND
ENVIRONMENTAL FACTORS.

Presentata da: Chiara Suanno

Coordinatore Dottorato

Maria Giovanna Belcastro

Supervisore

Stefano Del Duca

Co-supervisore

Stefania Biondi

Esame finale anno 2022

Ringraziamenti

Vorrei ringraziare tutte le persone che mi hanno accompagnato e supportato durante questo percorso di crescita personale e professionale, nel bel mezzo di una pandemia.

Ringrazio il prof. Stefano Del Duca per l'umanità, gentilezza e professionalità con cui mi ha seguita durante questi anni, e per la sua disponibilità ad accogliere e incentivare tutte le mie idee e proposte su questo progetto. Ringrazio Iris e Luigi per l'infinita pazienza nel rispondere ai miei dubbi, e ai miei dubbi sulle risposte ai miei dubbi (e così via), ma soprattutto per la dedizione che hanno nel loro lavoro e per la loro capacità di insegnare e di collaborare. Mi sono sentita parte del gruppo di ricerca sin da subito, e questo ha fatto la differenza.

Ringrazio le professoresse Anna Maria Mercuri, Delia Fernández-González, Elisabetta Verderio e Stefania Biondi, e per aver contribuito alla mia formazione e al mio progetto di ricerca, mettendomi a disposizione i loro strumenti e le loro conoscenze.

Ringrazio tutta la comitiva dell'Orto Botanico per aver trasformato il posto di lavoro in una seconda casa, un habitat dove le idee fermentano e la stanchezza si tampona con pause caffè, tè, yerba mate – insomma, caffeina in compagnia.

Ringrazio ovviamente la mia famiglia che crede sempre in me, anche quando antepongo la carriera accademica al fantomatico "posto fisso"; e che si sorbisce le mie nevrosi quando gli esperimenti non vanno, le ultracentrifughe si rompono, gli anticorpi non funzionano. Grazie mamma e papà.

Grazie a Giulio per avermi supportato durante l'eterna lotta contro il Revisore 2, e per essere stato sempre al mio fianco e pronto ad aiutarmi.
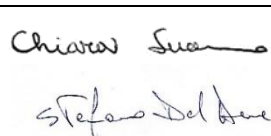
E grazie a Boogey, che c'è stato finché ha potuto.

Spero che questa sia la prima di tante raccolte di articoli Suanno et al.

Abstract

This thesis is a collection of scientific papers resulting from my research activity during the PhD course in Earth, Life, and Environmental Sciences. The main subject of the thesis is the capability of pollen to trigger a hypersensitive reaction in different environmental conditions, and the need to better characterise such allergenicity in order to measure it. This topic is discussed from different perspectives, using ecological, morphological, and molecular approaches. The thesis starts by summarising the importance of green infrastructures in the cities, from economical and conservational perspectives. It then focalises on the lesser-known ecosystem disservices urban vegetation can provide, and in particular on pollen allergy, exploring its causes and illustrating possible ways to monitor, foresee, and mitigate the allergenic risk. The possibility to monitor the allergenicity of urban green areas is then examined in depth, with an original research paper that proposes a method standardisation for existing allergenicity indices (Specific Allergenic Index and Urban Green Zones Allergenicty Index), and compares the indices results to evaluate their effectiveness. At the end of the thesis, pollen allergenicity is also approached from a molecular perspective, by investigating pollen allergens release mechanisms in the context of pollen hydration and germination. In particular, in an unpublished original research paper, the nature of allergen-carrying extracellular nanovesicles (pollensomes) released by pollen is extensively studied on a non-allergenic pollen model, to understand their biological role and thus the environmental conditions that trigger their release. Moreover, the last paper reported in the thesis demonstrates the secretion of a potential pollen allergen, a low-molecular weight cyclophilin, during pollen germination under stressful conditions. The thesis concludes with a brief description of other scientific activities carried on during the PhD, that still need more scientific corroboration to be published.

Co-author declaration

This declaration states the independent research contribution of the PhD candidate for each paper compiled in the thesis.

Paper No.	Title and full bibliographic reference
Paper I	**"More nature in the city"** G Capotorti, S Bonacquisti, L Abis, I Aloisi, F Attorre, G Bacaro, G Balletto, E Banfi, E Barni, F Bartoli, E Bazzato, M Beccaccioli, R Braglia, F Bretzel, M. A Brighetti, G Brundu, M Burnelli, C Calfapietra, V. E Cambria, G Caneva, A Canini, S Caronni, M Castello, C Catalano, L Celesti-Grapow, E Cicinelli, L Cipriani, S Citterio, G Concu, A Coppi, E Corona, S Del Duca, Vico E Del, E Di Gristina, G Domina, L Faino, E. A Fano, S Fares, E Farris, S Farris, M Fornaciari, M Gaglio, G Galasso, M Galletti, M. L Gargano, R Gentili, A. P Giannotta, C Guarino, R Guarino, G Iaquinta, G Iiriti, A Lallai, E Lallai, E Lattanzi, S Manca, F Manes, M Marignani, F Marinangeli, M Mariotti, F Mascia, P Mazzola, G Meloni, P Michelozzi, A Miraglia, C Montagnani, L Mundula, A. N Muresan, F Musanti, A Nardini, E Nicosia, L Oddi, F Orlandi, R Pace, M. E Palumbo, S Palumbo, L Parrotta, S Pasta, K Perini, L Poldini, A Postiglione, A Prigioniero, C Proietti, F. M Raimondo, A Ranfa, E. L Redi, M Reverberi, E Roccotiello, L Ruga, V Savo, P Scarano, F Schirru, R Sciarrillo, F Scuderi, A Sebastiani, C Siniscalco, A Sordo, C Suanno, M Tartaglia, A Tilia, C Toffolo, E Toselli, A Travaglini, F Ventura, G Venturella, F Vincenzi & C Blasi (2020) More nature in the city, Plant Biosystems - An International Journal Dealing with all Aspects of Plant Biology, 154:6, 1003-1006, DOI: 10.1080/11263504.2020.1837285

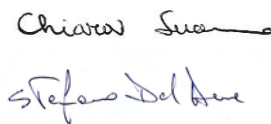| Role of PhD candidate	Type of contribution	Overall contribution (%)	Signature of PhD candidate and tutor
Other position	Writing	<15%	*Chiara Suanno* *Stefano Del Duca*

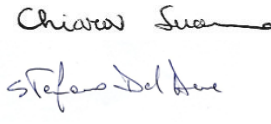| Paper No.	Title and full bibliographic reference
Paper II	**"Monitoring techniques for pollen allergy risk assessment"** C Suanno, I Aloisi, D Fernández-González, S Del Duca (2021) Monitoring techniques for pollen allergy risk assessment, Environmental Research, 197:111109, DOI: 10.1016/j.envres.2021.111109. Epub 2021 Apr 10. PMID: 33848553.

Role of PhD candidate	Type of contribution	Overall contribution (%)	Signature of PhD candidate and tutor
First author	Concept, literature research, writing.	>75%	*Chiara Suanno* *Stefano Del Duca*

Paper No.	Title and full bibliographic reference
Paper III	**"Pollen forecasting and its relevance in pollen allergen avoidance"** C Suanno, I Aloisi, D Fernández-González, S Del Duca (2021) Pollen forecasting and its relevance in pollen allergen avoidance, Environmental Research, 200:111150. DOI: 10.1016/j.envres.2021.111150. Epub 2021 Apr 21.

Role of PhD candidate	Type of contribution	Overall contribution (%)	Signature of PhD candidate and tutor
First author	Concept, literature research, writing.	>75%	*Chiara Suanno* *Stefano Del Duca*

Paper No.	Title and full bibliographic reference
Paper IV	**"Allergenic risk assessment of urban parks: Towards a standard index"** C Suanno, I Aloisi, L Parrotta, D Fernández-González, S Del Duca (2021) Allergenic risk assessment of urban parks: Towards a standard index, Environmental Research, 200:111436. doi: 10.1016/j.envres.2021.111436. Epub 2021 Jun 2.

Role of PhD candidate	Type of contribution	Overall contribution (%)	Signature of PhD candidate and tutor
First author	Experimental design, fieldwork, data analysis, writing.	>75%	*Chiara Suanno* *Stefano Del Duca*

Paper No.	Title and full bibliographic reference
Paper V (preprint)	**"A possible endocytic origin for pollen-derived extracellular nanovesicles"** C Suanno, E Tonoli, E Fornari, M. P Savoca, I Aloisi, L Parrotta, C Faleri, G Cai, E Verderio-Edwards, S Del Duca Ready for submission

Role of PhD candidate	Type of contribution	Overall contribution (%)	Signature of PhD candidate and tutor
First author	Experimental design, fieldwork, data analysis, writing.	>75%	*Chiara Suanno* *Stefano Del Duca*

Paper No.	Title and full bibliographic reference
Paper VI	**"A low molecular-weight cyclophilin localizes in different cell compartments of Pyrus communis pollen and is released in vitro under Ca2+ depletion"** L Parrotta, I Aloisi, C Suanno, C Faleri, A Kiełbowicz-Matuk, L Bini, G Cai, S Del Duca (2019) A low molecular-weight cyclophilin localizes in different cell compartments of Pyrus communis pollen and is released in vitro under Ca2+ depletion, Plant Physiology and Biochemistry, 144:197-206, DOI: 10.1016/j.plaphy.2019.09.045. Epub 2019 Sep 27.

Role of PhD candidate	Type of contribution	Overall contribution (%)	Signature of PhD candidate and tutor
Other position	Experiments, data analysis.	<15%	*Chiara Suanno* *Stefano Del Duca*

Summary

1. Introduction

1.1 Preface

My PhD project revolved around pollen, its relationships with environmental conditions, and the hypersensitivity reaction it can cause in allergic subjects. This thesis is a collection of the scientific papers that resulted from my research activity during the three years of PhD course. In the following paragraphs, I will synthetically introduce some key concepts on pollen development and pollen function, that are not extensively treated in the published papers but are nonetheless pivotal for the full understanding of the thesis subject. Chapter 2, a coral paper stemmed from the 115th Congress of the Italian Botanical Society, gives an overview on the role of the urban vegetation in the biodiversity conservation and on the ecosystem services it provides, delineating the state of the art of green infrastructures monitoring, implementation, and maintenance in Italy. The paper also addresses ecosystem disservices that can be caused by an incautious selection of the ornamental plants, such as alien species invasions or pollen allergies. The latter disservice is examined in depth in Chapter 3, a review that aims to classify and compare all the existing approaches for the monitoring of local pollen allergenicity. Unfortunately, monitoring alone is not useful in the short term to pollen-allergic subjects, who need to know allergic pollen concentrations in advance to plan their activities and medications. Hence, Chapter 4 investigates the available methods for pollen forecasting, their forecasting skills, and their usefulness to allergic patients. Inside the cities, where the vegetation distribution is discrete, the calculation of allergenic indices might help allergic subjects as well, informing them on the risk they take by accessing a certain green area. For this purpose, Chapter 5 proposes a method standardisation and results comparison for two popular allergenicity indices. Chapter 6, a preprint, moves the focus form the ecological to the cellular and molecular point of view in the study of pollen allergenicity. In this manuscript, the nature of extracellular nanovesicles carrying pollen allergens is investigated using a non-allergenic pollen model, to understand their biological function. Finally, Chapter 7 describes another possible mechanism of allergen release during pollen germination. After some conclusive remarks on the work presented, other research activities carried out during my PhD course are presented in section 9.1.

1.2 Key concenpts

1.2.1 A microgametophyte called pollen

Pollen is a living, microscopic organism, representing the male gametophyte of spermatophytes (seed plants). In fact, plant sexual reproduction is characterised by a unique alternation between two astonishingly different generations: the sporophyte, a diploid organism that originates from a zygote and produces haploid spores by meiosis; and the gametophyte, a haploid organism that originates from a spore and produces gametes by mitosis. For the spermatophyte clade, the sporophyte is the macroscopic, visible generation. Spores produced by these plants are not released in the environment, but instead they germinate inside the sporophyte reproductive structures, a phenomenon called endospory. Spermatophytes also show heterospory, producing two different types of spores:

- microspores, that are produced in the microsporangium and originate a microgametophyte (pollen), which is mobile and produces male gametes;

- megaspores, that are produced in the megasporangium inside the ovule and originate a megagametophyte, which remains inside the sporophyte tissues of the ovule and produces oocytes.

While all spermatophytes produce pollen, pollen production and sexual reproduction differ between gymnosperms (naked-seed plants) and angiosperms (flowering plants). Briefly, gymnosperm pollen is formed after 3 to 5 mitoses of the microspore, that can happen when pollen is still inside the microsporangia contained in the male cones, or after its release. Since number and timing of these divisions however vary between taxa, mature pollen of different gymnosperms has a different number of cells, ranging from 1 to 5. In most gymnosperms, upon its release into the environment pollen is formed at least by one tube cell and one antheridial cell, but there are some exceptions (*e.g. Juniperus* spp.). Spermatic cells are produced after pollination, when pollen reaches the ovule containing the megagametophyte, inside the female cone (Breygina et al., 2021). Angiosperms appeared later in the evolution of land plants (around 130 million years ago), and they introduced the reproductive specialisation of the flower. Flowers have peculiar organs allocating micro- and megasporangia: pollen is produced in structures called anthers, that form the androecium, while the ovules containing the megagametophytes are enveloped in modified leaves called carpels, that form the gynoecium. Evolution of angiosperms also involved a simplification in

pollen structure, that at maturity is made of one germinative cell and two spermatic cells (Adhikari et al., 2020; Hafidh and Honys, 2021; Mauseth, 2019).

1.2.2 Pollination

To achieve a successful reproduction, pollen must reach a macrogametophyte belonging to its same species and deliver two spermatic cells to the oocyte (Adhikari et al., 2020; Mauseth, 2019). It requires special adaptations for pollen to facilitate such dispersal, to endure abiotic stresses during the journey, to recognise its target, and to finally achieve the double fertilisation.

The first challenge for pollen is to reach the megagametophyte, a process called pollination. The duration of this journey is greatly variable, and it mainly depends on reproductive barriers, pollen vectors, and population density of the taxon considered. In taxa where self-pollination is allowed, pollen journey is minimal: pollination can happen inside the flower (autogamy) for hermaphrodite species, since they have both gynoecium and androecium on the same flower; or it can happen across the sporophyte (geitonogamy) for monoecious species, that have distinct male and female reproductive structures coexisting on the same individual. While self-pollination maximises the chances of a successful fertilisation, it does not significantly contribute to the genetic variability of the offspring. Hence, in many spermatophytes self-pollination is avoided using temporal or molecular reproductive barriers, and pollen must travel to the closest macrogametophyte of the same species to fulfil its biological function (Fattorini and Glover, 2020). In this case, the population density needs to be proportionate to the distance pollen can cover. The most evident pollen adaptations to dispersal are its microscopic dimensions and the evolution of a peculiar double-layered wall. The internal wall layer, called intine, has a cellulose-pectic composition similar to other plant cell walls, but the external layer, called exine, is mainly made of the toughest biopolymer on Earth, sporopollenin, which is capable to withstand harsh physical and chemical conditions, thus preserving the viability of the pollen grain in the atmosphere (Grienenberger and Quilichini, 2021).

The two vectors mainly employed by pollen for its dispersal are wind (anemophily) and insects (entomophily). While anemophily is prevalent in gymnosperms, with 98% of the existing gymnosperm species adopting this strategy (Breygina et al., 2021), angiosperm evolution was initially guided by the coevolution with pollinators, with the development of rewards and

attractive features for the insects, and then some clades independently evolved a wind pollination strategy. To date, 18% of the angiosperm families are known to have anemophilous pollination. However, many angiosperms are considered ambophilous, meaning that they adopt a combination of anemophily and entomophily where one of the two strategies can be prevalent, but not exclusive (Culley et al., 2002). Similarly, anemophilous gymnosperms can be occasionally pollinated by insects, attracted by the pollination drop on their ovules (Hafidh and Honys, 2021).

Pollen features such as its shape, dimensions, and the ornamentations and structures of the exine, can enhance pollination effectiveness. For example, anemophilous pollen is usually aerodynamic and it may present exine structures that are flight adaptations, like the air sacs (*sacci*) of Pinaceae pollen. On the other hand, entomophilous pollen is usually larger, with thicker exine and rougher ornamentations than anemophilous pollen, as it happens for the Asteraceae pollen grains (Accorsi et al., 1994; Culley et al., 2002; Forlani L., 1992; Lu et al., 2021).

1.2.3 Pollen germination

Another challenge for pollen grains is the energy supply. In fact, pollen is not photosynthetic and thus cannot self-sustain its metabolism for long, relying on its carbohydrate reserves only. For this reason, mature pollen is released into the environment dehydrated, in a quiescent state, and it is programmed to reactivate its metabolism upon its arrival on the ovule. In gymnosperms, dehydration can be extreme, and pollen can remain viable for long periods while traveling for several kilometres. In this clade, pollination is successful when pollen reaches the ovule in the female cone. In most species, it lands on a pollination drop secreted by the receptive ovule, that is an apoplastic fluid containing minerals, carbohydrates, and proteins. Some gymnosperms can produce other ovular secretions to capture the pollen grains, as in *Larix* spp., or not have any secretion at all (Breygina et al., 2021; Hafidh and Honys, 2021). At this point, pollen needs to deliver the sperm cells to the megagametophyte inside the ovule. First, pollen rehydrates and reactivates its metabolism, usually helped by the moisture and the substrates provided by the ovule, a process requiring hours to months. After this stage, fertilisation strategies vary among gymnosperm taxa. For example, *Ginkgo biloba* L. has motile sperm cells that are released in the pollination drop and independently reach the megagametophyte. The vast majority of existing gymnosperms however produces

immotile sperm cells that need to be actively transported to the oocyte by the pollen. Pollen accomplishes this task using a singular mechanism known as pollen germination: the tube cell initiates a polarised apical growth by transporting new membrane and depositing cell wall at the growing pole, forming a cylindric tube that makes its way through the ovule tissues and contact the megagametophyte. Pollen tube growth is remarkably slow in gymnosperms: its emergence requires at least few days, and the elongation is completed in a timespan variable from several weeks to one year, according to the species (Breygina et al., 2021; Mauseth, 2019). Pollen tubes emerge preferentially from areas of the wall where exine layer is thinner or absent, termed apertures. Such apertures can be *colpi* (furrows) if they are significantly more developed in one dimension than the other, *pori* (pores) if they are almost rounded, or *colpori* if there is a *porus* in the middle of the *colpus* (Forlani L., 1992). While Pinoideae and Abetoideae pollen grains have a furrow between the air sacks, other gymnosperm species have inaperturate pollen grains, and the position of pollen tube emergence depends on the pollen polarity, where present. Pollen tube in gymnosperms contains an uninterrupted stream of cytoplasm. Its central part, called body, contains most of the organelles, the tube cell nucleus, and the germinative cell derived from the antheridial cell, which will eventually produce two sperm cells by mitosis. The tube tip, called apex, is rich of mitochondria and endomembranes: an intense vesicular trafficking is in fact needed to sustain the tube elongation (Breygina et al., 2021).

Angiosperm pollen quest for the macrogametophyte is fundamentally similar, but it has to overcome additional obstacles. Angiosperm pollination ends with the arrival of pollen on the stigma, which is the receptive component of the carpel. In angiosperm pollen, exine is covered with a coat made of wax and other lipids, proteins, and sometimes volatile compounds. Based on the pollen coat composition, stigmatic papillae can operate a selection on pollen grains, possibly activating rejection pathways (Broz and Bedinger, 2021). If the stigmatic papillae activate the reception pathways, the stigma microenvironment promotes pollen rehydration and metabolism reactivation, similarly to the gymnosperm ovule secretions. Angiosperm pollen commonly has at least one aperture, with some exceptions, which facilitates pollen tube emergence. At this point, pollen tubes enter the stigma and grow through a narrow and elongated portion of the carpel, called style, towards the ovule which is situated at the base of the carpel. The carpel structure requires angiosperm pollen tubes to be significantly longer than the ones of the gymnosperms. Nonetheless, they emerge and grow in a matter of hours.

To make this extreme elongation possible, pollen cytoplasm progresses towards the tip of the tube, while older portions of the tubes are isolated by callose plugs (Mauseth, 2019).

Pollen tube journey is guided by chemical gradients and molecular signals deriving from carpel (in angiosperms), ovule, and megagametophyte cells. This implies a constant and precise communication between pollen and female structures (Çetinbaş-Genç et al., 2022; Cheung and Wu, 2008).

When pollen is accidentally inhaled, small pollen proteins involved in these interactions that are present in the pollen coat or secreted during pollen hydration and germination, can be released in the human respiratory mucosa, triggering allergic reactions in sensitive subjects (Mothes et al., 2004).

1.2.4 Bibliography

Accorsi, C.A., Mazzanti, M.B., Forlani, L., Randazzo, G., 1994. Flora Palinologica Italiana, Sezione Aeroplainologica: S 205 - Pinus pinea L. (Pinaceae). Aerobiologia (Bologna). 10, 97–111.

Adhikari, P.B., Liu, X., Wu, X., Zhu, S., Kasahara, R.D., 2020. Fertilization in flowering plants: an odyssey of sperm cell delivery. Plant Mol. Biol. 103, 9–32. https://doi.org/10.1007/S11103-020-00987-Z

Breygina, M., Klimenko, E., Schekaleva, O., 2021. Pollen Germination and Pollen Tube Growth in Gymnosperms. Plants 10, 1301. https://doi.org/10.3390/PLANTS10071301

Broz, A.K., Bedinger, P.A., 2021. Pollen-Pistil Interactions as Reproductive Barriers. Annu. Rev. Plant Biol. 72, 615–639. https://doi.org/10.1146/ANNUREV-ARPLANT-080620-102159

Çetinbaş-Genç, A., Conti, V., Cai, G., 2022. Let's shape again: the concerted molecular action that builds the pollen tube. Plant Reprod. 1, 1–27. https://doi.org/10.1007/S00497-022-00437-4

Cheung, A.Y., Wu, H.M., 2008. Structural and signaling networks for the polar cell growth machinery in pollen tubes. Annu. Rev. Plant Biol. 59, 547–572. https://doi.org/10.1146/annurev.arplant.59.032607.092921

Culley, T.M., Weller, S.G., Sakai, A.K., 2002. The evolution of wind pollination in angiosperms. Trends Ecol. Evol. 17, 361–369. https://doi.org/10.1016/S0169-5347(02)02540-5

Fattorini, R., Glover, B.J., 2020. Molecular Mechanisms of Pollination Biology. Annu. Rev. Plant Biol. 71, 487–515. https://doi.org/10.1146/ANNUREV-ARPLANT-081519-040003

Forlani L., 1986. La morfologia del polline. Boll. dell'accademia Gioenia di Sci. Nat. Catania 19, 525–631.

Hafidh, S., Honys, D., 2021. Reproduction Multitasking: The Male Gametophyte. Annu. Rev. Plant Biol. 72, 581–614. https://doi.org/10.1146/ANNUREV-ARPLANT-080620-021907

Lu, X., Ye, X., Liu, J., 2021. Morphological differences between anemophilous and entomophilous pollen. Microsc. Res. Tech. https://doi.org/10.1002/JEMT.23975

Mauseth, J.D., 2019. Botany: An Introduction To Plant Biology, 2019th ed. Jones and Bartlett Publishers, Inc.

Mothes, N., Horak, F., Valenta, R., 2004. Transition from a botanical to a molecular classification in tree pollen allergy: Implications for diagnosis and therapy. Int. Arch. Allergy Immunol. 135, 357–373. https://doi.org/10.1159/000082332

2. More nature in the city

Abstract

According to projects and practices that the Italian botanists and ecologists are carrying out for bringing "*more nature in the city*", new insights for a factual integration between ecological perspectives and more consolidated aesthetic and agronomic approaches to the sustainable planning and management of urban green areas are provided.

Keywords: Ecosystem services, human well-being, green infrastructure, urban green areas, urban biodiversity.

1. Introduction

Biodiversity strategies are increasingly focused on ecosystems and their services (IPBES 2019). In Europe, the MAES (Mapping and Assessment of Ecosystems and their Services) process has been expressly designed for addressing these targets and also provides essential knowledge for the deployment of Green Infrastructure (GI). Actually, GI is defined as "a strategically planned network of natural and semi-natural areas with other environmental features designed and managed to deliver a wide range of ecosystem services" that, on land, concerns rural as well as urban areas (EC 2013). Especially in cities, one of the main Ecosystem Services (ES) demands that GI is claimed to address is the improvement of citizen health with respect to environmental pollution. To this aim, the increase of vegetation cover has been prompted by the Italian Committee for Green Public Development as an effective solution to be adopted

across Italian cities and metropolitan areas (CVP 2018). The vision of the Committee consists of three main actions: i) significantly improve the coverage of plant communities, including woodlands but also shrublands and grasslands, ii) remove asphalt and concrete, in order to recover pervious surfaces, and iii) bring back forests to the cities. Forests were adopted as a benchmark because they represent complex systems, with a high species richness and marked structural, functional and temporal variability (Marchetti et al. 2010), just as complex, rich and variable are the urban green areas (FAO 2016). Consequently, in order to properly design and manage the urban green, a new and factual integration between ecological perspectives and more consolidated aesthetic and agronomic approaches is needed. Planning processes should increasingly become interdisciplinary and take into account important principles, such as a clear definition of the ES to be provided (e.g., improvement of air quality through PM removal) by "the right plant in the right place" (consistently with the potential vegetation of the site and with the varying performance of different species, e.g., deciduous vs evergreen ones) and avoiding potential disservices (e.g., those caused by the introduction of non-native species) (Celesti-Grapow and Blasi 2004). Knowledge on plant biology, auto- and syn-ecology, and on the varying performance of single taxa and communities in providing desired services should, therefore, be deepened and disseminated. The present work is aimed at facilitating this process, by showing to the international scientific community the more recent advances made by Italian botanists and ecologists in bringing "more nature in the city".

2. More nature in the city under a botanical and ecological perspective

A collection of different activities that are being carried out in Italy for promoting sustainable, effective and efficient improvement of urban green areas was made available by the symposium "More Nature in the City", within the 115th Congress of the Italian Botanical Society (AA.VV. 2020). The present overview is based on the research keywords and concepts adopted in the 26 contributions to the symposium (Figure 1) and is organised around the topics of Urban Biodiversity, Green Infrastructure and Ecosystem Services, and Human Health and Well-being (see the Appendix 1 in the Supplemental Materials).

Figure 1 *Visual representation of text data (word cloud) based on the keywords and terms adopted in the 26 contributions to the symposium "More Nature in the City", within the 115th Congress of the Italian Botanical*

3.   Urban biodiversity

The topic of Urban Biodiversity was especially addressed in terms of native/non-native species, plant diversity - ecological functions - ecosystem services - human well-being chain, ecological connectivity and typology of green areas. The emerging issues relate to: (i) sustainable use of non-native trees and the need for global guidelines for enhancing their utility while reducing risks of invasion and damages (Brundu et al. 2020); (ii) identification of ecosystem services and disservices related to varying composition of street trees across different cities, including the cultural values facilitated by the reconnection between community gardens and the local territory, history and traditions (Caneva, Bartoli, et al. 2020); (iii) innovative ways of measuring the quality of life with respect to environmental and botanical features, such as the sentiment analysis tool (Ladle et al. 2016; Schwartz et al. 2019); (iv) the pivotal role that public green spaces, such as university and botanical gardens, tree-lines and residual natural forests, may exert in terms of native species conservation, ecological connectivity, natural and cultural heritage valorisation and citizen well-being (Bressan and Poldini 2007; Poldini 2016); (v) the contribution of micro-habitats, such as those

joined to transportation networks, in guaranteeing refuge for native plant diversity (Plowes et al. 2007).

4.   Green infrastructure and ecosystem services

The topic of GI and ES was addressed in terms of biodiversity conservation and multi-disciplinary planning, urban forest restoration, compensation measures, green-grey solutions, and supply, flow, synergies and trade-offs of ES. Specifically, the contributions provided original hints on: (i) how to integrate floristic, vegetation and landscape scales approaches for supporting biodiversity conservation in planning processes (Capotorti et al. 2016; 2019) and how to deploy multi-disciplinary approaches for enhancing multi-functionality; (ii) methods for enhancing the success of forest restoration and promoting related investments by means of compensation measures; (iii) selection of suitable species and habitat templates for designing sustainable and efficient green roofs (Oberndorfer et al. 2007; Nardini et al. 2012; Catalano et al. 2016; 2018); (iv) development and application of eco-physiology approaches for enhancing supply and flow of regulat- ing ES, such as air and soil pollution removal, local climate regulation (Maragno et al. 2018), flooding prevention and carbon sequestration (Manes et al. 2016; Cristaldi et al. 2017; Pace et al. 2018); (v) development of urban green management strategies for supporting climate change adaptation and mitigation (Tsitsoni et al. 2015; Perini et al. 2017; Marando et al. 2019; Ferrini et al. 2020).

5.   Human health and well-being

The topic of Human Health and Well-being was addressed in terms of synergic relationships between urban green and health, recreation, social cohesion, food security, as well as potential trade-offs in terms of health hazards or risk (Lorenzini 1999). Specific contributions relate to: (i) education of new generations to road safety and environmental and health culture by means of participative projects (Domina et al. 2020); (ii) tools for planning and management of historic gardens in order to combine aesthetic and religious values with educational fruition; (iii) models for improving social and environmental conditions by means of new technologies applied to urban farming (Braglia et al. 2016; Caneva, Cicinelli, et al. 2020); (iv) formulation of reliable indicators for assessing and mitigating the allergenic

potential of urban green areas while valorising the phyto-resources for respiratory well-being (Hruska 2003; Cariñanos et al. 2014; Marinangeli and Fares 2020).

6.   Concluding remarks

In keeping with the growing strategic attention to urban sustainability (UN Habitat 2019), an overview is provided on the more recent advances in scientific knowledge and implementation activities carried out by Italian botanists and ecologists. The report presents an inventory of research projects and good practices that is useful at a national level, but is also likely to be of interest to an international audience. Actually, by means of the varied contributions relating to urban biodiversity, GI planning, and ES and associated benefits to human health and well-being, it allows to move forward with respect to pilot studies, such as those developed within the framework of the European EnRoute (Enhancing Resilience of Urban Ecosystems through Green Infrastructure) Project (Maes et al. 2019). Many of the inputs are feeding the design of a national plan on GI, which is intended to combine ecoregional and local approaches (Blasi 2018) in order to activate urban resilience and respond to many of the challenges posed by the COVID-19 pandemic (e.g., by improving air quality in the cities). It is hoped that this plan will inspire a proper use of the Disaster Resilience and Recovery Fund towards the sustainable and inclusive growth prompted by the European Green Deal.

7.   Bibliography

AA.VV. 2020. 115o Congresso della Società Botanica Italiana. Volume degli abstract [In Italian]; [accessed 2020 Sept 15]. http://www.societa-botanicaitaliana.it/115/img/Volume_115_Congresso_SBI.pdf.

Blasi C, Capotorti G, Copiz R, Mollo B. 2018. A first revision of the Italian Ecoregion map. Plant Biosystems. 152(6):1201–1204.

Braglia R, Redi EL, Scuderi F, Canini A. 2016. Il Ruolo Sociale degli Orti Botanici in Orti Botanici Eccellenze Italiane. Nuove Direzioni ed. Città di Castello (PG). 129–133.

Bressan E, Poldini L. 2007. La biodiversità nel Friuli Venezia Giulia e la sua integrazione nel paesaggio. Agribus Paesaggio Ambiente. 10(3): 202–208.

Brundu G, Pauchard A, Pyšek P, Pergl J, Bindewald AM, Brunori A, Canavan S, Campagnaro T, Celesti- Grapow L, Dechoum M de S, et al. 2020. Global guidelines for the sustainable use of non-native trees to prevent tree invasions and mitigate their negative impacts. NB. 61: 65–116.

Caneva G, Bartoli F, Zappitelli I, Savo V. 2020. Street trees in Italian cities: story, biodiversity and integration within the urban environment. Rendiconti Lincei. Scienze Fisiche e Naturali. 1–7.

Caneva G, Cicinelli E, Scolastri A, Bartoli F. 2020. Guidelines for urban community gardening: proposal of preliminary indicators for several ecosystem services (Rome, Italy). Urban Urban Greening. 126866.

Capotorti G, De Lazzari V, Alós Ortí M. 2019. Local scale prioritisation of green infrastructure for enhancing biodiversity in peri-urban agroeco- systems: a multi-step process applied in the Metropolitan City of Rome (Italy). Sustainability. 11(12):3322.

Capotorti G, Del Vico E, Anzellotti I, Celesti-Grapow L. 2016. Combining the conservation of biodiversity with the provision of ecosystem services in urban green infrastructure planning: critical features arising from a case study in the metropolitan area of Rome. Sustainability. 9(1):10.

Cariñanos P, Casares-Porcel M, Quesada-Rubio JM. 2014. Estimating the allergenic potential of urban green spaces: a case-study in Granada, Spain. Landscape Urban Plann. 123:134–144.

Catalano C, Marceno C, Laudicina VA, Guarino R. 2016. Thirty years unmanaged green roofs: ecological research and design implications. Landscape Urban Plann. 149:11–19.

Catalano C, Badalucco L, Laudicina VA, Guarino R. 2018. Some European green roof norms and guidelines through the lens of biodiversity: do ecoregions and plant traits also matter? Ecol Eng. 115:15–26.

Celesti-Grapow L, Blasi C. 2004. The role of alien and native weeds in the deterioration of archaeological remains in Italy. Weed Technol. 18(1):1508–1513.

Cristaldi A, Oliveri Conti G, Jho EH, Zuccarello P, Grasso A, Copat C, Ferrante M. 2017. Phytoremediation of contaminated soils by heavy metals and PAHs. A brief review. Environ Technol Innovation. 8: 309–326.

Comitato del Verde Pubblico - Italian Public Green Committee (CVP). 2018. Strategia Nazionale del Verde Urbano. [accessed 2020 Sept 15]. http://www.minambiente.it/sites/default/files/archivio/allegati/comitato%20verde%20pubblico/strategia_verde_urbano.pdf.

Domina G, Di Gristina E, Scafidi F, Calvo R, Venturella G, Gargano ML. 2020. The urban vascular flora of Palermo (Sicily, Italy). Plant Biosystems. 154(5):627–634.

European Commission (EC). 2013. Communication from the Commission to the European Parliament, the Council, the European Economic and Social Committee and the Committee of the Regions 'Green Infrastructure (GI)—Enhancing Europe's Natural Capital' (COM(2013) 249 Final of 6 May 2013).; [accessed 2020 Sept 15]. http://eur-lex.europa.eu/LexUriServ/LexUriServ.do?uri=COM:2013:0249:FIN:EN:PDF.

FAO. 2016. Guidelines on urban and peri-urban forestry. by Salbitano F, Borelli S, Conigliaro SM, Chen Y. FAO Forestry Paper No. 178. Rome. Food and Agriculture Organization of the United Nations.

Ferrini F, Fini A, Mori J, Gori A. 2020. Role of vegetation as a mitigating factor in the urban context. Sustainability. 12(10):4247.

Hruska K. 2003. Assessment of urban allergophytes using an allergen index. Aerobiologia (Bologna). 19(2):107–111.

IPBES. 2019. Global assessment report on biodiversity and ecosystem services of the Intergovernmental Science-Policy Platform on Biodiversity and Ecosystem Services. Brondizio ES, Settele J, D´ıaz S, Ngo HT (editors). IPBES secretariat, Bonn, Germany.

Ladle RJ, Correia RA, Do Y, Joo GJ, Malhado ACM, Proulx R, Roberge JM, Jepson P. 2016. Conservation culturomics. Front Ecol Environ. 14(5): 269–275. https://doi.org/10.1002/fee.1260.

Lorenzini G. 1999. Le piante e l'inquinamento dell'aria. Edagricole, Bologna. 335. pp.

Maes J, Zulian G, Gûnther S, Thijssen M, Raynal J. 2019. Enhancing Resilience Of Urban Ecosystems through Green Infrastructure. Final Report, EUR 29630 EN. Publications Office of the European Union, Luxembourg. JRC115375.

Manes F, Marando F, Capotorti G, Blasi C, Salvatori E, Fusaro L, Ciancarella L, Mircea M, Marchetti M, Chirici G, et al. 2016. Regulating ecosystem services of forests in ten Italian metropolitan cities: air quality improvement by PM10 and O3 removal. Ecol Indic. 67: 425–440.

Maragno D, Gaglio M, Robbi M, Appiotti F, Fano EA, Gissi E. 2018. Fine- scale analysis of urban flooding reduction from green infrastructure: an ecosystem services approach for the management of water flows. Ecol Modell. 386:1–10. https://doi.org/10.1016/j.ecolmodel.2018.08. 002.

Marando F, Salvatori E, Sebastiani A, Fusaro L, Manes F. 2019. Regulating ecosystem services and green infrastructure: assessment of urban heat island effect mitigation in the municipality of Rome, Italy. Ecol Modell. 392:92–102.

Marchetti M, Tognetti R, Lombardi F, Chiavetta U, Palumbo G, Sellitto M, Colombo C, Iovieno P, Alfani A, Baldantoni D, et al. 2010. Ecological portrayal of old-growth forests and persistent woodlands in the Cilento and Vallo di Diano National Park (southern Italy). Plant Biosystems. 144(1):130–147.

Marinangeli F, Fares S. 2020. Bosco polmone urbano: calendario dei servizi e disservizi del verde arboreo in un parco sanitario a Perugia per una fruizione funzionale. 115° Congresso della Società Botanica Italiana onlus, on line. VII International Plant Science Conference (IPSC).

Nardini A, Andri S, Crasso M. 2012. Influence of substrate depth and vegetation type on temperature and water runoff mitigation by extensive green roofs: shrubs versus herbaceous plants. Urban Ecosyst. 15(3):697–708.

Oberndorfer E, Lundholm J, Bass B, Coffman RR, Doshi H, Dunnett N, Gaffin S, Ko€hler M, Liu KKY, Rowe B. 2007. Green roofs as urban eco- systems: ecological structures, functions, and services. BioScience. 57(10):823–833.

Pace R, Biber P, Pretzsch H, Grote R. 2018. Modeling ecosystem services for park trees: sensitivity of i-Tree Eco simulations to light exposure and tree species classification. Forests. 9(2):89.

Perini K, Ottel´e M, Giulini S, Magliocco A, Roccotiello E. 2017. Quantification of fine dust deposition on different plant species in a vertical greening system. Ecol Eng. 100:268–276.

Plowes RM, Dunn JM, Gilbert LE. 2007. The urban fire ant paradox: Native fire ants persist in an urban refuge while invasive fire ants dominate natural habitats. Biol Invasions. 9(7):825–836. DOI:10.1007/ s10530-006-9084-7

Poldini L. 2016. Flora e vegetazione quali indicatori dello stato dell'ambiente e strumenti di pianificazione delle risorse naturali, Il caso studio del Carso dinarico nel Friuli Venezia Giulia. Mem. Accad. Lunigianese Sci. "G. Capellini". La Spezia. 82-83(2013-2013):27-47,

Schwartz AJ, Dodds PS, O'Neil-Dunne JPM, Danforth CM, Ricketts TH. 2019. Visitors to urban greenspace have higher sentiment and lower negativity on Twitter. People Nat. 1(4):476–485.

Tsitsoni T, Gounaris N, Kontogianni AB, Xanthopoulou-Tsitsoni V. 2015. Creation of an integrated system model for governance in urban MTEs and for adapting cities to climate change: preliminary results. ECMED. 41(2):33–44.

UN HABITAT. 2019. Flagship Programme 5. SDG Cities; [accessed 2020 Sept 15]. https://unhabitat.org/sdg-cities.

3. Monitoring techniques for pollen allergens risk assessment

Abstract

Understanding airborne pollen allergens trends is of great importance for the high prevalence and the socio-economic impact that pollen-related respiratory diseases have on a global scale. Pursuing this aim, aeropalynology evolved as a broad and complex field, that requires multidisciplinary knowledge covering the molecular identity of pollen allergens, the nature of allergen-bearing particles (pollen grains, pollen sub-particles, and small airborne particles), and the distributions of their sources. To estimate the health hazard that urban vegetation and atmospheric pollen concentrations pose to allergic subjects, it is pivotal to develop efficient and rapid monitoring systems and reliable allergic risk indices. Here, we review different pollen allergens monitoring approaches, classifying them into I) vegetation-based, II) pollen-based, and III) allergen-based, and underlining their advantages and limits. Finally, we discuss the outstanding issues and directions for future research that will further clarify our understanding of pollen aeroallergens dynamics and allergen avoidance strategies.

Keywords: pollen, aeroallergens, monitoring, pollinosis, allergenicity index, air samplers.

Abbreviations: AR, Allergic Rhinitis; PM, Particulate Matter; SAI, Specific Allergenic Index; I_{UGZA}, Urban Green Zones Allergenicity Index; AIROT, Aerobiological Index of Risk for Ornamental Trees; CNN**,** Convolutional Neural Networks; RT, real-time; LIF, laser (or light) induced fluorescence; qPCR, quantitative PCR; cpDNA, chloroplast DNA; NGS, Next Generation Sequencing; CE, Capillary electromigration.

1. Introduction

Allergic rhinitis (AR), allergic rhino conjunctivitis and asthma affect a significant share of the global population, with a higher prevalence in developed countries. It is estimated that over 300 million people worldwide suffer from asthma, while AR occurs in about 500 million

people, out of whom 200 million have asthma as a comorbidity (Ozdoganoglu and Songu, 2012; Simunovic et al., 2020).

Pollen is a common cause of these respiratory diseases, as more than 150 pollen proteins have been proven to cause allergic sensitisation (Xie et al., 2019). Allergenic plants are mostly wind-pollinated species, that have to release huge amounts of pollen in the atmosphere to reach a successful reproduction. This exposes sensitive subjects to pollen allergens for several months of the year, increasing their probability to become sensitised against one or more pollen types (D'Amato et al., 2007). Pollen sensitisation occurs when the subject inhales a quantity of allergenic pollen exceeding a certain threshold level, that variates according to the individual genetic background, the pollen type, and environmental factors. Sensitisation usually takes place in the respiratory mucosa, where humidity causes inhaled pollen to hydrate. Hydrated pollen releases some proteins (pollen allergens) that are misidentified by the immune system as possible antigens, activating an IgE-mediated hypersensitivity reaction against them (Asam et al., 2015; Mothes et al., 2004). This causes an inflammation of the upper airways symptomatic of the seasonal AR commonly known as "hay fever" or more properly "pollinosis" (D'Amato et al., 2007). According to the International Study of Asthma and Allergies in Childhood (ISAAC), the global prevalence of pollinosis at the beginning of this century was 22.1% in older children (13- to 14-yr-old) and 11.8% in younger ones (6- to 7-yr-old), with an annual increment of 0.3% in both age groups (Björkstén et al., 2008). These values however variate greatly between different geographic regions, because pollen allergy incidence is influenced by environmental and bioclimatic conditions that define allergenic plants distribution.

Pollen grains diameter ranges from 5 to 200 μm, so they can only enter the upper airways. Nonetheless, in the last decades it was proven that pollen allergens can also be carried by small particles of 2–5 μm in diameter, such as particulate matter (PM) and plant fragments. In this way, they can reach the lower, narrower airways, triggering allergic asthma. This situation often occurs during thunderstorms, when higher concentrations of pollen are resuspended in the air, and meteorological conditions promote the transfer of its allergens to other particles (Burge and Rogers, 2000; D'Amato, 2001; Harun et al., 2019). This "thunderstorm asthma" also occurs in pollinosis sufferers with no prior diagnosis of asthma. Furthermore, high pollen days during peak pollen season (≥50 grains/m^3) can increase the number of emergency department presentations for asthma attacks (Erbas et al., 2018). Some

authors also recorded a dose-response association between pollen exposure and asthma symptoms, suggesting threshold concentrations for different pollen types (Erbas et al., 2012; Galan et al., 2010; Tobias et al., 2004). High atmospheric levels of grass pollen, in particular, seem to be positively associated with severe asthmatic reactions in temperate climates, according to some authors (Erbas et al., 2018). However, this correlation is not always apparent, especially in subtropical areas (Ridolo et al., 2007; Simunovic et al., 2020). In European countries, also tree pollen seems to be positively related to asthma onsets (Guilbert et al., 2018; Ridolo et al., 2007).

The swelling of the upper airways caused by pollen in allergic subjects might explain asthma symptoms exacerbation. Besides, since the majority of asthmatics have rhinitis and up to 40% of patients with rhinitis have asthma, it cannot be ruled out that the two diseases sometimes exist as a continuum of inflammation, due to the functional complementarity of upper and lower airways, their interactions, and the similarity of their mucosae. This concept is known as "one airway, one disease" (Bousquet et al., 2008; Grossman, 1997).

Even if the role of pollen allergy in the global burden of asthma is yet to be comprehended, it is clear that both allergic asthma and pollinosis heavily affect the quality of life of pollen allergy sufferers, impairing their mental health, compromising their education and professional careers through presenteeism and absenteeism, and consequently lowering their productivity (Zuberbier et al., 2014).

Due to the high prevalence, the ubiquitous diffusion, and the medical and social burden of pollen allergies, their management is of global relevance. Nonetheless, to date there is still no decisive cure for this disease, hence it is important for pollen allergic subjects to be constantly aware of atmospheric pollen allergens level during the pollen season, in order to plan their movements and medications accordingly (Geller-Bernstein and Portnoy, 2019).

The regional nature of allergenic plants distribution, and the different biology fields involved in this topic, have promoted the development of a broad range of techniques and approaches to pollen allergenicity monitoring. This proliferation of methodologies for pollen allergy risk assessment calls for periodic literature reviews to summarise and classify them, and to address their optimal applications. With the present work, we propose a classification of pollen allergy monitoring methods based on their subject: (I) "vegetation-based" for ecological approaches focusing on allergenic plants; (II) "pollen-based" for aeropalynologycal approaches monitoring airborne pollen; (III) "allergen-based" for molecular approaches

detecting airborne pollen allergens. We discuss their viability for risk assessment and the better context for their implementation, prospecting possible improvements and future developments.

It is however important to remark that the methods hereby presented are not exhaustive, since they are not comprehensive of the whole literature on aerobiology studies and approaches. In fact, due to the vastity of the topic, in some cases it has been necessary to limit the discussion to the most common or promising techniques.

2. Vegetation-based approach

2.1 Vegetation-based monitoring: allergenicity indices

Distribution of allergenic pollen can be the result of natural floristic patterns, or a consequence of human landscaping. Landscaping and gardening strongly influence the vegetation diversity of an area, by introducing alien species or boosting the dominance of few native species, changes that are reflected by the air biota (Burge and Rogers, 2000; Capotorti et al., 2020; Cariñanos and Casares-Porcel, 2011). While many of the ornamental native trees are highly allergenic (Thompson and Thompson, 2003), exotic pollen types are usually not problematic because the locals have never been exposed to them. Nonetheless, pollen allergens from different plants can be cross-reactive, triggering allergic symptoms in patients that have been directly sensitised only against one of them (Mothes et al., 2004). Moreover, the massive introduction of a wind-pollinated exotic plant can lead over time to the sensitisation of susceptible subjects against it, as it happened for elm trees in eastern U.S.A., Australian pine in Spain, and cypress in Italy (Cariñanos and Casares-Porcel, 2011; Mothes et al., 2004; Sposato and Scalese, 2013). To understand the allergenicity potential of the urban green areas, three main allergencity indices have been proposed in the last 20 years.

The first one published is called AI (Allergenic Index) or SAI (Specific Allergenic Index), and has been tested on urban spontaneous and anthropogenic vegetation in Italy and Serbia (Ciferri et al., 2006; Hruska, 2003; Mrđan et al., 2017). By this method, urban ecosystems are sampled along gradients to identify ecological drivers of allergophytes distribution. Then, SAI is calculated for each plant species as the sum of values attributed to life cycle, phenology, cross

reactivity and abundance (Tab. 1). SAI for the whole green area is assumed to be the average SAI value of the individual species (Hruska, 2003), and it is calculated as follows:

$$SAI = \frac{\sum_{i=1}^{n} lc_i + pp_i + cr_i + a_i}{n} \ ;$$

with *n*= number of allergenic species, and the other parameters calculated for each species as explained in Tab.1.

Table 1 *SAI parameters, with their levels and related arbitrary numerical value* (Hruska, 2003)

Life cycle (lc)		Phenanthesic period (pp)		Cross reactivity (cr)		Abundance (a)	
Definition	Value	Duration	Value	Presence	Value	Cover %	Value
Annual	1	Less than 1 month	0.5	None present	0	<1	0.5
Biennial	2	More than 1 month	2	Present	1	1-25	1
Perennial	3					25-50	2
						50-75	3
						75-100	4

This index ranges between 2 and 10, and plants or parks are considered slightly allergenic with SAI up to 3, moderately allergenic from 4 to 6, and strongly allergenic from 6 to 10. This ranking shows a positive correlation with the pathological picture of pollen-sensitized patients (Hruska, 2003). SAI has the advantage to acknowledge both cross-allergenicity and the ephemeral contribution of non-perennial species to the airborne pollen load. On the other hand, it does not refer to the actual allergenicity of plants, in terms of sensitisation incidence. Furthermore, in this index all the phenanthesis periods are considered overlapping, so it must be associated with phenograms.

Recently, Cariñanos and colleagues have proposed the Urban Green Zones Allergenicity Index (I_{UGZA}). First published in 2014, it has been fine-tuned and applied to various city parks in many European cities (Cariñanos et al., 2014, 2017, 2019; Jochner-Oette et al., 2019; Kasprzyk et al., 2019b). The formula underwent through some changes over the years, but it can be generalized as it follows:

$$I_{UGZA} = \frac{1}{H_{max} * PAV_{max} * S_T} * \sum_{i=1}^{k} n_i * PAV_i * V_i$$

I_{UGZA} parameters, classified in biometric and biological, are explained in Tab. 2a and Tab. 2b. The theoretical maximum value for I_{UGZA} is 1, ideally representing a surface entirely covered by the most allergenic plants at their maximum height. This assumption however is in contrast with the decision of the authors to not take into account the "exceptional values" (H=18 m, ap= 4) when calculating H_{max} and PAV_{max} (Cariñanos et al., 2016, 2014). Minimum I_{UGZA} value is 0, attainable when all the plant species are non-allergenic, or when they do not produce pollen.

Table 2a *Definition and values of biometric parameters for Urban Green Zones Allergenicity Index (IUGZA)* (Cariñanos et al., 2014; Kasprzyk et al., 2019b)

Parameter	Definition		Arbitrary values (proposed by the authors)	
H_{max}	Maximum height reachable by pollen-producing vegetation. It can be evaluated accurately in situ, or it can arbitrarily be considered as the maximum height potentially reachable by the park vegetation.		14 m	
S_T	Total surface of the urban green area studied.			
n_i	Number of individuals of the i-species in the green area.			
V_i	Average volume of pollen-producing vegetation for each individual of the i-species (*i.e.* tree crowns, bushes, turfs). Foliage shape is simplified into one of the following regular geometric shapes:			
	Cylinder:	$V_i = H_i * S_i$		
	Cone:	$V_i = H_i * \dfrac{S_i}{3}$		
	Sphere:	$V_i = \dfrac{4}{3}\pi r^2$		
	Emisphere:	$V_i = \dfrac{2}{3}\pi r^2$		
	Cuboid:	$V_i = H_i * S_i$		
H_i	Average height of pollen-producing vegetation for each individual of the i-species. It can be evaluated accurately in situ, or it can be assumed to be the maximum height reported for the species. In the last case, arbitrary height categories are proposed.		Trees and shrubs:	2 m
				6 m
				10 m
				14 m
				18 m
			Herbs:	0.25 m
S_i	Average surface covered by each individual of the i-species (crown projection for trees). It is measured in situ.			

Table 2b *Definition and values of biologic parameters for Urban Green Zones Allergenicity Index (IUGZA)* (Cariñanos et al., 2014; Kasprzyk et al., 2019b)

Parameter	Definition	Arbitrary values (proposed by the authors)	
PAV (or VPA)	Allergenicity Potential Value of each species. PAV= tp*ap*dpp	$PAV_{max} = 9$	
Tpv2:	Type of pollination. Drawn from literature.	Sterile, cleistogamous or female	0
		Entomophilous	1
		Amphiphilic	2

		Anemophilous	3
Ap	Allergenicity potential of the plant species relative to the study area. Drawn from literature and databases.	Nonallergenic	0
		Low	1
		Moderate	2
		High	3
		Major allergen in the region	4
Dpp	Duration of pollination period. Pollen grains belonging to the same pollen type are considered as a single pollination event.	1-3 weeks	1
		4-6 weeks	2
		>6 weeks	3

Vegetation sampling strategies proposed by the authors range from a tree census of the whole park, to a selection of relevant species, to a combination of census for arboreal species and systematic sampling for herbaceous ones. Advantages of this method are the scalability (Cariñanos et al., 2017), and the evaluation of important allergenic features. There is also the possibility to simplify the method to a point that it might be applied almost directly on the floristic census of the area, on remote, without the guidance of experts.

There are anyway some downsides. First, I$_{UGZA}$ assumes the hypothesis of a positive correlation between vegetation volume and pollen production, which to this date has not been proven. Hence, it is necessary to associate the evaluation of local airborne pollen concentrations to the allergenicity index, since I$_{UGZA}$ alone is not always accurate in stating the real hazard posed to subjects with pollinosis by an urban green area (Kasprzyk et al., 2019a). Another improvable aspect is the standardization of sampling and calculation methods, to make the results comparable.

In 2019, Pecero-Casimiro and collaborators published the Aerobiological Index of Risk for Ornamental Trees (AIROT), merging plant biological features with non-biological factors that influence pollen production and dispersal, such as geographical features and urban landscape (Tab. 3) (Pecero-Casimiro et al., 2020, 2019). To do so, AIROT is combined with LiDAR remote sensing and Kriging interpolation, creating risk maps of pollen concentrations in urban environments, based on the distribution of allergenic ornamental trees and the presence of physical obstacles. This index can be calculated for individual plant species in different city areas, using the formula:

$$AIROT = \sum_{i=1}^{n} \frac{(PD_i \times (N_i \times \alpha_i) \times M_i \times Sh_i \times H_i)}{ST}$$

The results can be normalised on a scale from 0 (minimum risk) to 1 (maximum risk), creating a legend for risk maps and safe itineraries. However, the actual influence of its parameters on

pollen concentrations is still unclear, therefore a comparison with observed airborne pollen concentrations is needed to assess this method reliability.

Table 3 *Definition and values of Aerobiological Index of Risk for Ornamental Trees (AIROT) parameters (Pecero-Casimiro et al., 2019)*

Parameter	Definition	Arbitrary values	
PD_i	Potential Dispersability of the i-area. It is calculated by visibility analysis, using GIS and LiDAR to map all the potential obstacles to pollen dispersion.	0 - 10	
N_i	Density of the species in the i-area (trees/ha)		
α_i	pollen production according to the species and use	0.001, 0.01, 0.05, 0.1, 1	
M_i	Average maturity degree of individuals of the studied i-species in the i-area, calculated measuring trunk diameter and branch development	Young (<1 year)	1
		Adult (between 1 and 10 years)	5
		Mature (>10 years)	10
SH_i	Incidence of urban landscape on pollen dispersion in the i-area	residential/office/commercial/industrial street	1
		parkway	2
		boulevard	4
		main street	6
		wide avenue	8
		parks or public squares	10
H	Height above see level of the i-area	>1500 m.a.s.l	1
		<1500 m.a.s.l	5
ST	Total surface of the city in km^2		

2.2 Vegetation-based prevention: gardening guidelines and plant control

Since urban vegetation is anthropogenic, the impact of urban greenery on public health can be reduced by adopting hypoallergenic gardening guidelines (Thompson and Thompson, 2003). The most direct way to reduce allergenic pollen availability is to avoid planting potentially allergenic species. The American Academy of Asthma and Immunology advices gardeners to only use entomophilous, non-toxic and non-invasive plants, and offers a list of recommended low-allergenic plants suitable for different regions (Green et al., 2018). Another option is to prefer sterile varieties or species with low to moderate pollen productivity. For dioecious species, mainly female individuals should be selected, whether this does not pose substantial problems of fruits and seeds littering. When utter omission of

allergenic plants is impossible, it is important to not associate cross-allergenic species, to avoid potentially invasive species, and to adopt an appropriate pruning schedule to reduce or prevent the blooming (Cariñanos and Casares-Porcel, 2011; Green et al., 2018). These guidelines hardly apply to lawns, where grass allergens can also be aerosolised with mowing, even when flowers are absent. Hence, low-allergenic herbs and shrubs should preferred, along with hardscaping alternatives (Green et al., 2018). These guidelines however are difficult to apply to the existing urban vegetation.

In fact, removal of healthy trees from a landscape because of their allergenicity is not convenient from a cost-benefit point of view. Even when planning new public green areas, enforcing these guidelines in plant selection over aesthetic and practical criteria might be challenging. First, it would require a politic action (Cariñanos and Casares-Porcel, 2011), and secondly, sometimes hypoallergenic alternatives might not meet environmental sustainability criteria for urban greenery selection (Grote et al., 2016). However, hypo-allergenic gardening might not be decisive, because of allergenic pollen sources in the surrounding areas (Green et al., 2018). Moreover, it is impossible to rule out the allergenicity, and pollen from entomophilous species such as Indian bean (*Catalpa speciosa*) and horse chestnut (*Aesculus hippocastanum*) have shown cross-reactivity with common allergens (Green et al., 2018). Some countries tried to achieve allergen pollen reduction by promoting laws that forbid the planting of pollen-rich trees. This is the case of the mulberry (*Morus* sp.) in the Southwestern United States. Another approach is to control ruderal allergenic species, such as ragweed, but this is made difficult by the rapid and intense proliferation of these weeds on disturbed ground, that are typical of urban areas (Burge and Rogers, 2000).

3.   Pollen-based approach

3.1   Airborne pollen sampling

3.1.1 *Samplers for outdoor monitoring*

Airborne pollen concentrations in a specific area are not influenced by the local vegetation alone. Pollen can be transported by wind and dispersed by turbulences within the lowest atmospheric layer, from where it can be uplifted to free atmosphere by convection and enter air masses moved by synoptic systems. This way, pollen can undergo long distance dispersal, traveling for dozens of kilometres (D'Amato et al., 2007; Green et al., 2018; Sofiev et al.,

2006). Furthermore, even sedimented pollen grains can be secondarily re-suspended into the atmosphere, contributing more than once to airborne pollen load (Bastl et al., 2017).

Thus, airborne pollen monitoring has always been considered the most reliable and feasible method to evaluate allergic hazard for pollinosis sufferers. To maximise the usefulness of their information, monitoring stations are generally located into urbanised, densely populated areas. They collect atmospheric pollen through air samplers placed on the rooftop, between 15 and 20 m from the ground level, raised at least 1 m off the floor, and distant from any airflow barrier. This placement, along with a vegetation and geo-climatic evaluation of the monitored area, is important to reduce sampling biases, and should be kept similar between stations to enhance results comparability (Bucher et al., 2015; Galán et al., 2014). Since the beginning of aeropalynology, many pollen samplers have been proposed (Mullins and Emberlin, 1997). This review will explore only the ones still commonly employed for airborne pollen monitoring (Tab. 4).

Oldest and simplest pollen monitoring devices are the passive sedimentation samplers, in which pollen naturally settles on the collecting surface due to gravity. Examples of sedimentation samplers are Durham (Durham, 1946; O'Rourke, 1990), Cour Grovette (Belmonte et al., 2000; Cour, 1974), and Sigma-2-like (Miki et al., 2019; Mimić and Šikoparija, 2021; VDI 2119, 2013) samplers, that can collect daily or weekly pollen samples. For longer monitoring periods, various passive samplers collecting pollen in a jar have been developed at the end of the last century, such as Tauber (Cundill, 1991), Oldfield (Bush, 1992; Flenley, 1973), and Behling (Behling et al., 2001) traps, but they are mainly employed in environmental studies (Jantz et al., 2013; Poska, 2013). However, sedimentation samplers have been progressively abandoned in aerobiology, except for peculiar applications (Levetin, 2004).

Table 4 Description of air samplers currently used for outdoor continuous pollen monitoring

Sampler type	Sedimentation sampler			Impaction sampler		
Collection method	Passive sedimentation			Slit impaction		Rotating impaction
Sampler name	Durham sampler	Cour Grovette sampler	Sigma-2-like sampler	Hirst-type pollen and spore trap		Rotorod®
Sampling surface	Glass slide coated with grease	Cellulose garze impregnated in silicon oil	Adhesive slide or foil	Polyester tape coated with silicon oil or petroleum jelly	Adhesive-coated glass slide	Two plastic rods of 1.52 x 1.52 x 32 mm, coated with silicone grease

volumetric	No	Yes	Yes	Yes	Yes	Yes
*d50**	Not specified	Not specified	2.5 µm	3.7 - 5 µm		10 µm
Air intake velocity	-	Wind speed	Wind speed	10 l/min		Calculated with Pappus's Theorem for Volumes
Pollen collection efficiency	Not evaluated	Not evaluated	Variable	80%		80%
Time progression record	None	None	None	Hourly		None
Bibliography	(Durham, 1946; O'Rourke, 1990)	(Belmonte et al., 2000; Cour, 1974)	(Hofmann et al., 2014; Miki et al., 2019; Mimić and Šikoparija, 2021; VDI 2119, 2013)	(Frenz and Boire, 1999; Hirst, 1952; Levetin, 2004; Mandrioli and Puppi, 1978)		(Frenz and Boire, 1999)

*** d50**: value of the particle diameter at 50% in the cumulative distribution

Nowadays, airborne pollen is routinely sampled through volumetric impaction samplers that offer a steadier and controllable capture. They are based on the principle that when the air stream encounters an obstacle, it tends to drift away and bypass it, while airborne solid particles inertially collide against the surface of the obstacle (Levetin, 2004). The first instrument ever used for continuous pollen recording is in fact an impactor sampler, the volumetric Hirst-type pollen and spore trap (Mandrioli and Puppi, 1978). It is still the most widely used pollen sampler, chosen by 70% of the pollen monitoring stations worldwide (Buters et al., 2018). Hirst-type samplers are defined slit impactors because the air is aspired through a narrow inlet with a collecting surface behind. They can collect airborne pollen for either one week, on a polyester sticky tape mounted on a rotating drum, or one day, directly on a glass slide. A clockwork mechanism makes the collecting surface slide away from the inlet every hour, keeping track of the time progression. Daily samples are eventually prepared for light microscopy, usually applying glycerine jelly with basic fuchsin (Bucher et al., 2015; Levetin, 2004).

Other valid options for air quality monitoring are the rotating impaction samplers. While different models have been developed, such as Rotoslide and Rotobar (Ogden and Raynor, 1967; Solomon et al., 1968), the rotating arm impactor Rotorod® (Sampling Technologies Inc., Minnetonka (MN), 1998) is the most popular, mainly employed in U.S.A. and Canada. Particles suspended in the air around the Rotorod® impact against its two rotating rods, sticking to their collecting surface (Frenz, 1999; Heffer et al., 2005). At the end of the sampling the rods are placed in a special microscope slide, and Calberla's stain is applied (Levetin, 2004).

Hirst-type and Rotorod® provide similar results on daily pollen concentrations when compared side-by-side, and they both show an overall efficiency in pollen capture of about 80%. Nonetheless, their performance is differently affected by meteorological factors, being Hirst-type samplers more reliable with low wind speed, and Rotorod® ones with moderate wind speed (between 3 and 6 m/s). When the wind speed is higher than its air intake velocity, Hirst-type sampler might also significantly overestimate concentrations for some pollen types (Frenz, 1999; Geller-Bernstein and Portnoy, 2019; Heffer et al., 2005). For these reasons, before comparing data collected with different devices, it is important to adjust them using inter-sampler conversion factors and considering wind speed (Peel et al., 2014). Furthermore, while Hirst-type traps can sample continuously for one week without human intervention, the Rotorod® system is prone to overloading hence its duty cycle is usually kept at 10%, and adjusted according to the sampling duration and the expected pollen concentration. Therefore, Rotorod® samplers are rarely employed for continuous multiple-day sampling (Frenz, 1999; Frenz and Boire, 1999).

3.1.2 *Samplers for indoor and personal monitoring*

Pollen spectra vary at different heights and locations, and between indoor and outdoor environments. Even if there is a positive correlation between pollen concentrations recorded on the roofs of monitoring stations with those recorded at ground level, airborne pollen is generally more abundant at lower heights, and shows variations in species composition at different heights (Bastl et al., 2017; de Weger et al., 2020; Kasprzyk et al., 2019a; Rojo et al., 2019). In particular, it has been demonstrated that when the sampler is placed up to 10 meters above the ground level, its height is inversely proportional to the pollen concentrations recorded. Pollen concentrations at near-ground level also show great fluctuations, due to local events of emission, deposition, or resuspension of the pollen grains, or to microscale environmental dynamics (Rojo et al., 2019). To assess pollen concentrations at human height, portable samplers can be employed (Tab. 5).

Portable Hirst-type samplers are the most dependable choice for daily continuous records at ground level, but they operate in a fixed position. To evaluate the pollen exposure of a subject throughout the day, compact and wearable pollen personal samplers have been developed. In this case, the air intake velocity of the instrument tends to mimic the human breath rate. Common examples are the sampling cassettes, available as impaction or filtration samplers.

In the first case, particles impact against a glass slide, and the sample can be promptly analysed under light microscopy. Conversely, in filtration samplers, air flows through a porous membrane that captures airborne particles, with a diameter cut-off defined by the filter texture. Pollen is then recovered from the membrane using a detergent, and mounted on a light microscopy slide (Heffer et al., 2005; Levetin, 2004).

Other wearable impaction samplers have been invented throughout the years, either passive like the Personal Aeroallergen Sampler (PAAS) (Yamamoto et al., 2007), or connected to a pump like the Partrap FA52 (Coppa, Biella, Italy) (Berger et al., 2014; Fiorina et al., 1999). Unfortunately, most of them are not commercially available (de Weger et al., 2020). A recently proposed, purchasable portable sampler is the Pollator (Werchan et al., 2018), an active impactor that has a capture efficiency lower than the Hirst-type trap, but a comparable sensitivity to variations and trends in airborne pollen concentrations. It can also record meteorological parameters and keep track of the position via GPS while collecting pollen. A similar device that will likely be soon in commerce is the Pollensniffer (de Weger et al., 2020). This active impactor sampler seems to have a higher collecting efficiency than the 7-days Hirst-type trap for most pollen types, and a desirable user-friendliness.

To attain a precise quantification of the pollen actually inhaled by someone, another option is the nasal air sampler (NAS), an impaction sampler worn inside the nares (Graham et al., 2000). Despite its high-declared efficiency in particle capture, this approach is limited by nasal configuration and function. In general, the reliability of personal samplers alone is disputed, but they are considered a useful complement to routine diagnostic allergy tests. Significant obstacles to their application in wide epidemiological studies however are posed by their relatively high costs, the user engagement they require, and the massive data analysis that should follow (Berger et al., 2014).

Table 5 Description of different portable and personal samplers available on the market.

Sampler type	Slit impaction sampler					Filtration sampler
Sampler name	Hirst-type pollen and spore trap	Sampling cassette	Pollator	Pollensniffer	NAS	Sampling cassette

Sampling surface	Adhesive-coated glass slide	Adhesive-coated glass	Adhesive tape on a cartridge	Vaseline-coated Melinex® strip on a glass slide	Acrylic pressure-sensitive adhesive tape	Filter membrane
Wearable	No	Yes	Yes	Yes	Yes	Yes
*d50**	3.7 μm	1.7-2.8 μm	Not specified	Not specified	5 μm	Adjustable
Sampling duration	24 h	10 min	16 h	5–6 h	20 min	10 min
Optimal air intake velocity	10 l/min	15 l/m	6 l/min	7.5–9.2 l/min	25 l/min	15 l/m
Pollen collection efficiency	80-90%	95%	Not specified	Not specified	100%	65%
Time progression record	Yes	No	No	No	No	No
Bibliography	(Heffer et al., 2005; Hirst, 1952)	(Grinshpun et al., 2007; Heffer et al., 2005)	(Werchan et al., 2018)	(de Weger et al., 2020)	(Graham et al., 2000)	(Heffer et al., 2005)

***d50**: value of the particle diameter at 50% in the cumulative distribution

3.2 Pollen analysis

3.2.1 *Manual pollen counts*

Once collected with air samplers, pollen can be analysed by different means, according to the research purpose. The main aim of pollen sampling is to inform allergic patients about its atmospheric concentration, hence pollen counts are the most common analysis. While duration and frequency of air sampling are decided by each station, pollen counts are usually performed on 24 hours samples. This also means that pollen concentrations are necessarily at least 1 day old when they get published (Geller-Bernstein and Portnoy, 2019). Total number of pollen grains can be determined by optical microscopy, using a haemocytometer (Heffer et al., 2005), but it is common procedure to identify and quantify only pollen from plant species that are clinically relevant in the studied area. Allergenic pollen identification is accomplished by trained personnel in light microscopy, at 400x magnification, based on the overall grain morphology (exine, intine, cytoplasm). This method seldomly allows species identification, and airborne pollen grains are commonly identified at family or genus level, or assigned to a non-phylogenetic group called "pollen type" that includes different plant species with pollen grains morphologically indistinguishable from each other (D'Amato et al., 2007).

For timing reasons, only a subset of the sample is analysed, chosen by random fields or transect sub-sampling. According to the European Aerobiology Society, for daily samples collected with a slit impactor the subset should include at least 10% of the surface to minimise

the estimation error, as explained in the European Standard EN16868 (EN16868, 2019; Galán et al., 2014). In fact, the results obtained by reading 10% of the slide surface have been proven to fall within the thresholds of Relative errors in a quality control and reproducibility analysis (Galán et al., 2014). Random field sub-sampling is not recommended because it misses the time progression, and it might be biased by swift changes in pollen concentrations. The International Association for Aerobiology poses as minimum requirements to read 3 horizontal transepts, that account for the whole day, or 12 vertical transepts, that evaluate pollen abundance in certain moments of the day (Gharbi et al., 2017). The latter appears to be the most accurate approximation of the entire slide, but short pollination peaks could be missed if they fall between transepts. Moreover, the number of sweeps needed to cover 10% of the sample surface also depends on the microscope field of view dimension, that is affected by the objective magnification and diameter. Hence, the area to be analysed remains a better reference than the number of transepts (Galán et al., 2014). Pollen counts precision also depends on sampled pollen concentration, hence estimations of daily pollen concentrations are reliable only when 50 pollen grains or more are counted in longitudinal sweeps (Gharbi et al., 2017; Levetin, 2004).

Once pollen grains in the subsample have been identified and counted, raw abundance data of each taxon are multiplied by a conversion factor to obtain average daily concentrations expressed as particles per cubic meter of air (P/m^3) (Bucher et al., 2015; Galán et al., 2014). For long-term monitoring, these concentrations can be elaborated into their integral over time, called Annual (or Seasonal) Pollen Integral (APIn or SPIn) (Galán et al., 2017). Counting pollen grains while still fresh is time-effective, but it does not provide a good image resolution. When a more accurate identification is needed, pollen can be acetolysed to better visualise exine diagnostic details. Acetolysis consists of a dehydration by glacial acetic acid (CH$_3$COOH), followed by an acetylation with acetic anhydride (C$_4$H$_6$O$_3$) and sulfuric acid (H$_2$SO$_4$) in a 9:1 ratio, at 100°C for 10 minutes. Samples are then washed, dehydrated in ethanol, and resuspended in glycerine, so they can be mounted on microscope slides. This treatment removes non-sporopollenic and non-chitinous organic components from the sample, including intine and cytoplasm of the pollen grains, and it gives an amber shade to the exine, enhancing its features (Erdtman, 1969, 1943; Hesse et al., 2009). During acetolysis, known amounts of a marker are usually added to the sample. These markers can be exotic fern spores (e.g. *Lycopodium*) (Stockmarr, 1971), plastic microbeads (Ogden III, 1986), or black

ceramic spheres (Kitaba and Nakagawa, 2017). In this approach, pollen grains are usually counted up to 150, and their concentrations in the sample are expressed as relative frequencies, based on the number of marker units counted (Erdtman, 1943). Being a slow and demanding process, acetolysis should be applied only to small aerobiological samples, sporadically collected for brief studies. Examples of aerobiological samples fit for this treatment are those gathered by filtration (*e.g.* sampling cassettes and air filters), sedimentation (e.g. Cour sampler, Tauber, Oldfield, and Behling traps), or other sampling methods lacking time progression. For instance, to evaluate personal exposure to airborne pollen, hair can be used as a sampling surface, making the volunteers wash their hair weekly and collect the rinsing water. Pollen is then concentrated, acetolysed and mounted on a glass slide (Charpin et al., 2010; Penel et al., 2017). Another non-conventional approach is to collect the dust sedimented on surfaces by vacuum, and then to concentrate and acetolyse the pollen present in the sample (Bastl et al., 2017; Gore et al., 2006).

3.2.2 *Automatic pollen counts*

Pollen counting is a labour-intensive and time-consuming process, that requires a specific expertise gained by technicians over a long training period. Another downside of manual counts is the subjective component of pollen identification, that tends to lower the between-analysts reproducibility (Galán et al., 2014). From the beginning of this century several attempts have been made to create a reliable automatic system for pollen recognition (Holt and Bennett, 2014). The integration of microscopy with pollen identification software allowed to automatically simulate the whole counting process, limiting the human intervention to labelling the libraries used to train the recognition algorithms, and checking their results. The first instrument produced for this purpose, to our knowledge, is the Classifynder (Holt et al., 2011). It combines robotics, image processing and neural networks to find pollen on the slide, capture, analyse and store its image, and identify its type. On fresh pollen slides with few different types, its results are consistent with those of palynologists, even if its pollen counts are lower. It also takes a slightly longer time than humans to read a slide, but compensate with a considerably higher accuracy, especially because it cannot read the same grain twice (Holt et al., 2011).

With digital microscopes becoming more common, and machine learning technologies making significant improvements, there has been an increase in efficiency of automatic pollen

recognition, that is now based on more sophisticated feature extractors and supervised learning techniques (also called classifiers). For example, in 2016 Gonçalves and collaborators proposed a computer vision system to identify acetolysed pollen images, using Color, Shape and Texture (CST) and Bag of Visual Words (BOW) feature extraction algorithms, and the C-Support Vector Classification (C-SVC) classifier. They obtained an overall pollen classification accuracy greater than 64%, close to non-expert human performance, over 23 different pollen types (Gonçalves et al., 2016). However, progresses in this field have always been obstructed by the complexity of exine structure, the subtle differences between some pollen types, and the variability within type caused by grain orientation, pollen clumps, or wall rupture. Moreover, discriminating features are decided *a priori* by the researchers, a process that is time-consuming, requires informatics knowledge, and can bias the identification. In fact, human discrimination limits are reflected by the algorithm results, especially with high numbers of pollen types (Gonçalves et al., 2016; Holt et al., 2011). Deep learning algorithms can solve this problem, being able to autonomously identify and learn discriminating features of images from different classes. In particular, pre-trained convolutional neural networks (CNN) such as Alexnet can be employed for automatic feature extraction over large pollen images databases, a quicker approach than training a CNN from scratch. A setup where Alexnet extracts features from a pollen database, it is then retrained by transfer learning, and the features extracted thereafter are categorised using a linear discriminant classifier, allowed to correctly classify 97% of acetolysed pollen images from the same database of 23 pollen types used by Gonçalves and collaborators. It also showed a high processing speed, producing 170 predictions per second (Sevillano and Aznarte, 2018). A similar setup, associated with image pre-processing and data augmentation, led to an even better performance, exactly classifying 98% of the acetolysed pollen images tested, over a dataset produced by the Classifynder classification system containing 46 pollen classes (Sevillano et al., 2020).

Besides, it is not clear how these algorithms would perform with fresh pollen slides containing mixtures of unknown pollen types. Another limit is that automatic counts are still performed after pollen is sampled and mounted on the slide. To remove the delay between the air sampling and the publication of pollen bulletins, it is necessary to implement a real-time (RT) sampling and recognition system. This approach is already well established in Asia (Buters et al., 2018), while Europe is currently working towards an international RT pollen monitoring

network with the EUMETNET AutoPollen programme (Clot et al., 2020). Although different technologies have been applied to automatic aerosol analysis, image recognition and laser (or light) induced fluorescence (LIF) have proven to be the most effective (Tab. 6). Image recognition technology was the first to be applied to RT pollen analysis (Bennett, 1990; Šauliene et al., 2019). Japan pioneered this approach, building the first national automated pollen monitoring and forecasting network, Hanakosan, mostly based on the KH-3000 sensor (Yamatronics, Yokosuka, Japan). This sensor uses laser beam scattering to reconstruct and recognise the pollen grain morphology, but it is unable to distinguish between pollen types with the same scattering profile. Hence, while these devices optimally identify the main Asian allergenic pollen (*Cryptomeria japonica*), they still do not perform as well with more complex and diversified pollen spectra (Buters et al., 2018; Huffman et al., 2019; Kawashima et al., 2017). In other countries, where allergenic pollen grains are more variable, other instruments are preferred. For instance, in the USA a compact image-based RT pollen sensor, APS by PollenSense™ (Lucas et al., 2016), has been recently launched and commercialised (https://www.pollensense.com/). In Europe, the German ePIN automatic pollen monitoring network employs image-based BAA500 detectors (Hund-Wetzlar, Wetzlar, Germany), that use light microscopy mimicking the workflow of classic pollen counts. Their recognition algorithm can even be manually trained by experts (Huffman et al., 2019; Oteros et al., 2019; Šauliene et al., 2019).

However, in Europe LIF techniques have been historically preferred for aerosol monitoring. LIF-based sensors expose airborne particles to monochromatic light, inducing and detecting the autofluorescence typical of some organic molecules. This way, they can distinguish between bioaerosol and inorganic air pollutants (Huffman et al., 2019). Since related organisms may have similar LIF spectra, a precise identification of pollen types by fluorescence alone is challenging, and LIF-based instruments like the Wideband Integrated Bioaerosol Spectrometer or WIBS (Droplet Measurement Technologies, Longmont, Colorado) can only assess whether a biological particle could be pollen, based on its size and autofluorescent molecules combination. Other limits to this approach are the possible interference of inorganic particles containing aromatic hydrocarbons, and a change in biomolecules fluorescence properties due to growth conditions, agglomeration, or physical and chemical modifications (Calvo et al., 2018).

Nonetheless, the method can be significantly improved using multiple excitation wavelengths, and coupling LIF with other technologies (Huffman et al., 2019). It is the case of PA-300 last model, Rapid-E (Plair SA, Geneva, Switzerland), a LIF-based sensor that provides RT airborne pollen concentrations by combining a detailed autofluorescence analysis with light scattering. It is considered to date the most effective RT device, and it can distinguish between four macro-groups: (I) Grass pollen, (II) *Alnus*, *Corylus*, *Betula* and *Quercus*; (III) *Salix* and *Populus*; (IV) *Festuca*, *Artemisia* and *Juniperus*. This technology has the potential for a better resolution, but more research efforts are needed (Šauliene et al., 2019).

Another peculiar combination of LIF and image-based technology is the Poleno (Swisens AG, Horw, Switzerland). In this case, pollen identification strongly relies on the light scattering, thanks to convolutional neural networks trained with palynological databases. This device is also the first one capable of reproducing a holographic image of the pollen grain, allowing the user to verify the results or to train the algorithm by manual labelling. On one hand, an evolving algorithm can constantly improve the identification skills of the instrument, but on the other hand it reduces the reproducibility of results between individual stations. This technology is however limited by the risk of overloading at high atmospheric pollen concentrations, and by a size-dependent particle loss (Huffman et al., 2019; Sauvageat et al., 2020).

Results provided by RT automatic sensors have been compared to the traditional monitoring approach (Tab. 6), showing variable correlation with manual pollen count results, depending on the instrument, the pollen type, and the time interval considered. Although these correlations are not always directly comparable, automatic pollen counters that best approximate the daily pollen concentrations estimated by traditional approach to date appear to be BA500 and Rapid-E (Crouzy et al., 2016; Oteros et al., 2020; Tešendić et al., 2020). New information is expected in the near future as these sensors are being improved, calibrated and compared (Tummon et al., 2020).

Other RT approaches have been applied to pollen recognition, but they are not implemented in automatic sensors yet. It is the case of Raman and Fourier transform infrared spectroscopies, that use a photon beam to collect chemical information from a given sample. To distinguish different pollen spectra, it is necessary to use infrared light, avoiding the interference of pollen autofluorescence. Microspectroscopy methods in particular can provide pollen identification with high taxonomic resolution. In lab tests, near-infrared Raman

microspectroscopy identified 13 plant species from pollen mixtures with 96% precision. It is however unclear if this performance could be maintained with real airborne samples (Huffman et al., 2019; Rittenour et al., 2012).

Table 6 Real-time sensors employed for automatic recognition of airborne pollen grains.

Sampler type	Image-based			LIF-based		
Sampler name	KH-3000	BAA500	APS by PollenSense™	WIBS	PA-300 Rapid-E	Poleno
Recognition principle	Forward- and side-scattering from IR-A laser beam	Optical microscopy	Image capture in a lighting environment Convolutional neural networks	Elastic scattering from red laser beam, UV laser-induced fluorescence, Machine learning	Multi-angle scattering from near-UV laser beam, Deep-UV laser-induced fluorescence, Artificial neural networks	Light scattering, Holography, UV laser-induced fluorescence, Convolutional neural networks
Air intake velocity	4.1 l/min	100 l/min	Not specified	2.4 l/min	2.8 l/min	40 l/min
Processing time	Results in real-time	Pollen counts every 3 hours	Results in near real-time	Results in real-time	Up to 4500 particles processed per minute	Results in real-time, hourly resolution
Human intervention	None	Manual labelling (Optional)	None	Data analysis (Optional)	None	Manual labelling (Optional)
Recognition accuracy	Can effectively discriminate *Cryptomeria japonica* from other pollen types	Can recognise at least 11 pollen types with over 70% accuracy	Can identify pollen groups to order and genus 92.5% of the time, with variable accuracy for different types.	Can effectively distinguish pollen in aerosol samples	Can recognise at least 5 pollen types with 80% accuracy; can identify grass pollen and 3 macro-groups of non-grass pollen	Can recognise at least 6 pollen types with over 90% accuracy
Manual check	None	Pollen micrographs from 8 focal positions	None	None	Pollen sampled on adhesive-coated slides	Holographic reconstruction of the pollen grain, Pollen samples (Optional)
Comparison with Hirst-type sampler	Pearson's correlation coefficient for total daily pollen concentrations: 0.52	Spearman's correlation coefficient for total daily pollen concentrations: 0.84	Pearson's correlation coefficient for total daily pollen concentrations: 0.5	Total pollen concentrations of the same magnitude, same average, higher maximum than Hirst-type	Correlation coefficients for total pollen on the whole sampling period: - Pearson's: 0.95 - Spearman's: 0.82 - Kendall's: 0.65	Not available
Bibliography	(Huffman et al., 2019; Kawashima et al., 2017)	(Huffman et al., 2019; Oteros et al., 2020, 2019, 2015)	(Dalan et al., 2020; Lucas et al., 2021, 2016; Lucas and Bunderson, 2019)	(Calvo et al., 2018; Huffman et al., 2019; Ruske et al., 2018)	(Crouzy et al., 2016; Huffman et al., 2019; Šauliene et al., 2019)	(Huffman et al., 2019; Sauvageat et al., 2020)

3.2.3 *Molecular pollen analysis*

Another precise and objective method to identify pollen taxa is using DNA markers. In the last decade there have been a few attempts to combine genomics with aeropalynology, and even if this field is still at an early stage, its near future prospective is promising. One of the first genomic approaches applied to airborne pollen monitoring is the real-time quantitative PCR (qPCR), that provides pollen spectra just 2.5 hours after the sampling. To apply this method, it is necessary to select DNA sequences suitable as species-specific markers for every allergenic plant studied, and to establish qPCR standard curves for each one of them. Airborne pollen samples compatible with this analysis can be collected with different instruments (Tab. 7), DNA is then extracted from the sample and added to the qPCR reagents mixture. This mixture contains species-specific or genus-specific primer/probe sets. Thus, qPCR is run with a standard program and pollen loads of each sample are eventually calculated inserting cycle threshold values into the standard curve equations (Longhi et al., 2009; Rittenour et al., 2012).

Qualitative and quantitative results obtained by qPCR with TaqMan technology showed a positive and highly significant correlation with manual pollen counts of the same samples, with the advantage of a higher taxonomic resolution. Using single- or low-copy nuclear genes as markers allowed to distinguish all the 18 species present in the sample, including pollen types that can be only identified to the Family level in light microscopy, like Poaceae or Cupressaceae (Longhi et al., 2009). Highly preserved markers like nuclear genes grant precise species recognition and reliable pollen quantification (Longhi et al., 2009; Müller-Germann et al., 2015), but they require a minimum pollen quantity that is almost tenfold the one needed for visual counts (Rittenour et al., 2012).

Sensitivity can be improved targeting DNA multi-copy sequences such as the ribosomal ITS region of the nuclear genome (Müller-Germann et al., 2015; Rittenour et al., 2012), or chloroplast DNA (cpDNA) regions like maturase K (*matK*) genes (Mohanty et al., 2017a). ITS markers however might flaw quantitative results, due to differences in ploidy, or due to their copy number variability between species, within species, and even within individuals (Bell et al., 2016). Applications of cpDNA markers in palynology are also problematic, because plastids are inherited maternally and they are mostly degraded in the male gametophyte (Bell et al., 2016; Núñez et al., 2016). While it is possible to detect and analyse cpDNA in pollen grains

(Galimberti et al., 2014), its copy number is likely to vary between species due to different plastid inheritance strategies. These dynamics are yet to be comprehended and they might bias pollen detection and quantification when using cpDNA markers. This issue can be overcome by collecting pollen samples from different individuals, preparing two standard curves of the cpDNA marker per species, and testing the covariance between pollen grains and cycle threshold value (Mohanty et al., 2017b).

When targeting fast-evolving sequences, DNA barcoding is another valid option for pollen recognition. This method is based on the detection of a standardised DNA region, called DNA barcode, that is preserved within species and variable among species (Bell et al., 2016; Valentini et al., 2008). Although a univocal barcode marker for plant species has not been found yet, some cpDNA sequences and the ribosomal Internal Transcribed Spacer (ITS) region are good candidates, used alone or in combination (Bell et al., 2016; Hollingsworth et al., 2009). A recent application of DNA barcoding, called DNA metabarcoding (or targeted amplicon parallel sequencing), allows to simultaneously identify and quantify biological components of small environmental samples containing mixed DNA of different species, using high-throughput sequencing techniques (Banchi et al., 2019; Bell et al., 2016; Hollingsworth et al., 2009). In 2015, Kraaijeveld and collaborators proved that DNA metabarcoding can be effectively applied to airborne pollen samples, using next-generation sequencing (NGS) (Kraaijeveld et al., 2015). Since NGS cannot integrate two distant markers simultaneously, molecular markers are analysed one at a time (Núñez et al., 2016). The sequence of interest is amplified by single or dual index PCR, using universal primers for all the plant genera present in the sample. Then, the DNA is sequenced and aligned by bioinformatic analysis, to identify the plant taxa (Sickel et al., 2015). NGS analysis of the cpDNA locus *trnL* led to unambiguous identification of various European allergenic pollen genera in airborne samples, with a greater resolution than the microscopic counts. In particular, it can confidently distinguish Poaeceae members *Holcus, Hordeum, Phleum* and *Dactilis* (Kraaijeveld et al., 2015). Ribosomal subunit ITS2 instead allowed to effectively identify 99.7% of the sampled spermatophytes on a genus level (Korpelainen and Pietiläinen, 2017), and in some cases even on the species level (Banchi et al., 2020), providing results in good concordance with morphological identification (Korpelainen and Pietiläinen, 2017; Núñez et al., 2017; Núñez and Moreno, 2020; Sánchez-Parra et al., 2021). A recent study suggested that also RuBisCO chloroplast gene (*rbcL*) could be used as barcode for NGS analysis on aeropalynologycal

samples to detect short-term temporal changes in pollen spectra composition throughout the pollen season (Campbell et al., 2020). Although *trnL,* ITS2 and *rbcL* can identify pollen genera often overlooked in morphological analysis, used alone they are not fit for a thorough species-level identification and pollen quantification. For these reasons, the standard barcode for land plants requires a two-loci DNA barcode, including sequences of chloroplast markers *rbcL* and *matK* (Hollingsworth et al., 2009). *matK* has not been used for airborne pollen metagenomics yet, mainly because it is not very efficient in dealing with multiple plant families (Korpelainen and Pietiläinen, 2017). In 2019 a two-loci metabarcoding was performed on airborne grass pollen, combining ITS2 with *rbcL* (Brennan et al., 2019). This study identified to the genus level *Festuca*, *Holcus*, *Alopecurus, Lolium* and *Poa*, showing a higher resolution potential than *trnL* marker (Kraaijeveld et al., 2015). NGS studies on artificial pollen mixtures have proven that the combination of ITS2 and *rbcL* markers enables the taxonomic assignment of many pollen types to the species level, but both markers might miss or misclassify some species, especially rare ones (Bell et al., 2019; Campbell et al., 2020). However, it is not economically advantageous yet to implement metabarcoding with two markers in routine aerobiological monitoring (Campbell et al., 2020).

***Table 7** Real-time quantitative PCR approaches to airborne pollen monitoring*

Application	Evaluating qPCR efficiency	*Betula pendula,* *Artemisia vulgaris* and *Ambrosia artemisiifolia* pollen monitoring	Distinguishing *Juniperus ashei,* *Juniperus pinchotii,* and *Juniperus virginiana* in air samples
Sampler	Hand-sampled pollen from local allergenic plants	High-volume dichotomous sampler (self-constructed)	Hirst-type sampler
Sampling substrate	Polyester tape coated with silicon oil	2 glass fibre filters (diameter cut-off: >3μm and <3 μm)	Polyester tape coated with silicon oil
Sample dimension	-	7-days samples (375 m³ of air)	24-h samples (14.4 m³ of air)
Marker	Single- or low-copy nuclear genes	Nuclear DNA: BP8 and ITS for *Betula;* ITS for *Artemisia* and *Ambrosia*	cpDNA: *matK*
Probes	TaqMan probe dual labelled with a 6-carboxy-fluorescein group and Black Hole Quencher	SYBR® Green	TaqMan probe dual labelled with a 6-carboxy-fluorescein group and Black Hole Quencher
Termocycler	Light-Cycler 480 thermocycler (Roche Diagnostics)	Real-Time PCR MiniOpticon™ System (Biorad)	Step One Plus Real-Time PCR System (Applied Biosystems Inc)

Database	NCBI	NCBI, Genbank	Genbank
Taxonomic level	Species	Genus	Species
Bibliography	(Longhi et al., 2009)	(Müller-Germann et al., 2017, 2015)	(Mohanty et al., 2017b)

Table 8 *NGS metabarcoding approaches to airborne pollen monitoring*

Application	Outdoor airborne pollen monitoring						Indoor deposited pollen monitoring
Sampler	Hyrst-type sampler	Hyrst-type sampler	Cyclone sampler	Hyrst-type sampler	Impaction sampler (DUO SAS Super 360)	Hyrst-type sampler	Filtration sampler
Sampling substrate	Polyester tape coated with silicon oil	Melinex® tape coated with pharmaceutical sterile Vaseline	1.5 ml plastic vial	Melinex® tape coated with silicon-based adhesive	Petri dishes covered with sterile Vaseline	Melinex® tape coated with adhesive	Nylon filter
Sample dimension	1 longitudinal half of a 24-h sampling tape (7.2 m³ of air)	1 longitudinal half of a 7-days sampling tape (50.4 m³ of air)	24-h samples (23.7 m³ of air)	1 longitudinal half of a 24-h sampling tape (7.2 m³ of air)	1-h samples (10.8m³ of air)	6 24-h samples pooled together per week (86.4 m³ of air)	Vacuumed surfaces of 2 m² each
Marker	*trnL*	ITS2	*rbcL*, ITS2	*rbcL*	ITS2	ITS2	ITS2
NGS platform	Ion Torrent/Proton (Thermo Fisher Scientific)	MiSeq (Illumina)	MiSeq (Illumina)	MiSeq (Illumina)	MiSeq (Illumina)	Ion Torrent PGM (Thermo Fisher Scientific)	454 FLX pyrosequencing (Life Science, Roche), MiSeq (Illumina)
Database	Genbank	Custom database with data from Genebank and NCBI	Genbank	NCBI, Atlas of Living Australia	Custom database with data from Genebank and NCBI	PLANiTS2	Genbank
Bioinformatic pipeline	TSSV	Qiime	Python scripts	Qiime	Qiime	Qiime	Mothur
Taxonomic level	Genus	Genus	Genus	Genus	Family, genus	Genus, species	Genus
Bibliography	(Kraaijeveld et al., 2015)	(Núñez et al., 2017)	(Brennan et al., 2019)	(Campbell et al., 2020)	(Núñez and Moreno, 2020; Sánchez-Parra et al., 2021)	(Banchi et al., 2020)	(Korpelainen and Pietiläinen, 2017)

Overall, from published literature (Tab. 8), NGS appears a precise and detailed method to assess the pollen composition of air samples. It is more time-effective than traditional pollen

counts and does not require highly trained personnel. Moreover, it can also detect pollen debris and cytoplasm, potential bearers of pollen allergens that cannot be accounted for in visual pollen counts (Bell et al., 2019; Kraaijeveld et al., 2015). On the other hand, it can lead to misrepresentation of some pollen types when airborne non-pollinic plant material is sampled (Núñez et al., 2017). Additionally, NGS is inaccurate in evaluating pollen content, due to several potential biases at isolation, preservation and amplification levels (Bell et al., 2019). In particular, the PCR amplification step might cause misrepresentation of some taxa, because it conceals the original number of the markers, and because the amplification efficiency of different polymorphisms may vary. When the relative abundance of DNA reads positively correlates with the relative abundance of pollen grains, as it is for *tnrL*, the solution might be correcting the number of DNA sequences by the total number of sampled pollen grains (Baksay et al., 2020; Kraaijeveld et al., 2015). Nevertheless, this correlation is still debated, especially for *rbcL* and ITS2 sequences. Banchi and collaborators reduced some of these uncertainties for ITS2 marker by selecting the primer combinations and PCR approaches that captured the highest plant diversity, and by creating a mock pollen community as control (Banchi et al., 2020). Nonetheless, quantitative biases cannot be ruled out, and they may also differ among markers. Thus, while some authors consider NGS a semi-quantitative method (Banchi et al., 2020), others propose to infer quantitative data by aggregation of presence-absence data from different samples instead (Bell et al., 2019).

PCR-free NGS techniques are also being developed to avoid these complications, such as shotgun metagenomics, based on shotgun sequencing (Bell et al., 2016; Kraaijeveld et al., 2015; Núñez et al., 2016). Yet, this would not entirely solve the problem, and a better understanding of quantitative biases in mixed-pollen DNA barcoding is needed (Bell et al., 2019).

Genomic analysis on airborne pollen in general would surely benefit from a method standardisation, starting from the type and duration of the pollen sampling, that are likely to influence the outcomes. Furthermore, some authors object that the adhesive tape used for Hirst-type traps may contain PCR inhibitors, compromising sequencing outputs (Banchi et al., 2019). PCR inhibitors in air samples might be detected by adding an exogenous standard, and removed through appropriate DNA extraction methods (Rittenour et al., 2012). Another source of bias lays in the DNA isolation. In fact, differences in pollen wall resistance can make DNA extraction uneven between species, and it is also still unclear if results

obtained with different extraction strategies and isolation kits are comparable (Bell et al., 2016). Moreover, DNA metabarcoding on airborne pollen needs the development of a common bioinformatic pipeline and the creation of *ad hoc* databases (Banchi et al., 2019). Another significant limit to pollen genomics is the shortage of marker sequences deposited in genomic databases for some species (Banchi et al., 2019; Bell et al., 2016). However, with the constant update of genomic libraries and the rapid evolution of sequencing and amplification technologies, these approaches will likely become more efficient and affordable in the near future, and therefore suitable for rapid airborne pollen monitoring on a large scale (Bell et al., 2016; Kraaijeveld et al., 2015; Sickel et al., 2015).

4. Allergen-based approach

4.1 Airborne pollen allergens

Conventional allergenic pollen monitoring does not thoroughly describe pollen allergenicity. In fact, allergen content might variate quantitatively and qualitatively within one pollen type (Cecchi, 2013; D'Amato et al., 2007). Because of this variability, a more operational classification for pollen allergens was suggested, based on cross-reactivity rather than botanical origin (Mothes et al., 2004). In fact, atmospheric patterns of cross-reactive allergens can be more clinically relevant than airborne pollen types combinations (Aloisi et al., 2018; Fernández-González et al., 2020).

Allergen content per pollen grain, defined pollen potency, may also vary between individuals of the same species differing in cultivar, age, or growing conditions. For example, there is evidence for tree pollen to be significantly more allergenic with warmer temperatures (Cecchi, 2013; D'Amato et al., 2007; Mothes et al., 2004). Meteorological conditions before and during the pollen season in particular seem to affect pollen potency (Buters et al., 2015). Additionally, since allergens are often involved in pollen-stigma recognition, stressed plants can compensate low pollen production with high expression of these molecules, to maximise reproduction effectiveness (Fernández-González et al., 2011, 2010). When pollen with high potency reaches regions where the same pollen type is usually less allergenic, it creates an allergic hazard undetectable by pollen counts (Galan et al., 2013). Moreover, when interacting with human respiratory mucosa, different pollen taxa may release allergens with variable intensity and speed. Allergen release mechanisms are still largely unknown, but they might

attribute to each species peculiar levels of sensitization or elicitation (Hoidn et al., 2005; Mothes et al., 2004).

Pollen allergens can also be released directly into the atmosphere. In fact, allergens can be removed from pollen surface by friction or leaching, and transferred to other aerosol components such as plants fragments or air pollutants (D'Amato et al., 2007). Moreover, when exposed to rainwater, pollen can undergo germinative abortion, with emergence and subsequent rupture of the pollen tube, releasing submicronic particles that contain cytoplasmic allergens. Emission of such particles can also happen by simple osmotic rupture (Grote et al., 2003, 2000). Furthermore, fully germinated pollen can emit putative nanovesicles called pollensomes (diameter around 30-60 nm), that could act as airborne carrier of allergens (Prado et al., 2015, 2014). It is also possible that allergens are eluted directly into the atmosphere during pollen rehydration, then diffusing in droplets (D'Amato, 2001).

Genetic analysis has attested the existence of allergenic plants debris in the finest aerosol (Müller-Germann et al., 2015), that could derive from either the ruptured pollen or its source plant. Pollen allergens however are also present in the sporophyte tissues, from which they can disperse carried by plant fragments, starch granules, or, according to some authors, Ubish bodies (D'Amato, 2001). All this implies that low airborne pollen concentrations are not necessarily proof of low allergic risk, and vice versa. In fact, substantial quantities of airborne pollen allergens have been detected outside the pollen season, and this could explain the temporal mismatch between pollen exposure and allergic symptoms often reported in epidemiological studies (Cecchi, 2013; D'Amato, 2001; D'Amato et al., 2007).

Besides the abovementioned pollen-related aspects affecting airborne allergens concentrations, also external factors might lead to a misalignment between pollen and aeroallergens peaks, such as meteorological factors (Aloisi et al., 2018; Fernández-González et al., 2020).

Overall, the correlation between airborne pollen and allergens concentrations is not always significant, therefore allergenicity cannot be deducted by pollen concentrations alone (Plaza et al., 2016).

4.2   Pollen allergens sampling

Several studies in the last decade have focused on monitoring airborne pollen allergens and comparing them with pollen spectra. Pollen allergens can be carried by particles significantly smaller than pollen grains, so they require samplers with high intake velocity and low diameter cut-off. However, they seem to be detectable only in particles over 2.5 µm diameter, possibly because particles under this threshold are often diesel particulate, that tends to absorb them (Plaza et al., 2017).

The two devices usually employed for allergens monitoring are Cyclone samplers and cascade (or sieve) impactors (Tab. 9), placed on a rooftop following similar criteria to those used for pollen traps. Cyclone sampler is a volumetric air sampler that conveys the air into a rotating stream within a cylindrical or conical tube, where airborne particles adhere to the walls due to centrifugal force. This technology allows to sort out particles based on their mass, shape and size (Lippmann and Chan, 1979). Cyclone samplers can be employed in either pollen or allergens monitoring, since their particle size selectivity can be regulated (Brennan et al., 2019). However, Cyclone air samplers are designed to collect small particles with diameter of 1 µm or less, so they are mainly employed to collect pollen debris and aeroallergens rather than whole grains. Studies on aeroallergens often adopt multi-vial Cyclone samplers that grant a customisable time resolution and a longer sampling autonomy (Plaza et al., 2017, 2016). At the end of the sampling, the vials are centrifuged, and pollen allergens are isolated from the sample with an appropriate extraction buffer (Aloisi et al., 2019; García-Sánchez et al., 2019; Plaza et al., 2017).

Cascade impactors are multi-stage impaction samplers that capture particles with different aerodynamic properties on separate collecting surfaces. Its diameter cut-off and number of stages are customisable, and the last stage is usually a filtration sampler, to ensure the capture of finest particles (May, 1945). Different versions of cascade impactors have been proposed, with variable collection media and air intake velocities (Alan et al., 2020; Choël et al., 2020; Schäppi et al., 1999), but nowadays the two most popular are Andersen-like samplers (Andersen, 1958; Mitchell and Pilcher, 1959), and high-volume cascade impactors like the ChemVol® (Butraco, Son, The Netherlands) (Buters et al., 2015, 2008). Andersen-like samplers are the first cascade impactors developed, they have relatively low air intake velocity (28 l/min) and use glass fibre filters as impacting surface. After sampling, it

is possible to dry, condition and weight these filters to evaluate the sample mass concentration (Schäppi et al., 1996). Whole filters or their sub-sections are then submerged in the desired buffer to resuspend the captured particles (De Linares et al., 2019, 2007; Schäppi et al., 1996).

ChemVol-like impactors are a more recent invention (Buters et al., 2008), they are designed to collect high air volumes (800 l/min), and they use polyurethane foam as sampling substrate. Allergens can be retrieved either by immersion in the appropriate buffer solution, or by incubating the substrate in ammonium hydrogen carbonate with bovine serum albumin, lyophilising the extract for storage and resuspending it before the analysis. Unlike extraction buffers, the latter treatment removes components that could interfere with analysis, and it also increases test sensitivity. However, extraction buffers are more effective at isolating allergens from the sample (Plaza et al., 2017).

In a side-by-side comparison, trends recorded by the two devices are similar, but Cyclone samplers tend to record higher concentrations of aeroallergens than cascade impactors, and they are more sensitive to low concentrations occurring outside the pollen season (Plaza et al., 2017). Conversely, allergen data obtained by cascade impactors tend to better correlate with pollen concentrations. This might imply that the two devices have comparable efficiency in collecting pollen grains, but Cyclone sampler performs better in capturing smaller aeroallergen carriers as well, maybe due to its wind-orienting vane. Nonetheless, both devices proved to be reliable for airborne allergens sampling (Plaza et al., 2017). Throughout the years, other devices have been proposed for aeroallergen sampling, but they never became of common use, probably because they are not practical, and because they often rely on homemade samplers that would need standardisation. It is the case of electrostatic precipitation samplers (Plaza et al., 2017), and different models of virtual impactors with low flow rate that collect particles on filters or in water (Plaza et al., 2017; Takahashi et al., 2001). Other more generic sampling methods can be found in literature, such as adaptations of Hirst-type traps for immunoblotting analysis (Razmovski et al., 2000), or dust filters from ventilation systems (Sázelova et al., 2002). Meanwhile, new aeroallergen samplers are being developed, such as the one presented by De Linares and collaborators at the 7th European Symposyum on Aerobiology, based on a High-Volume TSP Sampler that collects particles on a glass fibre filter (De Linares et al., 2020).

Table 9 Description of most common aeroallergen samplers employed for pollen allergens monitoring

Sampler type	Cyclone sampler	Cascade (or sieve) impactor	
Collection method	Centrifugal force	Multi-stage impaction	
Common models	Low-volume Burkard multi-vial Cyclone sampler	ChemVol® high-volume cascade impactor	Andersen sampler
Sampling surface	1.5 ml plastic test tubes	Toroid-shaped pieces of polyurethane foam, up to 3 stages	Glass fibre filters, up to 8 stages
Air intake velocity	16.5 l/min	800 l/min	28 l/min
Particle collection efficiency	99% up to 1.06 µm 93% in the range 0.82 - 0.75 µm	Not specified for these substrates	
Time progression record	Adjustable	No	
Bibliography	(Brennan et al., 2019; Fernández-González et al., 2019; Lippmann and Chan, 1979; Plaza et al., 2017)	(Levetin, 2004; Menetrez et al., 2001; Mitchell and Pilcher, 1959; Plaza et al., 2017, 2016; Schäppi et al., 1999)	

4.3 Pollen allergens analysis

First studies on pollen aeroallergens employed passive transfer antigen neutralization techniques or RAST-type analysis. Nowadays, those methods have been abandoned and aeroallergens are usually identified and quantified by Double-sandwich ELISA (García-Sánchez et al., 2019). In this approach, the wells of a microplate are coated with monoclonal antibodies able to specifically recognise the allergen of interest. Once aeroallergens have been captured into the wells, polyclonal primary antibodies are added to detect them. These antibodies can be biotinylated or enzyme-conjugated; in the first case, the plate is then incubated with peroxidase-conjugate streptavidine. Eventually, the plate is developed with a suitable substrate, and allergen concentrations are evaluated measuring the absorbance at substrate-specific wavelength. Calculations are calibrated by using purified allergens as standard (García-Sánchez et al., 2019; Plaza et al., 2017). Some studies also applied indirect ELISA, coating the microplate wells directly with the sampled allergens, adding primary antibodies specific for the studied allergen and then enzyme-conjugated secondary antibodies, and developing the plate with the appropriate substrate (De Linares et al., 2019). With an estimated error of approximately 20%, ELISA assay is considered reliable and it is

regarded as the standard method for aeroallergen monitoring (Buters et al., 2015). However, other approaches have been attempted, like the basophil degranulation assay. This assay evaluates air samples allergenicity based on their capability to induce mediator release from an FcεRI-humanized rat basophil cell line. The cells are passively sensitised with sera of pollen allergic subjects, and then exposed to sequential dilutions of the sampled aeroallergens extract. Levels of β-hexosaminidase are then measured as indicator for histamine release (Buters et al., 2015). Since these techniques require at least one day of processing, some authors tried to develop RT quantification methods.

One option is to evaluate aeroallergens with the BIACORE system, based on surface plasmon resonance. In this method, monoclonal antibodies against target allergens are immobilised on a sensor chip placed in the system. Then, sampled aeroallergens suspended in HEPES buffer are injected in the instrument, and their bond with the antibodies is measured in RT. It is possible to quantify sampled allergens using progressive dilutions of the purified molecules as standard. This instrument can measure up to four different allergens simultaneously, but unfortunately it needs to operate in a controlled environment, hence cannot be connected to the outdoor air sampler. Capillary electromigration (CE) instead can be performed outside, thus could be implemented in an automatic aeroallergen sensor that provides airborne allergens profiles immediately after sampling. After they are extracted from the sampled particles, aeroallergens can be separated by CE techniques such as zone electrophoresis or micellar electrokinetic chromatography, and quantified measuring the UV absorbance at 206 nm (Sázelova et al., 2002).

Another interesting approach is to associate manual pollen counts with aeroallergen quantification, as proposed by Razmovski and collaborators (Razmovski et al., 2000). They used a Hirst-type sampler with transparent, acrylic pressure-sensitive adhesive tapes, that can collect half the pollen grains but twice the smaller particles (1-20 μm) than typical adhesive-coated polyester tapes. After the sampling, the tape is adhered to a polyvinylidene difluoride or nitrocellulose membrane, creating a sandwich, to transfer eluted allergens on the membrane. Finally, the sandwich is immunostained, obtaining a more sensitive allergen detection than ELISA immunoassay. Observing the sandwich in light microscopy with the tape upwards, it is possible to visualise allergens on the membrane as coloured halos behind their carriers on the tape. Furthermore, halo intensity can be used for protein quantification by image analysis.

Regardless of the method used to calculate them, aeroallergens concentrations can eventually be expressed in picograms of allergen per cubic meter of air (pg/m^3), or elaborated into annual and seasonal indices or integrals (eg. AI or SAIn) expressed in $pg*day/m^3$. Allergy Potency (AP) is instead obtained as the ratio of allergens to pollen daily concentrations (Fernández-González et al., 2019; Plaza et al., 2017). These indices are useful to evaluate the relation between aeroallergens, airborne pollen concentrations, meteorological parameters and pollinosis outbursts. However, being retrospective, they cannot be used for allergen avoidance. Airborne allergens are also difficult to forecast because of their marked interannual variability and their unclear relationship with meteorological conditions (De Linares et al., 2019; Plaza et al., 2016). If aeroallergens were carried by pollen grains only, their concentrations could be estimated using pollen dispersal models to map pollen potency (Buters et al., 2015). Besides, in reality the estimation of their dispersal dynamics is complicated by the dimensional variability of their carriers, that have diameters ranging from a hundred microns for pollen to dozens nanometres for nanovesicles (Plaza et al., 2016; Prado et al., 2015; Schäppi et al., 1996). In addition, to date aeroallergens emission is impossible to model since little is still known about the events underlying their expression and release (Cecchi, 2013; Plaza et al., 2017).

5.   Conclusion and future perspectives

Pollen allergenicity monitoring is an old problem that requires new solutions. However, sometimes the will to innovate the field tends to overcome the necessity of standardised, comparable data. Nowadays there is a wide range of different methods available for pollen monitoring, but their relative efficiency is sometimes unclear. This divergence of approaches is partly rooted in the geographical variability of pollen allergies and plant diversity, that makes it difficult to extend local results to other regions, confining aeropalynological research on a national level (Buters et al., 2018). The rapid technological progress of the last decades also participated in this diversification, providing affordable and efficient instruments for numerous applications, and allowing quick data collection and computation (Huffman et al., 2019). However, the technological progress is also providing tools with the potential to improve the standardisation of data collection even in areas with different biogeography, such as remote sensing technologies, or automated pollen monitoring networks (Caparros-Santiago et al., 2021; Huffman et al., 2019; Pecero-Casimiro et al., 2019).

This review attempts to classify and compare all these diverse techniques, in the light of their usefulness to allergic subjects, the main aim of aeropalynology. Airborne pollen counts have always been considered the most reliable option for this purpose. They have been carried on for almost 70 years, helping to comprehend pollen spatial and temporal dynamics and to forecast its future patterns, simultaneously providing important ecological insights. Despite their long-term continuity, aeropalynologycal data collections may often result spatially and temporally incomplete, mostly because traditional pollen analysis is labour-intensive. Progresses in machine learning, in particular with deep learning technologies like CNN, might soon relieve the workload of palynologists, granting at the same time a more rapid, accurate, and precise morphological identification of pollen grains, even to the species level (Sevillano et al., 2020). The implementation of automatic pollen counting systems, in combination with the production of affordable portable pollen samplers, might also promote epidemiological studies based on individual pollen exposure, that are still not cost and time effective with current technology. To date, RT automatic pollen monitoring networks exist in Switzerland, Germany and Japan, but they still yield satisfactory results only with low allergenic species richness. The progressive training of the machine learning algorithms associated to RT pollen sensors might soon lead to the publication of precise pollen bulletins only moments after air sampling.

Thanks to computational intelligence, morphological approach seems to be the most reliable and efficient proxy for pollen identification at the moment. While DNA markers have the potential to identify pollen to the species level, they cannot be used for routine airborne pollen monitoring just yet. In fact, even if DNA metabarcoding by NGS analysis can efficiently and simultaneously discriminate almost all the plant genera even in a small aerobiological sample, it cannot evaluate their concentrations. Furthermore, metabarcoding standard for land plants requires the use of at least 2 markers in combination, complicating NGS analysis and raising its cost (Banchi et al., 2019). On the other hand, qPCR allows to precisely identify and quantify several species of airborne pollen, but its application to daily airborne monitoring is still unlikely as well, due to its expensiveness and technical limits (Rittenour et al., 2012).

Overall, in the near future applications of LIF, spectroscopy, genomics and automated image-recognition might be the common procedure for pollen counts. While this would be a great advance for the discipline, in the perspective of allergen avoidance it might not be worth the

effort. In fact, many studies reported a discrepancy between allergenic airborne pollen levels and pollen allergy manifestations (Cecchi, 2013; D'Amato et al., 2007). Clear associations between these two factors however are difficult to assess for a number of reasons. First, it is almost impossible to clinically define allergic rhinitis in large populations, and this impairs epidemiological studies since unrelated symptoms might be mistakenly attributed to the disease. Even when pollen allergy is diagnosed, reported symptom intensity after pollen exposure remains subjective, and it can also be influenced by biological or environmental factors, like air pollution levels (Ozdoganoglu and Songu, 2012). Furthermore, individual reactions to a certain pollen exposure may also vary according to allergen sensitisation, cross-reactivity and pollen potency. Hence, to objectively evaluate the allergic risk for pollinosis sufferers, IgE levels against a specific allergen of monosensitised subjects should be compared to atmospheric levels of that allergen. Airborne allergen monitoring is feasible and reliable, and unlike pollen counts it can also quantify the risk caused by aeroallergen carriers other than pollen grains (Fernández-González et al., 2011). Implementation of ELISA in routine air quality monitoring however might require some time, and it would be likely focused only on the most important aeroallergens in the region. Besides, ELISA results are produced with one or more days of delay from the actual sampling, hence cannot be used to alert the population. Moreover, they do not take into account the differences in potential allergenicity among allergen isoforms (Wolf et al., 2017). Additionally, predicting future pollen aeroallergen patterns appears even more challenging than pollen forecasting, due to the variability of their carriers and the lack of knowledge about their production and release.

Hence, it is apparent that more basic research is needed to best exploit all the available technology. Understanding how environment and genetics influence allergens production, and characterising pollen allergens release mechanisms, would lead the way to the integration of pollen and allergen quantification into a comprehensive air allergenicity monitoring and forecasting system. To do so, standardised studies comparing airborne pollen spectra, aeroallergen levels, meteorological conditions and allergic reactions are needed. Still, this might not be enough for pollen allergy prevention. Allergen avoidance is often unpractical, because it would heavily interfere with the daily life of allergic subjects, who are more eager to take medicines than to follow such preventive measure (Ozdoganoglu and Songu, 2012). The best way to help them might be to provide a hypoallergenic urban environment, by selecting non-allergenic plants for landscaping, controlling allergenic weeds,

and adopting appropriate maintenance schedules. An allergic risk assessment of existing recreational green areas should also be performed, to warn sensitive visitors against the seasonal allergenicity potential of the park, and to evaluate future interventions (Cariñanos and Casares-Porcel, 2011).

6. Bibliography

Alan, Ş., Sarışahin, T., Acar Şahin, A., Kaplan, A., Pınar, N.M., 2020. An assessment of ragweed pollen and allergen loads in an uninvaded area in the Western Black Sea region of Turkey. Aerobiologia (Bologna). 36, 183–195. https://doi.org/10.1007/s10453-019-09620-z

Aloisi, I., Del Duca, S., De Nuntiis, P., Mandrioli, P., Fernández-González, D., 2019. Comparison of extraction methods for Poaceae pollen allergens. Aerobiologia (Bologna). 35, 195–200. https://doi.org/10.1007/s10453-018-9538-2

Aloisi, I., Del Duca, S., De Nuntiis, P., Vega Maray, A.M., Mandrioli, P., Gutiérrez, P., Fernández-González, D., 2018. Behavior of profilins in the atmosphere and in vitro, and their relationship with the performance of airborne pollen. Atmos. Environ. 178, 231–241. https://doi.org/10.1016/j.atmosenv.2018.01.051

Andersen, A.A., 1958. New sampler for the collection, sizing, and enumeration of viable airborne particles. U. S. Army Chem. Corps Proving Gr. 76, 471–484.

Asam, C., Hofer, H., Wolf, M., Aglas, L., Wallner, M., 2015. Tree pollen allergens - An update from a molecular perspective. Allergy Eur. J. Allergy Clin. Immunol. 70, 1201–1211. https://doi.org/10.1111/all.12696

Baksay, S., Pornon, A., Burrus, M., Mariette, J., Andalo, C., Escaravage, N., 2020. Experimental quantification of pollen with DNA metabarcoding using ITS1 and trnL. Sci. Rep. 10, 1–9. https://doi.org/10.1038/s41598-020-61198-6

Banchi, E., Ametrano, C.G., Tordoni, E., Stanković, D., Ongaro, S., Tretiach, M., Pallavicini, A., Muggia, L., Verardo, P., Tassan, F., Trobiani, N., Moretti, O., Borney, M.F., Lazzarin, S., 2020. Environmental DNA assessment of airborne plant and fungal seasonal diversity. Sci. Total Environ. 738. https://doi.org/10.1016/j.scitotenv.2020.140249

Banchi, E., Pallavicini, A., Muggia, L., 2019. Relevance of plant and fungal DNA metabarcoding in aerobiology. Aerobiologia (Bologna). 36, 9–23. https://doi.org/10.1007/s10453-019-09574-2

Bastl, K., Berger, U., Kmenta, M., Weber, M., 2017. Is there an advantage to staying indoors for pollen allergy sufferers ? Composition and quantitative aspects of the indoor pollen spectrum. Build. Environ. 123, 78–87. https://doi.org/10.1016/j.buildenv.2017.06.040

Behling, H., Cohen, M.C.L., Lara, R.J., 2001. Studies on Holocene mangrove ecosystem dynamics of the Bragança Peninsula in north-eastern Pará, Brazil. Palaeogeogr. Palaeoclimatol. Palaeoecol. 167, 225–242. https://doi.org/10.1016/S0031-0182(00)00239-X

Bell, K.L., Burgess, K.S., Botsch, J.C., Dobbs, E.K., Read, T.D., Brosi, B.J., 2019. Quantitative and qualitative assessment of pollen DNA metabarcoding using constructed species mixtures. Mol. Ecol. 28, 431–455. https://doi.org/10.1111/mec.14840

Bell, K.L., De Vere, N., Keller, A., Richardson, R.T., Gous, A., Burgess, K.S., Brosi, B.J., 2016. Pollen DNA barcoding: Current applications and future prospects. Genome 59, 629–640. https://doi.org/10.1139/gen-2015-0200

Belmonte, J., Canela, M., Guàrdia, R.A., 2000. Comparison between categorical pollen data obtained by Hirst and Cour sampling methods. Aerobiologia (Bologna). 16, 177–185. https://doi.org/10.1023/A:1007628214350

Bennett, B.Y.K.D., 1990. Pollen counting on a pocket computer. New Phytol. 114, 275–280.

Berger, U., Kmenta, M., Bastl, K., 2014. Individual pollen exposure measurements: Are they feasible? Curr. Opin. Allergy Clin. Immunol. 14, 200–205. https://doi.org/10.1097/ACI.0000000000000060

Björkstén, B., Clayton, T., Ellwood, Philippa, Stewart, A., Strachan, D., Ait-Khaled, N., Anderson, H.R., Asher, M.I., Beasley, R., Bjorkstén, B., Brunekreef, B., Cookson, W., Crane, J., Ellwood, P., Foliaki, S., Keil, U., Lai, C.K.W., Mallol, J., Robertson, C., Mitchell, E.A., Montefort, S., Odhiambo, J., Pearce, N., Shah, J., Stewart, A.W., Strachan, D.P., Von Mutius, E., Weiland, S.K., Williams, H., 2008. Worldwide time trends for symptoms of rhinitis and conjunctivitis: Phase III of the International Study of Asthma and Allergies in Childhood. Pediatr. Allergy Immunol. 19, 110–124. https://doi.org/10.1111/j.1399-3038.2007.00601.x

Bousquet, J., Khaltaev, N., Cruz, A.A., Denburg, J., Fokkens, W.J., Togias, A., Zuberbier, T., Canonica, G.W., Weel, C. Van, Agache, I., Bachert, C., 2008. Allergic Rhinitis and its Impact on Asthma (ARIA) 2008. Allergy 63, 8–160.

Brennan, G.L., Potter, C., de Vere, N., Griffith, G.W., Skjøth, C.A., Osborne, N.J., Wheeler, B.W., McInnes, R.N., Clewlow, Y., Barber, A., Hanlon, H.M., Hegarty, M., Jones, L., Kurganskiy, A., Rowney, F.M., Armitage, C., Adams-Groom, B., Ford, C.R., Petch, G.M., Consortium, T.P., Creer, S., 2019. Temperate airborne grass pollen defined by spatio-temporal shifts in community composition. Nat. Ecol. Evol. 3, 750–754.

Bucher, E., Bottarelli, L., De Gironimo, V., Ivaldi, C., Lessi, S., Moretti, O., Verardo, P., Anelli, P., Gottardini, E., Nardelli, V., Onorari, M., Pellegrini, E., Peana, I., Stenico, A., Tassan, F., 2015. POLLnet - Linee guida per il monitoraggio aerobiologico.

Burge, H.A., Rogers, C.A., 2000. Outdoor Allergens. Environ. Health Perspect. 108, 653–659. https://doi.org/10.1016/B978-0-323-29875-9.00020-3

Bush, M.B., 1992. A simple yet efficient pollen trap for use in vegetation studies. J. Veg. Sci. 3, 275–276. https://doi.org/10.2307/3235691

Buters, J.T.M., Antunes, C., Galveias, A., Bergmann, K.C., Thibaudon, M., Galán, C., Schmidt-Weber, C., Oteros, J., 2018. Pollen and spore monitoring in the world. Clin. Transl. Allergy 8, 1–5. https://doi.org/10.1186/s13601-018-0197-8

Buters, J.T.M., Kasche, A., Weichenmeier, I., Schober, W., Klaus, S., Traidl-Hoffmann, C., Menzel, A., Huss-Marp, J., Krämer, U., Behrendt, H., 2008. Year-to-year variation in release of Bet v 1 allergen from birch pollen: Evidence for geographical differences between west and south Germany. Int. Arch. Allergy Immunol. 145, 122–130. https://doi.org/10.1159/000108137

Buters, J.T.M., Prank, M., Sofiev, M., Pusch, G., Albertini, R., Annesi-Maesano, I., Antunes, C., Behrendt, H., Berger, U., Brandao, R., Celenk, S., Galan, C., Grewling, Ł., Jackowiak, B., Kennedy, R., Rantio-Lehtimäki, A., Reese, G., Sauliene, I., Smith, M., Thibaudon, M., Weber, B., Cecchi, L., 2015. Variation of the group 5 grass pollen allergen content of airborne pollen in relation to geographic location and time in season the HIALINE working group. J. Allergy Clin. Immunol. 136, 87-95.e6. https://doi.org/10.1016/j.jaci.2015.01.049

Calvo, A.I., Baumgardner, D., Castro, A., Fernández-González, D., Vega-Maray, A.M., Valencia-Barrera, R.M., Oduber, F., Blanco-Alegre, C., Fraile, R., 2018. Daily behavior of urban Fluorescing Aerosol Particles in northwest Spain. Atmos. Environ. 184, 262–277. https://doi.org/10.1016/j.atmosenv.2018.04.027

Campbell, B.C., Al Kouba, J., Timbrell, V., Noor, M.J., Massel, K., Gilding, E.K., Angel, N., Kemish, B., Hugenholtz, P., Godwin, I.D., Davies, J.M., 2020. Tracking seasonal changes in diversity of pollen allergen exposure: Targeted metabarcoding of a subtropical aerobiome. Sci. Total Environ. 747, 141189. https://doi.org/10.1016/j.scitotenv.2020.141189

Caparros-Santiago, J.A., Rodriguez-Galiano, V., Dash, J., 2021. Land surface phenology as indicator of global terrestrial ecosystem dynamics: A systematic review. ISPRS J. Photogramm. Remote Sens. 171, 330–347. https://doi.org/10.1016/j.isprsjprs.2020.11.019

Capotorti, G., Bonacquisti, S., Abis, L., Aloisi, I., Attorre, F., Bacaro, G., Balletto, G., Banfi, E., Barni, E., Bartoli, F., Bazzato, E., Beccaccioli, M., Braglia, R., Bretzel, F., Brighetti, M.A., Brundu, G., Burnelli, M., Calfapietra, C., Cambria, V.E., Caneva, G., Canini, A., Caronni, S., Castello, M., Catalano, C., Celesti-Grapow, L.,

Cicinelli, E., Cipriani, L., Citterio, S., Concu, G., Coppi, A., Corona, E., Del Duca, S., Del, V.E., Di Gristina, E., Domina, G., Faino, L., Fano, E.A., Fares, S., Farris, E., Farris, S., Fornaciari, M., Gaglio, M., Galasso, G., Galletti, M., Gargano, M.L., Gentili, R., Giannotta, A.P., Guarino, C., Guarino, R., Iaquinta, G., Iiriti, G., Lallai, A., Lallai, E., Lattanzi, E., Manca, S., Manes, F., Marignani, M., Marinangeli, F., Mariotti, M., Mascia, F., Mazzola, P., Meloni, G., Michelozzi, P., Miraglia, A., Montagnani, C., Mundula, L., Muresan, A.N., Musanti, F., Nardini, A., Nicosia, E., Oddi, L., Orlandi, F., Pace, R., Palumbo, M.E., Palumbo, S., Parrotta, L., Pasta, S., Perini, K., Poldini, L., Postiglione, A., Prigioniero, A., Proietti, C., Raimondo, F.M., Ranfa, A., Redi, E.L., Reverberi, M., Roccotiello, E., Ruga, L., Savo, V., Scarano, P., Schirru, F., Sciarrillo, R., Scuderi, F., Sebastiani, A., Siniscalco, C., Sordo, A., Suanno, C., Tartaglia, M., Tilia, A., Toffolo, C., Toselli, E., Travaglini, A., Ventura, F., Venturella, G., Vincenzi, F., Blasi, C., 2020. More nature in the city. Plant Biosyst. 154, 1003–1006. https://doi.org/10.1080/11263504.2020.1837285

Cariñanos, P., Adinolfi, C., Díaz de la Guardia, C., De Linares, C., Casares-Porcel, M., 2016. Characterization of Allergen Emission Sources in Urban Areas. J. Environ. Qual. 45, 244. https://doi.org/10.2134/jeq2015.02.0075

Cariñanos, P., Casares-Porcel, M., 2011. Urban green zones and related pollen allergy: A review. Some guidelines for designing spaces with low allergy impact. Landsc. Urban Plan. 101, 205–214. https://doi.org/10.1016/j.landurbplan.2011.03.006

Cariñanos, P., Casares-Porcel, M., Díaz de la Guardia, C., Aira, M.J., Belmonte, J., Boi, M., Elvira-Rendueles, B., De Linares, C., Fernández-Rodriguez, S., Maya-Manzano, J.M., Pérez-Badía, R., Rodriguez-de la Cruz, D., Rodríguez-Rajo, F.J., Rojo-Úbeda, J., Romero-Zarco, C., Sánchez-Reyes, E., Sánchez-Sánchez, J., Tormo-Molina, R., Vega Maray, A.M., 2017. Assessing allergenicity in urban parks: A nature-based solution to reduce the impact on public health. Environ. Res. 155, 219–227. https://doi.org/10.1016/j.envres.2017.02.015

Cariñanos, P., Casares-Porcel, M., Quesada-Rubio, J.M., 2014. Estimating the allergenic potential of urban green spaces: A case-study in Granada, Spain. Landsc. Urban Plan. 123, 134–144. https://doi.org/10.1016/j.landurbplan.2013.12.009

Cariñanos, P., Grilo, F., Pinho, P., Casares-Porcel, M., Branquinho, C., Acil, N., Andreucci, M.B., Anjos, A., Bianco, P.M., Brini, S., Calaza-Martínez, P., Calvo, E., Carrari, E., Castro, J., Chiesura, A., Correia, O., Gonçalves, A., Gonçalves, P., Mexia, T., Mirabile, M., Paoletti, E., Santos-Reis, M., Semenzato, P., Vilhar, U., 2019. Estimation of the allergenic potential of urban trees and urban parks: Towards the healthy design of urban green spaces of the future. Int. J. Environ. Res. Public Health 16. https://doi.org/10.3390/ijerph16081357

Cecchi, L., 2013. From pollen count to pollen potency: the molecular era of aerobiology. Eur. Respir. J. 42, 898–900. https://doi.org/10.1183/09031936.00096413

Charpin, D.A., Penel, V., Charpin-Kadouch, C., Pichot, C., Calleja, M., 2010. Recovery Of Pollen From Hair Washes According To Hair Characteristics. J. Allergy Clin. Immunol. 125, AB19. https://doi.org/10.1016/j.jaci.2009.12.106

Choël, M., Ivanovsky, A., Roose, A., Hamzé, M., Blanchenet, A.M., Deboudt, K., Visez, N., 2020. Evaluation of hirst-type sampler and PM10 impactor for investigating adhesion of atmospheric particles onto allergenic pollen grains. Aerobiologia (Bologna). 36, 657–668. https://doi.org/10.1007/s10453-020-09662-8

Ciferri, E., Torrisi, M., Staffolani, L., Hruska, K., 2006. Ecologiacal study of the urban allergenic flora of central Italy. J. Mediterr. Ecol. 7, 15–21.

Clot, B., Gilge, S., Hajkova, L., Magyar, D., Scheifinger, H., Sofiev, M., Bütler, F., Tummon, F., 2020. The EUMETNET AutoPollen programme: establishing a prototype automatic pollen monitoring network in Europe. Aerobiologia (Bologna). 4. https://doi.org/10.1007/s10453-020-09666-4

Cour, P., 1974. Nouvelles techniques de détection des fl ux et retombées polliniques: étude de la sédimentation des pollens et des spores à la surface du sol. Pollen spores XVI 1, 103–141.

Crouzy, B., Stella, M., Konzelmann, T., Calpini, B., Clot, B., 2016. All-optical automatic pollen identi fi cation :

Towards an operational system 140, 202–212. https://doi.org/10.1016/j.atmosenv.2016.05.062

Cundill, P., 1991. Comparisons of moss polster and pollen trap data: A pilot study. Grana 30, 301–308. https://doi.org/10.1080/00173139109431984

D'Amato, G., 2001. Airborne paucimicronic allergen-carrying particles and seasonal respiratory allergy. Allergy Eur. J. Allergy Clin. Immunol. 56, 1109–1111. https://doi.org/10.1034/j.1398-9995.2001.00317.x

D'Amato, G., Cecchi, L., Bonini, S., Nunes, C., Annesi-Maesano, I., Behrendt, H., Liccardi, G., Popov, T., Van Cauwenberge, P., 2007. Allergenic pollen and pollen allergy in Europe. Allergy Eur. J. Allergy Clin. Immunol. 62, 976–990. https://doi.org/10.1111/j.1398-9995.2007.01393.x

Dalan, D., Bunderson, L., Anderson, J., Lucas, R., 2020. Results of a Beta Test Evaluating Automated Pollen Identification During Ragweed Pollen Season. J. Allergy Clin. Immunol. 145, AB36. https://doi.org/10.1016/j.jaci.2019.12.738

De Linares, C., Alcázar, P., Valle, A.M., Díaz de la Guardia, C., Galán, C., 2019. Parietaria major allergens vs pollen in the air we breathe. Environ. Res. 176, 1–7.

De Linares, C., Nieto-Lugilde, D., Alba, F., Díaz de la Guardia, C., Galán, C., Trigo, M.M., 2007. Detection of airborne allergen (Ole e 1) in relation to Olea europaea pollen in Clinical and Experimental Allergy. Clin. Exp. Allergy 125–132.

De Linares, C. De, Belmonte, J., Delgado, R., 2020. New methodology for the measurement of airborne allergens, in: 7th European Symposium on Aerobiology - Bioaereosols and Environmental Impacts. p. 119.

de Weger, L.A., Molster, F., de Raat, K., den Haan, J., Romein, J., van Leeuwen, W., de Groot, H., Mostert, M., Hiemstra, P.S., 2020. A new portable sampler to monitor pollen at street level in the environment of patients. Sci. Total Environ. 741, 1–9. https://doi.org/10.1016/j.scitotenv.2020.140404

Durham, O.C., 1946. The volumetric incidence of atmospheric allergens: IV. A proposed standard method of gravity sampling, counting, and volumetric interpolation of results. J. Allergy 17, 79–86.

EN16868, 2019. Ambient air - Sampling and analysis of airbone pollen grains and fungal spores for networks related to allergy - Volumetric Hirst method, European Standard.

Erbas, B., Akram, M., Dharmage, S.C., Tham, R., Dennekamp, M., Newbigin, E., Taylor, P., Tang, M.L.K., Abramson, M.J., 2012. The role of seasonal grass pollen on childhood asthma emergency department presentations. Clin. Exp. Allergy 42, 799–805. https://doi.org/10.1111/j.1365-2222.2012.03995.x

Erbas, B., Jazayeri, M., Lambert, K.A., Katelaris, C.H., Prendergast, L.A., Tham, R., Parrodi, M.J., Davies, J., Newbigin, E., Abramson, M.J., Dharmage, S.C., 2018. Outdoor pollen is a trigger of child and adolescent asthma emergency department presentations: A systematic review and meta-analysis. Allergy Eur. J. Allergy Clin. Immunol. https://doi.org/10.1111/all.13407

Erdtman, G., 1969. Handbook of Palynology. Morphology – Taxonomy – Ecology. An Introduction to the Study of Pollen Grains and Spores.

Erdtman, G., 1943. An Introduction To Pollen Analysis. Chronica Botanica Company.

Fernández-González, D., González-Parrado, Z., Vega-Maray, A.M., Valencia-Barrera, R.M., Camazón-Izquierdo, B., De Nuntiis, P., Mandrioli, P., 2010. Platanus pollen allergen, Pla a 1: Quantification in the atmosphere and influence on a sensitizing population. Clin. Exp. Allergy 40, 1701–1708. https://doi.org/10.1111/j.1365-2222.2010.03595.x

Fernández-González, D., Rajo, F.J.R., Parrado, Z.G., Barrera, R.M.V., Jato, V., Grau, S.M., 2011. Differences in atmospheric emissions of Poaceae pollen and Lol p 1 allergen. Aerobiologia (Bologna). 27, 301–309. https://doi.org/10.1007/s10453-011-9199-x

Fernández-González, M., Álvarez-López, S., González-Fernández, E., Aira, M.J., Rodríguez-Rajo, F.J., 2020. Cross-reactivity between the Betulaceae family and fallout in the real atmospheric aeroallergen load. Sci. Total Environ. 715, 1–9. https://doi.org/10.1016/j.scitotenv.2020.136861

Fernández-González, M., Ribeiro, H., Pereira, J.R.S., Rodríguez-Rajo, F.J., Abreu, I., 2019. Assessment of the potential real pollen related allergenic load on the atmosphere of Porto city. Sci. Total Environ. 668, 333–341. https://doi.org/10.1016/j.scitotenv.2019.02.345

Fiorina, A., Mincarini, M., Sivori, M., Brichetto, L., Scordamaglia, A., Canonica, G.W., 1999. Aeropollinic sampling at three different heights by personal volumetric collector (Partrap FA 52). Allergy Eur. J. Allergy Clin. Immunol. 54, 1309–1315.

Flenley, J.R., 1973. The use of modern pollen rain samples in the study of the vegetational history of tropical regions. Quat. Plant Ecol. 14-H, 131–141.

Frenz, D.A., 1999. Comparing pollen and spore counts collected with the Rotorod Sampler and Burkard spore trap. Ann. Allergy, Asthma Immunol. 83, 341–349. https://doi.org/10.1016/S1081-1206(10)62828-1

Frenz, D.A., Boire, A.A., 1999. Pollen recovery in atmospheric samples collected with the Rotorod Sampler over multiple-day periods such as weekends. Ann. Allergy, Asthma Immunol. 83, 217–221. https://doi.org/10.1016/S1081-1206(10)62643-9

Galan, C., Antunes, C., Brandao, R., Torres, C., Caeiro, E., Ferro, R., Prank, M., Reese, G., Sauliene, I., Smith, M., Thibaudon, M., Weber, B., Kennedy, R., Rantio-lehtim, A., Reese, G., Sauliene, I., Smith, M., Thibaudon, M., Weber, B., Weichenmeier, I., Pusch, G., Buters, J.T.M., 2013. Airborne olive pollen counts are not representative of exposure to the major olive allergen Ole e 1. Allergy Eur. J. Allergy Clin. Immunol. 68, 809–812. https://doi.org/10.1111/all.12144

Galán, C., Ariatti, A., Bonini, M., Clot, B., Crouzy, B., Dahl, A., Fernandez-González, D., Frenguelli, G., Gehrig, R., Isard, S., Levetin, E., Li, D.W., Mandrioli, P., Rogers, C.A., Thibaudon, M., Sauliene, I., Skjoth, C., Smith, M., Sofiev, M., 2017. Recommended terminology for aerobiological studies. Aerobiologia (Bologna). 33, 293–295. https://doi.org/10.1007/s10453-017-9496-0

Galán, C., Smith, M., Thibaudon, M., Frenguelli, G., Oteros, J., Gehrig, R., Berger, U., Clot, B., Brandao, R., 2014. Pollen monitoring : minimum requirements and reproducibility of analysis. Aerobiologia (Bologna). 30, 385–395. https://doi.org/10.1007/s10453-014-9335-5

Galan, I., Prieto, A., Rubio, M., Herrero, T., Cervigo, P., Martı, I., Cantero, J.L., Gurbindo, M.D., Martinez, M.I., Aurelio, T., 2010. Association between airborne pollen and epidemic asthma in Madrid , Spain : a case e control study. Thorax 65, 398–402. https://doi.org/10.1136/thx.2009.118992

Galimberti, A., Mattia, F. De, Bruni, I., Scaccabarozzi, D., Sandionigi, A., Barbuto, M., Casiraghi1, M., Labra, M., 2014. A DNA Barcoding Approach to Characterize Pollen Collected by Honeybees. PLoS One 9, 1–13. https://doi.org/10.1371/journal.pone.0109363

García-Sánchez, J., Trigo, M. del M., Recio, M., 2019. Extraction and quanti fi cation of Ole e 1 from atmospheric air samples : An optimized protocol. Chemosphere 225, 490–496. https://doi.org/10.1016/j.chemosphere.2019.02.155

Geller-Bernstein, C., Portnoy, J.M., 2019. The Clinical Utility of Pollen Counts. Clin. Rev. Allergy Immunol. 57, 340–349. https://doi.org/10.1007/s12016-018-8698-8

Gharbi, D., Brighetti, M.A., Travaglini, A., Trigo, M.M., 2017. Comparison between the counting methods used by two aerobiology networks in southern Europe (Spain and Italy). Aerobiologia (Bologna). 33, 87–92. https://doi.org/10.1007/s10453-016-9452-4

Gonçalves, A.B., Souza, J.S., Da Silva, G.G., Cereda, M.P., Pott, A., Naka, M.H., Pistori, H., 2016. Feature extraction and machine learning for the classification of Brazilian Savannah pollen grains. PLoS One 11, 1–20. https://doi.org/10.1371/journal.pone.0157044

Gore, R.B., Curbishley, L., Truman, N., Hadley, E., Woodcock, A., Langley, S.J., Custovic, A., 2006. Intranasal air sampling in homes: Relationships among reservoir allergen concentrations and asthma severity. J. Allergy Clin. Immunol. 117, 649–655. https://doi.org/10.1016/j.jaci.2005.12.1351

Graham, J.A.H., Pavlicek, P.K., Sercombe, J.K., Xavier, M.L., Tovey, E.R., 2000. The nasal air sampler: A device for sampiing inhaled aeroallergens. Ann. Allergy, Asthma Immunol. 84, 599–604.

https://doi.org/10.1016/S1081-1206(10)62410-6

Green, B.J., Levetin, E., Horner, W.E., Codina, R., Barnes, C.S., Filley, W. V, 2018. Landscape Plant Selection Criteria for the Allergic Patient. J. Allergy Clin. Immunol. Pract. 6, 1869–1877. https://doi.org/10.1016/j.jaip.2018.05.020

Grinshpun, S.A., Adhikai, A., Cho, S.-H., Kim, K.-Y., Lee, T., Reponen, T., 2007. A small change in the design of a slit bioaerosol impactor significantly improves its collection characteristics. J. Environ. Monit. 9, 855–861.

Grossman, J., 1997. One Airway, One Disease. Chest 111, 11S-16S. https://doi.org/10.1378/chest.111.2

Grote, M., Valenta, R., Reichelt, R., 2003. Abortive pollen germination: A mechanism of allergen release in birch, alder, and hazel revealed by immunogold electron microscopy. J. Allergy Clin. Immunol. 111, 1017–1023. https://doi.org/10.1067/mai.2003.1452

Grote, M., Vrtala, S., Niederberger, V., Valenta, R., Reichelt, R., 2000. Expulsion of allergen-containing materials from hydrated rye grass (Lolium perenne) pollen revealed by using immunogold field emission scanning and transmission electron microscopy. J. Allergy Clin. Immunol. 105, 1140–1145. https://doi.org/10.1067/mai.2000.107044

Grote, R., Samson, R., Alonso, R., Amorim, J.H., Cariñanos, P., Churkina, G., Fares, S., Thiec, D. Le, Niinemets, Ü., Mikkelsen, T.N., Paoletti, E., Tiwary, A., Calfapietra, C., 2016. Functional traits of urban trees: air pollution mitigation potential. Front. Ecol. Environ. 14, 543–550. https://doi.org/10.1002/fee.1426

Guilbert, A., Cox, B., Bruffaerts, N., Hoebeke, L., Packeu, A., Hendrickx, M., De Cremer, K., Bladt, S., Brasseur, O., Van Nieuwenhuyse, A., 2018. Relationships between aeroallergen levels and hospital admissions for asthma in the Brussels-Capital Region: A daily time series analysis. Environ. Heal. A Glob. Access Sci. Source 17, 1–12. https://doi.org/10.1186/s12940-018-0378-x

Harun, N.-S., Lachapelle, P., Douglass, J., 2019. Thunderstorm-triggered asthma: what we know so far. J. Asthma Allergy 12, 101–108. https://doi.org/10.2147/JAA.S175155

Heffer, M.J., Ratz, J.D., Miller, J.D., Day, J.H., 2005. Comparison of the Rotorod to other air samplers for the determination of Ambrosia artemisiifolia pollen concentrations conducted in the Environmental Exposure Unit. Aerobiologia (Bologna). 21, 233–239. https://doi.org/10.1007/s10453-005-9007-6

Hesse, M., Halbritter, H., Zetter, R., Weber, M., Buchner, R., Frosch-Radivo, A., Ulrich, S., 2009. Pollen Terminology: an Illustrated Handbook. Springer-Verlag, Wien.

Hirst, J.M., 1952. An automatic volumetric spore trap. Ann. Appl. Biol. 39, 257–265.

Hofmann, F., Otto, M., Wosniok, W., 2014. Maize pollen deposition in relation to distance from the nearest pollen source under common cultivation - results of 10 years of monitoring (2001 to 2010). Environ. Sci. Eur. 26, 1–14. https://doi.org/10.1186/s12302-014-0024-3

Hoidn, C., Puchner, E., Pertl, H., Holztrattner, E., Obermeyer, G., 2005. Nondiffusional release of allergens from pollen grains of Artemisia vulgaris and Lilium longiflorum depends mainly on the type of the allergen. Int. Arch. Allergy Immunol. 137, 27–36. https://doi.org/10.1159/000084610

Hollingsworth, P.M., Forrest, L.L., Spouge, J.L., Hajibabaei, M., Ratnasingham, S., van der Bank, M., Chase, M.W., Cowan, R.S., Erickson, D.L., Fazekas, A.J., Graham, S.W., James, K.E., Kim, K.-J., Kress, W.J., Schneider, H., van AlphenStahl, J., Barrett, S.C.H., vanden Berg, C., Bogarin, D., Burgess, K.S., Cameron, K.M., Carine, M., Chacon, J., Clark, A., Clarkson, J.J., Conrad, F., Devey, D.S., Ford, C.S., Hedderson, T.A.J., Hollingsworth, M.L., Husband, B.C., Kelly, L.J., Kesanakurti, P.R., Kim, J.S., Kim, Y.-D., Lahaye, R., Lee, H.-L., Long, D.G., Madrinan, S., Maurin, O., Meusnier, I., Newmaster, S.G., Park, C.-W., Percy, D.M., Petersen, G., Richardson, J.E., Salazar, G.A., Savolainen, V., Seberg, O., Wilkinson, M.J., Yi, D.-K., Little, D.P., 2009. A DNA barcode for land plants. PNAS 106, 12794–12797.

Holt, K., Allen, G., Hodgson, R., Marsland, S., Flenley, J., 2011. Progress towards an automated trainable pollen location and classifier system for use in the palynology laboratory. Rev. Palaeobot. Palynol. 167, 175–183. https://doi.org/10.1016/j.revpalbo.2011.08.006

Holt, K.A., Bennett, K.D., 2014. Principles and methods for automated palynology. New Phytol. 203, 735–742. https://doi.org/10.1111/nph.12848

Hruska, K., 2003. Assessment of urban allergophytes using an allergen index. Aerobiologia (Bologna). 19, 107–111. https://doi.org/10.1023/A:1024450601697

Huffman, J.A., Perring, A.E., Savage, N.J., Clot, B., Tummon, F., Shoshanim, O., Damit, B., Schneider, J., Sivaprakasam, V., Zawadowicz, M.A., Crawford, I., Topping, D., Doughty, D.C., Hill, S.C., Pan, Y., Huffman, J.A., Perring, A.E., Savage, N.J., Clot, B., Crouzy, B., Tummon, F., Shoshanim, O., Damit, B., Schneider, J., Zawadowicz, M.A., Crawford, I., Gallagher, M., Topping, D., David, C., Crawford, I., Gallagher, M., Topping, D., Doughty, D.C., Steven, C.H., 2019. Real-time sensing of bioaerosols : Review and current perspectives. Aerosol Sci. Technol. 0, 1–31. https://doi.org/10.1080/02786826.2019.1664724

Jantz, N., Homeier, J., León-Yánez, S., Moscoso, A., Behling, H., 2013. Trapping pollen in the tropics - Comparing modern pollen rain spectra of different pollen traps and surface samples across Andean vegetation zones. Rev. Palaeobot. Palynol. 193, 57–69. https://doi.org/10.1016/j.revpalbo.2013.01.011

Jochner-Oette, S., Menzel, A., Gehrig, R., Clot, B., 2019. Decrease or increase? Temporal changes in pollen concentrations assessed by Bayesian statistics. Aerobiologia (Bologna). 35, 153–163. https://doi.org/10.1007/s10453-018-9547-1

Kasprzyk, I., Ćwik, A., Kluska, K., Wójcik, T., Cariñanos, P., 2019a. Allergenic pollen concentrations in the air of urban parks in relation to their vegetation. Urban For. Urban Green. 46, 126486. https://doi.org/10.1016/j.ufug.2019.126486

Kasprzyk, I., Wójcik, T., Cariñanos, P., Borycka, K., Ćwik, A., 2019b. Evaluation of the allergenicity of various types of urban parks in a warm temperate climate zone. Aerobiologia (Bologna). 35, 57–71. https://doi.org/10.1007/s10453-018-9537-3

Kawashima, S., Thibaudon, M., Matsuda, S., Fujita, T., Lemonis, N., Clot, B., Oliver, G., 2017. Automated pollen monitoring system using laser optics for observing seasonal changes in the concentration of total airborne pollen. Aerobiologia (Bologna). 33, 351–362. https://doi.org/10.1007/s10453-017-9474-6

Kitaba, I., Nakagawa, T., 2017. Black ceramic spheres as marker grains for microfossil analyses, with improved chemical, physical, and optical properties. Quat. Int. 455, 166–169. https://doi.org/10.1016/j.quaint.2017.08.052

Korpelainen, H., Pietiläinen, M., 2017. Biodiversity of pollen in indoor air samples as revealed by DNA metabarcoding. Nord. J. Bot. 35, 602–608. https://doi.org/10.1111/njb.01623

Kraaijeveld, K., de Weger, L.A., Ventayol García, M., Buermans, H., Frank, J., Hiemstra, P.S., den Dunnen, J.T., 2015. Efficient and sensitive identification and quantification of airborne pollen using next-generation DNA sequencing. Mol. Ecol. Resour. 15, 8–16. https://doi.org/10.1111/1755-0998.12288

Levetin, E., 2004. Methods for Aeroallergen Sampling. Curr. Allergy Asthma Rep. 4, 376–383.

Lippmann, M., Chan, T.L., 1979. Cyclone sampler performance. Staub, Reinhaltung der Luft 39, 7–11.

Longhi, S., Cristofori, A., Gatto, P., Cristofolini, F., Grando, M.S., Gottardini, E., 2009. Biomolecular identification of allergenic pollen : a new perspective for aerobiological monitoring ? Ann. Allergy, Asthma Immunol. 103, 508–514. https://doi.org/10.1016/S1081-1206(10)60268-2

Lucas, R., Bunderson, L., 2019. Initial results from an automated near-real time pollen collection device. Ann. Allergy, Asthma Immunol. 123, S22. https://doi.org/10.1016/j.anai.2019.08.240

Lucas, R., Bunderson, L., Allan, N., Lambson, K., 2016. Automated airborne particulate matter collection, imaging, identification, and analysis. WO 2016/073745 A3.

Lucas, R., Bunderson, L., Anderson, J., Dalan, D., 2021. Visual Machine Learning and Artificial Intelligence Application in Aeroallergen Identification During Spring, Summer, and Fall Pollen Season. J. Allergy Clin. Immunol. 147, AB80. https://doi.org/10.1016/j.jaci.2020.12.309

Mandrioli, P., Puppi, G., 1978. Method for sampling airborne pollen grains and fungal spores. In: Aerobiological

monitoring in the Emilia-Romagna Region. Ser. Stud. Doc. Emilia-Romagna, Italy 13.

May, K.R., 1945. The cascade impactor: An instrument for sampling coarse aerosols. J. Sci. Instrum. 22, 187–195.

Menetrez, M.Y., Foarde, K.K., Ensor, D.S., 2001. An analytical method for the measurement of nonviable bioaerosols. J. Air Waste Manag. Assoc. 51, 1436–1442. https://doi.org/10.1080/10473289.2001.10464365

Miki, K., Kawashima, S., Clot, B., Nakamura, K., 2019. Comparative efficiency of airborne pollen concentration evaluation in two pollen sampler designs related to impaction and changes in internal wind speed. Atmos. Environ. 203, 18–27. https://doi.org/10.1016/j.atmosenv.2019.01.039

Mimić, G., Šikoparija, B., 2021. Analysis of airborne pollen time series originating from Hirst-type volumetric samplers—comparison between mobile sampling head oriented toward wind direction and fixed sampling head with two-layered inlet. Aerobiologia (Bologna). 7. https://doi.org/10.1007/s10453-021-09695-7

Mitchell, R.I., Pilcher, J.M., 1959. Improved Cascade Impactor for Measuring Aerosol Particle Sizes in Air pollutants, Commercial aerosols, Cigarette smoke. Ind. Eng. Chem. 51, 1039–1042. https://doi.org/10.1021/ie51396a041

Mohanty, R.P., Buchheim, M.A., Anderson, J., Levetin, E., 2017a. Molecular analysis confirms the long-distance transport of Juniperus ashei pollen. PLoS One 12, 1–13. https://doi.org/10.1371/journal.pone.0173465

Mohanty, R.P., Buchheim, M.A., Levetin, E., 2017b. Molecular approaches for the analysis of airborne pollen: A case study of Juniperus pollen. Ann. Allergy, Asthma Immunol. 118, 204-211.e2. https://doi.org/10.1016/j.anai.2016.11.015

Mothes, N., Horak, F., Valenta, R., 2004. Transition from a botanical to a molecular classification in tree pollen allergy: Implications for diagnosis and therapy. Int. Arch. Allergy Immunol. 135, 357–373. https://doi.org/10.1159/000082332

Mrđan, S., Ljubojević, M., Orlović, S., Čukanović, J., Dulić, J., 2017. Poisonous and allergenic plant species in preschool's and primary school's yards in the city of Novi Sad. Urban For. Urban Green. 25, 112–119. https://doi.org/10.1016/j.ufug.2017.05.007

Müller-Germann, I., D.A., P., H., P., Alberternst, B., Pöschl, U., Fröhlich-Nowoisky, J., Després, V.R., 2017. Allergenic Asteraceae in air particulate matter : quantitative DNA analysis of mugwort and ragweed. Aerobiologia (Bologna). 33, 493–506. https://doi.org/10.1007/s10453-017-9485-3

Müller-Germann, I., Vogel, B., Vogel, H., Pauling, A., Fröhlich-Nowoisky, J., Pöschl, U., Després, V.R., 2015. Quantitative DNA Analyses for Airborne Birch Pollen. PLoS One 10, 1–17. https://doi.org/10.1371/journal.pone.0140949

Mullins, J., Emberlin, J., 1997. Sampling pollens. J. Aerosol Sci. 28, 365–370.

Núñez, A., de Paz, G.A., Ferencova, Z., Rastrojo, A., Guantes, R., García, A.M., Alcamí, A., Gutiérrez-Bustillo, A.M., Moreno, D.A., 2017. Validation of the Hirst-type spore trap for simultaneous monitoring of prokaryotic and eukaryotic biodiversities in urban air samples by next-generation sequencing. Appl. Environ. Microbiol. 83, 1–38. https://doi.org/10.1128/AEM.00472-17

Núñez, A., de Paz, G.A., Rastrojo, A., García, A.M., Alcamí, A., Gutiérrez-Bustillo, A.M., Moreno, D.A., 2016. Monitoring of airborne biological particles in outdoor atmosphere . Part 2 : Metagenomics applied to urban environments. Int. Microbiol. 19, 69–80. https://doi.org/10.2436/20.1501.01.265.

Núñez, A., Moreno, D.A., 2020. The Differential Vertical Distribution of the Airborne Biological Particles Reveals an Atmospheric Reservoir of Microbial Pathogens and Aeroallergens. Microb. Ecol. 80, 322–333. https://doi.org/10.1007/s00248-020-01505-w

O'Rourke, M.K., 1990. Comparative pollen calendars from Tucson, Arizona: Durham vs. Burkard samplers. Aerobiologia (Bologna). 6, 136–140. https://doi.org/10.1007/BF02539105

Ogden, E.C., Raynor, G.S., 1967. A new sampler for airborne pollen: The rotoslide. J. Allergy 40, 1–11.

Ogden III, J.G., 1986. An alternative to exotic spore or pollen addition in quantitative microfossil studies. Can. J. Earth Sci. 23, 102–106.

Oteros, J., Pusch, G., Weichenmeier, I., Heimann, U., Möller, R., Röseler, S., Traidl-Hoffmann, C., Schmidt-Weber, C., Buters, J.T.M., 2015. Automatic and Online Pollen Monitoring. Int. Arch. Allergy Immunol. 167, 158–166. https://doi.org/10.1159/000436968

Oteros, J., Sofiev, M., Smith, M., Clot, B., Damialis, A., Prank, M., Werchan, M., Wachter, R., Weber, A., Kutzora, S., Heinze, S., Herr, C.E.W., Menzel, A., Bergmann, K., Traidl-hoffmann, C., Schmidt-Weber, C.B., Buters, J.T.M., 2019. Building an automatic pollen monitoring network (ePIN): Selection of optimal sites by clustering pollen stations. Sci. Total Environ. 688, 1263–1274. https://doi.org/10.1016/j.scitotenv.2019.06.131

Oteros, J., Weber, A., Kutzora, S., Rojo, J., Heinze, S., Herr, C., Gebauer, R., Schmidt-Weber, C.B., Buters, J.T.M., 2020. An operational robotic pollen monitoring network based on automatic image recognition. Environ. Res. 191, 110031. https://doi.org/10.1016/j.envres.2020.110031

Ozdoganoglu, T., Songu, M., 2012. The burden of allergic rhinitis and asthma. Ther. Adv. Respir. Dis. 6, 11–23. https://doi.org/10.1177/1753465811431975

Pecero-Casimiro, R., Fernández-Rodríguez, S., Tormo-Molina, R., Monroy-Colín, A., Silva-Palacios, I., Cortés-Pérez, J.P., Gonzalo-Garijo, Á., Maya-Manzano, J.M., 2019. Urban aerobiological risk mapping of ornamental trees using a new index based on LiDAR and Kriging: A case study of plane trees. Sci. Total Environ. 693, 1–12. https://doi.org/10.1016/j.scitotenv.2019.07.382

Pecero-Casimiro, R., Fernández-Rodríguez, S., Tormo-Molina, R., Silva-Palacios, I., Gonzalo-Garijo, Á., Monroy-Colín, A., Coloma, J.F., Maya-Manzano, J.M., 2020. Producing urban aerobiological risk map for cupressaceae family in the SW iberian peninsula from LiDAR technology. Remote Sens. 12, 1–19. https://doi.org/10.3390/rs12101562

Peel, R.G., Kennedy, R., Smith, M., Hertel, O., 2014. Relative efficiencies of the Burkard 7-Day , Rotorod and Burkard Personal samplers for Poaceae and Urticaceae pollen under field conditions. Ann. Agric. Environ. Med. 21, 745–752. https://doi.org/10.5604/12321966.1129927

Penel, V., Calleja, M., Pichot, C., Charpin, D., 2017. Static and elevated pollen traps do not provide an accurate assessment of personal pollen exposure. Eur. Ann. Allergy Clin. Immunol. 49, 59–65.

Plaza, M.P., Alcázar, P., Hernández-Ceballos, M.A., Galán, C., 2016. Mismatch in aeroallergens and airborne grass pollen concentrations. Atmos. Environ. 144, 361–369. https://doi.org/10.1016/j.atmosenv.2016.09.008

Plaza, M.P., Alcázar, P., Velasco-Jiménez, M.J., Galán, C., 2017. Aeroallergens : a comparative study of two monitoring methods. Aerobiologia (Bologna). 33, 363–373. https://doi.org/10.1007/s10453-017-9475-5

Poska, A., 2013. Surface Samples and Trapping, 2nd ed, Encyclopedia of Quaternary Science: Second Edition. Elsevier B.V. https://doi.org/10.1016/B978-0-444-53643-3.00179-5

Prado, N., De Dios Alché, J., Casado-Vela, J., Mas, S., Villalba, M., Rodríguez, R., Batanero, E., 2014. Nanovesicles are secreted during pollen germination and pollen tube growth: A possible role in fertilization. Mol. Plant 7, 573–577. https://doi.org/10.1093/mp/sst153

Prado, N., De Linares, C., Sanz, M.L., Gamboa, P., Villalba, M., Rodríguez, R., Batanero, E., 2015. Pollensomes as Natural Vehicles for Pollen Allergens. J. Immunol. 195, 445–449. https://doi.org/10.4049/jimmunol.1500452

Razmovski, V., O'Meara, T.J., Taylor, D.J.M., Tovey, E.R., 2000. A new method for simultaneous immunodetection and morphologic identification of individual sources of pollen allergens. J. Allergy Clin. Immunol. 105, 725–731. https://doi.org/10.1067/mai.2000.105222

Ridolo, E., Albertini, R., Giordano, D., Soliani, L., Usberti, I., Dall'Aglio, P.P., 2007. Airborne pollen

concentrations and the incidence of allergic asthma and rhinoconjunctivitis in northern Italy from 1992 to 2003. Int. Arch. Allergy Immunol. 142, 151–157. https://doi.org/10.1159/000096441

Rittenour, W.R., Hamilton, R.G., Beezhold, D.H., Green, B.J., 2012. Immunologic, spectrophotometric and nucleic acid based methods for the detection and quantification of airborne pollen. J. Immunol. Methods 383, 47–53. https://doi.org/10.1016/j.jim.2012.01.012

Rojo, J., Oteros, J., Pérez-Badia, R., Cervigón, P., Ferencova, Z., Gutiérrez-Bustillo, A.M., Bergmann, K.C., Oliver, G., Thibaudon, M., Albertini, R., Rodríguez-De la Cruz, D., Sánchez-Reyes, E., Sánchez-Sánchez, J., Pessi, A.M., Reiniharju, J., Saarto, A., Calderón, M.C., Guerrero, C., Berra, D., Bonini, M., Chiodini, E., Fernández-González, D., García, J., Trigo, M.M., Myszkowska, D., Fernández-Rodríguez, S., Tormo-Molina, R., Damialis, A., Kolek, F., Traidl-Hoffmann, C., Severova, E., Caeiro, E., Ribeiro, H., Magyar, D., Makra, L., Udvardy, O., Alcázar, P., Galán, C., Borycka, K., Kasprzyk, I., Newbigin, E., Adams-Groom, B., Apangu, G.P., Frisk, C.A., Skjøth, C.A., Radišić, P., Šikoparija, B., Celenk, S., Schmidt-Weber, C.B., Buters, J., 2019. Near-ground effect of height on pollen exposure. Environ. Res. 174, 160–169. https://doi.org/10.1016/j.envres.2019.04.027

Ruske, S., Topping, D.O., Foot, V.E., Morse, A.P., Gallagher, M.W., 2018. Machine learning for improved data analysis of biological aerosol using the WIBS. Atmos. Meas. Tech. 11, 6203–6230.

Sánchez-Parra, B., Núñez, A., García, A.M., Campoy, P., Moreno, D.A., 2021. Distribution of airborne pollen, fungi and bacteria at four altitudes using high-throughput DNA sequencing. Atmos. Res. 249, 105306. https://doi.org/10.1016/j.atmosres.2020.105306

Šauliene, I., Šukiene, L., Daunys, G., Valiulis, G., Vaitkevičius, L., Matavulj, P., Brdar, S., Panic, M., Sikoparija, B., Clot, B., Crouzy, B., Sofiev, M., 2019. Automatic pollen recognition with the Rapid-E particle counter: The first-level procedure, experience and next steps. Atmos. Meas. Tech. 12, 3435–3452. https://doi.org/10.5194/amt-12-3435-2019

Sauvageat, E., Zeder, Y., Auderset, K., Calpini, B., Clot, B., Crouzy, B., Konzelmann, T., Lieberherr, G., Tummon, F., Vasilatou, K., 2020. Real-time pollen monitoring using digital holography. Atmos. Meas. Tech. 13, 1–20.

Sázelova, P., Kašička, V., Koval, D., Prusík, Z., Peltre, G., 2002. Evaluation of the efficiency of extraction of ultraviolet-absorbing pollen allergens and organic pollutants from airborne dust samples by capillary electromigration methods. J. Chromatogr. B 770, 303–311.

Schäppi, G.F., Monn, C., Wüthrich, B., Wanner, H.U., 1996. Direct Determination of Allergens in Ambient Aerosols: Methodological Aspects. Int. Arch. Allergy Immunol. 110, 364–370. https://doi.org/10.1159/000237329

Schäppi, G.F., Taylor, P.E., Pain, M.C.F., Cameron, P.A., Dent, A.W., Staff, I.A., Suphioglu, C., 1999. Concentrations of major grass group 5 allergens in pollen grains and atmospheric particles: Implications for hay fever and allergic asthma sufferers sensitized to grass pollen allergens. Clin. Exp. Allergy 29, 633–641. https://doi.org/10.1046/j.1365-2222.1999.00567.x

Sevillano, V., Aznarte, J.L., 2018. Improving classification of pollen grain images of the POLEN23E dataset through three different applications of deep learning convolutional neural networks. PLoS One 13, 1–18. https://doi.org/10.1371/journal.pone.0201807

Sevillano, V., Holt, K., Aznarte, J.L., 2020. Precise automatic classification of 46 different pollen types with convolutional neural networks. PLoS One 15. https://doi.org/10.1371/journal.pone.0229751

Sickel, W., Ankenbrand, M.J., Grimmer, G., Holzschuh, A., Härtel, S., Lanzen, J., Steffan-Dewenter, I., Keller, A., 2015. Increased efficiency in identifying mixed pollen samples by meta-barcoding with a dual-indexing approach. BMC Ecol. 15, 1–9. https://doi.org/10.1186/s12898-015-0051-y

Simunovic, M., Dwarakanath, D., Addison-Smith, B., Susanto, N.H., Erbas, B., Baker, P., Davies, J.M., 2020. Grass pollen as a trigger of emergency department presentations and hospital admissions for respiratory conditions in the subtropics: A systematic review. Environ. Res. 182, 109125. https://doi.org/10.1016/j.envres.2020.109125

Sofiev, M., Siljamo, P., Ranta, H., Rantio-Lehtimäki, A., 2006. Towards numerical forecasting of long-range air transport of birch pollen: Theoretical considerations and a feasibility study. Int. J. Biometeorol. 50, 392–402. https://doi.org/10.1007/s00484-006-0027-x

Solomon, W.R., Stohrer, A.W., Gilliam, J.A., 1968. The "fly-shield" rotobar: A simplified impaction sampler with motion-regulated shielding. J. Allergy 41, 290–296.

Sposato, B., Scalese, M., 2013. Prevalence and real clinical impact of Cupressus sempervirens and Juniperus communis sensitisations in Tuscan '" Maremma "', Italy. Allergol. Immunopathol. (Madr). 41, 17–24. https://doi.org/10.1016/j.aller.2011.08.001

Stockmarr, J., 1971. Tablets with spores used in absolute pollen analysis. Pollen et Spores XIII, 615–621.

Takahashi, Y., Ohashi, T., Nagoya, T., Sakaguchi, M., Yasueda, H., Nitta, H., 2001. Possibility of real-time measurement of an airborne Cryptomeria japonica pollen allergen based on the principle of surface plasmon resonance. Aerobiologia (Bologna). 17, 313–318.

Tešendić, D., Boberić Krstićev, D., Matavulj, P., Brdar, S., Panić, M., Minić, V., Šikoparija, B., 2020. RealForAll: real-time system for automatic detection of airborne pollen. Enterp. Inf. Syst. 1–17. https://doi.org/10.1080/17517575.2020.1793391

Thompson, J.L., Thompson, J.E., 2003. The urban jungle and allergy. Immunol. Allergy Clin. North Am. 23, 371–387. https://doi.org/10.1016/S0889-8561(03)00006-7

Tobias, A., Galan, I., Banegas, J.R., 2004. Non-linear short-term effects of airborne pollen levels with allergenic capacity on asthma emergency room admissions in Madrid , Spain. Clin. Exp. Allergy 34, 871–878. https://doi.org/10.1111/j.1365-2222.2004.01983.x

Tummon, F., Clot, B., Crouzy, B., Lieberherr, G., Kawashima, S., Manzano, J., O'Connor, D., 2020. What's really in the air? A season of pollen counts from automatic instruments, in: 7th European Symposium on Aerobiology - Bioaereosols and Environmental Impacts. p. 132.

Valentini, A., Pompanon, F., Taberlet, P., 2008. DNA barcoding for ecologists. Trends Ecol. Evol. 24, 110–117. https://doi.org/10.1016/j.tree.2008.09.011

VDI 2119, 2013. Ambient air measurements sampling of atmospheric particles > 2.5 µm on an acceptor surface using the Sigma-2 passive sampler. Characterization by optical microscopy and calculation of number settling rate and mass concentration 1–4.

Werchan, M., Sehlinger, T., Goergen, F., Bergmann, K.-C., 2018. The pollator: a personal pollen sampling device. Allergo J. Int. 27, 1–3. https://doi.org/10.1007/s40629-017-0034-y

Wolf, M., Twaroch, T.E., Huber, S., Reithofer, M., Steiner, M., Aglas, L., Hauser, M., Aloisi, I., Asam, C., Hofer, H., Parigiani, M.A., Ebner, C., Bohle, B., Briza, P., Neubauer, A., Stolz, F., Jahn-Schmid, B., Wallner, M., Ferreira, F., 2017. Amb a 1 isoforms: Unequal siblings with distinct immunological features. Allergy Eur. J. Allergy Clin. Immunol. 72, 1874–1882. https://doi.org/10.1111/all.13196

Xie, Z.-J., Guan, K., Yin, J., 2019. Advances in the clinical and mechanism research of pollen induced seasonal allergic asthma. Am. J. Clin. Exp. Immunol. 8, 1–8.

Yamamoto, N., Matsuki, H., Yanagisawa, Y., 2007. Application of the personal aeroallergen sampler to assess personal exposures to Japanese cedar and cypress pollens. J. Expo. Sci. Environ. Epidemiol. 17, 637–643. https://doi.org/10.1038/sj.jes.7500549

Zuberbier, T., Lotvall, J., Simoens, S., Subramanian, S. V, Church, M.K., 2014. Economic burden of inadequate management of allergic diseases in the European Union : a GA 2 LEN review. Allergy 69, 1275–1279. https://doi.org/10.1111/all.12470

4. Pollen forecasting and its relevance in pollen allergen avoidance

Abstract

Pollinosis and allergic asthma are respiratory diseases of global relevance, heavily affecting the quality of life of allergic subjects. Since there is not a decisive cure yet, pollen allergic subjects need to avoid exposure to high pollen allergens concentrations. For this purpose, pollen forecasting is an essential tool that needs to be reliable and easily accessible. While forecasting methods are rapidly evolving towards more complex statistical and physical models, the use of simple and traditional methods is still preferred in routine predictions. In this review, we summarise and explain the main parameters considered when forecasting pollen, and classify the different forecasting methods in two groups: observation-based and process-based. Finally, we compare these approaches based on their usefulness to allergic patients, and discuss possible future developments of the field.

Keywords: pollen, aeroallergens, pollen forecasting, pollinosis, allergen avoidance.

Abbreviations: AR, Allergic Rhinitis; APIn, Annual Pollen Integral; CAMS, Copernicus Atmosphere Monitoring Service; CI, Computational Intelligence; DA, Data Assimilation; FAR, False Alarm Ratio; GS, Gerrity Score; LAI, Leaf Area Index; LDD, Long Distance Dispersal; LiDAR, Light Detection and Ranging; LS, Lagrangian stochastic; POD, Probability of Detection; POFD, Probability of False Detection ; QoL, Quality of Life; RMSE, Root Mean Squared Error; SPIn, Seasonal Pollen Integral.

1.   Introduction

During the reproductive season, seed-plants produce and release male gametophytes in the form of pollen grains, that may carry allergenic molecules. Wind-pollinated plants in particular have to release huge amounts of pollen in the atmosphere to reach a successful reproduction, accidentally exposing the human population to high quantities of pollen allergens for several

months of the year. During this period, the immune system of susceptible subjects might start to recognise the inhaled pollen molecules as antigens and produce a hypersensitivity reaction against them, a phenomenon called sensitisation (D'Amato et al., 2007; Erbas et al., 2012). Pollen sensitisation leads to pollen allergy, that can result in two types of symptomatology: an allergic rhinitis (AR) called "hay fever" or pollinosis, or less frequently, allergic asthma (D'Amato et al., 1991; Erbas et al., 2007).

According to the International Study of Asthma and Allergies in Childhood (ISAAC), the global prevalence of pollinosis at the beginning of this century was 22.1% in older children (13- to 14-yr-old) and 11.8% in younger ones (6- to 7-yr-old), with an overall increase per year around 0.3% in both age groups (Björkstén et al., 2008a). The incidence of pollen allergies however displays geographic variability, being influenced by bioclimatic conditions and allergenic plants distribution (Björkstén et al., 2008b).

The perspective of a constant increase in pollen allergy prevalence is concerning because, even if it is not life-threatening per se, AR can lead to illness and disability, and it can affect the quality of life (QoL) in general (Bousquet et al., 2008). According to their duration, severity and frequency, AR symptoms can compromise performance, quality of sleep, cognitive function and work productivity of the allergic subjects. Furthermore, anxiety and depression appear to be common comorbidities to AR, especially when the symptoms are persistent (Canonica et al., 2007). AR can also have indirect implications on apparently unrelated aspects of human health. For instance, epidemiological data show a link between osteoporosis and pollen allergy, along with other hyper-IgE syndromes, and common AR prescriptions can lead to other bone pathologies (Sirufo et al., 2020).

Allergic asthma has a similar effect to AR on mental health, but it causes a more severe inflammation of the lower airways, that may become fatal. Asthma in general is estimated to account for about 1 in every 250 deaths worldwide (Masoli et al., 2004), with an average of over 1300 deaths per day (European Respiratory Society, 2017). The causes behind asthma onset are often difficult to investigate; therefore the exact mortality of allergic asthma alone remains unknown.

Because of this deteriorating effect on QoL, and the high prevalence recorded in some countries, respiratory allergies costs in medical care for both individuals and society can be elevated (Canonica et al., 2007). The major monetary burden of these diseases, however, derives from productivity loss. In 2014, the Global Allergy and Asthma European Network

evaluated the socio-economic damage provoked by AR in Europe, in terms of direct, indirect and intangible costs, and missed opportunities. According to the study, the European prevalence of airways allergies (between 20% and 35%) can lead to a loss in productivity from €55 to €151 billion per annum. These figures are higher than in other diseases, even if AR has milder consequences on health. This is because AR and asthma develop at an early age, therefore compromising the entire career of the sufferers through absenteeism or presenteeism (Zuberbier et al., 2014).

Due to this social burden, the possibility to cure and prevent pollen allergies would be beneficial for both the individual and the society. However, an effective therapy to treat the disease is yet to come. Currently, treatment of allergic rhinitis usually combines allergen avoidance, pharmacotherapy, immunotherapy and education (Bousquet et al., 2008). Pharmacotherapy aims to symptomatic treatment and inflammation reduction, and involves H1-anti-histamines, intranasal corticosteroids, topical cromoglycate and oral leukotriene-receptor antagonists (Roberts et al., 2018; Santos et al., 2015). Even severe allergic asthma symptoms can be soothed, using humanised monoclonal antibodies against IgE (Omalizumab) to reduce inflammation of the airway mucosa (Djukanović et al., 2004). Although there is evidence that these therapies can improve QoL of pollen allergies sufferers, patients taking these medications often do not consider their symptoms as completely under control (Canonica et al., 2007).

Allergen-specific immunotherapy is the only AR treatment that acts on the causes of the disease, having the potential to desensitise the patient (Roberts et al., 2018) and to prevent further allergic sensitisation and the development of asthma (Santos et al., 2015). Although it can substantially enhance patients QoL (Niederberger et al., 2018; Novakova et al., 2017; Pfaar et al., 2019), immunotherapy alone at the moment is not sufficient to treat every kind of pollinosis or to completely control AR symptoms (Demoly et al., 2016), so avoidance of the allergens is always required (Bastl et al., 2017c; Canonica et al., 2007; Mothes et al., 2004). An accurate allergic risk assessment is believed to help pollen allergy sufferers planning their movements, precautions and medications in order to avoid pollen allergens or at least mitigate their effect (Burge and Rogers, 2000). While aerobiological monitoring is common practice in several cities worldwide, it can only provide an estimation of allergenic pollen concentrations in retrospective, or in real-time at best (Huffman et al., 2019). Such information cannot be used for the prevention of allergy outbursts as it is, but it must be

elaborated into forecasting models to predict the future pollen loads. To our knowledge, the last thorough review on pollen forecasting has been published in 2013 by Scheifinger and colleagues (Scheifinger et al., 2013). Since then, many progresses have been made in the fields of artificial intelligence, remote sensing, computer modelling, Mobile Health and Crowdsensing. This deeply contributed to the fast evolution of pollen and phenological forecasting, allowing to extend old models to new regions (Hall et al., 2020; Oteros et al., 2019), to create new models for wider geographic areas (Sofiev et al., 2020, 2017), and to improve the time resolution of the forecasting (Sofiev et al., 2017). This review aims to give a comprehensive overview on the forecasting models available, and to discuss whether and how they are useful to the allergic subjects in the management of their disease.

2.   Pollen indices

To date, monitoring airborne allergenic pollen concentrations is considered the most reliable way to assess the health hazard for pollinosis sufferers worldwide (Galán et al., 2014). Ideally, pollen monitoring networks should have the highest spatial density and temporal continuity possible. In fact, airborne pollen spectra show a spatial variation that depends on geographic position and bioclimatic features of the monitored area, and temporal variation throughout the year, according to plant phenology and pollen morphology. They are also influenced by weather conditions that can modify pollen productivity, emission and dispersion (Bastl et al., 2017c). Moreover, pollen spectra are likely to undergo interannual variations, for example because of irregular flowering cycles (masting), shifts in species composition or meteorological variability (Brennan et al., 2019; Burge and Rogers, 2000; Geller-Bernstein and Portnoy, 2019). To compare pollen data over time, daily pollen concentrations can be summarised into standard indices, such as the Annual Pollen Integral (APIn) and the Seasonal Pollen Integral (SPIn). They are expressed in pollen*day/m^3 and calculated as the sum of the average daily pollen concentrations over the chosen timespan, or the average pollen concentration over the chosen period multiplied by the period duration in days (Galán et al., 2017). Comparison between these indices from different years allows to detect shifts in airborne pollen seasonality and concentrations for a specific region, helping for example to evaluate the effects of a changing climate on the air quality (Anderegg et al., 2021; Clò et al., 2016; Ziello et al., 2012).

Another important parameter derived from aeropalynological data is the pollen season, that positively correlates with pollen allergies outbursts (Erbas et al., 2018, 2012, 2007; Galan et al., 2010; Geller-Bernstein and Portnoy, 2019; Simunovic et al., 2020). There is no academic consensus over its definition, and according to the literature it can be calculated assuming as start and end day specific percentages of APIn or SPIn, considering threshold levels of daily pollen concentrations, or establishing a number of consecutive days during which a certain pollen type is detected (Bastl et al., 2018b; Pfaar et al., 2017).

However, since the majority of monitoring stations still rely on manual pollen counts, airborne pollen concentrations are provided with at least one day of delay and are not helpful for allergen avoidance. Hence, these data must be translated into a temporally resolved pollen forecast (Šikoparija et al., 2018).

3.   Parameters for pollen forecasting

To accurately predict pollen trends, it is useful to consider not only aeropalynological data, but also phenological, meteorological and ecological ones.

Aeropalynological records usually derive from manual pollen counts, and can be accessed through local or international databases (Galán et al., 2014; Scheifinger et al., 2013). However, the majority of pollen and spore monitoring networks are privately owned and therefore their data might not be freely available (Buters et al., 2018). Moreover, monitoring methods have not been standardised between different networks yet, so pollen data from different regions are usually not directly comparable (Bastl et al., 2018b). Another issue with airborne pollen data collection is that monitoring stations are present only in few major cities, hence atmospheric pollen concentrations remain unknown for vast geographic areas. Furthermore, not all of the existing stations perform a continuous monitoring. To overcome these problems, some attempts have been made in the last years to infer airborne pollen concentrations from the number of internet searches and tweets about pollen allergy, but this field is still far from being accurate (Gesualdo et al., 2015; Hall et al., 2020; Kmenta et al., 2016). On one hand, the number of tweets and Google Trends searches on allergic rhinoconjunctivitis was proven to correlate with pollen concentrations, especially during the early pollen season, when there is also a clear causality between the two parameters (Gesualdo et al., 2015; Hall et al., 2020). On the other hand, this approach suffers from various biases associated with the exact geo-localisation of the allergic subject, the local internet

consumption, and the keywords used to detect tweets and searches (Gesualdo et al., 2015). Moreover, when applying this method to sparsely populated areas, the sampled population might not be statistically relevant.

A more robust solution to fill in spatial gaps in pollen monitoring, not explored in Scheifinger's work, is to employ a group of statistic interpolation techniques, called kriging techniques. They are probabilistic methods that can model the spatial behaviour of pollen concentrations in unmonitored areas, using pollen records from adjacent monitoring stations. The high spatial autocorrelation of daily pollen concentrations in fact makes them fit for the application of these geostatistical methods (Della Valle et al., 2012; Oteros et al., 2019; Picornell et al., 2019). Multivariate kriging (cokriging) in particular has been used for this purpose, assuming as covariable a parameter that characterises sites with similar pollen emissions, such as the altitude or meteorological factors (Oteros et al., 2019; Picornell et al., 2019; Rojo and Pérez-Badia, 2015). Cokriging can also be combined with other models to weight in additional factors influencing the spatial distribution of airborne pollen, like the rainfall effect (Oteros et al., 2019). For each pollen type, internal validation of cokriging results can be performed calculating the determination coefficient R^2, the Root Mean Squared Error (RMSE), or the Mean Absolute Error (MAE); while external full cross-validation usually relies on Leave-one-out cross-validation (LOOCV) methods, and the results can be expressed as accuracy rates. According to these metrics, cokriging provides an accurate estimation of mean daily pollen concentrations in unmonitored areas, with relatively high spatial resolution (1 Km^2) but low time resolution (24-hour intervals). The atmospheric concentration of some pollen types however cannot be accurately described by cokriging, because the spatial distribution of their sources is driven by factors that are difficult to model (*e.g.* ruderal, ornamental or endemic species). For this reason, spatial interpolation could benefit from an accurate vegetation inventory of the region (Oteros et al., 2019; Picornell et al., 2019). Another promising approach for spatial interpolation of pollen data is the use of convolutional neural networks, that can predict pollen concentrations faster than kriging, and with similar or higher accuracy (Navares and Aznarte, 2019).

An interesting new source of aeropalynological data for pollen forecasting comes from the automatic pollen monitoring networks, that can provide real-time airborne pollen concentrations with high temporal resolution and continuity. Considered as a future possibility in Scheifinger and colleagues review (Scheifinger et al., 2013), in the last years

automatic pollen sensors have been rapidly gaining accuracy and precision in pollen classification, and their results have already been employed in forecasting studies (Clot et al., 2020; Huffman et al., 2019; Sofiev, 2019).

As an alternative to aeropalynology, pollen forecasting can rely on phenological data providing the timing of pollen emission. Phenological data are collected worldwide by national networks using different technologies, from the traditional systematic observations *in situ* and *ex situ* (*e.g.* the International Phenological Gardens) to the most advanced techniques of citizen science and remote sensing (Scheifinger et al., 2013). Remote sensing in particular is a rapid-evolving field that allows to collect ecological vegetation data using satellites and unmanned aerial vehicles (Maes and Steppe, 2019). In fact, these instruments can be equipped with sensors that provide high resolution aerial photographs, multi-spectral or hyper-spectral composite images, or Light Detection and Ranging (LiDAR) data. The analysis of different spectral wavelengths and geometric features, often elaborated into ecological indices, allows to describe many aspects of the vegetation, such as the taxa composition or the plant physiological and phenological state. To date, the most advanced technology for remote species recognition is the combination of hyperspectral sensors and LiDAR sensors: the former can identify plant species by their spectral features even in areas with high plant diversity, while the latter analyse the plant structure and the geometry of its components. While this approach is still under development and improvement, several studies successfully employed it to create or update vegetation inventories (Pecero-Casimiro et al., 2020, 2019; Rocchini et al., 2018; Shi et al., 2018). This approach can also help overcoming the problems created by different national data collection approaches when forecasting pollen concentrations over vast geographic regions (Sofiev et al., 2006). Moreover, the possibility offered by the remote sensing to frequently monitor vast areas with a standard approach, gives the opportunity to better understand the relationship between variations in plant distribution and phenological state, and airborne pollen concentrations (Huete et al., 2019). Unfortunately, the remote monitoring of plant phenology is still problematic because it requires multi-seasonal satellite observations to match with ground-based visual analysis. The relationship between the phenology signature, derived from the spectral analysis of the leaves, and the actual phenological stage recorded in the filed, in fact, does not always hold true, and it requires specific expert knowledge to be interpreted (Tomaselli et al., 2017). However, it has been recently demonstrated that satellite data from the sensor MODIS,

elaborated into the Enhanced Vegetation Index (EVI), tend to correlate with pollen concentrations on a local level, and that the use of Machine Learning techniques can help combining satellite data with ground-based data, with the potential to implement this relationship in pollen forecasting (Huete et al., 2019).

Both phenology and plant species composition vary between different sites, therefore forecasting models are usually developed for specific plant groups and regions (Levetin and Van de Water, 2003). Since phenology networks have more densely distributed stations and older records than air quality networks, they can supply to spatial and temporal gaps in the airborne pollen data series. Besides, the independent evolution of the two networks implies that their monitoring is not coordinated, with palynological records accounting for a higher botanical diversity than phenological ones (Scheifinger et al., 2013). Pollen production and dispersion is also influenced by environmental factors, that are accounted for by many forecasting approaches. Meteorological parameters for pollen forecasting can be either actual values from historical records or real-time monitoring, collected by meteorological stations, or future values estimations (Norris-Hill, 1995). These parameters are usually evaluated individually, but they can also be elaborated into bioclimatic indices. Bioclimatic indices could be more useful than individual meteorological variables when forecasting the pollen pre-season, since in this period they show a better correlation with mean daily pollen concentrations (Valencia-Barrera et al., 2002). Furthermore, since bioclimatic features modify plants phenology, it is important to assess bioclimatic similarity when comparing pollen forecasting models applied in different regions (Valencia-Barrera et al., 2001).

4.   Observation-based forecasting

Pollen forecasting is based on two broad categories of models: observation-based and process-based. The proportion of papers mentioning the different types of forecasting are represented in the Supplementary Figure 1. Observation-based models, sometimes referred as empirical models, are statistic elaborations of real aeropalynological, phenological and environmental data, collected in a specific region for several years (Tab. 1, Fig. S1A). They are also called receptor-oriented models, because they aim to estimate pollen concentrations that pollen traps (receptors) will record, without making assumptions on their sources and atmospheric dynamics (Norris-Hill, 1995; Ranzi et al., 2003; Scheifinger et al., 2013; Šikoparija et al., 2018). Depending on the application, these predictions can be short-term, seasonal, or

long-term. Short-term pollen forecasting is performed during the main pollen season, when meteorological conditions can cause daily variations. Seasonal forecasts are the most common, and they calculate start date, severity and peak levels of pollen season. Long-term forecasts aim to detect trends in seasonal pollen levels due to large-scale environmental modifications, and they require at least 20-years records of airborne pollen (Levetin and Van de Water, 2003).

The most popular and simple observation-based model is the calendar forecast. It uses flowering seasonality or aeropalynological data from the past years to find a medium trend. Pollen calendars are commonly presented as graphical descriptions of airborne concentrations for different pollen types during the year, outlining the shape and the duration of pollen seasons (Ranzi et al., 2003; Šikoparija et al., 2018). For a more accurate forecasting, records of meteorological parameters can be included in the calculation. Factors that could affect pollen trends are for example temperature, rainfall, hours of sunshine, cloud cover, relative humidity, wind speed and wind direction. Depending on the context and the pollen type, variations in one of these parameters may explain most of the pollen concentrations variability (Norris-Hill, 1995). The simplest way to evaluate these relations are regression and correlation analysis, that model past pollen concentrations relationship with one or more meteorological factors. Correlation or regression coefficients are then used to estimate future pollen concentrations. The same approach can be used to forecast the pollen season based on shifts in plant phenology (Scheifinger et al., 2013). However, calendar models seem to be nearly as efficient (Šikoparija et al., 2018).

A downside of the all the previous models is that they do not consider the timescale. When focusing on this aspect, time-series models are generally preferred. The Box-Jenkins method, an autoregressive moving average (ARMA) model, is regarded as a standard time-series model in aerobiology. Nonetheless, more advanced approaches are available, such as the Holt-Winters method (Aznarte et al., 2007; Ranzi et al., 2003; Scheifinger et al., 2013). However, because of the chaotic component in pollen time-series, Computational Intelligence (CI) will probably be the turning point for the observation-based models since it appears to better describe complex and non-linear phenomena than statistical models. Common CI applications in pollen forecasting are machine learning models such as the neural networks or the random forests. Neural nets can also be combined with fuzzy-rule based systems to obtain neuro-fuzzy models. Neural and neuro-fuzzy models a higher forecasting accuracy than

traditional linear approaches in the comparison between predicted and measured pollen concentrations, especially with pollen concentrations higher than 50 grains/m^3 (Aznarte et al., 2007). To date, different machine learning and advanced machine learning models are available for pollen forecasting, considering phenological and environmental parameters as well, often measured via satellite (Aznarte et al., 2007; Huete et al., 2019; Zewdie et al., 2019). Another innovative approach is the Hidden Markov Model (HMM), a stochastic model that uses the current state of the system to predict the probability of different future scenarios. The peculiarity of this method is to contemplate stochastic variations caused by mast cycling, particularly useful in *Betula* pollen forecasting (Levetin and Van de Water, 2003; Tseng et al., 2020).

Table 1 *Main features of observation-based pollen forecasting models*

	Observation-based forecasting				
Approach	Simple statistical analysis		Time-series analysis			Stochastic approach
Method	Calendar	Regression analysis, correlation	ARMA	Time-series decomposition	Machine-learning	Hidden Markov Model (HMM)
Examples	Pollen calendar, phenological calendar	-	Box-Jenkins method	Holt-Winters method	Neural networks, Random forests, Neuro-fuzzy models	-
Input	Past pollen concentrations, Past phenological observations	Past pollen concentrations, Past phenological observations, Meteorological parameters (past or forecasted)	Past pollen concentrations, seasonality	Past pollen concentrations, seasonality, cycle, random perturbation	Past pollen concentrations, Past phenological observations, Meteorological parameters and their thresholds	Past pollen concentrations, plant phenology, Past meteorological parameters
Output	Shape and duration of future pollen season	Shape and duration of future pollen season	Future atmospheric concentrations of some pollen types	Future airborne pollen concentrations	Probability of future scenarios	Future SPIn, considering mast cycle
Applicability	Routine seasonal forecasting	Seasonal forecasting when there is strong inter-annual meteorological variability	Pollen forecasting for specific studies where the timescale is important			Seasonal forecasting when pollen concentrations are influenced by stochastic variations
Bibliography	(D'Amato et al., 1991; Šikoparija et al., 2018)	(Norris-Hill, 1995; Scheifinger et al., 2013)	(Ranzi et al., 2003; Scheifinger et al., 2013)	(Aznarte et al., 2007)	(Arizmendi et al., 1993; Aznarte et al., 2007; Huete et al., 2019; Lops et al., 2020; Ranzi et al., 2003; Zewdie et al., 2019).	(Tseng et al., 2020)

5. Process-based forecasting

Process-based models, also known as simulation models, are built on a-priori assumptions about pollen dispersal and plant phenological responses to environmental factors. These models aim to forecast pollen production and release by the source plant and to reconstruct its journey from the source to the air sampler, therefore they are also defined source-oriented (Ranzi et al., 2003; Scheifinger et al., 2013; Šikoparija et al., 2018).

5.1 Process-based phenological models

Some process-based methods start from the assumption that pollen season overlaps with flowering season. They are defined process-based phenological models, and predict the beginning, the peak and the end of the pollen season as a function of environmental factors (Tab. 2, Fig. S1B) (Scheifinger et al., 2013). Two main events are thought to influence flowering season entrance: chilling temperature, that breaks bud dormancy, and forcing temperature (or thermal forcing), that stimulates bud development. The timing of these events can be elaborated into bud-burst models to produce a phenological forecast. While temperature appears to be the main driver of flowering for temperate climate trees, pollen season of herbaceous taxa and tropical and Mediterranean trees tends to correlate more with precipitations and photoperiod instead. Photoperiod in particular can be assumed to determine the moment when temperatures start to affect bud development (Migliavacca et al., 2012; Siniscalco et al., 2015). More flexible and generalised models, able to detect the principal phenological control in a certain dataset, are also available (Scheifinger et al., 2013). These phenological projections hold some degrees of uncertainty, associated to parameters, structure and drivers of the model (Migliavacca et al., 2012). Since each species has its peculiar environmental requirements, specific models and parameters should be selected for different plant groups (Scheifinger et al., 2013; Siniscalco et al., 2015). Nevertheless, different studies have observed interannual changes in environmental requirements for the same species, underlining how the relations between phenology and environment are yet to be fully understood (Siniscalco et al., 2015). The less controllable and quantifiable uncertainty associated to phenological models however is due to model drivers, and it is mainly caused by unpredictable changes in the future climate. All these problems can be minimised by using a model-data fusion approach that accounts for the overall model uncertainty (Migliavacca et al., 2012). Another major issue of phenological forecasting is that local flowering and pollen

seasons match only when long distance dispersal (LDD) contribution to the pollen records is negligible (Scheifinger et al., 2013).

5.2   Process-based dispersal models

Although around 90% of wind-borne (anemophilous) pollen grains falls within 100 m and 2.7 km from its source, the remaining 10% might travel from hundreds to thousands of kilometres (Green et al., 2018). Pollen dispersion is promoted by air masses movements and turbulences, opposed by gravity (dry deposition) and rain (wet deposition), and it is influenced by the chemico-physical modifications pollen can undergo during the process. In dry atmospheric conditions, around 50% of the total pollen emitted by anemophilous species is estimated to be transported more than 10000 km further from its source, with a half-lifetime of at least 1 day (Sofiev et al., 2006). In some cases, this LDD component can significantly alter local pollen records, for example when wind-pollinated species have dense extra-regional populations (Sofiev et al., 2006; Zink et al., 2012).

Thus, to better approximate future pollen concentrations, it is useful to model pollen emission and pollen dispersion as separate events (Kawashima and Takahashi, 1995; Sofiev et al., 2006).

First emission models developed for this type of process-based forecasting estimate pollen emission based on the relationship between weather conditions and quantity of pollen released into the atmosphere, derived from experimental data (Cai et al., 2019). Kawashima and Takahashi (Kawashima and Takahashi, 1999) pioneered this approach, calculating the potential pollen emission of a uniformly flowering source, based on its correlation with hourly measures of air temperature and wind speed, and on the number of male flowers estimated from the variations in summer temperatures. Similarly, Schueler and Schlünzen (Schueler and Schlünzen, 2006) considered the pollen emission as a function of the pollen production over a certain period. The pollen production in this case was estimated from the relationship between actual pollen concentrations in the tree crown, and three meteorological parameters (wind speed, relative humidity, and temperature), measured with a two-hour resolution. Comparison with actual pollen levels recorded at the source site proved this estimation acceptable, although not very precise. More articulate emission models based on empirical data have been developed, that pay more attention to the biological and biometric features of the source plant. An early example of this approach is provided by Hidalgo and

colleagues (Hidalgo et al., 2002), who employed neural networks to calculate the emission sub-model, based on three parameters: (I) the characteristics of the previous pollen seasons, formulated as the relationships between past pollen counts and meteorological data; (II) the dispersion factors, that included meteorological conditions, source plants abundance and distribution, and local topography; (III) the total pollen production, estimated empirically as the number of flowers per tree, anthers per flower, and pollen grains per anther. Another empirical emission model was proposed by Helbig and collaborators in 2004 (Helbig et al., 2004), that has the advantage to be very general, so that it can be adapted to different plant species. This model starts from the definition of pollen production as the maximum number of pollen grains recorded for a plant species during the pollen season. This maximum quantity is emitted in time by the source plant, according to the characteristics of the species, and in particular: (I) the likelihood to bloom in a certain day of the season; (II) the maximum pollen quantity that can be emitted from a certain area minus the pollen already emitted, that depends on the LAI and the height of the canopy; (III) the friction velocity required for the pollen release; (IV) the threshold temperature, humidity and wind speed required for pollen emission (Cai et al., 2019; Helbig et al., 2004). Starting from the same inputs, a semi-mechanistic emission model based on the mass balance of pollen emission fluxes from all the sides of the crown has been recently proposed (Cai et al., 2019). Some of the parameters and assumptions of this model however are associated with significant uncertainties, and the modelled emissions have only a medium correlation with actual pollen records for the area. Emission models can also be based on long-term phenological observations (Sofiev et al., 2006) and on the aforementioned phenological models (Duhl et al., 2013; Siljamo et al., 2013; Sofiev et al., 2015a, 2006). For instance, the "double-threshold air temperature sum" is a phenological emission model built on the direct proportionality between the flowering stage and the heat sum accumulation occurred between two temperature thresholds, and it allows to model the probability of an individual tree to enter the flowering stage. It takes into account other meteorological factors as well: ambient humidity and precipitations, that decrease the pollen emission; wind speed, that promotes it; and atmospheric turbulence, that has significant positive impact on pollen emission only in a scenario close to free convection. The accuracy of this method varies according to the study area (Sofiev et al., 2015a). Phenological emission models can also be calculated by CI, using for example the Random Forest machine learning technique, that was proven to explain 50% of the variance when

comparing the predicted and recorded pollen concentrations over a missing test year (Huete et al., 2019).

Atmospheric pollen dynamics instead are described by dispersal models, considering both environmental factors and pollen features, such as shape, density, dimension, and viability (Tab. 3, Fig. S1C) (Sofiev et al., 2006; Zhang et al., 2014). Distant pollen sources can be mapped using vegetation inventories or solving the inverse dispersion problem. In the latter case, when a pollen monitoring station records a possible LDD event, the source is identified by reconstructing the pollen trajectory from the source to the air sampler (Sofiev et al., 2013, 2006).

First pollen dispersion models were based on statistic elaborations (Helbig et al., 2004; Kuparinen, 2006). They can be integrated as sub-models in more complex, fully mechanistic dispersion models. The latter derive from the atmospheric physics principles that describe the motion of airborne particles. They consider factors such as gravity, wind speed, and turbulence, to explain pollen dynamics based on concurrent environmental conditions. More specifically, they are based on the advection-diffusion equation, that is an accurate approximation of pollen noninertial motion, approached with Eulerian or Lagrangian methods (Kuparinen, 2006; Nguyen et al., 1997; Sofiev et al., 2006).

In general, inputs required by mechanistic dispersal models are: a map of the source plants distribution, the pollen emission sub-model, knowledge on the features of the past pollen seasons, and the meteorological forecasting (Sofiev et al., 2013).

In the Eulerian approach, airborne particles are treated as a continuum (Zhang and Chen, 2007), and they are modelled as concentration fields on a grid that is fixed in space and time (Jia et al., 2021; Nguyen et al., 1997; Young et al., 2000). This method allows to predict the mean concentration of airborne particles for each point of the grid by solving the advection-diffusion equation, mainly using one of the following advection schemes: flux-form finite volume, that calculates the particles transport by mass fluxes at the borders of the grid cells; semi-Lagrangian, that considers the transport from departure points of the grid to an arrival point, and calculates the particle concentrations at the grid points closest to the arrival; or expansion-function, that calculates the solution of the equation using different sets of basis functions (Sofiev et al., 2015b).

Eulerian models for pollen forecasting are usually adapted from existing mesoscale models for air pollutants dispersal, combined with meteorological models. A valid example of the

Eulerian approach is the KAMM/DRAIS/MADEsoot, a comprehensive mesoscale model system for aerosol dispersion that produces a three-dimensional forecasting of temporal and spatial distribution of pollen grains (Helbig et al., 2004). Perquisites of this method are to take into account geomorphological heterogeneity, meteorological spatial variability, species-specific pollen emissions, wet deposition and resuspension. Other examples of Eulerian models are mentioned in Table 3. A multi-model ensemble has been published as well, calculated as the arithmetic average and median of the results from seven Eulerian models fields per hour. This ensemble, now implemented in the Copernicus Atmosphere Monitoring Service (CAMS) forecast (www.regional.atmosphere.copernicus.eu), showed higher correlation coefficients with observed daily mean pollen concentrations than the individual models alone (Sofiev et al., 2015a).

However, the Eulerian approach requires a number of simplifications that can limit the use of the model in many occasions (Kuparinen, 2006). For example, they do not take into account the effect of tree canopies. In fact, variations in leaf-area index and the foliage shedding of deciduous trees have been proven to strongly influence the turbulences within the canopy and therefore to affect pollen dispersion (Nathan and Katul, 2005). Furthermore, the application of Eulerian models is still hindered by their huge computational costs, and by the numerical diffusion effect produced by the grid system (Jia et al., 2021).

Another way to predict mean pollen concentrations in a specific area is the Lagrangian approach, that considers airborne particles as a discrete phase, and models their individual paths in a continuous space by applying a deformation to either the grid or the coordinates of a fixed grid (Nguyen et al., 1997; Young et al., 2000; Zhang and Chen, 2007). Lagrangian models for pollen forecasting are usually based on the "Lagrangian particle random-walk" method, that calculates the trajectory of thousands to millions particles, with the advection modelled on the wind dynamics and the diffusion simulated by random relocation (Nguyen et al., 1997; Sofiev et al., 2013). In particular, the Lagrangian Stochastic (LS) turbulence model is considered to give a realistic simulation of temporary airflows. An example of LS model for pollen dispersal is the SMOP-2D, that simulates individual pollen grains path from their emission to their deposition, considering wind turbulence, pollen aerodynamic features, canopy structure and landscape heterogeneity (Jarosz et al., 2004; Kuparinen, 2006). Using surface pollen spectra and vegetation data as input, it has been proven that LS models can give a more accurate approximation of the observed pollen concentration than some classical

Eulerian models when considering long-range events of pollen dispersal (Theuerkauf et al., 2016). Other examples of Lagrangian models are listed in Table 3. In general, Lagrangian models account for different factors that drive LDD events, including the irregular and autocorrelated turbulent fluctuations, and this tends to give a better approximation of the dispersal curve (Kuparinen, 2006). However, the potential of this approach is hampered by the topographical complexity of the study area, that can significantly complicate the modelling of the particles path (Sofiev et al., 2013).

There is not common agreement over the better approach to choose when forecasting pollen concentrations based on their dispersal. While some authors consider Lagrangian models to be more realistic in describing pollen atmospheric dynamics (Kuparinen, 2006; Theuerkauf et al., 2016), others prefer a more comprehensive Eulerian approach that seems a better fit especially in areas where airflow movements are difficult to predict, such as the mountains (Sofiev et al., 2013). In general, all the models have some limits, and the model choice is guided by the features of the study area or the data available. It is interesting to notice that SILAM, a global-to-meso-scale model for pollen forecasting, has been developed with both Eulerian and Lagrangian approaches, allowing to choose the better option for the study (Sofiev et al., 2015b; Veriankaitė et al., 2010).

Quasi-mechanistic models have also been proposed to explain pollen dispersion. They consider pollen dynamics to be probabilistic, describing pollen dispersion as a Brownian motion with drift, integrated with biological and aerodynamic factors (Klein et al., 2003).

While pollen dispersal can be approximated with a certain accuracy, however, this type of forecasting is still limited by the uncertainties associated with the emission sub-model. In fact, unpredictable changes in the future weather or in the plant physiology can substantially modify the starting day of the flowering season, or the pollen productivity, compromising pollen forecasting reliability. While the knowledge of the characteristic of the past pollen season can be useful to train the model, long-term averages of past observed data are not good predictors of the future pollen concentrations (Ranta et al., 2006; Sofiev et al., 2006).

This problem can be approached by calculating the probability of the pollen produced by a certain source (*e.g.* forests, prairies) to affect a receptor area, with the source considered constant in time, and not taking into account the seasonality and the variations in pollen production and release. This way, it is possible to define areas of risk that are likely to be reached by allergenic pollen via LDD. This information is then manually integrated with

updated qualitative data on the phenological state of the plant sources: if the flowering has started, then the probability is converted into forecasted pollen concentrations. This approach was proven to better approximate the observed pollen concentrations than the deterministic approach to pollen emission, although it still was not very accurate in some cases (Sofiev et al., 2006). Other options to improve the predictions of mechanistic forecasting models could be the use of either the "dynamic phenological emission" approach, that is an observation-based phenological model including real-time meteorological data, or the "emission data assimilation" approach, that relies on real-time phenological or aeropalynologycal data assimilation (DA) (Sofiev, 2019; Sofiev et al., 2006). The latter option has been recently tested using real-time aerobiological records for data assimilation in the SILAM model. DA is a relatively recent technology that allows to bring the model predictions closer to the observations, and it could be potentially used to improve the pollen forecasting quality throughout the season, predicting accurate airborne pollen concentrations several days ahead. Unfortunately, the atmospheric lifetime of pollen grains turned out to be too short for DA corrections, making them ineffective in a few hours when applied to forecasting (Sofiev, 2019).

Table 2 *Description of the principal process-based phenological models used in pollen forecasting*

	Process-based phenological models					
Model type	Thermal forcing only	Chilling only	Forcing temperature and chilling	Models including photoperiod	Models including photoperiod and water availability	Generalised Phenological Models
Examples	Spring warming (SW), Growing Degree Day (GDD)	-	Sequential, Parallel, Alternating, Deepening Rest, Four Phases	-	-	Unified model, Promotor-Inhibitor model
Input	Starting day of temperature accumulation, Spring daily temperatures, Plant phenology, Plant distribution	Starting day of temperature accumulation, Winter daily temperatures, Plant phenology, Plant distribution	Starting day of temperature accumulation, Winter and spring daily temperatures, Plant phenology, Plant distribution	Winter and spring daily temperatures, Plant phenology, Photoperiod, Plant distribution	Winter and spring daily temperatures, Plant phenology, Photoperiod, Soil water availability, Plant distribution	Environmental and phenological data, plant dataset
Assumptions	Pollen season begins when the sum of forcing units reaches a threshold value	Pollen season begins a certain time after the sum of chilling units reaches a threshold value	Pollen season start is defined by a combination of chilling and forcing units	Photoperiod defines the starting day of temperature accumulation, pollen season start is defined by a combination of chilling and forcing units	Photoperiod defines the starting day of temperature accumulation, pollen season start is defined by a combination of meteorological factors	Plant responses to a combination of environmental factors can be calculated with flexibles models
Best fit	Late-flowering trees in temperate regions	*Olea europaea* and *Alnus glutinosa* in Mediterranean reagions	Early-flowering trees in temperate regions (*e.g. Alnus* sp., *Acer* sp.)	Tropical and Mediterranean trees	Herbaceous species, tropical and Mediterranean trees	Complex datasets
Output	Starting date, peak and end of the next pollen season					
Bibliography	(Scheifinger et al., 2013; Siniscalco et al., 2015)					

Table 3 *Description of principal pollen dispersion models used in process-based pollen forecasting*

Model type	Numerical models	Fully mechanistic models		Quasi-mechanistic models
		Pollen dispersion models		
Approach	Statistic	Eulerian	Lagrangian	Probabilistic
Examples	Multiple regression equation	ADMS, CHIMERE, COSMO-ART, EURAD-IM, KAMM/DRAIS/MADEsoot, Kawashima & Takahashi model, LOTOS-EUROS, MATCH, METRAS, MOCAGE, SILAM Eulerian, WRF-MEGAN-CMAQ	CALMET/CALPUFF, HYSPLIT, PAPPUS, SILAM Lagrangian, SMOP-2D	-
Input	Past pollen concentrations, Meteorological parameters	Source plants distribution, Information on plant phenology and pollen season characteristics, Emission model, Meteorological model, Boundary layer, diffusion intensity, turbulent mixing.	Source plants distribution, Information on plant phenology and pollen season characteristics, Emission model, Meteorological model, Horizontal and vertical dimensions of the grid.	Male flowers height, Pollen settling velocity, Wind direction and speed, Turbulence
Principle	Pollen dispersion is modelled from the relation between pollen concentrations and meteorological factors.	Analytical approach. Pollen is modelled as a continuum, and its future concentrations in a certain point of a fixed grid are calculated by analytically resolving an advection-diffusion equation with Eulerian approach.	Simulation approach. Pollen dispersion is modelled by simulating the trajectories of individual particles.	Pollen dispersion is modelled as a three-dimensional Brownian motion with drift.
Output	Future pollen concentrations in a certain area	Future pollen concentrations in a certain area		Probability that a pollen grain falls in a certain point
Limits	Useful as sub-models for more complex models	Problems in evaluating pollen emissions, difficulties in simplifying biological factors, high computational costs, numerical diffusion effect.	Problems in evaluating pollen emissions, difficulties in modelling pollen trajectories in areas with complex topography.	Designed to model pollen dispersion in pollination events
Bibliography	(Helbig et al., 2004; Kuparinen, 2006; Scheifinger et al., 2013)	(Helbig et al., 2004; Hunt et al., 2001; Kawashima and Takahashi, 1999, 1995; Müller-Germann et al., 2015; Schueler and Schlünzen, 2006; Siljamo et al., 2013; Sofiev et al., 2015a, 2015b; Veriankaitė et al., 2010; Zhang et al., 2014; Zink et al., 2012)	(Hidalgo et al., 2002; Jarosz et al., 2004; Kuparinen, 2006; Müller-Germann et al., 2017; Sofiev et al., 2013, 2006; Zhang and Han, 2008)	(Klein et al., 2003)

6. Pollen loads and forecasting skills

To be disseminated to the public, predicted pollen concentrations must be translated into discrete categories indicating the allergenic risk they pose. This is not an easy task, because the physical response to aeroallergens exposure depends on many factors: aeroallergens concentrations, air pollution levels, meteorological parameters, and other environmental factors (Caillaud et al., 2014; Cecchi, 2013; D'Amato et al., 2007; Karatzas et al., 2013; Mothes et al., 2004). Genetics and epigenetics of the subject also play an important role in the manifestation of allergic symptoms. Thus, even when considering pollen exposure alone, *e.g.* exposing the subjects to fixed pollen concentrations in a controlled environment (pollen chamber), there is a certain subjectivity in the timing and the intensity of the allergic reaction (De Weger et al., 2013; Mothes et al., 2004).

Threshold values for symptom development have been defined throughout the years, to help allergic patients and medical personnel to understand pollen information and manage allergy symptoms. These thresholds have been established by evaluating the reactions of allergic patients to pollen exposure in "real life" conditions (De Weger et al., 2013). The most common method to achieve this is by asking the subjects to record their symptoms in a diary, and then correlating these symptoms to daily pollen levels (Bastl et al., 2014; De Weger et al., 2013; Kmenta et al., 2014). In some cases, this correlation is corroborated by weekly information provided by a network of allergologists (De Weger et al., 2013). During the last decade, interactive symptom diaries accessible to allergic patients and their physicians have been developed. They can be websites, such as www.pollendiary.com, www.airrater.org, www.allergymap.gr, and www.allergieradar.nl (Bastl et al., 2020, 2018a; Jones et al., 2020; Kalogiros et al., 2018; Pfaar et al., 2017); or specific apps like ARIA, MASK-air, and Allergy Diary (Bousquet et al., 2019; Caimmi et al., 2018; Clot et al., 2020; Kalogiros et al., 2018). While this Crowdsensing approach provides real-time and standardised data, the determination of pollen threshold levels for symptoms development remains problematic, and there is no general consensus on how they should be calculated (De Weger et al., 2013). Moreover, although there is a proven correlation between allergic symptoms and mean daily pollen concentrations, personal exposure of the subject likely differs from the pollen concentrations recorded by the monitoring station (Berger et al., 2014; De Weger et al., 2013; Levetin, 2004). The variability in pollen monitoring approaches adopted by different stations also represents

an important limit to the standardisation of pollen risk thresholds (Levetin, 2004). Moreover, the exposure level that can cause an allergic reaction also depends on the pollen type. In general, average daily airborne pollen concentrations that can trigger an allergic reaction range from 0 to 100 pollen grains/m^3 (Pfaar et al., 2017), but there is a variety of scales and categories that can be used to describe the airborne pollen concentrations and their associated risk. These values are accurately described and summarised by de Weger and colleagues (De Weger et al., 2013). Hence, while it is common to classify pollen loads using "Very Low", "Low", "Medium", "High", and "Very High" (or "Extreme") categories, it is important to acknowledge that the pollen concentration range included in the same level might variate among monitoring and forecasting providers, and aeroallergen considered (De Weger et al., 2013; Gehrig et al., 2018; Silver et al., 2020; Sofiev et al., 2020).

Another problem to address when disseminating pollen forecast for health managing purposes is its accuracy.

When estimating a model performance, the most common statistics employed to compare observed and predicted pollen concentrations are the correlation coefficients and the RMSE. Some authors also applied other metrics like Theil's U statistic, to obtain a scale-free measure, or MAE that is less sensitive to large errors than RMSE (Aznarte et al., 2007; Dennis et al., 2009; Picornell et al., 2019; Sofiev et al., 2017; Valencia-Barrera et al., 2002). Another useful metric is the accuracy rate or model accuracy (MA), that can be calculated as the relationship between the number of correct forecasts and the number of total forecasts (Picornell et al., 2019; Siljamo et al., 2013).

When the aim of the forecast is to inform the public on the allergic risk, however, it is important to evaluate mode accuracy and consistency in predicting different pollen levels. While the aforementioned statistics can also be applied to categorical pollen concentrations, for this purpose probabilistic skill-based indices and threshold-based statistics are preferred (Emmerson et al., 2019; Ritenberga et al., 2016; Siljamo et al., 2013; Zink et al., 2013). These metrics can be calculated for all the pollen load levels estimated by the forecast (Bastl et al., 2017b), or they can be based on a single threshold separating low and high daily pollen concentrations (De Weger et al., 2013; Siljamo et al., 2013).

When considering just one threshold, the Hit Rate (HR) or Probability of Detection (POD) is used to estimate the fraction of high pollen levels predictions that are correct (high predicted and high observed), while the False Alarm Ratio (FAR) identifies the fraction of incorrect high-

level predictions (high predicted and low observed). A complementary measure is the Probability of False Detection (POFD), that calculates the fraction of observed low-concentration days predicted as high. To evaluate the reliability of the predicted high-level days more comprehensively, the relationship between POD and POFD can be estimated through the Odds Ratio (OR) or the Hansen-Kuiper (or True Skill) Score, estimating the chances to observe a high-concentration day when it has been predicted (Emmerson et al., 2019; Gerrity, 1992; Siljamo et al., 2013). Some metrics also evaluate the performance of the forecasting against the probability to obtain the correct prediction by chance. Examples are the Equitable Threat Score (ETS), that measures the skill of a forecast to correctly predict high pollen days, adjusted for the probability to randomly obtain correct forecasts (Emmerson et al., 2019); and the Peirce Skill Score (PSS), that compares the performance of the model to that of a random forecast (Peirce, 1884; Zink et al., 2013).

When evaluating forecasting skills for more than two categories of pollen concentrations, all these metrics should be calculated for each category, considering the occurrence of the desired category as an event, and the occurrence of any other category as a non-event. This means that, when a non-event is both predicted and observed (correct negative), the prediction cannot be automatically assumed as correct (Emmerson et al., 2019; Zink et al., 2013). In this case, the Threat Score (TS) can be applied to evaluate the fraction of correct forecasts, ignoring the correct negatives (Zink et al., 2013).

A limit of these threshold-based metrics is that they do not consider how close the incorrect forecast was to the observed pollen level, in terms of pollen concentrations. For this reason, categorical forecasting evaluation is usually supported by the aforementioned non-categorical evaluation methods (Zink et al., 2013). To avoid low performance estimations of a model due to slight differences between predicted and observed concentrations, it is possible to assume an interval of tolerance around the threshold values, so that the categories have a slight overlap (Bastl et al., 2017b).

Another useful metric is the Gerrity Score (GS) (Gerrity, 1992), that attributes different weights to incorrect predictions, depending on how much they differ from the observed values. This score also evaluates the forecasting skill relative to the random chance, by rewarding the correct prediction of rare events more than the correct prediction of common events (Emmerson et al., 2019; Gerrity, 1992).

To be useful for allergic patients, pollen forecasting should have high POD and GS, accurately predicting days with high or very high pollen loads, that can cause relevant allergic reactions (Zink et al., 2013). On the other hand, the FAR of the forecasting model should be low, since incorrectly predicting high pollen loads can lead allergic patients to assume unnecessary medications or to avoid outdoor activities (Bastl et al., 2017a).

How these metrics could be clearly communicated to the public along with the forecast, however, is still debated (Bastl et al., 2017b).

7. Dissemination of pollen forecasts

Allergic symptoms can be exacerbated by different environmental and genetic components, but pollen exposure is certainly the most important risk factor for pollen allergic subjects (Bousquet et al., 2019). Aeroallergen monitoring and avoidance in fact represent a primary and secondary prevention strategy respectively for an individual decrease of the risks to develop allergic illnesses (Reid and Gamble, 2009). Knowledge of future pollen loads is perceived by pollen allergy sufferers to be useful for prevention and avoidance, as well as preparation and planning, highlighting a public demand for pollen information (Medek et al., 2019). This information is usually integrated with weather or air quality forecasting, and provided to the public via newspapers and television on a national scale, by websites on a regional scale, and by smartphone applications (apps) on a personal scale (Karatzas et al., 2013). Public consumption of pollen forecasting during the pollen season, recorded by forecasting websites, underlines the concern pollen allergy causes to sensitive subjects, and their need to monitor the situation (Kmenta et al., 2016).

While public access to air quality information is ensured by Governments and international organisations (Karatzas et al., 2013; Monfort et al., 2002) both as ordinary monitoring and incident-event alerts, pollen monitoring and forecasting tend to be overlooked by these regulations (Karatzas et al., 2013).

Nonetheless, in the last decades different Countries have joined efforts in common aerobiology networks and projects, with the creation of national and international websites designed for pollen allergic subjects, that provide daily pollen counts and pollen forecast at different time and spatial resolutions. Examples are www.polleninfo.org for Eurasian countries (Kmenta et al., 2016), www.pollen.com for the USA (Geller-Bernstein and Portnoy, 2019), and www.pollenforecast.com.au for Australian regions. Smartphone apps providing

daily pollen forecasts and monitoring allergy symptoms are also available in many countries (Bastl et al., 2017b; Bousquet et al., 2019; Jones et al., 2020; Kmenta et al., 2016), and many weather forecasting websites offer pollen information. All these tools are part of the Electronic Health (eHealth) and Mobile Health (mHealth), defined by the WHO as the medical and public health practice supported by information and communication technologies, and by wireless mobile devices, respectively (Bastl et al., 2020; WHO, 2018).

During the last century, the pollen calendar has been the main source of pollen forecasting available to the public (Fig. S1A), with the advantage to be intuitive and clearly understandable (D'Amato et al., 1991; Gehrig et al., 2018), but with the downsides of a low time resolution and the impossibility to predict uncommon and swift events. Pollen calendars are still employed to disseminate general, long-term information about the future pollen seasons by pollen-monitoring networks, patient organizations, and for medical information purposes (Gehrig et al., 2018), but they are progressively being substituted or flanked by more comprehensive approaches. To better exploit the informative potential of the pollen calendar, a recent study (Gehrig et al., 2018) developed a new form of it, intended for the public consumption as complementary to other forms of forecast. This pollen calendar is based on users' expectation to know the possible occurrence of high pollen levels during a certain period, instead of the mean pollen season. For this purpose, it is not calculated as an average value, but as the 90% quantile of the daily pollen concentrations for each day of the year, in a moving 9-day time window, over 20 years of data. These pollen concentrations are automatically calculated and regularly updated on the website (www.meteoswiss.ch/pollen-calendar), presented as pollen loads levels (low, moderate, high, very high), and can be visualised for individual monitoring stations, regions, or pollen type (Gehrig et al., 2018). Another way to disseminate long-term pollen information is a table with the starting date of the pollen season for the major pollen allergens, obtained by past pollen data and phenological observations. This information is embedded only in few pollen apps, e.g. Pollen and Pollen News, but it tends to be more accurate than daily or hourly forecasts (higher POD), and may help pollen allergic patients to prepare for the pollen season (Bastl et al., 2017b).

However, in the last decades a broad variety of pollen forecasting models have been proposed, in the attempt to obtain more accurate and precise predictions (Fig. S1), although just some of them have been made available for public consumption. Observation-based forecasting methods other than pollen calendars have been employed to disseminate short-

term pollen forecasts: for instance, the Spanish Aerobiology Network (REA) offers three-day forecasts generated on a national scale by the University of Cordoba using time-series (Fernández-Rodríguez et al., 2016; Oteros et al., 2019), that are available on the website www.uco.es/investiga/grupos/rea or on the Pollen REA app. Within the possible observation-based approaches, CI seems to give the best approximation of future pollen concentrations, in particular when using machine learning models with a non-linear behaviour, such as neural nets (Aznarte et al., 2007). This approach has been preferred by some pollen forecasting providers, such as the Danish patient association Asthma-Allergy, with their smartphone app Dagens Pollental.

Unfortunately, due to their regional and empirical nature, observation-based models cannot be generalised to wide geographic areas. Furthermore, they rely on real pollen records, usually expressed as mean daily pollen concentrations. This limits the time resolution of these approaches, since they can predict at best the daily concentrations or the starting, peak and end date of the pollen season, but they cannot give detailed information to pollen allergic subjects on the variations of the risk they are exposed to throughout the day (Scheifinger et al., 2013).

Process-based forecasting models instead have higher temporal and spatial resolution than the observation-based ones, and some of them can even weight in the effect of LDD events (Ranzi et al., 2003). In particular, some process-based dispersal models can now estimate future concentrations of 6 pollen types up to 5 days, for wide geographic regions (Sofiev et al., 2020). On the other hand, these models are associated with various uncertainties (Migliavacca et al., 2012), they do not run operationally and are not calculated for all the allergic pollen types (Maya-Manzano et al., 2021). This reduces the value of these forecasts for pollen allergic subjects, making this approach mainly limited to scientific research applications.

Nevertheless, some process-based dispersal models are starting to be employed by forecasting providers as informative tools to alert the public about possible future pollen concentrations, even with hourly resolution. For example, Swiss Federal Office of Climatology and Meteorology MeteoSwiss offers both the aforementioned user-oriented pollen calendar, and hourly three-day pollen forecasts calculated using COSMO-ART model. Similarly, Austrian website www.pollenwarndienst.at allows to choose among various pollen forecasts elaborated by the Medical University of Vienna: phenological calendars indicating the starting

date of the pollen season, three-day forecasts in the form of daily pollen concentration maps or daily pollen loads estimated by COSMO-ART, and daily forecasts with hourly resolution created with SILAM. Some of these forecasts are also available for other European countries at the website www.polleninfo.org. Furthermore, the ensemble model embedded in the CAMS website offers a 5-day global pollen forecasting and a 3-day forecasting on a European scale (Sofiev et al., 2020, 2017). CAMS also provides 3-day pollen forecasts to several apps designed for pollen allergic patients, such as BreezoMeter and MeteoPollen (Tab. 4) (Bousquet et al., 2019). The app PASYFO recently developed for Lithuania and Latvia by The Copernicus Project combines SILAM model and CAMS forecasts (Sofiev et al., 2020), while the Austrian app Pollen relies on the SILAM model for daily forecasts (Kmenta et al., 2014), achieving hit rates of 60% on the predicted pollen loads (Bastl et al., 2017b).

These examples, listed in Table 4, are excellences in their field. In fact, many pollen forecasting sources do not specify the method applied, nor they are associated to scientific publications or official institutions. This makes it difficult to evaluate their factual utility to allergic patients. In fact, pollen information disseminated by private or unofficial entities might be subject to conflict of interest or affected by poor data quality (Bastl et al., 2017a, 2017b). Health-related mobile apps in particular often lack of clinical evidence and validation (Matricardi et al., 2020a), and their pollen forecasts tend to have low performance and to be discontinuous, especially when they are published by private companies (Bastl et al., 2017b). Deliberate inaccuracy in pollen forecasting leads to avoidable under- and overestimations of the allergenic risk, because the public is not aware of the forecast performance, resulting in what can be considered a physical injury of the allergic subjects (Bastl et al., 2017a; Bousquet et al., 2019).

Another problem when evaluating the utility of pollen forecasting for allergic patients is the subjectivity of the symptoms, that partly depends on the personal exposure to the allergen. This problem has been addressed with the development of interactive symptom diaries, that allow to produce individual, user-specific symptom forecasting using CI to model the relationship between recorded symptoms, associated pollen counts, and concurrent environmental parameters (Bastl et al., 2014; Kmenta et al., 2014; Voukantsis et al., 2013). A continuous personal monitoring of allergic symptoms and pollen exposure could be the key to improve pollen forecasting in a way that is useful to allergy sufferers, and that can also help health workers to foresee pollen allergy outbreaks and emergency room accesses (Bastl et

al., 2014; Pfaar et al., 2017). For this reason, many apps providing pollen information have also integrated a symptom monitoring and forecasting service (Tab. 4) (Kmenta et al., 2016, 2014; Sofiev et al., 2020). It is however important to investigate whether the knowledge of pollen forecasts can have the psychological effect of anticipating pollen symptoms (Pfaar et al., 2017). Moreover, it is challenging to evaluate the real benefits provided by mobile apps to allergy sufferers, especially because of their discontinuous engagement with the app and the impossibility to detect subjective biases in their perception of the symptoms (Bousquet et al., 2019).

Table 4 *Description of mobile applications and websites cited in literature, that provide pollen forecasting to the public specifying the forecasting method applied.*

App	Website	Availability	Observation-based forecast	Process-based forecast	Day forecasted	Symptoms forecast	Pollen types	Bibliography
BreezoMeter	www.breezometer.com	International	No	CAMS ensemble	3	No	13+	(Bousquet et al., 2019)
Dagens Pollental	www.astma-allergi.dk/dagens	Denmark	Neural Networks	No	5	No	6	(Bousquet et al., 2019)
Meteo Allergie	http://www.pollinieallergia.net/	Italy	Pollen calendar, time series	No	7	No	11	(Mateo Pla et al., 2016)
MétéoPollen	www.meteopollen.com	France	No	CAMS ensemble	3	No	Not specified	(Bousquet et al., 2019)
PASYFO	https://atmosphere.copernicus.eu	Lithuania, Latvia	Pollen calendar	CAMS ensemble, SILAM	CAMS: 4 SILAM: 2	Yes	Calendar: 23 CAMS: 4 SILAM: 6	(Sofiev et al., 2020)
Pollen	www.pollenwarndienst.at www.polleninfo.org	Europe	Starting date of the pollen season	SILAM	3	Yes	25	(Bastl et al., 2017b; Bousquet et al., 2019; Kmenta et al.,)
Pollenflug Vorhersage	www.wetteronline.de	Germany	Pollen calendar, algorithms	No	7	No	14	(Bastl et al., 2017b)
Pollen-News	www.aha.ch/swiss-allergy-centre	Switzerland	No	COSMO-ART	3	No	14	(Bastl et al., 2017b)
	www.meteoswiss.ch	Switzerland	Pollen calendar	COSMO-ART	3	No	4	(Gehrig et al., 2018)
	www.polleninfo.org	Europe	Starting date of the pollen season	COSMO-ART, SILAM	3	No	COSMO-ART: 4 SILAM: 6	(Bousquet et al., 2019; Sofiev et al., 2006)
	www.regional.atmosphere.copernicus.eu	International	No	CAMS ensemble	5	No	5	(Sofiev et al., 2017)
	https://silam.fmi.fi	Europe	No	SILAM	4	Yes	6	(Sofiev et al., 2017)
	www.uco.es/investiga/grupos/rea	Spain	Time series	No	3	No	14	(Fernández-Rodríguez et al., 2016; Oteros et al., 2019)

8.   Conclusions

Pollen forecasting is an active research ground that conjugates aerobiology, engineering, physics, and informatics to approximate the complex phenomena of pollen emission and dispersion. To date, many approaches and models are available to forecast future pollen concentrations and the risk they pose to pollen allergic subjects. Observation-based models are the first type of pollen forecasting developed, based on past pollen concentrations and phenological observations (Fig. S1A). They are still employed to provide accurate pollen calendars and pollen season starting dates, allowing allergic subjects to plan in advance their movements and medications. On the other hand, the information is local, averaged, and expressed as weekly or daily values (Scheifinger et al., 2013). In the last two decades there has been a great effort to model the complex relationships between plants and the environment, that influence pollen emission and dispersal (Fig. S1B, C). This approach, called process-based, allows to simulate future pollen dynamics, given the initial conditions of the system. On a direct comparison, process-based models have more potential than the observation-based ones, and some of them can even weight in the effect of LDD events. Nonetheless, their use may be hindered by the computational effort and the amount of data they require (Ranzi et al., 2003). In fact, they need detailed information on geographical and meteorological features of the study area, and a deep knowledge of plant phenology and distribution (Norris-Hill, 1995; Šikoparija et al., 2018; Skjøth et al., 2010). This problem could be partially solved by preparing local or global allergenic plant inventories (Skjøth et al., 2010; Sofiev et al., 2006). Another major issue of process-based models is the uncertainty associated with pollen emission modelling, due to both a lack of knowledge about the process and the unpredictability of future climate scenarios (Migliavacca et al., 2012).

A common problem to all these forecasting approaches is that the airborne pollen data they elaborate are temporally and spatially scattered, and they do not accurately reflect individual exposure. Furthermore, since pollen sampling and counting methods may vary between different monitoring stations (Buters et al., 2018), real and forecasted pollen concentrations calculated in different areas might not be comparable. Comparability issues also arise from the long data collection and the massive computational effort these models require, that discourage the comparison between different models on the same dataset.

Because of all these issues, high forecasting accuracy is difficult to achieve. Complex dispersal models are not run routinely for many pollen types and locations yet, and their application is often limited to scientific research purposes. Process-based dispersion models like SILAM, COSMO-ART, and the CAMS ensemble, are being used by forecasting websites and mobile apps to inform the public on the allergenic risk, often with hourly resolution (Bousquet et al., 2019; Sofiev et al., 2020). Nonetheless, the usefulness of these instruments to pollen allergic subjects is still uncertain. On one hand, pollen information consumption is perceived as important and beneficial by allergic patients, because Electronic Health can help them self-manage their disease and reduce the symptom severity, a crucial issue especially for those living in rural or remote areas (Kmenta et al., 2016; Matricardi et al., 2020b; Sofiev et al., 2020). On the other hand, forecasting pollen levels in remote and underpopulated areas, where no pollen monitoring is in place, is still problematic (Hall et al., 2020; Oteros et al., 2019; Sofiev et al., 2020; Wakamiya et al., 2019). Furthermore, it is difficult to evaluate the reliability of the pollen forecast provided by many apps and websites, since they do not indicate their sources, their data are not be scientifically validated, and they tend to have temporal gaps (Bastl et al., 2017b). If the allergic subject relies on these instruments for his wellbeing, unaware of their probabilistic nature, unreliable pollen forecasting might be even detrimental to his health (Bastl et al., 2017a).

To enhance the value of pollen forecasting, more epidemiological studies correlating allergic symptoms and pollen concentrations are needed, because the severity of the allergic reaction also depends on other factors (Bastl et al., 2018a; Caillaud et al., 2014; De Weger et al., 2013; Sofiev et al., 2020). These studies need to be performed on a global scale, since pollination varies with plant abundance and microclimate, resulting in regionally differences in pollen emission that could affect both the pollen forecasting models and the individual exposure (Bastl et al., 2017b; Reid and Gamble, 2009). For these reasons, a portfolio of quality criteria for pollen monitoring and forecasting was recently suggested in the interest and for the protection of people affected by a pollen allergy (Bastl et al., 2017a).

9.   Bibliography

Anderegg, W.R.L., Abatzoglou, J.T., Anderegg, L.D.L., Bielory, L., Kinney, P.L., Ziska, L., 2021. Anthropogenic climate change is worsening North American pollen seasons. Proc. Natl. Acad. Sci. U. S. A. 118, e2013284118. https://doi.org/10.1073/pnas.2013284118

Arizmendi, C.M., Sanchez, J.R., Ramos, N.E., Ramos, G.I., 1993. Time series predictions with neural nets: application to airborne pollen forecasting. Int. J. Biometeorol. 37, 139–144.

Aznarte, J.L., Benitez Sanchez, J.M., Nieto Lugilde, D., de Linares Fernandez, C., Diaz de la Guardia, C., Alba Sanchez, F., 2007. Forecasting airborne pollen concentration time series with neural and neuro-fuzzy models. Expert Syst. Appl. 32, 1218–1225. https://doi.org/10.1016/j.eswa.2006.02.011

Bastl, K., Bastl, M., Bergmann, K.C., Berger, M., Berger, U., 2020. Translating the Burden of Pollen Allergy Into Numbers Using Electronically Generated Symptom Data From the Patient's Hayfever Diary in Austria and Germany: 10-Year Observational Study. J. Med. Internet Res. 22, e16767. https://doi.org/10.2196/16767

Bastl, K., Berger, M., Bergmann, K.C., Kmenta, M., Berger, U., 2017a. The medical and scientific responsibility of pollen information services. Wien. Klin. Wochenschr. 129, 70–74. https://doi.org/10.1007/s00508-016-1097-3

Bastl, K., Berger, U., Kmenta, M., 2017b. Evaluation of Pollen Apps Forecasts:The Need for Quality Control in an eHealth Service. J. Med. Internet Res. 19, 1–8. https://doi.org/10.2196/jmir.7426

Bastl, K., Berger, U., Kmenta, M., Weber, M., 2017c. Is there an advantage to staying indoors for pollen allergy sufferers ? Composition and quantitative aspects of the indoor pollen spectrum. Build. Environ. 123, 78–87. https://doi.org/10.1016/j.buildenv.2017.06.040

Bastl, K., Kmenta, M., Berger, M., Berger, U., 2018a. The connection of pollen concentrations and crowd-sourced symptom data: New insights from daily and seasonal symptom load index data from 2013 to 2017 in Vienna. World Allergy Organ. J. 11, 1–8. https://doi.org/10.1186/s40413-018-0203-6

Bastl, K., Kmenta, M., Berger, U.E., 2018b. Defining Pollen Seasons : Background and Recommendations. Curr. Allergy Asthma Rep. 18, 73.

Bastl, K., Kmenta, M., Jäger, S., Bergmann, K.-C., EAN, Berger, U., 2014. Development of a symptom load index: enabling temporal and regional pollen season comparisons and pointing out the need for personalized pollen information. Aerobiologia (Bologna). 30, 269–280. https://doi.org/10.1007/s10453-014-9326-6

Berger, U., Kmenta, M., Bastl, K., 2014. Individual pollen exposure measurements: Are they feasible? Curr. Opin. Allergy Clin. Immunol. 14, 200–205. https://doi.org/10.1097/ACI.0000000000000060

Björkstén, B., Clayton, T., Ellwood, P., Stewart, A., Strachan, D., Phase III Study Group, the I., 2008a. Worldwide time trends for symptoms of rhinitis and conjunctivitis: Phase III of the International Study of Asthma and Allergies in Childhood. Pediatr. Allergy Immunol. 19, 110–124. https://doi.org/10.1111/j.1399-3038.2007.00601.x

Björkstén, B., Clayton, T., Ellwood, Philippa, Stewart, A., Strachan, D., Ait-Khaled, N., Anderson, H.R., Asher, M.I., Beasley, R., Bjorkstén, B., Brunekreef, B., Cookson, W., Crane, J., Ellwood, P., Foliaki, S., Keil, U., Lai, C.K.W., Mallol, J., Robertson, C., Mitchell, E.A., Montefort, S., Odhiambo, J., Pearce, N., Shah, J., Stewart, A.W., Strachan, D.P., Von Mutius, E., Weiland, S.K., Williams, H., 2008b. Worldwide time trends for symptoms of rhinitis and conjunctivitis: Phase III of the International Study of Asthma and Allergies in Childhood. Pediatr. Allergy Immunol. 19, 110–124. https://doi.org/10.1111/j.1399-3038.2007.00601.x

Bousquet, J., Ansotegui, I.J., Anto, J.M., Arnavielhe, S., Bachert, C., Basagaña, X., Bédard, A., Bedbrook, A., Bonini, M., Bosnic-Anticevich, S., Braido, F., Cardona, V., Czarlewski, W., Cruz, A.A., Demoly, P., De Vries, G., Dramburg, S., Mathieu-Dupas, E., Erhola, M., Fokkens, W.J., Fonseca, J.A., Haahtela, T., Hellings, P.W., Illario, M., Ivancevich, J.C., Jormanainen, V., Klimek, L., Kuna, P., Kvedariene, V., Laune, D., Larenas-Linnemann, D., Lourenço, O., Onorato, G.L., Matricardi, P.M., Melén, E., Mullol, J., Papadopoulos, N.G., Pfaar, O., Pham-Thi, N., Sheikh, A., Tan, R., To, T., Tomazic, P.V., Toppila-Salmi, S., Tripodi, S., Wallace, D., Valiulis, A., van Eerd, M., Ventura, M.T., Yorgancioglu, A., Zuberbier, T., 2019. Mobile Technology in Allergic Rhinitis: Evolution in Management or Revolution in Health and Care? J. Allergy Clin. Immunol. Pract. 7, 2511–2523. https://doi.org/10.1016/j.jaip.2019.07.044

Bousquet, J., Khaltaev, N., Cruz, A.A., Denburg, J., Fokkens, W.J., Togias, A., Zuberbier, T., Canonica, G.W., Weel, C. Van, Agache, I., Bachert, C., 2008. Allergic Rhinitis and its Impact on Asthma (ARIA) 2008. Allergy 63, 8–160.

Brennan, G.L., Potter, C., de Vere, N., Griffith, G.W., Skjøth, C.A., Osborne, N.J., Wheeler, B.W., McInnes, R.N., Clewlow, Y., Barber, A., Hanlon, H.M., Hegarty, M., Jones, L., Kurganskiy, A., Rowney, F.M., Armitage, C.,

Adams-Groom, B., Ford, C.R., Petch, G.M., Consortium, T.P., Creer, S., 2019. Temperate airborne grass pollen defined by spatio-temporal shifts in community composition. Nat. Ecol. Evol. 3, 750–754.

Burge, H.A., Rogers, C.A., 2000. Outdoor Allergens. Environ. Health Perspect. 108, 653–659. https://doi.org/10.1016/B978-0-323-29875-9.00020-3

Buters, J.T.M., Antunes, C., Galveias, A., Bergmann, K.C., Thibaudon, M., Galán, C., Schmidt-Weber, C., Oteros, J., 2018. Pollen and spore monitoring in the world. Clin. Transl. Allergy 8, 1–5. https://doi.org/10.1186/s13601-018-0197-8

Cai, T., Zhang, Y., Ren, X., Bielory, L., Mi, Z., Nolte, C.G., Gao, Y., Leung, L.R., Georgopoulos, P.G., 2019. Development of a semi-mechanistic allergenic pollen emission model. Sci. Total Environ. 653, 947–957. https://doi.org/10.1016/j.scitotenv.2018.10.243

Caillaud, D., Martin, S., Segala, C., Besancenot, J.P., Clot, B., Thibaudon, M., 2014. Effects of airborne birch pollen levels on clinical symptoms of seasonal allergic rhinoconjunctivitis. Int. Arch. Allergy Immunol. 163, 43–50. https://doi.org/10.1159/000355630

Caimmi, D., Baiz, N., Sanyal, S., Banerjee, S., Demoly, P., Annesi-Maesano, I., 2018. Discriminating severe seasonal allergic rhinitis. Results from a large nation-wide database. PLoS One 13, 1–11. https://doi.org/10.1371/journal.pone.0207290

Canonica, G.W., Bousquet, J., Mullol, J., Scadding, G.K., Virchow, J.C., 2007. A survey of the burden of allergic rhinitis in Europe. Allergy 62, 17–25. https://doi.org/10.1111/j.1398-9995.2007.01548.x

Cecchi, L., 2013. From pollen count to pollen potency: the molecular era of aerobiology. Eur. Respir. J. 42, 898–900. https://doi.org/10.1183/09031936.00096413

Clò, E., Torri, P., Florenzano, A., Mercuri, A.M., 2016. Global warming and Annual Pollen Index of Poaceae. Atti della Soc. dei Nat. e Mat. di Modena 147, 183–193.

Clot, B., Gilge, S., Hajkova, L., Magyar, D., Scheifinger, H., Sofiev, M., Bütler, F., Tummon, F., 2020. The EUMETNET AutoPollen programme: establishing a prototype automatic pollen monitoring network in Europe. Aerobiologia (Bologna). 4. https://doi.org/10.1007/s10453-020-09666-4

D'Amato, G., Cecchi, L., Bonini, S., Nunes, C., Annesi-Maesano, I., Behrendt, H., Liccardi, G., Popov, T., Van Cauwenberge, P., 2007. Allergenic pollen and pollen allergy in Europe. Allergy Eur. J. Allergy Clin. Immunol. 62, 976–990. https://doi.org/10.1111/j.1398-9995.2007.01393.x

D'Amato, G., Spieksma, F.T.M., Bonini, S., 1991. Allergenic pollen and pollinosis in Europe. Oxford: Blackwell Sci. Publ.

De Weger, L.A., Bergmann, K.C., Rantio-Lehtimäki, A., Dahl, A., Buters, J., Déchamp, C., Belmonte, J., Thibaudon, M., Cecchi, L., Besancenot, J.P., Galán, C., Waisel, Y., 2013. Impact of pollen, in: Allergenic Pollen: A Review of the Production, Release, Distribution and Health Impacts. Springer Netherlands, pp. 161–215. https://doi.org/10.1007/978-94-007-4881-1_6

Della Valle, C.T., Triche, E.W., Bell, M.L., 2012. Spatial and temporal modeling of daily pollen concentrations. Int. J. Biometeorol. 56, 183–194. https://doi.org/10.1007/s00484-011-0412-y

Demoly, P., Passalacqua, G., Pfaar, O., Sastre, J., Wahn, U., 2016. Management of the polyallergic patient with allergy immunotherapy : a practice - based approach. Allergy, Asthma Clin. Immunol. 12, 1–13. https://doi.org/10.1186/s13223-015-0109-6

Dennis, R., Fox, T., Fuentes, M., Gilliland, A., Hanna, S., Hogrefe, C., Irwin, J., Rao, S.T., Scheffe, R., Schere, K., Steyn, D., Venkatram, A., 2009. On the Evaluation of Regional-Scale Photochemical Air Quality Modeling Systems 78. https://doi.org/https://doi.org/10.1007/s10652-009-9163-2

Djukanović, R., Wilson, S.J., Kraft, M., Jarjour, N.N., Steel, M., Chung, K.F., Bao, W., Fowler-Taylor, A., Matthews, J., Busse, W.W., Holgate, S.T., Fahy, J. V., 2004. Effects of treatment with anti-immunoglobulin E antibody omalizumab on airway inflammation in allergic asthma. Am. J. Respir. Crit. Care Med. 170, 583–893. https://doi.org/10.1164/rccm.200312-1651OC

Duhl, T.R., Zhang, R., Guenther, A., Chung, S.H., Salam, M.T., House, J.M., Flagan, R.C., Avol, E.L., Gilliland, F.D., Lamb, B.K., VanReken, T.M., Zhang, Y., Salathé, E., 2013. The Simulator of the Timing and Magnitude of Pollen Season (STaMPS) model: a pollen production model for regional emission and transport modeling. Geosci. Model Dev. Discuss. 6, 2325–2368. https://doi.org/10.5194/gmdd-6-2325-2013

Emmerson, K.M., Silver, J.D., Newbigin, E., Lampugnani, E.R., Suphioglu, C., Wain, A., Ebert, E., 2019. Development and evaluation of pollen source methodologies for the Victorian Grass Pollen Emissions Module VGPEM1.0. Geosci. Model Dev. 12, 2195–2214. https://doi.org/10.5194/gmd-12-2195-2019

Erbas, B., Akram, M., Dharmage, S.C., Tham, R., Dennekamp, M., Newbigin, E., Taylor, P., Tang, M.L.K., Abramson, M.J., 2012. The role of seasonal grass pollen on childhood asthma emergency department presentations. Clin. Exp. Allergy 42, 799–805. https://doi.org/10.1111/j.1365-2222.2012.03995.x

Erbas, B., Chang, J.-H., Dharmage, S., Ong, E.K., Hyndman, R., Newbigin, E., Abramson, M., 2007. Do levels of airborne grass pollen influence asthma hospital admissions ? Clin. Exp. Allergy 37, 1641–1647. https://doi.org/10.1111/j.1365-2222.2007.02818.x

Erbas, B., Jazayeri, M., Lambert, K.A., Katelaris, C.H., Prendergast, L.A., Tham, R., Parrodi, M.J., Davies, J., Newbigin, E., Abramson, M.J., Dharmage, S.C., 2018. Outdoor pollen is a trigger of child and adolescent asthma emergency department presentations: A systematic review and meta-analysis. Allergy Eur. J. Allergy Clin. Immunol. https://doi.org/10.1111/all.13407

European Respiratory Society, 2017. The Global Impact of Respiratory Disease- Second Edition, Forum of International Respiratory Societies.

Fernández-Rodríguez, S., Durán-Barroso, P., Silva-Palacios, I., Tormo-Molina, R., Maya-Manzano, J.M., Gonzalo-Garijo, Á., 2016. Regional forecast model for the Olea pollen season in Extremadura (SW Spain). Int. J. Biometeorol. 60, 1509–1517. https://doi.org/10.1007/s00484-016-1141-z

Galán, C., Ariatti, A., Bonini, M., Clot, B., Crouzy, B., Dahl, A., Fernandez-González, D., Frenguelli, G., Gehrig, R., Isard, S., Levetin, E., Li, D.W., Mandrioli, P., Rogers, C.A., Thibaudon, M., Sauliene, I., Skjoth, C., Smith, M., Sofiev, M., 2017. Recommended terminology for aerobiological studies. Aerobiologia (Bologna). 33, 293–295. https://doi.org/10.1007/s10453-017-9496-0

Galán, C., Smith, M., Thibaudon, M., Frenguelli, G., Oteros, J., Gehrig, R., Berger, U., Clot, B., Brandao, R., 2014. Pollen monitoring : minimum requirements and reproducibility of analysis. Aerobiologia (Bologna). 30, 385–395. https://doi.org/10.1007/s10453-014-9335-5

Galan, I., Prieto, A., Rubio, M., Herrero, T., Cervigo, P., Martı, I., Cantero, J.L., Gurbindo, M.D., Martinez, M.I., Aurelio, T., 2010. Association between airborne pollen and epidemic asthma in Madrid , Spain : a case e control study. Thorax 65, 398–402. https://doi.org/10.1136/thx.2009.118992

Gehrig, R., Maurer, F., Schwierz, C., 2018. Designing new automatically generated pollen calendars for the public in Switzerland. Aerobiologia (Bologna). 34, 349–362. https://doi.org/10.1007/s10453-018-9518-6

Geller-Bernstein, C., Portnoy, J.M., 2019. The Clinical Utility of Pollen Counts. Clin. Rev. Allergy Immunol. 57, 340–349. https://doi.org/10.1007/s12016-018-8698-8

Gerrity, J.P., 1992. A Note on Gandin and Murphy's Equitable Skill Score. Mon. Weather Rev. 120, 2709–2712. https://doi.org/10.1175/1520-0493(1992)120<2709:anogam>2.0.co;2

Gesualdo, F., Stilo, G., D'Ambrosio, A., Carloni, E., Pandolfi, E., Velardi, P., Fiocchi, A., Tozzi, A.E., 2015. Can twitter be a source of information on allergy? Correlation of pollen counts with tweets reporting symptoms of allergic rhinoconjunctivitis and names of antihistamine drugs. PLoS One 10, 1–11. https://doi.org/10.1371/journal.pone.0133706

Green, B.J., Levetin, E., Horner, W.E., Codina, R., Barnes, C.S., Filley, W. V, 2018. Landscape Plant Selection Criteria for the Allergic Patient. J. Allergy Clin. Immunol. Pract. 6, 1869–1877. https://doi.org/10.1016/j.jaip.2018.05.020

Hall, J., Lo, F., Saha, S., Vaidyanathan, A., Hess, J., 2020. Internet searches offer insight into early-season pollen patterns in observation-free zones. Sci. Rep. 10, 1–10. https://doi.org/10.1038/s41598-020-68095-y

Helbig, N., Vogel, B., Vogel, H., Fiedler, F., 2004. Numerical modelling of pollen dispersion on the regional scale. Aerobiologia (Bologna). 2, 3–19.

Hidalgo, P.J., Mangin, A., Galán, C., Hembise, O., Vázquez, L.M., Sanchez, O., 2002. An automated system for surveying and forecasting Olea pollen dispersion. Aerobiologia (Bologna). 18, 23–31. https://doi.org/10.1023/A:1014997310925

Huete, A., Nguyen Ngoc, T., Nguyen, H., Xie, Q., Katelaris, C., 2019. Forecasting Pollen Aerobiology with Modis EVI, Land Cover, and Phenology Using Machine Learning Tools. Int. Geosci. Remote Sens. Symp. 5429–5432. https://doi.org/10.1109/IGARSS.2019.8898796

Huffman, J.A., Perring, A.E., Savage, N.J., Clot, B., Crouzy, B., Tummon, F., Shoshanim, O., Damit, B., Schneider, J., Sivaprakasam, V., Zawadowicz, M.A., Crawford, I., Gallagher, M., Topping, D., Doughty, D.C., Hill, S.C., Pan, Y., 2019. Real-time sensing of bioaerosols: Review and current perspectives. Aerosol Sci. Technol. 54, 465–495. https://doi.org/10.1080/02786826.2019.1664724

Hunt, J.C.R., Higson, H.L., Walklate, P.J., Sweet, J.B., 2001. Modeling the dispersion and cross-fertilisation of pollen from GM crops.

Jarosz, N., Loubet, B., Huber, L., 2004. Modelling airborne concentration and deposition rate of maize pollen. Atmos. Environ. 38, 5555–5566. https://doi.org/10.1016/j.atmosenv.2004.06.027

Jia, M., Huang, X., Ding, K., Liu, Q., Zhou, D., Ding, A., 2021. Impact of data assimilation and aerosol radiation interaction on Lagrangian particle dispersion modelling. Atmos. Environ. 247, 118179. https://doi.org/10.1016/j.atmosenv.2020.118179

Jones, P.J., Koolhof, I.S., Wheeler, A.J., Williamson, G.J., Lucani, C., Campbell, S.L., Bowman, D.M.J.S., Johnston, F.H., 2020. Can smartphone data identify the local environmental drivers of respiratory disease? Environ. Res. 182, 109118. https://doi.org/10.1016/j.envres.2020.109118

Kalogiros, L.A., Lagouvardos, K., Nikoletseas, S., Papadopoulos, N., Tzamalis, P., 2018. Allergymap: A Hybrid mHealth Mobile Crowdsensing System for Allergic Diseases Epidemiology : multidisciplinary case study. 2018 IEEE Int. Conf. Pervasive Comput. Commun. Work. PerCom Work. 2018 597–602. https://doi.org/10.1109/PERCOMW.2018.8480280

Karatzas, K.D., Riga, M., Smith, M., 2013. Presentation and dissemination of pollen information, in: Allergenic Pollen: A Review of the Production, Release, Distribution and Health Impacts. Springer Netherlands, pp. 217–247. https://doi.org/10.1007/978-94-007-4881-1_7

Kawashima, S., Takahashi, Y., 1999. An improved simulation of mesoscale dispersion of airborne cedar pollen using a flowering-time map. Grana 38, 316–324. https://doi.org/10.1080/001731300750044555

Kawashima, S., Takahashi, Y., 1995. Modelling and simulation of mesoscale dispersion processes for airborne cedar pollen. Grana 34, 142–150. https://doi.org/10.1080/00173139509430003

Klein, E.K., Lavigne, C., Foueillassar, X., Gouyon, P.-H., Larédo, C., 2003. Corn pollen dispersal: quasi-mechanicistic models and field experiments. Ecol. Monogr. 73, 131–150.

Kmenta, M., Bastl, K., Jäger, S., Berger, U., 2014. Development of personal pollen information-the next generation of pollen information and a step forward for hay fever sufferers. Int. J. Biometeorol. 58, 1721–1726. https://doi.org/10.1007/s00484-013-0776-2

Kmenta, M., Zetter, R., Berger, U., Bastl, K., 2016. Pollen information consumption as an indicator of pollen allergy burden. Wien. Klin. Wochenschr. 128, 59–67. https://doi.org/10.1007/s00508-015-0855-y

Kuparinen, A., 2006. Mechanistic models for wind dispersal. Trends Plant Sci. 11, 296–301. https://doi.org/10.1016/j.tplants.2006.04.006

Levetin, E., 2004. Methods for Aeroallergen Sampling. Curr. Allergy Asthma Rep. 4, 376–383.

Levetin, E., Van de Water, P.K., 2003. Pollen count forecasting. Immunol. Allergy Clin. North Am. 23, 423–442. https://doi.org/10.1016/S0889-8561(03)00019-5

Lops, Y., Choi, Y., Eslami, E., Sayeed, A., 2020. Real-time 7-day forecast of pollen counts using a deep convolutional neural network. Neural Comput. Appl. 32, 11827–11836. https://doi.org/10.1007/s00521-019-04665-0

Maes, W.H., Steppe, K., 2019. Perspectives for Remote Sensing with Unmanned Aerial Vehicles in Precision Agriculture. Trends Plant Sci. 24, 152–164. https://doi.org/10.1016/j.tplants.2018.11.007

Masoli, M., Fabian, D., Holt, S., Beasley, R., 2004. The global burden of asthma: Executive summary of the GINA Dissemination Committee Report. Allergy Eur. J. Allergy Clin. Immunol. 59, 469–478. https://doi.org/10.1111/j.1398-9995.2004.00526.x

Mateo Pla, M.A., Lemus-Zúñiga, L.G., Montañana, J.M., Pons, J., Garza, A.A., 2016. A review of mobile apps for improving quality of life of asthmatic and people with allergies. Smart Innov. Syst. Technol. 45, 51–64. https://doi.org/10.1007/978-3-319-23024-5_5

Matricardi, P.M., Dramburg, S., Alvarez-Perea, A., Antolín-Amérigo, D., Apfelbacher, C., Atanaskovic-Markovic, M., Berger, U., Blaiss, M.S., Blank, S., Boni, E., Bonini, M., Bousquet, J., Brockow, K., Buters, J., Cardona, V., Caubet, J., Cavkaytar, Ö., Elliott, T., Esteban-Gorgojo, I., Fonseca, J.A., Gardner, J., Gevaert, P., Ghiordanescu, I., Hellings, P., Hoffmann-Sommergruber, K., Fusun Kalpaklioglu, A., Marmouz, F., Meijide Calderón, Á., Mösges, R., Nakonechna, A., Ollert, M., Oteros, J., Pajno, G., Panaitescu, C., Perez-Formigo, D., Pfaar, O., Pitsios, C., Rudenko, M., Ryan, D., Sánchez-García, S., Shih, J., Tripodi, S., Van der Poel, L., Os-Medendorp, H., Varricchi, G., Wittmann, J., Worm, M., Agache, I., 2020a. The role of mobile health technologies in allergy care: An EAACI position paper. Allergy 75, 259–272. https://doi.org/10.1111/all.13953

Matricardi, P.M., Potapova, E., Forchert, L., Dramburg, S., Tripodi, S., 2020b. Digital allergology: Towards a clinical decision support system for allergen immunotherapy. Pediatr. Allergy Immunol. 31, 61–64. https://doi.org/10.1111/pai.13165

Maya-Manzano, J.M., Smith, M., Markey, E., Hourihane Clancy, J., Sodeau, J., O´Connor, D.J., 2021. Recent developments in monitoring and modelling airborne pollen, a review. Grana 60, 1–19. https://doi.org/10.1080/00173134.2020.1769176

Medek, D.E., Simunovic, M., Erbas, B., Katelaris, C.H., Lampugnani, E.R., Huete, A., Beggs, P.J., Davies, J.M., 2019. Enabling self-management of pollen allergies: a pre-season questionnaire evaluating the perceived benefit of providing local pollen information. Aerobiologia (Bologna). 35, 777–782. https://doi.org/10.1007/s10453-019-09602-1

Migliavacca, M., Sonnentag, O., Keenan, T.F., Cescatti, A., O'Keefe, J., Richardson, A.D., 2012. On the uncertainty of phenological responses to climate change, and implications for a terrestrial biosphere model. Biogeosciences 9, 2063–2083. https://doi.org/10.5194/bg-9-2063-2012

Monfort, J., Haas, P., Harrison, K., Roe, D., Wates, J., Wiener, J., 2002. The Right to Know: Environmental Information Disclosure by Government and Industry, in: Zaelke, D., Kaniaru, D., Kruziková, E. (Eds.), Making Law Work: Environmental Compliance and Sustainable Development, Vol. 2. Cameron May Ltd, pp. 17–48. https://doi.org/10.1007/s10098-006-0033-z

Mothes, N., Horak, F., Valenta, R., 2004. Transition from a botanical to a molecular classification in tree pollen allergy: Implications for diagnosis and therapy. Int. Arch. Allergy Immunol. 135, 357–373. https://doi.org/10.1159/000082332

Müller-Germann, I., D.A., P., H., P., Alberternst, B., Pöschl, U., Fröhlich-Nowoisky, J., Després, V.R., 2017. Allergenic Asteraceae in air particulate matter : quantitative DNA analysis of mugwort and ragweed. Aerobiologia (Bologna). 33, 493–506. https://doi.org/10.1007/s10453-017-9485-3

Müller-Germann, I., Vogel, B., Vogel, H., Pauling, A., Fröhlich-Nowoisky, J., Pöschl, U., Després, V.R., 2015. Quantitative DNA Analyses for Airborne Birch Pollen. PLoS One 10, 1–17. https://doi.org/10.1371/journal.pone.0140949

Nathan, R., Katul, G.G., 2005. Foliage shedding in deciduous forests lifts up long-distance seed dispersal by wind. Proc. Natl. Acad. Sci. U. S. A. 102, 8251–8256. https://doi.org/10.1073/pnas.0503048102

Navares, R., Aznarte, J.L., 2019. Geographical imputation of missing poaceae pollen data via convolutional neural networks. Atmosphere (Basel). 10, 1–10. https://doi.org/10.3390/atmos10110717

Nguyen, K.C., Noonan, J.A., Galbally, I.E., Physick, W.L., 1997. Predictions of plume dispersion in complex terrain: Eulerian versus Lagrangian models. Atmos. Environ. 31, 947–958. https://doi.org/10.1016/S1352-2310(96)00292-0

Niederberger, V., Neubauer, A., Gevaert, P., Zidarn, M., Worm, M., Aberer, W., Malling, H.J., Pfaar, O., Klimek, L., Pfützner, W., Ring, J., Darsow, U., Novak, N., Gerth van Wijk, R., Eckl-Dorna, J., Focke-Tejkl, M., Weber, M., Müller, H.H., Klinger, J., Stolz, F., Breit, N., Henning, R., Valenta, R., 2018. Safety and efficacy of immunotherapy with the recombinant B-cell epitope–based grass pollen vaccine BM32. J. Allergy Clin. Immunol. 142, 497-509.e9. https://doi.org/10.1016/j.jaci.2017.09.052

Norris-Hill, J., 1995. The modelling of daily Poaceae pollen concentrations The modelling of daily Poaceae pollen concentrations. Grana 34, 182–188. https://doi.org/10.1080/00173139509429041

Novakova, S.M., Staevska, M.T., Novakova, P.I., Yoncheva, M.D., Bratoycheva, M.S., Musurlieva, N.M., Tzekov, V.D., Nicolov, D.G., 2017. Quality of life improvement after a three-year course of sublingual immunotherapy in patients with house dust mite and grass pollen induced allergic rhinitis: Results from real-life. Health Qual. Life Outcomes 15, 1–6. https://doi.org/10.1186/s12955-017-0764-z

Oteros, J., Bergmann, K.C., Menzel, A., Damialis, A., Traidl-Hoffmann, C., Schmidt-Weber, C.B., Buters, J., 2019. Spatial interpolation of current airborne pollen concentrations where no monitoring exists. Atmos. Environ. 199, 435–442. https://doi.org/10.1016/j.atmosenv.2018.11.045

Pecero-Casimiro, R., Fernández-Rodríguez, S., Tormo-Molina, R., Monroy-Colín, A., Silva-Palacios, I., Cortés-Pérez, J.P., Gonzalo-Garijo, Á., Maya-Manzano, J.M., 2019. Urban aerobiological risk mapping of ornamental trees using a new index based on LiDAR and Kriging: A case study of plane trees. Sci. Total Environ. 693, 1–12. https://doi.org/10.1016/j.scitotenv.2019.07.382

Pecero-Casimiro, R., Fernández-Rodríguez, S., Tormo-Molina, R., Silva-Palacios, I., Gonzalo-Garijo, Á., Monroy-Colín, A., Coloma, J.F., Maya-Manzano, J.M., 2020. Producing urban aerobiological risk map for cupressaceae family in the SW iberian peninsula from LiDAR technology. Remote Sens. 12, 1–19. https://doi.org/10.3390/rs12101562

Peirce, C.S., 1884. The numerical measure of the success of predictions. Science (80-.). https://doi.org/10.1126/science.ns-4.93.453-a

Pfaar, O., Bachert, C., Kuna, P., Panzner, P., Džupinová, M., Klimek, L., van Nimwegen, M.J., Boot, J.D., Yu, D., Opstelten, D.J.E., de Kam, P.J., 2019. Sublingual allergen immunotherapy with a liquid birch pollen product in patients with seasonal allergic rhinoconjunctivitis with or without asthma. J. Allergy Clin. Immunol. 143, 970–977. https://doi.org/10.1016/j.jaci.2018.11.018

Pfaar, O., Bastl, K., Berger, U., Buters, J., Calderon, M.A., Clot, B., Darsow, U., Demoly, P., Durham, S.R., Galán, C., Gehrig, R., Gerth van Wijk, R., Jacobsen, L., Klimek, L., Sofiev, M., Thibaudon, M., Bergmann, K.C., 2017. Defining pollen exposure times for clinical trials of allergen immunotherapy for pollen-induced rhinoconjunctivitis – an EAACI position paper. Allergy Eur. J. Allergy Clin. Immunol. 72, 713–722. https://doi.org/10.1111/all.13092

Picornell, A., Oteros, J., Trigo, M.M., Gharbi, D., Docampo Fernández, S., Melgar Caballero, M., Toro, F.J., García-Sánchez, J., Ruiz-Mata, R., Cabezudo, B., Recio, M., 2019. Increasing resolution of airborne pollen forecasting at a discrete sampled area in the southwest Mediterranean Basin. Chemosphere 234, 668–681. https://doi.org/10.1016/j.chemosphere.2019.06.019

Ranta, H., Kubin, E., Siljamo, P., Sofiev, M., Linkosalo, T., Oksanen, A., Bondestam, K., 2006. Long distance pollen transport cause problems for determining the timing of birch pollen season in Fennoscandia by using phenological observations. Grana 45, 297–304. https://doi.org/10.1080/00173130600984740

Ranzi, A., Lauriola, P., Marletto, V., Zinoni, F., 2003. Forecasting airborne pollen concentrations : Development of local models. Aerobiologia (Bologna). 19, 39–45.

Reid, C.E., Gamble, J.L., 2009. Aeroallergens, allergic disease, and climate change: Impacts and adaptation. Ecohealth 6, 458–470. https://doi.org/10.1007/s10393-009-0261-x

Ritenberga, O., Sofiev, M., Kirillova, V., Kalnina, L., Genikhovich, E., 2016. Statistical modelling of non-stationary processes of atmospheric pollution from natural sources: Example of birch pollen. Agric. For. Meteorol. 226–227, 96–107. https://doi.org/10.1016/j.agrformet.2016.05.016

Roberts, G., Pfaar, O., Akdis, C.A., Ansotegui, I.J., Durham, S.R., Gerth van Wijk, R., Halken, S., Larenas-Linnemann, D., Pawankar, R., Pitsios, C., Sheikh, A., Worm, M., Arasi, S., Calderon, M.A., Cingi, C., Dhami, S., Fauquert, J.L., Hamelmann, E., Hellings, P., Jacobsen, L., Knol, E.F., Lin, S.Y., Maggina, P., Mösges, R., Oude Elberink, J.N.G., Pajno, G.B., Pastorello, E.A., Penagos, M., Rotiroti, G., Schmidt-Weber, C.B., Timmermans, F., Tsilochristou, O., Varga, E.M., Wilkinson, J.N., Williams, A., Zhang, L., Agache, I., Angier, E., Fernandez-Rivas, M., Jutel, M., Lau, S., van Ree, R., Ryan, D., Sturm, G.J., Muraro, A., 2018. EAACI Guidelines on Allergen Immunotherapy: Allergic rhinoconjunctivitis. Allergy Eur. J. Allergy Clin. Immunol. 73, 765–798. https://doi.org/10.1111/all.13317

Rocchini, D., Bacaro, G., Chirici, G., Da Re, D., Feilhauer, H., Foody, G.M., Galluzzi, M., Garzon-Lopez, C.X., Gillespie, T.W., He, K.S., Lenoir, J., Marcantonio, M., Nagendra, H., Ricotta, C., Rommel, E., Schmidtlein, S., Skidmore, A.K., Van De Kerchove, R., Wegmann, M., Rugani, B., 2018. Remotely sensed spatial heterogeneity as an exploratory tool for taxonomic and functional diversity study. Ecol. Indic. 85, 983–990. https://doi.org/10.1016/j.ecolind.2017.09.055

Rojo, J., Pérez-Badia, R., 2015. Spatiotemporal analysis of olive flowering using geostatistical techniques. Sci. Total Environ. 505, 860–869. https://doi.org/10.1016/j.scitotenv.2014.10.022

Santos, A.F., Borrego, L.M., Rotiroti, G., Scadding, G., Roberts, G., 2015. The need for patient-focused therapy for children and teenagers with allergic rhinitis:A case-based review of current European practice. Clin. Transl. Allergy 5, 1–6. https://doi.org/10.1186/s13601-014-0044-5

Scheifinger, H., Belmonte, J., Buters, J., Celenk, S., Damialis, A., Dechamp, C., García-Mozo, H., Gehrig, R., Grewling, L., Halley, J.M., Hogda, K.-A., Jäger, S., Karatzas, K., Karlsen, S.-R., Koch, E., Pauling, A., Peel, R., Sikoparija, B., Smith, M., Galán-Soldevilla, C., Thibaudon, M., Vokou, D., de Weger, L.A., 2013. Monitoring, Modelling and Forecasting of the Pollen Season, in: Sofiev, M., Bergmann, K.-C. (Eds.), Allergenic Pollen: A Review of the Production, Release, Distribution and Health Impacts. Springer Science+Business Media, Dordrech, pp. 71–126. https://doi.org/10.1007/978-94-007-4881-1

Schueler, S., Schlünzen, K.H., 2006. Modeling of oak pollen dispersal on the landscape level with a mesoscale atmospheric model. Environ. Model. Assess. 11, 179–194. https://doi.org/10.1007/s10666-006-9044-8

Shi, Y., Skidmore, A.K., Wang, T., Holzwarth, S., Heiden, U., Pinnel, N., Zhu, X., Heurich, M., 2018. Tree species classification using plant functional traits from LiDAR and hyperspectral data. Int. J. Appl. Earth Obs. Geoinf. 73, 207–219. https://doi.org/10.1016/j.jag.2018.06.018

Šikoparija, B., Marko, O., Panić, M., Jakovetić, D., Radišić, P., 2018. How to prepare a pollen calendar for forecasting daily pollen concentrations of Ambrosia, Betula and Poaceae? Aerobiologia (Bologna). 34, 203–217. https://doi.org/10.1007/s10453-018-9507-9

Siljamo, P., Sofiev, M., Filatova, E., Grewling, Ł., Jäger, S., Khoreva, E., Linkosalo, T., Ortega Jimenez, S., Ranta, H., Rantio-Lehtimäki, A., Svetlov, A., Veriankaite, L., Yakovleva, E., Kukkonen, J., 2013. A numerical model of birch pollen emission and dispersion in the atmosphere. Model evaluation and sensitivity analysis. Int. J. Biometeorol. 57, 125–136. https://doi.org/10.1007/s00484-012-0539-5

Silver, J.D., Spriggs, K., Haberle, S., Katelaris, C.H., Newbigin, E.J., Lampugnani, E.R., 2020. Crowd-sourced allergic rhinitis symptom data: The influence of environmental and demographic factors. Sci. Total Environ. 705, 135147. https://doi.org/10.1016/j.scitotenv.2019.135147

Simunovic, M., Dwarakanath, D., Addison-Smith, B., Susanto, N.H., Erbas, B., Baker, P., Davies, J.M., 2020. Grass pollen as a trigger of emergency department presentations and hospital admissions for respiratory conditions in the subtropics: A systematic review. Environ. Res. 182, 109125. https://doi.org/10.1016/j.envres.2020.109125

Siniscalco, C., Caramiello, R., Migliavacca, M., Busetto, L., Mercalli, L., Colombo, R., Richardson, A.D., 2015. Models to predict the start of the airborne pollen season. Int. J. Biometeorol. 59, 837–848. https://doi.org/10.1007/s00484-014-0901-x

Sirufo, M.M., Suppa, M., Ginaldi, L., De Martinis, M., 2020. Does allergy break bones? Osteoporosis and its connection to allergy. Int. J. Mol. Sci. 21, 1–15. https://doi.org/10.3390/ijms21030712

Skjøth, C.A., Smith, M., Sikoparija, B., Stach, A., Myszkowska, D., Kasprzyk, I., Radisic, P., Stjepanovic, B., Hrga, I., Apatini, D., Magyar, D., Páldy, A., Ianovici, N., 2010. A method for producing airborne pollen source inventories : An example of Ambrosia (ragweed) on the Pannonian Plain. Agric. For. Meteorol. J. 150, 1203–1210. https://doi.org/10.1016/j.agrformet.2010.05.002

Sofiev, M., 2019. On possibilities of assimilation of near-real-time pollen data by atmospheric composition models. Aerobiologia (Bologna). 35, 523–531. https://doi.org/10.1007/s10453-019-09583-1

Sofiev, M., Belmonte, J., Gehrig, R., Izquierdo, R., Smith, M., Dahl, Å., Siljamo, P., 2013. Airborne Pollen Transport, in: Sofiev, M., Bergmann, K.-C. (Eds.), Allergenic Pollen: A Review of the Production, Release, Distribution and Health Impacts. Springer Science+Business Media, Dordrech, pp. 127–159. https://doi.org/10.1007/978-94-007-4881-1

Sofiev, M., Berger, U., Prank, M., Vira, J., Arteta, J., Belmonte, J., Bergmann, K.C., Chéroux, F., Elbern, H., Friese, E., Galan, C., Gehrig, R., Khvorostyanov, D., Kranenburg, R., Kumar, U., Marécal, V., Meleux, F., Menut, L., Pessi, A.M., Robertson, L., Ritenberga, O., Rodinkova, V., Saarto, A., Segers, A., Severova, E., Sauliene, I., Siljamo, P., Steensen, B.M., Teinemaa, E., Thibaudon, M., Peuch, V.H., 2015a. MACC regional multi-model ensemble simulations of birch pollen dispersion in Europe. Atmos. Chem. Phys. 15, 8115–8130. https://doi.org/10.5194/acp-15-8115-2015

Sofiev, M., Palamarchuk, Y., Bédard, A., Basagana, X., Anto, J.M., Kouznetsov, R., Urzua, R.D., Bergmann, K.C., Fonseca, J.A., De Vries, G., Van Erd, M., Annesi-Maesano, I., Laune, D., Pépin, J.L., Jullian-Desayes, I., Zeng, S., Czarlewski, W., Bousquet, J., 2020. A demonstration project of Global Alliance against Chronic Respiratory Diseases: Prediction of interactions between air pollution and allergen exposure-the Mobile Airways Sentinel NetworK-Impact of air POLLution on Asthma and Rhinitis approach. Chin. Med. J. (Engl). 133, 1561–1567. https://doi.org/10.1097/CM9.0000000000000916

Sofiev, M., Ritenberga, O., Albertini, R., Arteta, J., Belmonte, J., Bernstein, C.G., Bonini, M., Celenk, S., Damialis, A., Douros, J., Elbern, H., Friese, E., Galan, C., Oliver, G., Hrga, I., Kouznetsov, R., Krajsek, K., Magyar, D., Parmentier, J., Plu, M., Prank, M., Robertson, L., Marie Steensen, B., Thibaudon, M., Segers, A., Stepanovich, B., Valdebenito, A.M., Vira, J., Vokou, D., 2017. Multi-model ensemble simulations of olive pollen distribution in Europe in 2014: Current status and outlook. Atmos. Chem. Phys. 17, 12341–12360. https://doi.org/10.5194/acp-17-12341-2017

Sofiev, M., Siljamo, P., Ranta, H., Rantio-Lehtimäki, A., 2006. Towards numerical forecasting of long-range air transport of birch pollen: Theoretical considerations and a feasibility study. Int. J. Biometeorol. 50, 392–402. https://doi.org/10.1007/s00484-006-0027-x

Sofiev, M., Vira, J., Kouznetsov, R., Prank, M., Soares, J., Genikhovich, E., 2015b. Construction of the SILAM Eulerian atmospheric dispersion model based on the advection algorithm of Michael Galperin. Geosci. Model Dev. 8, 3497–3522. https://doi.org/10.5194/gmd-8-3497-2015

Theuerkauf, M., Couwenberg, J., Kuparinen, A., Liebscher, V., 2016. A matter of dispersal : REVEALSinR introduces state-of-the-art dispersal models to quantitative vegetation reconstruction. Veg. Hist. Archaeobot. 25, 541–553. https://doi.org/10.1007/s00334-016-0572-0

Tomaselli, V., Adamo, M., Veronico, G., Sciandrello, S., Tarantino, C., Dimopoulos, P., Medagli, P., Nagendra, H., Blonda, P., 2017. Definition and application of expert knowledge on vegetation pattern, phenology, and seasonality for habitat mapping, as exemplified in a Mediterranean coastal site. Plant Biosyst. 151, 887–899. https://doi.org/10.1080/11263504.2016.1231143

Tseng, Y.T., Kawashima, S., Kobayashi, S., Takeuchi, S., Nakamura, K., 2020. Forecasting the seasonal pollen index by using a hidden Markov model combining meteorological and biological factors. Sci. Total Environ. 698, 134246. https://doi.org/10.1016/j.scitotenv.2019.134246

Valencia-Barrera, R.M., Comtois, P., Fernández-gonzález, D., 2002. Bioclimatic indices as a tool in pollen forecasting. Int. J. Biometeorol. 46, 171–175. https://doi.org/10.1007/s00484-002-0138-y

Valencia-Barrera, R.M., Comtois, P., Fernández-González, D., 2001. Biogeography and bioclimatology in pollen forecasting - An example of grass in Leon (Spain) and Montreal (Canada). Grana 40, 223–229. https://doi.org/10.1080/001731301317223259

Veriankaitė, L., Siljamo, P., Sofiev, M., Šaulienė, I., Kukkonen, J., 2010. Modelling analysis of source regions of long-range transported birch pollen that influences allergenic seasons in Lithuania. Aerobiologia (Bologna). 26, 47–62. https://doi.org/10.1007/s10453-009-9142-6

Voukantsis, D., Karatzas, K., Jaeger, S., Berger, U., Smith, M., 2013. Analysis and forecasting of airborne pollen-induced symptoms with the aid of computational intelligence methods. Aerobiologia (Bologna). 29, 175–185. https://doi.org/10.1007/s10453-012-9271-1

Wakamiya, S., Matsune, S., Okubo, K., Aramaki, E., 2019. Causal relationships among pollen counts, tweet numbers, and patient numbers for seasonal allergic rhinitis surveillance: Retrospective analysis. J. Med. Internet Res. 21, 1–12. https://doi.org/10.2196/10450

WHO, 2018. mHealth, use of appropriate digital technologies for public health., Seventy-first World Health Assembly - Provisional agenda item 12.4 (A71/20).

Young, D.L., Wang, Y.F., Eldho, T.I., 2000. Solution of the advection-diffusion equation using the Eulerian-Lagrangian boundary element method. Eng. Anal. Bound. Elem. 24, 449–457. https://doi.org/10.1016/S0955-7997(00)00026-6

Zewdie, G.K., Lary, D.J., Levetin, E., Garuma, G.F., 2019. Applying deep neural networks and ensemble machine learning methods to forecast airborne ambrosia pollen. Int. J. Environ. Res. Public Health 16, 1–14. https://doi.org/10.3390/ijerph16111992

Zhang, L., Han, D.M., 2008. [An introduction of allergic rhinitis and its impact on asthma (ARIA) 2008 update]. Zhonghua Er Bi Yan Hou Tou Jing Wai Ke Za Zhi 43, 552–557.

Zhang, R., Duhl, T., Salam, M.T., House, J.M., Flagan, R.C., Avol, E.L., Gilliland, F.D., Guenther, A., Chung, S.H., Lamb, B.K., VanReken, T.M., 2014. Development of a regional-scale pollen emission and transport modeling framework for investigating the impact of climate change on allergic airway disease. Biogeosciences 11, 1461–1478. https://doi.org/10.5194/bg-11-1461-2014

Zhang, Z., Chen, Q., 2007. Comparison of the Eulerian and Lagrangian methods for predicting particle transport in enclosed spaces. Atmos. Environ. 41, 5236–5248. https://doi.org/10.1016/j.atmosenv.2006.05.086

Ziello, C., Sparks, T.H., Estrella, N., Belmonte, J., Bergmann, K.C., Bucher, E., Brighetti, M.A., Damialis, A., Detandt, M., Galán, C., Gehrig, R., Grewling, L., Gutiérrez Bustillo, A.M., Hallsdóttir, M., Kockhans-Bieda, M.-C., De Linares, C., Myszkowska, D., Pàldy, A., Sánchez, A., Smith, M., Thibaudon, M., Travaglini, A., Uruska, A., Valencia-Barrera, R.M., Vokou, D., Wachter, R., de Weger, L.A., Menzel, A., 2012. Changes to Airborne Pollen Counts across Europe. PLoS One 7, e34076. https://doi.org/10.1371/journal.pone.0034076

Zink, K., Pauling, A., Rotach, M.W., Vogel, H., Kaufmann, P., Clot, B., 2013. EMPOL 1.0: A new parameterization of pollen emission in numerical weather prediction models. Geosci. Model Dev. 6, 1961–1975. https://doi.org/10.5194/gmd-6-1961-2013

Zink, K., Vogel, H., Vogel, B., Magyar, D., Kottmeier, C., 2012. Modeling the dispersion of Ambrosia artemisiifolia L . pollen with the model system COSMO-ART. Int. J. Biometeorol. 56, 669–680. https://doi.org/10.1007/s00484-011-0468-8

Zuberbier, T., Lötvall, J., Simoens, S., Subramanian, S. V., Church, M.K., 2014. Economic burden of inadequate management of allergic diseases in the European Union: A GA2LEN review. Allergy Eur. J. Allergy Clin. Immunol. 69, 1275–1279. https://doi.org/10.1111/all.12470

5. Allergenic risk assessment of urban parks: towards a standard index

Abstract

Allergenicity indices are a powerful tool to assess the health hazard posed by urban parks to pollen allergic subjects. Nonetheless, only few indices have been developed and applied to urban vegetation in the last decade, and they were never compared nor standardised over the same dataset. To address this issue, in this paper the two best-known allergenicity indices, the Urban Green Zones Allergenicity Index (I_{UGZA}) and the Specific Allergenicity Index (SAI), have been calculated for the same park (the Botanical Garden of Bologna), collecting vegetation data through both systematic sampling and arboreal census. The results obtained with the two data collection methods were comparable for both indices, indicating systematic sampling as a reliable approximation of the total census. Besides, the allergenic risk resulted moderate to high according to SAI, and very low according to I_{UGZA}. Since SAI does not consider the total volume of the vegetation, it was deemed less reliable than I_{UGZA} in evaluating the allergenicity of an enclosed green space.

Keywords: I_{UGZA}, SAI, allergenicity, urban park, ecological index, pollen allergy.

Abbreviations: SAI, Specific Allergenicity Index; I_{UGZA} **,** Urban Green Zones Allergenicity Index; AIROT **,** Aerobiological Index of Risk for Ornamental Trees; NP **,** nano-phanerophytes; P scap **,** scapose phanerophytes; P caesp **,** cespitose phanerophytes; H-Index **,** Shannon-Wiener diversity index; ARPAE **,** Regional Agency for Prevention and Environment of Emilia-Romagna; WAO **,** World Allergy Organisation.

1.   Introduction

Pollen is a major source of airborne allergens. It causes seasonal allergic rhinitis (pollinosis) in a significant share of the human population, and it can occasionally trigger allergic asthma. According to the latest broad epidemiological studies, the prevalence of pollen allergy in

Europe is up to 40% (D'Amato et al., 2007), and it seems to be raising over time. The progressive worsening of pollen allergy burden is partly a consequence of modern environmental problems such as air pollution and climate change, that can impact morbidity, mortality, incidence, and prevalence of the disease (D'Amato et al., 2016). In fact, air pollutants have been proven to exacerbate rhinitis symptoms by direct interaction with pollen allergens and the respiratory mucosa. Particulate matter also appears to affect human exposure to pollen allergens, possibly acting as carrier and keeping them airborne even outside the pollen season (Aloisi et al., 2018; Cecchi, 2013; D'Amato, 2001). On the other hand, air pollution also contributes to climate change. Higher mean temperatures, heat waves and heavy rainfalls associated to climate change tend to alter spatial and temporal distribution of airborne pollen, potentially anticipating the pollen season and extending its duration (D'Amato et al., 2016). Moreover, all these abiotic stressors can also modify the pollen potency, by enhancing the expression of allergenic proteins (Cecchi, 2013; Fernández-González et al., 2010, 2011).

All these dynamics play an important role in the urban environment, where air pollution and climate change effects are heavier than in less anthropogenic environments. The health of pollinosis sufferers in urban centres is also threatened by gardening choices enhancing the potential allergenicity of green spaces, such as the plant species selection, association, and maintenance (Capotorti et al., 2020; Cariñanos and Casares-Porcel, 2011). This picture is worsened by the increased likelihood for city inhabitants to develop pollen allergies than people living in the countryside (Patel et al., 2018).

While the ecosystem disservice provided by allergenic ornamental species has been taken into account in the UE environmental policies (Science for Environment Policy, 2012) and in some European national regulations, guidelines for hypoallergenic trees selection can only be applied to future green infrastructures. In fact, the substitution of existing allergenic trees in parks and streets would not be convenient from an economic and ecological point of view (Cariñanos and Casares-Porcel, 2011). Hence, it is important to assess the allergenicity of existing urban vegetation in order to plan an appropriate maintenance, and to alert the allergic subjects of the risk it poses (Suanno et al., 2021). For this purpose, to our knowledge three allergenicity indices have been proposed in the last decade: the Specific Allergenicity Index (SAI) (Hruska, 2003), the Urban Green Zones Allergenicity Index (I_{UGZA}) (Cariñanos et al., 2014) and the Aerobiological Index of Risk for Ornamental Trees (AIROT) (Pecero-Casimiro et

al., 2019). AIROT calculates the allergenicity potential of a single plant species over large a study area, combining LiDAR remote sensing and Kriging interpolation. Its estimation involves biological features of the species and aspects of the surrounding environment that may influence pollen dispersal. SAI and I_{UGZA} instead are applied to smaller patches of urban vegetation, but they include all the allergenic species present in the area, providing a complete picture of the allergic risk. These two indices take into account different biological and biometric parameters of the vegetation that are related to pollen production, dispersal an allergenicity. While SAI has been employed only few times and mainly on anthropogenic, spontaneous vegetation, I_{UGZA} had a considerable success after its publication and it has been applied to many urban parks in several European cities (Cariñanos et al., 2016, 2019; Kasprzyk et al., 2019). However, the rapid spread of this index was not preceded by a method standardisation, especially for the sampling design, making it difficult to compare results obtained from incomparable datasets. In this work, the two indices SAI and I_{UGZA} were calculated for the same urban park (Botanical Garden of Bologna, Italy) using different sampling methods and inclusion criteria. One aim of this study is to evaluate the consistency between the two indices, and, in case they results are in disagreement, to indicate which one is more adequate to describe the allergenicity of a circumscribed green area. This kind of comparison, to our knowledge, has never been performed, and it would be of great importance to help in the choice of the appropriate metrics to apply to the urban vegetation. The other aim of the present work is to test the comparability between different data collection approaches, in order to corroborate the results from previous studies applying the indices, and to suggest a standard sampling method that is both time efficient and reliable. Thus, this study will provide an example of sampling design choice and validation for allergenicity indices, to give them a greater ecological value, and to ensure their reproducibility and the comparability between different datasets.

2. Materials and methods

2.1 Study area

This research was conducted in the metropolitan city of Bologna (44°29'N 11°20'E), capital of the Emilia-Romagna region, Italy. Bologna is situated at the foot of the Tuscan-Emilian Apennine, and it extends for 140.7 km² along the southern edge of the Po plain, where Reno and Savena valleys merge. This location entails a humid temperate climate, with the average

annual minimum temperature of 10°C and maximum temperature of 19°C, and mean annual rainfalls of 768.7 mm (data from the Regional Agency for Prevention and Environment of Emilia-Romagna (ARPAE, 2019), measured over the period 1991–2015).

Bologna is densely populated, hosting 384202 inhabitants. Since municipal vegetation covers around 9% of the city surface, there are 29 m^2 of public greenery per person. Public parks are mainly distributed in the more densely inhabited areas, but they are scarce in the city centre (data from the National Statistic Institution of Italy, ISTAT, relative to the year 2016 (ISTAT, 2016)).

The urban green area chosen for this study is the Botanical Garden of Bologna (44°30'00''N 11°21'14''E). This park belongs to the museum system of the University of Bologna (SMA), and it is one of the oldest Botanical Gardens in Italy, founded in 1568 and then moved into its current location in 1803 (Fig. 1). The park extends for 1.8 ha, and it gathers a great diversity of both native and exotic plant species.

Since it is one of the few public parks located in the city centre, and a tourist attraction with free access, it is frequently visited by city dwellers and foreigners, with 55338 visitors counted during the year 2019. It is therefore important to assess its allergenicity risk. Moreover, this park offers a good model for method standardisation, being relatively small and allowing to correctly identify plant species and to keep track of their maintenance. These aspects allowed to carry on a detailed and complete census of the arboreal species, that would not have been possible in wider areas with unknown and unmaintained vegetation. While the presence of exotic and uncommon plant species implies that the Botanical Garden is not representative of common urban parks, the plant collection is mainly composed by native species, indigenous of the region, and some zones of the Botanical Garden even recreate the local natural habitats. In fact, the vegetation is organised in different habitats and exhibitions: a wooded garden at the entrance, with the prevalence of evergreen species; a wooded hill frequently pruned and managed, with the prevalence of indigenous herbs, trees and shrubs; two small orchards with edible and medical species, surrounded by spontaneous weeds and grasses; vast areas with a frequently mowed lawn and individual trees spaced apart; patches with unmaintained weeds and grasses, for conservation and experimental purposes; the recreation of a local riparian forest, with the prevalence of old silver poplars (*Populus alba* L.); a system of small lakes with freshwater plants and algae; an exhibition of rocky vegetation; and the recreation of a local continental forest, with low levels of maintenance and

characterised by the presence of indigenous species of the region. Greenhouses and temporary exhibitions are also present, but they were not considered in this study.
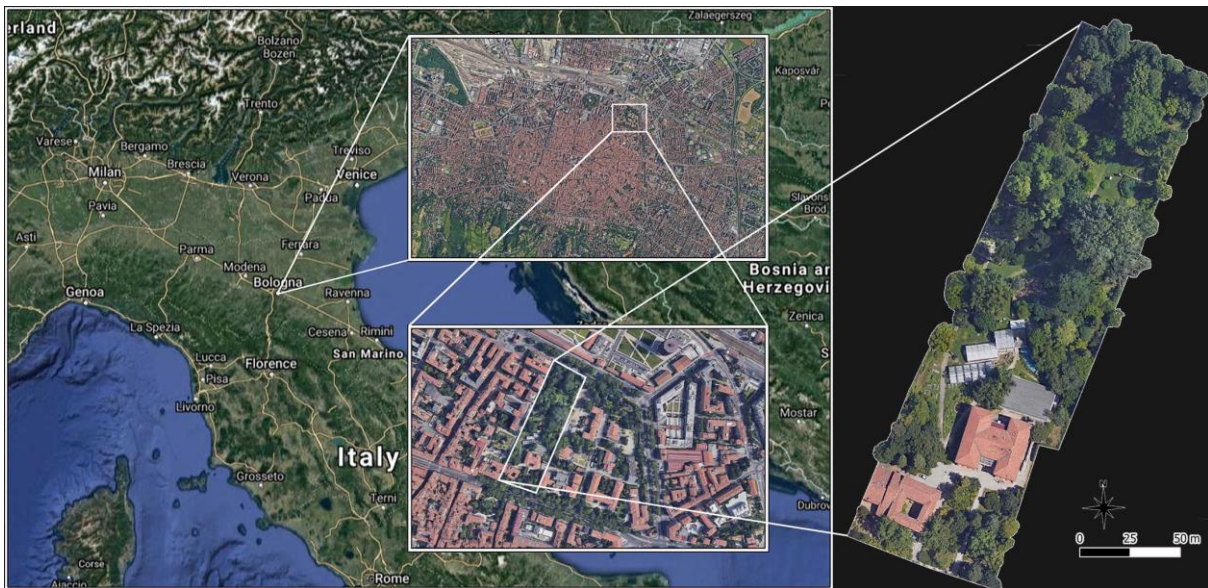
Figure 1: "Botanical Garden of Bologna" – Map of the Botanical Garden of Bologna and its geographic context, created using satellite images in QGIS and Adobe Photoshop.

2.2   Data collection

Vegetation data were collected in 2019 and 2020, form spring to summer. The vegetation considered in this study included not only the ornamental species displayed in the Garden, but also the spontaneous flora present therein, in form of grass, weeds, or shrubs. In fact, for educational and scientific purposes, some areas of the Botanical Garden are subject to low levels of maintenance, allowing spontaneous grass and weed to grow and bloom, and local trees to reproduce from seeds.

In 2019 the vegetation was sampled by systematic sampling, considered by the authors the fittest objective method to apply because of the highly heterogeneous structure of the park vegetation. The whole surface of the park was divided with a 30x30 m grid in Quantum Geographic Information System (QGIS) (QGIS Association, 2021), selecting the centre of each square as centre of the 10x10 m plots (Fig. S1). Plots falling outside the park perimeter or over the buildings were excluded from the sampling. Eventually, the vegetation was sampled in 18 plots representing 10% of the whole garden surface. For each plot, all the spermatophytes were identified using the Botanical Garden inventory and monographic flora, and they were

measured. Data on herbaceous and arboreal vegetation were collected separately, as shown in Table 1.

In 2020 a census of the "arboreal species" (trees and shrubs) present in the Botanical Garden was carried out. To attain an objective definition of arboreal species, only the plant species included in the Raunkiær classifications of nano-phanerophytes (NP), scapose phanerophytes (P scap) and cespitose phanerophytes (P caesp) (Raunkiaer, 1934) were considered. Woody climbers (P lian) were excluded from the census, due to difficulties in defining their shape and height. Since no woody climber produces a pollen considered allergenic in Emilia Romagna, their exclusion avoided overestimations of the crown volume without compromising the allergenic indices results. For all the arboreal species, only individuals taller than 1 m were censed, in order to simplify the task and to exclude spontaneous young seedlings that would have been removed during the ordinary maintenance of the park. All the specimens that met these requirements were identified up to the species level, using the Botanical Garden plant inventory and monographic flora, and measured as indicated in Table 1.

Table 1 *Scheme for data collection in the field to calculate SAI and I_{UGZA}*

PARAMETERS COLLECTED IN THE FIELD		
	Parameter	**Calculation**
Herbaceous species	Maximum height	Average height of the taller plants for each species.
	Relative abundance	Measured as percent surface cover.
Arboreal species	Crown volume	Estimated approximating the crown shape to the geometrical figure of parallelepipedon, sphere, cone, and cylinder (Cariñanos et al., 2014; Kasprzyk et al., 2019).
	Crown base	Calculated as the crown projection on the ground, measuring its diameters or sides with a metric tape.

Crown height	Measured by clinometer or telemeter. Height was always considered the highest point of the crown, even when it did not fall inside the survey area.
Sex	Female, male, dioecious/hermaphrodite. Evaluated by analysing the flowers.
Fertility	Presence/absence of flowers and fruits throughout the year.

Additional information on maintenance and vegetation structure was also collected, but it was not used for indices calculation.

The other parameters required by allergenicity indices were drawn from literature, as indicated by their authors (Cariñanos et al., 2014; Hruska, 2003), and are reported in Table 2.

Table 2 *Scheme of parameters drawn from literature to calculate SAI and I_{UGZA}*

PARAMETERS DRAWN FROM LITERATURE	
Parameter	**Sources**
Allergenicity	ARPAE list of allergenic species in the region (ARPAE, 2020a), WAO list of allergenic plants in Italy (WAO, 2012), systematic reviews on allergenic species in Italy (Ortolani et al., 2015), allergen databases (Allergome Team and Collaborators, 2021), books (Oh, 2018).
Cross-allergenicity	Published literature on cross-reactivity among pollen allergens (Cancelliere et al., 2020; Gadermaier et al., 2014; Gangl et al., 2015; Gastaminza et al., 2009; Lombardero et al., 2002; López-Matas et al., 2016; Moraes et al., 2018; Mothes et al., 2004; Panzani et al., 1986; Schwietz et al., 2000; Weber, 2003).
Pollination strategy	Published literature on individual species pollination, when it was not apparent from the flower structure (Anderson, 1976; Meeuse, 1984; Ortolani et al., 2015).

Duration of pollination period / phenanthesic period	ARPAE pollen calendar for Bologna (ARPAE, 2020b), monographic flora (Conti et al., 2005; Pignatti, 2017).
Life cycle	Monographic flora (Conti et al., 2005; Pignatti, 2017).

2.3   Data analysis

Species richness, Shannon-Wiener diversity index (H-Index) (Shannon, 1948), and Pielou's evenness (Pielou, 1966) were calculated for both data collections. For the systematic sampling, analyses were carried out separately on either all the spermatophytes, or "arboreal species" (NP, P scap, P caesp) only.

Individual plants were included in the allergenicity indices calculations if they were fertile (flowers/fruits present), pollen-producing (males, hermaphrodites, or monoecious), and belonging to an allergenic species. Species were considered allergenic if they met one of the following criteria: (I) listed as allergenic in Emilia Romagna by the ARPAE website www.arpae.it (ARPAE, 2020a); (II) listed as allergenic in Italy by the World Allergy Organisation (WAO) website www.worldallergy.org (WAO, 2012); (III) listed as allergenic in Italy by systematic reviews on the matter (Ortolani et al., 2015); (IV) not reported as allergenic in Italy, but showing cross-reactivity with pollen allergens that are clinically relevant in Italy (Tab. 2). The workflow followed to evaluate the allergenicity of each plant species is illustrated in Figure S2. When the taxonomic determination was not achievable to the species or genus level, the individual was considered allergenic if its genus or family included species that are allergenic in Emilia Romagna.

Hence, allergenicity indices were calculated for both data sets using Formulae (1) (Hruska, 2003) and (2) (Cariñanos et al., 2014).

$$(1) \quad SAI = \frac{\sum_{i=1}^{n} lc_i + pp_i + cr_i + a_i}{N}$$

In (1): **i**= i-species, **N**= total number of allergenic species, **lc**= life cycle, **pp**= phenanthesic period, **cr**= cross reactivity, **a**= abundance. Parameters calculation is explained in Table 3.

Table 3 *Estimation of SAI parameters according to Hruska (Hruska, 2003). Abundance is expressed as percent surface cover.*

Life cycle (lc)	Phenanthesic period (pp)	Cross reactivity (cr)	Abundance (a)
Annual =1	Less than 1 month = 0.5	None = 0	<1% = 0.5
Biennial = 2	More than 1 month = 2	Present = 1	1-25% = 1
Perennial = 3			25-50% = 2
			50-75% = 3
			75-100% = 4

SAI ranges between 2 and 10. Values below 4 are associated with a low allergic risk, from 4 to 6 with a moderate risk, and above 6 with a high risk (Hruska, 2003). This index is calculated considering allergenic species only.

$$(2) \quad I_{UGZA} = \frac{1}{H_{max}*PAV_{max}*S_T} * \sum_{i=1}^{k} n_i * PAV_i * V_i$$

In (2): **H_max**=maximum height reached by vegetation; **PAV**= allergenicity potential value (Tab. 4); **S_T**= total surface of the green area; **i**= i-species; **n**=total number of individuals; **V**= average vegetation volume.

Table 4 Allergenicity Potential Value (PAV) parameters for IUGZA calculation, according to Cariñanos and collaborators (Cariñanos et al., 2014), with minor modifications.

Parameter	Definition	Arbitrary values
PAV (or VPA)	Allergenicity Potential Value of each species. PAV= tp*ap*dpp	PAV_max = 27
Tp	Type of pollination.	Sterile, cleistogamous or female = 0
		Entomophilous = 1
		Amphiphilic = 2
		Anemophilous = 3
Ap	Allergenicity potential of the plant species relative to the study area.	Nonallergenic = 0
		Low = 1
		Moderate = 2
		High = 3
Dpp	Duration of pollination period. Pollen grains belonging to the same pollen type are considered as a single pollination event.	1-3 weeks = 1
		4-6 weeks = 2
		>6 weeks = 3

I_UGZA ranges from 0 to 1, with values lower than 0.3 indicating a low allergic risk, from 0.3 to 0.5 a moderate risk, and a high risk above 0.5 (Cariñanos et al., 2014).

In this work, the maximum value assigned to Ap is 3, instead of attributing an exceptional value of Ap=4 to the main local allergens. In fact, to assume Ap=4 while keeping and PAV_max = 27 would imply that I_UGZA can theoretically exceed the value of 1. On the other hand, using

Ap=4 and assuming PAV$_{max}$ = 36 would significantly lower the final I$_{UGZA}$ result, because the number of main local allergens is usually very small. However, calculations using both of these combinations were carried on for comparison, and are reported in Table S3.

For both systematic sampling and census datasets, SAI and I$_{UGZA}$ were calculated on (I) all the allergenic species; (II) arboreal species only.

Since during the census only arboreal species were measured, some approximations were made to extend data of herbaceous species from the sampling to the whole park surface, in order to obtain a complete, albeit rough picture of the park allergenicity. This was realised by extending the percent surface cover of herbaceous species from the total sampled surface of the plots, to the entire vegetated area of the park, as explained by Kasprzyk and collaborators (Kasprzyk et al., 2019). The vegetated area in this case was estimated in QGIS by subtracting the surface occupied by buildings, paths, and the lake, from the total park area. This approach however implies an extreme simplification of the herbaceous vegetation diversity and distribution. In particular, it assumes plants to be evenly distributed along the Garden surface, ignoring that spontaneous plants tend to be aggregated in plant communities. Nonetheless, this simplification appeared acceptable for the purposes of the present study, and it avoided the introduction of subjectivity in the sampling.

On the systematic sampling dataset, species richness, H-index and allergenicity indices were also calculated per plot, to test the linear regression between species richness and allergenic species, and between species diversity and allergenicity indices, using the "lm" function in RStudio (RStudio Team, 2020).

3. Results

During the systematic sampling of 2019, 328 different species were identified, belonging to 86 plant families. They showed high H-index and evenness, as expected for a Botanical Garden (Tab. 5). Of the species sampled, around 69% were herbaceous, 30% were arboreal, and the remaining 1% were woody climbers (Tab. 5, Fig. 2A). Among these species, only 46 were allergenic, equally divided between arboreal and herbaceous (Tab. 5, Fig. 2B), and 21 of them are considered major allergens in the region (Tab. S1, S2).
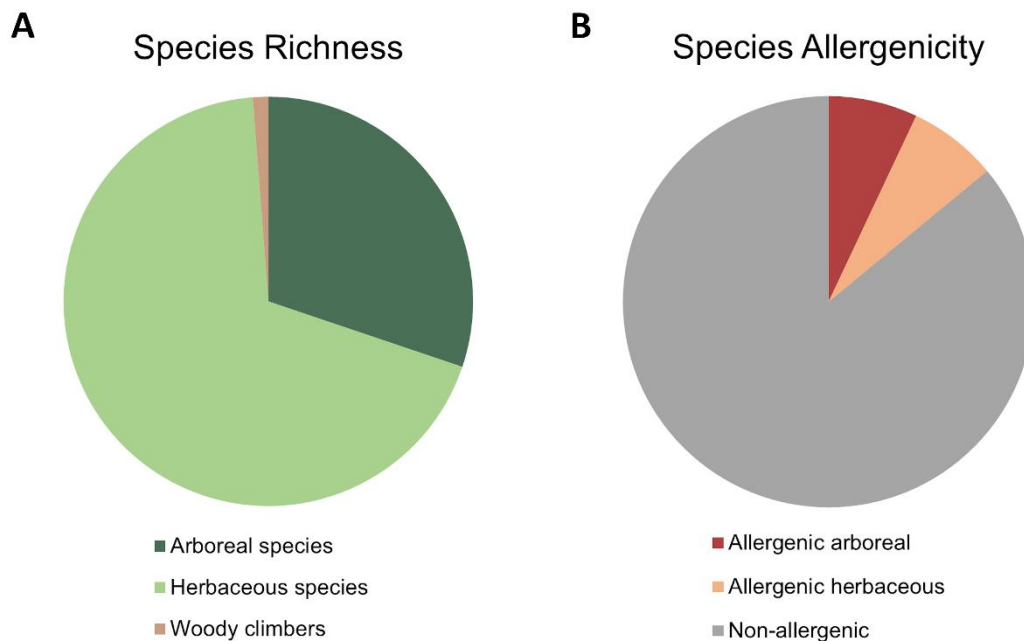
Figure 2: "Species richness" *- Distribution of the species richness among three groups of vegetation (A), and partition of allergenic and non-allergenic species (B) in the Botanical Garden of Bologna, according to the systematic sampling of 2019.*

The arboreal species census of 2020 also revealed a high level of diversity and evenness, comparable with the systematic sampling. This approach detected an arboreal species richness of 226, more than double the one recorded by systematic sampling, divided among 56 plant families. Only 19% of the species censed were classified as allergenic (Tab. 5, Fig. 3). Overall, both methods revealed a share of allergenic species lower than a quarter of the total richness. The complete list of allergenic species identified in the Botanical Garden is reported in Tables S1 and S2. The most abundant allergenic species in the park, in terms of percent surface cover, are rough meadow-grass (*Poa trivialis* L., 19.6%), perennial ryegrass (*Lolium perenne* L., 9.8%), upright pellitory (*Parietaria officinalis* L., 1.7%), annual meadow-grass (*Poa annua* L., 0.8%), and mouse barley (*Hordeum murinum* L., 0.5%) for the herbaceous species (Tab. S2); and silver poplar (*Populus alba* L., 10.9%), hazel (*Corylus avellana* L., 6%), paper mulberry (*Broussonetia papyrifera* (L.) L'Hér. ex Vent., 3.6%), box elder (*Acer negundo* L., 3.4%), and field maple (*Acer campestre* L., 3.3%) for the arboreal species (Tab. S1). Hazel and field maple have the habitus of small trees and shrubs, thus their high surface cover corresponds to a high number of individuals (56 and 48 respectively). On the contrary, the other arboreal species with high surface cover are represented by a small number of individuals. Allergenic arboreal species with an high number of individuals are instead broad-

leaf privet (*Ligustrum lucidum* W.T.Aiton, 173), common privet (*Ligustrum vulgare* L., 119), and field elm (*Ulmus minor* Mill., 30). However, it was not possible to assess whether the plants counted as different individuals could be ramets of a clonal colony, hence the percent surface cover was used as measure of abundance in all the calculations, instead of the number of individuals.

The areas of the Botanical Garden with a higher number of allergenic species, according to the systematic sampling, were a wooded hill (Fig. S1, plot 8), hosting 13 allergenic species in 100 m^2, both herbaceous and arboreal; the recreation of a local forest (Fig. S1, plot 16), with 12 herbaceous and arboreal allergenic species; and the orchard of edible and medicinal plants Fig. S1, plot 14), that harboured 11 allergenic herbaceous species, 8 of which were spontaneous grasses and weeds.

The linear regression calculated on the number of species per plot from the systematic sampling, suggests a significant positive correlation (p-value<0.05) between total species and allergenic species richness, and between non-allergenic and allergenic species richness. However, in both cases the dispersion was too high (adjusted R^2<0.4) to confirm the relationship (Fig. S3).

Allergenicity potential estimations were consistent between systematic sampling and census, for both I$_{UGZA}$ and SAI. Moreover, the results of the two indices did not change significantly when considering all the spermatophytes, or arboreal species only. Nonetheless, it is worth noting that I$_{UGZA}$ was slightly lower when considering only the arboreal species of the systematic sampling, while SAI was slightly higher for the arboreal species of both the systematic sampling and the census (Tab. 5, Fig. 4). However, the major difference between the two indices is the estimated risk level. In fact, while SAI pointed towards a moderate to high allergenic risk for the park, with values around 6, I$_{UGZA}$ values lower than 0.1 suggested a very low allergenicity potential, well under the threshold of 0.3 indicated by I$_{UGZA}$ authors as a trigger for allergic reactions (Tab. 5). Results of the alternative formulations of I$_{UGZA}$ with ap=4 for the main allergens can be found in Table S3 and agree with this allergenicity level. In fact, I$_{UGZA}$ resulted 0.01 units lower when using PAVmax=36, and 0.01 units higher when using PAVmax=36, for all the datasets.

When focusing on the most problematic allergenic species of the park, results are less clear. In fact, while systematic sampling and census led to the same allergenicity indices values, they notably differed in identifying the main plant species responsible for it. This discrepancy is

present in both indices (examples in Tab. 6, 7), but it is more pronounced in I_{UGZA}, where systematic sampling overestimated the importance of some allergenic species such as European hop-hornbeam (*Ostrya carpinifolia* Scop.*)* and field elm (*Ulmus minor* Mill.), that resulted less influent on the allergenicity when considering the whole arboreal vegetation. In fact, the census revealed that the most problematic species for the allergenicity of the Botanical Garden are silver poplar (*Populus alba* L.) and hazel (*Corylus avellana* L.). On the other hand, both data collection methods and allergenicity indices agreed in indicating the narrow-leafed ash (*Fraxinus angustifolia* Vahl), a major allergen of the region, as one of the main contributors to the park allergenicity. These differences are explained by the lower species richness detected by the systematic sampling, and the different relative abundances reported for the same species between the sampling and the census.

 H-index, I_{UGZA}, and SAI were also calculated for each plot from the systematic sampling dataset. A linear regression test was performed to further investigate the relationship between plant diversity and allergenicity (Fig. S4), obtaining no significant correlation between H-Index and the two allergenicity indices (p-value>0.1).
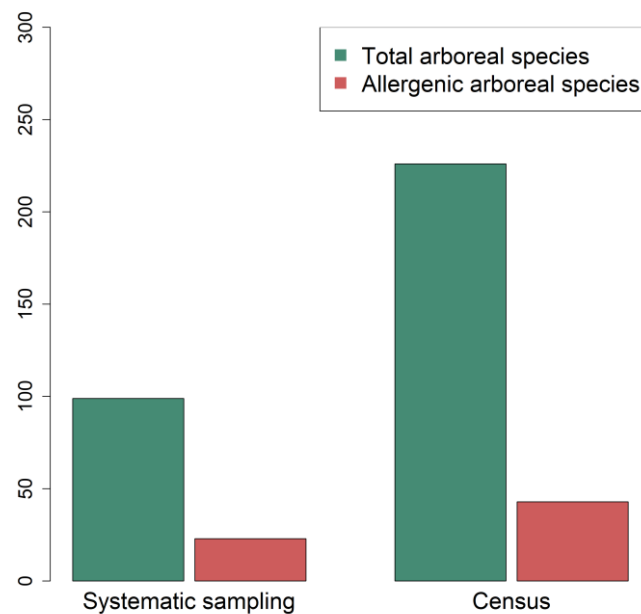
Figure 3: *"Allergenic species" - Comparison between total and allergenic arboreal species for the Botanical Garden of Bologna, according to the systematic sampling of 2019 and the census of 2020.*
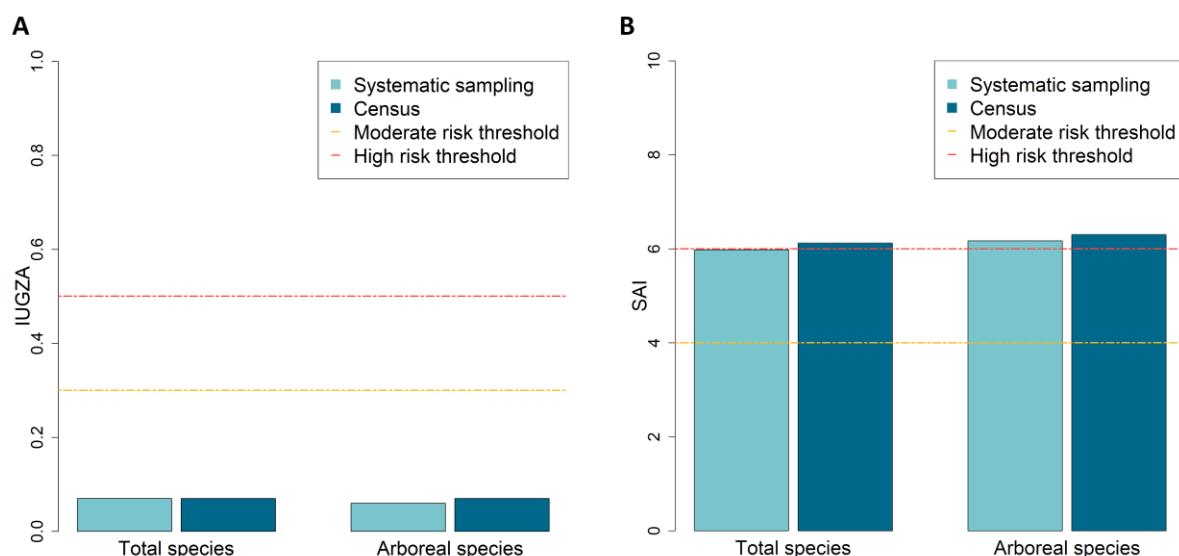
Figure 4: "Allergenicity indices" - *Comparison of IUGZA (A) and SAI (B) values for the Botanical Garden of Bologna, calculated on different datasets and vegetation groups. Light blue bars: data from systematic sampling of 2019; dark blue bars: data from arboreal census of 2020. Dotted lines indicate the risk thresholds: yellow for moderate and red for high risk.*

Table 5 *Species richness, species diversity, evenness, I_{UGZA}, and SAI values for the Botanical Garden of Bologna, according to the systematic sampling of 2019 and the arboreal species census of 2020.*

Parameter	Plant type	Systematic sampling	Census
Species richness	All spermatophytes	328	-
	Arboreal species	99	226
	Herbaceous species	225	-
	Woody climbers	4	-
Allergenic species richness	All spermatophytes	46	-
	Arboreal species	23	43
	Herbaceous species	23	-
Shannon-Wiener index (H-index)	All spermatophytes	4.21	-
	Arboreal species	3.65	4.45
Evenness	All spermatophytes	0.73	-
	Arboreal species	0.79	0.82
I_{UGZA}	All spermatophytes	0.07	0.07
	Arboreal species	0.06	0.07
SAI	All spermatophytes	5.98	6.12

	Arboreal species	6.17	6.30

Table 6 *List of the three main arboreal and herbaceous species contributing to I_{UGZA} for the Botanical Garden of Bologna with their percent cover on the total park surface (% cover). Species are ordered from higher to lower I_{UGZA} values. Allergenic levels for the Emilia Romagna region: * slightly allergenic; ** moderately allergenic; *** extremely allergenic.*

Importance	Family	Species	% cover
Arboreal species from census			
1	Salicaceae	*Populus alba* L. **	10.9
2	Betulaceae	*Corylus avellana* L. ***	6.0
3	Oleaceae	*Fraxinus angustifolia* Vahl ***	2.2
Arboreal species from systematic sampling			
1	Oleaceae	*Fraxinus angustifolia* Vahl ***	2.2
2	Betulaceae	*Ostrya carpinifolia* Scop. *	1.4
3	Ulmaceae	*Ulmus minor* Mill. *	2.0
Herbaceous species from systematic sampling			
1	Poaceae	*Poa trivialis* L. ***	19.6
2	Poaceae	*Lolium perenne* L. ***	9.8
3	Urticaceae	*Parietaria officinalis* L. ***	1.7

Table 7 *List of the plant species with the highest SAI value (SAI=7) for the Botanical Garden of Bologna, with their percent cover on the total park surface (% cover). Allergenic levels for the Emilia Romagna region: * slightly allergenic; ** moderately allergenic; *** extremely allergenic.*

Family	Species	% cover
Systematic sampling		
Betulaceae	*Corylus avellana* L. ***	6.0
Betulaceae	*Ostrya carpinifolia* Scop. *	1.4
Cupressaceae	*Cupressus sempervirens* L. ***	0.5
Oleaceae	*Fraxinus angustifolia* Vahl ***	2.2
Pinaceae	*Pinus nigra* J.F.Arnold *	0.7
Poaceae	*Poa trivialis* L. ***	19.6
Poaceae	*Lolium perenne* L. ***	9.8
Urticaceae	*Parietaria officinalis* L. ***	1.7
Census		
Betulaceae	*Corylus avellana* L. ***	6.0
Betulaceae	*Ostrya carpinifolia* Scop. *	1.4
Cupressaceae	*Sequoia sempervirens* (D.Don) Endl. *	1.1
Fagaceae	*Quercus ilex* L. **	1.6
Fagaceae	*Quercus robur* L. *	1.5
Oleaceae	*Fraxinus angustifolia* Vahl ***	2.2
Pinaceae	*Pinus nigra* J.F.Arnold *	1.2
Taxaceae	*Taxus baccata* L. *	0.4

4.   Discussion

This study-case is peculiar due to the nature of the park, that is conceived to host a great diversity of plant species in a relatively narrow space, and to reproduce various habitats. While the Botanical Garden was otherwise a good model for method standardisation, these characteristics complicated the sampling design, that needed to be optimised to be suitable for both the dense and variable vegetation of the Garden, and the more sparse and uniform vegetation of other urban parks. A common feature of all these green areas however is their anthropogenic nature, that implies an artificial distribution of the individual ornamental plants, creating aggregations of some species in structures such as living screens, groves, and rows. While the distribution of spontaneous plants like weeds tends to be random, ornamental species distribution in urban parks is usually planned, and a random sampling would probably miss most of the plant diversity. Hence, the systematic sampling was chosen as fittest method to reduce the time and effort needed to analyse the vegetation, while still obtaining objective data suitable for statistical analysis. Nonetheless, possible sampling issues might occur when the systematic sampling grid overlaps with geometric features of the park design. This can be avoided with a careful placement of the grid in the GIS environment, considering vegetation structure and paths distribution, or by modifying the mesh dimension. In this study, systematic sampling covered only 10% of the park total surface. Nevertheless, it provided half of the arboreal species richness recorded by the complete census. It also allowed to estimate species diversity and evenness values comparable to those of the census, and compatible with the heterogeneity of the park (Tab. 5). Most importantly, the systematic sampling estimated not only the same allergenic risk level, but almost the same allergenicity potential values than those calculated on the complete census dataset (Tab. 5, Fig. 3). This suggests that the sampling method hereby proposed could offer a reliable approximation of the park allergenicity, by analysing as little as 10% of the park extension. However, it is important to reproduce this study in other urban parks, to verify and corroborate the consistency between the results obtained by systematic sampling and census. If these results will be confirmed, this approach could offer a quick way to obtain reliable and comparable allergenic levels in future studies.

The main problem of systematic sampling revealed by this study is the misidentification of the main allergenic plant species. This can be explained by the fact that individuals of the

same species are not evenly or randomly distributed along the park, but instead they tend to be aggregated in the recreation of small habitats. Hence, the higher surface cover of a species does not always correspond to a higher probability to be sampled. This caused the systematic sampling to miss entirely some allergenic species that were instead identified as the main drivers of the Botanical Garden allergenicity by the census. This problem could be avoided by increasing the percentage of the park surface sampled.

The two allergenicity indices consistently pointed towards two different allergenicity levels for the park, for all the datasets considered (Tab. 5). While SAI indicated a moderate to high allergenicity potential, I_{UGZA} reported allergenicity values that are lower than most of those published for Mediterranean parks (Cariñanos et al., 2017; Kasprzyk et al., 2019). The extremely low values of I_{UGZA} could depend on the fact that this study employed the first version of the index (Cariñanos et al., 2014), keeping the maximum height in the numerator (2), and considering it to be the height of the tallest individual plant in the dataset. In recent papers, I_{UGZA} formula is presented without the maximum height in the numerator (Cariñanos et al., 2017; Velasco-Jiménez et al., 2020), but this would impair the index reliability since the maximum I_{UGZA} value could exceed 1, and the index would have the unit of measurement of the height (m). Another difference of the I_{UGZA} formula employed in this work with those employed in literature was the choice to not consider extreme values of Ap=4, but this did not have a significant impact on the results (Tab. S3).

Assuming a comparability between the results of the present study with those published in literature for other green areas, I_{UGZA} values for the Botanical Garden are consistent with those obtained for other public and private parks evaluated in Central Italy (Rome), such as Villa Sciarra, Parco Centrale del Lago, and Parco San Sebastiano (Cariñanos et al., 2019), and with the Spanish historic park Parque de los Pinos, that also has a similar tree density (Cariñanos et al., 2017). On the other hand, the allergenicity potential of the Garden is lower than other Mediterranean urban green areas of comparable extension, like the Spanish parks Campus Norte (Orense), Jardín de Ajora (Valencia), and La Alamedilla (Salamanca) (Cariñanos et al., 2017).

It is apparent that the Botanical Garden has a low number of allergenic species, none of which shows a spatial dominance since Pielou's evenness is very high, despite the presence of clustered habitats. While this justifies the low allergenicity level detected by I_{UGZA}, it disagrees with SAI results. This inconsistency does not seem to be linked to the peculiar heterogeneity

the study area, since no correlation between the plant diversity and the results of the allergenic indices has been detected in this study (Fig. S4). Moreover, in this study, the behaviour of the two indices was not affected by the species richness considered (Tab. 5, Fig. 4). Hence, the difference between I_{UGZA} and SAI results is likely explained by the different parameters they consider. In order to choose which index is to be trusted, it is important to notice that some of these parameters might not be strictly related to the allergenicity potential, such as the duration of the life cycle (lc) in SAI; while others, like the local allergenicity (ap) in I_{UGZA}, can be considered more accurate (Tab. 3, 4). SAI in fact lacks such parameter, and thus assumes all the species to be equally allergenic, even though the allergenic species of the Botanical Garden displayed a wide range of allergenicity levels. Another limit of SAI is that being an average value, it can overestimate the allergenicity of a green area when considering only a subset of allergenic species that are perennial or have higher surface cover. This explains why the allergenicity of the park appears higher according to SAI when considering arboreal species only, compared to the allergenicity calculated on all spermatophytes (Tab. 5, Fig. 3B). In conclusion, I_{UGZA} seems more reliable than SAI in estimating the allergenicity potential of a green area, hence the Botanical Garden of Bologna may be considered safe for pollen-allergic visitors, based on the local vegetation. However, neither of the two allergenicity indices takes into account the extra-local component of airborne pollen, that could affect the air quality of the park. Hence, to thoroughly assess the allergenicity risk of the area, airborne pollen sampling at ground and roof level should be carried out as well.

Another interesting finding of this research is that the allergenicity potential of the Botanical Garden is mostly driven by trees and shrubs, even though herbaceous species are more than double the arboreal species sampled, and they cover almost the same surface. This finding is in agreement with previous statements by Cariñanos and collaborators (Cariñanos et al., 2016, 2017), and it suggests that the systematic sampling of only arboreal species may be an accurate way to simplify and speed up the data collection. However, this hypothesis needs to be tested on other parks that have a sparser tree canopy.

Finally, the systematic sampling allowed to test the relationship between plant diversity and allergenicity. A possible positive linear relationship between species richness and number of allergenic species is not supported by the adjusted R^2, while there is no relationship between H-Index and I_{UGZA} values. This was expected since the distribution of plant species in urban

parks is intentional and driven by aesthetical or practical motives, hence the presence of allergenic species is aleatory. Moreover, with equal plant diversity, the allergenicity potential of an area can change according to the number and the volume of the allergenic species present in the area. Vice versa, if the whole volume of the vegetation is made of plants having the same PAV (Tab. 4), the allergenicity potential would be the same whether all the individuals belong to the same species, or if each one of them belongs to a different species. These hypotheses however need to be supported by further studies on wider areas.

5.   Conclusions

Testing two data collection methods and two allergenicity indices on the same urban park allows to validate the sampling methods and the reliability of the indices. The present work shows that systematic sampling and complete census of selected phanerophytes provide comparable results, hence the systematic sampling could be a valid and rapid option for data collection when calculating allergenicity indices. Moreover, vegetation sampling to calculate allergenicity indices could be limited to trees and shrubs, since they seem to drive the allergenicity of the park. However, these hypotheses need to be confirmed by further studies on different urban parks. Nonetheless, plant checklists and inventories should be compiled for the park, in order to detect allergenic species possibly missed by the sampling.

While the data collection methods are comparable, the two indices led to opposite risk evaluations. According to I_{UGZA}, the allergenicity of the Botanical Garden of Bologna is very low, while according to SAI it ranges from moderate to high. Since I_{UGZA} behaviour on different datasets appeared more consistent than the one of SAI, it was hereby considered more reliable. To corroborate this hypothesis, allergenicity indices should be compared to the allergic symptomatology reported by the Botanical Garden visitors in future studies.

6.   Bibliography

Allergome Team and Collaborators, 2021. Allergome [WWW Document]. URL https://www.allergome.org/ (accessed 4.15.21).

Aloisi, I., Del Duca, S., De Nuntiis, P., Vega Maray, A.M., Mandrioli, P., Gutiérrez, P., Fernández-González, D., 2018. Behavior of profilins in the atmosphere and in vitro, and their relationship with the performance of airborne pollen. Atmos. Environ. 178, 231–241. https://doi.org/10.1016/j.atmosenv.2018.01.051

Anderson, G.. J.., 1976. The Pollination Biology of Tilia. Am. J. Bot. 63, 1203–1212.

ARPAE, 2020a. Schede botaniche — Arpae Emilia-Romagna [WWW Document]. URL https://www.arpae.it/it/temi-ambientali/pollini/schede-botaniche (accessed 4.9.21).

ARPAE, 2020b. Calendario pollinico Bologna — Arpae Emilia-Romagna [WWW Document]. URL https://www.arpae.it/it/temi-ambientali/pollini/calendari-pollinici/bologna (accessed 4.9.21).

ARPAE, 2019. Clima — Arpae Emilia-Romagna [WWW Document]. URL https://www.arpae.it/it/temi-ambientali/clima (accessed 4.9.21).

Cancelliere, N., Iglesias, I., Ayuga, Á., Miranda, E.E., 2020. Cross-reactivity between Parietaria Judaica and Parietaria officinalis in immunotherapy extracts for the treatment of allergy to Parietaria. Biomed. Reports 12, 326–332. https://doi.org/10.3892/br.2020.1297

Capotorti, G., Bonacquisti, S., Abis, L., Aloisi, I., Attorre, F., Bacaro, G., Balletto, G., Banfi, E., Barni, E., Bartoli, F., Bazzato, E., Beccaccioli, M., Braglia, R., Bretzel, F., Brighetti, M.A., Brundu, G., Burnelli, M., Calfapietra, C., Cambria, V.E., Caneva, G., Canini, A., Caronni, S., Castello, M., Catalano, C., Celesti-Grapow, L., Cicinelli, E., Cipriani, L., Citterio, S., Concu, G., Coppi, A., Corona, E., Del Duca, S., Del, V.E., Di Gristina, E., Domina, G., Faino, L., Fano, E.A., Fares, S., Farris, E., Farris, S., Fornaciari, M., Gaglio, M., Galasso, G., Galletti, M., Gargano, M.L., Gentili, R., Giannotta, A.P., Guarino, C., Guarino, R., Iaquinta, G., Iiriti, G., Lallai, A., Lallai, E., Lattanzi, E., Manca, S., Manes, F., Marignani, M., Marinangeli, F., Mariotti, M., Mascia, F., Mazzola, P., Meloni, G., Michelozzi, P., Miraglia, A., Montagnani, C., Mundula, L., Muresan, A.N., Musanti, F., Nardini, A., Nicosia, E., Oddi, L., Orlandi, F., Pace, R., Palumbo, M.E., Palumbo, S., Parrotta, L., Pasta, S., Perini, K., Poldini, L., Postiglione, A., Prigioniero, A., Proietti, C., Raimondo, F.M., Ranfa, A., Redi, E.L., Reverberi, M., Roccotiello, E., Ruga, L., Savo, V., Scarano, P., Schirru, F., Sciarrillo, R., Scuderi, F., Sebastiani, A., Siniscalco, C., Sordo, A., Suanno, C., Tartaglia, M., Tilia, A., Toffolo, C., Toselli, E., Travaglini, A., Ventura, F., Venturella, G., Vincenzi, F., Blasi, C., 2020. More nature in the city. Plant Biosyst. 154, 1003–1006. https://doi.org/10.1080/11263504.2020.1837285

Cariñanos, P., Adinolfi, C., Díaz de la Guardia, C., De Linares, C., Casares-Porcel, M., 2016. Characterization of Allergen Emission Sources in Urban Areas. J. Environ. Qual. 45, 244. https://doi.org/10.2134/jeq2015.02.0075

Cariñanos, P., Casares-Porcel, M., 2011. Urban green zones and related pollen allergy: A review. Some guidelines for designing spaces with low allergy impact. Landsc. Urban Plan. 101, 205–214. https://doi.org/10.1016/j.landurbplan.2011.03.006

Cariñanos, P., Casares-Porcel, M., Díaz de la Guardia, C., Aira, M.J., Belmonte, J., Boi, M., Elvira-Rendueles, B., De Linares, C., Fernández-Rodriguez, S., Maya-Manzano, J.M., Pérez-Badía, R., Rodriguez-de la Cruz, D., Rodríguez-Rajo, F.J., Rojo-Úbeda, J., Romero-Zarco, C., Sánchez-Reyes, E., Sánchez-Sánchez, J., Tormo-Molina, R., Vega Maray, A.M., 2017. Assessing allergenicity in urban parks: A nature-based solution to reduce the impact on public health. Environ. Res. 155, 219–227. https://doi.org/10.1016/j.envres.2017.02.015

Cariñanos, P., Casares-Porcel, M., Quesada-Rubio, J.M., 2014. Estimating the allergenic potential of urban green spaces: A case-study in Granada, Spain. Landsc. Urban Plan. 123, 134–144. https://doi.org/10.1016/j.landurbplan.2013.12.009

Cariñanos, P., Grilo, F., Pinho, P., Casares-Porcel, M., Branquinho, C., Acil, N., Andreucci, M.B., Anjos, A., Bianco, P.M., Brini, S., Calaza-Martínez, P., Calvo, E., Carrari, E., Castro, J., Chiesura, A., Correia, O., Gonçalves, A., Gonçalves, P., Mexia, T., Mirabile, M., Paoletti, E., Santos-Reis, M., Semenzato, P., Vilhar, U., 2019. Estimation of the allergenic potential of urban trees and urban parks: Towards the healthy design of urban green spaces of the future. Int. J. Environ. Res. Public Health 16. https://doi.org/10.3390/ijerph16081357

Cecchi, L., 2013. From pollen count to pollen potency: the molecular era of aerobiology. Eur. Respir. J. 42, 898–900. https://doi.org/10.1183/09031936.00096413

Conti, F., Abbate, G., Alessandrini, A., Blasi, C., 2005. An Annotated Checklist of the Italian Vascular Flora 420.

D'Amato, G., 2001. Airborne paucimicronic allergen-carrying particles and seasonal respiratory allergy. Allergy Eur. J. Allergy Clin. Immunol. 56, 1109–1111. https://doi.org/10.1034/j.1398-9995.2001.00317.x

D'Amato, G., Cecchi, L., Bonini, S., Nunes, C., Annesi-Maesano, I., Behrendt, H., Liccardi, G., Popov, T., Van Cauwenberge, P., 2007. Allergenic pollen and pollen allergy in Europe. Allergy Eur. J. Allergy Clin. Immunol. 62, 976–990. https://doi.org/10.1111/j.1398-9995.2007.01393.x

D'Amato, G., Pawankar, R., Vitale, C., Lanza, M., Molino, A., Stanziola, A., Sanduzzi, A., Vatrella, A., D'Amato, M., 2016. Climate change and air pollution: Effects on respiratory allergy. Allergy, Asthma Immunol. Res. 8, 391–395. https://doi.org/10.4168/aair.2016.8.5.391

Fernández-González, D., González-Parrado, Z., Vega-Maray, A.M., Valencia-Barrera, R.M., Camazón-Izquierdo, B., De Nuntiis, P., Mandrioli, P., 2010. Platanus pollen allergen, Pla a 1: Quantification in the atmosphere and influence on a sensitizing population. Clin. Exp. Allergy 40, 1701–1708. https://doi.org/10.1111/j.1365-2222.2010.03595.x

Fernández-González, D., Rajo, F.J.R., Parrado, Z.G., Barrera, R.M.V., Jato, V., Grau, S.M., 2011. Differences in atmospheric emissions of Poaceae pollen and Lol p 1 allergen. Aerobiologia (Bologna). 27, 301–309. https://doi.org/10.1007/s10453-011-9199-x

Gadermaier, G., Eichhorn, S., Vejvar, E., Weilnböck, L., Lang, R., Briza, P., Huber, C.G., Ferreira, F., Hawranek, T., 2014. Plantago lanceolata: An important trigger of summer pollinosis with limited IgE cross-reactivity. J. Allergy Clin. Immunol. 134, 472-475.e5. https://doi.org/10.1016/j.jaci.2014.02.016

Gangl, K., Niederberger, V., Valenta, R., Nandy, A., 2015. Marker allergens and panallergens in tree and grass pollen allergy. Allergo J. Int. 24, 158–169. https://doi.org/10.1007/s40629-015-0055-3

Gastaminza, G., Lombardero, M., Bernaola, G., Antepara, I., Muñoz, D., Gamboa, P.M., Audicana, M.T., Marcos, C., Ansotegui, I.J., 2009. Allergenicity and cross-reactivity of pine pollen. Clin. Exp. Allergy 39, 1438–1446. https://doi.org/10.1111/j.1365-2222.2009.03308.x

Hruska, K., 2003. Assessment of urban allergophytes using an allergen index. Aerobiologia (Bologna). 19, 107–111. https://doi.org/10.1023/A:1024450601697

ISTAT, 2016. Statistiche Istat [WWW Document]. URL http://dati.istat.it/Index.aspx (accessed 4.9.21).

Kasprzyk, I., Wójcik, T., Cariñanos, P., Borycka, K., Ćwik, A., 2019. Evaluation of the allergenicity of various types of urban parks in a warm temperate climate zone. Aerobiologia (Bologna). 35, 57–71. https://doi.org/10.1007/s10453-018-9537-3

Lombardero, M., Obispo, T., Calabozo, B., Lezaún, A., Polo, F., Barber, D., 2002. Cross-reactivity between olive and other species. Role of Ole e 1-related proteins. Allergy Eur. J. Allergy Clin. Immunol. 57, 29–34. https://doi.org/10.1034/j.1398-9995.2002.057s71029.x

López-Matas, M.A., Moya, R., Cardona, V., Valero, A., Gaig, P., Malet, A., Viñas, M., García-Moral, A., Labrador, M., Alcoceba, E., Ibero, M., Carnés, J., 2016. Relevance of allergenic sensitization to Cynodon dactylon and Phragmites communis: Cross-reactivity with pooideae grasses. J. Investig. Allergol. Clin. Immunol. 26, 295–303. https://doi.org/10.18176/jiaci.0049

Meeuse, A.D.J., 1984. Rate of dependence of Plantago media L. on entomophilous reproduction – preliminary report. Acta Bot. Neerl. 33, 129–130.

Moraes, A.H., Asam, C., Almeida, F.C.L., Wallner, M., Ferreira, F., Valente, A.P., 2018. Structural basis for cross-reactivity and conformation fluctuation of the major beech pollen allergen Fag s 1. Sci. Rep. 8, 1–10. https://doi.org/10.1038/s41598-018-28358-1

Mothes, N., Horak, F., Valenta, R., 2004. Transition from a botanical to a molecular classification in tree pollen allergy: Implications for diagnosis and therapy. Int. Arch. Allergy Immunol. 135, 357–373. https://doi.org/10.1159/000082332

Oh, J.-W., 2018. Pollen Allergy in a Changing World, Pollen Allergy in a Changing World. https://doi.org/10.1007/978-981-10-5499-0

Ortolani, C., Previdi, M., Sala, G., Bozzoli Parasacchi, V., Ortolani, A., Minella, C., 2015. Allergenicity of trees and shrubbery to use in the italian urban green. Systematic review and evidence-based reccomandations. Eur. J. Aerobiol. Environmetal Med. XI.

Panzani, R., Yasueda, H., Shimizu, T., Shida, T., 1986. Cross-reactivity between the pollens of Cupressus sempervirens (common cypress) and of Cryptomeria japonica (Japanese cedar). Ann. Allergy 57, 26–30.

Patel, N.P., Prizment, A.E., Thyagarajan, B., Roberts, E., Nelson, H.H., Church, T.R., Lazovich, D., 2018. Urban versus Rural Residency and Allergy Prevalence among Adult Women: Iowa Women's Health Study. Ann. Allergy, Asthma Immunol. 120, 654–660. https://doi.org/10.1016/j.anai.2018.03.029.

Pecero-Casimiro, R., Fernández-Rodríguez, S., Tormo-Molina, R., Monroy-Colín, A., Silva-Palacios, I., Cortés-Pérez, J.P., Gonzalo-Garijo, Á., Maya-Manzano, J.M., 2019. Urban aerobiological risk mapping of ornamental trees using a new index based on LiDAR and Kriging: A case study of plane trees. Sci. Total Environ. 693, 1–12. https://doi.org/10.1016/j.scitotenv.2019.07.382

Pielou, E., 1966. The measurement of diversity in different types of biological collections. J. Theor. Biol. 13, 131–144.

Pignatti, S., 2017. Flora d'Italia. Edagricole-New Business Media.

QGIS Association, 2021. QGIS Geographic Information System [WWW Document]. URL https://www.qgis.org/en/site/ (accessed 4.9.21).

Raunkiaer, C., 1934. The life forms of plants and statistical plant geography; being the collected papers of C. Raunkiaer. Clarendon Press, Oxford.

RStudio Team, 2020. RStudio: Integrated Development for R. [WWW Document]. URL http://www.rstudio.com/.

Schwietz, L.A., Goetz, D.W., Whisman, B.A., Reid, M.J., 2000. Cross-reactivity among conifer pollens. Ann. Allergy, Asthma Immunol. 84, 87–93. https://doi.org/10.1016/S1081-1206(10)62746-9

Science for Environment Policy, 2012. The Multifunctionality of Green Infrastructure.

Shannon, C.E., 1948. A mathematical theory of communication. Bell Syst. Tech. J. 27, 379–423.

Suanno, C., Aloisi, I., Fernández-González, D., Del Duca, S., 2021. Monitoring techniques for pollen allergy risk assessment. Environ. Res. https://doi.org/10.1016/j.envres.2021.111109

Velasco-Jiménez, M.J., Cariñanos, P., Galán, C., 2020. Allergenicity of the urban green areas in the city of Córdoba (Spain). Urban For. Urban Green. 49, 1–8. https://doi.org/10.1016/j.ufug.2020.126600

WAO, 2012. Italy | World Allergy Organization [WWW Document]. URL https://www.worldallergy.org/resources/world-atlas-of-aeroallergens/italy (accessed 4.9.21).

Weber, R.W., 2003. Patterns of pollen cross-allergenicity. J. Allergy Clin. Immunol. 112, 229–239. https://doi.org/10.1067/mai.2003.1683

6. A possible endocytic origin for pollen-derived extracellular nanovesicles

This chapter is a preprint of an original research article.
Authors: C Suanno, E Tonoli, E Fornari, M. P Savoca, I Aloisi, L Parrotta, C Faleri, G Cai, E Verderio-Edwards, S Del Duca

Abstract

It has been recently discovered that extracellular nanovesicles, termed "pollensomes", are released by pollen during germination. These vesicles may play an important role in pollen-pistil interaction during fertilisation, stabilising the secreted bioactive molecules and allowing long-distance signaling. However, the nature of these vesicles is still unclear. In this work, putative pollensomes are isolated from hydrated and germinated kiwi (*Actinidia chinensis* Planch.) pollen, and characterised using imaging techniques, immunoblotting, and proteomics. This analysis confirms that only germinated pollen releases pollensomes in detectable concentrations, and that these vesicles may have endocytic origins. The presence of plant homologs of ALIX, a well-recognised and accepted marker of exosomes in mammals, is consistent with the hypothesis that these vesicles may be exosomes.

Keywords: pollensomes, nanovesicles, pollen tube, pollination, exosomes, signaling, ALIX, MVB

Abbreviations: AFM, Atomic force microscopy; EVF, vesicle-free supernatant; EVs, putative extracellular nanovesicles; EXPO, Exocyst-Postive Organelle; GKP, Germinated kiwi pollen; HKP, Hydrated kiwi pollen; ILV, Intraluminal vesicle; MVB, Multivesicular body; PKP, PBS-hydrated kiwi pollen; PTA, Particle tracking analysis; TL, Total Lysate.

1.   Introduction

It is widely known that protein secretion is needed for pollen-pistil communication during spermatophyte sexual reproduction, from the species-specific recognition, to the self-compatibility or incompatibility, to the pollen tube elongation (Cheung and Wu, 2008; Hafidh et al., 2014; Mandrone et al., 2019). However, proof that extracellular nanovesicles are

involved in such communication has been found only in the last two decades. In fact, in 2000 Grote and colleagues demonstrated that allergenic pollen, when hydrated in rainwater, can release nanoparticles bearing pollen allergens (Grote et al., 2000, 2003). In 2014, Prado and colleagues proved that allergen-bearing nanoparticles released by germinated pollen grains are extracellular nanovesicles, with diameter ranging from 28 to 60 nm, that they named "pollensomes" (Prado et al., 2014, 2015). Since pollensomes were isolated using a protocol designed to isolate mammalian exosomes, and since they were comparable in size with known exosomes, the researchers speculated that pollensomes could be plant exosomes (Prado et al., 2014). Exosomes are a relatively new concept in biology, and especially in plant science. They were first discovered in mammals, and the bulk of knowledge about them derives from the study of mammalian cells, but they have also been described in other animals, yeasts, and plants (Rutter and Innes, 2017; Kurian et al., 2021). Exosomes can be defined as small extracellular nanovesicles, between 30 and 150 nm in diameter, that have a lipidic double-layered membrane and endocytic origins. These features distinguish them from other known extracellular vesicles: nanovesicles derived by exocyst-positive organelles (EXPOs) have single-layered lipidic membranes (Wang et al., 2010), while extracellular microvesicles and apoptotic bodies are on average larger in size (50-1000 nm and 500-2000 nm, respectively) and originate by budding from the plasma membrane (Kurian et al., 2021). However, to date the release of microvesicles by budding from the plasma membrane has not been demonstrated for plants (Woith et al., 2021). Exosomes instead have a peculiar biogenesis, since they are produced by invagination in the membrane of the late endosome. At this stage, exosomes are called intraluminal vesicles (ILVs), and the organelle including them is called multivesicular body (MVB). The membrane of the MVB then fuses to the plasma membrane, releasing the ILVs in the extracellular environment as exosomes (Johnstone, 2006; Javeed and Mukhopadhyay, 2017). While exosomes are known to mediate cellular signaling and several other biological functions in mammals (Javeed and Mukhopadhyay, 2017), their role in plants is yet to be fully understood, but it is ascertained that plant exosomes are involved in stress responses and defence signaling, and it is speculated that they could mediate intercellular communication as well (An et al., 2007; Hansen and Nielsen, 2017; Rutter and Innes, 2017; Woith et al., 2021). Moreover, there is evidence that stigmatic papillae of *Brassica napus* L. secrete exosomes to communicate with pollen during pollen hydration and pollen tube entry (Goring, 2017), and it is reasonable to wonder whether this

type of communication might be adopted by the pollen as well, since exosomes are known to enhance the effectiveness of signaling by protecting their cargo from degradation in the extracellular environment (Akuma et al., 2019).

An extracellular vesicle can be defined exosome if: (I) it can be isolated by ultracentrifugation at 100000 x g, (II) its dimensions fall within the accepted range for exosomes (30-150 nm), (III) it is released by MVBs, (IV) it contains accepted molecular markers for exosomes (Kurian et al., 2021). The latter requirement is particularly difficult to meet for plant exosomes, since no universal molecular marker has been described yet, although some attempts have been made (Regente et al., 2009; Hafidh et al., 2016; Rutter and Innes, 2017; Woith et al., 2021). Widely accepted molecular markers for mammalian exosomes are ALIX (Apoptosis-Linked gene-2 Interacting protein X), Tsg101 (Tumor Susceptibility Gene 101), tetraspanins (CD81, CD63, CD9), and flotillin (Kurian et al., 2021).

ALIX domain Bro1 is highly preserved in the evolution of eucaryotic organisms, and Bro1 domain containing proteins are present in yeasts and plants. ALIX and its homologs are known to be involved in the formation of ILVs and in the sorting of their cargo (Bissig and Gruenberg, 2014; Kalinowska et al., 2015; García-León and Rubio, 2020), making plant homologs of a ALIX a good candidate for exosome markers.

In this study, kiwi (*Actinidia chinensis* Planch.) pollen has been the experimental model to investigate the conditions that stimulate pollensomes release, and the nature of these nanovesicles, following the working hypothesis that they could be exosomes. For this purpose, diverse imaging techniques and a qualitative proteomic analysis have been applied to the putative pollensomes. Moreover, plant homologs of ALIX have been tested as a possible molecular marker for plant exosomes.

2.   Materials and Methods

2.1   Plant material

Kiwi pollen has been chosen as model for this study because it is easily available, shows a high *in vitro* germination rate in only two hours, and it can be stored for several years without a significant decrease in viability and germinability. Kiwi pollen used in these experiments was purchased in 2019 from Azienda Agricola Tabanelli Pierino, Mirko e C. (Castel Bolognese, Bologna, Italy). Pollen was then dried and stored at -20°C.

2.2   Sample treatment

Each sample was made of 10 mg dry pollen for particle tracking analysis, atomic force microscopy, immunofluorescence, and immunogold. For western blot analysis and FM4-64™ staining, samples were made of 20 mg dry pollen, whereas 40 mg dry pollen samples were used for total proteomics. All the samples were initially rehydrated for 30 min at 30°C in a humid chamber with 100% relative humidity, and their viability was checked by MTT assay (Paris et al., 2017). Pollen was then resuspended in germination medium (10% sucrose, 324 µM H_3BO_3, 1.27 mM $Ca(NO_3)_2$) at concentrations of 1 mg/ml, and incubated in a petri dish for 2 h at 30°C (germinated kiwi pollen, GKP); alternatively, pollen was hydrated in the humid chamber, at the same conditions and for the same time of GKP, and was eventually resuspended in particle-free PBS at concentrations of 0.5 mg/ml (hydrated kiwi pollen, HKP). For FM4-64 staining, a third treatment group was added (PBS-hydrated kiwi pollen, PKP), by resuspending the rehydrated pollen in particle-free PBS (Dubecco's PBS 1x, Capricorn Scientific, Italy) at concentrations of 1 mg/ml, and incubating it in a petri dish for 2 h at 30°C. For all groups, viability and germinability were estimated in light field microscopy with a Leica DM750 microscope, equipped with a Leica ICC50 W camera, using Leica AirLab software. Only pollen that had a viability rate over 80%, a germination rate over 60% for GKP, and a germination rate of 0% for HKP and PKP was used for subsequent analyses.

2.3   Nanovesicles isolation

Nanovesicles isolation was carried out as previously described (Prado et al., 2014, 2015; Furini et al., 2018), with minor modifications. Briefly, pollen grains were pelleted at 5000 x g for 15 min at 4°C and the supernatant was collected, filtered twice in 0.22 µm syringe filters, and then ultra-centrifuged at 100000 x g at 4°C for 1h, to pellet the putative extracellular nanovesicles (EVs).

2.4   Particle tracking analysis

Particle tracking analysis (PTA) was performed using ZetaView® Basic-NTA (Particle Metrix, Germany). Pelleted EVs were resuspended in particle-free PBS and analysed in measurement mode "Size Distribution", 2 Cycles, 11 Positions. Germination medium and particle-free PBS were used as blank for the treatment and the control group respectively, and the measurements were performed in triplicate for each group.

2.5   Atomic force microscopy

Atomic force microscopy (AFM) was performed using a Dimension ICON atomic force microscope equipped with a Nanoscope V controller operating in ScanAsyst tapping mode air environment. Standard silicon nitride triangular cantilevers (ScanAsyst-air, Bruker, U.K.), with resonant frequencies ranging between 45 and 95kHz, and spring constants ranging between 0.2 and 0.8 N/m, were used. Imaging was performed at a rate of 0.7Hz. All measurements were performed in temperature (23 °C ± 1 °C) controlled laboratories.

EVs were resuspended in particle-free PBS at concentrations of $10.4 \cdot 10^4$ particles/µl (calculated using ZetaView™) for both treatment and control group. Particle-free PBS was used as negative control to rule out contamination. Slides were then prepared under laminar flow hood according to literature (Sebaihi et al., 2017), with some modifications. 35µl of sample were added on a $5cm^2$ polylysine-coated MICA. After 1 h of incubation the samples were gently rinsed with ultrapure water and let dry overnight at room temperature. 10×10 μm^2, $2 \times 2 \ \mu m^2$ and $500 \times 500 \ nm^2$ AFM images were recorded at 512 sample lines. All the images were analysed using Nanoscope software. A first order flattening was applied to AFM images and the section analysis function of Nanoscope software was used to detect and measure the size of the particles.

2.6   Fluorescence microscopy

Fluorescence microscopy was performed using a NEXCOPE NE920 microscope equipped with a mercury short-arc lamp Osram HBO 103 and a 20 Mpx cooled colour camera with C-MOS 1" sensor (TiEsseLab, Italy).

To prove the vesicular nature of the isolated nanoparticles, both germinated pollen grains and EVs from GKP and HKP were resuspended in PBS and added with 2 µM FM™ 4-64 (also known as SynaptoRed™ C2) fluorescent dye (Tocris, Italy) and observed at the fluorescence microscope using TRIC filter.

For immunolocalisation of ALIX-homologs, ARF1, and Clathrin, only germinated samples were analysed. Germination medium was discarded after a light centrifugation (1000 x g), and pelleted pollen grains were then processed as described in literature (Parrotta et al., 2018; Mandrone et al., 2019), with some modifications. Briefly, pelleted pollen grains were fixed with PME buffer (4% formaldehyde, 50 mM PIPES pH 6.8, 1 mM $MgSO_4$, 5 mM EDTA) for 1 h, digested by pectinase and cellulase for 7 min, permeabilised with 0.5% Triton X-100 for 30

min, and eventually dehydrated in cold methanol (-20°C) for 10 min. Samples were blocked with 3% BSA in PBS, and then incubated with the primary antibodies (1:50 dilution of anti-ALIX, 1:300 dilution of anti-ARF1, or 1:700 dilution of anti-Clathrin, in PBS) at 4°C overnight. Samples used as negative controls were incubated with PBS only. All samples were thus incubated with a goat polyclonal anti-rabbit IgG, FITC-conjugated (dilution 1:200, SouthernBiotech, Italy), and 3% BSA in PBS, for 2 h at room temperature, in the dark. Finally, samples were washed in PBS, added with 10% glycerol, and mounted on glass slides. Fluorescence was observed at 600X magnification using the FITC filter.

2.7   Electron microscopy

For electron microscopy, the transmission electron microscope (TEM) Philips Morgagni 268 D set at 80 kV was employed, and images were captured with a MegaView II CCD Camera (Philips Electronics, The Netherlands) and analysed with the microscope software (AnaliSYS). Immunogold labelling was carried out following Parrotta and colleagues protocol (Parrotta et al., 2019). Briefly, germinated pollen was dehydrated in growing concentrations of ethanol, and then infiltrated with LR White resin. Thus, the resin was incapsulated and polymerised in oven at 40°C for 2 days. The resin was then sectioned, and the sections were blocked in 5% normal goat serum (Invitrogen, Italy) for 20 min and then incubated in a 1:50 dilution of the anti-ALIX antibody for 1 h. Three sections were selected as negative controls and they were not incubated with the primary antibody. Finally, the excess of primary antibody was washed in 50 mM Tris–HCl pH 7.6, 0.9% NaCl, 0.1% Tween, and all the sections were incubated for 45 min with a dilution 1:20 of goat anti-rabbit secondary antibody conjugated with 15 nm gold particles (BioCell, Italy). Sections were washed with distilled water and counterstained first with 2% uranyl acetate for 10 min, and then with lead citrate for 5 min. At least 50 pollen tubes and grains were analysed per sample.

2.8   Protein isolation and quantification

Total proteins were isolated from whole pollen grains as shown in literature (Mandrone et al., 2019), with minor modifications. Briefly, pelleted pollen was resuspended in pollen extraction buffer (PEB) (Tris-HCl 20 mM pH 8.5, DTT 2mM, protease inhibitors cocktail 1:100) and pottered 80 times. Wall and membrane debris were discarded afterwards by spinning the samples at 1000 x g for 10 min, and the supernatant (total lysate, TL) was then collected. Total proteins were extracted from the pelleted EVs by resuspending them in PEB.

Proteins in the vesicle-free supernatant (EVF) were precipitated with 10% TCA and washed with acetone at -20°C, pelleted by centrifuge at 15000 x g for 5 min at 4°C, and then resuspended in PEB (Furini et al., 2018).

Protein content was quantified by Bradford assay (Bradford Reagent, Sigma-Aldrich, Italy).

2.9   Immunoblotting

Total proteins from TLs, EVs, and EVFs of both treatment and control groups were resolved in one-dimensional SDS-PAGE and blotted onto nitrocellulose membrane. The membrane was then blocked in 5% Blotting Grade Blocker (BioRad, Italy) in TBS for 30 min, and thus incubated at 4°C overnight with one of the following rabbit polyclonal antibodies: 1:2000 dilution of anti-Clathrin Heavy Chain (Agrisera), 1:5000 dilution of anti-H$^+$ATPase (Agrisera, Italy), 1:500 dilution of anti-COXII (Agrisera, Italy), 1:5000 dilution of anti-UGPase (Agrisera, Italy), 1:1000 dilution of anti-ARF1 (Agrisera, Italy), or 1:1000 dilution of anti-ALIX (Covalab, Italy). All membranes were then washed in TBS-Tween (0.05% v/v) and TBS, and they were incubated at room temperature for 2 h with 1:5000 goat polyclonal anti-rabbit IgG peroxidase conjugated (Sigma-Aldrich, Italy). Finally, the membranes were developed with Amersham™ ECL Prime Western Blotting Reagents (GE Healthcare, Italy) and read in chemiluminescence with Azure 280 (Azure Biosystems, California). Experiments were repeated in triplicate for each target protein.

2.10   Proteomics

EVs from 3 germinated samples were lysed in RIPA buffer (25 mM TrisHCl pH 7.2, 150 mM NaCl, 2 mM EDTA, 5% Sodium deoxycholate, 1% NP40, 0.1% SDS), and their protein content was quantified by Bradford assay, BCA assay, and 2-D Quant Kit (GE Healthcare, Italy), resulting in an average of 40 µg per sample. Proteins were lyophilised and stored at -80°C until analysis. EVs protein lysates were processed and trypsinised using S-trap micro methodology (Protifi, UK). Samples were resuspended to 1ug/uL in 5% acetonitrile and 0.1% formic acid in a two-stage process. Individual samples and a pool of all three samples were analysed by RP-HPLC-ESI-MS/MS using a TripleTOF 6600+ mass spectrometer in data dependent acquisition mode, according to literature (Furini et al., 2018) with some modifications. RP-HPLC mobile phases were solvent A (0.1% (v/v) formic acid in LC/MS grade water) and solvent B (LC/MS grade acetonitrile containing 0.1% (v/v) formic acid). Samples were injected (trap/elute via 5 x 0.3µm YMC Triart C18 trap column) onto a YMC Triart-C18

column (15 cm, 3μm, 300 um i.d) at 5 μL/min using a microflow LC system (Eksigent ekspert nano LC 425) with an increasing linear gradient of B going from 3% to 30% in 68 min; to 40% at 73 min then washing to 80% for 3 min before re-equilibration in a total time of 87 min. Mass calibration (TOF-MS and Product ion) was performed by the MS every 4 samples using an injection of a standard of 40 fmol PepCal mix (Sciex, Canada) digest. Ionisation was via the Sciex DuoSpray™ source, using a 50 μm electrode at +5500 V. A spectral library was produced by DDA of all samples, in high sensitivity mode. DDA mass spectrometry files were searched using ProteinPilot 4 (SCIEX, U.K.) and the analysis was conducted by the software with an exhaustive identification strategy, searching the UniProt/Swiss-Prot database (January 2019 release) for *Actinidia* genus. Protein families, cellular localisations and functions were drawn from UniProtKB (UniProt Consortium, 2021) and from literature (Kawai and Uchimiya, 1995; Anderson et al., 2004; Tiwari et al., 2005; Al-Whaibi, 2011; Olvera-Carrillo et al., 2011; Lu et al., 2012; Suhandono et al., 2014a; Dumont et al., 2016; Kuttiyatveetil and Sanders, 2017; Saqib et al., 2019).

2.11 Statistical analysis

Statistical analysis was carried out in RStudio (RStudio Team, 2020). To test datasets for normality, Shapiro-Wilk test was applied, using shapiro.test() function. To evaluate the statistical significance (p-value <0.05) of the differences between GKP and HKP samples, t-test and two-way ANOVA were performed on protein concentrations, using t.test(), lm(), and anova() functions with default settings, followed by a post-hoc pairwise t-test with Bonferroni correction using paiwise.t.test() function. Kruskal-Wallis test was performed on ZetaView™ measurements using kruskal.test() function.

3. Results

3.1 Nanovesicles visualisation and measurments

ZetaView® particle tracker was able to detect nanoparticles ranging between 266 and 1 nm in diameter in both GKP and HKP EVs samples. However, the vast majority of particles (>95%) had a diameter comprised between 120 and 209 nm. While median and peak diameter did not vary between the two groups, of nanoparticles were isolated from GKP showed a significantly higher concentration than those in EVs isolated from HKP (Fig 1).

In AFM analysis, nanoparticles were visible in both GKP and HKP EVs, while they were absent in the negative control. Many particles appeared to be aggregated (Fig. 2), having diameter and height of respectively 40.4 nm ± 60.4 nm and 10.7 nm for HKP, and of 78.1 nm ± 57.4 nm and 9.8nm for GKP.

EVs from GKP emitted a clear fluorescent signal after FM4-64™ staining (Fig. 3B), indicating the presence of vesicles with double-layered lipidic membrane in this fraction. Excessive dimensions of the fluorescent spots compared to the maximum expected (220 nm) was likely due to aggregation of the vesicles (as shown also by AFM) and to the diffusion of fluorescent light. On the contrary, EV fractions from HKP and PKP did not show any fluorescence after FM4-64™ dyeing. Intact germinated pollen grains were stained as well, as a positive control (Fig. 3A), showing uniform fluorescent spotting along the pollen tube, and the characteristic intense coloration on the tube apex, due to vesicle accumulation (Parton et al., 2003).

3.2 Characterisation of nanovesicles proteins

Total protein concentration resulted significantly higher (p-value<0.02) for GKP EVs, than for HKP EVs and EVFs from both groups, while protein concentration of GKP EVFs, GHP EVFs, and GHP EVs was comparable (Fig. 4).

Clathrin heavy chain was chosen as marker for vesicular compartments, H^+ATPase as plasma membrane marker, COXII (Plant Cytochrome oxidase subunit II) as mitochondrial marker, UGPase (UDP-glucose phosphorylase) as cytoplasmic marker, and ARF1 (ADP-ribosylation factor 1) as marker for the Golgi membrane. All the markers were found in the TLs, while they were all absent from the other fractions (EVs and EVFs) of both experimental groups, except for Clathrin heavy chain, that was present in GKP EVs (Fig. 5).

Western blot analysis also revealed the presence of enriched levels of possible plant homologs of ALIX in the EVs of germinated kiwi pollen, with a molecular weight around 40 kDa. This protein was present in both TLs but was not detectable in the EVFs fractions and in the EVs from HKP (Fig. 6).

The RP-HPLC-ESI-MS/MS provided a list of 2945 accession numbers matching with the peptides sequenced from EVs of GKP, corresponding to 1203 different proteins (Tab. S1, Supplementary). Out of these proteins, only 56 were present in all three replicas, were identified using at least 2 peptides, and had a 95% coverage over 70% of the peptide length (Tab. 1). The majority of the proteins listed in Table 1 is involved in catabolic and biosynthetic

processes, which is compatible with the high metabolic activity in the pollen cytoplasm during pollen tube elongation. Three proteins of this list are involved in stress response: the Late embryogenesis abundant protein, the Stress-induced protein, and the Heat shock protein 70 (Hsp70) family protein. Others are involved in transport and signaling, like the Guanosine nucleotide diphosphate dissociation inhibitor, and the Clathrin heavy chain like protein (UniProt Consortium, 2021).
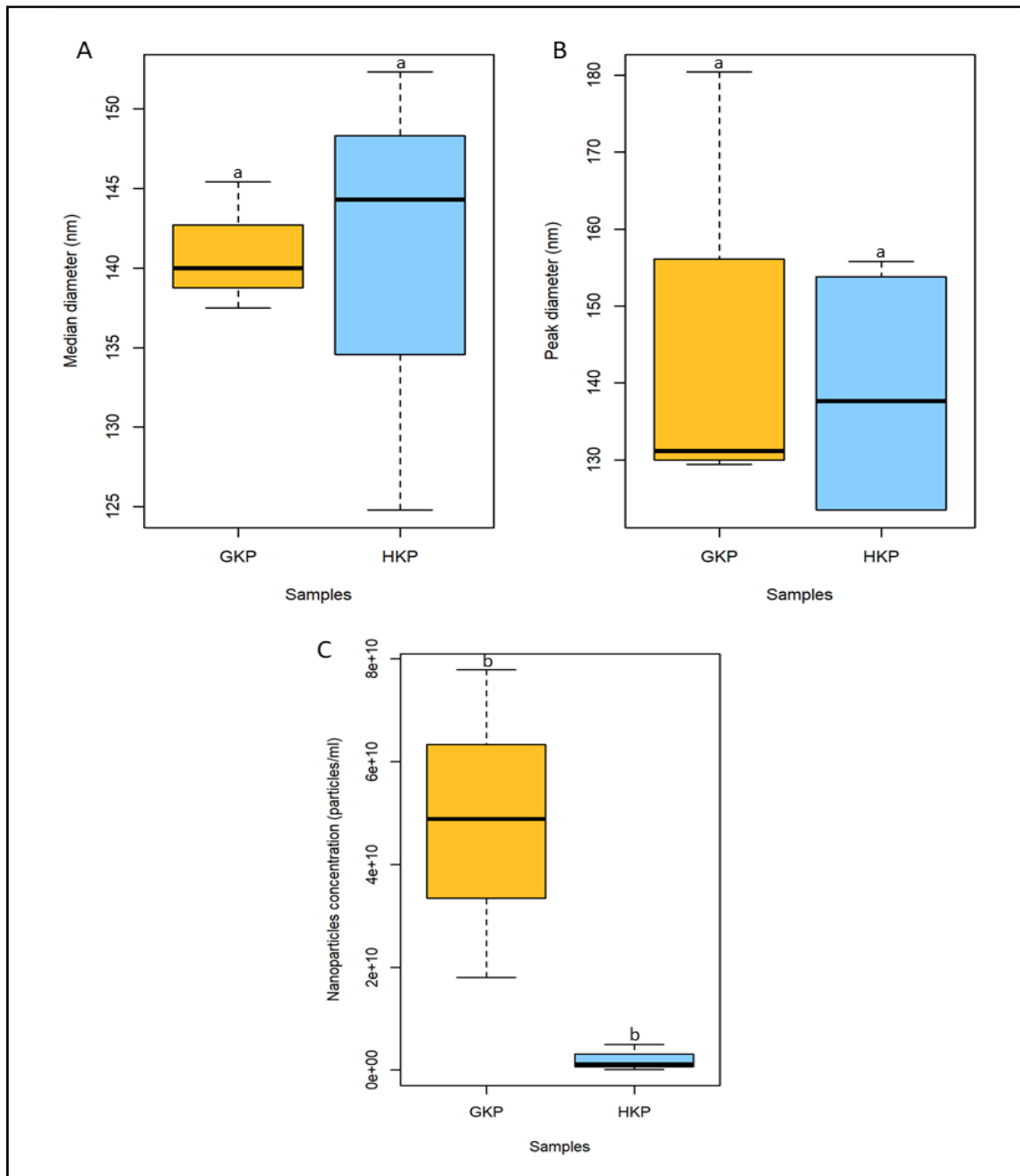
Figure 2 Boxplot representation (± SD) of median (A) and peak (B) diameters (nm), and concentration (particle/ml) (C) of nanoparticles in EVs from GKP and HKP. Kruskal-Wallis test indicated no significant difference between a and a, and significant difference (p-value<0.05) between b and b.
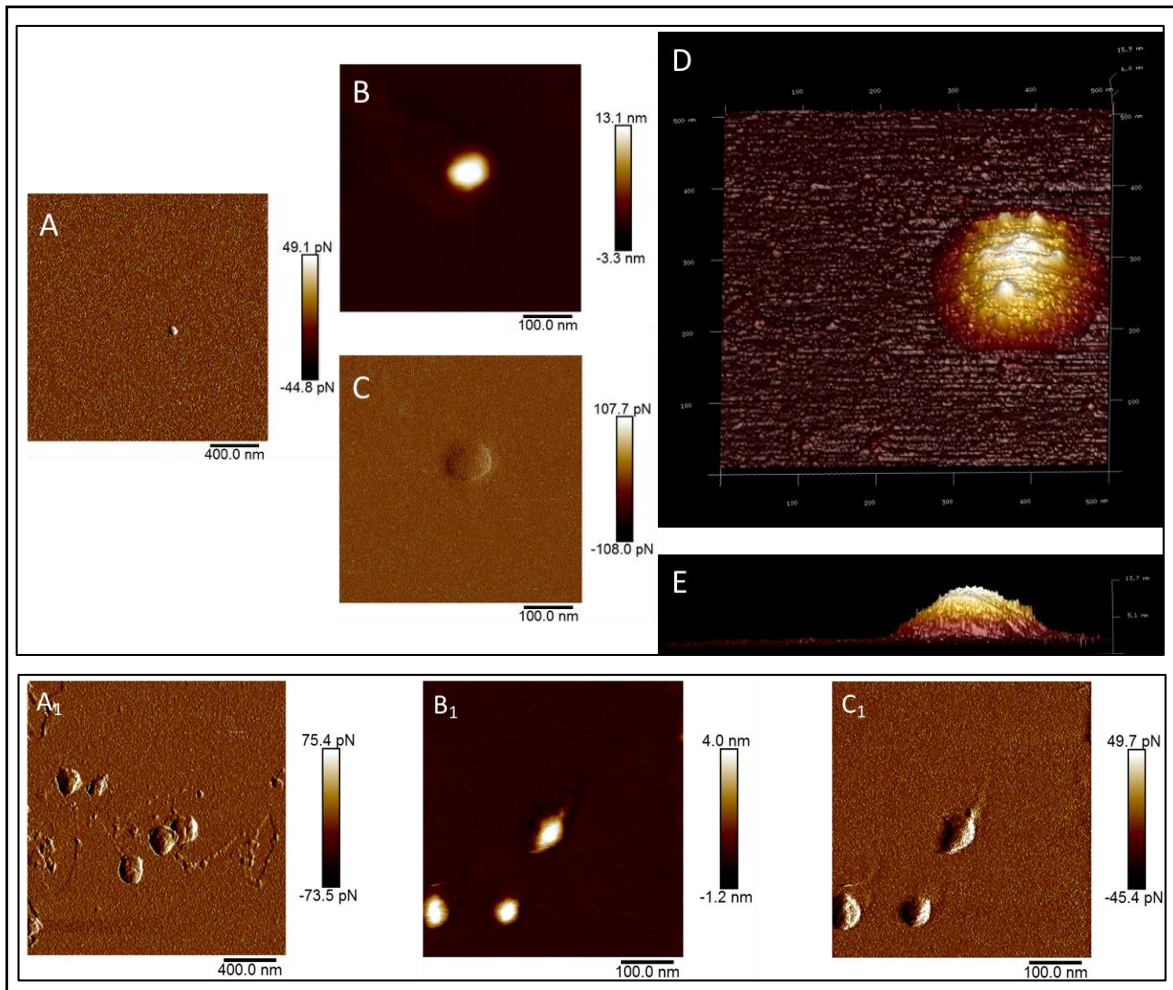
Figure 4 *AFM images of EVs from hydrated (A, B,C,D, E) and germinated (A1,B1,C1) kiwi. A, B, C, D, and E picture the same nanoparticle. B1 and C1 picture the same group of nanoparticles. B and B1 are represented in height mode. A, A1, C, and C1 are represented in peak force error mode. D and E are 3D images.*
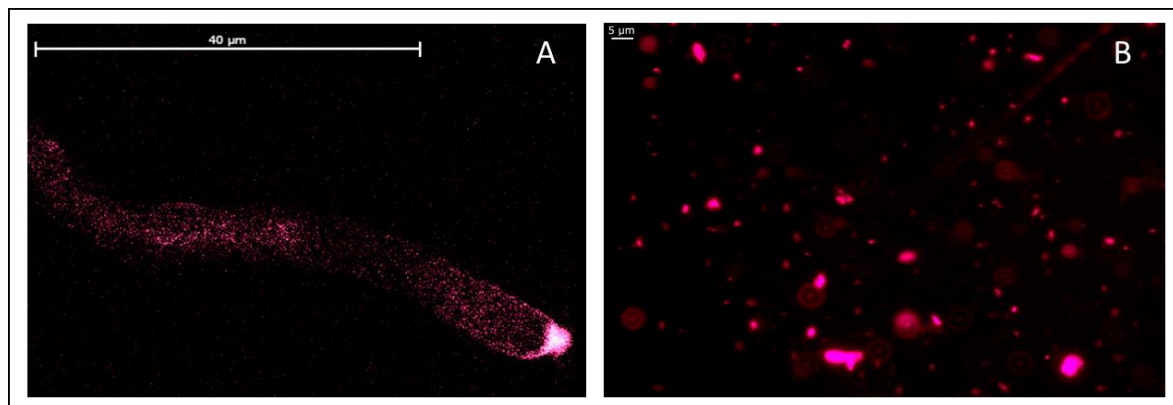
Figure 3 *Pollen tube (A) and EVs (B) of germinated kiwi pollen, dyed with FM4-64™ to enhance the presence of double-layered vesicles.*
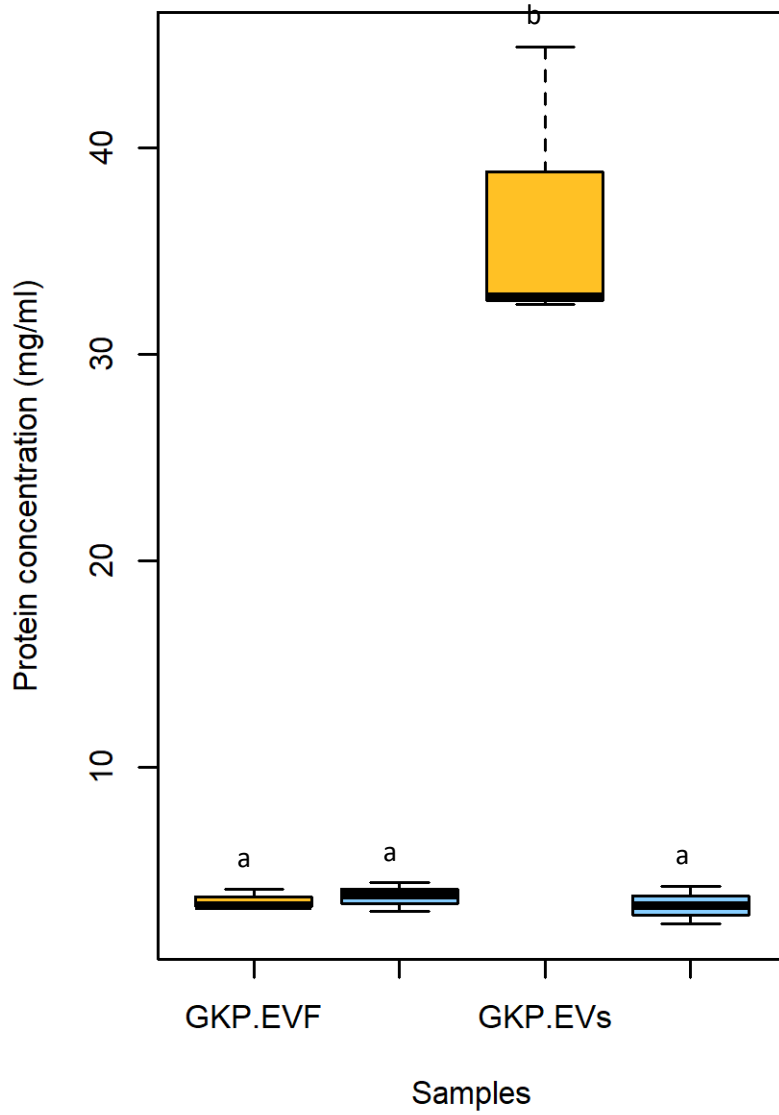
Figure 4 *Mean protein content (± SD) for EVs and EVF from germinated and hydrated samples. ANOVA and t-test were significant between a and b (p-value < 0.05) and non-significant between a and a (p-value > 0.5).*
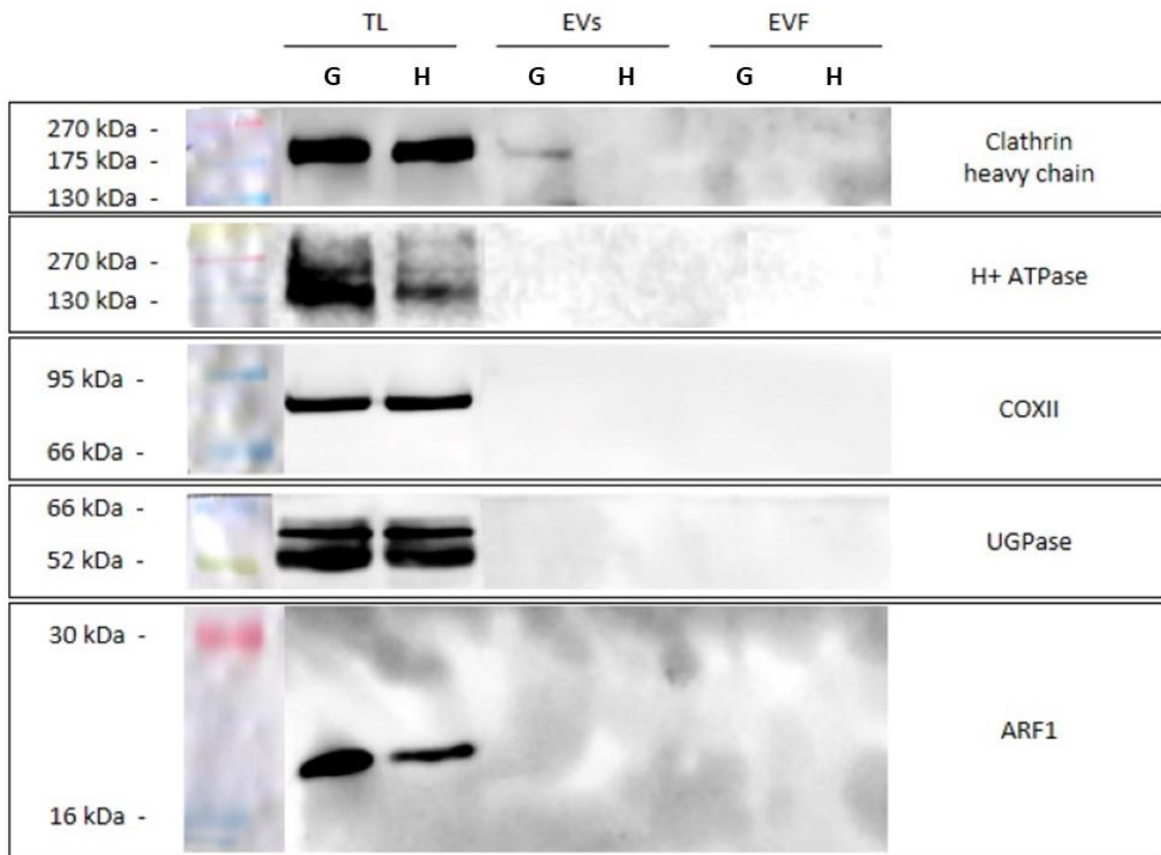
Figure 5 *Western blot analysis of TL, EV and EVF fractions from hydrated (H) and germinated (G) pollen samples.*
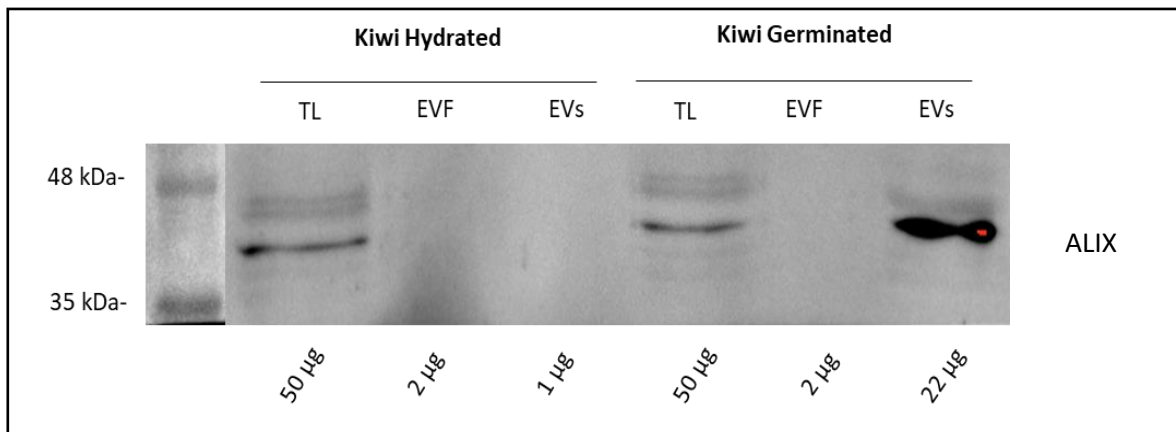
Figure 6 *Western blot analysis of TL, EV, and EVF fractions from hydrated and germinated kiwi pollen, probed for ALIX.*

Table 8 List of the proteins identified in all three replicas of germinated kiwi pollen EV samples, identified using 2 or more peptides and with 95% coverage over 70% of the length of the peptides. Proteins are ordered by decreasing values of maximum length of 95% coverage and maximum number of peptides. Information not available on UniProtKB and/or in literature were marked as "Unknown".

Protein	Family	Cellular localisation	Biological process
Late embryogenesis abundant protein	Late embryogenesis abundant protein (LEA) family protein (90% homology)	Plasma membrane	Response to dehydration
Fructose-bisphosphate aldolase	Class I fructose-bisphosphate aldolase family	Cytoplasm, plastids	Glycolytic process
Stress-induced protein	Late embryogenesis abundant protein (LEA) family protein (90% homology)	Unknown	Stress response
S-adenosylmethionine synthase	Adomet synthase family	Cytoplasm	One-carbon metabolic process, s-adenosylmethionine biosynthetic process
UDP-arabinopyranose mutase	Reversibly Glycosylated Proteins (RGP) family	Cytoplasm	Plant-type cell wall organization or biogenesis
Proteasome subunit alpha type (Fragment)	Peptidase T1A family	Cytoplasm, nucleus	Ubiquitin-dependent protein catabolic process
Carbonic anhydrase	Beta-class carbonic anhydrase family	Cytoplasm, plastids	Carbon utilization
Adenosylhomocysteinase	Adenosylhomocysteinase family	Cytoplasm, plasma membrane, vacuole, tonoplast	One-carbon metabolic process
Adenylate kinase (Fragment)	Adenylate kinase family	Cytoplasm, plastids	'De novo' pyrimidine nucleobase biosynthetic process
Inorganic diphosphatase	Ppase family	Cytoplasm	Phosphate-containing compound metabolic process
Calcium-binding protein	EF hand calcium-binding protein family (90% homology)	Unknown	Calcium ion binding
Fructokinase-2 like	Carbohydrate kinase pfkB family	Unknown	Starch biosynthetic process
Serine hydroxymethyltransferase	SHMT family	Cytoplasm, mitochondrion	Glycine biosynthetic process from serine, methylation, tetrahydrofolate interconversion

Proteasome subunit beta	Peptidase T1B family	Cytoplasm, nucleus	Proteolysis involved in cellular protein catabolic process
26S proteasome non-ATPase regulatory subunit 8 A like	Proteasome subunit S14 family	Proteasome, membrane	Proteolysis
Phosphoglycerate kinase	Phosphoglycerate kinase family	Chloroplast, cytoplasm, nucleus	Glycolytic process
UTP--glucose-1-phosphate uridylyltransferase	UDPGP type 1 family (50% similarity)	Unknown	Uridylyltransferase activity
UDP-glucuronate decarboxylase	NAD(P)-dependent epimerase/dehydratase family UDP-glucuronic acid decarboxylase subfamily	Membrane	D-xylose metabolic process, UDP-d-xylose biosynthetic process
Proteasome subunit alpha type	Peptidase T1A family	Nucleus, cytoplasm	Ubiquitin-dependent protein catabolic process
Triosephosphate isomerase	Triosephosphate isomerase family	Cytoplasm, plastids	Glycolytic process
Phosphopyruvate hydratase	Enolase family	Cytoplasm, nucleus	Glycolytic process
26S protease regulatory subunit 6A (Fragment)	AAA ATPase family	Cytoplasm, proteasome	Protein catabolic process
Phosphoglucomutase (alpha-D-glucose-1,6-bisphosphate-dependent)	Phosphohexose mutase family	Cytoplasm, plastids	Glucose metabolic process
Glyceraldehyde-3-phosphate dehydrogenase	Glyceraldehyde-3-phosphate dehydrogenase family	Cytoplasm, plastids	Glucose metabolic process
Tubulin beta chain	Tubulin family	Cytoskeleton	Microtubule-based process
Eukaryotic initiation factor 4A-14	Eukaryotic initiation factor 4A-14 family	Unknown	Protein biosynthesis
Actin-depolymerizing factor 7 like (Fragment)	Actin-binding proteins ADF family	Cytoskeleton	Actin filament depolymerization
Profilin	Profilin family	Cytoskeleton	Actin-binding

Glutaredoxin like	Glutaredoxin family CPYC subfamily	Unknown	Electron transport
26S protease regulatory subunit 6A like	AAA ATPase family	Cytoplasm, proteasome	Protein catabolic process
Heat shock protein 70 family protein	Heat shock protein 70 family	Cytoplasm, nucleus, mitochondria	Stress response
UDP-glucose 6-dehydrogenase	UDP-glucose/GDP-mannose dehydrogenase family	Cell wall, cytoplasm, nucleus, secretory vesicles	UDP-glucuronate biosynthetic process
Guanosine nucleotide diphosphate dissociation inhibitor	Rab GDI family	Cytoplasm, apoplast, plasmodesma	Protein transport, small GTPase mediated signal transduction
Mediator of RNA polymerase II transcription subunit 37e	Heat shock protein 70 family	Unknown	ATPase activity
Eukaryotic initiation factor 4A-11	DEAD box helicase family	Unknown	Protein biosynthesis
Methylenetetrahydrofolate reductase	Methylenetetrahydrofolate reductase family	Unknown	Methionine metabolic process, tetrahydrofolate interconversion
UDP-4-keto-6-deoxy-D-glucose 3,5-epimerase/UDP-4-keto-L-rhamnose 4-keto-reductase	Unknown	Nucleus, cytoplasm, plasmodesma	Nucleotide-sugar metabolic process
Elongation factor 1-alpha	TRAFAC class translation factor GTPase superfamily Classic translation factor GTPase family, EF-Tu/EF-1A subfamily	Cytoplasm	Unknown
Actin-97	Actin family	Cytoskeleton	ATP-binding
Pyrophosphate--fructose 6-phosphate 1-phosphotransferase subunit alpha	Phosphofructokinase type A (PFKA) family, ppi-dependent PFK group II subfamily Clade 'Long' sub-subfamily	Cytoplasm	Glycolytic process
Actin-7	Actin family	Cytoskeleton	ATP-binding
Pyrophosphate--fructose 6-phosphate 1-phosphotransferase subunit beta	Phosphofructokinase type A (PFKA) family, ppi-dependent PFK group II subfamily Clade 'Long' sub-subfamily	Cytoplasm	Fructose 6-phosphate metabolic process (glycolytic process)
14-3-3-like protein	14-3-3 family	Unknown	Unknown

Glycine-rich RNA-binding protein	Unknown	Unknown	RNA-bidning
Bifunctional dTDP-4-dehydrorhamnose 3,5-epimerase/dTDP-4-dehydrorhamnose reductase	dTDP-4-dehydrorhamnose reductase family	Cytoplasm, plasma membrane, plasmodesma	Cell wall organization, dTDP-rhamnose biosynthetic process, UDP-rhamnose biosynthetic process
26S proteasome non-ATPase regulatory subunit like	Proteasome subunit S9 family Proteasome subunit S5A family	Proteasome	Protein catabolic process
Peptidyl-prolyl cis-trans isomerase	Cyclophilin-type ppiase family	Unknown	Protein folding
Fructokinase-4 like	Carbohydrate kinase pfkb family	Unknown	Starch biosynthetic process
Acetyl-CoA acetyltransferase	Thiolase family	Cytoplasm	Acyltransferase
T-complex protein 1 subunit delta	TCP-1 chaperonin family	Cytoplasm	Protein folding
Elongation factor (Fragment)	Classic translation factor GTPase family, EF-G/EF-2 subfamily	Cytoplasm	Protein biosynthesis
CCT-beta (Fragment)	TCP-1 chaperonin family	Unknown	Protein folding
Clathrin heavy chain like	Clathrin heavy chain family	TGN, plasma membrane	Intracellular protein transport, vesicle-mediated transport
Calmodulin	Unknown	Unknown	Calcium ion binding
26S protease regulatory subunit 7	AAA ATPase family	Cytoplasm, proteasome	Protein catabolic process
26S protease regulatory subunit 7B	AAA ATPase family	Cytoplasm, proteasome	Protein catabolic process

3.3   Localization of Chlatrin, ALIX and ARF1 in the pollen tube
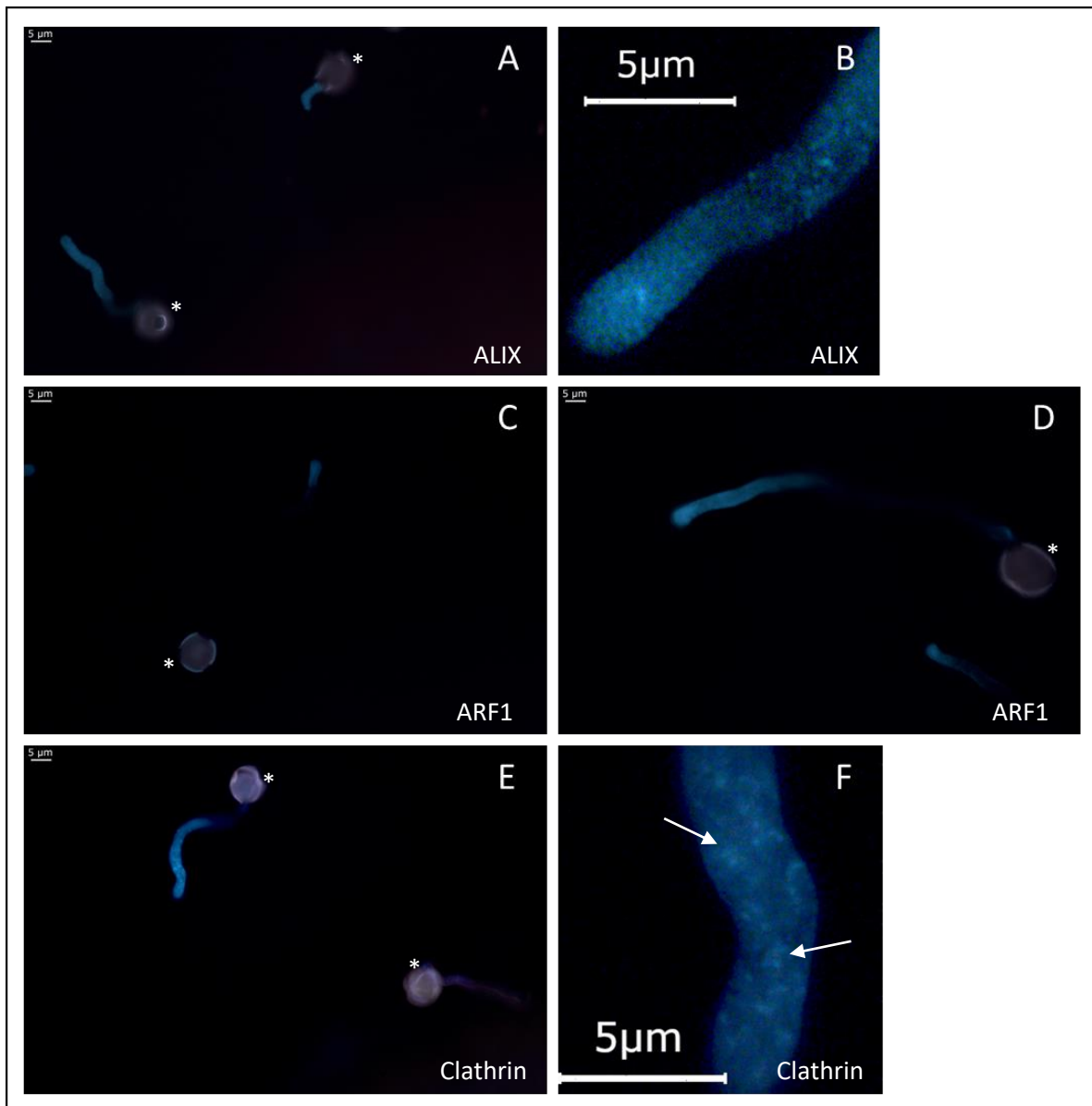
Figure 5 *Indirect immunofluorescence labelling of germinated kiwi pollen with FITC-conjugated secondary antibodies, probed for ALIX (A, B), ARF1 (C, D), and Clathrin heavy chain (E, F). The autofluorescence of the pollen wall is visible in violet (*), while in blue is pictured the fluorescent labelling of the target proteins. F shows a detail of the clustering for Clathrin heavy chain spots (indicated by the arrows).*

Immunofluorescence labelling revealed the presence of ALIX-homologs, ARF1, and Clathrin heavy chain in the pollen tube (Fig. 7). In particular, ALIX-homologs seemed to be localised

almost homogeneously in all the metabolically active portion of the pollen tube (Fig. 7A and 7B), while ARF1 appeared to be more concentrated towards the tube tip (Fig. 7C and 7D). Clathrin heavy chain had a localisation compatible with that shown by ALIX (Fig. 7E), but it appeared to form clusters compatible with its function and localisation on the plasma membrane (Fig. 7F). The negative control excluded nonspecific fluorescence for the pollen tube.

Immunogold labelling allowed to investigate the distribution of possible ALIX-homologs on a subcellular level. The negative control confirmed that nonspecific binding of gold-conjugated secondary antibodies did not impair the analysis. ALIX-homologs were distributed in the pollen tube cytoplasm, but also associated with small vesicles near the plasma membrane (Fig. 8).
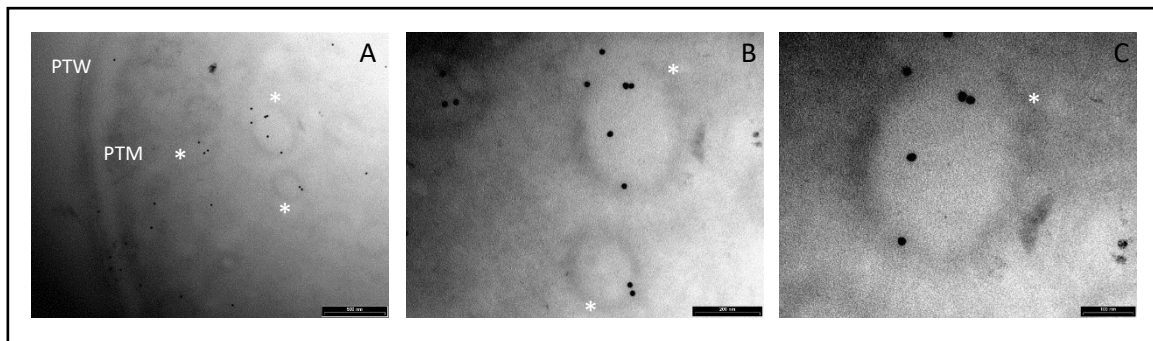
Figure 6 *Immunogold labelling of ALIX-homologs in a transverse section of kiwi pollen tube. Pictures A, B, and C represent a progressive zoom on one of the subcellular structures compatible with vesicles (*), near the plasma membrane. PTW= pollen tube wall, PTM= pollen tube plasma membrane.*

4.   Discussion

4.1   Nanoparticles can be isolated from kiwi pollen after ultracentrifugation

This study demonstrated that nanoparticles can be isolated from kiwi pollen samples after ultracentrifugation at 10000 x g (Fig. 1, 2). While this has already been established for germinated pollen of other species (Prado et al., 2014, 2015), it is to our knowledge the first time that such nanoparticles have been also isolated from hydrated pollen, although Grote and colleagues described similar nanoparticles released after hydration in rainwater by birch,

alder, hazel, and ryegrass pollen, using electron microscopy (Grote et al., 2000, 2003). However, while pollen studied by Grote and colleagues underwent germinative abortion during hydration, kiwi pollen used in this study showed 0% germination rate after hydration, performed either in humid chamber or in PBS. It is clear however that hydrated kiwi pollen releases a significantly smaller amount of nanoparticles than germinated kiwi pollen (Fig. 1). When samples containing the same concentration of nanoparticles isolated from HKP and GKP were visualised in AFM, it was possible to appreciate rounded, vesicle-like structures (Fig. 2) in both groups, compatible for dimensions and shape with small extracellular vesicles (Prado et al., 2014, 2015; Kurian et al., 2021).

4.2 Nanoparticles released by germinated kiwi pollen are nanovesicles

When EVs isolated from the same sample size of GKP, HKP, and PKP were stained with FM4-64™, only GKP EVs showed a detectable fluorescent signal, meaning that the nanoparticles isolated were nanovesicles with a double-layered lipidic membrane (Fig. 3). The absence of a fluorescent signal in PKP EVs indicates that the secretion of such vesicles is not promoted by the resuspension of pollen in a liquid medium, but rather by the germination process itself. The relatively high protein content of GKP EV (Fig. 4) corroborates the idea that GKP secretes nanovesicles, and the low protein concentrations in EVF fractions seem to exclude the possibility of a significant contamination of the EV fraction by secreted proteins. While in the light of particle tracking analysis and AFM results (Fig. 1, 2) it is not possible to rule out that HKP can secrete extracellular nanovesicles, it is apparent that, if present, its secretion rate is very low and almost undetectable.

To furtherly assess that proteins and membranes found in GKP EV fraction did not derive from pollen tube rupture and cell debris, total protein content of TL, EV, and EVF fractions from both GKP and HKP was probed for known molecular markers of different organelles. The immunoblotting analysis excluded the presence of contaminations from plasma membrane, mitochondria, cytoplasm, and Golgi apparatus in EV and EVF fractions (Fig. 5), confirming that pollen integrity was preserved throughout the EVs isolation process.

Proteomic analysis of GKP EVs revealed the presence in all three replicas of Ole e 1 (Table 1S), which was described as a pollensome molecular marker by Prado and colleagues (Prado et al., 2014; Hafidh et al., 2016), thus validating the presence of extracellular nanovesicles in the GKP EVs. Like those found in pollensomes (Prado et al., 2014), the majority of proteins identified in GKP EVs are involved in metabolic and biosynthetic processes, cell signaling, vesicular trafficking, cytoskeletal movements, and stress response (Tab. 1). Moreover, proteins that are thought to be involved in the cell wall reorganisation needed for vesicles secretion, like α-L-arabinofuranosidase, Glucosidases, Galactosidases, and Pectinases (Woith et al., 2021), have been identified in GKP EVs (Tab. 1S).

4.3 Nanovesicles secreted by germinated kiwi pollen could be exosomes

The EV isolation employed hereby was originally designed for mammalian exosomes (Prado et al., 2014; Furini et al., 2018; Kurian et al., 2021). The nanoparticles isolated in this study resulted on average larger in size than those described as pollensomes (Prado et al., 2014), but nonetheless their peak and median diameters fell within the accepted range for exosomes (Fig. 1) and are compatible with published plant exosomes dimensions (Rutter and Innes, 2017). The tendency to aggregation shown by these particles during particle tracking analysis, AFM, and FM4-64™ staining (Fig. 2, 3), might explain the difference with the published pollensomes dimensions.

Immunoblotting revealed the presence of Clathrin heavy chain in GKP EV fraction, while this protein was absent from HKP EVs and EVFs of both samples (Fig. 5). Clathrin light and heavy chains, Clathrin heavy chain like proteins, Clathrin coat assembly proteins, and Clathrin interactors EPSIN like where also identified in GKP EVs by RP-HPLC-ESI-MS/MS analysis (Tab. 1, S1). Since Clathrin is involved in endocytic processes (Narasimhan et al., 2020), its presence in the EV fraction may support the hypothesis of Prado and collaborators that these extracellular nanovesicles could have an endocytic origin (An et al., 2007; Prado et al., 2014). In fact, while it is not considered an exosome marker, Clathrin heavy chain is often found in exosomes (Woith et al., 2021). It is possible that during the formation of exosomes, Clathrin triskelions derived from the disassembly of endocytic vesicles coatings are still present in the

cytoplasm near the endosome, and might be incorporated in the ILVs lumina, as it happens for other cytoplasmic molecules (Kurian et al., 2021). In fact, in GKP EVs proteome Dynamin and Dynamin-related protein like were also identified (Tab. 1s), which are involved in the removal of Clathrin coating from endocytic vesicles. The fluorescence immunolabelling of Clathrin heavy chain highlighted its presence in clusters along the pollen tube, suggesting the possibility of ongoing endocytic events (Fig. 7E, 7F), thus supporting this hypothesis.

The proteomic analysis identified the presence of ARFs, ARF-GAPs, and ARF-GEFs in GKP EVs (Tab. S1). However, ARF1, that is considered a molecular marker for Golgi membranes (Robinson et al., 2011), was not detected in EVs by immunoblotting (Fig. 5). The fluorescence immunolabelling of ARF1 on germinated pollen grains showed its presence in particular towards the tip of the pollen tube (Fig. 7C, 7D), describing the distribution of the Golgi apparatus during the apical growth, but also likely indicating the presence of vesicles that have been processed in the TGN, and are involved in the intense intracellular trafficking observed during pollen tube growth. The absence of Golgi markers in GKP EVs could imply that these nanovesicles bypassed the Golgi apparatus and underwent unconventional secretion (Del Duca et al., 2013; Hafidh et al., 2016; Rabouille, 2017), which is in line with the exosome hypothesis. In fact, the proteomic analysis revealed the presence of proteins that have been found to be unconventionally secreted during pollen tube growth, such as Actin, Adenosine kinase (ADK), ARF/ARFGAP, Gp-dh-C domain containing proteins, HSP70, proteasome subunits, Ras, Ribonucleosid-diphospate reductase large subunit (RRM1), UDP-arabinopyranose mutase, and the translationally controlled tumor protein (NtTCTP) which is thought to be involved in pollen tube guidance and ovule targeting (Tab. 1, S1). Contrarily, only few proteins known to be conventionally secreted and abundant in germinated pollen secretome were found in EVs proteome (Hafidh et al., 2016). An Exocyst subunit Exo70 was identified in the GKP EVs (Tab S1), but their staining with FM4-64™ (Fig. 3) indicates the presence of a lipidic bilayer, excluding the unconventional secretion by EXPOs, that produces single-layered extracellular vesicles (Wang et al., 2010; Hafidh et al., 2016). EVs proteomic analysis also identified proteins involved in signal transduction, *e.g.* a total of 277 Kinases, and

a Cysteine protease family protein that could act as a ligand (Hafidh et al., 2016), and this is consistent with the role of exosomes in cell-cell communication.

Proteomic analysis also revealed the presence in GKP EVs of proteins that are common in either plant or mammalian exosomes, like HSP70, Chaperones, Syntaxins, Tetraspanins, Ubiquine-like proteins, and Ubiquitin-related enzymes (Tab. 1, 1S) (Johnstone, 2006; Rutter and Innes, 2017; Kurian et al., 2021). Ras-related Rab proteins (Tab. 1S), that have been described as possible markers for plant exosomes (Regente et al., 2009), were also found. Moreover, using a polyclonal anti-ALIX antibody it was possible to detect the presence of putative ALIX-homologs in GKP EVs (Fig. 6). This protein was clearly more concentrated in EVs than in TL, suggesting a possible role of this protein in the formation or secretion of the nanovesicles. In fact, plant homologs of ALIX are known to participate in the differentiation of MVBs and to be involved in vesicular trafficking (Kalinowska et al., 2015; Cui et al., 2016; García-León and Rubio, 2020). The protein band had a molecular weight of about 43 kDa, that is compatible with the molecular weight estimated for ALIX-homolog encoded by the gene CEY00_Acc28537 of *Actinidia chinensis* var. *chinensis* (UniProt Consortium, 2021). The immunofluorescence labelling of ALIX-homologs allowed to visualise their homogeneous distribution in the metabolically active portion of the elongating pollen tube (Fig. 7A, 7B). This was confirmed by immunogold labelling that localised the proteins both in the cytoplasm and associated with vesicle-like structures near the pollen tube membrane (Fig. 8), which is compatible with the known subcellular localisation and mechanisms of ALIX and BRO1-domain containing proteins (Bissig and Gruenberg, 2014; García-León and Rubio, 2020), and with the observed localisation of Ole e 1 in the pollen tubes (Prado et al., 2014). However, as for Prado and colleagues it was not possible in this study to visualise putative ILVs inside the vesicle-like structures associated with ALIX-homologs, and thus it is not possible to assess the presence of an MVB with the imaging techniques employed hereby. However, the presence of ESCRT-related proteins in GKP EVs proteome reinforces the idea that pollen extracellular nanovesicles could derive from MVBs, since ESCRT known functions in plant cells are related

to the ILVs formation and possibly to the MVB fusion with the plasma membrane (Gao et al., 2017).

5.   Conclusions

Pollen-pistil interactions have always been a fascinating yet elusive topic in plant molecular biology. Studies on pollen secretome are starting to shade light on the molecules involved in pollen hydration, pollen-stigma compatibility, pollen tube entrance, and tube guidance through the style (Del Duca et al., 2010; Hafidh et al., 2014, 2016; Mandrone et al., 2019). Since intercellular communication is fundamental for a successful fertilisation, it is plausible that bioactive molecules might be secreted by pollen through vesicles, to stabilise them during their journey towards their target. In this study, a population of extracellular nanovesicles released by kiwi pollen during *in vitro* germination was isolated and characterised using different proxies. These vesicles appeared to be consistent with the pollensomes described by Prado and colleagues (Prado et al., 2014, 2015), and also met several criteria in the definition of exosomes (Suhandono et al., 2014b; Kurian et al., 2021). In fact, they were isolated by centrifugation at 10000 x g, had a diameter of 150 nm (Fig. 1), a rounded shape (Fig. 2), and a double-layered lipidic membrane (Fig. 3). They also carried proteins involved in endocytosis such as Clathrin, ESCRT-related proteins, and Dynamin, suggesting an endocytic origin (Tab. S1). This thesis is supported by the presence in their proteome of proteins that are usually unconventionally secreted, and the absence of the TGN marker ARF1, suggesting that they followed an unconventional secretion route. Several proteins and protein families known to be common in exosomes were found (Tab. 1, Tab. S1), including Ras-related Rab proteins, that are a possible plant exosome marker (Regente et al., 2009). Moreover, immunoblotting revealed an enrichment in plant homologs of a well-known mammalian exosome marker, ALIX, that are proven to be involved in ILVs formation and cargo sorting (Fig. 6). Immunolocalisation revealed the presence of ALIX homologs along the growing pollen tube (Fig. 7A, 7B), and they were associated with vesicle-like organelles near the pollen tube wall (Fig. 8). However, it was not possible to visualise MVBs in electron microscopy, hence it is still difficult to assess the exact biogenesis of these vesicles. Nonetheless, the presence of Clathrin

clusters along the pollen tube (Fig. 7E, 7F) might indicate the presence of ongoing endocytic events, thus supporting the theory that pollensomes derive from ILVs and explaining the presence of Clathrin heavy chain in the vesicles (Fig. 5).

While further investigation into these vesicles is surely needed to characterise their biogenesis and secretion route, this work contributes to amplify the still scarce knowledge on pollen extracellular nanovesicles features, and on the proteins that are possibly involved in their formation, release, and biological function.

6. Bibliography

Akuma, P., Okagu, O. D., and Udenigwe, C. C. (2019). Naturally Occurring Exosome Vesicles as Potential Delivery Vehicle for Bioactive Compounds. Front. Sustain. Food Syst. 3, 1–8. doi:10.3389/fsufs.2019.00023.

Al-Whaibi, M. H. (2011). Plant heat-shock proteins: A mini review. J. King Saud Univ. - Sci. 23, 139–150. doi:10.1016/J.JKSUS.2010.06.022.

An, Q., Van Bel, A. J. E., and Hückelhoven, R. (2007). Do plant cells secrete exosomes derived from multivesicular bodies? Plant Signal. Behav. 2, 4–7. doi:10.4161/psb.2.1.3596.

Anderson, L. E., Bryant, J. A., and Carol, A. A. (2004). Both chloroplastic and cytosolic phosphoglycerate kinase isozymes are present in the pea leaf nucleus. Protoplasma 2004 2232 223, 103–110. doi:10.1007/S00709-004-0041-Y.

Bissig, C., and Gruenberg, J. (2014). ALIX and the multivesicular endosome: ALIX in Wonderland. Trends Cell Biol. 24, 19–25. doi:10.1016/J.TCB.2013.10.009.

Cheung, A. Y., and Wu, H. M. (2008). Structural and signaling networks for the polar cell growth machinery in pollen tubes. Annu. Rev. Plant Biol. 59, 547–572. doi:10.1146/annurev.arplant.59.032607.092921.

Cui, Y., Shen, J., Gao, C., Zhuang, X., Wang, J., and Jiang, L. (2016). Biogenesis of Plant Prevacuolar Multivesicular Bodies. Mol. Plant 9, 774–786. doi:10.1016/j.molp.2016.01.011.

Del Duca, S., Cai, G., Di Sandro, A., and Serafini-Fracassini, D. (2010). Compatible and self-incompatible pollination in Pyrus communis displays different polyamine levels and transglutaminase activity. Amino Acids 38, 659–667. doi:10.1007/S00726-009-0426-5.

Del Duca, S., Serafini-Fracassini, D., and Cai, G. (2013). An unconventional road for the secretion of transglutaminase in pollen tubes? Plant Signal. Behav. 8, 8–11. doi:10.4161/psb.24446.

Dumont, S., Bykova, N. V., Pelletier, G., Dorion, S., and Rivoal, J. (2016). Cytosolic triosephosphate isomerase from Arabidopsis thaliana is reversibly modified by glutathione on cysteines 127 and 218. Front. Plant Sci. 7, 1942. doi:10.3389/FPLS.2016.01942/BIBTEX.

Furini, G., Schroeder, N., Huang, L., Boocock, D., Scarpellini, A., Coveney, C., et al. (2018). Proteomic profiling reveals the transglutaminase-2 externalization pathway in kidneys after unilateral ureteric obstruction. J. Am. Soc. Nephrol. 29, 880–905. doi:10.1681/ASN.2017050479.

Gao, C., Zhuang, X., Shen, J., and Jiang, L. (2017). Plant ESCRT Complexes: Moving Beyond Endosomal Sorting. Trends Plant Sci. 22, 986–998. doi:10.1016/J.TPLANTS.2017.08.003/ATTACHMENT/C7A3A70E-8C86-4FBC-90E0-E335130913E1/MMC1.MP4.

García-León, M., and Rubio, V. (2020). Biochemical and Imaging Analysis of ALIX Function in Endosomal Trafficking of Arabidopsis Protein Cargoes. Methods Mol. Biol. 2177, 49–58. doi:10.1007/978-1-0716-0767-1_5.

Goring, D. R. (2017). Exocyst, exosomes, and autophagy in the regulation of Brassicaceae pollen-stigma interactions. J. Exp. Bot. 69, 69–78. doi:10.1093/jxb/erx340.

Grote, M., Valenta, R., and Reichelt, R. (2003). Abortive pollen germination: A mechanism of allergen release in birch, alder, and hazel revealed by immunogold electron microscopy. J. Allergy Clin. Immunol. 111, 1017–1023. doi:10.1067/mai.2003.1452.

Grote, M., Vrtala, S., Niederberger, V., Valenta, R., and Reichelt, R. (2000). Expulsion of allergen-containing materials from hydrated rye grass (Lolium perenne) pollen revealed by using immunogold field emission scanning and transmission electron microscopy. J. Allergy Clin. Immunol. 105, 1140–1145. doi:10.1067/mai.2000.107044.

Hafidh, S., Potěšil, D., Fíla, J., Čapková, V., Zdráhal, Z., and Honys, D. (2016). Quantitative proteomics of the tobacco pollen tube secretome identifies novel pollen tube guidance proteins important for fertilization. Genome Biol. 17, 1–29. doi:10.1186/s13059-016-0928-x.

Hafidh, S., Potěšil, D., Fíla, J., Fecikova, J., Čapková, V., Zdráhal, Z., et al. (2014). In search of ligands and receptors of the pollen tube: the missing link in pollen tube perception. Biochem. Soc. Trans. 42, 388–394. doi:10.1042/BST20130204.

Hansen, L. L., and Nielsen, M. E. (2017). Plant exosomes: Using an unconventional exit to prevent pathogen entry? J. Exp. Bot. 69, 59–68. doi:10.1093/jxb/erx319.

Javeed, N., and Mukhopadhyay, D. (2017). Exosomes and their role in the micro-/macro-environment: A comprehensive review. J. Biomed. Res. 31, 386–394. doi:10.7555/JBR.30.20150162.

Johnstone, R. M. (2006). Exosomes biological significance: A concise review. Blood Cells, Mol. Dis. 36, 315–321. doi:10.1016/j.bcmd.2005.12.001.

Kalinowska, K., Nagel, M. K., Goodman, K., Cuyas, L., Anzenberger, F., Alkofer, A., et al. (2015). Arabidopsis ALIX is required for the endosomal localization of the deubiquitinating enzyme AMSH3. Proc. Natl. Acad. Sci. U. S. A. 112, E5543–E5551. doi:10.1073/PNAS.1510516112/-/DCSUPPLEMENTAL.

Kawai, M., and Uchimiya, H. (1995). Biochemical properties of rice adenylate kinase and subcellular location in plant cells. Plant Mol. Biol. 27, 943–951. doi:10.1007/BF00037022.

Kurian, T. K., Banik, S., Gopal, D., Chakrabarti, S., and Mazumder, N. (2021). Elucidating Methods for Isolation and Quantification of Exosomes: A Review. Mol. Biotechnol. 63, 249–266. doi:10.1007/s12033-021-00300-3.

Kuttiyatveetil, J. R. A., and Sanders, D. A. R. (2017). Analysis of plant UDP-arabinopyranose mutase (UAM): Role of divalent metals and structure prediction. Biochim. Biophys. Acta - Proteins Proteomics 1865, 510–519. doi:10.1016/J.BBAPAP.2017.02.005.

Lu, W., Tang, X., Huo, Y., Xu, R., Qi, S., Huang, J., et al. (2012). Identification and characterization of fructose 1,6-bisphosphate aldolase genes in Arabidopsis reveal a gene family with diverse responses to abiotic stresses. Gene 503, 65–74. doi:10.1016/J.GENE.2012.04.042.

Mandrone, M., Antognoni, F., Aloisi, I., Potente, G., Poli, F., Cai, G., et al. (2019). Compatible and incompatible pollen-styles interaction in Pyrus communis l. Show different transglutaminase features, polyamine pattern and metabolomics profiles. Front. Plant Sci. 10, 1–13. doi:10.3389/FPLS.2019.00741/BIBTEX.

Narasimhan, M., Johnson, A., Prizak, R., Kaufmann, W. A., Tan, S., Casillas-Pérez, B., et al. (2020). Evolutionarily unique mechanistic framework of clathrin-mediated endocytosis in plants. Elife 9. doi:10.7554/ELIFE.52067.

Olvera-Carrillo, Y., Reyes, J. L., and Covarrubias, A. A. (2011). Late embryogenesis abundant proteins: Versatile players in the plant adaptation to water limiting environments. Plant Signal. Behav. 6, 586. doi:10.4161/PSB.6.4.15042.

Paris, R., Pagliarani, G., Savazzini, F., Aloisi, I., Iorio, R. A., Tartarini, S., et al. (2017). Comparative analysis of allergen genes and pro-inflammatory factors in pollen and fruit of apple varieties. Plant Sci. 264, 57–68. doi:10.1016/J.PLANTSCI.2017.08.006.

Parrotta, L., Aloisi, I., Suanno, C., Faleri, C., Kiełbowicz-Matuk, A., Bini, L., et al. (2019). A low molecular-weight cyclophilin localizes in different cell compartments of Pyrus communis pollen and is released in vitro under Ca2+ depletion. Plant Physiol. Biochem. 144, 197–206. doi:10.1016/J.PLAPHY.2019.09.045.

Parrotta, L., Faleri, C., Duca, S. Del, and Cai, G. (2018). Depletion of sucrose induces changes in the tip growth mechanism of tobacco pollen tubes. Ann. Bot. 122, 23–43. doi:10.1093/aob/mcy043.

Parton, R. M., Fischer-Parton, S., Trewavas, A. J., and Watahiki, M. K. (2003). Pollen tubes exhibit regular periodic membrane trafficking events in the absence of apical extension. J. Cell Sci. 116, 2707–2719. doi:10.1242/jcs.00468.

Prado, N., De Dios Alché, J., Casado-Vela, J., Mas, S., Villalba, M., Rodríguez, R., et al. (2014). Nanovesicles are secreted during pollen germination and pollen tube growth: A possible role in fertilization. Mol. Plant 7, 573–577. doi:10.1093/mp/sst153.

Prado, N., De Linares, C., Sanz, M. L., Gamboa, P., Villalba, M., Rodríguez, R., et al. (2015). Pollensomes as Natural Vehicles for Pollen Allergens. J. Immunol. 195, 445–449. doi:10.4049/jimmunol.1500452.

Rabouille, C. (2017). Pathways of Unconventional Protein Secretion. Trends Cell Biol. 27, 230–240. doi:10.1016/J.TCB.2016.11.007.

Regente, M., Corti-Monzón, G., Maldonado, A. M., Pinedo, M., Jorrín, J., and de la Canal, L. (2009). Vesicular fractions of sunflower apoplastic fluids are associated with potential exosome marker proteins. FEBS Lett. 583, 3363–3366. doi:10.1016/j.febslet.2009.09.041.

Robinson, D. G., Scheuring, D., Naramoto, S., and Friml, J. (2011). ARF1 Localizes to the Golgi and the Trans-Golgi Network. Plant Cell 23, 846. doi:10.1105/TPC.110.082099.

RStudio Team (2020). RStudio: Integrated Development for R. Available at: http://www.rstudio.com/.

Rutter, B. D., and Innes, R. W. (2017). Extracellular vesicles isolated from the leaf apoplast carry stress-response proteins. Plant Physiol. 173, 728–741. doi:10.1104/pp.16.01253.

Saqib, A., Scheller, H. V., Fredslund, F., and Welner, D. H. (2019). Molecular characteristics of plant UDP-arabinopyranose mutases. Glycobiology 29, 839. doi:10.1093/GLYCOB/CWZ067.

Sebaihi, N., De Boeck, B., Yuana, Y., Nieuwland, R., and Pétry, J. (2017). Dimensional characterization of extracellular vesicles using atomic force microscopy. Meas. Sci. Technol. 28, 1–8. doi:10.1088/1361-6501/28/3/034006.

Suhandono, S., Apriyanto, A., and Ihsani, N. (2014a). Isolation and characterization of three cassava elongation factor 1 alpha (MeEF1A) promoters. PLoS One 9. doi:10.1371/JOURNAL.PONE.0084692.

Suhandono, S., Apriyanto, A., and Ihsani, N. (2014b). Isolation and Characterization of Three Cassava Elongation Factor 1 Alpha (MeEF1A) Promoters. PLoS One 9, e84692. doi:10.1371/JOURNAL.PONE.0084692.

Tiwari, A., Kumar, P., Singh, S., and Ansari, S. A. (2005). Carbonic anhydrase in relation to higher plants. Photosynthetica 43, 1–11.

UniProt Consortium (2021). https://www.uniprot.org/uniprot/. Available at: https://www.uniprot.org/uniprot/.

Wang, J., Ding, Y., Wang, J., Hillmer, S., Miao, Y., Lo, S. W., et al. (2010). EXPO, an exocyst-positive organelle distinct from multivesicular endosomes and autophagosomes, mediates cytosol to cell wall exocytosis in Arabidopsis and tobacco cells. Plant Cell 22, 4009–4030. doi:10.1105/TPC.110.080697.

Woith, E., Guerriero, G., Hausman, J. F., Renaut, J., Leclercq, C. C., Weise, C., et al. (2021). Plant extracellular vesicles and nanovesicles: Focus on secondary metabolites, proteins and lipids with perspectives on their potential and sources. Int. J. Mol. Sci. 22, 1–20. doi:10.3390/ijms22073719.

7. A low molecular-weight cyclophilin localizes in different cell compartments of *Pyrus communis* pollen and is released in vitro under Ca2+ depletion

Abstract

Cyclophilins (CyPs) are ubiquitous proteins involved in a wide variety of processes including protein maturation and trafficking, receptor complex stabilization, apoptosis, receptor signaling, RNA processing, and spliceosome assembly. The ubiquitous presence is justified by their peptidyl-prolyl *cis-trans* isomerase (PPIase) activity, catalyzing the rotation of X-Pro peptide bonds from a *cis* to a *trans* conformation, a critical rate-limiting step in protein folding, as over 90% of proteins contain trans prolyl imide bonds. In Arabidopsis 35 CyPs involved in plant development have been reported, showing different subcellular localizations and tissue- and stage-specific expression. In the present work, we focused on the localization of CyPs in pear (*Pyrus communis*) pollen, a model system for studies on pollen tube elongation and on pollen-pistil self-incompatibility response. Fluorescent, confocal and immuno-electron microscopy showed that this protein is present in the cytoplasm, organelles and cell wall, as confirmed by protein fractionation. Moreover, an 18-kDa CyP isoform was specifically released extracellularly when pear pollen was incubated with the Ca^{2+} chelator EGTA.

Keywords: Cyclophilin, Pollen tube, *Pyrus communis*, EGTA.

Abbreviations: CyP, Cyclophilin; LC-ESI/MS-MS, Liquid chromatography electrospray ionization-tandem MS; MS, Mass spectrometry; PMF, Peptide mass finger-

printing; PPIase, Peptidyl-prolyl cis-TRANS isomerase; TEM, Transmission electron microscope.

1. Introduction

Cyclophilins (CyPs) were first described as intracellular target proteins for the immunosuppressive drug cyclosporin. These proteins play an active role in protein folding insofar as they catalyze the isomerization of peptidyl-prolyl bonds from the *cis-* to the *trans-* conformation (PPIase activity). Consequently, they are included in the protein family of molecular chaperones (Schreiber, 1991). Multiple CyPs in plants have been reported to have different tissue and cellular locations and to be associated with a multitude of functions and regulatory pathways through their foldase, scaffolding, chaperoning or other unknown activities. Many functions of plant CyPs have been proposed, but their physiological relevance in pollen germination or stress responses is still largely unknown (Kumari et al., 2013).

Plant CyPs were first identified in 1990 with the isolation of CyP cDNA sequences from tomato (*Solanum lycopersicum*), maize (*Zea mays*) and oilseed rape (*Brassica napus*) (Gasser et al., 1990). Later, the presence of CyPs was also demonstrated in carrot, pumpkin, raspberry, periwinkle, and rye grass pollen (Cadot et al., 2000, 2006; Marzban et al., 2008; De Canio et al., 2009; de Olano et al., 2010). CyP isoforms are usually encoded by large gene families (*e.g.* 35 genes in the Arabidopsis genome, 28 in rice) and classified according to whether they have a single CyP domain or additional functional domains (Trivedi et al., 2012). Plant CyPs localize in distinct cellular compartments or organelles, such as the cytosol, mitochondria and chloroplasts and their expression is modulated by different abiotic stresses such as heat-, cold-, drought, and salt stress, suggesting a role of these proteins in stress responses (Kumari et al., 2013). The role of CyPs in abiotic stress tolerance is further supported by recent studies demonstrating that the ectopic expression of CyP genes enhance tolerance to multiple abiotic stress conditions (Kaur et al., 2016; Romano et al., 2004). Plant development also requires several and specific CyP isoforms, *e.g.* in Arabidopsis CyP40 is specifically required for vegetative growth, but not for reproductive maturation of the shoot (Berardini et al., 2001),

while CyP5 is mainly involved in the coordination of cell polarity along the apical-basal embryo axis (Grebe et al., 2000).

Cadot and co-workers (Cadot et al., 2000) first showed the existence of CyPs in birch pollen and their extractability at alkaline pH, although it is not yet clear whether these CyPs are secreted from pollen grains or are pollen-coated proteins. In pollen, CyPs also localize in the cytosol, vegetative nuclei of grains, and generative cells, suggesting that CyPs are not exclusively pollen-coated proteins.

CyPs have been the subject of considerable scientific interest due to their high biochemical and clinical relevance. Being an IgE-binding protein, CyP is an allergen (Ghosh et al., 2014). CyP has a high homology with Bet v 7, one of the main birch pollen allergens (Cadot et al., 2000). Indeed, during the last decades CyP has been identified as a novel allergen also from olive, carrot, pumpkin, raspberry, periwinkle and rye grass pollen (Cadot et al., 2000, 2006; Fujita et al., 2001; San Segundo-Acosta et al., 2019; Marzban et al., 2008; de Olano et al., 2010; De Canio et al., 2009). Thus, CyP has been confirmed to be a pan-allergen and found to be cross-reactive across species, including humans (Fluckiger et al., 2002).

Numerous metabolic and cytosolic processes sustain the tip growth of pollen tubes (Cheung and Wu, 2008), among which the maintenance of a tip-focused cytosolic Ca^{2+} gradient, which is generally supported by an influx of Ca^{2+} through the apical plasma membrane (Steinhorst and Kudla, 2013). The tip-focused Ca^{2+} gradient is indispensable for pollen tube tip growth and orientation, as it regulates actin organization, protein kinase activities and exocytosis (Cardenas et al., 2008). In fact, the oscillatory increase of Ca^{2+} influx follows tube elongation but precedes the fusion of secretory vesicles (Coelho and Malho, 2006). While investigating the release of the extracellular Ca^{2+} signal transducer calmodulin (CaM) (Shang et al., 2005), Yokota and colleagues (Yokota et al., 2004) found that a 21-kDa CyP was specifically released into the extracellular medium when lily pollen was incubated in the presence of EGTA or at low concentrations of Ca^{2+}. However, the release mechanism of CyP from pollen grains and their role once released remains to be elucidated, even if an involvement in signal transduction during pollen tube growth in the style was hypothesized (Ghosh et al., 2014).

In spite of all this evidence regarding the role of CyPs in pollen tube growth, the distribution of CyPs in pollen remains to be elucidated. Therefore, in this work, we investigated for the first time, the localization of CyPs in pear pollen using several microscopy techniques and the different distribution of specific isoforms in grains and pollen tubes by chromatographic, electrophoretic, and immunological approaches.

2.   Materials and Methods

2.1   Plant material and pollen germination

Mature pollen of pear (*Pyrus communis* cv. Williams) was collected from plants grown in experimental plots at the University of Bologna (Department of Agricultural and Food Sciences). Pollen handling, storage, hydration and germination were performed as previously reported (Aloisi et al., 2015). After 1 h of germination, the medium was supplemented with different concentrations of EGTA (0.4 mM, 1 mM and 5 mM) up to 2 h. In control samples, pollen was allowed to germinate up to 2 h without any EGTA supplementation. For germination tests, pollen grains were gently washed with germination medium or HEMS buffer (25 mM Hepes pH 7.5, 3 mM EDTA, 2 mM $MgCl_2$, 15% sucrose) supplemented or not with EGTA and allowed to germinate in standard conditions for 2 h. Pollen was visualized under a light microscope (Nikon Eclipse E600) equipped with a digital camera (Nikon DXM1200). At least 100 pollen grains were counted to determine pollen tube length and percentage germination.

2.2   Fluorescence and confocal microscopy

Indirect immunofluorescence microscopy in pollen tubes was performed according to standard procedures (Cai et al., 2011). Briefly, germinated pollen samples were fixed with 3% paraformaldehyde in PM buffer (50 mM Pipes, pH 6.9, 1 mM EGTA, 0.5 mM $MgCl_2$) for 30 min, then cell wall digestion was performed with 1.5% cellulase. After two washes with PM buffer, samples were incubated with the primary antibodies. The anti-CyP CYP-18 antibody (Kielbowicz-Matuk et al., 2007) was used at 1:100 dilution, and incubated at 4°C overnight. Following two washes with PM buffer, samples were incubated with a goat anti-rabbit Alexa

Fluor 488nm (Invitrogen) as secondary antibodies for 45 min in the dark at 37°C. After two washes in PM buffer, samples were placed on slides and covered with a drop of Citifluor and observations were made using a Zeiss Axio Imager fluorescence microscope equipped with a 63x objective. Images were captured with an MRm AxioCam video camera using AxioVision software. Reconstruction of tube sections was done from Z-series images obtained with the Zeiss Apotome (0.5 µm between each Z image) using the LOCI Import filter and the Reslice command of ImageJ software (https://imagej.nih.gov/ij/). As a control, fixed pollen was directly incubated with a secondary antibody.

2.3 Immunogold electron microscopy

Immunogold labelling on pear pollen tubes was performed according to the protocol described in (Li et al., 1995). The anti-CyP antibody was used at the dilution of 1:300 in 50 mM Tris–HCl pH 7.6, 0.9% NaCl, 0.1% Tween-20, 0.2% BSA. The goat anti-rabbit secondary antibody, diluted 1:20 for 45 min at room temperature, was conjugated with 15 nm gold particles (BioCell). Images were captured with a transmission electron microscope (TEM) Philips Morgagni 268 D set at 80 kV and equipped with a MegaView II CCD Camera (Philips Electronics, Eindhoven, The Netherlands). Samples were incubated with 5% normal goat serum (Invitrogen) for 20 min at room temperature to prevent binding to unspecific sites. Sections were incubated with the primary antibody for 1 h and then washed (3-4 times) in 50 mM Tris–HCl pH 7.6, 0.9 % NaCl, 0.1% Tween 20 for 30 min. After drying, samples were incubated with the gold-conjugated secondary antibody for 15 min at room temperature. After washing for 30 min as described above and for further 10 min with dH_2O (distilled H_2O), sections were counterstained with 2% uranyl acetate in H_2O for 10-20 min, carefully washed in dH_2O for 15 min and then counterstained with lead citrate for 5-10 min. Scaling was done using the scale bar generated by the microscope software (AnaliSYS). For each experimental condition, at least 50 pollen tubes and grains were analyzed.

2.4 Extraction of proteins from cytosol, membrane, and cell wall fractions

Sequential fractionation and isolation of subcellular proteins from germinated pollen was performed as described by Parrotta et al. (2016) with some modifications. Briefly, after hydration, pollen tubes were incubated for 90 min in growth medium, while treated samples were supplemented with 3 mM EGTA after 45 min of incubation. Pollen tubes from each sample (control and supplemented with EGTA), were collected by low speed centrifugation and washed with HM buffer (50 mM Hepes pH 7.5, 2 mM $MgCl_2$) containing 10% sucrose. Then, pollen was lysed in a cold room (4 °C) using a Potter-Elvehjem homogenizer (40 strokes); the lysis buffer was HM supplemented with 0.1% Triton. After centrifugation at 500g for 10 min (4 °C), the supernatant was removed and centrifuged at high speed (100,000g for 45 min at 4 °C). The resulting pellet (Mem-Org fraction) was resuspended in 1 M Tris HCl pH 7.4; samples were then centrifuged at 15,000g for 5 min in a microfuge and the supernatant was directly used. The supernatant from the high-speed centrifugation (cytosolic fraction) was then resuspended in suitable buffers for either 1-D or 2-D electrophoresis. The pellet from the initial low-speed centrifugation (cell wall fraction) was washed several times with HM buffer to remove contaminating proteins. The last pellet was resuspended in 1 M Tris HCl pH 7.4. Protein concentration was determined using a commercial kit (BCA Protein Assay, Thermo Fisher), according to the manufacturer's instructions. Each sample was analyzed in three replicates.

2.5 1-D and 2-D electrophoresis

Separation of proteins by 1-D electrophoresis was performed on 15% mini gels using a Mini-Protean cell (Bio-Rad) equipped with a Power Pac Bio-Rad 300 at 200 V for approximately 50 min. Forty μg of proteins were loaded per lane. Gels were stained with Bio-Safe Coomassie blue (Bio-Rad).

For 2-DE analysis, 11-cm IPG Strips with a 6–11 pH gradient (Bio-Rad) were used in combination with 18% Criterion XT gels (Bio-Rad). Strips were rehydrated in the solubilization buffer (40 mM Tris, 8 M urea, 2 M thiourea, 2% CHAPS, and traces of bromophenol blue) to which 18 mM DTT and 20 μL/mL IPG buffer were added. Samples were dissolved at 1 mg/mL

in the solubilization buffer. Strips were rehydrated overnight in Immobiline Dry Strip Reswelling Tray (GE HealthCare) and covered with the Dry Strip Cover PlusOne (GE HealthCare). Strips were run using a Protean IEF Cell (Bio-Rad) through six different steps:

- From 0 to 500 V for 30 min.

- From 500 V to 1000 for 30 min.

- From 1000 to 8000 V for 3 h.

- 8000 V until a total of 15,000 Vhr (Volts h^{-1}).

- From 8000 to 500 V for 10 min.

- Hold step of 500 V until use of strips.

Strips were stored at -80 °C or used immediately. In both cases, they were equilibrated for 15 min in equilibration buffer (50 mM Tris-HCl, pH 8.8 containing 6 M urea, 30% glycerol, 2% SDS, bromophenol blue, 10 mg/mL DTT). Proteins were then separated in the second dimension based on a Bis-Tris buffer system. Molecular weight standards of the Precision series (Bio-Rad) were run in parallel.

2.6 Western blotting and image analysis

Electroblotting of proteins to nitrocellulose membrane was performed using a Trans-Blot Turbo Transfer System (Bio-Rad) according to the manufacturer's instructions. Quality of blotting was determined by checking the transfer of precision pre-stained molecular standards (Bio-Rad). After blotting, membranes were blocked overnight at 4 °C in 5% Blocking-Grade Blocker (Bio-Rad) in TBS (20 mM Tris pH 7.5, 150 mM NaCl) plus 0.1% Tween-20. After washing with TBS, membranes were incubated with the primary antibody (anti CYP-18 diluted at 1:1000) for 1 h. A goat anti-rabbit IgG (Bio-Rad) diluted 1:3000 was used as secondary antibody. After rinsing the membranes with TBS, the immunological reactions were visualized with ImmunStar (Bio-Rad). Images of gels and blots were acquired using a Fluor-S apparatus (Bio-Rad) and analyzed with the Quantity One software (Bio-Rad). Exposure times were 30-60 s for blots and 5-7 s for Coomassie-stained gels.

All blots were developed using identical conditions, from substrate incubation to exposure time. All images were processed correspondingly using the Autoscale command (to improve the quality of gels and blots) and the Background Subtraction command (to remove the background noise). The relative intensity of single spots was calculated with the Volume tool of Quantity One software. Blots were performed in triplicate.

2.7   CyP purification and mass spectrometry identification

The supernatant obtained after washing with HEMS buffer containing 1 mM EGTA was collected for gel filtration chromatography using a Superdex 75 10/300 GL column (GE Healthcare) equilibrated with 25 mM Tris-HCl pH 7.5, 1 mM PMSF, 1 mM DTT, 3 mM EDTA, and 1 mM PMSF, before loading the protein sample. Elution was performed at a constant flow rate of 0.5 mL/min; a UV detector at 280 nm was used to check fractions eluted from the column. Eluted fractions showing protein peaks were separated by SDS-PAGE (15% acrylamide) and/or blotted on nitrocellulose and stained by iodine-starch staining (Kumar et al., 1985).

Protein identification was performed as previously described (Hellman et al., 1995; Soskic et al., 1999). The electrophoretic lane of interest was manually excised and processed as reported elsewhere (Aloisi et al., 2016). Acquisition of mass spectra was performed using an Ultraflex III MALDI-TOF/TOF mass spectrometer (Bruker Daltonics, Billerica, MA, United States) in reflector positive mode. Spectra were analyzed by Flex Analysis software v. 3.0. Peptide mass fingerprinting (PMF) database searching was carried out in NCBInr and/or Swiss-Prot databases using Mascot (Matrix Science Ltd., London, UK, http://www.matrixscience.com) on-line available software. The search settings were as follows: mass tolerance was set at 100 ppm, trypsin as the digestion enzyme with one allowed missed cleavage and oxidation of methionine as a variable modification. In order to accept identifications, the number of matched peptides, the extent of sequence coverage, and the probabilistic score were considered. Peptide digests that did not give unambiguous identifications were subjected to peptide sequencing by tandem MS. MS/MS analysis was performed on the Ultraflex III MALDI-TOF/TOF instrument. Two to three PMF peaks showing

a high intensity were CID (Collision Induced Dissociation) fragmented using Argon as collision gas, and MALDI-TOF/TOF tandem MS was performed in LIFT mode by software-controlled data acquisition. Fragmented ions were analyzed using the Flex Analysis software v. 3.0. The MS/MS database search was carried out in NCBInr and/or Swiss-Prot databases using the on-line MASCOT MS/MS ion search software. The following parameters were applied for the database search: trypsin specificity, one missed cleavage allowed, peptide precursor mass tolerance: ±100 ppm, fragment mass tolerance ±0.6 Da, peptide precursor charge state +1, carbamidomethylation of cysteine as a fixed modification, oxidation of methionine as a possible modification. Protein identification was considered significant based on Mascot ion score, peptide coverage by "b" and "y" ions, and expected value.

Liquid chromatography electrospray ionization-tandem MS (LC-ESI/MS-MS) was performed with a Micro-HPLC Pump Phoenix 40 (Thermo Finnigan, San Jose, CA, USA) equipped with the LCQ DECA IT mass spectrometer (Thermo Finnigan). The TurboSEQUEST algorithm (Thermo Finnigan) analyzed spectra. Using the online MASCOT MS/MS ion search software, an MS/MS database search was carried out in the NCBI nr or Swiss-ProtKB databases. Only peptides with individual ion scores of less than 0.05 (p < 0.05) were considered significant.

2.8 Bioinformatic analysis

A bioinformatic annotation of CyP genes from pear was performed by comparing the FASTA sequence of CyP from *Phaseolus vulgaris*, present in NCBI databases, to the pear genome (Jung et al., 2019). We performed a tblastn (search translated nucleotide databases using a protein query) on *Pyrus Communis* cv. Bartlett DH Genome v2.0 transcripts. mRNA sequences of the corresponding genes were blasted on protein databases available online at NCBI (blastx; search protein databases using a translated nucleotide query), in order to confirm that the identified sequences correspond to CyPs. Alignments, target name, E-Value, % of identity and chromosomal coordinates for putative CyP genes are reported.

2.9   Statistical analysis

Pollen germination rate, pollen tube length and band intensity analysis were analyzed using ImageJ software (http://rsbweb.nih.gov/ij/index.html). Differences between sample sets were determined by analysis of variance (one-way ANOVA, with a threshold P-value of 0.05) using R.

3.   Results

3.1   CyP localizes in several pollen compartments

In order to investigate the localization of CyP, several microscopy techniques were used. First, in order to discriminate whether pollen CyP localizes within the cytoplasm or in the cell wall, germinated pollen was treated or not with cell wall-degrading enzymes and CyP localization was performed by immunofluorescence. Immunolocalization of CyP in pollen treated with cell wall degrading enzymes showed a diffuse and uniform signal, mostly localized in the apical and subapical region of the pollen tube (Figure 1B and 1C); when the pollen cell wall was not digested, cells showed a regular distribution of CyP along the cell wall, mostly with a dot-like appearance (Figure 1E-1F). Detection of CyP in pollen with both digested or undigested cell walls suggested that CyP localizes both in the cytoplasm and in the cell wall of pear pollen. No unspecific signal was detected, either in pollen with undigested cell wall nor in pollen with digested cell wall (Figure 1A and 1D). In order to confirm the localization of CyP in the cell wall, confocal microscopy was performed in germinated pollen not treated with cell wall-degrading enzymes. A distribution of CyP all along the outer layer of the tube was observed (arrows in Figure 2A). Along the pollen tube, the signal exhibited mainly a dot-like appearance and looked more intense in the apical region, confirming the results obtained by fluorescence microscopy (Figure 2A and 2B). The distribution of CyP was also analyzed by a tube sections reconstruction of the cross sections in two different points of the pollen tube (indicated by dotted lines), which highlighted the distribution of CyP along the cell edge, suggesting its association with the cell wall (Figure 2B, inserts). A similar distribution was found in pollen grains (Figure 2C). The distribution of CyP was further analyzed by immunoelectron microscopy. In the

apex/subapex region of pollen tubes, gold particles were found mostly in association with the plasma membrane and in the cell wall, but gold particles were also found in the cytosol, presumably associated to organelles or vesicles. The signal was evident in association with the cell wall at the tube apex (Figure 2D, arrows). A similar distribution was found along the pollen tube. Again, CyPs were mainly associated with the plasma membrane, the cell wall and the cytosol, probably in association with organelles and vesicles (arrow in Figure 2E). No unspecific signal was detected, neither in fluorescence acquisition nor in TEM analysis (Supplementary material 1).

The localization of CyPs in different cellular compartments was also analyzed by pollen sub-fractionation followed by western blotting. Sub-fractionation and isolation of subcellular proteins was performed in order to isolate proteins bound to the cell wall (**CW**), soluble cytosolic proteins (**CYT**) and transmembrane proteins with strong interactions to the intracellular membrane-bound organelles (**Mem-Org**). Results indicated that CyP accumulated in all compartments to different levels, as highlighted by western blot data (Figure 3A), and confirmed after quantification of single band intensities. Analysis of band intensity indicated that EGTA increased CyP accumulation in this fraction (Figure 3B). In the Mem-Org fraction as well as in the cytosol fraction, control and EGTA-treated samples did not show any statistically relevant differences (Figure 3C and 3D). This result was made even more evident after a similar electrophoretic separation followed by coomassie blue staining (Supplementary material 2). CyP antibody recognized a single band with a molecular weight of *ca*. 18 kDa (Figure 3E), while 2-D electrophoretic separation followed by immunodetection revealed two different spots in pollen tubes grown in standard condition (Figure 3F); spots

differed for the pI value (pH range 8.5/8.7), suggesting the presence of at least two protein isoforms in pear pollen.
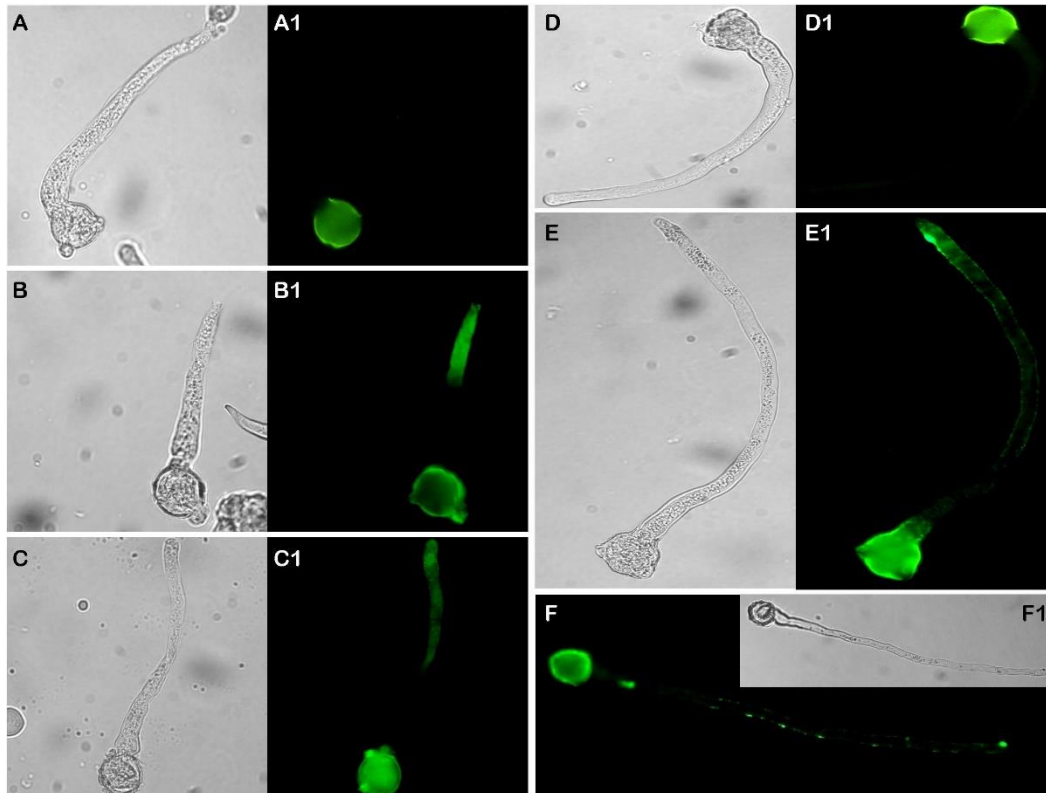
Figure 1: CyP localizes in the cytoplasm and in the pollen tube cell wall. CyP immunolocalization by fluorescence microscopy of pollen tubes probed with CYP-18 antibody and a secondary Alexa Fluor 488 antibody, after cell wall digestion (B1, C1) and without cell wall digestion (E1, F). B,C, E and F1 bright field images of the corresponding germinated pollen reported in the fluorescence images. Autofluorescence is visible in the pollen grain but a specific signal of primary antibody was detected along the tube, neither in pollen whose cell wall was digested (A1), nor in pollen whose cell wall was not digested (D1). A and D, control pollen, respectively with digested and not digested cell wall, in bright field.
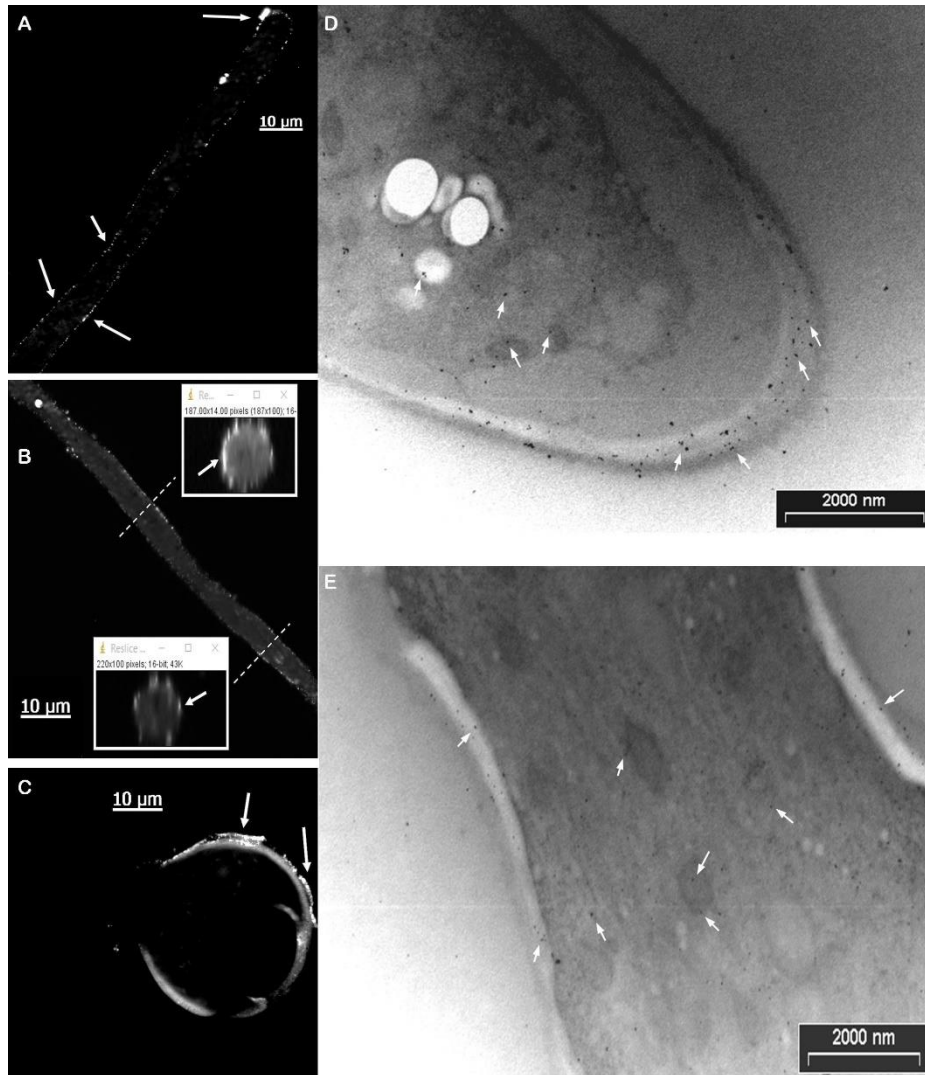
Figure 2*: Distribution of CyP within the pollen tube. Confocal microscopy of germinated pollen not treated with cell wall degrading enzymes (A-C). Arrows highlight distribution of CyP all along the outer layer of pollen tube (A). Cross sections (inserts) at two different points of the pollen tube (indicated by dotted lines) highlight the distribution of CyP in the cell edge (B). A similar distribution was found in pollen grains (C). CyP distribution detected by immunoelectron microscopy in the apex/subapex region of pollen tubes (D) and in the pollen tube shank (E). Gold particles were found mostly in association with the plasma membrane, in the cell wall and in the cytosol, presumably associated with organelles or vesicles (arrows).*
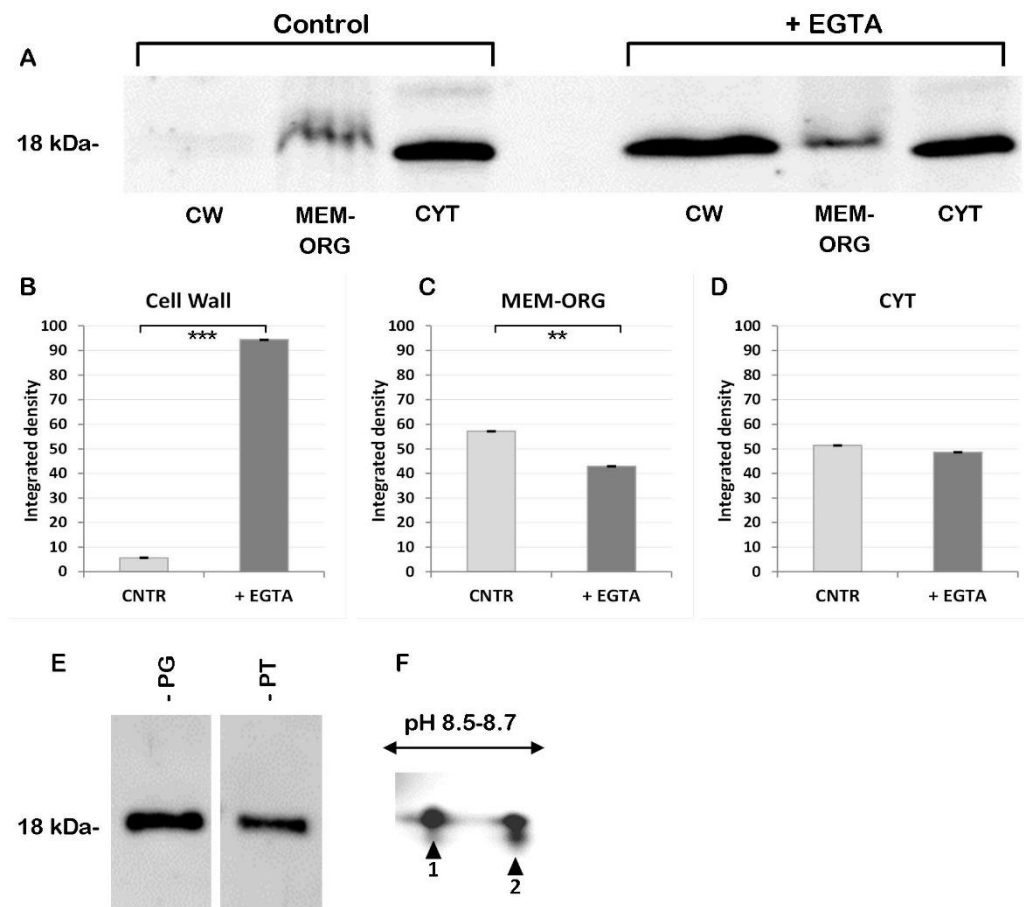
Figure 3: *Western blotting analysis of CyP confirms its localization in several cell compartments and the presence of two different isoforms. Sub-fractionation of pollen cell compartments followed by western blotting (A) and relative quantification (B, C and D). Three compartments (cell wall, cytosol and membrane-organelles) are shown by representative images. Values are mean ± SD of three replicates analyzed in duplicate. Means were compared by one way ANOVA. ** = p ≤ 0.01;*** = p ≤ 0.001. The cell wall compartments showed the marked significant differences between control and EGTA treated samples. Immunoblot analysis of CyP in pollen grains (PG) and pollen tubes (PT) (E). 2D electrophoresis followed by immunoblot analysis of proteins extracted from pollen tubes (F).*

3.2   Ca2+-depletion induces the release of CyP from pear pollen

In order to understand the effect of EGTA on the release of CyP in pollen growth medium, the tube length of pollen grown in the presence of 0.4 mM, 1 mM and 5 mM EGTA was analyzed. The presence of EGTA, even at the lowest concentration, significantly reduced the growth rate of pollen tubes; no significant differences between tube growth in the presence of 1 mM and

5 mM of EGTA were observed (Figure 4A). The presence of EGTA also affected germination, since washing pollen grains with HEMS buffer supplemented with EGTA decreased the germination rate from 80% (no EGTA) to 25%. The washing step also reduced the germination rate in the absence of EGTA, but to a significantly lesser extent (from 80% to 60%) (Figure 4B). The distribution of CyP was analyzed by immunoelectron microscopy after treatment with EGTA showing that the density of gold particles was lower than in the controls (Figure 4C). In particular, we found that gold particles were predominantly associated with the plasma membrane and the inner layer of the cell wall, and not with the cytoplasm (Figure 4D).

The 2-D electrophoretic separation followed by immunodetection revealed only one spot with a pI value around 8.7 in tubes (TPT - Total Pollen Tubes) and grains (TPG - Total pollen Grains) washed with HEMS buffer. This was different from control pollen grains (WPG - Washed Pollen Grains) and tubes (WPT - Washed Pollen Tubes), where two isoforms were detectable (Figure 4E and its quantification 4F) suggesting the presence of only one protein isoform in pear pollen treated with EGTA and thus the release of CyP in the germination medium.

To confirm the EGTA-induced release of CyP, proteins present in the supernatant obtained after washing with HEMS buffer containing 1 mM EGTA were processed for purification and then analyzed by MS. After gel filtration chromatography, SDS-PAGE separation, and transfer of proteins to nitrocellulose followed by iodine-starch staining, we found five fractions (fractions 33-37) showing mainly one band of *ca.* 18 kDa (Figure 5). These five fractions were collected and electrophoretically separated, thus the 18 kDa band has been cut from the gel and analyzed by MS.

The 18-kDa protein was demonstrated to be a CyP by MALDI-TOF (Table 1) and confirmed by LC-MS/MS (Table 2 reports the comparison by Mascot software). This confirmed the release of one CyP isoform into the growing medium under Ca^{2+}-depletion conditions.
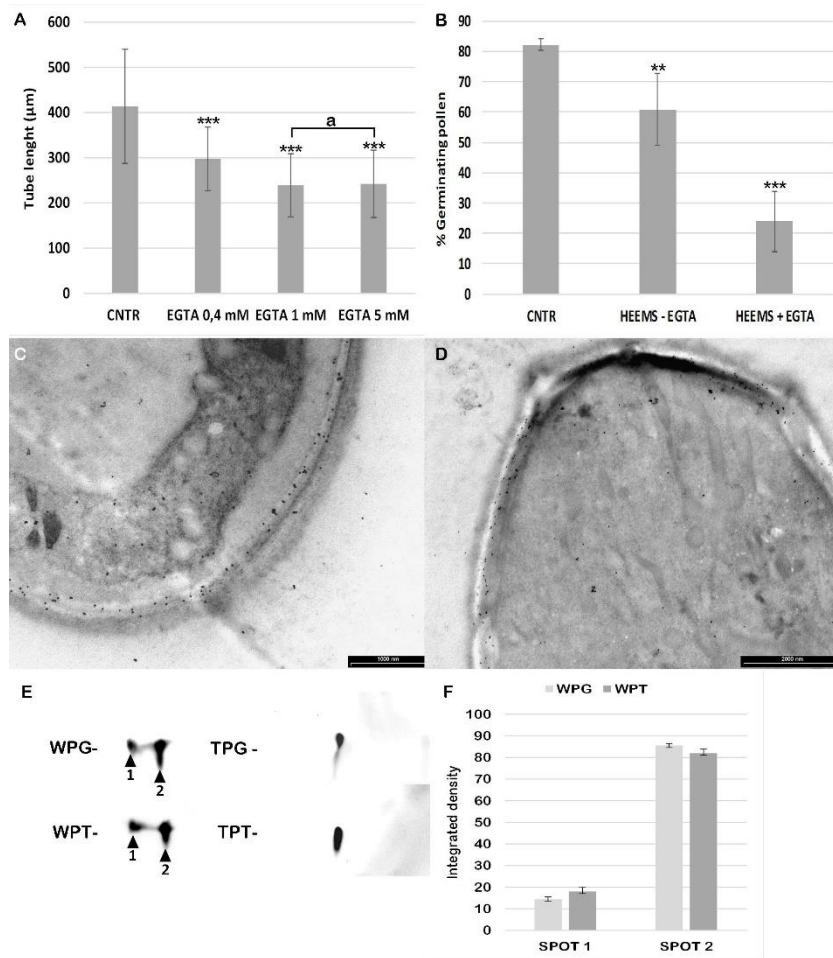
Figure 4*: EGTA inhibits pollen germination and pollen tube elongation and determines the release of CyP. EGTA (0.4 mM, 1 mM and 5 mM) arrested pollen tube elongation in a dose-dependent manner. The means of tube length derive from at least 100 measurements in three independent experiments. Means of treated and not treated (control) samples after 2 h germination by one way ANOVA. ** = p ≤ 0.01;*** = p ≤ 0.001. Bars indicate standard deviation. Samples marked with "a" are not significantly different (A). Analysis of germination of pollen after EGTA treatment. Pollen was gently washed with HEMS buffer supplemented or not with 3 mM EGTA and allowed to germinate in standard medium for 2 h. Means derive from at least 100 measurements and the experiment was repeated three times. Means of samples were compared with control sample after 2 h germination by one way ANOVA. ** = P < 0.01; *** = P < 0.001. Bars indicate standard deviation (B). Distribution of CyP by immunoelectron microscopy in control pollen (C) and after EGTA, showing a lower density of gold particles (D). 2D electrophoresis followed by immunoblot analysis of both EGTA-released and EGTA-unreleased (TPG - Total pollen Grains and TPT - Total Pollen Tubes) proteins from both pollen grains and pollen tubes. (E). Relative quantitation of the two CyP spots of Fig 4E. No significant differences were detected between EGTA-washed pollen grains (WPG - Washed Pollen Grains) and EGTA-washed pollen tubes (WPT - Washed Pollen Tubes) (F).*
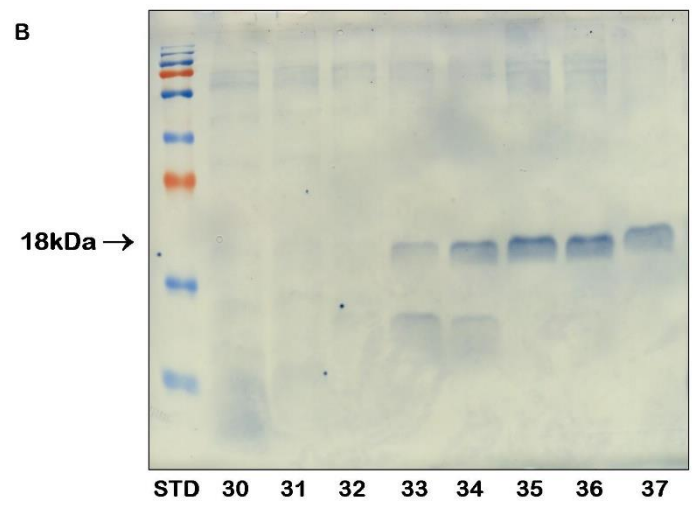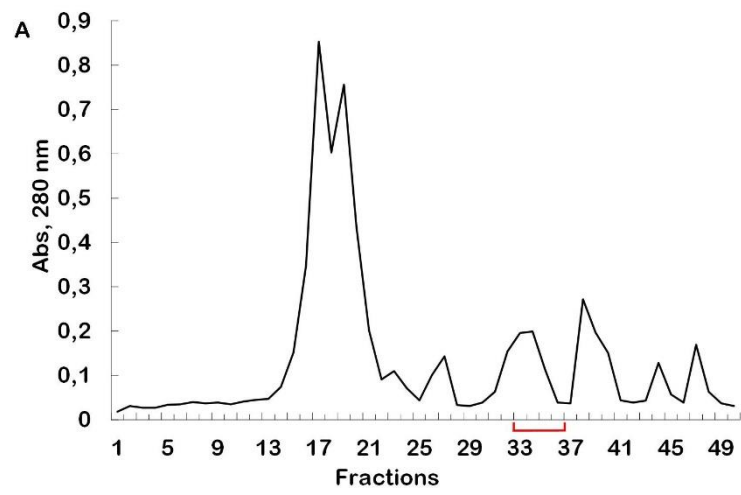
***Figure 5**: Chromatographic separation of pollen proteins released after washing pollen grains with HEMS buffer containing EGTA. Chromatogram of gel filtration chromatography using a Superdex 75 10/300 GL column. Fractions have been eluted with HEMS buffer supplemented with 1 mM EGTA and checked for absorbance (Abs) at 280 nm. Red bar indicate a peak of Abs at 280 nm (A); when these fractions were run on SDS-PAGE (15%) and transferred to nitrocellulose, after iodine starch staining, they appeared definitely enriched in one band with 18 kDa (B).*

***Table 1:** EGTA-released proteins identified by MALDI-TOF MS.*

Description	Accession number	Database	Peptide	Organism
CyP	gi|829119	NCBInr	HVVFGQVVEGLDVVK	*Phaseolus vulgaris*
CyP	gi|829119	NCBInr	VFFDMTIGGQPAGR	*Phaseolus vulgaris*

Table 2: *EGTA-released proteins identified by LC-MS/MS.*

Description	Accession number	Database	Peptide	Organism
Peptidyl-prolyl *cis-trans* isomerase CYP18-3 (CyP) Peptidyl-prolyl *cis-trans* isomerase CYP19-2 (CyP)	CP18C_ARATH CP19B_ARATH	Swiss-Prot	K.HVVFGQVVEGLDVVK.A	*Arabidopsis thaliana*
Peptidyl-prolyl *cis-trans* isomerase 1 (Cyclophilin)	CYP1_SOYBN	Swiss-Prot	K.HVVFGQVIEGLNVVK.D	*Glycine max*
Peptidyl-prolyl *cis-trans* isomerase CYP18-3 (CyP) Peptidyl-prolyl *cis-trans* isomerase CYP19-2 (CyP)	CP18C_ARATH CP19B_ARATH	Swiss-Prot	K.HVVFGQVVEGLDVVK.A	*Arabidopsis thaliana*

A bioinformatic analysis of the NCBI database showed that CyPs are not annotated for *Pyrus communis*. For this reason, we compared the FASTA sequence of *Phaseolus vulgaris* to the entire genome of *P. communis*.

Results of Blast analysis highlighted the presence of 33 putative genes corresponding to CyPs (Table 3). Each sequence was analyzed, the corresponding mRNA sequence downloaded and reported on NCBI database to confirm the correspondence to CyPs already annotated in other plant species.

Table 3. *Putative CyPs identified in Pyrus communis cv. Bartlett based on DH Genome v2.0 transcripts.*

N°	Target Name	E-Value	Identity	Chromosome alignment
1	pycom05g11090	4.69409E-95	156/172 (90.7%)	Chr5:14565526..14566044+
2	pycom10g10310	1.83384E-88	150/172 (87.21%)	Chr10:13611493..13612254+
3	pycom12g22510	3.87554E-72	130/171 (76.02%)	Chr12:23381723..23382987+
4	pycom04g20270	8.96782E-68	121/155 (78.06%)	Chr12:23381723..23382987+
5	pycom11g06130	5.04152E-64	117/170 (68.82%)	Chr11:4728747..4731377+
6	pycom03g05580	4.91214E-62	114/170 (67.06%)	Chr3:4421561..4423606+
7	pycom01g17040	1.55409E-59	111/170 (65.29%)	Chr1:16437708..16439668-
8	pycom16g10580	4.07188E-54	112/171 (65.5%)	Chr16:7251810..7254139-
9	pycom15g24270	1.40401E-53	104/174 (59.77%)	Chr15:18478393..18479270+
10	pycom17g28180	2.44746E-52	102/168 (60.71%)	Chr17:26204064..26206132+
11	pycom02g13470	3.78116E-52	103/174 (59.2%)	Chr2:10000668..10003665+

12	pycom05g06840	3.94678E-52	104/174 (59.77%)	Chr5:9651006..9654480+
13	pycom07g03370	3.25961E-51	101/171 (59.06%)	Chr7:2786574..2789287+
14	pycom02g23890	7.04685E-51	103/175 (58.86%)	Chr2:21983699..21986377+
15	pycom13g10750	2.79206E-50	105/159 (66.04%)	Chr13:7241405..7243784-
16	pycom07g20020	7.02564E-50	103/175 (58.86%)	Chr7:22220925..22222910-
17	pycom03g20370	4.1466E-48	100/141 (70.92%)	Chr3:20862051..20866253-
18	pycom10g10540	1.85793E-45	94/171 (54.97%)	Chr10:13910258..13913098+
19	pycom15g10880	1.05727E-44	89/169 (52.66%)	Chr15:7309999..7314262+
20	pycom05g11340	4.05245E-44	93/171 (54.39%)	Chr5:14882526..14885427+
21	pycom08g12230	5.74429E-44	87/173 (50.29%)	Chr8:10534103..10540454+
22	pycom11g24550	1.39269E-29	60/90 (66.67%)	Chr11:27467528..27470983-
23	pycom02g16470	1.01918E-24	69/143 (48.25%)	Chr2:13622162..13623645+
24	pycom14g02830	3.64173E-24	68/148 (45.95%)	Chr14:2163415..2166024-
25	pycom12g02890	5.94354E-23	72/161 (44.72%)	Chr12:2613417..2615911-
26	pycom02g15080	6.48339E-21	64/132 (48.48%)	Chr2:11798030..11802120+
27	pycom15g26020	1.19076E-20	64/132 (48.48%)	Chr15:20657508..20661646+
28	pycom11g21670	1.42082E-15	61/111 (54.95%)	Chr11:24744737..24745960+
29	pycom03g09380	2.00947E-14	35/56 (62.5%)	Chr3:7892245..7892819+
30	pycom15g05220	1.55074E-13	53/150 (35.33%)	Chr15:3121075..3122688-
31	pycom07g05380	3.18915E-13	46/67 (68.66%)	Chr7:4652891..4653133-
32	pycom07g05330	3.18915E-13	46/67 (68.66%)	Chr7:4612297..4612539-
33	pycom05g20510	5.25035E-10	49/140 (35%)	Chr5:23291697..23297603+

4. Discussion

Although the pear genome has been sequenced, to date there are no CyPs annotated in the NCBI database. A bioinformatic analysis based on the draft of the pear genome (Chagne et al., 2014), allowed the identification of 33 possible genes that correspond to CyPs in the NCBI database. The number of putative CyPs was similar to the number of in other plant species, such as Arabidopsis (35 genes) and in rice (28 genes), where CyPs constitute a family of highly conserved proteins encoded by multigenic families. The phylogenetic analysis of rice and Arabidopsis CyP family members indicate high sequence variation in the proteins (Trivedi et al., 2012), however CyPs can be classified according to whether they have a single CyP domain or they possess additional functional domains (Romano et al., 2004). In general low molecular-weight CyPs possess peptidyl-prolyl *cis-trans* isomerase activities thought to play an important

role in protein folding and processing (Yokota et al., 2004), however a higher molecular weight CyP (*ca.* 40 kDa) in *Spinacia oleracea* was also possess a isomerase activity (Fulgosi et al., 1998).

In this work, we analyzed the localization of CyP in pollen grains and tubes of pear, first using fluorescent microscopy that indicated a dot-spot localization along the cell edge, probably in association with the plasma membrane or the cell wall; the signal appeared more intense in the apical region. These evidences were confirmed by subsequent analysis with immunogold electron microscopy. In this case, gold particles specifically localized in the cytosol, the plasma membrane and the cell wall. Distribution of CyP in different compartments was confirmed by protein differential extraction followed by immunoblot detection; those tests highlighted specific accumulation of CyP isoforms. CyPs localized mainly in the membrane/organelle fraction, followed by the cytosol compartment. CyPs were less abundant in the cell wall fraction. However, the increase in CyP accumulation in cell wall fraction after the addition of EGTA in the growth medium, indicated that CyPs were targeted towards the cell wall compartment in the presence of EGTA. These data are in agreement with the localization of CyPs in other plant cells, where they are known to be targeted to different subcellular compartments such as the cytoplasm, nucleus, endoplasmic reticulum, mitochondria and chloroplasts (Kielbowicz-Matuk et al., 2007; Romano et al., 2005; Vasudevan et al., 2015).

CyP was localized in the cytosol and vegetative nuclei of pollen grains and generative cells, indicating that it is not a pollen-coated protein. It was suggested that CyPs released from rice pollen is involved in signal transduction during pollen tube growth (Dai et al., 2006). The release mechanism and the role of the pollen-released protein remain both to be elucidated. Moreover, it is not clear whether pollen contains several isoforms; the only evidence of several isoforms in pollen derives from studies in *Oryza sativa*, where three different CyPs were identified with a proteomics approach (Dai et al., 2006). In our study, we found at least two different isoforms in pear pollen after 2-D electrophoretic separation followed by immunoblot detection in control pollen tubes.

In the present study, we showed that the Ca^{2+} chelator EGTA causes a significant reduction of pear pollen tube length, even at low concentration (< 0.4 mM), while concentrations above 1 mM totally blocked tube growth, in agreement with earlier work (Picton and Steer, 1983) and with our recent data (Aloisi et al., 2017). Washing grains with EGTA also significantly reduced pollen germination rate. Apart from the cessation of tube elongation, no other morphological changes were detected. EGTA also induced protein release into the medium, among which a low molecular-weight CyP was abundant. This 18-kDa CyP was homologous to a CyP of *Phaseolus vulgaris* (identified with MALDI-TOF analysis). This finding was confirmed by subsequent analysis with LC-MS/MS spectrometry, which highlighted homology with CyPs from *Arabidopsis thaliana* and *Glycine max*. The role of Ca^{2+} and, in particular, of the tip-focused cytosolic Ca^{2+} gradient (supported by an influx of Ca^{2+} through the apical plasma membrane) is well known to be essential for the growth and orientation of pollen tubes (Franklin- Tong, 1999). Yokota and coworkers showed that a 21-kDa CyP was released from pollen grains into the extracellular medium *in vitro* at low concentrations of Ca^{2+}. This was confirmed for pollen of lily, *Nicotiana tabacum* and *Tradescantia,* while CyP release from pollen of the gymnosperm *Cryptomeria japonica* required alkaline pH besides Ca^{2+} depletion (Yokota et al., 2004). Several articles report a quick release of cytoplasmic proteins upon pollen hydration. This release can happen in the atmosphere after contact with air humidity, in aqueous media (during fertilization or in-vitro pollen rehydration) but also after the interaction of pollen with human mucosa (Morales et al., 2008; Aloisi et al., 2018; Zaidi et al., 2012). Among proteins released, also pollen allergens belonging to different protein families were found in different pollen (Alche et al., 2004; Grote et al., 1993; Vega-Maray et al., 2006; Vrtala et al., 1993) and CyPs are not an exception (Zaidi et al., 2012). For this reason, pollen allergy can be triggered not only by whole pollen grains, but also from sub-particles and fragments. Pollen CyPs have been speculated to serve a protective role during pollen dehydration and to be involved in signal transduction during pollen tube growth in the style once released in the extracellular medium (Dai et al., 2006). Moreover, plant CyPs belong to the group of stress-induced proteins. They are involved in responding to various

environmental stimuli including wounding and exposure to chemicals (Zaidi et al., 2012), Ca^{2+} depletion induced by EGTA, could have favored CyP release in the extracellular medium. EGTA could, on the other hand, loosen the pollen tube cell wall thus favoring the release of cytoplasmic material from the pollen tube. In fact Ca^{2+} ions are needed to cross-link acid pectins at the subapex edge of the pollen tube (Rockel et al., 2008) where they bind Ca^{2+}, thereby contributing to strengthen the cell wall (Palin and Geitmann, 2012; Wolf and Greiner, 2012). If Ca^{2+} ions are not present, newly synthetized ductile methyl-esterified pectins are secreted at the tube apex they are chemically converted into acid pectins, but do not cross-link and form a stiff net.

This specific localization was apparently similar in control samples (pollen tubes grown in the absence of EGTA) and in EGTA-washed pollen tubes. EGTA caused a decrease of protein content mostly in the cytosolic compartment of the pollen tube; Ca^{2+}-depletion did not release cell wall-associated CyP. This evidence was confirmed by the presence of only one isoform in pollen after treatment with EGTA. Currently, we can only speculate that EGTA washing caused the release of only one isoform, but we still do not know which done. We can hypothesize that the isoform indicated by "1" in figure 4E was released completely into the growth medium. This evidence confirms earlier data showing that lily pollen grown in an EGTA- containing medium releases CyP, mainly from the cytoplasm, while CyPs were not released from the vegetative nucleus and the generative cell (Yokota et al., 2004).

The cellular function of CyP remains essentially unknown, although a role as molecular chaperones or folding catalysts was suggested, especially under stress condition. The role of CyPs in abiotic stress tolerance is further supported by recent studies which demonstrate that the ectopic expression of CyP genes enhance tolerance to multiple abiotic stress conditions (Kaur et al., 2016; Romano et al., 2004). In plants, their presence has been reported in almost all organs studied (*e.g*. roots, leaves, stems, buds, and anthers) and have been hypothesized to be involved in intracellular signaling pathways by reacting with calcineurin, a calcium-binding protein (Cadot et al., 2000). However, only a few studies have focused on the presence of CyPs in pollen (Cadot et al., 2000). Because of the poor knowledge of the cellular function

of CyPs, it is difficult to predict their role in pollen. CyPs may enhance the tolerance capacity of pollen against environmental stress because their synthesis in maize and bean has been shown to be up-regulated in response to some selective stress conditions, such as heat, chemical exposure, and infection by pathogens (Cadot et al., 2000).

5. Bibliography

Alche, J.D., M'rani-Alaoui, M., Castro, A.J., Rodriguez-Garcia, M.I., 2004. Ole e 1, the major allergen from olive (Olea europaea L.) pollen, increases its expression and is released to the culture medium during in vitro germination. Plant Cell Physiol. 45, 1149–1157.

Aloisi, I., Cai, G., Tumiatti, V., Minarini, A., Del Duca, S., 2015. Natural polyamines and synthetic analogs modify the growth and the morphology of Pyrus communis pollen tubes affecting ROS levels and causing cell death. Plant Sci. 239, 92–105.

Aloisi, I., Parrotta, L., Ruiz, K.B., Landi, C., Bini, L., Cai, G., Biondi, S., Del Duca, S., 2016. New insight into quinoa seed quality under salinity: changes in proteomic and amino acid profiles, phenolic content, and antioxidant activity of protein extracts. Front. Plant Sci. 7.

Aloisi, I., Cai, G., Faleri, C., Navazio, L., Serafini-Fracassini, D., Del Duca, S., 2017. Spermine regulates pollen tube growth by modulating Ca2+-dependent actin orga- nization and cell wall structure. Front. Plant Sci. 8.Aloisi, I., Del Duca, S., De Nuntiis, P., Maray, A.M.V., Mandrioli, P., Gutierrez, P., Fernandez-Gonzalez, D., 2018. Behavior of profilins in the atmosphere and in vitro, and their relationship with the performance of airborne pollen. Atmos. Environ. 178, 231–241.

Berardini, T.Z., Bollman, K., Sun, H., Poethig, R.S., 2001. Regulation of vegetative phase change in Arabidopsis thaliana by cyclophilin 40. Science 291, 2405–2407.

Cadot, P., Diaz, J.F., Proost, P., Van Damme, J., Engelborghs, Y., Stevens, E.A.M., Ceuppens, J.L., 2000. Purification and characterization of an 18-kd allergen of birch (Betula verrucosa) pollen: identification as a cyclophilin. J. Allergy Clin. Immunol. 105, 286–291.

Cadot, P., Nelles, L., Srahna, M., Dilissen, E., Ceuppens, J.L., 2006. Cloning and expres- sion of the cyclophilin Bet v 7, and analysis of immunological cross-reactivity among the cyclophilin A family. Mol. Immunol. 43, 226–235.

Cai, G., Faleri, C., Del Casino, C., Emons, A.M.C., Cresti, M., 2011. Distribution of callose synthase, cellulose synthase, and sucrose synthase in tobacco pollen tube is controlled in dissimilar ways by actin filaments and microtubules. Plant Physiol. 155, 1169–1190.

Cardenas, L., Lovy-Wheeler, A., Kunkel, J.G., Hepler, P.K., 2008. Pollen tube growth oscillations and intracellular calcium levels are reversibly modulated by actin poly- merization. Plant Physiol. 146, 1611–1621.

Chagne, D., Crowhurst, R.N., Pindo, M., Thrimawithana, A., Deng, C., Ireland, H., Fiers, M., Dzierzon, H., Cestaro, A., Fontana, P., Bianco, L., Lu, A., Storey, R., Knabel, M.,

Saeed, M., Montanari, S., Kim, Y.K., Nicolini, D., Larger, S., Stefani, E., Allan, A.C., Bowen, J., Harvey, I., Johnston, J., Malnoy, M., Troggio, M., Perchepied, L., Sawyer, G., Wiedow, C., Won, K., Viola, R., Hellens, R.P.,

Brewer, L., Bus, V.G.M., Schaffer, R.J., Gardiner, S.E., Velasco, R., 2014. The draft genome sequence of European pear (Pyrus communis L. 'Bartlett'). PLoS One 9.

Cheung, A.Y., Wu, H.M., 2008. Structural and signaling networks for the polar cell growth machinery in pollen tubes. Annu. Rev. Plant Biol. 59, 547–572.

Coelho, P.C., Malho, R., 2006. Correlative analysis of [Ca](C) and apical secretion during pollen tube growth and reorientation. Plant Signal. Behav. 1, 152–157.

Dai, S., Li, L., Chen, T., Chong, K., Xue, Y., Wang, T., 2006. Proteomic analyses of Oryza sativa mature pollen reveal novel proteins associated with pollen germination and tube growth. Proteomics 6, 2504–2529.

De Canio, M., D'Aguanno, S., Sacchetti, C., Petrucci, F., Cavagni, G., Nuccetelli, M., Federici, G., Urbani, A., Bernardini, S., 2009. Novel IgE recognized components of Lolium perenne pollen extract: comparative proteomics evaluation of allergic pa- tients sensitization profiles. J. Proteome Res. 8, 4383–4391.

de Olano, D.G., Gonzalez-Mancebo, E., Macadan, S.S., Cano, M.G., Perez-Gordo, M., Ortega, B.C., Vivanco, F., Vargas, C.P., 2010. Allergy to pumpkin with cyclophilin as the relevant allergen. Ann. Allergy Asthma Immunol. 104, 98–99.

Fluckiger, S., Fijten, H., Whitley, P., Blaser, K., Crameri, R., 2002. Cyclophilins, a new family of cross-reactive allergens. Eur. J. Immunol. 32, 10–17.

Franklin-Tong, V.E., 1999. Signaling and the modulation of pollen tube growth. Plant Cell 11, 727–738.

Fujita, C., Moriyama, T., Ogawa, T., 2001. Identification of cyclophilin as an IgE-binding protein from carrots. Int. Arch. Allergy Immunol. 125, 44–50.

Fulgosi, H., Vener, A.V., Altschmied, L., Herrmann, R.G., Andersson, B., 1998. A novel multi-functional chloroplast protein: identification of a 40 kDa immunophilin-like protein located in the thylakoid lumen. EMBO J. 17, 1577–1587.

Gasser, C.S., Gunning, D.A., Budelier, K.A., Brown, S.M., 1990. Structure and expression of cytosolic cyclophilin peptidyl-prolyl cis-trans isomerase of higher-plants and pro- duction of active tomato cyclophilin in Escherichia-coli. P Natl Acad Sci USA 87, 9519–9523.

Ghosh, D., Mueller, G.A., Schramm, G., Edwards, L.L., Petersen, A., London, R.E., Haas, H., Bhattacharya, S.G., 2014. Primary identification, biochemical characterization, and immunologic properties of the allergenic pollen cyclophilin cat r 1. J. Biol. Chem. 289, 21374–21385.

Grebe, M., Gadea, J., Steinmann, T., Kientz, M., Rahfeld, J.U., Salchert, K., Koncz, C., Jurgens, G., 2000. A conserved domain of the arabidopsis GNOM protein mediates subunit interaction and cyclophilin 5 binding. Plant Cell 12, 343–356.

Grote, M., Vrtala, S., Valenta, R., 1993. Monitoring of 2 allergens, Bet-V-I and profilin, in Dry and rehydrated birch pollen by immunogold electron-microscopy and im- munoblotting. J. Histochem. Cytochem. 41, 745–750.

Hellman, U., Wernstedt, C., Gonez, J., Heldin, C.H., 1995. Improvement of an in-gel di- gestion procedure for the micropreparation of internal protein-fragments for amino- acid sequencing. Anal. Biochem. 224, 451–455.

Jung, S., Lee, T., Cheng, C.H., Buble, K., Zheng, P., Yu, J., Humann, J., Ficklin, S.P., Gasic, K., Scott, K., Frank, M., Ru, S.S., Hough, H., Evans, K., Peace, C., Olmstead, M., DeVetter, L.W., McFerson, J., Coe, M., Wegrzyn, J.L., Staton, M.E., Abbott, A.G., Main, D., 2019. 15 years of GDR: new data and functionality in the genome database for rosaceae. Nucleic Acids Res. 47, D1137–D1145.

Kaur, G., Singh, S., Dutta, T., Kaur, H., Singh, B., Pareek, A., Singh, P., 2016. The peptidyl- prolyl cis-trans isomerase activity of the wheat cyclophilin, TaCypA-1, is essential for inducing thermotolerance in Escherichia coli. Biochim Open 2, 9–15.

Kielbowicz-Matuk, A., Rey, P., Rorat, T., 2007. The abundance of a single domain cy- clophilin in Solanaceae is regulated as a function of organ type and high temperature and not by other environmental constraints. Physiol. Plant. 131, 387–398.

Kumar, B.V., Lakshmi, M.V., Atkinson, J.P., 1985. Fast and efficient method for detection and estimation of proteins. Biochem. Biophys. Res. Commun. 131, 883–891.

Kumari, S., Roy, S., Singh, P., Singla-Pareek, S.L., Pareek, A., 2013. Cyclophilins: proteins in search of function. Plant Signal. Behav. 8, e22734.

Li, Y.Q., Faleri, C., Geitmann, A., Zhang, H.Q., Cresti, M., 1995. Immunogold localization of arabinogalactan proteins, unesterified and esterified pectins in pollen grains and pollen tubes of nicotiana-tabacum-L. Protoplasma 189, 26–36.

Marivet, J., Margispinheiro, M., Frendo, P., Burkard, G., 1994. Bean cyclophilin gene- expression during plant development and stress conditions. Plant Mol. Biol. 26, 1181–1189.

Marzban, G., Herndl, A., Kolarich, D., Maghuly, F., Mansfeld, A., Hemmer, W., Katinger, H., Laimer, M., 2008. Identification of four IgE-reactive proteins in raspberry (Rubus ideaeus L.). Mol. Nutr. Food Res. 52, 1497–1506.

Morales, S., Jimenez-Lopez, J.C., Castro, A.J., Rodriguez-Garcia, M.I., Alche, J.D., 2008. Olive pollen profilin (Ole e 2 allergen) co-localizes with highly active areas of the actin cytoskeleton and is released to the culture medium during in vitro pollen ger- mination. J Microsc-Oxford 231, 332–341.

Palin, R., Geitmann, A., 2012. The role of pectin in plant morphogenesis. Biosystems 109, 397–402.

Parrotta, L., Faleri, C., Cresti, M., Cai, G., 2016. Heat stress affects the cytoskeleton and the delivery of sucrose synthase in tobacco pollen tubes. Planta 243, 43–63.

Picton, J.M., Steer, M.W., 1983. Evidence for the role of Ca 2+ ions in tip extension in pollen tubes. Protoplasma 115, 7.

Rockel, N., Wolf, S., Kost, B., Rausch, T., Greiner, S., 2008. Elaborate spatial patterning of cell-wall PME and PMEI at the pollen tube tip involves PMEI endocytosis, and reflects the distribution of esterified and de-esterified pectins. Plant J. 53, 133–143.

Romano, P.G., Horton, P., Gray, J.E., 2004. The Arabidopsis cyclophilin gene family. Plant Physiol. 134, 1268–1282.

Romano, P., Gray, J., Horton, P., Luan, S., 2005. Plant immunophilins: functional ver- satility beyond protein maturation. New Phytol. 166, 753–769.

San Segundo-Acosta, P., Oeo-Santos, C., Benede, S., de los Rios, V., Navas, A., Ruiz-Leon, B., Moreno, C., Pastor-Vargas, C., Jurado, A., Villalba, M., Barderas, R., 2019. Delineation of the olive pollen proteome and its allergenome unmasks cyclophilin as a relevant cross-reactive allergen. J. Proteome Res. 18, 3052–3066.

Schreiber, S.L., 1991. Chemistry and biology of the immunophilins and their im- munosuppressive ligands. Science 251, 283–287.

Shang, Z.L., Ma, L.G., Zhang, H.L., He, R.R., Wang, X.C., Cui, S.J., Sun, D.Y., 2005. Ca2+ influx into lily pollen grains through a hyperpolarization-activated Ca2+-permeable channel which can be regulated by extracellular CaM. Plant Cell Physiol. 46, 598–608.

Soskic, V., Gorlach, M., Poznanovic, S., Boehmer, F.D., Godovac-Zimmermann, J., 1999. Functional proteomics analysis of signal transduction pathways of the platelet-de- rived growth factor beta receptor. Biochemistry 38, 1757–1764.

Steinhorst, L., Kudla, J., 2013. Calcium - a central regulator of pollen germination and tube growth. Biochim. Biophys. Acta 1833, 1573–1581.

Trivedi, D.K., Yadav, S., Vaid, N., Tuteja, N., 2012. Genome wide analysis of Cyclophilin gene family from rice and Arabidopsis and its comparison with yeast. Plant Signal. Behav. 7, 1653–1666.

Vasudevan, D., Gopalan, G., Kumar, A., Garcia, V.J., Luan, S., Swaminathan, K., 2015. Plant immunophilins: a review of their structure-function relationship. Biochim. Biophys. Acta 1850, 2145–2158.

Vega-Maray, A.M., Fernandez-Gonzalez, D., Valencia-Barrera, R., Suarez-Cervera, M., 2006. Detection and release of allergenic proteins in Parietaria judaica pollen grains. Protoplasma 228, 115–120.

Vrtala, S., Grote, M., Duchene, M., Vanree, R., Kraft, D., Scheiner, O., Valenta, R., 1993. Properties of tree and grass-pollen allergens - reinvestigation of the linkage between solubility and allergenicity. Int. Arch. Allergy Immunol. 102, 160–169.

Wolf, S., Greiner, S., 2012. Growth control by cell wall pectins. Protoplasma 249, 169–175.

Yokota, E., Ohmori, T., Muto, S., Shimmen, T., 2004. 21-kDa polypeptide, a low-mole- cular-weight cyclophilin, is released from pollen of higher plants into the extra- cellular medium in vitro. Planta 218, 1008–1018.

Zaidi, M.A., O'Leary, S., Wu, S.B., Gleddie, S., Eudes, F., Laroche, A., Robert, L.S., 2012. A molecular and proteomic investigation of proteins rapidly released from triticale pollen upon hydration. Plant Mol. Biol. 79, 101–121.

8. Final remarks

Spermatophytes reproductive biology is a fascinating yet elusive subject, that often crosses paths with human health. While human coexistence with plants is both desirable and necessary, plants might provide ecosystem disservices, such as pollen allergies. Allergic rhinoconjuctivites and asthma can significantly impair the quality of life of the individual, and thus the allergenic risk posed by airborne pollen needs to be monitored, forecasted, and prevented. Recent advances in basic science knowledge, in technology, and in computational intelligence, have revolutionised the approach to allergenic pollen monitoring and forecasting, improving their temporal and spatial resolution, and making them faster and more precise. Nevertheless, allergenic pollen production and dispersal dynamics are influenced by a multitude of intrinsic and extrinsic factors, making them difficult to generalise and thus to predict. Furthermore, mechanisms underlying pollen sensitisation and pollen allergy outbursts are still unclear: allergenic pollen can carry different concentrations of pollen allergens, which can be released either directly in the respiratory mucosa, or in the atmosphere first, and then inhaled. These events however are strongly influenced by the concurring environmental conditions. Moreover, the release mechanism of pollen allergens in the human airways is still largely unknown. All these uncertainties and variabilities make almost impossible to estimate a precise and generalised allergenic pollen risk using a single approach, and they require a multidisciplinary and multiproxy effort instead.

At the end of this research project, it is apparent how a detailed investigation on pollen molecular biology, pollen productivity, and pollen potency, could really make a difference in the understanding of the relationships amongst air pollutants, adverse meteorological conditions, and severeness of pollen allergic reactions.

9. PhD candidate scientific and academic activity

9.1   Other experimental activities

Apart from the conceptual, experimental, and analytical work that led to the papers collected in this thesis, during my PhD course I followed and contributed to other lines of research that still need additional experiments for their results to be presented to the scientific community. In particular, the study reported in Chapter 4 was followed by a further investigation on the allergenicity of the Botanical Garden of Bologna, that I am briefly describing in this section. One approach to this subject was to prepare a questionnaire with 35 questions, starting from the available literature on the monitoring of pollen allergies around the world. The questionnaire was administrated online to a random sample of 255 adults (>18 yo) living in Bologna province, and it aimed to evaluate the percentage of pollen-allergic people in the city and the impact this disease has on their daily lives, but also to assess whether visiting the Botanical Garden can cause a symptom outbreak in pollen allergic subjects. The results of the questionnaire were in line with the European data: 24.2% of respondents declared to have a pollen allergy diagnosis, and 44.2% had relatives suffering from pollen allergies. The most common allergy was to Poaceae pollen, followed by Cupressaceae and Betulaceae. According to the survey, out of 27 diagnosed pollen-allergic subjects, only 6 experienced allergic symptoms after visiting the park, corroborating the low allergenicity of the park and the higher reliability of I_{UGZA} compared to SAI. These 6 people were mainly allergic to Betulaceae, Poaceae, Cupressaceae, Oleaceae, Salicaceae, and Urticaceae pollen, which agrees with the most important allergenic species indicated by the calculation of IUGZA on the complete census of the Botanical Garden wooden flora. After this pilot-study, the questionnaire is ready to be administered to the park visitors during different pollen seasons, in order to gain statistical significance and to track the allergic symptoms back to their causes.

Another approach to test the allergenicity of the park was to conduct a comprehensive monitoring of the airborne pollen in the surroundings of the botanical garden, identifying and quantifying allergenic pollen collected by:

176

- a volumetric Hirst-type air sampler, VPPS 2000 (Lanzoni, Italy), placed on the rooftop of the nearby Physics department in Via Irnerio 46, that operated continuously from February to July 2021, providing an image of the average airborne pollen spectra nearby the park;

- natural gravimetric traps (moss polsters), sampled inside the plots described in Chapter 4, that should provide an image of the pollen spectra the park visitors are realistically exposed to.

However, as explained in Chapter 2, pollen counts are a labour-intensive process and to this date the analysis of these samples is still ongoing. Preliminary results are suggesting that the airborne concentrations of allergenic pollen near the Botanical Garden significantly differ from those recorded by ARPAE for the city of Bologna. These concentrations seem to be affected not only by the vegetation in the proximity of the sampler, but also by medium and long-distance dispersal events, and by the presence of physical barriers in the city centre that create peculiar atmospheric dynamics influencing particle dispersal, as described in Chapter 3. The presence of allergenic pollen originating from outside the park is evident also in samples from moss polsters, thus underlying the importance to associate pollen analysis to the allergenic indices elaboration.

9.2   Education

o   **Seminars attended:**

- "Postglacial colonization and island biogeography in alpine vegetation of Southern Europe", Borja Jiménez-Alfaro PhD (29/11/2018, 2 h)

- "A Matrix of life and death", Prof. Elisabetta Verderio (19/12/2018, 2 h)

- "Selling Science to politicians and publics – communicating technical science to non-technical audiences", Prof. Iain Stewart (25/02/2019, 6 h)

- "Predator-prey Interactions in the Fossil Record", Prof. Michal Kowalewski (11/03/2019, 6 h)

- "The Origin of Life, Early Evolution, and Endosymbiosis", Prof. William F. Martin (18/03/2019 – 19/03/2019, 6 h)

- "Evolutionary Genomics: Methods and Case Studies", Prof. Fabrizio Ghiselli (09/05/2019, 4 h)

- "Biodiversity and bioindicators in a climate change perspective", Prof. Juri Nascimbene (18/06/2019, 4 h)

- "Scientometry and Bibliometry", prof. Alessandro Chiarucci (1/10/2019, 4 h)

- "Transposable Element repression in the germline: piRNAs as guardians of the germline genome integrity", Dr Emilie Brasset (23/10/2019, 1 h)

- "Targeting muscle and metabolic pathologies to develop new treatment strategies for spinal muscular atrophy", Melissa Bowerman (6/11/2019, 1 h)

- "Signalling with ubiquitin—communication between metabolism and immune responses and DNA damage repair", Dr Elton Zeqiraj (13/11/2019, 1 h)

- "Host and HPV methylation play a cornerstone role in HPV-related cancer progression", Dr. Belinda Nedja (19/11/2019, 1 h)

- "More than neuropsychiatry: Emerging implications for trace amine pharmacology in breast cancer, immune modulation and nutrient-induced hormone secretion", Prof. Mark Berry (4/12/2019, 1 h)

- "Links between diet, the gut microbiota, and health", Alan Walker (13/12/2019, 1 h)

- "Novel (lymph)angiogenic factors and their receptors in human endothelial cells - from discovery towards translational research", Leonid Nikitenko (15/01/2020, 1 h)

- "Transglutaminase 2 in calcium homeostasis and neurodegeneration", Dr. Elisa Tonoli (22/01/2020, 1 h)

- "Remote sensing", Prof. Duccio Rocchini (17/04/2020, 4 h)

- "LaTeX: scientific formatting for lazy people... like scientists!", Prof. Duccio Rocchini (28/05/2020, 4 h)

- "Ugly but amazing: serpentinization, energy, and life (and new frontiers from the deep Earth and other planetary bodies)", Prof. Alberto Vitale Brovarone (19/02/2021, 2.5 h)

- "Funzioni, cause, meccanismi", Prof. Raffaella Campaner (19/03/2021, 10.5 h)

- "Etica e scienza (ed etica della scienza)", Prof. Maria Giovanna Belcastro, Prof. Fabrizio Rufo, Prof. Federico Fanti (23/04/2021, 3.5 h)

- "Epigenetic inheritance: neo-Lamarckism?", Prof. Liliana Milani (29/04/2021, 3 h)

- o Courses attended:
  - "72910 – Laboratorio di Cartografia Numerica e GIS", Prof. Luigi Cantelli (52 h)

  - "Statistics for STVA PhD course", Prof. Andrea Luchetti and Prof. Alessio Boattini (35 h)

- o Workshops attended:
  - "Workshop: Understand your data", Erika Brattich PhD (10/12/2018, 2 h)

  - "Workshop on plant & vegetation effects in urban environments" (14/12/2018, 2 h)

  - Academic simulation "Scientific Journalist for a day" (06/06/2019, 4 h)

  - "Connecting Nature – Business Model Canvas, Financing and Entrepreneurship Workshop" (01/06/2019 – 02/06/2019, 13 h)

9.3   Congress attendance and Posters/Abstracts presented

- o 115th Congress of the Italian Botanical Society (SBI) (24 h), with poster presentation/video contribution: "Allergenic potential of urban green areas: methods standardisation applied to the Botanical Garden of Bologna" (9-11/09/2020).

- o 7th European Symposium on Aerobiology (ESA2020) (40 h), with poster presentation/video contribution: "Pollensome: a new unexplored topic of aerobiology and allergology" (16-20/11/2020).

- o VI edition: States General of the Urban Greenery, Ministry of the Environment, ISPRA, SNPA (23-24/11/2020, 10 h).

- o Annual meeting of the SBI 2021 working groups (16-18/06/2021, 13 h).

- o Scheduled: MedPalynos2021, with oral presentation: "Does pollen release exosomes?" (6-8/09/2021).

- o Scheduled: 116th Congress of the Italian Botanical Society (SBI), with poster presentation/video contribution: "Allergenic risk assessment of urban parks: towards a standard index" (8-10/09/2021).

9.4   Awards

o   MedPlaynos2021 best speech prize in S1: Pollen Biology And Structure, with the work entitled: Does Pollen Release Exosomes?

9.5   Publications on IF Journals

1.   Luigi Parrotta, Iris Aloisi, Chiara Suanno, Claudia Faleri, Agnieszka Kiełbowicz-Matuk, Luca Bini, Giampiero Cai, Stefano Del Duca, "A low molecular-weight cyclophilin localizes in different cell compartments of Pyrus communis pollen and is released in vitro under Ca2+ depletion", Plant Physiology and Biochemistry, 2019, ISSN 0981-9428, https://doi.org/10.1016/j.plaphy.2019.09.045.

2.   Capotorti G., Bonacquisti S., Abis L., Aloisi I., Attorre F., Bacaro G., Balletto G., Banfi E., Barni E., Bartoli F., Bazzato E., Beccaccioli M., Braglia R., Bretzel F., Brighetti M. A., Brundu G., Burnelli M., Calfapietra C., Cambria V. E., Caneva G., Canini A., Caronni S., Castello M., Catalano C., Celesti-Grapow L., Cicinelli E., Cipriani L., Citterio S., Concu G., Coppi A., Corona E., Del Duca S., Del V. E., Di Gristina E., Domina G., Faino L., Fano E. A., Fares S., Farris E., Farris S., Fornaciari M., Gaglio M., Galasso G., Galletti M., Gargano M. L., Gentili R., Giannotta A. P., Guarino C., Guarino R., Iaquinta G., Iiriti G., Lallai A., Lallai E., Lattanzi E., Manca S., Manes F., Marignani M., Marinangeli F., Mariotti M., Mascia F., Mazzola P., Meloni G., Michelozzi P., Miraglia A., Montagnani C., Mundula L., Muresan A. N., Musanti F., Nardini0 A., Nicosia E., Oddi L., Orlandi F., Pace R., Palumbo M. E., Palumbo S., Parrotta L., Pasta S., Perini K., Poldini L., Postiglione A., Prigioniero A., Proietti C., Raimondo F. M., Ranfa A., Redi E. L., Reverberi M., Roccotiello E., Ruga L., Savo V., Scarano P., Schirru F., Sciarrillo R., Scuderi F., Sebastiani A., Siniscalco C., Sordo A., Suanno C., Tartaglia M., Tilia A., Toffolo C., Toselli E., Travaglini A., Ventura F., Venturella G., Vincenzi F., Blasi C. , "More nature in the city", PLANT BIOSYSTEMS, 2020, ISSN 1126-3504, https://doi.org/10.1080/11263504.2020.1837285.

3.   Chiara Suanno, Iris Aloisi, Delia Fernández-González, Stefano del Duca, "Monitoring techniques for pollen allergy risk assessment", Environmental Research, 2021, ISSN: 0013-9351, https://doi.org/10.1016/j.envres.2021.111109.

4.   Chiara Suanno, Iris Aloisi, Delia Fernández-González, Stefano del Duca, "Pollen forecasting and its relevance in pollen allergen avoidance", Environmental Research, 2021, ISSN: 0013-9351, https://doi.org/10.1016/j.envres.2021.111150.

5.   Chiara Suanno, Iris Aloisi, Luigi Parrotta, Delia Fernández-González, Stefano del Duca, "Allergenic risk assessment of urban parks: Towards a standard index", Environmental Research, 2021, ISSN: 0013-9351, https://doi.org/10.1016/j.envres.2021.111436.

9.6   Other publications

1.   Battistini R., Castrignanò M., Bergamaschi M., Daconto L., Del Duca S., Aloisi I., Suanno C., Parrotta L., Tositti L., Patuelli R., Pietrantoni L., Tria A., Rainieri G., "Studio di benchmarking e di definizione di indicatori per l'analisi di impatto della linea tranviaria", report dell'Alma Mater Studiorum – Università di Bologna, 27 novembre 2019.

9.7   Didactic activity

o   Lab demonstrations (tutor) for the academic discipline BIO/01 General Botany (60 h, 2019; 60 h 2020; 60 h, 2021).

o   Lab demonstrations (tutor) for the academic discipline BIO/10 Biochemistry (36 h, 2020, 24h, 2021).

o   Co-tutoring for 1 undergraduate student (Sara Quartieri, Biology, 2020) and 4 postgraduate students (Sciences and Management of Nature: Giovanna Iaquinta (2019), Giada Domeniconi (2020), Flavia Ruggirello (2021); Biodiversity and Evolution: Anna Sirigu (2021)).

9.8   Period abroad

o   **Research project:** "Study on secretion of respirable size nanovesicles delivering allergens during pollen germination".

o   **Facility:** Nottingham Trent University (Clifton, Nottingham NG11 8NS, United Kingdom).

o   **Period:** from 1/10/2019 to 31/01/2020.

o   **Tutor:** Prof. Elisabetta Verderio-Edwards (Associate Professor and Reader in Medical Biochemistry, Research Coordinator for REF, School of Science and Technology, Nottingham Trent University. E-mail: elisabetta.verderio-edwards@ntu.ac.uk).

o   **Funding:** Marco Polo scholarship.

10.   Supplementary material

Supplementary to chapter 4

Fig. S1: *"Number of articles on forecasting in Scopus"* - *Pie charts of the number of papers published since 2010, found in Scopus with the reported keywords in the title, abstract and keyword sections. Observation-based forecasting (A), Process-based phenological models (B), and Pollen dispersion models (C).*
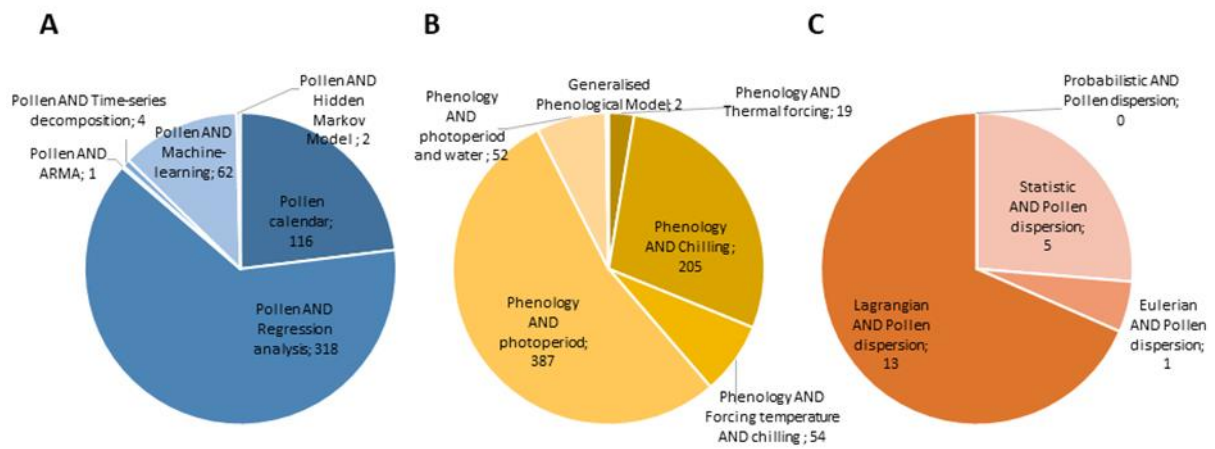
Supplementary to chapter 5

Figure S1 *Map of the Botanical Garden of Bologna divided in 30x30 m squares for the systematic sampling, with the centre of the plot indicated by the blue dot. The map is produced in QGIS*
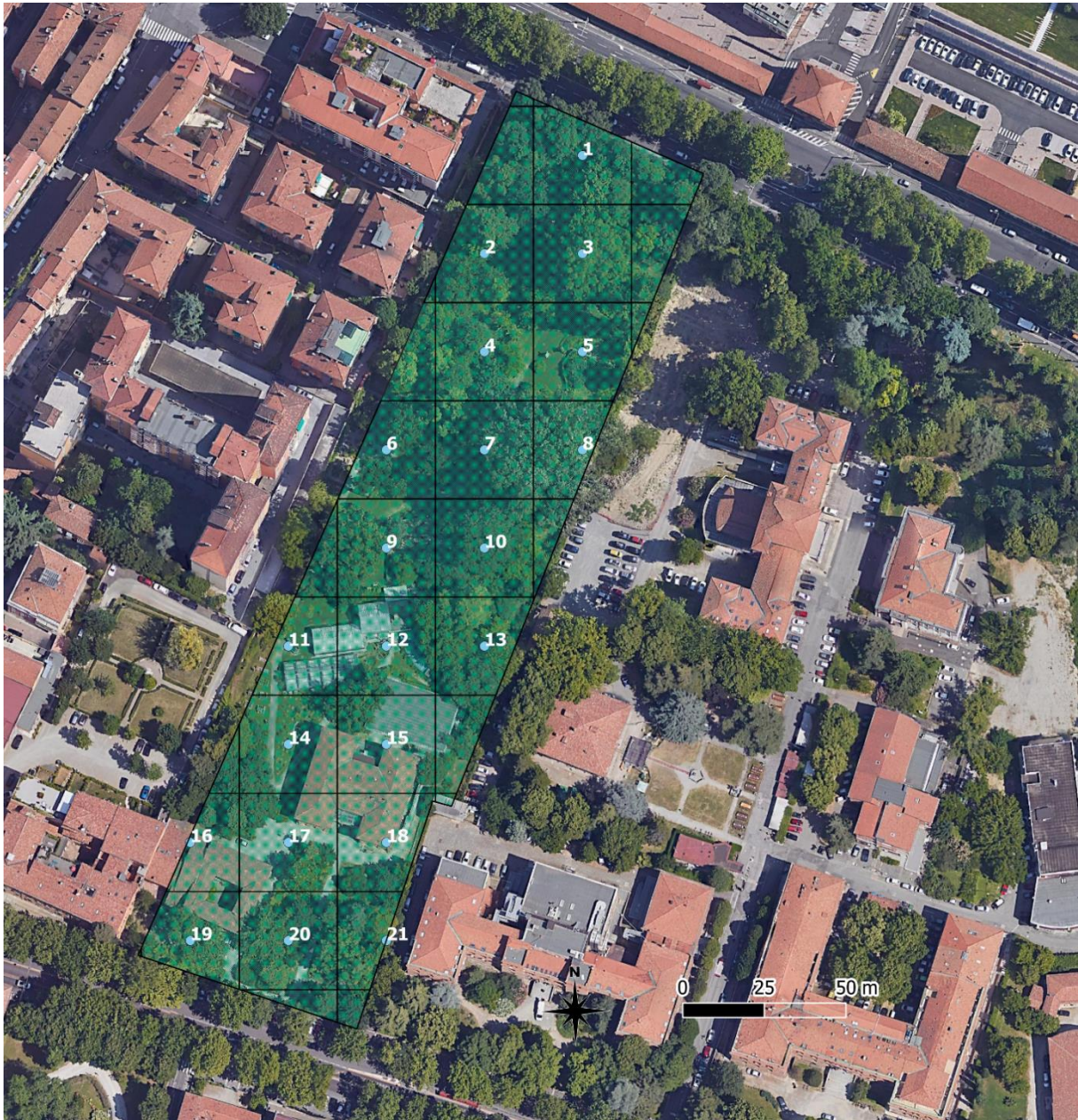
environment.

Figure S2 *Workflow of the allergenic species evaluation employed in this work.*
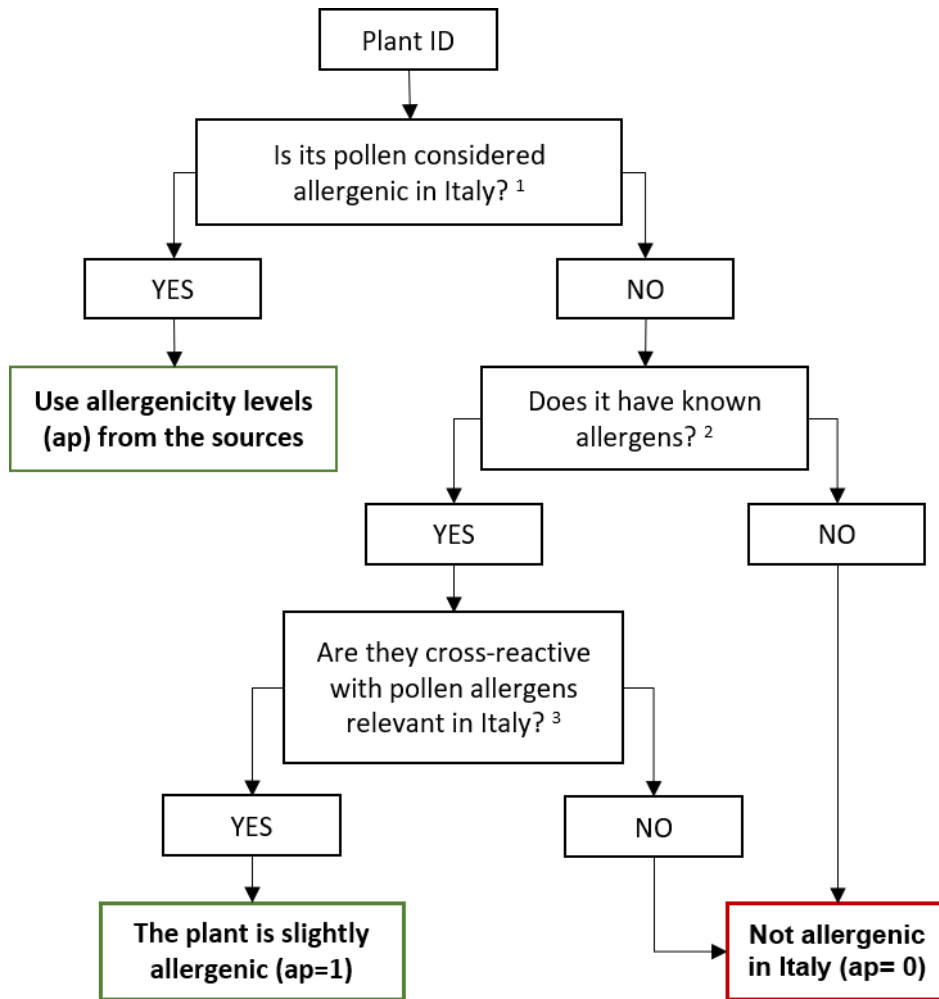
[1] **Sources:** ARPAE list of allergenic species in the region (ARPAE, 2020), WAO list of allergenic plants in Italy (WAO, 2012), systematic reviews on allergenic species in Italy (Ortolani et al., 2015).

[2] **Sources**: allergen databases (Allergome Team and Collaborators, 2021)

[3] **Sources**: scientific papers (Cancelliere et al., 2020; Gadermaier et al., 2014; Gangl et al., 2015; Gastaminza et al., 2009; Lombardero et al., 2002; López-Matas et al., 2016; Moraes et al., 2018; Mothes et al., 2004; Panzani et al., 1986; Schwietz et al., 2000; Weber, 2003), books (Oh, 2018).

Table S9 List of allergenic arboreal taxa present in the Botanical Garden of Bologna according to the 2020 census, with their number of individuals (N. individuals) and their percent cover over the total park surface (% cover). The list includes individuals identified to the genus level that did not belong to any of the other species mentioned. Colours represent the reported allergenicity for the region. Violet: main allergens of the region; red: extremely allergenic; orange: moderately allergenic; yellow: slightly allergenic. Last column reports the status for each species in the Italian Region Emilia Romagna: i=indigenous; ac=alien, casual; an=alien, naturalised; ai=alien, invasive.

FAMILY	TAXONOMIC IDENTIFICATION	N. individuals	% cover	Status
Betulaceae	*Alnus glutinosa* (L.) Gaertn.	1	0.08	i
Betulaceae	*Carpinus orientalis* Mill.	1	0.58	i
Betulaceae	*Corylus avellana* L.	56	6.04	i
Betulaceae	*Corylus maxima* Mill.	3	0.33	ac
Betulaceae	*Ostrya carpinifolia* Scop.	1	1.41	i
Cupressaceae	*Cryptomeria japonica* (Thunb. Ex L.f.) D.Don	2	0.78	ac
Cupressaceae	*Cupressus sempervirens* L.	2	0.47	ac
Cupressaceae	*Juniperus communis* L.	1	0.02	i
Cupressaceae	*Platycladus orientalis* (L.) Franco	1	0.02	ac
Cupressaceae	*Sequoia sempervirens* (D.Don) Endl.	1	1.08	ac
Fagaceae	*Fagus sylvatica* L.	1	0.09	i
Fagaceae	*Quercus ilex* L.	5	1.57	i
Fagaceae	*Quercus robur* L.	4	1.52	i
Juglandaceae	*Juglans regia* L.	2	0.65	an
Malvaceae	*Tilia americana* L.	1	1.03	ac
Malvaceae	*Tilia cordata* L.	2	1.00	i
Moraceae	*Broussonetia papyrifera* (L.) L'Hér. Ex Vent.	3	3.65	an
Oleaceae	*Fraxinus angustifolia* Vahl	6	2.21	i
Oleaceae	*Fraxinus* sp.	2	0.88	
Oleaceae	*Fraxiuns ornus* L.	1	0.39	i
Oleaceae	*Ligustrum lucidum* W.T.Aiton	173	0.44	ac
Oleaceae	*Ligustrum vulgare* L.	119	0.19	i
Oleaceae	*Olea europaea* L.	1	0.04	ac
Oleaceae	*Syringa vulgaris* L.	2	0.06	ac
Pinaceae	*Picea abies* (L.) H.Karst.	1	0.64	i
Pinaceae	*Pinus halepensis* Mill.	1	0.31	i
Pinaceae	*Pinus pinea* L.	3	0.71	an
Pinaceae	*Pinus nigra* J.F.Arnold	1	1.20	an
Pinaceae	*Pinus sylvestris* L.	1	0.09	i
Platanaceae	*Platanus acerifolia* (Aiton) Willd.	1	2.54	ac
Salicaceae	*Populus alba* L.	11	10.86	i

Salicaceae	*Populus nigra* L.	1	1.43	i
Sapindaceae	*Acer campestre L.*	48	3.34	i
Sapindaceae	*Acer monspessulanum* L.	1	0.04	i
Sapindaceae	*Acer negundo* L.	7	3.38	an
Sapindaceae	*Acer opalus* Mill.	2	2.12	i
Sapindaceae	*Acer palmatum* Thunb.	1	0.30	an
Sapindaceae	*Acer platanoides* L.	6	1.67	i
Sapindaceae	*Acer pseudoplatanus* L.	3	2.13	i
Sapindaceae	*Acer saccharinum* L.	1	0.52	ac
Sapindaceae	*Acer* sp.	2	0.89	
Taxaceae	*Taxus baccata* L.	3	0.42	i
Ulmaceae	*Ulmus minor* Mill.	30	1.96	i

Table S10 *List of allergenic herbaceous species present in the Botanical Garden of Bologna according to the 2019 systematic sampling census, with their percent cover of the plot surface (% cover). The list includes individuals identified to the genus or family level that did not belong to any of the other species mentioned. Colours represent the reported allergenicity for the region. Violet: main allergens of the region; red: extremely allergenic; orange: moderately allergenic; yellow: slightly allergenic. Last column reports the status for each species in the Italian Region Emilia Romagna: i=indigenous; ac=alien, casual; an=alien, naturalised; ai=alien, invasive.*

FAMILY	TAXONOMIC IDENTIFICATION	% cover	Status
Amaranthaceae	*Chenopodium album* L.	0.011	i
Asteraceae	*Artemisia dracunculus* L.	0.056	ac
Asteraceae	*Artemisia* sp.	0.003	
Asteraceae	*Taraxacum campylodes* G.E.Haglund	0.147	i
Plantaginaceae	*Plantago lanceolata* L.	0.017	i
Plantaginaceae	*Plantago major* L.	0.317	i
Poaceae	*Brachypodium pinnatum* (L.) P.Beauv	0.111	ac
Poaceae	*Brachypodium sylvaticum* (Huds.) P.Beauv.	0.478	i
Poaceae	*Bromus sterilis* L.	0.028	i
Poaceae	*Catapodium rigidum* (L.) C.E.Hubb.	0.278	i
Poaceae	*Cynodon dactylon* (L.) Pers.	0.084	i
Poaceae	*Dactylis glomerata* L.	0.111	i
Poaceae	*Hordeum murinum* L.	0.667	i
Poaceae	*Lolium perenne* L.	9.786	i
Poaceae	*Melica uniflora* Retz.	0.083	i
Poaceae	*Phragmites australis* (Cav.) Trin. ex Steud.	0.556	i
Poaceae	*Poa annua* L.	0.822	i
Poaceae	*Poa pratensis* L.	0.094	i
Poaceae	*Poa trivialis* L.	19.561	i

Poaceae	Poaceae	0.061	
Poaceae	*Zea mays* L.	0.017	ac
Poaceae	*Zea mexicana* (Schrad.) Kuntze	0.006	ac
Urticaceae	*Parietaria officinalis* L.	1.703	i

Table S11 I_{UGZA} values considering ap=4 for the major allergens in the region (*Corylus avellana* L., *Cupressus sempervirens* L, *Olea europaea* L., *Poa trivialis* L., *Lolium perenne* L., *Poa annua* L., *Dactylis glomerata* L., *Poa pratensis* L., *Cynodon dactylon* (L.) Pers., *Bromus sterilis* L., *Zea mays* L., *Zea mexicana* (Schrad.) Kuntze, *Parietaria officinalis* L.), with different PAV_{max} values.

Plant group	Approach	PAV$_{max}$	I$_{UGZA}$
All spermatophytes	Systematic sampling	27	0.07
All spermatophytes	Systematic sampling	36	0.05
All spermatophytes	Census	27	0.08
All spermatophytes	Census	36	0.06
Arboreal species	Systematic sampling	27	0.06
Arboreal species	Systematic sampling	36	0.04
Arboreal species	Census	27	0.08
Arboreal species	Census	36	0.06

Figure S3 Relationship between number of allergenic species and species richness (A) and between number of allergenic and non-allergenic species (B) per plot in the Botanical Garden of Bologna, according to the systematic sampling of 2019.
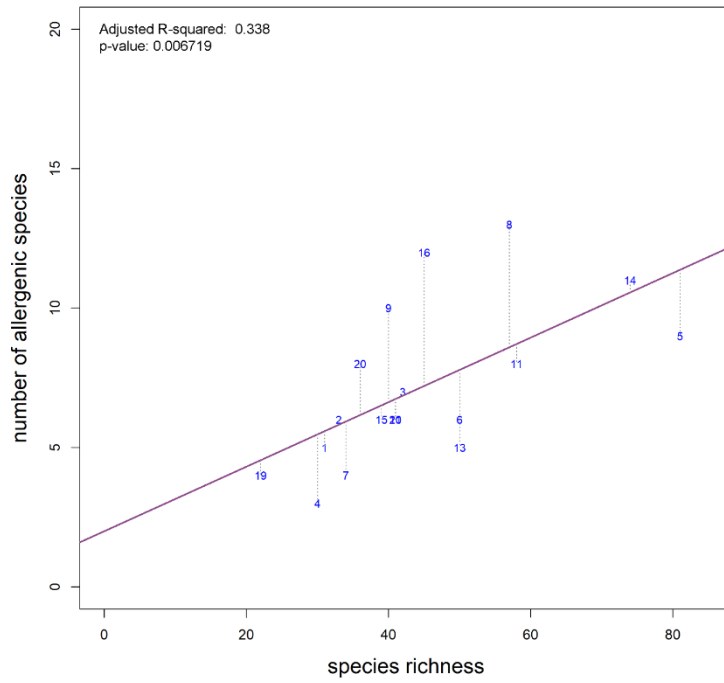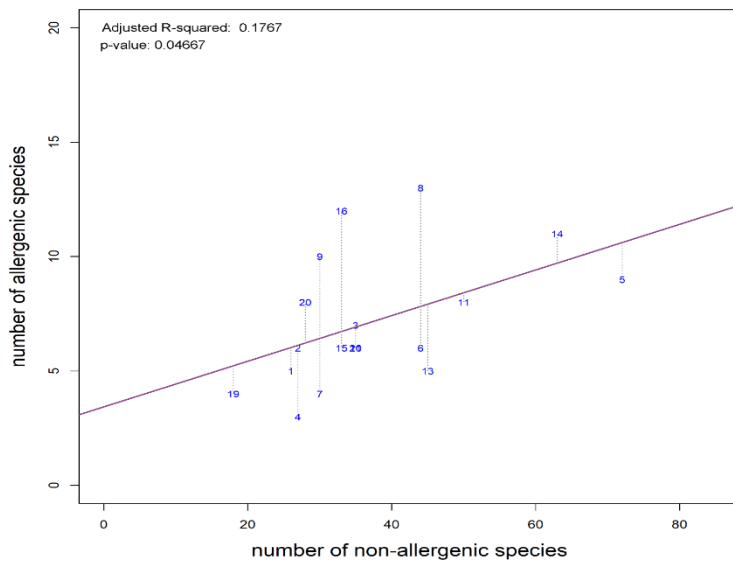
Figure S4 *Scatterplot of the relationship between Shannon-Wiener diversity index (H-index) and Urban Green Zones Allergenicity Index (I_{UGZA}) (A) or Specific Allergenic Index (SAI) (B) for the Botanical Garden of Bologna, calculated per plot on the 2019 systematic sampling dataset.*
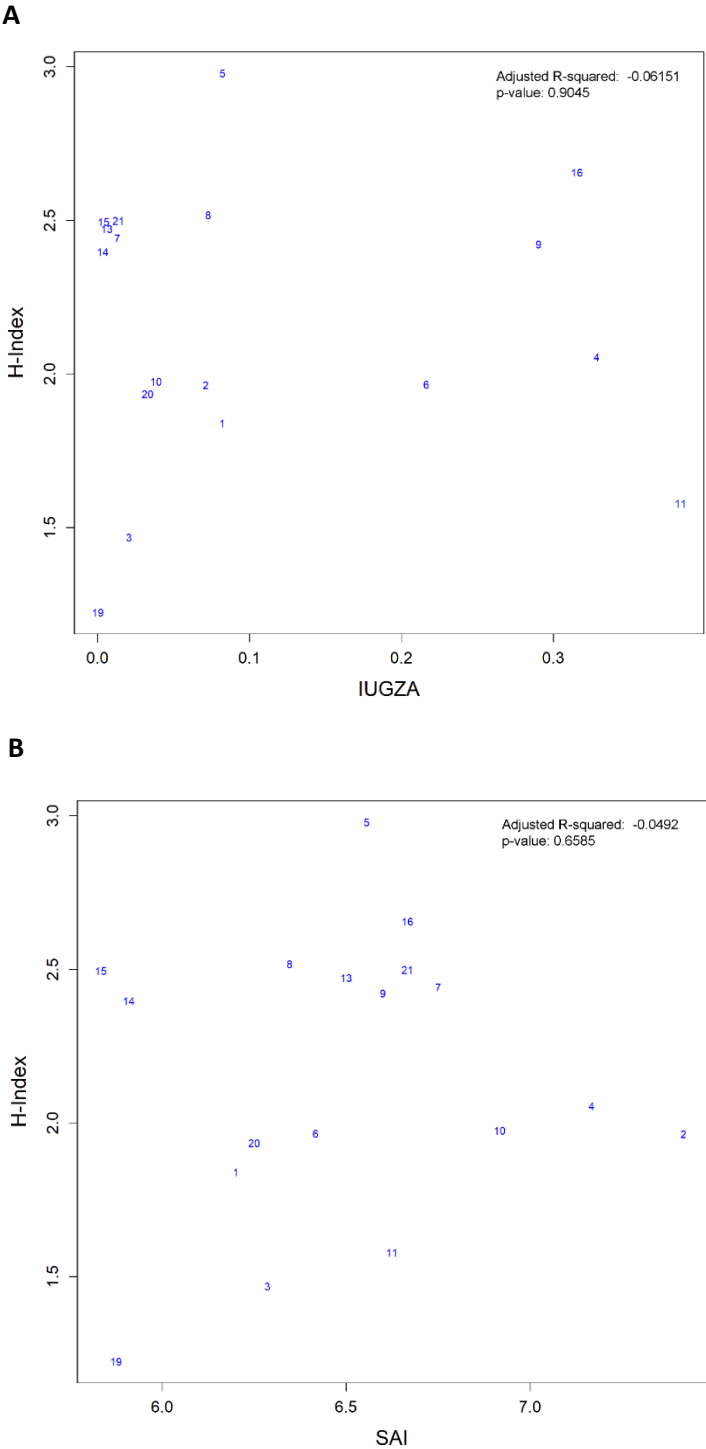
Bibliography

Allergome Team and Collaborators, 2021. Allergome [WWW Document]. URL https://www.allergome.org/ (accessed 4.15.21).

ARPAE, 2020. Schede botaniche — Arpae Emilia-Romagna [WWW Document]. URL https://www.arpae.it/it/temi-ambientali/pollini/schede-botaniche (accessed 4.9.21).

Cancelliere, N., Iglesias, I., Ayuga, Á., Miranda, E.E., 2020. Cross-reactivity between Parietaria Judaica and Parietaria officinalis in immunotherapy extracts for the treatment of allergy to Parietaria. Biomed. Reports 12, 326–332. https://doi.org/10.3892/br.2020.1297

Gadermaier, G., Eichhorn, S., Vejvar, E., Weilnböck, L., Lang, R., Briza, P., Huber, C.G., Ferreira, F., Hawranek, T., 2014. Plantago lanceolata: An important trigger of summer pollinosis with limited IgE cross-reactivity. J. Allergy Clin. Immunol. 134, 472-475.e5. https://doi.org/10.1016/j.jaci.2014.02.016

Gangl, K., Niederberger, V., Valenta, R., Nandy, A., 2015. Marker allergens and panallergens in tree and grass pollen allergy. Allergo J. Int. 24, 158–169. https://doi.org/10.1007/s40629-015-0055-3

Gastaminza, G., Lombardero, M., Bernaola, G., Antepara, I., Muñoz, D., Gamboa, P.M., Audicana, M.T., Marcos, C., Ansotegui, I.J., 2009. Allergenicity and cross-reactivity of pine pollen. Clin. Exp. Allergy 39, 1438–1446. https://doi.org/10.1111/j.1365-2222.2009.03308.x

Lombardero, M., Obispo, T., Calabozo, B., Lezaún, A., Polo, F., Barber, D., 2002. Cross-reactivity between olive and other species. Role of Ole e 1-related proteins. Allergy Eur. J. Allergy Clin. Immunol. 57, 29–34. https://doi.org/10.1034/j.1398-9995.2002.057s71029.x

López-Matas, M.A., Moya, R., Cardona, V., Valero, A., Gaig, P., Malet, A., Viñas, M., García-Moral, A., Labrador, M., Alcoceba, E., Ibero, M., Carnés, J., 2016. Relevance of allergenic sensitization to Cynodon dactylon and Phragmites communis: Cross-reactivity with pooideae grasses. J. Investig. Allergol. Clin. Immunol. 26, 295–303. https://doi.org/10.18176/jiaci.0049

Moraes, A.H., Asam, C., Almeida, F.C.L., Wallner, M., Ferreira, F., Valente, A.P., 2018. Structural basis for cross-reactivity and conformation fluctuation of the major beech pollen allergen Fag s 1. Sci. Rep. 8, 1–10. https://doi.org/10.1038/s41598-018-28358-1

Mothes, N., Horak, F., Valenta, R., 2004. Transition from a botanical to a molecular classification in tree pollen allergy: Implications for diagnosis and therapy. Int. Arch. Allergy Immunol. 135, 357–373. https://doi.org/10.1159/000082332

Oh, J.-W., 2018. Pollen Allergy in a Changing World, Pollen Allergy in a Changing World. https://doi.org/10.1007/978-981-10-5499-0

Ortolani, C., Previdi, M., Sala, G., Bozzoli Parasacchi, V., Ortolani, A., Minella, C., 2015. Allergenicity of trees and shrubbery to use in the italian urban green. Systematic review and evidence-based reccomandations. Eur. J. Aerobiol. Environmetal Med. XI.

Panzani, R., Yasueda, H., Shimizu, T., Shida, T., 1986. Cross-reactivity between the pollens of Cupressus sempervirens (common cypress) and of Cryptomeria japonica (Japanese cedar). Ann. Allergy 57, 26–30.

Schwietz, L.A., Goetz, D.W., Whisman, B.A., Reid, M.J., 2000. Cross-reactivity among conifer pollens. Ann. Allergy, Asthma Immunol. 84, 87–93. https://doi.org/10.1016/S1081-1206(10)62746-9

WAO, 2012. Italy | World Allergy Organization [WWW Document]. URL https://www.worldallergy.org/resources/world-atlas-of-aeroallergens/italy (accessed 4.9.21).

Weber, R.W., 2003. Patterns of pollen cross-allergenicity. J. Allergy Clin. Immunol. 112, 229–239. https://doi.org/10.1067/mai.2003.1683

Supplementary to chapter 6

Table S1 *Proteins identified by RP-HPLC-ESI-MS/MS in nanovesicles isolated from germinated kiwi (Actinidia chinensis Planch.) pollen using UniProt database, ordered by accession number. Samples were analysed in triplicate, and a pooling of the 3 biological replicas was analysed as well. Mean and maximum values are calculated for each accession number over the 4 total replicas. Mean Pep= mean number of peptides (95% confidence); Max Pep= maximum number of peptides (95% confidence); Mean %Cov= mean 95% coverage; Max %Cov= maximum 95% coverage.*

	Accession number	Protein name	Mean Pep	Max Pep	Mean %Cov	Max %Cov	N. replicas
1	A0A2R6P373	REVERSED Serine/threonine-protein kinase	1.00	1	2.41	2.41	1
2	A0A2R6P3Q0	REVERSED Piriformospora indica-insensitive protein	1.00	1	2.30	2.30	2
3	A0A2R6P5Q0	REVERSED Receptor-like serine/threonine-protein kinase	1.00	1	1.62	1.62	1
4	A0A2R6P788	REVERSED E3 ubiquitin-protein like	1.00	1	0.81	0.81	1
5	A0A2R6PE76	REVERSED Ribonuclease P protein subunit p25-like protein	1.00	1	3.32	3.32	1
6	A0A2R6PEL7	REVERSED Disease resistance protein	1.00	1	1.24	1.24	2
7	A0A2R6PER4	REVERSED Suppressor of gene silencing like protein	1.00	1	0.81	0.81	1
8	A0A2R6PF55	REVERSED E3 UFM1-protein like	1.00	1	1.69	1.69	1
9	A0A2R6PJD9	REVERSED GTP diphosphokinase	1.00	1	1.56	1.56	2
10	A0A2R6PJI8	REVERSED Serine/threonine-protein kinase	1.00	1	0.91	0.91	3
11	A0A2R6PJX7	REVERSED DnaJ subfamily B member like	1.00	1	1.44	1.44	1
12	A0A2R6PJZ5	REVERSED J domain-containing protein	1.00	1	1.15	1.15	1
13	A0A2R6PK49	REVERSED Protein ALWAYS EARLY like	1.00	1	1.00	1.00	1
14	A0A2R6PKE4	REVERSED Serine/threonine protein phosphatase 2A regulatory subunit B''gamma like	1.00	1	1.30	1.30	2
15	A0A2R6PMP6	REVERSED 28S rRNA (Cytosine-C(5))-methyltransferase	1.00	1	1.37	1.37	2
16	A0A2R6PPF8	REVERSED Receptor-like kinase	1.00	1	0.97	0.97	1
17	A0A2R6PW02	REVERSED Serine/threonine-protein kinase	1.00	1	0.92	0.92	3
18	A0A2R6PX74	REVERSED Serine/threonine protein phosphatase 2A regulatory subunit B''gamma like	1.00	1	1.30	1.30	2
19	A0A2R6PXE6	REVERSED Rhodanese-like domain-containing protein	1.00	1	9.26	9.26	2
20	A0A2R6PY60	REVERSED Cytochrome P450 87A3 like	1.00	1	2.74	2.74	1
21	A0A2R6PYM0	REVERSED Serine/threonine protein phosphatase 2A regulatory subunit B''gamma like	1.00	1	1.30	1.30	2
22	A0A2R6Q040	REVERSED DPH4 like	1.00	1	4.49	4.49	1
23	A0A2R6Q9X2	REVERSED Rhodanese-like domain-containing protein	1.00	1	9.26	9.26	2
24	A0A2R6QAV0	REVERSED Serine/threonine protein phosphatase 2A regulatory subunit B''gamma like	1.00	1	1.30	1.30	2
25	A0A2R6QD53	REVERSED Receptor-like serine/threonine-protein kinase	1.00	1	1.62	1.62	1
26	A0A2R6QDC0	REVERSED Disease resistance protein	1.00	1	0.96	0.96	1
27	A0A2R6QQS2	REVERSED Protein argonaute like	1.00	1	0.99	0.99	2
28	A0A2R6QVL9	REVERSED Protein DETOXIFICATION	1.00	1	2.23	2.23	1
29	A0A2R6QYY8	REVERSED Endonuclease	1.00	1	2.91	2.91	2
30	A0A2R6R486	REVERSED Zinc protease PQQL-like	1.00	1	0.99	0.99	4
31	A0A2R6R7P4	REVERSED Neuron navigator like	1.00	1	1.05	1.05	4
32	A0A2R6RA10	REVERSED Protein hemingway like	1.00	1	1.05	1.05	4
33	A0A2R6RA28	REVERSED Calcium-dependent protein kinase	1.00	1	1.50	1.50	1
34	A0A2R6RB28	REVERSED Microtubule-associated protein like	1.00	1	1.38	1.38	1
35	A0A2R6RB41	REVERSED Thioredoxin-like protein YLS8	1.00	1	8.45	8.45	1
36	A0A2R6RCG6	REVERSED Chaperone protein dnaJ 20 like	1.00	1	4.65	4.65	1

37	A0A2R6RD00	REVERSED Upstream activation factor subunit spp27 like	1	1	5.63	5.63	4
38	A0A2R6RQX4	REVERSED Receptor-like serine/threonine-protein kinase	1.00	1	1.13	1.13	1
39	A0A2R6RSB6	REVERSED Uncharacterized protein	1.00	1	2.43	2.43	1
40	A0A2R6RV83	REVERSED Acetylcholine receptor subunit beta-like	1.00	1	2.52	2.52	1
41	A0A2R6S0Y7	REVERSED GPI-anchored adhesin-like protein	1.00	1	0.61	0.61	1
42	A0A2R6S135	REVERSED Thioredoxin reductase	1.00	1	1.29	1.29	2
43	A0A0C5CH61	ATP synthase subunit beta, chloroplastic	1.00	1	2.21	2.21	2
44	A0A2R6NHF6	UDP-glucuronate decarboxylase	3.40	4	22.34	26.54	4
45	A0A2R6NNP9	Aspartic proteinase	1.00	1	5.44	5.44	2
46	A0A2R6NU89	40S ribosomal protein	4.40	6	21.48	26.85	4
47	A0A2R6NZ12	Universal stress protein	3.25	5	12.88	19.70	4
48	A0A2R6P1F0	Metal-nicotianamine transporter like	1.00	1	2.44	2.44	1
49	A0A2R6P248	ATP synthase subunit alpha (Fragment)	0.00	0	0.00	0.00	1
50	A0A2R6P2I1	DNA/RNA-binding protein Alba-like protein	6.00	7	39.54	42.64	3
51	A0A2R6P2K6	Ethanolamine kinase	3.50	5	10.96	16.04	4
52	A0A2R6P2P6	Galactinol--sucrose galactosyltransferase	1.00	1	1.93	1.93	1
53	A0A2R6P2Q1	Protein kinase	5.00	8	18.74	29.32	4
54	A0A2R6P2Q4	Late embryogenesis abundant protein	1.00	1	4.04	4.04	4
55	A0A2R6P2R4	Activator of Hsp90 ATPase	4.00	4	10.15	11.49	3
56	A0A2R6P2R8	CCT-theta	26.60	36	52.46	66.44	4
57	A0A2R6P2S2	Mucin-2 like (Fragment)	2.00	3	10.47	16.25	4
58	A0A2R6P2S5	Adenylyl-sulfate kinase	6.00	8	37.62	52.40	4
59	A0A2R6P2S9	Transcription factor MafB like	1.50	2	5.86	7.10	4
60	A0A2R6P2T6	Glucan endo-1,3-beta-D-glucosidase	4.50	5	9.32	10.35	2
61	A0A2R6P2Z4	Phosphoglycerate mutase (2,3-diphosphoglycerate-independent)	16.60	23	22.74	26.24	4
62	A0A2R6P321	Tubulin beta chain	13.00	14	51.30	56.03	4
63	A0A2R6P325	Phosphomethylethanolamine N-methyltransferase	16.00	24	31.73	42.36	4
64	A0A2R6P335	Actin-interacting protein like	5.00	8	10.66	17.87	2
65	A0A2R6P340	Guanine nucleotide-binding protein subunit beta-like protein	18.40	24	62.24	67.27	4
66	A0A2R6P341	Mitogen-activated protein kinase	20.00	31	31.58	43.47	4
67	A0A2R6P342	Guanine nucleotide-binding protein subunit beta-like protein	18.40	24	62.24	67.27	4
68	A0A2R6P344	Phospholipase D	4.60	5	6.44	6.93	4
69	A0A2R6P365	Eukaryotic peptide chain release factor GTP-binding subunit ERF3B like	8.33	11	17.81	22.90	3
70	A0A2R6P377	Pyruvate dehydrogenase E1 component subunit beta	1.00	1	2.88	2.88	3
71	A0A2R6P378	Exocyst subunit Exo70 family protein	5.00	8	9.57	14.55	2
72	A0A2R6P3B9	Proteasome subunit beta	12.40	16	51.23	59.85	4
73	A0A2R6P3C9	Glyceraldehyde-3-phosphate dehydrogenase	13.50	16	22.74	24.20	2
74	A0A2R6P3D8	60S ribosomal protein like (Fragment)	3.50	4	21.52	25.82	6
75	A0A2R6P3E9	Eukaryotic translation initiation factor 4B2 like	2.00	3	3.70	5.56	3
76	A0A2R6P3H0	ATP citrate synthase	13.00	18	35.18	43.97	4
77	A0A2R6P3H3	Ribose-phosphate pyrophosphokinase	2.00	2	4.91	4.91	1
78	A0A2R6P3H7	Carbonic anhydrase	19.40	24	67.80	74.83	4

79	A0A2R6P3I1	ADP-ribosylation factor	8.50	10	44.62	47.51	4
80	A0A2R6P3I9	Aldehyde dehydrogenase family 2 member like	1.00	1	1.68	1.68	2
81	A0A2R6P3J6	Protein argonaute 1B like	2.25	4	2.00	3.57	4
82	A0A2R6P3J7	AP-1 complex subunit gamma	14.25	22	17.45	24.52	4
83	A0A2R6P3K0	AD domain-containing protein	1.00	1	5.49	5.49	1
84	A0A2R6P3K7	Dynamin-related protein like	4.00	4	10.50	10.50	2
85	A0A2R6P3L3	Threonyl-tRNA synthetase	12.80	22	17.52	29.16	4
86	A0A2R6P3Q5	Eukaryotic initiation factor 4A-3	5.33	7	9.88	13.73	3
87	A0A2R6P3R1	Tetratricopeptide repeat protein like	19.20	27	46.51	59.20	4
88	A0A2R6P3U4	ACD11 protein	1.00	1	5.58	5.58	3
89	A0A2R6P3U8	Fructose-bisphosphate aldolase	3.50	6	11.57	20.31	4
90	A0A2R6P3V1	Fruit protein like	1.33	2	7.41	7.41	3
91	A0A2R6P3W2	Fruit protein like	3.00	4	13.29	14.69	4
92	A0A2R6P3X5	ATP synthase subunit beta	1.00	1	1.99	1.99	2
93	A0A2R6P3Z1	26S proteasome non-ATPase regulatory subunit like	24.20	35	58.20	73.29	4
94	A0A2R6P3Z3	14-3-3-like protein GF14 iota (Fragment)	18.50	20	64.15	64.34	2
95	A0A2R6P406	Nucleolar protein	1.00	1	1.24	1.24	1
96	A0A2R6P424	Spermidine synthase	1.00	1	3.79	3.79	4
97	A0A2R6P432	Glutathione S-transferase	5.50	6	24.35	25.32	4
98	A0A2R6P438	Tetratricopeptide repeat protein 38	1.00	1	1.71	1.71	2
99	A0A2R6P447	40S ribosomal protein like	7.33	9	29.95	37.56	3
100	A0A2R6P448	Serine/threonine-protein phosphatase	8.20	12	35.23	49.67	4
101	A0A2R6P454	Cullin-3A like	4.00	4	5.72	5.72	2
102	A0A2R6P484	GTP-binding protein like	3.75	4	27.59	30.05	4
103	A0A2R6P485	Galactokinase	19.00	26	48.46	66.13	4
104	A0A2R6P489	Pectinesterase	11.40	15	23.07	28.62	4
105	A0A2R6P496	Ribosomal protein L19	4.50	5	25.47	28.57	4
106	A0A2R6P4A1	Translationally-controlled tumor protein	9.00	12	61.67	68.45	4
107	A0A2R6P4B4	Exopolygalacturonase	1.00	1	3.55	3.55	3
108	A0A2R6P4D4	Protein-synthesizing GTPase	7.40	11	19.27	29.31	4
109	A0A2R6P4E1	40S ribosomal protein S21	4.20	8	40.49	58.54	4
110	A0A2R6P4F5	Protein like	1.00	1	1.74	1.74	4
111	A0A2R6P4G6	Procollagen-proline 4-dioxygenase	1.00	1	3.05	3.05	2
112	A0A2R6P4I0	BSD domain-containing protein	1.00	1	2.03	2.03	2
113	A0A2R6P4I1	ATP citrate synthase	10.50	11	20.37	20.37	2
114	A0A2R6P4I7	Receptor-like serine/threonine-protein kinase	1.00	1	3.66	3.66	2
115	A0A2R6P4K6	YTH domain-containing family protein	2.00	2	2.69	2.69	2
116	A0A2R6P4L1	Galacturonokinase	2.00	2	5.38	5.38	3
117	A0A2R6P4M7	ATP citrate synthase	20.00	20	40.79	40.79	1
118	A0A2R6P4N0	Actin cytoskeleton-regulatory complex protein	8.25	13	8.94	14.05	4
119	A0A2R6P4N7	Serine/threonine-protein kinase (Fragment)	4.33	7	5.87	9.24	3
120	A0A2R6P4P1	Proteasome subunit beta	12.80	15	46.61	50.85	4

121	A0A2R6P4P6	S-adenosylmethionine synthase	26.00	26	53.94	53.94	1
122	A0A2R6P4Q5	HEAT protein	26.00	36	51.17	63.03	4
123	A0A2R6P4Q6	Pectinesterase	15.00	18	34.91	41.87	4
124	A0A2R6P4S2	Rho GDP-dissociation inhibitor like	3.00	5	11.52	18.22	3
125	A0A2R6P4W4	EH domain-containing protein	2.75	5	5.81	10.62	4
126	A0A2R6P4Y4	Polyadenylate-binding protein (Fragment)	2.50	3	6.63	8.35	2
127	A0A2R6P502	Proteasome subunit beta	13.00	16	68.51	82.84	4
128	A0A2R6P568	Eukaryotic translation initiation factor 4C	2.50	4	17.76	24.83	4
129	A0A2R6P584	Ubiquitin-conjugating enzyme like	2.75	4	16.55	19.59	4
130	A0A2R6P587	DNA damage-inducible protein	2.50	4	9.83	14.99	4
131	A0A2R6P5B6	Adenylyltransferase and sulfurtransferase MOCS3	1.00	2	2.76	5.53	4
132	A0A2R6P5H9	5'-nucleotidase	1.00	1	2.60	2.60	3
133	A0A2R6P5L1	ADP-ribosylation factor (Fragment)	9.67	13	45.19	47.78	3
134	A0A2R6P5P2	CTP synthase (Fragment)	3.33	5	11.14	16.71	3
135	A0A2R6P5Q1	Exopolygalacturonase	1.50	2	3.37	4.29	4
136	A0A2R6P5Q2	Kinesin-like protein	1.00	1	1.49	1.49	2
137	A0A2R6P5S4	Universal stress protein	1.33	2	9.11	13.66	3
138	A0A2R6P5T7	Ribosomal protein L19	4.00	5	23.21	29.25	4
139	A0A2R6P5U8	Serine/threonine-protein phosphatase	1.00	1	1.25	1.25	1
140	A0A2R6P5V0	Methenyltetrahydrofolate cyclohydrolase	3.50	5	13.82	19.08	4
141	A0A2R6P5V9	HSP20-like chaperone protein	6.80	9	26.31	32.44	4
142	A0A2R6P5X4	OTU domain-containing protein	1.75	3	7.56	12.35	4
143	A0A2R6P5Y9	NPL4-like protein	1.00	1	3.14	3.14	1
144	A0A2R6P645	COMPASS-like H3K4 histone methylase component WDR5B	2.75	5	13.74	25.72	4
145	A0A2R6P664	Serine/threonine-protein phosphatase	4.00	6	20.00	29.35	4
146	A0A2R6P691	Peptidyl-prolyl cis-trans isomerase	2.67	4	14.45	21.67	3
147	A0A2R6P695	Ras-related protein like	4.00	4	19.91	19.91	1
148	A0A2R6P696	Pyridoxal 5'-phosphate synthase subunit PDX1.3 like	12.60	15	41.93	45.34	4
149	A0A2R6P6A1	Asparagine synthetase [glutamine-hydrolyzing]	4.00	4	8.89	8.89	1
150	A0A2R6P6A6	Alpha-1,4 glucan phosphorylase	1.75	3	3.03	5.18	4
151	A0A2R6P6B1	ABC transporter G family member 31 like	2.00	3	1.60	2.40	3
152	A0A2R6P6B4	Ran-binding protein 1 a like	1.00	1	9.46	9.46	1
153	A0A2R6P6I1	Nardilysin-like	2.00	2	2.42	2.42	2
154	A0A2R6P6I7	Non-specific serine/threonine protein kinase	1.00	1	2.04	2.04	1
155	A0A2R6P6J1	26S protease regulatory subunit 6B like	13.80	19	49.20	60.74	4
156	A0A2R6P6K6	Ubiquitin-conjugating enzyme like	3.80	6	28.11	37.84	4
157	A0A2R6P6M5	Ubiquitin carboxyl-terminal hydrolase (Fragment)	1.00	1	2.32	2.32	1
158	A0A2R6P6N9	BSD domain-containing protein	2.00	2	5.54	5.54	2
159	A0A2R6P6P5	60S ribosomal protein like	3.40	5	29.17	42.11	4
160	A0A2R6P6P6	Receptor-like kinase	1.00	1	1.53	1.53	2
161	A0A2R6P6Q2	Quinone-oxidoreductase	1.00	1	3.95	3.95	2
162	A0A2R6P6R8	Wound-induced basic protein	1.00	1	23.40	23.40	4

163	A0A2R6P6V4	E1 ubiquitin-activating enzyme	12.00	16	15.10	20.31	4
164	A0A2R6P6V6	Pectate lyase	1.00	1	1.81	1.81	4
165	A0A2R6P6V7	Serine/threonine-protein kinase	1.00	1	0.69	0.69	1
166	A0A2R6P6W7	Chaperonin CPN60-2 like	1.67	2	3.13	3.83	3
167	A0A2R6P6X5	Ribonuclease P protein subunit p25-like protein	4.50	5	24.71	27.17	2
168	A0A2R6P6Y4	Uncharacterized protein	5.20	6	25.84	27.92	4
169	A0A2R6P6Y6	Ras GTPase-activating protein-binding protein like	1.00	1	2.36	2.36	2
170	A0A2R6P6Y7	Serine/threonine-protein kinase	3.00	4	6.15	8.50	4
171	A0A2R6P704	Phosphatidylglycerol/phosphatidylinositol transfer protein	1.75	3	11.70	19.87	4
172	A0A2R6P730	Casein kinase 1-like protein (Fragment)	1.00	1	4.11	4.11	3
173	A0A2R6P763	Ribosomal protein	9.67	12	41.36	49.54	6
174	A0A2R6P797	Protein SUPPRESSOR OF K(+) TRANSPORT GROWTH DEFECT like	1.50	2	3.47	4.86	2
175	A0A2R6P7A0	Protein transport protein like	1.00	1	0.94	0.94	2
176	A0A2R6P7A2	UDP-D-apiose/UDP-D-xylose synthase	18.20	25	53.73	67.35	4
177	A0A2R6P7B4	AP-2 complex subunit alpha	8.33	11	9.69	12.18	3
178	A0A2R6P7E4	26S proteasome regulatory subunit 4 A like	21.50	31	44.70	56.29	4
179	A0A2R6P7G6	Serine/threonine-protein phosphatase 6 regulatory subunit like	2.00	2	2.35	2.35	2
180	A0A2R6P7G8	Cell division cycle protein (Fragment)	22.20	31	49.05	55.85	4
181	A0A2R6P7G9	RuvB-like helicase	5.75	9	13.39	21.47	4
182	A0A2R6P7H6	60S ribosomal protein like	6.40	8	46.15	54.82	4
183	A0A2R6P7J5	Serine/threonine-protein phosphatase	1.50	3	1.68	3.35	4
184	A0A2R6P7J6	Vicilin-like seed storage protein	7.00	9	17.00	20.17	4
185	A0A2R6P7L2	Proteasome subunit beta type-4 like (Fragment)	9.00	13	46.83	59.26	4
186	A0A2R6P7L3	L-ascorbate peroxidase	10.80	15	46.56	56.40	4
187	A0A2R6P7P1	60S ribosomal protein L35	2.60	3	20.32	22.76	4
188	A0A2R6P7Q4	D-amino-acid transaminase	1.00	1	2.76	2.76	3
189	A0A2R6P7Q8	40S ribosomal protein S15a	6.00	8	39.54	50.00	4
190	A0A2R6P7S0	Glutelin type-B 4 basic chain like	15.00	20	39.83	48.88	4
191	A0A2R6P7U0	Oxysterol-binding protein-related protein like	1.00	1	1.75	1.75	4
192	A0A2R6P7V0	Heat shock protein 70 family protein	44.80	61	56.61	67.18	4
193	A0A2R6P7V2	Ras-related protein like	7.33	9	34.11	41.67	3
194	A0A2R6P7V5	Actin	74.33	95	74.71	75.60	3
195	A0A2R6P7W0	Actin-depolymerizing factor 2 like (Fragment)	3.00	5	21.58	33.81	4
196	A0A2R6P7Y2	Protein argonaute like	6.50	11	7.65	13.16	4
197	A0A2R6P7Z0	Short-chain dehydrogenase/reductase	1.00	1	2.92	2.92	1
198	A0A2R6P7Z3	Proteasome subunit alpha type	19.00	29	54.54	67.87	4
199	A0A2R6P7Z4	Calcium-dependent protein kinase	1.50	2	4.88	5.80	4
200	A0A2R6P816	COP9 signalosome complex subunit 2 like	6.00	8	22.36	30.79	4
201	A0A2R6P853	Cysteine proteinase inhibitor	2.40	3	28.62	37.25	4
202	A0A2R6P862	Receptor-like protein kinase HERK	1.00	1	1.94	1.94	1
203	A0A2R6P874	Oxidoreductase, N-terminal protein	1.00	1	2.27	2.27	2
204	A0A2R6P8B2	Serine/threonine-protein phosphatase	10.67	14	40.04	48.24	6

205	A0A2R6P8B8	Enoyl-[acyl-carrier-protein] reductase	1.00	1	2.04	2.04	2
206	A0A2R6P8C9	Tubulin alpha chain	23.50	29	44.26	49.89	4
207	A0A2R6P8F5	L-ascorbate oxidase	23.00	32	40.71	45.37	4
208	A0A2R6P8F8	Transcription factor Pur-alpha like	7.60	10	30.21	39.16	4
209	A0A2R6P8G8	Calmodulin	7.20	12	52.48	70.47	4
210	A0A2R6P8J9	Rho GTPase-activating protein	2.00	2	1.95	1.95	4
211	A0A2R6P8K1	YTH domain-containing family protein	1.00	1	1.28	1.28	2
212	A0A2R6P8W9	BAR domain protein	1.00	1	1.86	1.86	1
213	A0A2R6P8X1	DEAD-box ATP-dependent RNA helicase	9.00	9	16.09	16.09	1
214	A0A2R6P8X8	Nuclear transport factor 2 like	1.00	1	11.38	11.38	4
215	A0A2R6P8Y1	Importin-5 like	11.75	17	12.54	18.26	4
216	A0A2R6P8Z1	60S ribosomal protein L7a (Fragment)	6.80	10	24.61	34.38	4
217	A0A2R6P8Z2	Exocyst subunit Exo70 family protein	17.80	28	27.56	41.27	4
218	A0A2R6P8Z4	Uridine kinase	3.20	4	6.84	8.49	4
219	A0A2R6P911	COP9 signalosome complex subunit 3 like	7.80	14	19.39	33.18	4
220	A0A2R6P913	Transcription factor like	1.00	1	1.12	1.12	1
221	A0A2R6P945	Glyceraldehyde-3-phosphate dehydrogenase	40.00	57	72.34	74.18	4
222	A0A2R6P958	Glucuronokinase	4.80	8	21.61	36.94	4
223	A0A2R6P979	Glucose-6-phosphate 1-dehydrogenase	3.75	6	8.65	14.31	4
224	A0A2R6P998	Glycerol-3-phosphate dehydrogenase [NAD(+)]	8.40	12	26.95	37.47	4
225	A0A2R6P999	Bidirectional sugar transporter SWEET6b like	1.00	1	3.93	3.93	3
226	A0A2R6P9A0	Non-specific serine/threonine protein kinase	1.00	1	2.19	2.19	3
227	A0A2R6P9A8	Glutaredoxin like	3.60	6	44.95	77.98	4
228	A0A2R6P9H9	60S ribosomal protein	2.00	2	16.67	16.67	4
229	A0A2R6P9K9	40S ribosomal protein S9-2	5.33	6	18.78	19.80	3
230	A0A2R6P9M0	Tubulin alpha chain	33.00	49	56.80	59.56	4
231	A0A2R6P9M4	Serine/threonine protein phosphatase 2A regulatory subunit	3.00	3	5.00	5.00	2
232	A0A2R6P9N1	UDP-glucose 6-dehydrogenase	40.20	55	73.84	76.88	4
233	A0A2R6P9T9	ATP synthase subunit beta	1.00	1	1.99	1.99	2
234	A0A2R6P9U1	UDP-arabinopyranose mutase	50.80	74	86.71	87.89	4
235	A0A2R6P9V8	Late embryogenesis abundant protein	7.20	10	83.64	93.94	4
236	A0A2R6P9W2	Endo-1,3(4)-beta-glucanase	2.25	3	3.84	5.07	4
237	A0A2R6P9X4	T-complex protein 1 subunit zeta	19.83	26	48.29	64.30	6
238	A0A2R6P9Y4	2,3-bisphosphoglycerate-independent phosphoglycerate mutase	2.75	5	8.23	15.56	4
239	A0A2R6P9Z7	Protein transport protein SEC13 B like	6.20	9	26.82	43.05	4
240	A0A2R6PA04	HEAT repeat-containing protein isoform 1	3.00	3	1.51	1.51	2
241	A0A2R6PA08	HEAT repeat-containing protein isoform 2	3.00	3	1.43	1.43	2
242	A0A2R6PA18	40S ribosomal protein S7	4.00	5	30.89	38.22	3
243	A0A2R6PA36	ATP synthase subunit beta	1.80	4	3.69	8.23	4
244	A0A2R6PA38	2-hydroxyacyl-CoA lyase	3.60	7	7.25	15.41	4
245	A0A2R6PA39	Protein RMD5 A like	2.67	4	8.63	12.95	3
246	A0A2R6PA48	Malate dehydrogenase	1.50	2	4.92	6.46	4

247	A0A2R6PA59	Protein C2-DOMAIN ABA-RELATED like	1.00	1	5.45	5.45	1
248	A0A2R6PA80	Eukaryotic translation initiation factor 4E-2 like (Fragment)	1.00	1	16.46	16.46	4
249	A0A2R6PA85	60S ribosomal protein like	2.67	4	17.81	21.92	3
250	A0A2R6PAA3	RuvB-like helicase	4.25	6	10.71	15.20	4
251	A0A2R6PAA6	Indole-3-acetic acid-amido synthetase	1.00	1	1.84	1.84	2
252	A0A2R6PAF0	Receptor-like protein kinase	1.00	1	1.44	1.44	1
253	A0A2R6PAF8	Peptidyl-prolyl cis-trans isomerase	4.00	5	10.81	13.78	4
254	A0A2R6PAG5	Serine/threonine-protein kinase	1.00	1	3.65	3.65	3
255	A0A2R6PAM5	Polyol transporter like	4.75	9	7.35	13.66	4
256	A0A2R6PAN7	Calcium-dependent protein kinase	5.50	6	12.87	13.60	2
257	A0A2R6PAQ7	Nuclease	1.00	1	2.16	2.16	2
258	A0A2R6PAR0	Inactive TPR repeat-containing thioredoxin like	2.00	2	3.83	3.83	2
259	A0A2R6PAT2	PLAT domain-containing protein	1.00	1	11.23	11.23	3
260	A0A2R6PAT3	Calcium-binding protein	1.67	2	7.14	8.67	3
261	A0A2R6PAT8	Trafficking protein particle complex subunit 12 like	1.33	2	3.24	4.87	3
262	A0A2R6PAV3	PLAT domain-containing protein	1.33	2	12.83	16.04	3
263	A0A2R6PAW9	Kirola like	1.00	1	7.33	7.33	4
264	A0A2R6PB13	Protein C2-DOMAIN ABA-RELATED 7, N-terminally processed like	4.50	6	29.74	39.08	4
265	A0A2R6PB61	Serine/threonine-protein like	10.25	15	17.46	24.53	4
266	A0A2R6PB67	Subtilisin-like protease	1.75	2	2.48	2.91	4
267	A0A2R6PB92	Cysteinyl-tRNA synthetase	8.75	10	18.37	20.52	4
268	A0A2R6PBC6	60S ribosomal protein	1.50	2	9.58	12.50	2
269	A0A2R6PBE6	WD repeat-containing protein	3.75	5	6.81	8.97	4
270	A0A2R6PBE7	Chaperone protein like	1.67	2	3.69	4.33	3
271	A0A2R6PBE8	Glutaminyl-tRNA synthetase	3.33	4	4.37	5.42	3
272	A0A2R6PBF9	Uncharacterized protein	1.75	2	5.10	5.90	4
273	A0A2R6PBG1	Paladin like	2.00	4	1.57	3.14	4
274	A0A2R6PBG5	Serine/threonine-protein phosphatase	7.75	11	33.66	47.06	4
275	A0A2R6PBI3	Phosphoglucomutase	16.40	23	48.14	62.19	4
276	A0A2R6PBL5	14-3-3-like protein GF14 iota	19.40	24	62.23	66.53	4
277	A0A2R6PBL8	Heparanase-like protein	8.40	11	20.61	26.44	4
278	A0A2R6PBN0	Eukaryotic translation initiation factor 5A	7.67	8	43.19	44.03	3
279	A0A2R6PBN1	60S ribosomal protein like	3.20	4	17.92	21.95	4
280	A0A2R6PBP9	Nodulin-related protein	1.50	2	17.94	22.90	4
281	A0A2R6PBQ5	Phospholipid-transporting ATPase	2.00	2	1.50	1.50	2
282	A0A2R6PBQ6	UDP-glucose 6-dehydrogenase	28.80	39	63.79	75.00	4
283	A0A2R6PBU3	Serine/threonine-protein kinase	1.33	3	2.59	5.72	3
284	A0A2R6PBV5	60S ribosomal protein like	2.00	2	11.59	11.59	1
285	A0A2R6PBW2	Dihydrolipoamide acetyltransferase component of pyruvate dehydrogenase complex	1.00	1	3.63	3.63	3
286	A0A2R6PCF1	Agmatine deiminase	1.00	1	3.21	3.21	4
287	A0A2R6PCF9	Serine/threonine-protein phosphatase	1.00	1	3.59	3.59	1
288	A0A2R6PCI2	ATP synthase subunit b like	1.67	2	5.18	6.36	3

289	A0A2R6PCJ3	UDP-arabinopyranose mutase	23.60	33	55.38	64.90	4
290	A0A2R6PCK9	40S ribosomal protein like	6.25	7	41.84	46.53	4
291	A0A2R6PCL6	T-complex protein 1 subunit delta	31.25	38	66.78	72.52	4
292	A0A2R6PCS2	Ubiquitin (Fragment)	10.20	12	60.38	60.76	4
293	A0A2R6PCS4	Prolyl-tRNA synthetase	5.20	9	13.37	22.55	4
294	A0A2R6PCS5	Non-specific serine/threonine protein kinase	1.00	1	2.23	2.23	3
295	A0A2R6PCT8	Serine/threonine-protein phosphatase 2A	27.60	39	51.52	62.69	4
296	A0A2R6PCT9	Kinesin-like protein (Fragment)	9.00	15	10.98	18.03	4
297	A0A2R6PCU6	Pyruvate kinase	2.20	3	4.15	5.76	4
298	A0A2R6PCU9	Pectinesterase	11.60	18	22.00	32.26	4
299	A0A2R6PCY1	Alpha,alpha-trehalose-phosphate synthase	6.00	6	8.07	8.07	1
300	A0A2R6PCZ9	Phosphomevalonate kinase (Fragment)	3.00	4	7.06	9.17	3
301	A0A2R6PD24	DEAD-box ATP-dependent RNA helicase	1.00	1	1.67	1.67	3
302	A0A2R6PD26	Eukaryotic initiation factor 4A-14	30.20	42	66.57	78.74	4
303	A0A2R6PD31	Cellulose synthase-like protein	1.00	1	0.80	0.80	1
304	A0A2R6PD33	Protein argonaute like	2.25	4	2.19	3.91	4
305	A0A2R6PD44	Inositol-tetrakisphosphate 1-kinase	3.00	4	7.16	9.64	4
306	A0A2R6PD48	Clathrin interactor EPSIN like	0.00	0	0.00	0.00	1
307	A0A2R6PD59	ATP-dependent 6-phosphofructokinase	6.00	6	13.64	13.64	1
308	A0A2R6PD62	26S proteasome non-ATPase regulatory subunit 13 A like (Fragment)	5.80	9	24.26	31.30	4
309	A0A2R6PD75	Glycerophosphodiester phosphodiesterase	3.40	4	11.71	13.55	4
310	A0A2R6PD83	40S ribosomal protein S12 (Fragment)	6.20	7	56.64	60.58	4
311	A0A2R6PD96	Stromal cell-derived factor 2-like protein	1.00	1	5.63	5.63	2
312	A0A2R6PDA0	Glycerol kinase	14.00	19	39.96	53.07	4
313	A0A2R6PDC0	Calnexin like	2.25	4	5.27	9.43	4
314	A0A2R6PDC2	Carbonyl reductase	9.60	15	33.92	46.31	4
315	A0A2R6PDD9	Serine/threonine-protein kinase (Fragment)	5.50	7	9.16	11.02	4
316	A0A2R6PDG4	CASP-like protein	1.00	1	4.40	4.40	2
317	A0A2R6PDG7	SWI/SNF complex subunit SWI3A like	1.00	1	1.24	1.24	2
318	A0A2R6PDH2	Diadenosine tetraphosphate synthetase	26.20	34	45.01	53.35	4
319	A0A2R6PDH4	V-type proton ATPase subunit C	2.20	3	6.63	8.29	4
320	A0A2R6PDI0	Ubiquitin receptor RAD23	0.67	1	2.14	3.22	3
321	A0A2R6PDI1	Dual specificity protein like	1.67	2	2.11	2.58	3
322	A0A2R6PDI7	DEAD-box ATP-dependent RNA helicase	2.00	2	3.60	3.60	1
323	A0A2R6PDJ0	Pyruvate dehydrogenase E1 component subunit beta	1.00	1	2.91	2.91	3
324	A0A2R6PDL5	Programmed cell death protein	12.50	18	20.83	29.00	4
325	A0A2R6PDM3	26S proteasome non-ATPase regulatory subunit like	12.20	15	35.28	42.23	4
326	A0A2R6PDN6	UDP-glucuronate decarboxylase	4.14	5	9.54	11.70	7
327	A0A2R6PDP2	60S ribosomal protein like (Fragment)	3.33	4	17.92	20.43	3
328	A0A2R6PDQ1	Kinesin-like protein	1.00	1	1.49	1.49	2
329	A0A2R6PDQ4	Kinesin-like protein (Fragment)	1.00	1	1.92	1.92	2
330	A0A2R6PDR1	60S ribosomal protein like	4.20	5	40.65	48.39	4

331	A0A2R6PDR2	Citrulline--aspartate ligase	7.67	11	15.00	22.00	3
332	A0A2R6PDR9	Pectinesterase	7.80	10	37.60	42.62	4
333	A0A2R6PDS4	Far upstream element-binding protein like	1.00	1	1.98	1.98	1
334	A0A2R6PDS7	Glyceraldehyde-3-phosphate dehydrogenase	31.80	44	63.55	72.19	4
335	A0A2R6PDS9	SNF1-related protein kinase regulatory subunit gamma-1 like	3.00	3	9.02	10.12	3
336	A0A2R6PDX3	AP-1 complex subunit mu-2 like	7.40	13	21.40	39.72	4
337	A0A2R6PDY5	Ribosomal protein L19	3.33	4	17.30	19.81	3
338	A0A2R6PE03	DnaJ subfamily B member 1 like	1.00	1	3.05	3.05	1
339	A0A2R6PE09	Plasma membrane ATPase	12.33	14	14.92	17.01	3
340	A0A2R6PE24	NAP1-related protein (Fragment)	1.00	1	5.39	5.39	1
341	A0A2R6PE29	60S ribosomal protein	2.60	3	20.17	22.50	4
342	A0A2R6PE31	Aldose 1-epimerase	4.50	7	23.75	35.69	4
343	A0A2R6PE33	ADP-ribosylation factor GTPase-activating protein	1.75	2	2.32	2.59	4
344	A0A2R6PE34	Transportin like	1.00	1	2.57	2.57	2
345	A0A2R6PE49	Methyltransferase	1.00	1	1.96	1.96	2
346	A0A2R6PE52	60S ribosomal protein like	7.40	9	33.11	39.32	4
347	A0A2R6PE64	Vacuolar protein sorting-associated protein 29	1.67	2	8.77	11.05	3
348	A0A2R6PE76	Ribonuclease P protein subunit p25-like protein	2.00	2	7.97	7.97	1
349	A0A2R6PE84	Protein DCL like	1.00	1	4.76	4.76	3
350	A0A2R6PE89	26S proteasome regulatory subunit 4 A like	27.50	34	58.78	62.39	4
351	A0A2R6PEB1	Pantoate--beta-alanine ligase	1.00	1	4.15	4.15	2
352	A0A2R6PEC1	60S ribosomal protein like (Fragment)	6.80	8	48.87	53.38	4
353	A0A2R6PEC4	Glutathione gamma-glutamylcysteinyltransferase	1.00	1	1.99	1.99	1
354	A0A2R6PEC9	1,3-beta-glucan synthase	2.50	3	1.42	1.73	2
355	A0A2R6PED4	Dihydroorotase	1.00	1	3.18	3.18	4
356	A0A2R6PED8	Aspartyl aminopeptidase	6.25	8	23.21	29.92	4
357	A0A2R6PEE3	60S ribosomal protein L23	4.60	6	39.72	49.29	4
358	A0A2R6PEF4	Glycolipid transfer protein	6.00	7	34.28	37.13	4
359	A0A2R6PEF6	60S ribosomal protein like (Fragment)	6.80	8	48.87	53.38	4
360	A0A2R6PEI7	Serine/threonine-protein kinase	3.00	4	6.15	8.50	4
361	A0A2R6PEJ2	Glycolipid transfer protein	5.33	6	31.85	37.13	3
362	A0A2R6PEJ5	Phosphatidylglycerol/phosphatidylinositol transfer protein	1.33	2	8.38	11.98	3
363	A0A2R6PEK3	Serine/threonine-protein phosphatase	1.00	1	1.32	1.32	2
364	A0A2R6PEN2	Sec23/Sec24, trunk domain protein	1.00	1	0.94	0.94	2
365	A0A2R6PEN9	Ribosomal protein	7.25	10	33.33	43.52	4
366	A0A2R6PEP7	Protein SUPPRESSOR OF K(+) TRANSPORT GROWTH DEFECT like	1.50	2	3.47	4.86	2
367	A0A2R6PER2	Pleiotropic drug resistance protein	2.50	3	2.00	2.35	2
368	A0A2R6PES4	AP-2 complex subunit alpha	9.75	14	11.24	15.31	4
369	A0A2R6PES9	UDP-D-apiose/UDP-D-xylose synthase	17.40	24	50.80	62.72	4
370	A0A2R6PEU5	Non-specific serine/threonine protein kinase	6.00	10	13.69	23.61	4
371	A0A2R6PEX0	Cell division cycle protein like	32.00	44	53.38	61.62	4
372	A0A2R6PEY7	Chaperonin CPN60-2 like	1.67	2	3.13	3.83	3

373	A0A2R6PEZ3	Serine/threonine-protein phosphatase 6 regulatory subunit like	2.00	2	2.53	2.53	2
374	A0A2R6PEZ9	60S ribosomal protein L12	6.40	8	46.15	54.82	4
375	A0A2R6PF15	Syntaxin-71 like	2.00	2	8.71	8.71	2
376	A0A2R6PF16	Proteasome subunit beta type-4 like (Fragment)	9.00	13	46.83	59.26	4
377	A0A2R6PF29	V-type proton ATPase subunit D like	1.00	1	5.36	5.36	2
378	A0A2R6PF49	Receptor-like protein kinase HERK	1.00	1	1.44	1.44	1
379	A0A2R6PF59	Glutelin type-A 2 basic chain like	14.80	19	41.01	48.88	4
380	A0A2R6PF60	60S ribosomal protein L35	2.60	3	20.32	22.76	4
381	A0A2R6PF61	P-loop NTPase domain-containing protein	1.00	1	1.37	1.37	1
382	A0A2R6PF75	D-amino-acid transaminase	1.67	2	5.41	6.67	3
383	A0A2R6PF76	40S ribosomal protein S15a	5.20	7	30.92	39.23	4
384	A0A2R6PF86	Actin-depolymerizing factor 2 like (Fragment)	3.50	5	26.83	35.77	4
385	A0A2R6PF90	Ras-related protein like	8.20	10	38.06	46.76	4
386	A0A2R6PF91	Heat shock protein 70 family protein	38.00	46	45.15	50.54	2
387	A0A2R6PF93	Actin-3 like	15.00	15	70.80	70.80	1
388	A0A2R6PFB1	Vicilin-like seed storage protein	6.60	7	17.80	18.82	4
389	A0A2R6PFC7	Homoserine dehydrogenase	3.50	5	9.38	13.30	4
390	A0A2R6PFD4	COP9 signalosome complex subunit 2 like	5.00	7	19.81	29.76	4
391	A0A2R6PFD7	Protein argonaute like	6.50	11	7.65	13.16	4
392	A0A2R6PFE1	Calmodulin	5.00	7	39.60	55.70	3
393	A0A2R6PFE5	Proteasome-associated protein	13.50	20	9.23	13.54	4
394	A0A2R6PFE7	Proteasome subunit alpha type	19.67	24	56.76	64.26	3
395	A0A2R6PFG4	Rho GTPase-activating protein	2.00	2	1.95	1.95	4
396	A0A2R6PFH4	Calcium-dependent protein kinase	1.50	2	3.47	4.13	4
397	A0A2R6PFI5	Cysteine proteinase inhibitor	1.67	2	17.61	22.64	3
398	A0A2R6PFK1	Oxysterol-binding protein-related protein like	1.00	1	1.75	1.75	4
399	A0A2R6PFL7	Cinnamoyl-CoA reductase	7.00	8	23.92	25.31	2
400	A0A2R6PFM5	Tetraketide alpha-pyrone reductase (Fragment)	5.50	6	24.19	24.19	2
401	A0A2R6PFR8	Enoyl-[acyl-carrier-protein] reductase	1.00	1	2.04	2.04	2
402	A0A2R6PFT1	DEAD-box ATP-dependent RNA helicase	12.33	15	31.57	35.10	3
403	A0A2R6PFU2	Importin-5 like (Fragment)	7.00	11	11.54	17.84	3
404	A0A2R6PFU5	Transcription repressor like	1.00	1	3.48	3.48	1
405	A0A2R6PFU9	Proteasome inhibitor	1.00	1	14.44	14.44	2
406	A0A2R6PFV3	YTH domain-containing family protein like	1.00	1	1.29	1.29	2
407	A0A2R6PFV5	Cinnamoyl-CoA reductase	7.00	11	26.91	39.51	4
408	A0A2R6PFX2	L-ascorbate oxidase	21.00	31	35.84	41.28	4
409	A0A2R6PFX3	Pyruvate kinase	17.60	26	46.04	61.23	4
410	A0A2R6PGC1	DEP domain-containing mTOR-interacting protein	1.00	1	1.62	1.62	3
411	A0A2R6PGD4	ATP synthase subunit beta	1.00	1	2.21	2.21	2
412	A0A2R6PGE0	WD repeat-containing protein	6.00	7	10.00	11.72	2
413	A0A2R6PGH2	Pyruvate kinase	20.00	30	47.22	63.92	4
414	A0A2R6PGJ5	Serine/threonine-protein phosphatase 2A activator	2.00	3	4.56	6.40	4

415	A0A2R6PGK7	Receptor protein kinase	1.00	1	1.47	1.47	2
416	A0A2R6PGN4	Calcium-binding protein	1.67	2	7.14	8.67	3
417	A0A2R6PGP8	Phosphoglucomutase (alpha-D-glucose-1,6-bisphosphate-dependent)	36.40	50	70.86	79.28	4
418	A0A2R6PGQ8	Kirola like	1.00	1	7.33	7.33	4
419	A0A2R6PGV1	ATP synthase subunit beta	1.00	1	1.98	1.98	2
420	A0A2R6PGV5	Fructose-bisphosphate aldolase	3.00	5	10.97	18.62	3
421	A0A2R6PGY6	Cysteinyl-tRNA synthetase	7.33	11	13.96	20.93	3
422	A0A2R6PH22	Dihydrolipoamide acetyltransferase component of pyruvate dehydrogenase complex	1.00	1	3.59	3.59	3
423	A0A2R6PH78	6-phosphogluconate dehydrogenase, decarboxylating	6.50	8	15.88	18.97	4
424	A0A2R6PH86	Phosphoenolpyruvate carboxylase	54.60	76	52.13	63.21	4
425	A0A2R6PH90	Eukaryotic translation initiation factor 3 subunit L	6.40	10	13.14	19.96	4
426	A0A2R6PH91	Proteasome inhibitor PI31 subunit like	1.50	2	7.59	11.48	2
427	A0A2R6PH97	La protein	1.00	1	2.94	2.94	4
428	A0A2R6PHB0	Hydrolase	1.00	1	2.51	2.51	2
429	A0A2R6PHC2	Malic enzyme	22.40	30	44.16	59.08	4
430	A0A2R6PHH1	Eukaryotic initiation factor 4A-14	27.20	36	55.79	61.59	4
431	A0A2R6PHJ6	AP-4 complex subunit epsilon	3.33	5	3.33	4.84	3
432	A0A2R6PHK2	TOM1-like protein	1.25	2	2.29	3.48	4
433	A0A2R6PHK7	Acyl-CoA-binding protein	1.00	1	8.89	8.89	3
434	A0A2R6PHN3	Glutaminyl-tRNA synthetase	2.67	3	4.44	5.13	3
435	A0A2R6PHN8	Ubiquitin carboxyl-terminal hydrolase	2.00	3	2.34	3.62	4
436	A0A2R6PHR1	Plant UBX domain-containing protein	2.00	3	4.33	6.71	4
437	A0A2R6PHR3	UPF0160 protein	1.00	1	2.71	2.71	2
438	A0A2R6PHR4	Luminal-binding protein	9.75	15	17.55	27.79	4
439	A0A2R6PHS6	26S proteasome non-ATPase regulatory subunit 8 A like	19.20	27	62.17	81.65	4
440	A0A2R6PHU0	4-coumarate--CoA ligase	2.33	3	4.20	5.62	3
441	A0A2R6PHV9	Ubiquitin-conjugating enzyme like	3.80	6	28.11	37.84	4
442	A0A2R6PHW0	Endoglucanase	1.00	1	2.08	2.08	2
443	A0A2R6PHW1	Reticulon-like protein	1.00	1	3.25	3.25	2
444	A0A2R6PHW5	Spastin like	12.00	18	19.47	28.52	4
445	A0A2R6PHX7	Endoglucanase	1.00	1	1.92	1.92	1
446	A0A2R6PHY2	Aspartate aminotransferase	13.33	18	31.10	40.85	3
447	A0A2R6PHZ1	Glutathione peroxidase	2.00	3	12.95	20.48	4
448	A0A2R6PHZ5	Tubulin beta chain	21.00	29	53.06	66.14	3
449	A0A2R6PI05	Glutathione S-transferase	1.00	1	9.17	9.17	3
450	A0A2R6PI07	UDP-glucose 4-epimerase	7.67	9	24.23	26.72	3
451	A0A2R6PI20	3-hydroxy-3-methylglutaryl coenzyme A synthase	13.50	16	33.69	37.37	4
452	A0A2R6PI62	Eukaryotic initiation factor 4A-15 like	13.33	14	60.21	60.21	3
453	A0A2R6PI69	Transaldolase	1.00	1	2.79	2.79	2
454	A0A2R6PI73	Beta-adaptin-like protein	15.00	24	21.25	32.21	3
455	A0A2R6PI74	Adenine phosphoribosyltransferase	1.00	1	8.24	8.24	2
456	A0A2R6PIA1	26S proteasome non-ATPase regulatory subunit 13 A like	10.60	16	25.90	35.67	4

457	A0A2R6PIA3	Phosphomevalonate kinase (Fragment)	2.50	4	6.52	10.18	4
458	A0A2R6PIB2	Inositol-tetrakisphosphate 1-kinase	2.50	3	6.61	8.11	2
459	A0A2R6PIB3	Cellulose synthase-like protein	1.00	1	0.61	0.61	1
460	A0A2R6PIC5	Alpha,alpha-trehalose-phosphate synthase	7.00	7	10.13	10.13	1
461	A0A2R6PIH7	GTP-binding protein YPTM2	8.80	12	49.66	69.46	4
462	A0A2R6PIH9	Regulator of nonsense transcripts like	1.00	1	0.79	0.79	2
463	A0A2R6PIJ7	Hyaluronan/mRNA-binding protein	1.00	1	2.26	2.26	2
464	A0A2R6PIM1	Acyl-CoA-binding protein	1.00	1	8.89	8.89	3
465	A0A2R6PIM8	Eukaryotic initiation factor 4A-14	29.00	39	60.27	70.77	4
466	A0A2R6PIN1	Glutathione S-transferase	1.00	1	4.45	4.45	3
467	A0A2R6PIP8	Pyruvate kinase	2.20	3	4.15	5.76	4
468	A0A2R6PIP9	Far upstream element-binding protein like	2.67	4	5.56	8.33	3
469	A0A2R6PIR3	Inositol oxygenase	1.75	3	8.95	14.32	4
470	A0A2R6PIR7	ATP-dependent 6-phosphofructokinase	7.20	12	16.95	25.98	4
471	A0A2R6PIT5	TOM1-like protein	1.25	2	2.24	3.41	4
472	A0A2R6PIT9	Hsp70-Hsp90 organizing protein	16.40	28	31.66	53.05	4
473	A0A2R6PIU5	Bark storage protein like	1.67	2	5.44	7.12	3
474	A0A2R6PIW4	GTP-binding nuclear protein (Fragment)	8.00	11	41.00	51.36	4
475	A0A2R6PIX2	Ribosomal protein L15 (Fragment)	4.25	7	20.14	31.22	4
476	A0A2R6PIY4	Serine/threonine protein phosphatase 2A regulatory subunit	2.50	3	5.34	6.05	2
477	A0A2R6PIY6	DEAD-box ATP-dependent RNA helicase (Fragment)	1.33	2	3.71	5.57	3
478	A0A2R6PIY8	Uncharacterized protein	4.50	7	24.83	39.52	4
479	A0A2R6PIZ2	26S protease regulatory subunit 8 A	24.00	32	54.24	64.76	4
480	A0A2R6PJ08	Trafficking protein particle complex II-specific subunit like	1.00	1	0.66	0.66	2
481	A0A2R6PJ16	Protein-serine/threonine phosphatase	2.00	3	5.82	8.03	4
482	A0A2R6PJ19	Malic enzyme	23.20	31	49.37	61.63	4
483	A0A2R6PJ20	AP-2 complex subunit mu	3.80	7	7.44	12.10	4
484	A0A2R6PJ39	Eukaryotic initiation factor 4A-14 like (Fragment)	7.00	7	42.86	42.86	1
485	A0A2R6PJ46	Photosystem II CP43 reaction center protein	1.00	1	6.97	6.97	2
486	A0A2R6PJ58	Protein arginine N-methyltransferase	3.75	6	6.15	9.91	4
487	A0A2R6PJD8	Stress-response A/B barrel domain-containing protein	1.00	1	11.71	11.71	2
488	A0A2R6PJH9	Ubiquitin	10.20	12	61.16	61.54	4
489	A0A2R6PJJ5	Receptor-like protein kinase	1.00	1	1.41	1.41	1
490	A0A2R6PJK5	Pectinesterase	3.60	5	18.87	20.30	4
491	A0A2R6PJL3	Universal stress protein	3.40	6	29.33	48.47	4
492	A0A2R6PJL4	Importin subunit alpha-2 like (Fragment)	1.50	2	7.32	10.04	2
493	A0A2R6PJP9	YTH domain-containing family protein	1.00	1	1.45	1.45	2
494	A0A2R6PJR0	Sperm-associated antigen 1A like	2.50	3	5.17	6.69	4
495	A0A2R6PJR8	Galactokinase	19.60	31	42.72	60.00	4
496	A0A2R6PJR9	3-hydroxyacyl-CoA dehydrogenase	1.00	1	1.39	1.39	1
497	A0A2R6PJS1	Phospholipase	1.00	1	0.77	0.77	2
498	A0A2R6PJU6	Dihydrolipoyl dehydrogenase	1.00	1	2.09	2.09	1

499	A0A2R6PJV0	Inosine-5'-monophosphate dehydrogenase	4.75	6	12.70	16.33	4
500	A0A2R6PJV1	3-deoxy-8-phosphooctulonate synthase	1.20	2	3.83	5.91	4
501	A0A2R6PJV6	Mitogen-activated protein kinase kinase kinase	1.00	1	4.40	4.66	2
502	A0A2R6PJW5	Histone-arginine methyltransferase	1.67	2	3.71	4.27	3
503	A0A2R6PJW7	Sucrose nonfermenting 4-like protein	2.50	4	5.48	8.81	4
504	A0A2R6PJY0	Serine/threonine-protein phosphatase 2A regulatory subunit B'' subunit like	1.00	1	2.10	2.10	2
505	A0A2R6PK00	60S ribosomal protein like	4.00	5	31.91	36.51	4
506	A0A2R6PK45	40S ribosomal protein S16	10.00	12	55.84	58.39	4
507	A0A2R6PK48	Sugar transport protein	1.00	1	2.80	2.80	1
508	A0A2R6PK53	NEDD8-activating enzyme E1 catalytic subunit	1.00	1	6.56	6.56	1
509	A0A2R6PK64	ADP-ribosylation factor (Fragment)	10.00	14	56.78	60.00	4
510	A0A2R6PK79	Putative GPI-anchored protein	1.75	2	11.06	13.07	4
511	A0A2R6PK82	40S ribosomal protein like (Fragment)	6.00	7	29.57	33.85	2
512	A0A2R6PK85	Proteasome subunit beta type-2-A like	5.00	5	51.69	51.69	1
513	A0A2R6PK88	Prefoldin subunit like	1.00	1	6.12	6.12	2
514	A0A2R6PK90	5'-nucleotidase	1.00	1	2.59	2.59	3
515	A0A2R6PKA5	Transmembrane emp24 domain-containing protein	1.00	1	5.00	5.00	2
516	A0A2R6PKB8	GDP-mannose 3,5-epimerase	18.00	24	49.36	60.64	4
517	A0A2R6PKB9	Stem-specific protein	4.60	7	21.29	32.53	4
518	A0A2R6PKD6	Diphthamide synthase	1.00	1	1.47	1.47	2
519	A0A2R6PKE4	Serine/threonine protein phosphatase 2A regulatory subunit B''gamma like	8.25	12	16.28	23.19	4
520	A0A2R6PKH5	Adenosine kinase	23.00	35	63.28	68.91	4
521	A0A2R6PKJ3	60S ribosomal protein L12	3.00	3	22.29	22.29	1
522	A0A2R6PKJ9	Malate dehydrogenase	19.80	24	48.07	50.30	4
523	A0A2R6PKK2	40S ribosomal protein S15-4 (Fragment)	2.00	3	21.00	29.33	4
524	A0A2R6PKK5	Methyltransferase	1.00	1	2.35	2.35	3
525	A0A2R6PKL7	Casein kinase 1-like protein	1.00	1	2.56	2.56	3
526	A0A2R6PKM3	Tetratricopeptide repeat protein like	4.00	6	6.44	9.67	4
527	A0A2R6PKR2	Basic leucine zipper and W2 domain-containing protein	7.00	9	20.32	24.57	4
528	A0A2R6PKR5	Aspartic proteinase-like protein	2.75	3	7.34	7.76	4
529	A0A2R6PKT4	Ubiquitinyl hydrolase 1	19.00	27	19.98	24.64	4
530	A0A2R6PKV1	Non-specific serine/threonine protein kinase	3.33	5	7.98	11.97	3
531	A0A2R6PKY4	Ubiquitin-like protein 5	2.00	2	24.66	24.66	2
532	A0A2R6PKZ6	Isopentenyl-diphosphate Delta-isomerase	3.25	4	13.13	19.87	4
533	A0A2R6PL09	Golgi to ER traffic protein	1.00	1	5.18	5.18	3
534	A0A2R6PL20	Regulator of nonsense transcripts like	1.00	1	0.84	0.84	2
535	A0A2R6PL37	Leukotriene A-4 hydrolase	5.60	11	9.54	20.00	4
536	A0A2R6PL62	Paramyosin like	3.00	3	6.63	6.63	1
537	A0A2R6PL76	Actin-depolymerizing factor 2 like (Fragment)	2.00	2	10.14	10.14	1
538	A0A2R6PL82	40S ribosomal protein S15a-1	5.83	8	40.39	50.00	6
539	A0A2R6PLA2	Glucan endo-1,3-beta-glucosidase	1.00	1	2.83	2.83	1
540	A0A2R6PLB0	Triosephosphate isomerase	21.80	31	75.06	77.65	4

541	A0A2R6PLB6	Thaumatin-like protein	1.00	1	8.40	8.40	1
542	A0A2R6PLC1	Tropinone reductase	2.33	3	6.74	8.61	3
543	A0A2R6PLC2	Mannose-1-phosphate guanylyltransferase	3.75	5	13.78	20.22	4
544	A0A2R6PLD8	Ras-related protein like	7.80	11	39.26	53.95	4
545	A0A2R6PLE4	Folylpolyglutamate synthase	2.33	4	4.67	8.10	3
546	A0A2R6PLF5	Alpha crystallin/Hsp20 domain protein	3.25	4	17.54	20.15	4
547	A0A2R6PLF6	60S ribosomal protein L35a-1	2.40	4	24.82	41.96	4
548	A0A2R6PLI0	Eukaryotic translation initiation factor 3 subunit F	4.00	6	17.28	27.72	4
549	A0A2R6PLJ2	Clathrin heavy chain like (Fragment)	32.80	46	48.08	57.32	4
550	A0A2R6PLJ6	Syntaxin-binding protein 5-like	2.00	3	2.06	3.17	4
551	A0A2R6PLK3	GDP-Man:Man(3)GlcNAc(2)-PP-Dol alpha-1,2-mannosyltransferase	1.00	1	1.88	1.88	4
552	A0A2R6PLK8	Eukaryotic translation initiation factor 3 subunit G	7.20	12	22.13	36.08	4
553	A0A2R6PLL1	Diphosphomevalonate decarboxylase	8.50	15	20.37	36.34	4
554	A0A2R6PLP1	Cation/H(+) antiporter like	2.50	4	3.27	5.44	4
555	A0A2R6PLT6	Ras-related protein like	7.75	10	40.15	51.23	4
556	A0A2R6PLV0	Autophagy-related protein	1.00	1	3.18	3.18	1
557	A0A2R6PLV8	Alpha-soluble NSF attachment protein	4.00	6	15.92	21.65	3
558	A0A2R6PLW8	60S ribosomal protein L35	1.67	2	14.36	16.26	3
559	A0A2R6PLX5	Ribosomal protein L15	5.60	8	28.14	39.22	4
560	A0A2R6PLX7	Aquaporin TIP5-1 like	1.00	1	4.43	4.44	2
561	A0A2R6PLY1	60S ribosomal protein like	4.60	7	23.90	32.47	4
562	A0A2R6PLY7	Transketolase	2.25	3	3.46	4.53	4
563	A0A2R6PLZ7	Heat shock protein 70 family protein (Fragment)	33.50	43	46.78	55.02	4
564	A0A2R6PM00	40S ribosomal protein S20-2	4.60	5	46.88	49.18	4
565	A0A2R6PM02	Serine/threonine protein kinase	1.00	1	0.89	0.89	2
566	A0A2R6PM03	Calcium-binding protein	11.60	13	76.87	84.35	4
567	A0A2R6PM29	Valine--tRNA ligase	1.00	1	1.58	1.58	2
568	A0A2R6PM34	Sorbitol dehydrogenase	2.00	2	9.47	9.47	4
569	A0A2R6PM47	Serine/threonine-protein phosphatase	1.00	1	6.19	6.19	4
570	A0A2R6PM48	RHOMBOID-like protein	2.25	3	5.41	7.21	4
571	A0A2R6PM58	ADP-ribosylation factor-related protein	1.00	1	6.37	6.37	2
572	A0A2R6PM77	Tubulin beta chain	30.80	46	64.65	74.72	4
573	A0A2R6PM79	Tripeptidyl-peptidase II	25.40	38	22.56	32.05	4
574	A0A2R6PM92	4-coumarate--CoA ligase	3.50	4	8.94	10.13	4
575	A0A2R6PM98	Hyaluronan/mRNA-binding protein	1.00	1	2.46	2.46	2
576	A0A2R6PMB2	Ras-related protein RABD2a	7.60	11	43.45	65.52	4
577	A0A2R6PME9	Phosphoacetylglucosamine mutase	1.75	3	3.76	6.45	4
578	A0A2R6PMF2	Regulator of nonsense transcripts like	1.00	1	0.79	0.79	2
579	A0A2R6PMF7	Haloacid dehalogenase-like hydrolase domain-containing protein	6.75	8	36.53	43.67	4
580	A0A2R6PMH0	AP-2 complex subunit mu like (Fragment)	1.00	1	9.01	9.01	1
581	A0A2R6PMH1	Acetylornithine deacetylase	3.60	7	10.09	20.32	4
582	A0A2R6PMI1	Gamma-glutamylcyclotransferase family protein	1.50	2	8.47	12.17	2

583	A0A2R6PMJ0	Inositol-tetrakisphosphate 1-kinase	3.67	5	10.10	13.77	3
584	A0A2R6PMK0	Binding partner of like (Fragment)	1.67	2	7.60	9.86	3
585	A0A2R6PML3	Aspartate--tRNA ligase	20.00	26	40.67	50.37	4
586	A0A2R6PML6	L-arabinokinase	3.75	6	4.32	7.11	4
587	A0A2R6PMM3	Serine/threonine-protein kinase	5.00	5	6.23	6.23	1
588	A0A2R6PMN9	Eukaryotic translation initiation factor 3 subunit C	13.80	24	15.72	26.38	4
589	A0A2R6PMP0	Ran-binding protein 1 b like	1.75	2	7.94	8.88	4
590	A0A2R6PNQ4	ADP-ribosylation factor	9.60	14	44.70	46.99	4
591	A0A2R6PNS8	Pectinesterase inhibitor domain protein	1.00	1	4.59	4.59	4
592	A0A2R6PNU1	Importin subunit alpha	3.00	4	8.08	10.96	4
593	A0A2R6PNV1	Lysyl-tRNA synthetase	21.25	26	38.50	43.16	4
594	A0A2R6PNV2	60S ribosomal protein like (Fragment)	3.60	5	21.40	27.96	4
595	A0A2R6PNW5	UDP-glucuronate decarboxylase	4.80	6	11.38	14.53	4
596	A0A2R6PNX7	UDP-glucuronate decarboxylase	4.00	5	8.63	11.06	4
597	A0A2R6PNX9	40S ribosomal protein S21	3.00	4	28.29	31.71	4
598	A0A2R6PP12	Cullin-1 like	9.25	14	13.90	21.11	4
599	A0A2R6PP24	Homocysteine S-methyltransferase	2.00	2	3.75	3.75	3
600	A0A2R6PP31	Indole-3-acetic acid-amido synthetase	1.00	1	1.56	1.56	1
601	A0A2R6PP39	Sucrose synthase (Fragment)	5.00	9	12.47	23.96	3
602	A0A2R6PP48	Protein transport protein Sec24-like	7.40	12	8.30	13.51	4
603	A0A2R6PP82	Flowering locus Ky domain like	1.00	1	2.20	2.20	2
604	A0A2R6PP88	Inorganic phosphate transporter 1-4 like	1.67	3	3.39	6.48	3
605	A0A2R6PP96	ABC transporter I family member 21 like	3.25	5	16.34	25.40	4
606	A0A2R6PPC8	Ribonuclease P protein subunit p25-like protein	1.67	2	6.05	6.93	3
607	A0A2R6PPC9	26S proteasome regulatory subunit 4 A like	22.80	33	50.43	61.57	4
608	A0A2R6PPD7	Signal recognition particle 9 kDa protein	1.00	1	10.68	10.68	2
609	A0A2R6PPE5	G3BP-like protein	1.00	1	2.16	2.16	2
610	A0A2R6PPE6	S-(hydroxymethyl)glutathione dehydrogenase	10.00	12	44.19	49.60	2
611	A0A2R6PPF4	AP2/ERF and B3 domain-containing transcription repressor like	1.00	1	5.96	5.96	1
612	A0A2R6PPF8	Receptor-like kinase	1.00	1	1.51	1.51	2
613	A0A2R6PPG3	Peptidylprolyl isomerase	2.80	4	22.55	33.12	4
614	A0A2R6PPG9	Peptidylprolyl isomerase	11.60	16	20.80	28.10	4
615	A0A2R6PPH0	Cytochrome b561 and DOMON domain-containing protein	1.00	1	4.10	4.10	3
616	A0A2R6PPH6	Glyoxalase-like domain protein	1.00	1	12.27	12.27	2
617	A0A2R6PPJ1	Quinone-oxidoreductase	1.00	1	3.93	3.93	1
618	A0A2R6PPJ6	Glyoxylate/succinic semialdehyde reductase	3.50	4	15.53	17.41	2
619	A0A2R6PPK5	60S ribosomal protein like (Fragment)	4.50	7	12.13	16.94	4
620	A0A2R6PPL5	Eukaryotic translation initiation factor 2 subunit beta like	4.33	6	18.06	22.91	3
621	A0A2R6PPM6	Acyl-coenzyme A thioesterase	1.00	1	2.73	2.73	2
622	A0A2R6PPP0	E1 ubiquitin-activating enzyme	14.75	20	15.68	20.60	4
623	A0A2R6PPP9	Ubiquitin-conjugating enzyme like	2.33	3	22.75	30.41	3
624	A0A2R6PPQ6	DEAD-box ATP-dependent RNA helicase	2.00	2	3.34	3.34	3

625	A0A2R6PPQ7	60S acidic ribosomal protein P0	11.20	14	47.72	52.02	4
626	A0A2R6PPR1	60S ribosomal protein like	4.20	7	31.28	47.37	4
627	A0A2R6PPR3	40S ribosomal protein S26 (Fragment)	3.80	4	35.68	37.60	4
628	A0A2R6PPS0	Proliferating cell nuclear antigen	2.00	3	7.58	10.61	3
629	A0A2R6PPS6	Pyruvate decarboxylase	25.20	38	42.59	52.07	4
630	A0A2R6PPT7	Tubulin beta chain	41.00	52	74.46	77.53	3
631	A0A2R6PPU3	Thioredoxin-like fold protein	0.00	0	0.00	0.00	1
632	A0A2R6PPX7	Actin	66.00	66	71.09	71.09	1
633	A0A2R6PQ01	Succinate--CoA ligase [ADP-forming] subunit beta, mitochondrial	1.33	2	3.32	4.98	3
634	A0A2R6PQ14	Proteasome subunit beta type-4 like (Fragment)	6.00	8	31.85	37.86	4
635	A0A2R6PQ21	L-ascorbate peroxidase	8.20	12	32.93	42.24	4
636	A0A2R6PQ23	Beta-galactosidase	1.00	1	1.30	1.30	1
637	A0A2R6PQ38	L-ascorbate peroxidase	3.67	4	55.45	61.39	3
638	A0A2R6PQ46	P-loop NTPase domain-containing protein	3.25	5	4.61	7.05	4
639	A0A2R6PQ52	ABC transporter F family member 1 like	7.00	12	13.37	22.83	4
640	A0A2R6PQ53	Ras-related protein like	7.33	9	34.11	41.67	3
641	A0A2R6PQ55	RuvB-like helicase	2.00	3	5.59	7.74	2
642	A0A2R6PQ86	ABC transporter G family member 28 like	1.00	1	0.86	0.86	2
643	A0A2R6PQ88	Uridine kinase	1.00	1	2.01	2.01	1
644	A0A2R6PQ99	Serine/threonine-protein kinase	7.00	10	13.80	19.31	4
645	A0A2R6PQA5	Proteasome activator subunit like	13.00	23	7.94	14.39	4
646	A0A2R6PQB8	Heat shock cognate protein	55.25	66	54.83	57.51	4
647	A0A2R6PQC0	Elongation factor 1-alpha	53.40	82	63.56	75.28	4
648	A0A2R6PQC2	Farnesyl pyrophosphate synthase	10.40	13	30.12	35.38	4
649	A0A2R6PQC6	UDP-D-apiose/UDP-D-xylose synthase	16.50	22	47.04	59.90	4
650	A0A2R6PQD5	3-hydroxyisobutyryl-CoA hydrolase-like protein	6.25	9	18.95	27.84	4
651	A0A2R6PQE4	Syntaxin-124 like	1.33	2	6.67	10.00	3
652	A0A2R6PQE8	Persulfide dioxygenase	1.00	1	3.94	3.94	4
653	A0A2R6PQF8	Ubiquitin-conjugating enzyme E2 11	2.33	3	22.75	30.41	3
654	A0A2R6PQG3	Clathrin coat assembly protein	1.00	1	1.70	1.70	2
655	A0A2R6PQI5	YTH domain-containing family protein	1.00	1	1.30	1.30	2
656	A0A2R6PQJ2	Calcium-binding protein	2.50	3	11.79	13.54	4
657	A0A2R6PQJ5	Adaptin ear-binding coat-associated protein 1 NECAP-1 protein	1.00	1	2.84	2.84	2
658	A0A2R6PQJ6	GPI-anchored protein	2.80	4	21.92	27.20	4
659	A0A2R6PQL2	Secretory carrier-associated membrane protein	1.00	1	2.60	2.60	2
660	A0A2R6PQL7	Metacaspase-4 subunit p10 like	2.50	3	7.69	9.79	4
661	A0A2R6PQM3	60S acidic ribosomal protein	1.00	1	6.61	6.61	4
662	A0A2R6PQM7	Tubulin alpha chain	21.00	21	38.68	40.31	2
663	A0A2R6PQN2	Oxysterol-binding protein-related protein like	1.00	1	1.75	1.75	4
664	A0A2R6PQN3	Serine/threonine-protein phosphatase	10.20	14	38.67	47.94	4
665	A0A2R6PQP5	DEAD-box ATP-dependent RNA helicase	8.00	10	14.52	18.11	2
666	A0A2R6PQP6	Formyltetrahydrofolate synthetase	3.00	4	4.74	6.47	2

667	A0A2R6PQS7	CCT-eta	29.80	43	53.07	66.96	4
668	A0A2R6PQT7	C2 domain-containing protein	1.00	1	2.63	2.63	3
669	A0A2R6PQV4	Molybdopterin molybdenumtransferase	1.75	2	3.03	3.50	4
670	A0A2R6PQY4	COP9 signalosome complex subunit 6	4.00	6	17.10	23.23	4
671	A0A2R6PQY9	Bifunctional nitrilase/nitrile hydratase	1.00	1	2.89	2.89	2
672	A0A2R6PQZ0	Elongation factor 1-beta 2 like	9.40	12	43.98	56.64	4
673	A0A2R6PQZ7	Elongation factor (Fragment)	54.60	78	56.01	63.90	4
674	A0A2R6PQZ8	Serine/threonine-protein phosphatase	1.50	3	1.66	3.33	4
675	A0A2R6PR00	Phosphoglycerate kinase	30.00	40	69.38	81.30	4
676	A0A2R6PR40	Heterogeneous nuclear ribonucleoprotein like	1.00	1	3.10	3.10	2
677	A0A2R6PR53	Heterogeneous nuclear ribonucleoprotein like	1.00	1	3.37	3.37	2
678	A0A2R6PR64	Phosphoglycerate kinase	34.40	49	63.94	73.07	4
679	A0A2R6PR95	Nuclear cap-binding protein like	1.00	1	1.04	1.04	2
680	A0A2R6PRA4	Polyadenylate-binding protein (Fragment)	1.75	2	4.24	4.77	4
681	A0A2R6PRA5	EH domain-containing protein	2.00	2	4.58	4.58	1
682	A0A2R6PRB6	Tryptophan synthase	1.00	1	2.61	2.61	2
683	A0A2R6PRE0	COBRA-like protein	1.20	2	2.30	3.51	4
684	A0A2R6PRE5	HECT-type E3 ubiquitin transferase	4.25	7	1.00	1.63	4
685	A0A2R6PRE8	26S proteasome non-ATPase regulatory subunit 2 homolog	20.60	29	22.85	29.26	4
686	A0A2R6PRG0	GTPase-activating protein like	2.00	2	4.72	4.72	1
687	A0A2R6PRG3	Aconitate hydratase	15.00	24	20.32	32.33	4
688	A0A2R6PRH3	Ubiquitin carboxyl-terminal hydrolase	4.00	6	5.15	7.57	4
689	A0A2R6PRI1	Probable bifunctional methylthioribulose-1-phosphate dehydratase/enolase-phosphatase E1	1.33	2	2.97	4.74	3
690	A0A2R6PRI7	ADP-ribosylation factor GTPase-activating protein	1.00	1	1.67	1.67	1
691	A0A2R6PRK0	Vesicle-fusing ATPase	7.50	13	12.53	21.97	4
692	A0A2R6PRM4	Early nodulin-like protein	10.20	12	55.40	55.40	4
693	A0A2R6PRN8	60S ribosomal protein	6.80	8	52.03	52.21	4
694	A0A2R6PRP1	UDP-arabinopyranose mutase	22.00	22	53.30	53.30	1
695	A0A2R6PRP4	Ras-related protein RABA1f	9.40	12	43.59	53.46	4
696	A0A2R6PRQ0	G3BP-like protein	2.00	3	3.91	5.86	3
697	A0A2R6PRT6	Tetraspanin-8 like	3.60	5	23.94	34.20	4
698	A0A2R6PRU0	Malate dehydrogenase (Fragment)	2.50	3	10.49	11.83	2
699	A0A2R6PRU4	Malate dehydrogenase	2.60	4	7.49	10.37	4
700	A0A2R6PRU6	40S ribosomal protein like	4.67	5	32.87	34.72	3
701	A0A2R6PS14	Pantothenate kinase 2	2.00	4	2.64	5.28	4
702	A0A2R6PS30	Plant intracellular Ras-group-related LRR protein	2.00	3	3.54	5.23	4
703	A0A2R6PS40	40S ribosomal protein S9-2	8.00	12	32.08	51.27	4
704	A0A2R6PS79	60S ribosomal protein like (Fragment)	3.80	5	21.00	26.52	4
705	A0A2R6PS92	Phosphopantothenoylcysteine decarboxylase	1.00	1	6.70	6.70	1
706	A0A2R6PSB6	NAD(P)H dehydrogenase (quinone)	2.00	3	11.57	17.73	2
707	A0A2R6PSC4	Glucose-6-phosphate 1-epimerase	1.00	1	2.83	2.83	3
708	A0A2R6PSD5	Protein-methionine-S-oxide reductase	1.00	1	4.64	4.64	1

709	A0A2R6PSD9	Proteasome subunit alpha type	9.80	12	60.64	65.78	4
710	A0A2R6PSE3	V-type proton ATPase subunit C	1.00	1	4.86	4.86	2
711	A0A2R6PSE5	Glyceraldehyde-3-phosphate dehydrogenase	36.20	56	71.69	78.64	4
712	A0A2R6PSF5	Elongation factor 1-delta like (Fragment)	7.40	11	33.31	51.74	4
713	A0A2R6PSH2	Phospholipase D	33.20	42	51.94	57.97	4
714	A0A2R6PSI1	GTP-binding nuclear protein (Fragment)	8.00	11	41.00	51.36	4
715	A0A2R6PSJ5	Calnexin like	1.67	3	4.35	7.72	3
716	A0A2R6PSJ7	DEAD-box ATP-dependent RNA helicase (Fragment)	1.33	2	3.47	5.20	3
717	A0A2R6PSK7	Phenylalanyl-tRNA synthetase beta subunit	18.00	27	36.96	51.99	4
718	A0A2R6PSL0	Serine-threonine kinase receptor-associated protein	6.80	11	24.12	40.67	4
719	A0A2R6PSL7	GTP-binding nuclear protein (Fragment)	7.20	10	35.91	45.00	4
720	A0A2R6PSM6	Plasma membrane ATPase	8.40	12	18.08	24.63	4
721	A0A2R6PSP9	Late embryogenesis abundant protein	4.67	6	58.93	58.93	3
722	A0A2R6PSQ7	DEAD-box ATP-dependent RNA helicase 15 (Fragment)	2.00	3	4.24	6.35	3
723	A0A2R6PSR0	Heat shock 70 protein	21.75	29	30.21	39.65	4
724	A0A2R6PSS1	Ribosomal protein L37 (Fragment)	3.40	4	29.36	34.04	4
725	A0A2R6PST7	Nuclear pore complex protein like	1.00	1	2.16	2.16	1
726	A0A2R6PST9	60S ribosomal protein like	4.40	7	31.94	48.61	4
727	A0A2R6PSV1	Ras-related protein Rab7	5.00	7	23.83	31.88	3
728	A0A2R6PSV5	Serine-threonine kinase receptor-associated protein	6.80	11	23.99	40.44	4
729	A0A2R6PSV8	Eukaryotic initiation factor 4A-8	32.75	38	71.61	73.85	4
730	A0A2R6PSW5	Early nodulin-like protein	1.00	1	4.32	4.32	2
731	A0A2R6PSX2	Ubiquitin carboxyl-terminal hydrolase	11.50	14	29.02	36.53	4
732	A0A2R6PSX5	Profilin	8.60	13	60.92	67.18	4
733	A0A2R6PSY1	Protein CDI like	5.00	7	18.84	26.43	4
734	A0A2R6PSY6	Serine/threonine-protein phosphatase 2A 55 kDa regulatory subunit B	5.80	9	12.39	18.45	4
735	A0A2R6PSY9	Oligouridylate-binding protein like	1.00	1	1.88	1.88	3
736	A0A2R6PSZ0	Coatomer subunit zeta	1.00	1	13.74	13.74	2
737	A0A2R6PSZ2	Nucleosome assembly protein like	3.40	5	11.92	17.82	4
738	A0A2R6PT00	40S ribosomal protein SA	12.60	15	40.88	42.09	4
739	A0A2R6PT01	Casein kinase 1-like protein	1.00	1	2.12	2.12	1
740	A0A2R6PT28	Heterogeneous nuclear ribonucleoprotein like	1.00	1	3.35	3.35	1
741	A0A2R6PT30	Proteasome subunit alpha type	14.60	18	63.33	68.29	4
742	A0A2R6PT33	MO25-like protein	2.25	4	6.61	10.63	4
743	A0A2R6PT36	Proteasome subunit alpha type	15.20	20	64.81	74.26	4
744	A0A2R6PT43	5'-nucleotidase	1.00	1	4.12	4.12	4
745	A0A2R6PT51	Glycylpeptide N-tetradecanoyltransferase	8.00	14	24.84	39.17	4
746	A0A2R6PT61	60S ribosomal protein like	7.50	8	35.57	37.40	2
747	A0A2R6PT81	Developmentally-regulated G-protein	2.75	5	8.46	15.54	4
748	A0A2R6PT95	EH domain-containing protein	2.00	2	4.58	4.58	1
749	A0A2R6PT98	Mitogen-activated protein kinase	1.50	2	3.93	5.14	2
750	A0A2R6PTA1	Polyadenylate-binding protein (Fragment)	1.75	2	4.22	4.75	4

751	A0A2R6PTB0	Ubiquitin carboxyl-terminal hydrolase	3.50	5	4.44	6.24	4
752	A0A2R6PTB4	Aconitate hydratase	9.50	14	12.99	20.83	2
753	A0A2R6PTB8	Protein-serine/threonine phosphatase	1.50	3	4.47	8.94	4
754	A0A2R6PTC3	NAD(P)H dehydrogenase (quinone)	2.00	3	11.57	17.73	2
755	A0A2R6PTD3	TBC1 domain family member 15 like	3.00	3	6.75	6.75	1
756	A0A2R6PTE9	40S ribosomal protein S8	8.00	8	36.07	36.07	2
757	A0A2R6PTF7	Ras-related protein RABA1f	7.80	10	37.60	48.39	4
758	A0A2R6PTG9	ADP-ribosylation factor GTPase-activating protein	1.00	1	1.66	1.66	1
759	A0A2R6PTH3	3'(2'),5'-bisphosphate nucleotidase	2.00	2	4.46	4.46	2
760	A0A2R6PTH6	Anther-specific protein	11.40	14	50.37	53.09	4
761	A0A2R6PTI4	Probable bifunctional methylthioribulose-1-phosphate dehydratase/enolase-phosphatase E1	1.33	2	2.80	4.47	3
762	A0A2R6PTJ2	Malate dehydrogenase	3.00	5	9.91	16.52	4
763	A0A2R6PTJ4	Glutathione S-transferase	1.00	1	4.11	4.11	1
764	A0A2R6PTK6	DNA/RNA-binding protein Alba-like protein	6.00	6	39.53	39.53	2
765	A0A2R6PTM1	Anther-specific protein	5.20	6	35.55	40.12	4
766	A0A2R6PTM5	Choline-phosphate cytidylyltransferase	1.50	2	3.73	4.97	2
767	A0A2R6PTP3	Transmembrane 9 superfamily member	1.00	1	1.21	1.21	1
768	A0A2R6PTP5	Nuclear polyadenylated RNA-binding protein like	1.00	1	3.09	3.09	2
769	A0A2R6PTR3	Vesicle-fusing ATPase	3.00	5	6.25	10.59	2
770	A0A2R6PTS6	Ras-related protein RABB1c	5.40	7	33.74	44.08	4
771	A0A2R6PTS7	Phosphoenolpyruvate carboxylase	35.00	50	43.47	59.64	4
772	A0A2R6PTT7	TBC1 domain family member protein	1.00	1	18.69	18.69	1
773	A0A2R6PTU2	Tyrosine--tRNA ligase	10.25	13	40.61	50.52	4
774	A0A2R6PTU8	Protein C2-DOMAIN ABA-RELATED like	1.00	1	5.20	5.20	1
775	A0A2R6PTU9	Tyrosine--tRNA ligase like	10.25	13	36.88	45.88	4
776	A0A2R6PTV1	Phosphoenolpyruvate carboxylase	24.40	36	36.63	52.33	4
777	A0A2R6PTV3	Serine/threonine-protein phosphatase	5.33	10	20.07	37.50	3
778	A0A2R6PTV5	Actin-interacting protein like	9.20	13	19.90	27.99	4
779	A0A2R6PTW2	Protein argonaute 1B like	2.25	4	3.17	5.78	4
780	A0A2R6PTW9	Ubiquitin-conjugating enzyme E2 36	4.25	6	37.09	54.90	4
781	A0A2R6PTX4	Phosphomethylethanolamine N-methyltransferase	11.00	15	27.26	34.54	4
782	A0A2R6PTY9	Zygote arrest protein	1.00	1	13.89	13.89	3
783	A0A2R6PTZ9	Glutamine synthetase	34.20	49	63.54	65.73	4
784	A0A2R6PU03	Mitogen-activated protein kinase	20.60	32	33.07	44.88	4
785	A0A2R6PU25	Phenylalanyl-tRNA synthetase beta subunit	19.50	23	34.83	38.64	2
786	A0A2R6PU27	G3BP-like protein	2.00	3	4.45	6.68	3
787	A0A2R6PU45	Guanine nucleotide-binding protein subunit beta-like protein	18.20	25	60.60	70.00	4
788	A0A2R6PU59	LON peptidase N-terminal domain and RING finger protein	2.00	2	3.29	3.29	2
789	A0A2R6PU68	Malate dehydrogenase	2.80	4	6.49	7.75	4
790	A0A2R6PU81	40S ribosomal protein like	5.00	5	34.72	34.72	2
791	A0A2R6PU88	COBRA-like protein	1.00	1	1.22	1.22	1
792	A0A2R6PU99	UDP-arabinopyranose mutase	20.00	27	49.32	58.24	4

793	A0A2R6PUB9	Universal stress protein	1.00	1	11.46	11.46	1
794	A0A2R6PUF7	40S ribosomal protein like	7.60	11	29.44	44.67	4
795	A0A2R6PUG8	Programmed cell death protein	8.75	13	13.53	19.44	4
796	A0A2R6PUH7	Mannose-1-phosphate guanyltransferase	7.67	8	22.09	22.17	3
797	A0A2R6PUI2	Ubiquitin-conjugating enzyme E2 36	3.75	5	30.88	42.48	4
798	A0A2R6PUM2	Phosphopantothenoylcysteine decarboxylase	1.00	1	7.11	7.11	1
799	A0A2R6PUN2	Protein-methionine-S-oxide reductase	1.00	1	15.52	15.52	1
800	A0A2R6PUP7	Glucose-6-phosphate 1-epimerase	1.00	1	2.55	2.55	3
801	A0A2R6PUP9	Proteasome subunit alpha type (Fragment)	9.20	11	83.53	88.24	4
802	A0A2R6PUQ8	30S ribosomal protein	1.00	1	4.26	4.26	1
803	A0A2R6PUT8	Serine/threonine-protein kinase	4.00	5	8.31	10.09	3
804	A0A2R6PUU9	Protein transport protein Sec24-like	9.75	14	9.67	13.54	4
805	A0A2R6PUV0	Calnexin like	2.25	4	5.79	10.09	4
806	A0A2R6PUV5	40S ribosomal protein S12 (Fragment)	5.20	6	42.78	46.72	4
807	A0A2R6PUW2	Profilin	8.80	14	59.70	67.18	4
808	A0A2R6PUX0	60S ribosomal protein like (Fragment)	3.25	4	19.48	25.97	4
809	A0A2R6PUX3	Coatomer subunit beta (Fragment)	10.00	10	14.46	14.46	2
810	A0A2R6PUY0	Stromal cell-derived factor 2-like protein	1.00	1	5.61	5.61	2
811	A0A2R6PUZ0	Nuclear pore complex protein like	1.00	1	2.18	2.18	1
812	A0A2R6PUZ6	Nucleosome assembly protein like	3.40	5	11.92	17.82	4
813	A0A2R6PV08	V-type proton ATPase subunit C	2.00	3	6.24	8.29	3
814	A0A2R6PV11	Hydroxyphenylpyruvate reductase	10.75	14	43.29	50.80	4
815	A0A2R6PV14	Diadenosine tetraphosphate synthetase	21.40	28	39.08	48.73	4
816	A0A2R6PV24	60S ribosomal protein like	4.40	7	31.94	48.61	4
817	A0A2R6PV26	Aldehyde dehydrogenase (NAD(+))	3.80	5	9.35	12.15	4
818	A0A2R6PV42	26S protease regulatory subunit 7 A like	7.50	9	47.78	54.81	2
819	A0A2R6PV46	40S ribosomal protein SA	12.60	15	40.47	41.67	4
820	A0A2R6PV48	5'-nucleotidase	1.00	1	3.87	3.87	2
821	A0A2R6PV64	Developmentally-regulated G-protein	2.75	5	8.46	15.54	4
822	A0A2R6PV65	Ubiquitin carboxyl-terminal hydrolase	4.33	5	58.50	63.73	3
823	A0A2R6PV69	Ribosomal protein L37 (Fragment)	3.25	4	28.19	34.04	4
824	A0A2R6PV71	Casein kinase 1-like protein	1.67	2	3.81	4.66	3
825	A0A2R6PV75	RING-box protein like	1.00	1	12.17	12.17	3
826	A0A2R6PV78	Oligouridylate-binding protein like	1.00	1	2.86	2.86	3
827	A0A2R6PV86	Vesicle transport protein	0.00	0	0.00	0.00	1
828	A0A2R6PVB5	Serine/threonine-protein phosphatase 2A 55 kDa regulatory subunit B	4.67	6	9.29	12.67	3
829	A0A2R6PVC5	Mitogen-activated protein kinase	1.00	1	2.38	2.38	1
830	A0A2R6PVD3	Coatomer subunit zeta	1.00	1	13.74	13.74	2
831	A0A2R6PVI9	60S ribosomal protein like	10.40	14	44.47	52.85	4
832	A0A2R6PVR0	Plasma membrane ATPase	23.40	36	28.04	37.42	4
833	A0A2R6PVS9	Pto-interacting protein like	1.00	1	2.77	2.77	1
834	A0A2R6PVV0	Importin subunit alpha	3.75	6	10.56	16.15	4

835	A0A2R6PVV5	Stress-response A/B barrel domain-containing protein	1.33	2	19.22	28.83	3
836	A0A2R6PVX1	ATP citrate synthase	31.00	39	53.98	59.87	4
837	A0A2R6PVY2	60S ribosomal protein like (Fragment)	6.80	8	48.87	53.38	4
838	A0A2R6PVY7	HECT-type E3 ubiquitin transferase	1.00	1	0.97	0.97	3
839	A0A2R6PVZ1	Eukaryotic initiation factor 4A-8 like (Fragment)	7.00	7	30.77	30.77	1
840	A0A2R6PW26	Vesicle-associated membrane protein	1.00	1	3.77	3.77	3
841	A0A2R6PW28	AMMECR1 protein	1.00	1	4.24	4.25	3
842	A0A2R6PW40	Sperm-associated antigen 1A like	2.50	3	5.15	6.67	4
843	A0A2R6PW50	40S ribosomal protein	4.80	7	29.32	45.89	4
844	A0A2R6PW68	Malate dehydrogenase	21.40	28	56.69	62.35	4
845	A0A2R6PW72	Universal stress protein	2.50	4	19.69	28.13	2
846	A0A2R6PW96	Diphosphomevalonate decarboxylase	8.40	16	20.10	36.87	4
847	A0A2R6PWA3	Methyltransferase	1.00	1	2.20	2.20	3
848	A0A2R6PWA4	Pleiotropic drug resistance protein	2.50	3	1.96	2.29	2
849	A0A2R6PWC9	Exocyst subunit Exo70 family protein	2.00	2	4.02	4.02	2
850	A0A2R6PWF7	Basic leucine zipper like	1.00	1	3.41	3.41	2
851	A0A2R6PWG2	DnaJ protein	7.20	11	26.12	41.63	4
852	A0A2R6PWG7	Phospholipase	1.00	1	0.72	0.72	2
853	A0A2R6PWH3	Basic leucine zipper and W2 domain-containing protein	8.00	10	22.81	27.01	4
854	A0A2R6PWK1	Beta-glucosidase	6.00	8	15.36	20.08	4
855	A0A2R6PWK8	Acyl-[acyl-carrier-protein] desaturase	1.50	2	4.67	6.31	4
856	A0A2R6PWL6	Adenosine kinase	24.75	33	68.47	68.91	4
857	A0A2R6PWM3	RBR-type E3 ubiquitin transferase	5.50	8	11.51	18.04	4
858	A0A2R6PWN1	60S ribosomal protein L12	3.00	3	22.29	22.29	1
859	A0A2R6PWP4	Isopentenyl-diphosphate Delta-isomerase	6.00	9	20.64	28.52	4
860	A0A2R6PWQ2	40S ribosomal protein S23 (Fragment)	3.80	5	37.86	41.43	4
861	A0A2R6PWQ4	Aspartic proteinase-like protein	5.75	8	15.64	22.18	4
862	A0A2R6PWQ9	Elongation factor 1-alpha	50.25	67	64.21	70.47	4
863	A0A2R6PWS7	Phosphatidate phosphatase	1.00	1	1.42	1.42	3
864	A0A2R6PWS9	Trafficking protein particle complex subunit like	2.00	3	23.35	34.91	4
865	A0A2R6PWT6	Phosphatidate phosphatase	1.00	1	3.27	3.27	3
866	A0A2R6PWT8	mRNA cap-binding protein	1.50	2	9.30	12.06	4
867	A0A2R6PWT9	Uveal autoantigen with coiled-coil domains and ankyrin repeats protein	10.50	16	14.15	20.26	4
868	A0A2R6PWU5	UDP-glucuronate decarboxylase	2.50	3	5.29	6.21	2
869	A0A2R6PWV9	60S ribosomal protein like (Fragment)	5.80	7	40.60	45.11	4
870	A0A2R6PWW6	Actin-depolymerizing factor 2 like (Fragment)	2.67	3	15.94	18.84	3
871	A0A2R6PWW8	60S ribosomal protein like	4.60	7	23.74	32.26	4
872	A0A2R6PWX0	Ras-related protein like	7.00	9	30.36	38.84	3
873	A0A2R6PWY3	ADP-ribosylation factor GTPase-activating protein	1.00	1	2.42	2.42	2
874	A0A2R6PWY9	Heat shock protein 70 family protein	46.60	64	62.16	76.89	4
875	A0A2R6PWZ6	60S ribosomal protein L38 (Fragment)	3.00	4	19.12	19.12	3
876	A0A2R6PX08	60S ribosomal protein	12.40	16	40.12	49.85	4

877	A0A2R6PX13	Fructokinase-4 like	29.80	38	71.73	72.64	4
878	A0A2R6PX42	Non-specific serine/threonine protein kinase	3.33	5	7.96	11.94	3
879	A0A2R6PX44	Pyruvate kinase	20.00	23	41.08	43.45	2
880	A0A2R6PX49	60S ribosomal protein (Fragment)	2.67	3	17.50	20.00	3
881	A0A2R6PX58	Phosphopyruvate hydratase	56.00	75	77.85	79.78	4
882	A0A2R6PX63	WD repeat-containing protein	1.50	2	2.01	2.79	4
883	A0A2R6PX66	Late embryogenesis abundant protein	4.00	5	40.35	41.05	3
884	A0A2R6PX74	Serine/threonine protein phosphatase 2A regulatory subunit B''gamma like	8.50	11	16.51	21.15	2
885	A0A2R6PX78	Cyclase-associated protein	18.00	24	40.97	52.85	4
886	A0A2R6PX84	Vesicle-associated membrane protein	2.67	4	11.06	15.00	3
887	A0A2R6PX86	Elongation factor 1-alpha	46.60	71	58.84	67.56	4
888	A0A2R6PXA0	Serine/threonine-protein kinase	1.00	1	0.80	0.80	1
889	A0A2R6PXA7	EH domain-containing protein	1.75	3	3.53	6.06	4
890	A0A2R6PXA8	Guanosine nucleotide diphosphate dissociation inhibitor	28.20	41	50.90	61.49	4
891	A0A2R6PXB4	Cysteine proteinase inhibitor 1 like	1.00	1	10.43	10.43	3
892	A0A2R6PXE8	Patatin	1.33	2	0.95	1.43	3
893	A0A2R6PXE9	Glutathione reductase	6.25	11	20.83	35.95	4
894	A0A2R6PXF4	Adenosine deaminase-like protein	1.00	1	2.98	2.98	2
895	A0A2R6PXF9	Guanosine nucleotide diphosphate dissociation inhibitor	18.00	22	33.86	41.22	3
896	A0A2R6PXG5	Cellulose synthase-like protein	6.25	11	5.64	9.27	4
897	A0A2R6PXH2	Glutathione reductase	9.67	11	27.04	31.64	3
898	A0A2R6PXH4	Vesicle-associated membrane protein	4.00	4	15.00	15.00	1
899	A0A2R6PXI0	26S proteasome non-ATPase regulatory subunit 1 homolog	22.20	29	26.82	33.30	4
900	A0A2R6PXI3	Serine/threonine-protein kinase	1.00	1	0.64	0.64	1
901	A0A2R6PXI5	Heterogeneous nuclear ribonucleoprotein like	1.00	1	3.48	3.48	2
902	A0A2R6PXI8	Inorganic diphosphatase	29.33	38	36.69	42.02	3
903	A0A2R6PXL4	3-ketoacyl-CoA thiolase 2, peroxisomal like	10.75	15	37.26	47.94	4
904	A0A2R6PXL7	Fructose-bisphosphate aldolase	41.00	56	73.46	79.89	4
905	A0A2R6PXM2	Polyadenylate-binding protein	5.33	7	8.50	10.73	3
906	A0A2R6PXM6	Ribosomal protein	6.00	8	27.96	35.19	4
907	A0A2R6PXP3	Pyruvate kinase	16.20	23	35.52	44.78	4
908	A0A2R6PXP8	V-type proton ATPase subunit H	3.00	4	7.64	10.57	3
909	A0A2R6PXQ9	L-ascorbate peroxidase	3.00	3	17.46	17.46	1
910	A0A2R6PXU2	VHS domain-containing protein	1.00	1	0.59	0.59	2
911	A0A2R6PXV0	UBX domain-containing protein	5.00	6	12.16	14.22	4
912	A0A2R6PXW8	Tropinone reductase-like	1.00	1	4.35	4.35	1
913	A0A2R6PXX5	Nucleic acid-binding, OB-fold protein	1.50	2	7.36	9.82	2
914	A0A2R6PXX8	Stem-specific protein	3.00	3	10.27	10.27	2
915	A0A2R6PY06	60S ribosomal protein like (Fragment)	6.00	7	31.05	33.70	4
916	A0A2R6PY32	Alpha,alpha-trehalose-phosphate synthase	20.25	28	32.23	44.73	4
917	A0A2R6PY47	3-oxoacyl-[acyl-carrier-protein] synthase	3.50	6	10.35	16.09	4
918	A0A2R6PY63	60S ribosomal protein L18a	6.60	9	36.41	50.00	4

919	A0A2R6PY67	Pyruvate dehydrogenase E1 component subunit beta	1.60	3	3.74	6.98	4
920	A0A2R6PY77	Cullin-4 like	1.00	1	1.41	1.41	1
921	A0A2R6PY80	CSC1-like protein	5.50	9	6.88	11.20	4
922	A0A2R6PY82	60S acidic ribosomal protein	2.50	3	16.50	21.00	2
923	A0A2R6PY85	40S ribosomal protein like (Fragment)	7.60	11	46.31	66.44	4
924	A0A2R6PY93	Serine/threonine-protein phosphatase 6 regulatory subunit like	5.50	7	7.48	9.89	4
925	A0A2R6PY98	Receptor-like protein kinase	1.00	1	1.38	1.38	1
926	A0A2R6PYB6	Cationic amino acid transporter like	1.67	2	2.52	2.96	3
927	A0A2R6PYB9	Obg-like ATPase 1	11.50	12	35.53	36.80	2
928	A0A2R6PYC3	Proteasome subunit alpha type	15.80	23	67.47	80.32	4
929	A0A2R6PYC7	UDP-arabinose 4-epimerase	2.75	4	7.53	11.24	4
930	A0A2R6PYD4	Ubiquitinyl hydrolase 1	2.25	3	12.50	18.63	4
931	A0A2R6PYG4	DnaJ protein	4.33	5	13.91	16.55	3
932	A0A2R6PYG5	Exocyst subunit Exo70 family protein	2.00	2	3.35	3.35	2
933	A0A2R6PYG8	Ubiquitinyl hydrolase 1	12.33	16	14.25	16.72	3
934	A0A2R6PYH6	Copper transport protein like	1.00	1	13.83	13.83	4
935	A0A2R6PYH8	Myosin-11 like (Fragment)	19.40	31	13.75	20.86	4
936	A0A2R6PYK7	Arabinose 5-phosphate isomerase	2.00	3	4.90	7.35	3
937	A0A2R6PYL4	Nascent polypeptide-associated complex subunit beta	1.33	2	10.77	16.15	3
938	A0A2R6PYL7	UDP-arabinopyranose mutase	6.75	13	19.75	38.35	4
939	A0A2R6PYM0	Serine/threonine protein phosphatase 2A regulatory subunit B''gamma like	11.80	20	22.56	36.92	4
940	A0A2R6PYN0	Protein pelota homolog	1.00	1	3.44	3.44	2
941	A0A2R6PYN9	Subtilisin-like protease	8.60	12	14.68	20.33	4
942	A0A2R6PYP9	V-type proton ATPase subunit	1.00	1	3.13	3.13	2
943	A0A2R6PYQ8	Uncharacterized protein	5.40	9	19.40	30.93	4
944	A0A2R6PYR0	Isopentenyl-diphosphate Delta-isomerase	6.20	9	26.81	35.74	4
945	A0A2R6PYR1	Uncharacterized protein	1.00	1	5.59	5.59	1
946	A0A2R6PYS4	Serine/threonine protein phosphatase 2A regulatory subunit	8.75	12	15.54	19.64	4
947	A0A2R6PYS9	Ras-related protein	2.00	2	11.00	11.00	1
948	A0A2R6PYT8	Ubiquitin-like protein	1.00	1	13.04	13.04	1
949	A0A2R6PYY4	Coatomer subunit epsilon	5.50	7	31.92	39.79	4
950	A0A2R6PZ72	Pyrophosphate--fructose 6-phosphate 1-phosphotransferase subunit alpha	40.40	56	62.17	71.96	4
951	A0A2R6PZC1	Catalase	4.20	5	10.37	11.74	4
952	A0A2R6PZD7	Small nuclear ribonucleoprotein Sm D3	1.50	2	10.60	14.39	4
953	A0A2R6PZH2	Ribonuclease P protein subunit p25-like protein	3.75	5	13.13	15.95	4
954	A0A2R6PZH8	Translation initiation factor IF-2 like (Fragment)	1.67	2	8.63	10.59	3
955	A0A2R6PZJ6	Tubulin beta chain	32.60	49	61.60	68.22	4
956	A0A2R6PZJ9	Endoplasmin like	3.60	5	4.07	5.21	4
957	A0A2R6PZL0	Sulfate adenylyltransferase	14.60	23	31.72	45.82	4
958	A0A2R6PZM4	Endoglucanase	2.00	2	3.63	3.63	1
959	A0A2R6PZS7	Isoflavone reductase-like protein	7.20	10	24.09	32.47	4
960	A0A2R6PZT2	Thioredoxin H-type like	4.60	6	46.45	52.07	4

961	A0A2R6PZT6	Proteasome subunit alpha type	12.40	14	40.29	45.05	4
962	A0A2R6PZW0	60S acidic ribosomal protein	3.40	5	31.38	48.28	4
963	A0A2R6PZW6	Serine/threonine protein kinase	1.00	1	0.80	0.80	1
964	A0A2R6PZY1	COP9 signalosome complex subunit like	11.25	15	36.59	47.10	4
965	A0A2R6Q004	Phosphoglycerate mutase-like protein isoform 2	2.00	2	6.78	6.78	2
966	A0A2R6Q015	Polyadenylate-binding protein	3.67	5	10.48	14.55	3
967	A0A2R6Q027	Alpha-amylase	1.00	1	2.42	2.42	1
968	A0A2R6Q035	Protein WEAK CHLOROPLAST MOVEMENT UNDER BLUE LIGHT 1 like	17.50	23	21.89	28.03	4
969	A0A2R6Q055	Protein like	1.00	1	1.87	1.87	1
970	A0A2R6Q056	Glycosyltransferase	1.75	2	4.13	4.69	4
971	A0A2R6Q073	Argininosuccinate lyase	2.25	4	6.17	11.01	4
972	A0A2R6Q090	Polyadenylate-binding protein	7.00	13	10.79	18.93	3
973	A0A2R6Q092	AP-4 complex subunit mu like	2.00	2	4.32	4.66	2
974	A0A2R6Q0A4	Esterase	1.00	1	6.44	6.44	4
975	A0A2R6Q0B0	14-3-3 protein	10.80	16	41.82	59.52	4
976	A0A2R6Q0C1	14-3-3-like protein	23.00	28	67.13	73.95	4
977	A0A2R6Q0C4	F-box protein	3.00	4	2.97	4.10	4
978	A0A2R6Q0D5	14-3-3 protein (Fragment)	6.00	9	19.84	27.95	4
979	A0A2R6Q0H1	Calcium-transporting ATPase	1.00	1	1.08	1.08	1
980	A0A2R6Q0H2	Myosin heavy chain kinase	1.50	2	3.79	4.90	2
981	A0A2R6Q0K0	Adenine phosphoribosyltransferase	3.00	4	20.83	27.17	3
982	A0A2R6Q0M4	Phosphoglycerate mutase-like protein isoform 1	2.00	2	7.97	7.97	2
983	A0A2R6Q0M8	Ubiquitin-fold modifier-conjugating enzyme 1	1.00	1	5.75	5.75	2
984	A0A2R6Q0N3	E3 ubiquitin-protein like	7.00	10	11.89	15.01	4
985	A0A2R6Q0N5	Phosphoglycerate mutase-like protein	3.00	3	10.16	10.31	2
986	A0A2R6Q0N6	Xylulose kinase	9.40	15	19.25	28.01	4
987	A0A2R6Q0R1	Phosphoenolpyruvate carboxykinase (ATP)	12.60	18	26.99	38.69	4
988	A0A2R6Q0S2	E3 ubiquitin-protein like (Fragment)	2.25	3	10.26	10.26	4
989	A0A2R6Q0S4	IST1-like protein	1.33	2	2.29	3.43	3
990	A0A2R6Q0T9	Programmed cell death protein	14.60	23	23.52	35.06	4
991	A0A2R6Q0V2	Ras-related protein like	1.00	1	10.59	10.59	1
992	A0A2R6Q0V8	GEM-like protein	1.00	1	3.96	3.96	1
993	A0A2R6Q0X5	V-type proton ATPase proteolipid subunit	1.00	1	10.91	10.91	3
994	A0A2R6Q0Y5	Deubiquitinating enzyme MINDY-3	1.00	1	1.46	1.46	2
995	A0A2R6Q0Y7	UPF0496 protein	1.00	1	1.79	1.79	1
996	A0A2R6Q117	Protein-serine/threonine phosphatase	4.00	5	12.46	16.20	2
997	A0A2R6Q141	TOM1-like protein	1.75	3	3.73	6.23	4
998	A0A2R6Q143	UDP-sugar pyrophosphorylase	15.25	20	28.95	37.54	4
999	A0A2R6Q164	Proteasome subunit beta (Fragment)	6.25	9	44.31	51.98	4
1000	A0A2R6Q182	Alkaline/neutral invertase	19.00	25	43.19	54.68	4
1001	A0A2R6Q183	Dihydrolipoamide acetyltransferase component of pyruvate dehydrogenase complex	2.00	2	5.96	5.96	2
1002	A0A2R6Q1A1	Calcium-dependent protein kinase	9.20	14	20.23	30.84	4

1003	A0A2R6Q1A5	Immune-associated nucleotide-binding protein	1.00	1	5.00	5.00	2
1004	A0A2R6Q1C5	Nascent polypeptide-associated complex subunit alpha-like protein	1.33	2	8.87	13.30	3
1005	A0A2R6Q1D7	60S ribosomal protein	15.00	21	35.84	44.99	4
1006	A0A2R6Q1E9	Late embryogenesis abundant protein	5.00	8	56.63	81.93	4
1007	A0A2R6Q1F2	Transcription factor like	1.00	1	2.92	2.92	3
1008	A0A2R6Q1I5	Protein DJ-1 D like	1.00	1	3.53	3.53	2
1009	A0A2R6Q1I6	Ras-related protein	2.33	3	11.50	14.50	3
1010	A0A2R6Q1J1	UTP--glucose-1-phosphate uridylyltransferase like (Fragment)	24.50	29	75.82	78.83	4
1011	A0A2R6Q1J5	Isocitrate dehydrogenase [NADP]	14.80	21	36.72	47.83	4
1012	A0A2R6Q1K8	UTP--glucose-1-phosphate uridylyltransferase	46.40	61	75.54	80.84	4
1013	A0A2R6Q1K9	Coatomer subunit delta (Fragment)	6.80	11	11.10	16.67	4
1014	A0A2R6Q1L3	Glutamate decarboxylase	14.00	16	31.13	35.74	2
1015	A0A2R6Q1L4	Transmembrane 9 superfamily member	2.00	2	3.24	3.24	2
1016	A0A2R6Q1N1	Ras-related protein RABA2a	6.33	7	32.09	35.81	3
1017	A0A2R6Q1P8	Cullin-associated NEDD8-dissociated protein	14.00	17	15.98	18.69	2
1018	A0A2R6Q1Q3	Methionine S-methyltransferase	12.80	21	12.34	19.98	4
1019	A0A2R6Q1S9	Thioredoxin reductase	6.75	9	27.64	37.89	4
1020	A0A2R6Q1V2	Serine/threonine-protein kinase	1.25	2	3.15	4.94	4
1021	A0A2R6Q1V3	EPS15 homologyprotein	1.00	1	1.44	1.44	2
1022	A0A2R6Q1X0	Phosphoinositide phosphatase	3.60	6	7.11	12.58	4
1023	A0A2R6Q1X4	AP complex subunit sigma (Fragment)	1.00	1	8.12	8.13	3
1024	A0A2R6Q1Z3	Protein disulfide-isomerase	2.00	3	4.95	7.27	2
1025	A0A2R6Q202	Phosphoserine aminotransferase	2.00	5	5.44	13.60	4
1026	A0A2R6Q211	Eukaryotic translation initiation factor 3 subunit J	1.50	2	9.42	12.56	4
1027	A0A2R6Q227	Vacuolar protein sorting-associated protein 35	3.67	6	5.59	10.09	3
1028	A0A2R6Q231	SKP1-like protein	1.00	1	8.39	8.39	2
1029	A0A2R6Q232	Elongation factor 1-gamma like (Fragment)	11.00	15	26.67	31.90	4
1030	A0A2R6Q233	Rac-like GTP-binding protein RHO1	9.20	13	31.57	40.10	4
1031	A0A2R6Q241	Protein EARLY-RESPONSIVE TO DEHYDRATION 7 like	3.00	3	7.74	7.74	1
1032	A0A2R6Q242	Protein EARLY-RESPONSIVE TO DEHYDRATION 7 like	3.00	4	7.61	10.20	3
1033	A0A2R6Q253	26S proteasome non-ATPase regulatory subunit like	7.50	8	22.32	23.45	4
1034	A0A2R6Q2C7	Catalase	6.50	8	16.87	20.53	4
1035	A0A2R6Q2D2	Coatomer subunit beta	10.00	17	13.14	22.36	4
1036	A0A2R6Q2E2	UDP-4-keto-6-deoxy-D-glucose 3,5-epimerase/UDP-4-keto-L-rhamnose 4-keto-reductase	15.20	20	34.76	43.62	4
1037	A0A2R6Q2E5	Sarcosine oxidase	1.00	1	2.55	2.55	1
1038	A0A2R6Q2F2	Protein-serine/threonine phosphatase	3.00	3	12.15	12.15	1
1039	A0A2R6Q2I1	Eukaryotic translation initiation factor 5A	7.80	9	48.62	55.62	4
1040	A0A2R6Q2J8	Protein-serine/threonine phosphatase	1.00	1	3.57	3.57	1
1041	A0A2R6Q2K5	HSP-interacting protein	1.33	2	1.61	2.41	3
1042	A0A2R6Q2K8	40S ribosomal protein	4.40	7	28.18	38.99	4
1043	A0A2R6Q2L8	Pentatricopeptide repeat-containing protein	1.00	1	1.95	1.95	2
1044	A0A2R6Q2M3	Clathrin assembly protein	1.00	1	1.23	1.23	2

1045	A0A2R6Q2M8	GDP-mannose 4,6-dehydratase	15.00	22	41.17	48.81	4
1046	A0A2R6Q2N2	DNA/RNA-binding protein Alba-like protein	4.00	5	29.20	36.00	4
1047	A0A2R6Q2P0	DEAD-box ATP-dependent RNA helicase 15 (Fragment)	2.00	3	4.24	6.35	3
1048	A0A2R6Q2Q3	26S protease regulatory subunit 8 A	23.33	33	51.82	66.43	3
1049	A0A2R6Q2R8	N-alpha-acetyltransferase	1.33	2	7.32	10.98	3
1050	A0A2R6Q2S5	DnaJ subfamily B member 5 like	1.00	1	3.05	3.05	2
1051	A0A2R6Q2T0	ADP-ribosylation factor GTPase-activating protein	1.00	1	1.52	1.52	1
1052	A0A2R6Q2T3	Eukaryotic translation initiation factor 3 subunit L	7.00	11	14.19	21.71	4
1053	A0A2R6Q2T8	La protein	1.00	1	2.92	2.92	4
1054	A0A2R6Q2U2	Aspartate aminotransferase	16.20	21	37.72	45.83	4
1055	A0A2R6Q2V0	Esterase	1.00	1	2.71	2.71	2
1056	A0A2R6Q2Y4	BTB/POZ domain and ankyrin repeat-containing protein	3.50	5	13.46	20.51	4
1057	A0A2R6Q323	Eukaryotic initiation factor 4A-14	32.25	39	59.97	63.29	4
1058	A0A2R6Q331	Alkylated DNA repair protein like	1.00	1	4.34	4.34	1
1059	A0A2R6Q351	AP-4 complex subunit epsilon	4.50	7	4.89	7.41	4
1060	A0A2R6Q354	Acyl-CoA-binding protein	1.00	1	8.89	8.89	3
1061	A0A2R6Q375	Clathrin assembly protein	4.25	7	7.11	11.99	4
1062	A0A2R6Q396	Villin-4 like	8.75	14	11.10	17.35	4
1063	A0A2R6Q3A4	TOM1-like protein	1.00	1	2.13	2.13	3
1064	A0A2R6Q3C0	Vacuolar protein sorting-associated protein	1.33	2	9.31	13.97	3
1065	A0A2R6Q3C1	26S proteasome non-ATPase regulatory subunit 13 A like	10.40	16	26.27	41.19	4
1066	A0A2R6Q3D8	Monodehydroascorbate reductase	5.50	9	14.74	24.65	2
1067	A0A2R6Q3G6	40S ribosomal protein S15 (Fragment)	3.00	4	30.80	40.67	4
1068	A0A2R6Q3H2	Proteasome subunit beta	13.40	17	68.04	82.84	4
1069	A0A2R6Q3H8	40S ribosomal protein like (Fragment)	11.00	11	49.81	49.81	2
1070	A0A2R6Q3N5	BSD domain-containing protein	1.00	1	2.05	2.05	2
1071	A0A2R6Q3N9	Procollagen-proline 4-dioxygenase	1.00	1	3.05	3.05	2
1072	A0A2R6Q3P2	Protein like	1.00	1	2.34	2.34	4
1073	A0A2R6Q3Q3	Translationally-controlled tumor protein	8.20	11	55.48	60.71	4
1074	A0A2R6Q3Q5	40S ribosomal protein S21	3.60	7	35.37	50.00	4
1075	A0A2R6Q3T0	Ribosomal protein L19	4.50	5	25.47	28.57	4
1076	A0A2R6Q3T3	ATP citrate synthase	38.80	49	59.67	65.13	4
1077	A0A2R6Q3T8	Pectinesterase	9.50	12	17.13	19.83	2
1078	A0A2R6Q3U7	GTP-binding protein like	3.75	4	27.59	30.05	4
1079	A0A2R6Q3V2	S-adenosylmethionine synthase	37.00	49	67.68	79.13	4
1080	A0A2R6Q3V8	YTH domain-containing family protein	2.00	2	2.84	2.84	2
1081	A0A2R6Q3X1	Pectinesterase	15.00	18	34.97	41.95	4
1082	A0A2R6Q3Y9	Hsp70-Hsp90 organizing protein	3.00	3	11.71	11.71	2
1083	A0A2R6Q3Z8	Sorting nexin like	2.33	3	5.24	6.73	3
1084	A0A2R6Q403	Proteasome subunit beta	12.80	15	46.61	50.85	4
1085	A0A2R6Q405	Ubiquitin-conjugating enzyme E2 variant 1C like	4.20	6	31.13	35.76	4
1086	A0A2R6Q408	Serine/threonine-protein kinase	4.33	7	6.09	9.58	3

1087	A0A2R6Q411	Ribosomal protein	6.80	10	29.45	38.89	4
1088	A0A2R6Q424	Trafficking protein particle complex subunit like	1.00	1	1.26	1.26	2
1089	A0A2R6Q429	7,8-dihydroneopterin aldolase	1.00	1	5.67	5.67	1
1090	A0A2R6Q431	40S ribosomal protein	4.40	6	21.62	27.03	4
1091	A0A2R6Q462	Sucrose-phosphatase	13.50	17	36.77	43.53	4
1092	A0A2R6Q465	Uncharacterized protein	1.00	1	12.50	12.50	2
1093	A0A2R6Q471	Ubiquitinyl hydrolase 1	17.75	25	17.86	23.09	4
1094	A0A2R6Q474	Syntaxin-131	0.00	0	0.00	0.00	1
1095	A0A2R6Q476	Protein-synthesizing GTPase	8.00	12	21.85	33.62	4
1096	A0A2R6Q478	5-methyltetrahydropteroyltriglutamate--homocysteine S-methyltransferase	67.60	97	60.73	66.27	4
1097	A0A2R6Q497	Random slug protein	6.25	8	16.71	20.41	4
1098	A0A2R6Q4B7	Exportin-7 like	5.25	8	5.25	8.17	4
1099	A0A2R6Q4D8	Protein-tyrosine-phosphatase	1.00	2	3.31	6.63	4
1100	A0A2R6Q4H6	Calcium-binding protein	1.00	1	3.29	3.29	4
1101	A0A2R6Q4H7	S-formylglutathione hydrolase	6.00	7	25.71	29.58	4
1102	A0A2R6Q4J9	Villin-3 like	5.75	8	5.75	7.97	4
1103	A0A2R6Q4L1	Exportin-2 like (Fragment)	3.00	3	5.81	5.81	1
1104	A0A2R6Q4L9	Reticulon-like protein	2.00	2	3.99	3.99	1
1105	A0A2R6Q4N3	Ras-related protein like	2.00	2	9.82	9.82	3
1106	A0A2R6Q4P1	N-alpha-acetyltransferase	1.00	1	4.88	4.88	1
1107	A0A2R6Q4Q9	TBCC domain-containing protein 1	6.67	7	13.25	14.03	3
1108	A0A2R6Q4V8	Protein CfxQ like	3.75	5	10.75	13.99	4
1109	A0A2R6Q4W5	Sugar transport protein	1.00	1	3.33	3.33	2
1110	A0A2R6Q4Z0	Profilin	10.80	16	40.90	43.61	4
1111	A0A2R6Q4Z7	Phosphotransferase	1.00	1	3.02	3.02	1
1112	A0A2R6Q4Z9	Vacuolar protein sorting-associated protein	1.00	1	4.61	4.61	1
1113	A0A2R6Q503	Asparagine--tRNA ligase	9.60	14	17.64	26.41	4
1114	A0A2R6Q505	Calcium-transporting ATPase	1.00	1	1.53	1.53	1
1115	A0A2R6Q512	Xaa-Pro dipeptidase	1.00	1	1.80	1.80	2
1116	A0A2R6Q513	Inorganic pyrophosphatase	1.00	1	3.13	3.13	1
1117	A0A2R6Q535	Guanylate kinase (Fragment)	1.33	2	4.30	6.45	3
1118	A0A2R6Q541	Casein kinase 1-like protein	1.67	2	3.86	4.72	3
1119	A0A2R6Q557	Hydrolase_4 domain-containing protein	2.25	4	7.06	13.02	4
1120	A0A2R6Q560	Vacuolar protein sorting-associated protein	1.00	1	4.48	4.48	3
1121	A0A2R6Q572	Serine/threonine protein phosphatase 2A regulatory subunit	1.00	1	2.22	2.22	2
1122	A0A2R6Q585	40S ribosomal protein (Fragment)	1.00	1	12.96	12.96	2
1123	A0A2R6Q586	Methylthioribose-1-phosphate isomerase	1.67	2	8.48	10.10	3
1124	A0A2R6Q587	40S ribosomal protein like	10.80	12	53.56	59.83	4
1125	A0A2R6Q589	RING-box protein like	1.00	1	11.20	11.20	3
1126	A0A2R6Q5A9	Pectinesterase	3.00	5	5.52	9.43	4
1127	A0A2R6Q5B0	Rho guanine nucleotide exchange factor like	1.00	1	2.21	2.21	2
1128	A0A2R6Q5B1	Proteasome subunit alpha type	15.20	20	64.55	72.36	4

1129	A0A2R6Q5C0	Oligouridylate-binding protein like	1.00	1	2.06	2.06	3
1130	A0A2R6Q5D3	Arginyl-tRNA synthetase (Fragment)	20.60	31	39.18	52.90	4
1131	A0A2R6Q5D8	Pectinesterase	3.00	5	5.52	9.43	4
1132	A0A2R6Q5E8	60S ribosomal protein	2.00	2	11.67	11.67	2
1133	A0A2R6Q5G9	Translation machinery-associated protein 22	1.00	1	4.15	4.15	4
1134	A0A2R6Q5K9	CTP synthase	1.67	2	2.98	3.53	3
1135	A0A2R6Q5L1	Cullin-4 like	1.00	1	1.34	1.34	1
1136	A0A2R6Q5N9	60S ribosomal protein L6	9.20	12	34.05	42.24	4
1137	A0A2R6Q5P5	Dynamin-related protein like	0.00	0	0.00	0.00	1
1138	A0A2R6Q5Q2	Beta-ureidopropionase	3.33	4	9.16	10.60	3
1139	A0A2R6Q5Q4	Eukaryotic translation initiation factor 3 subunit K	3.67	4	19.72	22.07	3
1140	A0A2R6Q5R1	Lysine ketoglutarate reductase (Fragment)	3.00	4	3.03	3.84	2
1141	A0A2R6Q5U6	Cation-chloride cotransporter like	3.00	4	4.17	5.35	3
1142	A0A2R6Q5W0	3-oxo-Delta(4,5)-steroid 5-beta-reductase	5.80	8	18.62	26.28	4
1143	A0A2R6Q5W5	COP9 signalosome complex subunit 5b like	6.00	11	19.11	36.01	4
1144	A0A2R6Q5Y7	26S proteasome non-ATPase regulatory subunit 13 A like	10.00	14	25.34	34.97	4
1145	A0A2R6Q5Z9	Serine/threonine-protein kinase	1.00	1	3.58	3.58	3
1146	A0A2R6Q603	Basic secretory protease	1.00	1	4.37	4.37	3
1147	A0A2R6Q605	40S ribosomal protein S16	10.00	10	56.94	56.94	1
1148	A0A2R6Q629	EKC/KEOPS complex subunit Tprkb like	1.00	1	4.65	4.65	2
1149	A0A2R6Q635	DnaJ protein	6.50	11	22.67	41.39	4
1150	A0A2R6Q640	Tubulin alpha chain	30.00	39	51.77	56.32	4
1151	A0A2R6Q657	L-galactose dehydrogenase	1.00	1	2.51	2.51	2
1152	A0A2R6Q658	Proline iminopeptidase	1.00	1	4.53	4.53	1
1153	A0A2R6Q666	Malate dehydrogenase	1.50	2	7.20	9.47	4
1154	A0A2R6Q669	14-3-3-like protein	23.80	29	68.89	73.95	4
1155	A0A2R6Q6B1	Peptidylprolyl isomerase	1.60	2	17.50	23.21	4
1156	A0A2R6Q6C1	Sugar transport protein	1.00	1	1.94	1.94	3
1157	A0A2R6Q6E5	Glycine-rich RNA-binding protein like	1.00	1	6.50	6.50	1
1158	A0A2R6Q6F3	COP9 signalosome complex subunit 8 like	2.00	3	11.42	16.75	4
1159	A0A2R6Q6G5	Subtilisin-like protease SBT4.15	4.60	7	7.08	11.05	4
1160	A0A2R6Q6J0	Uncharacterized protein (Fragment)	1.00	1	3.86	3.86	2
1161	A0A2R6Q6J6	Serine/threonine-protein kinase	2.00	3	6.34	9.01	4
1162	A0A2R6Q6K2	Dynamin-related protein like	0.00	0	0.00	0.00	1
1163	A0A2R6Q6L9	Ras-related protein like	5.67	6	28.06	29.77	3
1164	A0A2R6Q6P1	Dynamin GTPase	1.25	2	1.63	2.72	4
1165	A0A2R6Q6P5	60S ribosomal protein L18a	6.60	9	36.41	50.00	4
1166	A0A2R6Q6P9	3-oxoacyl-[acyl-carrier-protein] synthase	4.60	8	14.43	24.57	4
1167	A0A2R6Q6U3	Alpha,alpha-trehalose-phosphate synthase	15.50	16	21.99	22.46	2
1168	A0A2R6Q6X2	Non-specific serine/threonine protein kinase	1.00	1	1.82	1.82	1
1169	A0A2R6Q704	Phospholipase	1.00	1	0.72	0.72	2
1170	A0A2R6Q710	Translationally-controlled tumor protein	4.50	5	27.68	31.55	2

1171	A0A2R6Q713	Syntaxin-43 like	1.00	1	4.37	4.37	2
1172	A0A2R6Q721	Dihydrolipoyl dehydrogenase	1.00	1	2.10	2.10	1
1173	A0A2R6Q722	Calreticulin	3.50	6	8.83	15.40	4
1174	A0A2R6Q723	GTP-binding protein like	3.75	4	27.59	30.05	4
1175	A0A2R6Q729	Kinesin-like protein	1.00	1	1.49	1.49	2
1176	A0A2R6Q734	Importin subunit alpha	6.20	11	17.12	30.65	4
1177	A0A2R6Q758	ATP citrate synthase	11.00	14	30.02	35.70	4
1178	A0A2R6Q765	Golgi apparatus membrane protein TVP23	1.00	1	6.01	6.01	4
1179	A0A2R6Q767	Trafficking protein particle complex subunit	1.60	2	9.08	11.35	4
1180	A0A2R6Q768	ADP-ribosylation factor (Fragment)	9.60	14	45.45	47.78	4
1181	A0A2R6Q775	Non-specific serine/threonine protein kinase	1.00	1	2.21	2.21	3
1182	A0A2R6Q780	Small nuclear ribonucleoprotein-associated protein	1.00	1	2.89	2.89	4
1183	A0A2R6Q783	Serine/threonine-protein phosphatase	1.50	3	1.67	3.34	4
1184	A0A2R6Q7A2	Ribosomal protein	10.50	12	45.14	49.54	4
1185	A0A2R6Q7B4	F-box/LRR-repeat protein	2.00	3	5.57	8.35	3
1186	A0A2R6Q7S9	Protein kinase	2.00	2	2.79	2.79	2
1187	A0A2R6Q7T5	Ubiquitin-conjugating enzyme E2 10	2.75	4	16.55	19.59	4
1188	A0A2R6Q7T7	Eukaryotic translation initiation factor 4C	2.50	4	17.76	24.83	4
1189	A0A2R6Q7V9	Desiccation protectant protein like	9.40	12	62.73	64.29	4
1190	A0A2R6Q7W1	Exocyst complex component like	1.67	3	2.10	3.75	3
1191	A0A2R6Q811	Acyl-coenzyme A oxidase	3.75	6	6.70	11.14	4
1192	A0A2R6Q834	40S ribosomal protein like (Fragment)	3.67	4	25.27	28.02	3
1193	A0A2R6Q837	UPF0664 stress-induced protein like	2.00	3	10.78	15.20	4
1194	A0A2R6Q847	FAM10 family protein	7.60	12	19.70	31.31	4
1195	A0A2R6Q895	Bifunctional dTDP-4-dehydrorhamnose 3,5-epimerase/dTDP-4-dehydrorhamnose reductase	18.80	26	62.75	71.91	4
1196	A0A2R6Q899	60S ribosomal protein	3.40	4	21.84	25.15	4
1197	A0A2R6Q8A2	Sugar transport protein	3.60	6	6.80	11.13	4
1198	A0A2R6Q8A7	3-hydroxy-3-methylglutaryl coenzyme A synthase	15.60	23	31.91	43.86	4
1199	A0A2R6Q8C7	LIM domain-containing protein	1.33	2	8.77	11.84	3
1200	A0A2R6Q8D6	Glutathione peroxidase	1.00	1	8.85	8.85	4
1201	A0A2R6Q8E2	Glutamine amidotransferase	11.25	14	19.15	24.84	4
1202	A0A2R6Q8G0	Tubulin beta chain	30.80	46	64.95	75.06	4
1203	A0A2R6Q8G5	Golgin candidate like	3.00	3	3.93	3.93	2
1204	A0A2R6Q8H8	Beta-adaptin-like protein	13.25	21	16.45	24.92	4
1205	A0A2R6Q8I6	Serine/arginine repetitive matrix protein like	9.00	13	26.45	36.20	4
1206	A0A2R6Q8J4	6-phosphogluconate dehydrogenase, decarboxylating (Fragment)	8.80	13	24.37	36.08	4
1207	A0A2R6Q8J7	Ubiquitin-conjugating enzyme E2 28	3.80	6	28.11	37.84	4
1208	A0A2R6Q8K1	Puromycin-sensitive aminopeptidase	8.67	12	10.76	14.23	3
1209	A0A2R6Q8M9	Reticulon-like protein	1.00	1	3.25	3.25	2
1210	A0A2R6Q8P3	Luminal-binding protein 5precursor	12.00	18	16.98	25.34	4
1211	A0A2R6Q8Q1	Nucleoside diphosphate kinase	1.00	1	3.26	3.26	1
1212	A0A2R6Q8Q2	Protein YIP	1.00	1	3.36	3.36	3

1213	A0A2R6Q8Q8	Xylose isomerase	5.80	9	14.86	23.16	4
1214	A0A2R6Q8R0	ADP-ribosylation factor	1.00	1	6.04	6.04	2
1215	A0A2R6Q8U5	GDP-L-fucose synthase	3.50	5	15.94	23.75	4
1216	A0A2R6Q8V5	(+)-neomenthol dehydrogenase	1.00	1	2.96	2.96	1
1217	A0A2R6Q8X3	60S ribosomal protein L36	3.00	4	22.42	29.09	3
1218	A0A2R6Q912	Heat shock protein	25.20	40	26.75	39.43	4
1219	A0A2R6Q939	SUMO-conjugating enzyme UBC9	3.80	6	28.11	37.84	4
1220	A0A2R6Q948	Pyruvate kinase	1.00	1	1.93	1.93	1
1221	A0A2R6Q983	Protein BOBBER like	3.20	5	12.62	19.66	4
1222	A0A2R6Q985	Dipeptidyl aminopeptidase	2.00	2	2.71	2.71	2
1223	A0A2R6Q988	Importin subunit beta-1 like	3.00	3	10.70	10.70	1
1224	A0A2R6Q996	Oligopeptide transporter like	1.50	2	1.64	2.18	4
1225	A0A2R6Q9A3	Vacuolar protein sorting-associated protein like (Fragment)	2.00	2	9.84	9.84	1
1226	A0A2R6Q9D7	60S ribosomal protein	9.80	11	52.16	55.15	4
1227	A0A2R6Q9F2	60S ribosomal protein L13	8.00	11	39.90	50.72	4
1228	A0A2R6Q9G0	ADP-ribosylation factor like	1.00	1	8.29	8.29	1
1229	A0A2R6Q9G1	Protein EXPORTIN 1A like	7.67	12	9.06	14.19	3
1230	A0A2R6Q9H7	TOM1-like protein	1.00	1	3.03	3.03	3
1231	A0A2R6Q9I3	Binding partner of like (Fragment)	1.25	2	6.03	9.88	4
1232	A0A2R6Q9I4	TOM1-like protein	1.00	1	3.06	3.06	3
1233	A0A2R6Q9I9	Binding partner of like (Fragment)	1.00	1	5.53	5.53	2
1234	A0A2R6Q9J8	Protein EXORDIUM like	2.40	3	8.16	10.20	4
1235	A0A2R6Q9L5	Alanine--tRNA ligase	21.60	33	23.85	35.89	4
1236	A0A2R6Q9N1	FAD synthase	1.50	2	2.34	3.13	4
1237	A0A2R6Q9P3	Serine/threonine protein phosphatase 2A regulatory subunit	3.00	3	6.30	6.30	2
1238	A0A2R6Q9S4	WEB family protein	13.75	18	23.79	30.21	4
1239	A0A2R6Q9T6	Heterogeneous nuclear ribonucleoprotein like	1.00	1	3.46	3.46	2
1240	A0A2R6Q9U5	Fumarylacetoacetase	1.00	1	3.74	3.74	3
1241	A0A2R6Q9V5	Rho GDP-dissociation inhibitor like	4.60	6	19.92	24.90	4
1242	A0A2R6Q9V7	Malonyl-CoA decarboxylase	1.50	2	3.30	4.47	2
1243	A0A2R6Q9X5	Patatin	1.33	2	0.95	1.42	3
1244	A0A2R6Q9Y6	Protein translation factor SUI1	1.00	1	11.50	11.50	2
1245	A0A2R6Q9Z0	Adenosine deaminase-like protein	1.00	1	2.98	2.98	2
1246	A0A2R6QA19	NAD(P)H dehydrogenase (quinone)	2.00	3	11.57	17.73	2
1247	A0A2R6QA48	VHS domain-containing protein	1.00	1	0.59	0.59	2
1248	A0A2R6QAA0	Ras-related protein like	8.50	10	39.22	44.04	4
1249	A0A2R6QAC7	Alpha,alpha-trehalose-phosphate synthase	18.80	29	29.66	45.27	4
1250	A0A2R6QAF3	Cyclic phosphodiesterase	1.00	1	6.01	6.01	3
1251	A0A2R6QAG7	Calcyclin-binding protein	3.67	5	15.85	18.39	3
1252	A0A2R6QAG8	Prefoldin subunit like	1.00	1	8.46	8.46	3
1253	A0A2R6QAH6	40S ribosomal protein like (Fragment)	6.33	8	33.78	39.60	3
1254	A0A2R6QAI7	UDP-arabinose 4-epimerase	2.75	4	7.53	11.24	4

1255	A0A2R6QAI8	Pyruvate dehydrogenase E1 component subunit beta	1.60	3	3.74	6.98	4
1256	A0A2R6QAJ3	60S ribosomal protein L18a	6.60	9	36.41	50.00	4
1257	A0A2R6QAJ9	Receptor-like protein kinase	1.00	1	1.38	1.38	1
1258	A0A2R6QAK0	Obg-like ATPase 1	11.00	14	32.68	43.40	4
1259	A0A2R6QAL2	Serine/threonine-protein phosphatase 6 regulatory subunit like	2.00	2	3.33	3.33	3
1260	A0A2R6QAM0	Coatomer subunit epsilon	5.00	6	30.19	36.33	4
1261	A0A2R6QAM5	Ubiquitinyl hydrolase 1	1.67	2	18.03	23.77	3
1262	A0A2R6QAN0	CSC1-like protein	5.00	7	5.94	8.29	2
1263	A0A2R6QAN8	DNA double-strand break repair Rad50 ATPase	9.00	13	30.32	39.05	4
1264	A0A2R6QAP5	Proteasome subunit alpha type	14.20	21	57.19	69.48	4
1265	A0A2R6QAQ3	Diphosphomevalonate decarboxylase	3.33	4	7.21	8.55	3
1266	A0A2R6QAQ6	Uricase	2.00	3	7.38	11.07	3
1267	A0A2R6QAQ7	Exocyst subunit Exo70 family protein	2.00	2	3.35	3.35	2
1268	A0A2R6QAR0	AMMECR1 protein	1.00	1	4.24	4.24	1
1269	A0A2R6QAR6	Myosin-9 like (Fragment)	18.80	32	16.32	25.78	4
1270	A0A2R6QAR7	Copper transport protein like	1.00	1	13.83	13.83	4
1271	A0A2R6QAS3	Ubiquitinyl hydrolase 1	12.00	14	18.66	20.38	3
1272	A0A2R6QAU3	Peroxygenase	1.00	1	5.31	5.31	2
1273	A0A2R6QAU6	Arabinose 5-phosphate isomerase	2.00	3	4.90	7.35	3
1274	A0A2R6QAV0	Serine/threonine protein phosphatase 2A regulatory subunit B''gamma like	10.75	19	21.20	35.06	4
1275	A0A2R6QAV2	Nascent polypeptide-associated complex subunit beta	1.33	2	10.90	16.35	3
1276	A0A2R6QAV5	UDP-arabinopyranose mutase	7.00	13	20.88	38.64	4
1277	A0A2R6QAX7	Nascent polypeptide-associated complex subunit beta	1.33	2	10.90	16.35	3
1278	A0A2R6QAX8	V-type proton ATPase subunit	1.00	1	3.13	3.13	2
1279	A0A2R6QAY2	Serine/threonine protein phosphatase 2A regulatory subunit	5.00	5	9.84	9.84	1
1280	A0A2R6QAY9	Uncharacterized protein	5.20	8	20.26	30.32	4
1281	A0A2R6QB13	Ras-related protein	2.00	2	11.00	11.00	1
1282	A0A2R6QB23	Ubiquitin-like protein 5	2.00	2	24.66	24.66	2
1283	A0A2R6QB40	Inorganic diphosphatase	38.20	62	70.88	80.65	4
1284	A0A2R6QBP7	Patellin-4 like	18.20	27	35.58	48.32	4
1285	A0A2R6QBR0	NEDD8-like protein	8.67	9	46.79	46.79	3
1286	A0A2R6QBS4	Protein like	4.75	6	19.79	25.44	4
1287	A0A2R6QBS5	Elongation factor (Fragment)	56.20	80	60.10	71.62	4
1288	A0A2R6QBU4	Vesicle-fusing ATPase	2.50	4	4.14	6.78	2
1289	A0A2R6QBU7	60S ribosomal protein L27	3.00	5	23.56	38.52	4
1290	A0A2R6QBX0	Anamorsin like (Fragment)	1.00	1	5.45	5.46	2
1291	A0A2R6QBX7	60S ribosomal protein like (Fragment)	6.00	7	31.05	33.70	4
1292	A0A2R6QBZ3	Acetohydroxy-acid reductoisomerase	1.67	2	3.72	4.50	3
1293	A0A2R6QBZ4	Ubiquitin-conjugating enzyme E2 36	4.25	6	37.09	54.90	4
1294	A0A2R6QC06	Ras-related protein RABA1f	11.40	14	50.78	57.14	4
1295	A0A2R6QC08	Cysteine protease	10.20	15	32.38	39.54	4
1296	A0A2R6QC35	26S proteasome non-ATPase regulatory subunit 2 homolog	35.40	49	43.95	54.94	4

1297	A0A2R6QC51	Dihydroorotase	1.00	1	2.92	2.92	4
1298	A0A2R6QC74	Clathrin light chain	10.50	14	21.33	25.76	4
1299	A0A2R6QC95	Syntaxin-124 like	2.00	3	8.69	13.03	3
1300	A0A2R6QCC0	60S ribosomal protein L8-3	5.25	8	20.29	28.08	4
1301	A0A2R6QCD2	diacylglycerol kinase	7.00	11	17.54	26.58	4
1302	A0A2R6QCE5	Choline-phosphate cytidylyltransferase	1.50	2	3.90	5.20	2
1303	A0A2R6QCG0	GlcNAc kinase	1.00	1	3.75	3.75	2
1304	A0A2R6QCI1	Anthocyanidin 3-O-glucoside 2'''-O-xylosyltransferase	1.50	3	3.27	6.55	4
1305	A0A2R6QCI8	Malate dehydrogenase	0.67	1	2.34	3.51	3
1306	A0A2R6QCJ2	Olee1-like protein	4.00	5	29.75	32.50	4
1307	A0A2R6QCJ5	Phosphoglycerate mutase (2,3-diphosphoglycerate-independent)	43.80	60	58.21	62.43	4
1308	A0A2R6QCK2	14-3-3-like protein (Fragment)	4.00	4	13.13	13.13	2
1309	A0A2R6QCK3	Phosphoenolpyruvate carboxylase	35.60	49	40.29	52.23	4
1310	A0A2R6QCK7	Protein DJ-1 B like	4.20	7	12.13	20.05	4
1311	A0A2R6QCM2	Ras-related protein RABB1c	3.00	3	18.01	18.01	1
1312	A0A2R6QCQ9	UDP-4-keto-6-deoxy-D-glucose 3,5-epimerase/UDP-4-keto-L-rhamnose 4-keto-reductase	40.20	57	56.98	68.30	4
1313	A0A2R6QCT0	Pyrophosphate--fructose 6-phosphate 1-phosphotransferase subunit beta	43.40	64	67.64	75.00	4
1314	A0A2R6QCU0	Exopolygalacturonase	30.60	47	56.04	60.40	4
1315	A0A2R6QCV7	Rho GDP-dissociation inhibitor like	4.00	7	13.73	19.44	4
1316	A0A2R6QCX1	Exopolygalacturonase	30.60	47	56.04	60.40	4
1317	A0A2R6QCX5	TBC1 domain family member 2B like	1.67	2	4.17	4.85	3
1318	A0A2R6QCY3	Uridine kinase	6.00	6	12.63	12.63	2
1319	A0A2R6QCZ3	Dynein assembly factor 5, axonemal like	1.75	3	4.50	7.92	4
1320	A0A2R6QCZ8	Enhancer of mRNA-decapping protein	1.00	1	2.91	2.91	3
1321	A0A2R6QD18	Early nodulin-like protein	4.50	5	20.63	21.69	4
1322	A0A2R6QD26	Heat shock protein like (Fragment)	26.60	36	56.30	64.43	4
1323	A0A2R6QD56	UPF0664 stress-induced protein like	2.00	3	10.78	15.20	4
1324	A0A2R6QD67	Non-specific serine/threonine protein kinase	1.00	1	2.25	2.25	3
1325	A0A2R6QD70	40S ribosomal protein S8	10.60	15	43.65	52.05	4
1326	A0A2R6QD78	Eukaryotic translation initiation factor 4C	2.50	4	17.76	24.83	4
1327	A0A2R6QD80	Rho GDP-dissociation inhibitor like	2.67	4	11.37	17.97	3
1328	A0A2R6QD88	EH domain-containing protein	2.00	2	4.58	4.58	1
1329	A0A2R6QD96	Adenylyltransferase and sulfurtransferase MOCS3	1.00	2	2.38	4.76	4
1330	A0A2R6QDA6	Rab3 GTPase-activating protein catalytic subunit	1.00	1	1.44	1.44	2
1331	A0A2R6QDC3	Polyadenylate-binding protein (Fragment)	2.25	3	6.13	8.42	4
1332	A0A2R6QDH6	ADP-ribosylation factor GTPase-activating protein	1.00	1	2.06	2.06	1
1333	A0A2R6QDI2	Universal stress protein	4.20	7	20.08	31.06	4
1334	A0A2R6QDI4	Universal stress protein	1.50	2	7.76	9.94	2
1335	A0A2R6QDN8	Prolyl-tRNA synthetase	2.00	2	4.51	4.51	1
1336	A0A2R6QDP4	Cullin-1 like	9.00	9	12.04	12.04	1
1337	A0A2R6QDQ0	CTP synthase	3.75	5	7.52	10.32	4
1338	A0A2R6QDR3	Pectinesterase	12.20	19	23.88	34.74	4

1339	A0A2R6QDT4	Inosine-5'-monophosphate dehydrogenase	4.25	6	17.26	24.11	4
1340	A0A2R6QDU1	NAD(P)H dehydrogenase (quinone)	4.00	5	24.31	30.39	4
1341	A0A2R6QE08	Non-specific serine/threonine protein kinase	1.00	1	4.00	4.00	2
1342	A0A2R6QE11	60S ribosomal protein L8	4.75	7	21.06	28.08	4
1343	A0A2R6QE13	Serine/threonine-protein kinase	3.50	6	10.61	18.57	4
1344	A0A2R6QE27	40S ribosomal protein (Fragment)	7.75	13	43.04	56.95	4
1345	A0A2R6QE50	NPL4-like protein	2.67	3	9.74	10.71	3
1346	A0A2R6QE57	60S ribosomal protein L18a	4.00	4	21.63	26.97	2
1347	A0A2R6QEA0	Heterogeneous nuclear ribonucleoprotein like	1.00	1	3.20	3.20	2
1348	A0A2R6QEA8	40S ribosomal protein S24	2.60	3	19.56	21.01	4
1349	A0A2R6QEB7	Acetyl-CoA acetyltransferase	27.40	36	63.87	72.55	4
1350	A0A2R6QEE2	Glycerol-3-phosphate acyltransferase	1.33	2	10.79	16.18	3
1351	A0A2R6QF12	Histidine--tRNA ligase (Fragment)	1.00	1	1.01	1.01	1
1352	A0A2R6QF31	Serine/threonine-protein kinase	5.33	8	6.71	9.43	3
1353	A0A2R6QF35	Calcium-transporting ATPase	1.50	2	2.62	3.49	4
1354	A0A2R6QF39	Coatomer subunit beta	6.00	6	7.48	7.48	1
1355	A0A2R6QF46	V-ATPase 69 kDa subunit	16.80	27	31.89	49.58	4
1356	A0A2R6QF55	D-3-phosphoglycerate dehydrogenase	1.67	3	2.69	5.07	3
1357	A0A2R6QF56	Mitogen-activated protein kinase	1.00	1	2.20	2.20	1
1358	A0A2R6QF64	Plasma membrane ATPase	10.00	10	9.89	9.89	1
1359	A0A2R6QF70	Alanine aminotransferase	2.40	5	6.03	13.05	4
1360	A0A2R6QF74	Proteasome subunit alpha type	16.00	21	66.67	75.95	4
1361	A0A2R6QF75	26S protease regulatory subunit 7	26.40	37	58.03	70.42	4
1362	A0A2R6QF78	60S ribosomal protein like	9.00	11	39.19	41.87	4
1363	A0A2R6QF94	Vesicle transport protein	0.00	0	0.00	0.00	1
1364	A0A2R6QFB0	Pollen receptor-like kinase	1.00	1	1.46	1.46	2
1365	A0A2R6QFC0	Threonine synthase	1.00	1	1.92	1.92	1
1366	A0A2R6QFE0	Eukaryotic initiation factor 4A-11	13.00	13	36.80	36.80	1
1367	A0A2R6QFF5	DEAD-box ATP-dependent RNA helicase	1.00	1	2.19	2.19	1
1368	A0A2R6QFF9	Serine/threonine-protein phosphatase 2A 55 kDa regulatory subunit B	6.00	10	11.90	19.73	4
1369	A0A2R6QFG0	40S ribosomal protein SA	11.00	11	37.37	37.37	3
1370	A0A2R6QFG2	RWD domain-containing protein	1.00	1	4.31	4.31	1
1371	A0A2R6QFG3	60S ribosomal protein like	5.25	7	40.51	51.72	4
1372	A0A2R6QFG5	ESCRT-related protein like	2.33	3	12.38	15.35	3
1373	A0A2R6QFI9	Profilin	7.67	11	37.00	44.51	3
1374	A0A2R6QFJ8	Protein transport protein SEC13 B like	2.00	2	8.88	8.88	2
1375	A0A2R6QFL5	Nucleosome assembly protein like	3.00	4	10.89	14.96	4
1376	A0A2R6QFL7	VHS domain-containing protein	1.00	1	1.69	1.69	2
1377	A0A2R6QFN0	Glutaredoxin-dependent peroxiredoxin	5.60	7	47.65	58.02	4
1378	A0A2R6QFN3	Ras-related protein Rab7	5.80	9	27.54	40.58	4
1379	A0A2R6QFP1	Hydroxyphenylpyruvate reductase	5.40	9	19.36	28.43	4
1380	A0A2R6QFS0	Nuclear pore complex protein like	1.00	1	2.10	2.10	1

1381	A0A2R6QFT0	Heat shock 70 protein	21.00	30	25.45	34.91	4
1382	A0A2R6QFU3	N-alpha-acetyltransferase 15, NatA auxiliary subunit like	7.20	13	8.80	15.47	4
1383	A0A2R6QFU8	GTP-binding nuclear protein (Fragment)	8.00	11	41.00	51.36	4
1384	A0A2R6QFW1	Coatomer subunit beta-2 like (Fragment)	9.40	14	15.81	25.35	4
1385	A0A2R6QG00	Embryo-specific 3 protein	1.00	1	5.70	5.70	4
1386	A0A2R6QG04	Stromal cell-derived factor 2-like protein	1.00	1	5.63	5.63	2
1387	A0A2R6QG25	Glycerol kinase	11.60	17	31.26	47.70	4
1388	A0A2R6QG39	Calnexin like	2.33	3	5.55	7.21	3
1389	A0A2R6QG51	Carbonyl reductase	9.60	15	33.92	46.31	4
1390	A0A2R6QG61	Ribonuclease	26.00	39	28.68	39.78	4
1391	A0A2R6QG72	V-type proton ATPase subunit C	2.25	3	6.75	8.29	4
1392	A0A2R6QG73	Serine/threonine-protein kinase (Fragment)	6.50	10	10.49	15.98	4
1393	A0A2R6QG75	Pyruvate dehydrogenase E1 component subunit beta	1.00	1	2.93	2.93	3
1394	A0A2R6QG86	SWI/SNF complex subunit SWI3A like	1.00	1	1.24	1.24	2
1395	A0A2R6QG91	Dual specificity protein like	1.67	2	2.62	3.20	3
1396	A0A2R6QG96	Diadenosine tetraphosphate synthetase	26.40	35	45.14	55.43	4
1397	A0A2R6QGA0	Tetratricopeptide repeat protein like	1.00	1	2.91	2.91	1
1398	A0A2R6QGC9	60S ribosomal protein like (Fragment)	2.67	3	13.81	15.47	3
1399	A0A2R6QGD3	Citrulline--aspartate ligase	10.00	14	26.49	37.61	4
1400	A0A2R6QGD6	Purple acid phosphatase	4.80	9	8.70	17.15	4
1401	A0A2R6QGE0	Purple acid phosphatase	1.00	1	1.41	1.41	1
1402	A0A2R6QGE3	Aspartyl aminopeptidase	12.20	18	27.25	39.13	4
1403	A0A2R6QGE6	SNF1-related protein kinase regulatory subunit gamma-1 like	3.40	5	9.84	14.59	4
1404	A0A2R6QGF0	Spastin like	3.75	6	4.39	7.01	4
1405	A0A2R6QGG3	Glyceraldehyde-3-phosphate dehydrogenase	31.80	45	65.62	75.44	4
1406	A0A2R6QGH1	Adenosylhomocysteinase	9.00	9	22.39	22.39	1
1407	A0A2R6QGI4	Programmed cell death protein	5.00	5	8.63	8.63	1
1408	A0A2R6QGK4	AP-1 complex subunit mu-2 like	7.80	14	22.38	40.65	4
1409	A0A2R6QGK6	DEAD-box ATP-dependent RNA helicase	2.00	2	3.18	3.18	1
1410	A0A2R6QGP9	T-complex protein 1 subunit gamma	25.00	34	45.88	56.02	4
1411	A0A2R6QGS0	Betaine aldehyde dehydrogenase	7.00	10	18.62	28.32	4
1412	A0A2R6QGT3	Peroxidase	6.60	9	28.84	37.09	4
1413	A0A2R6QGU9	TNF receptor-associated factor like	3.00	3	7.63	7.63	2
1414	A0A2R6QGV5	Transportin like	1.00	1	1.54	1.54	2
1415	A0A2R6QGW4	40S ribosomal protein like	8.00	10	36.21	43.93	4
1416	A0A2R6QGX1	Plasma membrane ATPase	11.33	13	14.77	17.09	3
1417	A0A2R6QGX9	DnaJ subfamily B member like	1.00	1	3.05	3.05	1
1418	A0A2R6QGY5	Pectate lyase	1.40	2	4.14	6.98	4
1419	A0A2R6QGY8	Hypersensitive-induced response protein	1.00	1	4.22	4.23	2
1420	A0A2R6QH09	Methyltransferase	1.67	2	3.20	3.74	3
1421	A0A2R6QH14	NAP1-related protein	1.00	1	4.12	4.12	1
1422	A0A2R6QH16	60S ribosomal protein	2.60	3	20.17	22.50	4

1423	A0A2R6QH18	Protein DCL like	1.00	1	4.78	4.78	3
1424	A0A2R6QH20	Malate dehydrogenase	3.20	5	8.74	13.35	4
1425	A0A2R6QH43	LON peptidase N-terminal domain and RING finger protein	1.00	1	1.86	1.86	2
1426	A0A2R6QH58	Non-specific serine/threonine protein kinase	2.00	2	4.07	4.56	2
1427	A0A2R6QH63	Receptor-like protein kinase	1.00	1	1.39	1.39	1
1428	A0A2R6QH88	Glycerophosphodiester phosphodiesterase	2.75	3	10.36	11.00	4
1429	A0A2R6QHB2	40S ribosomal protein like	6.00	7	40.14	46.53	4
1430	A0A2R6QHD6	Protein argonaute 1B like	2.25	4	2.18	3.90	4
1431	A0A2R6QHF8	Annexin	1.00	1	3.48	3.48	2
1432	A0A2R6QHG4	UDP-arabinopyranose mutase	22.50	30	51.60	62.12	4
1433	A0A2R6QHH9	TPR repeat-containing thioredoxin TDX like	1.00	1	2.41	2.41	1
1434	A0A2R6QHJ3	VAMP-like protein	2.75	4	15.62	23.50	4
1435	A0A2R6QHK0	AAI domain-containing protein	3.60	5	29.22	40.41	4
1436	A0A2R6QHN1	Serine/threonine protein kinase	1.00	1	0.78	0.78	2
1437	A0A2R6QHN4	60S ribosomal protein like	4.60	6	42.74	49.19	4
1438	A0A2R6QHP0	Eukaryotic translation initiation factor 5A	8.33	9	54.79	55.62	3
1439	A0A2R6QHR2	Transmembrane 9 superfamily member	2.00	3	3.13	4.69	3
1440	A0A2R6QHS1	UDP-glucuronate decarboxylase	2.00	3	5.57	8.35	3
1441	A0A2R6QHU6	Fructose-bisphosphate aldolase	1.75	2	14.53	16.86	4
1442	A0A2R6QHU7	T-complex protein 1 subunit delta	26.40	35	56.00	67.66	4
1443	A0A2R6QHV0	Hydroxy monocarboxylic acid anion dehydrogenase, HIBADH-type protein (Fragment)	1.33	2	7.51	11.26	3
1444	A0A2R6QHV8	FGGY carbohydrate kinase domain-containing protein	3.75	6	7.89	12.66	4
1445	A0A2R6QHW1	Eukaryotic peptide chain release factor GTP-binding subunit ERF3A like	7.75	11	16.10	23.68	4
1446	A0A2R6QHX7	Tetraspanin-15 like	1.00	1	2.74	2.74	4
1447	A0A2R6QI12	Cellulose synthase-like protein	8.60	17	7.25	13.05	4
1448	A0A2R6QI40	2,3-bisphosphoglycerate-independent phosphoglycerate mutase	5.00	7	40.72	51.61	4
1449	A0A2R6QI79	Transmembrane 9 superfamily member	1.33	2	3.02	4.52	3
1450	A0A2R6QI84	Agmatine deiminase	1.00	1	2.89	2.89	4
1451	A0A2R6QI88	Serine/threonine-protein phosphatase	7.40	12	30.16	50.17	4
1452	A0A2R6QIB5	Protein YIP	1.00	1	3.27	3.27	3
1453	A0A2R6QID5	Trafficking protein particle complex subunit	2.00	3	13.31	19.89	4
1454	A0A2R6QIE5	3,4-dihydroxy-2-butanone kinase	5.00	7	12.12	17.85	4
1455	A0A2R6QIG1	Glutamyl-tRNA synthetase	25.80	39	32.26	45.10	4
1456	A0A2R6QIH5	Protein C2-DOMAIN ABA-RELATED like	3.25	5	18.79	23.64	4
1457	A0A2R6QII0	Nuclear distribution protein like	6.75	11	6.50	10.43	4
1458	A0A2R6QII2	ADP-ribosylation factor	1.00	1	6.04	6.04	2
1459	A0A2R6QII6	Sucrose-phosphate synthase like	8.50	11	13.48	15.98	4
1460	A0A2R6QIK8	L-cysteine desulfhydrase	2.75	4	8.26	11.45	4
1461	A0A2R6QIY3	Nucleoside diphosphate kinase	1.00	1	3.80	3.80	1
1462	A0A2R6QIZ5	26S proteasome non-ATPase regulatory subunit 8 A like	13.00	13	35.36	36.46	3
1463	A0A2R6QJ03	Endoglucanase	3.00	6	6.55	12.62	4
1464	A0A2R6QJ06	Beta-adaptin-like protein	13.25	18	18.12	23.86	4

1465	A0A2R6QJ34	Low-temperature-induced protein	1.67	2	4.73	5.80	3
1466	A0A2R6QJ67	Phosphopyruvate hydratase	7.25	11	15.77	24.26	4
1467	A0A2R6QJ76	Myosin-9 like (Fragment)	26.80	41	28.19	40.34	4
1468	A0A2R6QJ92	Alpha-1,4 glucan phosphorylase	1.33	2	2.52	3.78	3
1469	A0A2R6QJ96	5-methyltetrahydropteroyltriglutamate--homocysteine S-methyltransferase	35.00	45	29.24	30.84	2
1470	A0A2R6QJB2	Peptidyl-prolyl cis-trans isomerase	2.00	3	11.49	17.24	3
1471	A0A2R6QJB8	Pyridoxal 5'-phosphate synthase subunit PDX1.3 like	12.60	15	41.93	45.34	4
1472	A0A2R6QJC3	E1 ubiquitin-activating enzyme	10.33	12	12.99	15.33	3
1473	A0A2R6QJC4	Tubulin beta chain	33.80	51	68.18	77.08	4
1474	A0A2R6QJC5	Asparagine synthetase [glutamine-hydrolyzing]	7.25	11	16.24	21.37	4
1475	A0A2R6QJE3	Sorting nexin 2B like	1.00	1	1.78	1.78	2
1476	A0A2R6QJG1	Ran-binding protein 1 a like	2.00	3	13.18	19.82	4
1477	A0A2R6QJG9	40S ribosomal protein S26 (Fragment)	2.80	3	27.09	29.03	4
1478	A0A2R6QJI6	Ubiquitin carboxyl-terminal hydrolase	3.50	4	11.37	12.87	4
1479	A0A2R6QJJ3	Ubiquitin-conjugating enzyme like	3.80	6	28.11	37.84	4
1480	A0A2R6QJP1	60S ribosomal protein like	1.80	3	14.89	24.81	4
1481	A0A2R6QJP2	Receptor-like kinase	1.00	1	1.57	1.57	2
1482	A0A2R6QJP9	Peptidylprolyl isomerase	10.20	15	18.03	25.18	4
1483	A0A2R6QJR4	Wound-induced basic protein	1.00	1	23.40	23.40	4
1484	A0A2R6QJS0	40S ribosomal protein S8	5.00	5	26.48	26.48	1
1485	A0A2R6QJT2	Regulator of nonsense transcripts like	1.00	1	0.79	0.79	2
1486	A0A2R6QJV8	Hyaluronan/mRNA-binding protein	1.00	1	2.30	2.30	2
1487	A0A2R6QJW9	Ras-related protein like	8.80	12	49.66	69.46	4
1488	A0A2R6QJZ3	Adenine phosphoribosyltransferase	1.50	2	10.72	13.19	2
1489	A0A2R6QK08	Transaldolase	1.00	1	2.78	2.78	2
1490	A0A2R6QK30	Hsp70-Hsp90 organizing protein	17.20	28	33.27	52.53	4
1491	A0A2R6QK62	UDP-glucose 4-epimerase	9.25	11	30.53	36.21	4
1492	A0A2R6QK70	Plant intracellular Ras-group-related LRR protein	1.00	1	1.54	1.54	1
1493	A0A2R6QK77	DnaJ subfamily B member like	5.75	8	22.19	31.66	4
1494	A0A2R6QKA6	LIMR family protein	2.00	2	4.11	4.11	2
1495	A0A2R6QKB7	Delta-1-pyrroline-5-carboxylate synthase	9.25	13	15.64	22.02	4
1496	A0A2R6QKB8	3'(2'),5'-bisphosphate nucleotidase	1.50	2	4.70	6.97	2
1497	A0A2R6QKD3	Aldo-keto reductase family 4 member like	13.60	20	46.86	62.86	4
1498	A0A2R6QKE0	Oxysterol-binding protein-related protein like	1.00	1	1.78	1.78	3
1499	A0A2R6QKE2	ADP-ribosylation factor GTPase-activating protein	3.25	4	6.67	8.31	4
1500	A0A2R6QKF0	Mediator of RNA polymerase II transcription subunit 37e	48.00	67	63.02	76.12	4
1501	A0A2R6QKF5	Inorganic diphosphatase	35.00	44	40.74	49.54	2
1502	A0A2R6QKH4	Peptidyl-prolyl cis-trans isomerase	1.67	2	8.38	9.95	3
1503	A0A2R6QKI6	Nudix hydrolase	3.60	6	25.23	44.32	4
1504	A0A2R6QKL9	Disease resistance RPP13-like protein	1.00	1	0.90	0.90	4
1505	A0A2R6QKN4	Glutamine--fructose-6-phosphate transaminase (isomerizing)	7.75	11	13.35	19.76	4
1506	A0A2R6QKN8	Protein transport protein SEC31 B like	17.75	22	17.55	20.84	4

1507	A0A2R6QKP2	Serine carboxypeptidase-like (Fragment)	1.00	1	4.17	4.17	3
1508	A0A2R6QKP6	Carboxypeptidase	1.67	2	3.43	4.03	3
1509	A0A2R6QKS5	Thaumatin-like protein	2.80	4	14.87	19.33	4
1510	A0A2R6QKT9	Clustered mitochondria protein homolog	1.00	1	0.92	0.92	2
1511	A0A2R6QKW8	Serine/threonine-protein phosphatase	8.25	11	31.07	35.78	4
1512	A0A2R6QKZ6	Protein transport protein SEC23	2.00	3	3.85	5.77	3
1513	A0A2R6QL16	Adenylate kinase (Fragment)	17.80	25	75.65	85.99	4
1514	A0A2R6QL23	Eukaryotic translation initiation factor 4G like	1.00	1	0.70	0.70	2
1515	A0A2R6QL71	Sucrose nonfermenting 4-like protein	1.00	1	1.66	1.66	1
1516	A0A2R6QL91	Mevalonate kinase	1.00	1	2.33	2.33	2
1517	A0A2R6QLA6	Protein BONZAI like	1.00	1	2.06	2.06	2
1518	A0A2R6QLF6	Eukaryotic translation initiation factor 3 subunit D	4.33	7	9.86	17.16	3
1519	A0A2R6QLG0	Monothiol glutaredoxin-S17 like (Fragment)	1.33	2	3.83	5.75	3
1520	A0A2R6QLK2	Quinone oxidoreductase	3.00	4	12.10	15.69	3
1521	A0A2R6QLL2	ADP-ribosylation factor GTPase-activating protein AGD5	1.00	1	1.68	1.68	1
1522	A0A2R6QLM3	Sugar carrier protein like	1.00	1	1.34	1.34	2
1523	A0A2R6QLN7	Universal stress protein	4.60	8	19.83	30.58	4
1524	A0A2R6QLN9	Heat shock 70 protein (Fragment)	1.50	2	8.21	10.95	2
1525	A0A2R6QLS3	Protein translation factor like	1.00	1	11.40	11.40	2
1526	A0A2R6QLT1	Heat shock 70 protein	9.25	13	20.76	26.43	4
1527	A0A2R6QLV2	Aspartic proteinase	2.67	3	7.33	7.98	3
1528	A0A2R6QLZ2	Heterogeneous nuclear ribonucleoprotein like	1.00	1	3.38	3.38	2
1529	A0A2R6QM19	Subtilisin-like protease	8.00	11	14.85	20.37	4
1530	A0A2R6QMB9	CTP synthase	1.67	2	3.04	3.85	3
1531	A0A2R6QMD5	Proteasome subunit alpha type	14.00	20	60.87	71.15	4
1532	A0A2R6QME1	UDP-N-acetylglucosamine diphosphorylase	5.00	8	12.12	19.35	4
1533	A0A2R6QME7	Serine/threonine-protein kinase	1.00	1	0.61	0.61	1
1534	A0A2R6QMF6	60S ribosomal protein like	8.00	10	35.45	44.64	4
1535	A0A2R6QMG4	60S ribosomal protein like	7.00	7	29.18	29.18	1
1536	A0A2R6QMK1	DEAD-box ATP-dependent RNA helicase 15 (Fragment)	1.50	2	2.94	4.00	2
1537	A0A2R6QML0	DNA/RNA-binding protein Alba-like protein	4.00	4	27.95	28.35	2
1538	A0A2R6QMM0	Clathrin assembly protein	1.00	1	1.23	1.23	2
1539	A0A2R6QMN0	40S ribosomal protein	4.40	7	28.18	38.99	4
1540	A0A2R6QMN1	Sucrose-phosphate synthase	9.50	13	7.82	10.20	4
1541	A0A2R6QMN6	40S ribosomal protein	5.00	5	32.70	32.70	2
1542	A0A2R6QMQ3	Uncharacterized protein	2.33	3	13.87	17.84	3
1543	A0A2R6QMS4	Luminal-binding proteinprecursor	11.00	13	15.59	18.95	3
1544	A0A2R6QMT0	UPF0160 protein	1.00	1	2.72	2.72	2
1545	A0A2R6QMT3	26S proteasome non-ATPase regulatory subunit 8 A like	6.00	7	23.22	26.59	3
1546	A0A2R6QMU9	Plant UBX domain-containing protein	2.00	3	4.26	6.61	4
1547	A0A2R6QMV6	UDP-N-acetylglucosamine--peptide N-acetylglucosaminyltransferase	1.67	2	2.87	3.48	3
1548	A0A2R6QMW9	Ubiquitin carboxyl-terminal hydrolase	2.00	3	3.13	4.69	3

1549	A0A2R6QMX2	Endoglucanase	1.00	1	2.62	2.62	2
1550	A0A2R6QMX7	Inorganic diphosphatase	33.40	52	72.09	84.65	4
1551	A0A2R6QMY2	Cinnamyl alcohol dehydrogenase	2.67	4	10.14	15.21	3
1552	A0A2R6QMY5	Methyltransferase	2.80	6	5.77	12.44	4
1553	A0A2R6QN14	Endoglucanase	1.00	1	1.92	1.92	2
1554	A0A2R6QN17	Nucleoside diphosphate kinase	1.00	1	3.80	3.80	1
1555	A0A2R6QN19	UDP-glucose 4-epimerase	10.60	15	45.65	65.13	4
1556	A0A2R6QN30	Ubiquitin-conjugating enzyme like	3.80	6	28.11	37.84	4
1557	A0A2R6QN62	Reticulon-like protein	1.00	1	3.36	3.36	2
1558	A0A2R6QN69	G2-specific protein kinase	12.80	20	31.96	45.16	4
1559	A0A2R6QN70	40S ribosomal protein like (Fragment)	2.00	2	13.56	13.56	1
1560	A0A2R6QN93	Puromycin-sensitive aminopeptidase	13.25	20	17.68	25.43	4
1561	A0A2R6QN98	Golgin candidate like	3.00	3	3.92	3.92	2
1562	A0A2R6QNA6	Glutamine amidotransferase	10.25	13	21.63	28.09	4
1563	A0A2R6QNB3	Tubulin beta chain	31.60	47	66.77	77.35	4
1564	A0A2R6QND5	60S ribosomal protein	3.40	4	21.84	25.15	4
1565	A0A2R6QNE5	Sugar transport protein	9.40	18	9.83	11.61	4
1566	A0A2R6QNF0	3-hydroxy-3-methylglutaryl coenzyme A synthase	13.60	18	26.20	31.21	4
1567	A0A2R6QNI0	Bifunctional dTDP-4-dehydrorhamnose 3,5-epimerase/dTDP-4-dehydrorhamnose reductase	21.40	31	65.35	73.58	4
1568	A0A2R6QNK9	FAM10 family protein	7.80	12	17.54	24.88	4
1569	A0A2R6QNM0	Adenine phosphoribosyltransferase	1.00	1	8.24	8.24	2
1570	A0A2R6QNS1	Ubiquitin carboxyl-terminal hydrolase	3.00	5	18.11	27.16	4
1571	A0A2R6QNV5	Haloacid dehalogenase-like hydrolase domain-containing protein Sgpp	2.75	3	16.13	17.13	4
1572	A0A2R6QNW3	Phosphoacetylglucosamine mutase	1.67	2	3.49	4.11	3
1573	A0A2R6QNW4	Regulator of nonsense transcripts like	1.00	1	0.79	0.79	2
1574	A0A2R6QNY2	AP-2 complex subunit mu	3.80	7	7.99	12.99	4
1575	A0A2R6QNY8	Gamma-glutamylcyclotransferase family protein	3.00	4	15.71	21.99	4
1576	A0A2R6QNZ0	Acetylornithine deacetylase	3.60	7	10.09	20.32	4
1577	A0A2R6QP01	Pyruvate dehydrogenase E1 component subunit alpha	0.67	1	2.14	3.21	3
1578	A0A2R6QP08	RNA-binding protein like	1.00	1	4.21	4.21	2
1579	A0A2R6QP24	Alkaline/neutral invertase	13.00	18	23.20	31.90	4
1580	A0A2R6QP25	60S ribosomal protein	4.80	7	35.39	51.28	4
1581	A0A2R6QP32	40S ribosomal protein like (Fragment)	3.67	5	24.05	35.44	3
1582	A0A2R6QP59	DEAD-box ATP-dependent RNA helicase	2.00	2	5.07	5.07	2
1583	A0A2R6QP66	LIM domain-containing protein	6.25	8	32.59	41.79	4
1584	A0A2R6QP72	Digalactosyldiacylglycerol synthase	0.67	1	1.43	2.14	3
1585	A0A2R6QP80	ATPase	1.25	2	4.17	6.94	4
1586	A0A2R6QP81	Phospholipase D	2.00	2	2.57	2.57	2
1587	A0A2R6QP91	Non-specific serine/threonine protein kinase	1.00	1	1.90	1.90	3
1588	A0A2R6QPC7	Serine/threonine-protein kinase	8.75	15	11.39	18.32	4
1589	A0A2R6QPD1	Aspartate--tRNA ligase	20.20	27	41.15	52.70	4
1590	A0A2R6QPD9	Binding partner of like (Fragment)	1.67	2	5.62	6.81	3

1591	A0A2R6QPG3	Proteasome subunit beta	14.60	21	67.17	74.89	4
1592	A0A2R6QPG8	Inositol-tetrakisphosphate 1-kinase	2.00	3	5.23	7.71	2
1593	A0A2R6QPI7	CCT-alpha	25.00	31	54.18	65.02	4
1594	A0A2R6QPJ6	COP9 signalosome complex subunit 7 like	1.00	1	4.45	4.45	1
1595	A0A2R6QPJ9	Ras-related protein like	4.50	5	20.69	22.66	2
1596	A0A2R6QPK6	Hyaluronan/mRNA-binding protein	1.00	1	2.51	2.51	2
1597	A0A2R6QPN7	Vacuolar protein sorting-associated protein like (Fragment)	2.50	4	11.25	17.67	4
1598	A0A2R6QPN8	60S ribosomal protein L37a-1 (Fragment)	2.80	5	31.21	51.65	4
1599	A0A2R6QPP3	Nucleoside diphosphate kinase	8.20	10	50.54	56.08	4
1600	A0A2R6QPS0	60S ribosomal protein	8.00	9	41.58	48.97	3
1601	A0A2R6QPS7	Protein EXPORTIN 1A like	5.50	6	5.48	5.66	2
1602	A0A2R6QPT0	Nascent polypeptide-associated complex subunit alpha-like protein	2.60	4	13.78	18.66	4
1603	A0A2R6QPU1	Adenylate kinase (Fragment)	6.50	7	28.62	30.92	4
1604	A0A2R6QPV1	Ras-related protein RABH1b	7.75	9	40.63	48.08	4
1605	A0A2R6QPW7	Eukaryotic translation initiation factor 3 subunit B	16.20	25	28.15	44.66	4
1606	A0A2R6QQ33	N-alpha-acetyltransferase	1.50	2	9.90	13.02	4
1607	A0A2R6QQ45	Alkaline/neutral invertase	18.80	24	32.19	38.54	4
1608	A0A2R6QQ51	Eukaryotic translation initiation factor 4E-1 like	1.00	1	7.47	7.47	2
1609	A0A2R6QQ60	Glycine-rich protein	2.50	3	20.68	23.64	4
1610	A0A2R6QQ71	Triosephosphate isomerase	3.50	4	11.70	13.56	2
1611	A0A2R6QQA4	Ubiquitin-conjugating enzyme E2 28	1.00	1	7.43	7.43	1
1612	A0A2R6QQA8	Beta-galactosidase	8.00	14	11.80	19.47	4
1613	A0A2R6QQA9	SKP1-like protein	1.00	1	8.44	8.44	2
1614	A0A2R6QQB4	26S proteasome non-ATPase regulatory subunit 3 like	25.40	32	56.39	69.40	4
1615	A0A2R6QQC2	Calcium-dependent protein kinase	1.50	2	5.30	6.55	2
1616	A0A2R6QQC3	Vacuolar proton pump subunit B	13.40	18	31.84	41.39	4
1617	A0A2R6QQE5	Calcium-dependent protein kinase	1.00	1	4.77	4.77	2
1618	A0A2R6QQG8	Calcium-dependent protein kinase	4.75	8	11.04	16.31	4
1619	A0A2R6QQH5	Receptor protein kinase	1.00	1	1.46	1.46	2
1620	A0A2R6QQI7	Eukaryotic initiation factor 4A-3	5.33	7	9.88	13.73	3
1621	A0A2R6QQJ3	DUF89 domain-containing protein	1.33	2	3.09	4.63	3
1622	A0A2R6QQJ4	Binding partner of like (Fragment)	5.00	8	17.70	28.75	4
1623	A0A2R6QQK0	60S ribosomal protein L44 (Fragment)	2.20	3	13.66	16.35	4
1624	A0A2R6QQK4	Thioredoxin domain-containing protein	1.50	2	6.14	8.77	4
1625	A0A2R6QQP9	ATP synthase subunit beta	1.00	1	1.99	1.99	2
1626	A0A2R6QQQ6	Fructose-bisphosphate aldolase	4.50	9	13.79	26.80	4
1627	A0A2R6QQR6	26S proteasome non-ATPase regulatory subunit like	24.20	35	58.20	73.29	4
1628	A0A2R6QQU7	14-3-3-like protein GF14 iota (Fragment)	22.00	29	64.88	67.44	4
1629	A0A2R6QQV1	Proteasome assembly chaperone like	1.50	2	5.83	7.78	4
1630	A0A2R6QQX8	Cullin-3B like	2.00	2	5.42	5.42	2
1631	A0A2R6QQZ4	Tetratricopeptide repeat protein 38	1.75	2	3.79	4.48	4
1632	A0A2R6QR02	Cullin-3A like	4.00	4	5.72	5.72	2

1633	A0A2R6QR04	40S ribosomal protein like	7.25	10	30.33	46.19	4
1634	A0A2R6QR07	Glutathione S-transferase	8.00	11	37.01	45.30	4
1635	A0A2R6QR10	Serine/threonine-protein phosphatase	7.75	12	33.17	49.67	4
1636	A0A2R6QR17	Glutathione S-transferase like (Fragment)	1.00	1	8.05	8.05	2
1637	A0A2R6QR24	Spermidine synthase	1.00	1	3.79	3.79	4
1638	A0A2R6QR26	Protein LSM12 A like	1.00	1	5.49	5.49	1
1639	A0A2R6QR27	Uncharacterized protein	1.00	1	4.28	4.28	1
1640	A0A2R6QR42	Carbonic anhydrase	18.40	22	79.52	86.11	4
1641	A0A2R6QR46	ATP citrate synthase	13.20	19	36.17	46.57	4
1642	A0A2R6QR47	ADP-ribosylation factor	10.33	15	58.94	63.54	6
1643	A0A2R6QR59	AP-1 complex subunit gamma	11.25	18	14.71	20.87	4
1644	A0A2R6QR84	CCT-epsilon	21.25	28	42.80	56.07	4
1645	A0A2R6QRA1	Serine/threonine protein phosphatase 2A regulatory subunit	2.00	2	3.51	3.51	2
1646	A0A2R6QRA8	Eukaryotic translation initiation factor 4B2 like	2.00	3	3.75	5.62	3
1647	A0A2R6QRC7	60S ribosomal protein like (Fragment)	3.20	4	19.89	26.26	4
1648	A0A2R6QRF1	Exocyst subunit Exo70 family protein	5.75	9	11.29	16.69	4
1649	A0A2R6QRF4	Proteasome subunit beta	14.00	16	56.23	56.88	4
1650	A0A2R6QRI2	40S ribosomal protein S27 (Fragment)	3.60	5	40.71	44.71	4
1651	A0A2R6QRJ7	DNA-directed RNA polymerase II subunit like	1.50	2	5.16	6.25	2
1652	A0A2R6QRK3	Adenylyl-sulfate kinase	5.00	6	31.61	40.38	4
1653	A0A2R6QRK6	Glucan endo-1,3-beta-D-glucosidase	4.50	5	12.85	13.95	4
1654	A0A2R6QRK9	CCT-theta	24.40	31	56.77	68.62	4
1655	A0A2R6QRN5	Protein kinase	3.33	5	12.42	18.36	3
1656	A0A2R6QRP8	Activator of heat shock 90 protein like	4.33	6	12.10	17.58	3
1657	A0A2R6QRQ5	Late embryogenesis abundant protein	1.50	2	9.20	11.66	4
1658	A0A2R6QRS5	Serine-threonine kinase receptor-associated protein	2.00	2	6.82	6.82	1
1659	A0A2R6QRT2	GTP-binding nuclear protein (Fragment)	8.00	11	41.00	51.36	4
1660	A0A2R6QRU6	DNA/RNA-binding protein Alba-like protein	6.80	8	45.89	51.16	4
1661	A0A2R6QRW4	HSP20-like chaperone protein	1.00	1	7.64	7.64	1
1662	A0A2R6QRX1	WD repeat-containing protein	3.50	5	2.67	3.81	4
1663	A0A2R6QRY2	Sucrose-phosphate synthase	10.33	13	10.75	12.59	3
1664	A0A2R6QRZ7	Galactinol--sucrose galactosyltransferase	14.00	22	23.90	33.81	4
1665	A0A2R6QS00	Glutamyl-tRNA synthetase	22.40	33	28.80	39.65	4
1666	A0A2R6QS23	Plasma membrane ATPase	20.00	22	19.99	21.09	2
1667	A0A2R6QS36	Trafficking protein particle complex subunit	2.00	2	9.79	9.79	2
1668	A0A2R6QS40	Leucine aminopeptidase	21.80	28	47.57	58.46	4
1669	A0A2R6QS42	VAMP-like protein	2.25	3	11.63	15.50	4
1670	A0A2R6QS52	Eukaryotic translation initiation factor 4G-1 like	2.00	3	2.47	3.70	3
1671	A0A2R6QS57	Eukaryotic translation initiation factor 5A	8.75	9	55.00	55.62	4
1672	A0A2R6QS58	Transmembrane 9 superfamily member	2.00	3	3.15	4.72	3
1673	A0A2R6QS73	COP9 signalosome complex subunit 1 like	7.00	9	17.31	23.08	4
1674	A0A2R6QS83	Transmembrane 9 superfamily member	1.33	2	2.90	4.35	3

1675	A0A2R6QS86	Phospholipase D	1.00	1	1.49	1.49	2
1676	A0A2R6QSA2	Non-specific serine/threonine protein kinase	1.00	1	1.86	1.86	3
1677	A0A2R6QSA9	BEACH domain-containing protein	36.60	56	18.31	27.88	4
1678	A0A2R6QSB1	Inorganic phosphate transporter 1-4 like	3.20	6	7.57	14.88	4
1679	A0A2R6QSC1	P-loop NTPase domain-containing protein	3.25	5	4.60	7.04	4
1680	A0A2R6QSD8	ABC transporter F family member 1 like	6.60	11	12.50	20.67	4
1681	A0A2R6QSD9	Serine/threonine protein phosphatase 2A regulatory subunit B''alpha like	2.00	2	2.82	2.82	1
1682	A0A2R6QSE1	Succinate--CoA ligase [ADP-forming] subunit beta, mitochondrial	1.33	2	3.32	4.98	3
1683	A0A2R6QSE7	Casein kinase 1-like protein	1.00	1	2.64	2.64	3
1684	A0A2R6QSF6	60S ribosomal protein like (Fragment)	6.80	8	48.87	53.38	4
1685	A0A2R6QSG8	Uncharacterized protein	4.00	5	27.37	33.55	4
1686	A0A2R6QSH1	Ribonuclease P protein subunit p25-like protein	1.67	2	4.31	4.94	3
1687	A0A2R6QSH7	S-(hydroxymethyl)glutathione dehydrogenase	11.20	17	42.11	57.52	4
1688	A0A2R6QSJ0	26S proteasome regulatory subunit 4 A like	6.00	6	17.30	17.30	1
1689	A0A2R6QSJ1	60S ribosomal protein like	6.00	6	30.10	30.10	2
1690	A0A2R6QSK5	G3BP-like protein	1.00	1	2.14	2.14	2
1691	A0A2R6QSL0	Peptidylprolyl isomerase	2.00	3	17.45	26.75	4
1692	A0A2R6QSM2	Cytochrome b561 and DOMON domain-containing protein	1.00	1	2.53	2.53	4
1693	A0A2R6QSM3	Peptidylprolyl isomerase	12.50	14	22.38	27.57	4
1694	A0A2R6QSM6	Valyl-tRNA synthetase (Fragment)	10.50	16	11.49	16.87	4
1695	A0A2R6QSN5	Glyoxalase-like domain protein	1.00	1	12.27	12.27	2
1696	A0A2R6QSN6	Cytochrome b561 and DOMON domain-containing protein	1.00	1	4.03	4.03	3
1697	A0A2R6QSP7	60S ribosomal protein like (Fragment)	5.50	7	14.17	17.00	4
1698	A0A2R6QSQ9	Glyoxylate/succinic semialdehyde reductase	4.33	6	19.57	27.65	3
1699	A0A2R6QSR1	60S ribosomal protein L10 (Fragment)	9.20	11	44.63	51.85	4
1700	A0A2R6QSR9	Ubiquitin-conjugating enzyme like	3.80	6	28.11	37.84	4
1701	A0A2R6QSU6	Ran-binding protein 1 a like	1.00	1	3.60	3.60	2
1702	A0A2R6QSW0	ATP-dependent RNA helicase	2.00	2	3.34	3.34	3
1703	A0A2R6QSW5	Proliferating cell nuclear antigen	2.00	3	7.58	10.61	3
1704	A0A2R6QSX4	Tubulin beta chain	32.50	52	66.21	77.70	4
1705	A0A2R6QSX5	Serine/threonine-protein phosphatase	7.40	11	33.41	44.44	4
1706	A0A2R6QSY6	Ras-related protein like	5.00	6	24.23	29.17	3
1707	A0A2R6QT27	UDP-glucuronate decarboxylase	8.25	9	23.33	26.09	4
1708	A0A2R6QT30	Metacaspase-4 subunit p10 like	2.50	3	7.86	10.00	4
1709	A0A2R6QT48	Heat shock protein Hsp90 family protein	48.75	68	47.96	56.08	4
1710	A0A2R6QT50	Calcium-binding protein	2.50	3	11.79	13.54	4
1711	A0A2R6QT53	Farnesyl pyrophosphate synthase	10.60	14	29.36	35.38	4
1712	A0A2R6QT71	Ubiquitin-conjugating enzyme E2 11	1.00	1	7.43	7.43	1
1713	A0A2R6QT75	UDP-D-apiose/UDP-D-xylose synthase	3.50	4	19.05	21.16	2
1714	A0A2R6QT82	L-ascorbate peroxidase	7.20	10	36.08	48.00	4
1715	A0A2R6QT84	Serine/threonine-protein kinase	6.00	6	11.54	12.70	2
1716	A0A2R6QT86	Protein-tyrosine-phosphatase	1.00	1	4.07	4.07	3

1717	A0A2R6QTA5	TBC1 domain family member 2B like	1.67	2	4.19	4.87	3
1718	A0A2R6QTE4	NEDD8-like protein	8.67	9	46.79	46.79	3
1719	A0A2R6QTF1	60S ribosomal protein L27	2.67	4	19.51	28.15	3
1720	A0A2R6QTG2	Aconitate hydratase	9.00	11	13.17	16.33	4
1721	A0A2R6QTG5	Ras-related protein like	6.50	8	30.32	37.96	2
1722	A0A2R6QTI9	Universal stress protein (Fragment)	3.00	4	12.78	18.50	3
1723	A0A2R6QTJ9	Protein translation factor like	1.00	1	11.50	11.50	2
1724	A0A2R6QTL3	GPI-anchored protein	3.20	5	19.15	26.83	4
1725	A0A2R6QTN0	Aminotransferase	13.20	18	39.24	52.62	4
1726	A0A2R6QTN6	60S acidic ribosomal protein like	1.40	2	9.59	14.05	4
1727	A0A2R6QTP0	Adaptin ear-binding coat-associated protein 1 NECAP-1 protein	1.00	1	2.72	2.72	2
1728	A0A2R6QTP3	Importin-5 like	2.00	2	1.58	1.58	1
1729	A0A2R6QTP4	YTH domain-containing family protein	1.00	1	1.29	1.29	2
1730	A0A2R6QTP5	L-ascorbate oxidase	9.40	12	17.73	21.76	4
1731	A0A2R6QTP9	26S proteasome non-ATPase regulatory subunit 2 homolog	28.20	39	34.19	42.83	4
1732	A0A2R6QTQ1	Serine/threonine-protein phosphatase	10.00	14	37.57	48.24	4
1733	A0A2R6QTS2	Selenoprotein O	10.00	14	19.16	26.31	4
1734	A0A2R6QTU2	Formyltetrahydrofolate synthetase	5.25	7	10.26	14.31	4
1735	A0A2R6QTU6	Ubiquitinyl hydrolase 1	8.00	8	7.62	7.62	1
1736	A0A2R6QTV0	Mannan endo-1,4-beta-mannosidase	1.00	1	2.42	2.42	2
1737	A0A2R6QTV4	DEAD-box ATP-dependent RNA helicase	12.80	20	23.40	35.26	4
1738	A0A2R6QTW0	CCT-eta	30.00	43	48.76	61.04	4
1739	A0A2R6QTW2	Hyccin like	1.00	1	3.62	3.62	4
1740	A0A2R6QTW7	60S ribosomal protein	6.00	6	40.71	40.71	1
1741	A0A2R6QTW8	Short-chain dehydrogenase/reductase	1.00	1	2.80	2.80	1
1742	A0A2R6QTX1	Signal recognition particle 9 kDa protein	1.33	2	14.89	22.33	3
1743	A0A2R6QTX5	26S proteasome regulatory subunit 4 A like	8.00	8	43.79	43.79	1
1744	A0A2R6QTY3	Protein transport protein Sec24-like	5.33	8	6.90	10.30	3
1745	A0A2R6QTZ4	Non-specific serine/threonine protein kinase	1.00	1	3.98	3.98	2
1746	A0A2R6QU02	Homocysteine S-methyltransferase	2.00	2	6.92	6.92	3
1747	A0A2R6QU11	N-alpha-acetyltransferase	1.00	1	5.17	5.17	1
1748	A0A2R6QU18	40S ribosomal protein (Fragment)	7.40	8	53.78	56.95	4
1749	A0A2R6QU25	Glutathione peroxidase	1.00	1	5.88	5.88	3
1750	A0A2R6QU47	Endo-1,3 like	1.00	1	6.12	6.12	2
1751	A0A2R6QU62	Cullin-1 like	11.00	15	16.60	22.40	3
1752	A0A2R6QU84	Endo-1,3 like	1.00	1	5.00	5.00	2
1753	A0A2R6QU88	Endoglucanase	1.00	1	2.55	2.55	2
1754	A0A2R6QU90	UDP-glucuronate decarboxylase	4.80	6	10.57	13.50	4
1755	A0A2R6QU98	60S ribosomal protein like (Fragment)	3.80	5	22.80	27.96	4
1756	A0A2R6QUA0	Sucrose synthase	11.60	19	17.34	29.22	4
1757	A0A2R6QUB1	Importin subunit alpha	3.00	4	8.08	10.96	4
1758	A0A2R6QUB2	Lysine--tRNA ligase	19.75	24	35.00	40.17	4

1759	A0A2R6QUE0	Receptor-like protein kinase	1.67	2	2.47	3.02	3
1760	A0A2R6QUG7	ADP-ribosylation factor (Fragment)	9.60	14	45.45	47.78	4
1761	A0A2R6QUJ1	Lysine ketoglutarate reductase	3.00	4	2.80	3.61	4
1762	A0A2R6QUJ2	Brefeldin A-inhibited guanine nucleotide-exchange protein like	10.33	15	6.89	10.03	3
1763	A0A2R6QUL1	Beta-galactosidase	25.40	34	38.10	46.42	4
1764	A0A2R6QUL6	Eukaryotic translation initiation factor 3 subunit K	4.20	6	17.51	26.18	4
1765	A0A2R6QUM0	Proteasome subunit alpha type	14.20	18	54.80	61.38	4
1766	A0A2R6QUN4	Oligouridylate-binding protein like	1.00	1	2.42	2.42	3
1767	A0A2R6QUP2	40S ribosomal protein like	10.80	12	53.78	60.08	4
1768	A0A2R6QUR1	Serine/threonine-protein kinase	2.00	3	3.90	5.94	4
1769	A0A2R6QUS1	Casein kinase 1-like protein	1.67	2	3.75	4.58	3
1770	A0A2R6QUS3	Translation machinery-associated protein 22	1.00	1	4.15	4.15	4
1771	A0A2R6QUU5	Inorganic pyrophosphatase	1.00	1	2.60	2.60	1
1772	A0A2R6QUW1	40S ribosomal protein S30	1.00	1	16.13	16.13	4
1773	A0A2R6QUW5	Vacuolar protein sorting-associated protein	1.00	1	4.61	4.61	1
1774	A0A2R6QUW6	60S ribosomal protein like	1.00	1	17.39	17.39	1
1775	A0A2R6QUW8	Asparagine--tRNA ligase	9.50	13	16.89	22.84	4
1776	A0A2R6QUX8	Profilin	5.60	7	62.26	78.20	4
1777	A0A2R6QUY6	Hexokinase	1.00	1	2.25	2.25	1
1778	A0A2R6QUZ5	Arginyl-tRNA synthetase (Fragment)	23.80	38	43.68	63.31	4
1779	A0A2R6QV19	Protein CfxQ like	3.75	5	10.75	13.99	4
1780	A0A2R6QV46	Serine/threonine protein phosphatase 2A regulatory subunit	1.00	1	2.22	2.22	2
1781	A0A2R6QV55	TBCC domain-containing protein 1	4.75	6	8.86	11.15	4
1782	A0A2R6QV69	Ras-related protein like	2.00	2	9.21	9.21	3
1783	A0A2R6QV87	Guanylate kinase (Fragment)	1.33	2	4.32	6.48	3
1784	A0A2R6QV89	Insulin-degrading enzyme-like 1, peroxisomal	1.50	2	1.78	2.38	4
1785	A0A2R6QV90	40S ribosomal protein like	9.40	13	34.91	42.18	4
1786	A0A2R6QV92	Reticulon-like protein	4.00	4	7.99	7.99	2
1787	A0A2R6QV95	40S ribosomal protein like	9.20	13	34.71	43.12	4
1788	A0A2R6QVA7	Villin-3 like (Fragment)	3.00	3	44.12	44.12	1
1789	A0A2R6QVA9	Calcium-binding protein	1.40	2	5.38	6.91	4
1790	A0A2R6QVB3	Villin-3 like	3.75	5	7.21	9.36	4
1791	A0A2R6QVC6	Calcium-transporting ATPase	1.00	1	1.07	1.07	1
1792	A0A2R6QVI1	Amylomaltase	8.25	13	8.20	12.96	4
1793	A0A2R6QVI5	Exportin-7 like	4.67	7	6.52	10.15	3
1794	A0A2R6QVN2	5-methyltetrahydropteroyltriglutamate--homocysteine S-methyltransferase	70.00	101	64.76	67.97	4
1795	A0A2R6QVQ5	Syntaxin-132 like	0.00	0	0.00	0.00	1
1796	A0A2R6QVR5	Sucrose-phosphatase	9.50	11	29.90	32.82	2
1797	A0A2R6QVS1	Ubiquitinyl hydrolase 1	17.80	26	17.19	22.91	4
1798	A0A2R6QVT3	Ubiquitin carboxyl-terminal hydrolase	1.00	1	1.48	1.48	2
1799	A0A2R6QVU1	UDP-4-keto-6-deoxy-D-glucose 3,5-epimerase/UDP-4-keto-L-rhamnose 4-keto-reductase	35.50	46	50.70	55.70	4
1800	A0A2R6QVU3	Trafficking protein particle complex subunit like	2.00	3	1.63	2.49	4

1801	A0A2R6QVU8	Ubiquitin-conjugating enzyme E2 variant 1D like	4.50	6	33.74	36.99	4
1802	A0A2R6QVY1	Sorting nexin like	2.33	3	5.20	6.68	3
1803	A0A2R6QW07	Ribosomal protein	6.40	9	27.96	35.19	4
1804	A0A2R6QW25	Pleiotropic drug resistance protein	2.50	3	1.98	2.32	2
1805	A0A2R6QW32	Fructose-bisphosphate aldolase	33.20	45	75.03	86.59	4
1806	A0A2R6QW44	40S ribosomal protein (Fragment)	3.00	4	30.80	40.67	4
1807	A0A2R6QW47	Monodehydroascorbate reductase	8.00	14	20.65	36.41	4
1808	A0A2R6QW64	Phosphoenolpyruvate carboxylase	36.60	53	41.01	55.85	4
1809	A0A2R6QW92	60S ribosomal protein L8	6.00	8	23.21	28.08	3
1810	A0A2R6QWF2	Acetyl-CoA acetyltransferase	25.80	34	58.78	66.18	4
1811	A0A2R6QWG2	Ras-related protein RABB1c	5.00	6	31.51	38.39	2
1812	A0A2R6QWG6	Rho GDP-dissociation inhibitor like	3.40	6	12.51	17.28	4
1813	A0A2R6QWH7	Exopolygalacturonase	20.40	29	45.21	51.38	4
1814	A0A2R6QWI0	Fimbrin-5 like	10.25	16	15.92	22.62	4
1815	A0A2R6QWI1	Heterogeneous nuclear ribonucleoprotein like	1.00	1	3.15	3.15	2
1816	A0A2R6QWI5	TBC1 domain family member 2B like	1.67	2	4.16	4.83	3
1817	A0A2R6QWM7	Aconitate hydratase	8.00	13	8.39	13.29	4
1818	A0A2R6QWM8	NEDD8-activating enzyme E1 regulatory subunit	2.00	4	4.98	9.96	4
1819	A0A2R6QWP5	Vesicle-fusing ATPase	2.50	4	5.05	8.28	2
1820	A0A2R6QWS6	Receptor-like protein kinase THESEUS	1.00	1	1.43	1.43	1
1821	A0A2R6QWT9	ADP-ribosylation factor GTPase-activating protein	1.00	1	1.70	1.70	1
1822	A0A2R6QWU0	Trafficking protein particle complex II-specific subunit like	1.50	2	1.31	1.75	2
1823	A0A2R6QWW5	60S ribosomal protein L8	5.20	7	23.46	28.08	4
1824	A0A2R6QWX4	Universal stress protein	3.75	6	17.52	29.06	4
1825	A0A2R6QWX8	Hydrolase	1.00	1	2.80	2.80	1
1826	A0A2R6QWZ8	Tryptophan synthase	1.00	1	3.18	3.18	2
1827	A0A2R6QX03	TBC1 domain family member 15 like	3.75	5	10.20	13.59	4
1828	A0A2R6QX07	NAD(P)H dehydrogenase (quinone)	3.40	4	21.08	25.00	4
1829	A0A2R6QX28	LEA_2 domain-containing protein	1.00	1	5.93	5.93	4
1830	A0A2R6QX42	Clathrin light chain	10.75	15	22.92	28.94	4
1831	A0A2R6QX89	Anamorsin like (Fragment)	1.00	1	5.45	5.46	2
1832	A0A2R6QX93	Protein DJ-1 B like	6.67	9	15.65	21.07	3
1833	A0A2R6QX96	Serine/threonine-protein phosphatase 5	5.00	7	12.78	17.94	4
1834	A0A2R6QXA0	UDP-4-keto-6-deoxy-D-glucose 3,5-epimerase/UDP-4-keto-L-rhamnose 4-keto-reductase	46.00	59	62.42	67.26	4
1835	A0A2R6QXA2	60S ribosomal protein like (Fragment)	6.00	7	31.05	33.70	4
1836	A0A2R6QXA4	Alpha,alpha-trehalose-phosphate synthase	11.50	15	16.10	20.30	4
1837	A0A2R6QXF2	Ras-related protein like	8.00	10	46.34	57.30	2
1838	A0A2R6QXF9	26S proteasome non-ATPase regulatory subunit 2 homolog	30.00	42	36.80	45.46	4
1839	A0A2R6QXI3	Ketol-acid reductoisomerase	3.20	4	5.86	7.29	4
1840	A0A2R6QXJ1	Ubiquitin-conjugating enzyme E2 36	4.25	6	37.09	54.90	4
1841	A0A2R6QXP8	Small nuclear ribonucleoprotein Sm D3	1.50	2	10.60	14.39	4
1842	A0A2R6QXS3	AP complex subunit sigma (Fragment)	1.00	1	5.67	5.67	3

1843	A0A2R6QXS5	EPS15 homologyprotein	1.67	2	1.44	1.70	3
1844	A0A2R6QXT3	Chaperone protein like	1.00	1	7.50	7.50	4
1845	A0A2R6QXU1	Cytosolic purine 5'-nucleotidase like isoform 2	1.50	3	2.65	5.30	4
1846	A0A2R6QXW7	Maf-like protein	2.25	3	12.01	16.02	4
1847	A0A2R6QXX6	Protein WEAK CHLOROPLAST MOVEMENT UNDER BLUE LIGHT 1 like	2.67	4	3.12	4.62	3
1848	A0A2R6QXX7	Cytosolic purine 5'-nucleotidase like isoform 1	1.50	3	2.64	5.29	4
1849	A0A2R6QXY8	26S proteasome regulatory subunit RPN11	13.00	18	50.83	66.03	4
1850	A0A2R6QY00	Polyadenylate-binding protein	4.40	8	10.47	18.72	4
1851	A0A2R6QY05	Actinidain like	4.20	6	10.35	12.00	4
1852	A0A2R6QY14	Polyadenylate-binding protein	10.20	16	16.28	24.24	4
1853	A0A2R6QY36	Actinidain like	5.50	6	9.79	9.79	2
1854	A0A2R6QY57	Tubulin alpha chain	28.00	36	49.37	54.10	3
1855	A0A2R6QY61	HECT-type E3 ubiquitin transferase	27.50	39	8.45	11.28	4
1856	A0A2R6QY77	HECT-type E3 ubiquitin transferase	28.25	39	8.34	11.01	4
1857	A0A2R6QY89	14-3-3-like protein GF14 kappa	5.00	5	19.40	19.40	1
1858	A0A2R6QYA0	Protein NETWORKED 2A like	1.00	1	0.86	0.86	2
1859	A0A2R6QYA6	14-3-3-like protein	23.00	29	67.48	72.14	4
1860	A0A2R6QYB7	14-3-3 protein (Fragment)	4.50	6	18.32	24.89	2
1861	A0A2R6QYC0	Geranylgeranyl transferase type-2 subunit alpha like	1.00	1	1.68	1.68	3
1862	A0A2R6QYD0	AP-4 complex subunit mu like	3.75	6	8.59	13.97	4
1863	A0A2R6QYD4	Rho GTPase-activating protein	7.50	10	10.13	13.81	4
1864	A0A2R6QYD6	Eukaryotic peptide chain release factor subunit 1-3 like	1.00	1	8.94	8.94	1
1865	A0A2R6QYG1	60S ribosomal protein L30	5.67	7	41.66	41.96	3
1866	A0A2R6QYG2	Oxidoreductase, N-terminal protein	2.00	3	7.22	10.83	3
1867	A0A2R6QYH0	Annexin	10.75	15	31.72	43.35	4
1868	A0A2R6QYI3	Alkaline/neutral invertase	12.00	12	23.37	23.37	1
1869	A0A2R6QYJ6	D-fructose-1,6-bisphosphate 1-phosphohydrolase	1.00	1	4.88	4.88	1
1870	A0A2R6QYK1	Phosphopantothenate--cysteine ligase	1.67	2	6.83	7.95	3
1871	A0A2R6QYM5	Ribonuclease P protein subunit p25-like protein	3.40	5	14.70	18.18	4
1872	A0A2R6QYM9	Ras-related protein	3.50	4	17.15	20.00	2
1873	A0A2R6QYR7	Oxysterol-binding protein-related protein like	2.00	2	3.07	3.07	2
1874	A0A2R6QYS8	Proteasome subunit beta (Fragment)	7.67	9	44.88	47.52	3
1875	A0A2R6QYT3	SCY1-like protein	4.00	4	4.87	4.87	2
1876	A0A2R6QYU7	Eukaryotic translation initiation factor 3 subunit I	10.40	14	44.42	61.35	4
1877	A0A2R6QYU8	Methionyl-tRNA synthetase	24.67	28	33.66	38.90	3
1878	A0A2R6QYV1	Methionine aminopeptidase 2	1.00	1	2.05	2.05	1
1879	A0A2R6QYV9	Far upstream element-binding protein like	2.00	3	5.93	8.64	4
1880	A0A2R6QYW1	Aminopeptidase	13.50	15	16.27	17.80	2
1881	A0A2R6QYW5	Carboxylesterase 12	2.50	4	8.79	14.19	4
1882	A0A2R6QYW8	Ran-binding protein 1 c like	1.00	1	3.69	3.69	2
1883	A0A2R6QYZ9	Ribose-phosphate pyrophosphokinase	4.25	7	18.16	30.19	4
1884	A0A2R6QZ07	Neurofilament medium polypeptide like	1.00	1	2.55	2.55	2

1885	A0A2R6QZ19	Pre-mRNA-splicing factor cwc22 like	1.50	2	10.70	14.43	4
1886	A0A2R6QZ25	Acetylxylan esterase A	1.00	1	2.30	2.30	2
1887	A0A2R6QZ29	UDP-4-keto-6-deoxy-D-glucose 3,5-epimerase/UDP-4-keto-L-rhamnose 4-keto-reductase	45.80	67	64.17	75.89	4
1888	A0A2R6QZ32	Glutathione transferase	3.00	3	13.96	13.96	2
1889	A0A2R6QZ36	Serine/threonine-protein phosphatase 5	4.00	5	8.75	11.19	2
1890	A0A2R6QZ39	40S ribosomal protein (Fragment)	8.67	12	32.57	41.44	3
1891	A0A2R6QZ72	Vacuolar-sorting receptor 1 like	15.40	26	30.07	52.30	4
1892	A0A2R6QZ79	Receptor-like protein kinase	1.00	1	1.34	1.34	1
1893	A0A2R6QZ88	Retinal-binding protein	3.25	5	8.58	13.54	4
1894	A0A2R6QZD7	Trafficking protein particle complex II-specific subunit like	1.00	1	0.66	0.66	2
1895	A0A2R6QZG3	26S protease regulatory subunit 8 A	23.00	31	54.18	66.19	4
1896	A0A2R6QZI8	Ribosomal protein L37 (Fragment)	3.83	5	31.91	38.30	6
1897	A0A2R6QZJ0	Serine/threonine protein phosphatase 2A regulatory subunit	2.50	3	5.28	5.98	2
1898	A0A2R6QZJ4	TOM1-like protein	1.00	1	2.18	2.18	3
1899	A0A2R6QZL0	Malic enzyme	14.40	19	29.44	40.24	4
1900	A0A2R6QZM5	Beta-adaptin-like protein	2.00	3	3.32	5.31	4
1901	A0A2R6QZP1	Glucoamylase	1.00	1	5.45	5.45	4
1902	A0A2R6QZP9	DNA/RNA-binding protein Alba-like protein	6.60	8	46.32	54.89	4
1903	A0A2R6QZS8	N-alpha-acetyltransferase 15, NatA auxiliary subunit like	5.25	9	6.46	10.28	4
1904	A0A2R6QZT4	Heat shock 70 protein	17.75	22	33.09	38.86	4
1905	A0A2R6QZT7	Nuclear pore complex protein like	1.00	1	2.10	2.10	1
1906	A0A2R6QZW3	Hydroxyphenylpyruvate reductase	3.00	4	10.97	13.74	3
1907	A0A2R6QZX3	Glutaredoxin-dependent peroxiredoxin	5.60	7	47.65	58.02	4
1908	A0A2R6QZX6	Ribosomal protein L37 (Fragment)	3.00	4	26.24	34.04	3
1909	A0A2R6R005	Protein transport protein SEC13 B like	3.00	3	12.50	12.50	2
1910	A0A2R6R017	Tubulin beta chain	37.80	55	71.47	78.89	4
1911	A0A2R6R027	Ribonuclease P protein subunit p25-like protein	5.20	8	21.32	34.50	4
1912	A0A2R6R043	Malic enzyme	3.80	6	12.84	20.06	4
1913	A0A2R6R057	Prolyl endopeptidase	3.00	5	6.89	11.07	4
1914	A0A2R6R062	ESCRT-related protein like	2.33	3	16.24	20.13	3
1915	A0A2R6R069	Serine/threonine-protein phosphatase 2A 55 kDa regulatory subunit B	6.00	10	11.90	19.73	4
1916	A0A2R6R071	RWD domain-containing protein	1.00	1	4.53	4.53	1
1917	A0A2R6R080	CCT-beta (Fragment)	32.00	43	62.52	70.99	4
1918	A0A2R6R091	Nucleosome assembly protein like	2.00	2	6.86	6.86	2
1919	A0A2R6R095	DEAD-box ATP-dependent RNA helicase	1.00	1	2.21	2.21	1
1920	A0A2R6R097	60S ribosomal protein like	4.20	6	32.00	43.45	4
1921	A0A2R6R0A1	Casein kinase 1-like protein	1.67	2	3.81	4.65	3
1922	A0A2R6R0A2	Serine/threonine-protein kinase	2.00	2	2.55	2.55	1
1923	A0A2R6R0B3	Eukaryotic initiation factor 4A-11	33.50	40	73.49	76.03	4
1924	A0A2R6R0C7	Threonine synthase	1.00	1	1.92	1.92	1
1925	A0A2R6R0F9	Oligouridylate-binding protein like	1.00	1	1.93	1.93	3
1926	A0A2R6R0G5	Vesicle transport protein	0.00	0	0.00	0.00	1

1927	A0A2R6R0H9	Proteasome subunit alpha type	16.00	21	66.67	75.95	4
1928	A0A2R6R0I7	Alanine aminotransferase	2.00	3	13.60	19.90	3
1929	A0A2R6R0J8	Plasma membrane ATPase	7.00	7	7.47	7.47	1
1930	A0A2R6R0K5	Mitogen-activated protein kinase	1.00	1	2.22	2.22	1
1931	A0A2R6R0M1	60S ribosomal protein like	9.40	12	40.65	45.53	4
1932	A0A2R6R0M7	Putative helicase MAGATAMA 3 protein	1.00	1	0.51	0.51	1
1933	A0A2R6R0N0	26S protease regulatory subunit 7B	26.80	37	58.59	70.42	4
1934	A0A2R6R0P6	Sucrose nonfermenting 4-like protein	3.25	5	6.74	10.49	4
1935	A0A2R6R0Q9	Histidine--tRNA ligase	21.80	34	26.29	38.46	4
1936	A0A2R6R0S2	60S ribosomal protein L7a (Fragment)	4.00	4	15.56	15.56	1
1937	A0A2R6R0T0	Translocon-associated protein subunit beta like	1.00	1	8.12	8.12	2
1938	A0A2R6R137	Nascent polypeptide-associated complex subunit alpha-like protein	1.33	2	8.87	13.30	3
1939	A0A2R6R143	Importin subunit alpha	2.00	3	5.42	8.79	2
1940	A0A2R6R148	ABC transporter I family member 20 like	5.25	6	18.39	20.67	4
1941	A0A2R6R153	Non-specific serine/threonine protein kinase	1.00	1	2.21	2.21	3
1942	A0A2R6R177	Proteasome subunit alpha type-4 like	10.75	14	38.10	44.54	4
1943	A0A2R6R1A1	Cullin-associated NEDD8-dissociated protein	18.75	25	18.71	25.06	4
1944	A0A2R6R1A2	Ras-related protein like	5.33	6	27.44	31.16	3
1945	A0A2R6R1A9	Elongation factor 1-gamma 2 like (Fragment)	11.40	17	27.35	36.75	4
1946	A0A2R6R1B2	60S ribosomal protein like	12.00	13	28.54	31.06	2
1947	A0A2R6R1C2	Basic-leucine zipper domain protein	1.00	1	2.92	2.92	2
1948	A0A2R6R1D3	Coatomer subunit delta (Fragment)	7.20	12	11.86	18.56	4
1949	A0A2R6R1F7	Calreticulin like (Fragment)	2.75	5	5.95	10.71	4
1950	A0A2R6R1F9	40S ribosomal protein S24	2.60	3	19.71	21.17	4
1951	A0A2R6R1G1	Guanine deaminase	2.80	5	21.72	38.17	4
1952	A0A2R6R1H1	Cysteine synthase	3.00	3	11.08	11.08	1
1953	A0A2R6R1I4	Coatomer subunit alpha	13.00	24	13.14	24.22	4
1954	A0A2R6R1I9	26S protease regulatory subunit S10B B	18.00	27	49.62	67.92	3
1955	A0A2R6R1J5	Cysteine protease	1.00	1	4.40	4.40	2
1956	A0A2R6R1K7	SNF1-related protein kinase regulatory subunit gamma-1 like	3.00	3	7.24	7.24	2
1957	A0A2R6R1K8	NADP-dependent D-sorbitol-6-phosphate dehydrogenase	1.33	2	5.72	8.74	3
1958	A0A2R6R1K9	Beta-galactosidase	2.20	3	17.95	21.79	4
1959	A0A2R6R1M6	40S ribosomal protein S25 (Fragment)	3.00	3	29.91	29.91	4
1960	A0A2R6R1P0	Adenylyl cyclase-associated protein	6.75	8	13.42	15.51	4
1961	A0A2R6R1P5	Proteasome assembly chaperone 2	1.50	2	7.47	9.25	4
1962	A0A2R6R1Q6	Armadillo repeat-containing protein	5.50	8	12.47	19.26	4
1963	A0A2R6R1R2	Glycine-rich RNA-binding protein	8.40	10	50.82	54.11	4
1964	A0A2R6R1R5	Protein FAM114A2 like	2.00	3	4.27	6.53	4
1965	A0A2R6R1S2	Carboxylesterase 13	1.00	1	6.31	6.31	1
1966	A0A2R6R1T7	DNA-directed RNA polymerases II, IV and V subunit 3 like	1.00	1	4.08	4.08	2
1967	A0A2R6R1V5	LRR receptor-like serine/threonine-protein kinase	1.40	2	2.67	3.82	4
1968	A0A2R6R1V9	UDP-arabinose 4-epimerase	2.00	3	5.14	7.90	2

1969	A0A2R6R1W8	Basic secretory protease	1.00	1	4.46	4.46	3
1970	A0A2R6R1W9	Indole-3-acetic acid-amido synthetase	1.67	2	2.39	3.01	3
1971	A0A2R6R1X0	Thioredoxin domain-containing protein (Fragment)	1.50	2	7.11	8.82	4
1972	A0A2R6R1Y7	Glutamine-dependent NAD(+) synthetase	2.50	4	3.40	6.11	4
1973	A0A2R6R202	Nucleosome assembly protein like (Fragment)	3.40	5	15.72	23.51	4
1974	A0A2R6R225	Hsp70-Hsp90 organizing protein	2.00	2	6.42	6.42	1
1975	A0A2R6R235	Methionyl-tRNA synthetase	26.00	37	41.18	58.50	4
1976	A0A2R6R263	Endoglucanase	1.00	1	2.61	2.61	2
1977	A0A2R6R268	HSP20-like chaperone protein	1.00	1	7.64	7.64	1
1978	A0A2R6R269	Aminopeptidase	23.60	35	28.51	36.63	4
1979	A0A2R6R284	Methionine aminopeptidase 2	2.00	2	4.29	4.29	1
1980	A0A2R6R294	Proline-rich protein	2.00	2	13.51	13.51	2
1981	A0A2R6R299	SCY1-like protein	4.00	4	4.87	4.87	2
1982	A0A2R6R2A0	Eukaryotic translation initiation factor 3 subunit I	11.00	12	41.75	48.04	2
1983	A0A2R6R2A2	HSP20-like chaperone protein	1.00	1	7.64	7.64	1
1984	A0A2R6R2A8	Far upstream element-binding protein like	2.00	3	3.09	4.51	4
1985	A0A2R6R2B9	Tryptophanyl-tRNA synthetase (Fragment)	5.25	7	26.74	34.38	4
1986	A0A2R6R2D4	Alkaline/neutral invertase	22.40	29	44.42	54.53	4
1987	A0A2R6R2F2	AP complex subunit sigma (Fragment)	2.50	3	17.35	21.76	4
1988	A0A2R6R2G8	Flavonol synthase/flavanone 3-hydroxylase	1.00	1	2.96	2.96	2
1989	A0A2R6R2H0	Oxysterol-binding protein-related protein like	2.00	2	3.04	3.04	2
1990	A0A2R6R2J8	Carboxyvinyl-carboxyphosphonate phosphorylmutase	1.00	1	7.60	7.60	3
1991	A0A2R6R2L4	D-fructose-1,6-bisphosphate 1-phosphohydrolase	5.40	9	19.35	30.59	4
1992	A0A2R6R2L5	D-fructose-1,6-bisphosphate 1-phosphohydrolase	5.40	9	18.75	29.63	4
1993	A0A2R6R2L6	Exocyst complex component SEC5	1.33	2	1.18	1.78	3
1994	A0A2R6R2M0	Carboxypeptidase	2.00	4	4.63	9.42	4
1995	A0A2R6R2N7	Polypyrimidine tract-binding protein	2.00	2	7.62	7.62	2
1996	A0A2R6R2N9	Ras-related protein	1.67	2	20.66	23.97	3
1997	A0A2R6R2Q8	Serine decarboxylase	13.80	23	36.23	56.36	4
1998	A0A2R6R2Q9	Ras-related protein like	2.00	2	9.81	10.05	2
1999	A0A2R6R2T1	Annexin	8.80	13	30.22	44.53	4
2000	A0A2R6R2T5	60S ribosomal protein L30	5.67	7	41.66	41.96	3
2001	A0A2R6R2T6	Eukaryotic peptide chain release factor subunit 1-3 like	7.80	13	18.35	29.06	4
2002	A0A2R6R2T7	14-3-3 protein 7 (Fragment)	8.00	12	25.66	34.52	6
2003	A0A2R6R2U7	14-3-3-like protein	25.25	30	70.04	72.14	4
2004	A0A2R6R2X2	14-3-3-like protein GF14 kappa	10.80	16	41.46	60.73	4
2005	A0A2R6R2Y5	Serine/threonine-protein phosphatase	8.67	10	30.56	30.56	3
2006	A0A2R6R2Y6	Malignant T-cell-amplified sequence 1 like (Fragment)	2.33	3	14.50	18.08	3
2007	A0A2R6R310	Pectinesterase	9.60	13	17.15	20.57	4
2008	A0A2R6R317	AP-4 complex subunit mu like (Fragment)	3.00	5	7.28	12.41	4
2009	A0A2R6R319	Protein BONZAI like	1.00	1	2.24	2.24	2
2010	A0A2R6R327	26S protease regulatory subunit 6A like	32.67	39	62.22	69.88	3

2011	A0A2R6R332	Mevalonate kinase	1.00	1	2.33	2.33	2
2012	A0A2R6R339	GTP-binding protein like	3.00	3	20.21	20.21	3
2013	A0A2R6R340	Dihydrolipoyl dehydrogenase	1.25	2	2.48	3.89	4
2014	A0A2R6R342	Beta-galactosidase	2.00	3	5.05	7.82	4
2015	A0A2R6R349	C2 domain-containing protein	1.00	1	3.99	3.99	1
2016	A0A2R6R355	Importin subunit alpha	5.80	9	14.35	19.96	4
2017	A0A2R6R367	Protein YIP	1.40	2	5.91	9.96	4
2018	A0A2R6R388	Protein disulfide-isomerase	4.00	6	15.21	21.75	3
2019	A0A2R6R397	Carbohydrate esterase	1.00	1	3.50	3.50	2
2020	A0A2R6R3C3	Polyadenylate-binding protein	9.00	13	15.25	21.04	4
2021	A0A2R6R3F0	Protein WEAK CHLOROPLAST MOVEMENT UNDER BLUE LIGHT 1 like	3.00	4	3.75	4.75	3
2022	A0A2R6R3F2	Exocyst complex component SEC3A like	1.50	2	1.75	2.37	2
2023	A0A2R6R3H4	26S proteasome regulatory subunit RPN11	13.00	18	50.83	66.03	4
2024	A0A2R6R3I9	Cytosolic purine 5'-nucleotidase	1.00	1	1.62	1.62	1
2025	A0A2R6R3K9	CCT-beta (Fragment)	32.60	44	62.83	70.23	4
2026	A0A2R6R3M3	Ribonuclease P protein subunit p25-like protein	5.50	9	23.44	34.75	4
2027	A0A2R6R3N4	Tubulin beta chain	37.80	55	71.47	78.89	4
2028	A0A2R6R3N6	Naringenin,2-oxoglutarate 3-dioxygenase	2.00	3	7.10	10.38	3
2029	A0A2R6R3Q0	AP complex subunit sigma (Fragment)	1.00	1	5.67	5.67	3
2030	A0A2R6R3Q5	Small nuclear ribonucleoprotein Sm D3	1.50	2	9.72	13.19	4
2031	A0A2R6R3Q8	EPS15 homologyprotein	1.75	3	1.58	2.71	4
2032	A0A2R6R3R9	Chaperone protein like	1.00	1	7.50	7.50	4
2033	A0A2R6R3S0	Pyrophosphate--fructose 6-phosphate 1-phosphotransferase subunit alpha	34.80	48	56.21	68.88	4
2034	A0A2R6R3U4	Proline--tRNA ligase	2.00	3	11.39	17.09	3
2035	A0A2R6R3Y6	Leucyl-tRNA synthetase	13.20	20	16.49	24.26	4
2036	A0A2R6R406	Terpene cyclase/mutase family member	2.25	4	3.13	5.67	4
2037	A0A2R6R407	60S acidic ribosomal protein like	1.00	1	6.61	6.61	4
2038	A0A2R6R418	Oligouridylate-binding protein like	1.00	1	1.96	1.96	3
2039	A0A2R6R419	Calcium-transporting ATPase	1.00	1	0.73	0.73	2
2040	A0A2R6R439	RING-box protein like	1.00	1	11.76	11.76	3
2041	A0A2R6R484	Casein kinase 1-like protein	1.00	1	2.11	2.11	1
2042	A0A2R6R485	ATP-dependent 6-phosphofructokinase	2.00	2	4.54	4.54	1
2043	A0A2R6R498	Vacuolar protein sorting-associated protein	1.00	1	4.59	4.59	1
2044	A0A2R6R4B8	Malic enzyme	10.00	13	23.86	30.12	4
2045	A0A2R6R4D4	3-hydroxyacyl-CoA dehydrogenase	5.25	8	9.87	14.36	4
2046	A0A2R6R4D8	Rho guanine nucleotide exchange factor like	2.50	3	5.95	7.22	4
2047	A0A2R6R4E6	ARF guanine-nucleotide exchange factor like	2.00	3	1.54	2.31	3
2048	A0A2R6R4G3	Protein CfxQ like	2.00	3	4.24	6.88	3
2049	A0A2R6R4G8	GTP-binding nuclear protein (Fragment)	8.00	11	41.00	51.36	4
2050	A0A2R6R4H5	Ethanolamine kinase	3.50	6	12.40	21.87	4
2051	A0A2R6R4J3	TBC1 domain family member 15 like	1.00	1	1.37	1.37	2
2052	A0A2R6R4N2	Protein-serine/threonine phosphatase	1.00	1	3.57	3.57	1

2253	A0A2R6RBU8	NADP-dependent D-sorbitol-6-phosphate dehydrogenase	1.80	3	6.15	7.44	4
2254	A0A2R6RBW3	Phenylalanine--tRNA ligase	5.20	8	12.58	20.08	4
2255	A0A2R6RBW8	Adenylyl cyclase-associated protein	4.25	5	7.70	9.07	4
2256	A0A2R6RBX7	Cysteine protease	1.00	1	4.38	4.38	2
2257	A0A2R6RBY3	Kinesin-like protein	1.00	1	0.37	0.37	3
2258	A0A2R6RBY8	40S ribosomal protein S25 (Fragment)	3.00	3	29.91	29.91	4
2259	A0A2R6RBZ0	Carboxylesterase 13	8.80	15	37.20	60.33	4
2260	A0A2R6RBZ2	Ras-related protein Rab7	4.00	6	19.09	27.18	3
2261	A0A2R6RBZ6	2-hydroxyisoflavanone dehydratase	2.20	3	7.58	11.30	4
2262	A0A2R6RC05	Girdin like	2.00	3	4.28	6.54	4
2263	A0A2R6RC31	Thioredoxin domain-containing protein	1.50	2	6.84	8.49	4
2264	A0A2R6RC47	2-hydroxyisoflavanone dehydratase	1.00	1	2.94	2.94	2
2265	A0A2R6RC48	D-3-phosphoglycerate dehydrogenase	1.00	1	1.52	1.52	1
2266	A0A2R6RC54	Tubulin alpha chain	29.50	35	47.45	49.45	2
2267	A0A2R6RC63	DNA-directed RNA polymerases II, IV and V subunit 3 like	1.00	1	4.08	4.08	2
2268	A0A2R6RC71	Indole-3-acetic acid-amido synthetase	1.67	2	2.39	3.00	3
2269	A0A2R6RCA1	Protein FAM126B like	1.00	1	3.23	3.23	4
2270	A0A2R6RCB0	Alpha-L-arabinofuranosidase	10.80	14	16.80	22.32	4
2271	A0A2R6RCB4	Ubiquitin carboxyl-terminal hydrolase	1.00	1	2.99	2.99	2
2272	A0A2R6RCD9	(3R)-hydroxymyristoyl-[acyl-carrier-protein] dehydratase	1.80	3	7.59	13.50	4
2273	A0A2R6RCG5	Pyruvate dehydrogenase E1 component subunit alpha	0.67	1	2.14	3.20	3
2274	A0A2R6RCH0	RNA-binding protein ARP1	1.00	1	4.14	4.14	2
2275	A0A2R6RCH4	Alkaline/neutral invertase	4.00	4	6.66	6.66	1
2276	A0A2R6RCK5	40S ribosomal protein like (Fragment)	5.20	7	34.13	47.83	4
2277	A0A2R6RCL8	Eukaryotic translation initiation factor 4C	1.67	2	13.10	17.93	3
2278	A0A2R6RCM6	M cell-type agglutination protein like	1.00	1	12.77	12.77	2
2279	A0A2R6RCP1	ATPase	1.00	1	4.21	4.21	2
2280	A0A2R6RCQ7	Protein transport Sec1a like	10.50	14	19.84	26.03	4
2281	A0A2R6RCR2	Uncharacterized protein	1.00	1	5.77	5.77	3
2282	A0A2R6RCR4	Non-specific serine/threonine protein kinase	1.00	1	1.92	1.92	3
2283	A0A2R6RCV4	Ras-related protein like	4.50	5	20.69	22.66	2
2284	A0A2R6RCW8	CCT-alpha	25.80	32	55.75	66.85	4
2285	A0A2R6RCX1	Ras-related protein RABH1b	8.25	11	42.19	51.92	4
2286	A0A2R6RCX2	Nucleoside diphosphate kinase	8.20	10	50.54	56.08	4
2287	A0A2R6RCX9	Hyaluronan/mRNA-binding protein	1.00	1	2.51	2.51	2
2288	A0A2R6RD18	Thioredoxin-like protein	2.00	2	18.46	18.46	2
2289	A0A2R6RD33	N-alpha-acetyltransferase	1.50	2	10.27	13.51	4
2290	A0A2R6RD45	OMPdecase	10.60	16	28.93	41.54	4
2291	A0A2R6RD55	Protein transport protein SEC31 B like	5.20	7	5.03	6.60	4
2292	A0A2R6RD57	Dihydrolipoyl dehydrogenase	1.25	2	2.46	3.86	4
2293	A0A2R6RD58	GTP-binding protein like	3.75	4	27.59	30.05	4
2294	A0A2R6RD60	Protein disulfide-isomerase	3.67	6	9.81	14.72	3

2295	A0A2R6RD66	Importin subunit alpha-1a like	5.25	9	20.77	32.94	4
2296	A0A2R6RD69	Serine/threonine-protein phosphatase	10.00	13	38.43	43.21	4
2297	A0A2R6RD70	Malignant T-cell-amplified sequence 1 like (Fragment)	2.33	3	14.50	18.08	3
2298	A0A2R6RD71	Topless-related protein	9.80	15	10.67	15.39	4
2299	A0A2R6RD79	60S ribosomal protein like	4.25	5	38.48	46.88	4
2300	A0A2R6RD81	26S protease regulatory subunit 6A like	29.00	45	60.49	77.53	4
2301	A0A2R6RD87	Protein YIP	1.40	2	5.91	9.96	4
2302	A0A2R6RDA6	Branched-chain-amino-acid aminotransferase-like protein	3.00	5	5.95	10.32	4
2303	A0A2R6RDC1	Ras-related protein like	2.60	4	12.92	19.28	4
2304	A0A2R6RDC2	40S ribosomal protein (Fragment)	8.20	10	34.01	37.65	4
2305	A0A2R6RDD2	Ubiquitin carboxyl-terminal hydrolase	1.00	1	2.97	2.97	2
2306	A0A2R6RDG9	Methyltransferase	3.33	5	3.96	5.12	3
2307	A0A2R6RDH5	Aspartic proteinase	1.00	1	2.95	2.95	2
2308	A0A2R6RDH6	Seryl-tRNA synthetase	2.00	2	4.90	4.90	1
2309	A0A2R6RDI0	Ras-related protein	3.50	4	17.31	20.19	2
2310	A0A2R6RDJ2	1,3-beta-glucan synthase	2.75	5	1.51	2.71	4
2311	A0A2R6RDK3	Golgi apparatus membrane protein TVP23	1.00	1	6.15	6.15	4
2312	A0A2R6RDL6	Trafficking protein particle complex subunit	1.60	2	9.08	11.35	4
2313	A0A2R6RDL7	ADP-ribosylation factor (Fragment)	10.33	15	59.26	63.89	6
2314	A0A2R6RDM5	Alcohol dehydrogenase	4.25	6	10.33	14.21	4
2315	A0A2R6RDM6	Actin-7	57.00	88	70.34	75.07	4
2316	A0A2R6RDP7	Glucan endo-1,3-beta-D-glucosidase	7.20	10	17.61	24.11	4
2317	A0A2R6RDR1	26S proteasome non-ATPase regulatory subunit 12 A like (Fragment)	20.40	28	45.30	55.78	4
2318	A0A2R6RDS0	Protein BONZAI like	1.00	1	2.00	2.00	2
2319	A0A2R6RDT1	Calreticulin like (Fragment)	2.75	5	5.95	10.71	4
2320	A0A2R6RDT6	40S ribosomal protein S24	2.60	3	19.71	21.17	4
2321	A0A2R6RDT8	Cysteine synthase	10.60	16	43.14	59.69	4
2322	A0A2R6RDU8	Guanine deaminase	2.80	5	21.72	38.17	4
2323	A0A2R6RDW6	Basic-leucine zipper domain protein	1.00	1	2.77	2.77	2
2324	A0A2R6RDX9	Glutamine synthetase	35.20	52	65.84	68.82	4
2325	A0A2R6RDY7	Receptor protein kinase	1.00	1	1.48	1.48	2
2326	A0A2R6RE09	Mannitol dehydrogenase	9.60	15	39.67	57.78	4
2327	A0A2R6RE10	Guanosine nucleotide diphosphate dissociation inhibitor	45.80	64	69.62	76.63	4
2328	A0A2R6RE47	Protein NRT1/ PTR FAMILY 8.3 like	1.00	1	1.87	1.87	2
2329	A0A2R6RE59	DEP domain-containing mTOR-interacting protein	1.00	1	1.62	1.62	3
2330	A0A2R6RE77	Threonyl-tRNA synthetase	11.40	18	18.95	30.61	4
2331	A0A2R6RE82	Ubiquitin	10.20	12	61.16	61.54	4
2332	A0A2R6RE91	Type 1 phosphatases regulator like	1.00	1	10.17	10.17	2
2333	A0A2R6REA0	ATP citrate synthase	9.25	14	25.17	30.73	4
2334	A0A2R6REA7	Glutamate--glyoxylate aminotransferase	1.00	1	2.29	2.29	1
2335	A0A2R6REB0	Nuclear antigen	1.00	1	6.82	6.82	3
2336	A0A2R6REB1	60S ribosomal protein like	2.40	3	23.02	27.40	4

2337	A0A2R6REB5	Mannan endo-1,4-beta-mannosidase	1.50	2	2.95	4.11	4
2338	A0A2R6REB9	Proteasome subunit beta	10.20	13	41.98	51.10	4
2339	A0A2R6RED9	Glycosyltransferase	7.25	10	23.07	31.13	4
2340	A0A2R6REE0	Glyceraldehyde-3-phosphate dehydrogenase (Fragment)	29.00	29	44.25	44.25	1
2341	A0A2R6REF2	Urease	4.00	7	4.85	8.69	4
2342	A0A2R6REH3	60S ribosomal protein like (Fragment)	2.80	4	17.36	25.82	4
2343	A0A2R6REH9	Proteasome subunit beta	12.00	16	48.40	59.85	4
2344	A0A2R6REQ5	AP-1 complex subunit mu-2	0.00	0	0.00	0.00	1
2345	A0A2R6RER4	60S ribosomal protein like	1.50	2	15.75	19.18	4
2346	A0A2R6RER5	Glutamate--glyoxylate aminotransferase	1.00	1	2.29	2.29	1
2347	A0A2R6RES0	ATP citrate synthase	7.33	10	18.52	21.99	3
2348	A0A2R6RES1	Pectinesterase inhibitor 1 like	1.25	2	8.29	13.14	4
2349	A0A2R6REV0	Mannan endo-1,4-beta-mannosidase	1.00	1	1.77	1.77	3
2350	A0A2R6REV4	Proteasome subunit beta	10.20	13	41.98	51.10	4
2351	A0A2R6REV9	CCT-epsilon	24.80	37	49.57	65.23	4
2352	A0A2R6REW4	Ubiquitin-conjugating enzyme E2 protein	3.80	6	28.11	37.84	4
2353	A0A2R6REZ7	Pyruvate kinase	1.00	1	1.91	1.91	1
2354	A0A2R6RF14	Nucleoredoxin like	1.00	1	2.44	2.44	1
2355	A0A2R6RF31	Uncharacterized protein	1.00	1	2.42	2.42	3
2356	A0A2R6RF33	Type 1 phosphatases regulator like	1.00	1	10.00	10.00	2
2357	A0A2R6RF34	ADP-ribosylation factor (Fragment)	11.50	13	45.84	47.78	2
2358	A0A2R6RF52	Spermidine synthase	1.00	1	3.80	3.80	4
2359	A0A2R6RF68	14-3-3 protein	1.33	2	5.85	8.77	3
2360	A0A2R6RF69	HSP20-like chaperone protein	1.00	1	7.64	7.64	1
2361	A0A2R6RF90	14-3-3 protein	1.33	2	5.85	8.77	3
2362	A0A2R6RF94	Glutathione S-transferase	1.00	1	3.98	3.98	2
2363	A0A2R6RF95	Serine/threonine-protein phosphatase	8.25	12	37.75	55.23	4
2364	A0A2R6RFA2	SNF1-related protein kinase regulatory subunit gamma-1-like	3.75	5	11.01	15.58	4
2365	A0A2R6RFA3	Geranylgeranyl transferase type-2 subunit beta	1.00	1	4.70	4.70	2
2366	A0A2R6RFB1	Exocyst complex component EXO84A like	1.00	1	1.31	1.31	3
2367	A0A2R6RFB8	Uncharacterized protein	1.75	2	4.98	5.75	4
2368	A0A2R6RFB9	Methyltransferase	1.67	2	3.20	3.75	3
2369	A0A2R6RFD2	Pectate lyase	1.00	1	2.28	2.28	3
2370	A0A2R6RFD5	40S ribosomal protein like	4.50	5	13.45	14.21	2
2371	A0A2R6RFE6	60S ribosomal protein	1.00	1	12.77	12.77	1
2372	A0A2R6RFF3	26S proteasome non-ATPase regulatory subunit like	24.25	32	55.97	67.85	4
2373	A0A2R6RFG0	60S ribosomal protein	2.60	3	20.17	22.50	4
2374	A0A2R6RFH3	Serine/threonine-protein kinase	0.75	1	1.91	2.55	4
2375	A0A2R6RFI2	Dual specificity protein kinase	2.00	2	3.72	3.72	1
2376	A0A2R6RFN9	14-3-3-like protein GF14 iota (Fragment)	16.20	21	55.91	65.25	4
2377	A0A2R6RFP6	Kinesin-like protein	1.00	1	1.47	1.47	2
2378	A0A2R6RFR4	Importin subunit alpha	5.00	9	14.20	26.54	4

2379	A0A2R6RFR9	GTP-binding protein like	3.00	3	20.21	20.21	3
2380	A0A2R6RFS2	Syntaxin-41 like	1.00	1	4.37	4.37	2
2381	A0A2R6RFS8	S-adenosylmethionine synthase	5.50	7	17.88	21.99	2
2382	A0A2R6RFU3	Non-specific serine/threonine protein kinase	1.00	1	2.21	2.21	3
2383	A0A2R6RFW7	Hydrolase	1.00	1	2.80	2.80	2
2384	A0A2R6RG28	Sucrose-phosphate synthase	25.60	38	28.58	39.91	4
2385	A0A2R6RG49	3-oxoacyl-[acyl-carrier-protein] synthase (Fragment)	3.00	5	22.34	34.75	4
2386	A0A2R6RG74	Tubulin beta chain	29.00	38	59.52	67.57	4
2387	A0A2R6RG83	Cullin-4 like	1.00	1	1.33	1.33	1
2388	A0A2R6RG90	DNA damage-binding protein 1	0.00	0	0.00	0.00	1
2389	A0A2R6RGA1	Alpha,alpha-trehalose-phosphate synthase	13.00	17	19.56	25.26	4
2390	A0A2R6RGB8	Non-specific serine/threonine protein kinase	1.00	1	1.82	1.82	1
2391	A0A2R6RGC0	60S ribosomal protein like	2.75	4	21.48	26.56	4
2392	A0A2R6RGC1	26S protease regulatory subunit 6A (Fragment)	31.00	52	62.36	79.40	4
2393	A0A2R6RGC4	Stress-related protein	3.50	5	15.71	22.53	4
2394	A0A2R6RGD3	Translationally-controlled tumor protein	4.33	5	25.99	33.33	3
2395	A0A2R6RGE2	ABC transporter F family member 4 like (Fragment)	1.50	2	4.12	5.29	2
2396	A0A2R6RGF0	Dynamin GTPase	1.25	2	1.63	2.71	4
2397	A0A2R6RGF2	Methionine S-methyltransferase	3.00	4	2.67	3.66	2
2398	A0A2R6RGJ1	Serine/threonine-protein kinase	2.00	3	6.39	9.09	4
2399	A0A2R6RGJ7	Basic-leucine zipper domain protein	1.00	1	2.67	2.67	2
2400	A0A2R6RGM5	Glycine-rich RNA-binding protein like	1.00	1	6.50	6.50	1
2401	A0A2R6RGN5	Protein DMR6-LIKE OXYGENASE 2 like	6.00	9	13.90	20.00	4
2402	A0A2R6RGR6	14-3-3-like protein	24.40	30	66.92	71.98	4
2403	A0A2R6RGT4	Malate dehydrogenase	1.00	1	3.09	3.09	2
2404	A0A2R6RGU8	Proline iminopeptidase	1.33	2	6.62	9.92	3
2405	A0A2R6RGV6	Replication factor C subunit	0.00	0	0.00	0.00	1
2406	A0A2R6RGW4	40S ribosomal protein S29 (Fragment)	2.00	2	33.33	33.33	3
2407	A0A2R6RGX9	3-oxo-Delta(4,5)-steroid 5-beta-reductase	3.50	6	10.41	18.53	2
2408	A0A2R6RGZ4	Basic secretory protease	1.75	3	6.96	11.74	4
2409	A0A2R6RH04	S-methyl-5-thioribose kinase	1.67	2	6.21	7.88	3
2410	A0A2R6RH05	D-3-phosphoglycerate dehydrogenase	1.00	1	1.50	1.50	1
2411	A0A2R6RH10	Polyadenylate-binding protein	5.00	6	8.32	9.83	2
2412	A0A2R6RH14	Kynurenine formamidase	0.00	0	0.00	0.00	1
2413	A0A2R6RH21	COP9 signalosome complex subunit 5a like	6.00	11	19.94	37.12	4
2414	A0A2R6RH51	EKC/KEOPS complex subunit Tprkb like	1.00	1	4.65	4.65	2
2415	A0A2R6RH55	CD2 like	1.40	2	4.12	5.88	4
2416	A0A2R6RH68	F-box/WD repeat-containing protein	1.00	1	2.29	2.29	1
2417	A0A2R6RH70	VID27 domain-containing protein	1.00	1	2.22	2.22	1
2418	A0A2R6RH73	Pollen-specific leucine-rich repeat extensin-like protein	3.20	5	4.87	7.72	4
2419	A0A2R6RH75	La-related protein like	4.00	6	9.34	13.73	4
2420	A0A2R6RH78	Serine/threonine-protein kinase	1.33	2	4.22	5.51	3

2421	A0A2R6RHB4	Phosphatidylinositol 4-kinase alpha 1 like	7.75	13	4.68	7.78	4
2422	A0A2R6RHB7	Phospholipase A-2-activating protein	2.33	3	4.48	5.53	3
2423	A0A2R6RHC2	Ras-related protein Rab7	4.00	6	19.09	27.18	3
2424	A0A2R6RHD0	Coatomer subunit gamma	11.00	19	13.32	22.27	4
2425	A0A2R6RHD3	Bifunctional dihydrofolate reductase-thymidylate synthase	2.33	3	5.28	6.76	3
2426	A0A2R6RHD5	Glycine-rich RNA-binding protein	6.80	9	36.97	47.27	4
2427	A0A2R6RHD8	Ras-related protein Rab7	4.00	6	19.09	27.18	3
2428	A0A2R6RHE0	Phenylalanine--tRNA ligase	8.00	14	19.79	35.86	4
2429	A0A2R6RHE3	26S protease regulatory subunit 10B A	19.60	26	54.89	66.42	4
2430	A0A2R6RHE6	40S ribosomal protein S25 (Fragment)	3.00	3	29.91	29.91	4
2431	A0A2R6RHG5	Receptor-like protein kinase	2.50	4	3.73	6.08	4
2432	A0A2R6RHG8	Chaperone protein like	9.00	12	36.29	46.63	4
2433	A0A2R6RHJ3	SH3 domain-containing protein	5.33	9	16.04	27.03	3
2434	A0A2R6RHJ5	Alkaline/neutral invertase	16.00	16	30.18	30.18	1
2435	A0A2R6RHJ8	Vacuolar protein	1.00	1	1.98	1.98	3
2436	A0A2R6RHK8	Beta-galactosidase	10.00	17	11.96	19.13	4
2437	A0A2R6RHM4	Glycine-rich protein	4.50	5	28.57	29.87	4
2438	A0A2R6RHM5	Peptidyl-prolyl cis-trans isomerase	15.60	22	67.33	73.26	4
2439	A0A2R6RHN3	Trafficking protein particle complex subunit	1.00	1	7.69	7.69	3
2440	A0A2R6RHN4	Vacuolar proton pump subunit B	13.40	18	31.84	41.39	4
2441	A0A2R6RHP0	Transportin-1 like	9.00	13	10.93	15.30	2
2442	A0A2R6RHQ2	26S proteasome non-ATPase regulatory subunit 3 like	18.25	23	35.89	44.56	4
2443	A0A2R6RIS1	GDP-mannose 4,6-dehydratase	16.20	24	44.93	56.50	4
2444	A0A2R6RIS2	GDP-mannose 4,6-dehydratase	18.75	25	50.07	58.62	4
2445	A0A2R6RIS4	Serine protease	1.00	1	2.68	2.68	3
2446	A0A2R6RIS9	Glycine-rich protein	3.00	4	25.13	33.17	4
2447	A0A2R6RIV8	Phosphoserine aminotransferase	1.75	4	4.58	10.24	4
2448	A0A2R6RIX1	Serine/threonine-protein kinase	1.33	2	2.85	4.27	3
2449	A0A2R6RIX8	Catalase (Fragment)	5.67	6	16.11	17.74	3
2450	A0A2R6RIY0	Rac-like GTP-binding protein	9.20	13	31.57	40.10	4
2451	A0A2R6RJ03	Vacuolar protein sorting-associated protein 35	3.67	6	5.44	9.62	3
2452	A0A2R6RJ33	Mannitol dehydrogenase	5.00	7	17.99	21.67	4
2453	A0A2R6RJ37	Guanosine nucleotide diphosphate dissociation inhibitor	38.20	54	60.00	67.64	4
2454	A0A2R6RJ66	Glutamine synthetase	12.25	15	58.11	60.38	4
2455	A0A2R6RJ67	Glutamate decarboxylase	14.20	20	32.55	42.89	4
2456	A0A2R6RJ79	UTP--glucose-1-phosphate uridylyltransferase	45.00	61	70.57	76.63	4
2457	A0A2R6RJ80	Eukaryotic translation initiation factor 3 subunit J	1.67	2	10.32	12.56	3
2458	A0A2R6RJ82	Isocitrate dehydrogenase [NADP]	4.00	4	9.90	9.90	1
2459	A0A2R6RJ86	Transmembrane 9 superfamily member	2.00	2	3.24	3.24	2
2460	A0A2R6RJ92	Ras-related protein Rab5	2.33	3	12.63	15.93	3
2461	A0A2R6RJA2	Thioredoxin reductase	5.33	7	22.42	30.18	3
2462	A0A2R6RJA4	Protein DJ-1 D like	1.00	1	3.33	3.33	2

2463	A0A2R6RJD6	40S ribosomal protein (Fragment)	8.60	11	35.63	41.70	4
2464	A0A2R6RJE1	WEB family protein	3.75	6	5.08	7.73	4
2465	A0A2R6RJE3	Ras-related protein Rab11D	2.75	4	13.74	19.37	4
2466	A0A2R6RJE5	COP9 signalosome complex subunit 3 like	1.00	1	2.33	2.33	1
2467	A0A2R6RJE7	Ubiquitin carboxyl-terminal hydrolase	1.00	1	3.23	3.23	2
2468	A0A2R6RJG7	Glyceraldehyde-3-phosphate dehydrogenase	41.20	59	75.43	79.23	4
2469	A0A2R6RJH7	Glucose-6-phosphate 1-dehydrogenase	2.33	3	4.77	6.38	3
2470	A0A2R6RJH9	Early nodulin-like protein	6.40	9	27.95	31.06	4
2471	A0A2R6RJI5	Glycerol-3-phosphate dehydrogenase [NAD(+)]	8.60	13	26.31	37.47	4
2472	A0A2R6RJK1	Serine/threonine protein phosphatase 2A regulatory subunit	3.00	3	4.96	4.96	2
2473	A0A2R6RJM2	Glycerophosphodiester phosphodiesterase	1.67	2	3.04	3.73	3
2474	A0A2R6RJM9	Serine--tRNA ligase isoform 2	1.00	1	6.94	6.94	1
2475	A0A2R6RJN7	Ras-related protein	2.00	2	9.14	9.14	1
2476	A0A2R6RJP2	Methyltransferase	3.50	4	3.06	3.06	2
2477	A0A2R6RJQ1	PLAT domain-containing protein	2.25	4	19.09	29.57	4
2478	A0A2R6RJQ6	Serine--tRNA ligase isoform 1	1.00	1	6.79	6.79	1
2479	A0A2R6RJS7	26S proteasome non-ATPase regulatory subunit 12 A like (Fragment)	17.00	25	37.30	52.15	4
2480	A0A2R6RJT1	Actin-7	57.00	88	70.34	75.07	4
2481	A0A2R6RJV9	Exocyst subunit Exo70 family protein	21.20	32	33.66	49.14	4
2482	A0A2R6RJW5	60S ribosomal protein L7a (Fragment)	6.80	10	24.51	34.24	4
2483	A0A2R6RJY1	Nuclear transport factor 2 like	1.00	1	11.38	11.38	4
2484	A0A2R6RJY4	Uridine kinase	3.20	4	6.61	8.21	4
2485	A0A2R6RK09	Glutaredoxin like	5.00	6	60.55	66.06	4
2486	A0A2R6RK27	ADP-ribosylation factor (Fragment)	9.60	14	56.11	63.89	4
2487	A0A2R6RK34	Non-specific serine/threonine protein kinase	1.00	1	2.19	2.19	3
2488	A0A2R6RK54	Glucuronokinase	1.00	1	3.93	3.93	1
2489	A0A2R6RK58	Bidirectional sugar transporter SWEET6b like	1.00	1	3.93	3.93	3
2490	A0A2R6RK61	Uridine kinase	7.75	11	19.13	25.86	4
2491	A0A2R6RK67	Protein transport protein SEC13 B like	4.33	5	14.79	16.89	3
2492	A0A2R6RK70	Mannose-1-phosphate guanyltransferase	2.67	4	6.62	9.93	3
2493	A0A2R6RK86	Hypersensitive-induced response protein	2.00	2	8.59	8.59	2
2494	A0A2R6RK89	Inositol hexakisphosphate and diphosphoinositol-pentakisphosphate kinase	6.25	10	6.07	9.43	4
2495	A0A2R6RKA1	60S ribosomal protein	2.00	2	16.67	16.67	3
2496	A0A2R6RKB4	40S ribosomal protein S9-2	5.33	6	18.78	19.80	3
2497	A0A2R6RKG4	40S ribosomal protein like	3.00	3	21.68	21.68	1
2498	A0A2R6RKH1	UDP-glucose 6-dehydrogenase	39.60	54	73.21	76.88	4
2499	A0A2R6RKI7	UDP-arabinopyranose mutase	50.20	74	87.24	89.04	4
2500	A0A2R6RKJ4	Stress-induced protein	8.20	12	82.42	90.91	4
2501	A0A2R6RKJ5	Coatomer subunit zeta	1.00	1	6.12	6.12	2
2502	A0A2R6RKM7	T-complex protein 1 subunit zeta 1 like	20.40	27	52.30	68.92	4
2503	A0A2R6RKP0	LisH domain and HEAT repeat-containing protein	1.33	2	1.24	1.86	3
2504	A0A2R6RKQ7	Eukaryotic translation initiation factor 5 like	1.00	1	2.21	2.21	4

2505	A0A2R6RKR6	40S ribosomal protein S7	5.20	6	39.79	43.98	4
2506	A0A2R6RKS5	Organellar oligopeptidase	11.00	13	18.94	21.04	2
2507	A0A2R6RKT4	ATP synthase subunit beta	1.40	3	2.82	6.04	4
2508	A0A2R6RKU9	Malate dehydrogenase	1.50	2	4.92	6.46	4
2509	A0A2R6RKV6	Protein C2-DOMAIN ABA-RELATED like	1.00	1	5.45	5.45	1
2510	A0A2R6RKX9	RuvB-like helicase	4.25	6	10.71	15.20	4
2511	A0A2R6RKY6	60S ribosomal protein like	2.67	4	17.81	21.92	3
2512	A0A2R6RKZ6	Calcium-transporting ATPase	4.60	8	6.23	11.41	4
2513	A0A2R6RL22	Receptor-like protein kinase	1.00	1	1.44	1.44	1
2514	A0A2R6RL32	Phosphatidylinositol 3,4,5-trisphosphate 3-phosphatase and protein-tyrosine-phosphatase	2.50	4	4.89	7.79	4
2515	A0A2R6RL40	Nicotinate phosphoribosyltransferase	1.00	1	1.43	1.43	1
2516	A0A2R6RL52	Indole-3-acetic acid-amido synthetase	1.67	2	2.40	3.01	3
2517	A0A2R6RLA0	Serine/threonine-protein kinase	1.33	2	4.27	5.57	3
2518	A0A2R6RLF1	Suppressor of gene silencing like protein	1.00	1	1.86	1.86	3
2519	A0A2R6RM90	Pyrophosphate--fructose 6-phosphate 1-phosphotransferase subunit alpha	47.80	68	64.57	75.53	4
2520	A0A2R6RMD2	Catalase	5.80	7	13.19	15.26	4
2521	A0A2R6RMD6	Small nuclear ribonucleoprotein Sm D3	1.50	2	10.60	14.39	4
2522	A0A2R6RME8	Dehydrin like	2.75	4	14.71	23.04	4
2523	A0A2R6RMH6	Alpha-amylase	1.00	1	2.42	2.42	1
2524	A0A2R6RMI2	Endoplasmin like	4.40	7	5.04	7.80	4
2525	A0A2R6RMI3	Vacuolar protein sorting-associated protein 35	1.33	2	1.94	2.53	3
2526	A0A2R6RMJ6	Alkaline/neutral invertase	9.20	12	16.63	20.88	4
2527	A0A2R6RMK2	Endoglucanase	5.25	8	10.18	14.15	4
2528	A0A2R6RMK9	Sulfate adenylyltransferase	16.60	25	38.70	54.39	4
2529	A0A2R6RMP7	Thioredoxin H-type like	4.40	6	44.79	50.41	4
2530	A0A2R6RMR3	Proteasome subunit alpha type	12.75	14	42.31	45.05	4
2531	A0A2R6RMT0	Isoflavone reductase-like protein	6.00	8	18.04	22.46	4
2532	A0A2R6RMU9	COP9 signalosome complex subunit like	6.50	9	22.17	30.23	4
2533	A0A2R6RMV0	Glucose-6-phosphate isomerase	6.75	10	14.34	20.59	4
2534	A0A2R6RMV4	Methylthioribose-1-phosphate isomerase	1.00	1	13.07	13.07	2
2535	A0A2R6RMX9	Myosin heavy chain kinase	2.75	4	6.32	8.80	4
2536	A0A2R6RMY1	Serpin-ZX like	2.00	2	5.63	5.63	3
2537	A0A2R6RMY9	Polyadenylate-binding protein	3.67	5	10.07	13.91	3
2538	A0A2R6RMZ1	Serpin-ZX like	2.00	2	5.67	5.67	3
2539	A0A2R6RMZ3	60S acidic ribosomal protein	2.80	4	33.16	47.86	4
2540	A0A2R6RN29	Serpin-ZX like	2.00	2	5.64	5.64	3
2541	A0A2R6RN43	Polyadenylate-binding protein	7.60	12	13.61	20.80	4
2542	A0A2R6RN45	Protein WEAK CHLOROPLAST MOVEMENT UNDER BLUE LIGHT 1 like	11.50	12	13.97	14.41	2
2543	A0A2R6RN50	Protein like	2.33	3	6.76	8.62	3
2544	A0A2R6RN76	Adenine phosphoribosyltransferase	2.00	3	10.40	14.80	4
2545	A0A2R6RN77	Calcium-transporting ATPase	1.00	1	1.08	1.08	1
2546	A0A2R6RNB3	Xylulose kinase	12.20	17	25.97	33.81	4

2547	A0A2R6RNC2	Ubiquitin-fold modifier-conjugating enzyme 1	1.00	1	5.75	5.75	2
2548	A0A2R6RNC8	Phosphoglycerate mutase-like protein	4.25	6	12.35	16.95	4
2549	A0A2R6RNE7	Calcium-dependent protein kinase	4.80	8	10.88	16.14	4
2550	A0A2R6RNG3	Mechanosensitive ion channel protein	2.00	2	2.25	2.25	2
2551	A0A2R6RNG4	Phosphoenolpyruvate carboxykinase (ATP)	7.00	10	14.26	20.45	2
2552	A0A2R6RNG5	Metal-independent phosphoserine phosphatase	3.75	6	21.47	33.48	4
2553	A0A2R6RNG8	Argininosuccinate lyase	2.25	4	6.19	11.05	4
2554	A0A2R6RNI8	Mitochondrial phosphate carrier protein like	1.00	1	2.94	2.94	2
2555	A0A2R6RNL0	GEM-like protein	1.67	2	6.12	7.14	3
2556	A0A2R6RNM3	14-3-3-like protein	23.80	30	68.66	73.95	4
2557	A0A2R6RNM4	14-3-3 protein	9.60	14	33.36	46.25	4
2558	A0A2R6RNN3	Esterase	1.00	1	6.44	6.44	3
2559	A0A2R6RNP0	14-3-3 protein	7.33	10	25.29	35.02	3
2560	A0A2R6RNP2	Protein FAM91A1 like	3.67	5	3.59	4.85	3
2561	A0A2R6RNQ6	Eukaryotic peptide chain release factor subunit 1-3 like	5.00	5	11.90	11.90	1
2562	A0A2R6RNR4	60S ribosomal protein L30	5.00	7	41.96	52.68	4
2563	A0A2R6RNS7	IST1-like protein	1.33	2	2.27	3.41	3
2564	A0A2R6RNT6	Polyadenylate-binding protein like	12.20	21	19.59	32.58	4
2565	A0A2R6RNV2	Polypyrimidine tract-binding protein	1.00	1	2.70	2.70	2
2566	A0A2R6RNV9	Eukaryotic translation initiation factor 5B	4.50	5	4.67	5.26	2
2567	A0A2R6RNW1	Exocyst complex component SEC5	1.00	1	0.82	0.82	2
2568	A0A2R6RNW2	Ras-related protein like	2.00	2	9.76	9.76	1
2569	A0A2R6RNW4	UPF0496 protein	1.00	1	1.80	1.80	1
2570	A0A2R6RNW6	Transcription factor like	1.00	1	2.83	2.83	3
2571	A0A2R6RNW8	D-fructose-1,6-bisphosphate 1-phosphohydrolase	1.50	2	5.29	7.65	2
2572	A0A2R6RNY5	60S ribosomal protein	14.50	21	35.35	44.99	4
2573	A0A2R6RNY9	TOM1-like protein	1.75	3	3.73	6.24	4
2574	A0A2R6RP29	Ubiquitin-fold modifier 1	1.00	1	15.79	15.79	3
2575	A0A2R6RP30	Eukaryotic translation initiation factor 5-2 like	1.00	1	2.19	2.19	4
2576	A0A2R6RP36	Protein-serine/threonine phosphatase	3.00	3	8.72	8.72	1
2577	A0A2R6RP65	Protein disulfide-isomerase	3.00	6	7.50	14.11	4
2578	A0A2R6RP72	Calcium-dependent protein kinase	5.60	8	20.40	29.89	4
2579	A0A2R6RP74	Alkaline/neutral invertase	17.00	21	44.08	51.69	4
2580	A0A2R6RP87	Sucrose transport protein	6.80	10	14.43	20.04	4
2581	A0A2R6RP91	Sucrose transport protein	5.80	9	12.35	18.44	4
2582	A0A2R6RPA1	Ran-binding protein like	5.50	8	14.32	20.70	4
2583	A0A2R6RPD5	AP complex subunit sigma (Fragment)	1.60	2	13.75	17.50	4
2584	A0A2R6RPD9	Proteasome subunit beta (Fragment)	7.60	11	54.06	62.38	4
2585	A0A2R6RPE0	Elongation factor 1-gamma like (Fragment)	2.50	3	7.67	8.49	4
2586	A0A2R6RPE7	Beta-galactosidase	2.33	3	2.74	3.56	3
2587	A0A2R6RPF2	UDP-sugar pyrophosphorylase	9.40	12	18.50	23.16	4
2588	A0A2R6RQF6	Nascent polypeptide-associated complex subunit alpha-like protein	2.60	4	12.69	17.18	4

2589	A0A2R6RQG8	Protein EXPORTIN 1A like	7.33	11	7.44	11.34	3
2590	A0A2R6RQI4	Vacuolar protein sorting-associated protein like (Fragment)	2.50	4	11.25	17.67	4
2591	A0A2R6RQP4	Reticulon-like protein	1.00	1	3.18	3.18	2
2592	A0A2R6RQP6	Ubiquitin-conjugating enzyme E2 protein	3.80	6	28.11	37.84	4
2593	A0A2R6RQP9	Spastin like	9.00	11	14.61	17.43	3
2594	A0A2R6RQR3	C2 domain-containing protein	2.50	3	12.26	14.94	4
2595	A0A2R6RQS3	60S ribosomal protein L36	3.00	4	22.42	29.09	3
2596	A0A2R6RQS7	Trafficking protein particle complex subunit	1.33	2	7.49	11.24	3
2597	A0A2R6RQT3	Actin-depolymerizing factor 7 like (Fragment)	15.00	24	73.83	78.68	4
2598	A0A2R6RQT8	Receptor-like protein kinase	1.00	1	1.47	1.47	1
2599	A0A2R6RQW4	Sorbitol dehydrogenase	15.20	18	52.53	61.54	4
2600	A0A2R6RR05	Ras-related protein RABD2a	5.67	6	29.89	31.53	3
2601	A0A2R6RR06	Autophagy-related protein	1.00	1	3.18	3.18	1
2602	A0A2R6RR16	Protein-methionine-S-oxide reductase	1.00	1	4.37	4.37	1
2603	A0A2R6RR27	Pectinesterase	29.00	36	62.78	66.94	4
2604	A0A2R6RR54	Alpha-soluble NSF attachment protein	6.25	9	26.11	34.13	4
2605	A0A2R6RR68	Clathrin heavy chain like	39.60	55	57.13	70.68	4
2606	A0A2R6RR77	Eukaryotic translation initiation factor 2 subunit alpha like	8.20	13	26.46	39.83	4
2607	A0A2R6RR78	GDSL esterase/lipase	1.00	1	3.91	3.91	3
2608	A0A2R6RRA0	26S proteasome non-ATPase regulatory subunit 7 A like	9.00	13	35.29	51.61	4
2609	A0A2R6RRB5	Mannose-1-phosphate guanylyltransferase	4.50	6	17.52	24.93	4
2610	A0A2R6RRB7	60S ribosomal protein L35a-1	2.40	4	24.82	41.96	4
2611	A0A2R6RRD6	Glucan endo-1,3-beta-D-glucosidase	1.00	1	2.20	2.20	1
2612	A0A2R6RRE4	Actin-97 like	13.00	13	16.17	16.17	1
2613	A0A2R6RRE6	60S ribosomal protein like	4.60	7	24.21	32.89	4
2614	A0A2R6RRG4	Glutathione S-transferase	3.00	3	25.00	25.00	2
2615	A0A2R6RRH0	Macrophage erythroblast attacher like	2.00	3	4.82	7.23	3
2616	A0A2R6RRH2	Aldo-keto reductase	1.00	1	3.22	3.22	2
2617	A0A2R6RRH6	Protein transport protein SEC23	6.67	9	12.01	15.80	3
2618	A0A2R6RRI1	Aldo-keto reductase	1.00	1	3.33	3.33	2
2619	A0A2R6RRI2	60S ribosomal protein L35	1.80	2	15.12	16.26	4
2620	A0A2R6RRI4	Ras-related protein like	3.00	3	16.36	16.36	2
2621	A0A2R6RRI8	Proteasome inhibitor	1.00	1	4.45	4.45	2
2622	A0A2R6RRK6	Tubulin beta chain	27.00	27	64.21	64.21	1
2623	A0A2R6RRQ1	ERBB-3 BINDING PROTEIN 1 like	13.20	19	34.15	47.58	4
2624	A0A2R6RRQ2	Importin subunit beta-1 like	7.75	12	11.59	17.51	4
2625	A0A2R6RRQ8	40S ribosomal protein like	9.20	13	25.70	35.91	4
2626	A0A2R6RRR2	Uncharacterized protein	1.75	3	11.91	20.59	4
2627	A0A2R6RRV3	Receptor-like protein kinase	1.00	1	1.34	1.34	1
2628	A0A2R6RRV9	Ubiquitin-conjugating enzyme E2 28	3.80	6	28.11	37.84	4
2629	A0A2R6RRW2	Vacuolar-sorting receptor 1 like	4.80	7	7.85	10.36	4
2630	A0A2R6RRW5	26S protease regulatory subunit 6B	13.00	20	35.03	54.73	2

2631	A0A2R6RRX0	Eukaryotic translation initiation factor 2 subunit beta like	3.50	5	15.04	22.56	4
2632	A0A2R6RRX4	Calcium-binding protein	2.00	2	7.25	7.25	1
2633	A0A2R6RRY5	Peptidase	3.00	4	6.70	9.09	4
2634	A0A2R6RRY6	Receptor-like kinase	1.00	1	1.52	1.52	2
2635	A0A2R6RRY9	Glycine-rich RNA-binding protein	1.00	1	8.84	8.84	2
2636	A0A2R6RS13	DNA-directed RNA polymerases II and V subunit 8A like	1.50	2	9.72	13.19	4
2637	A0A2R6RS18	2-alkenal reductase	1.00	1	3.18	3.18	1
2638	A0A2R6RS20	Acyl-[acyl-carrier-protein] desaturase	1.50	2	4.67	6.31	4
2639	A0A2R6RS33	WEB family protein	5.75	8	15.59	22.31	4
2640	A0A2R6RS47	Eukaryotic translation initiation factor 2A	1.00	1	1.93	1.93	2
2641	A0A2R6RS66	Serine/threonine protein phosphatase 2A regulatory subunit	4.00	4	7.98	7.98	2
2642	A0A2R6RS85	Protein fluG like	30.60	50	43.04	59.19	4
2643	A0A2R6RSB7	S-adenosylmethionine synthase	48.40	72	78.68	84.43	4
2644	A0A2R6RSC6	Cell division cycle protein like	46.50	59	53.41	57.32	4
2645	A0A2R6RSD3	Protein EXPORTIN 1A like	7.00	12	7.87	14.00	4
2646	A0A2R6RSD5	60S ribosomal protein	9.60	11	50.41	55.15	4
2647	A0A2R6RSI1	Vacuolar protein sorting-associated protein like (Fragment)	2.00	3	9.42	14.00	4
2648	A0A2R6RSI3	Importin subunit beta-1 like	6.50	10	10.76	14.47	4
2649	A0A2R6RSI7	Probable 6-phosphogluconolactonase	1.00	1	2.51	2.51	1
2650	A0A2R6RSJ8	Dipeptidyl aminopeptidase	2.00	2	2.71	2.71	2
2651	A0A2R6RSK0	Protein BOBBER like	2.80	4	11.16	15.79	4
2652	A0A2R6RSM9	Heat shock protein	34.00	38	35.30	38.21	2
2653	A0A2R6RSR7	Tripeptidyl-peptidase	5.75	8	19.49	29.66	4
2654	A0A2R6RSR9	4-coumarate--CoA ligase	3.50	4	8.94	10.13	4
2655	A0A2R6RSS3	60S ribosomal protein L36	2.33	3	15.15	18.18	3
2656	A0A2R6RST2	Tubulin beta chain (Fragment)	14.25	19	66.92	75.78	4
2657	A0A2R6RST9	ADP-ribosylation factor-related protein like	1.00	1	6.37	6.37	2
2658	A0A2R6RSU6	Methyltransferase	2.00	2	4.12	4.12	1
2659	A0A2R6RSW6	Valyl-tRNA synthetase (Fragment)	8.50	10	9.78	10.75	2
2660	A0A2R6RSZ0	Phosphopyruvate hydratase	35.80	47	66.52	71.91	4
2661	A0A2R6RSZ4	Calcium-binding protein	11.50	13	75.00	84.35	4
2662	A0A2R6RT07	40S ribosomal protein S13	5.00	6	35.50	40.40	4
2663	A0A2R6RT17	Serine/threonine protein kinase	1.00	1	0.77	0.77	2
2664	A0A2R6RT35	PLAT domain-containing protein	1.00	1	4.97	4.97	4
2665	A0A2R6RT38	Fructokinase-7 like	13.40	18	46.03	61.14	4
2666	A0A2R6RT42	2-phosphoglycerate kinase	1.25	2	3.28	5.46	4
2667	A0A2R6RT49	Autophagy-related protein	1.00	1	3.22	3.22	1
2668	A0A2R6RT63	Protein-methionine-S-oxide reductase	1.00	1	3.49	3.49	1
2669	A0A2R6RT73	2-haloacrylate reductase	1.50	2	3.35	4.72	4
2670	A0A2R6RTB5	Alpha-soluble NSF attachment protein	2.00	2	14.84	14.84	1
2671	A0A2R6RTB6	Ras-related protein like	7.25	9	40.89	52.71	4
2672	A0A2R6RTC5	UDP-glucuronate decarboxylase	23.80	34	71.24	80.59	4

2673	A0A2R6RTD6	Actin-97	64.20	96	73.21	75.60	4
2674	A0A2R6RTD7	Triosephosphate isomerase	17.60	24	66.93	70.47	4
2675	A0A2R6RTE1	Methionine--tRNA ligase	10.25	14	27.55	35.98	4
2676	A0A2R6RTE2	Actin-depolymerizing factor (Fragment)	2.00	2	10.14	10.14	1
2677	A0A2R6RTF4	Clathrin heavy chain like	49.80	65	48.86	58.15	4
2678	A0A2R6RTH6	Eukaryotic translation initiation factor 3 subunit F	4.80	7	22.25	34.04	4
2679	A0A2R6RTJ6	Tropinone reductase	1.67	2	4.74	5.62	3
2680	A0A2R6RTK1	26S proteasome non-ATPase regulatory subunit 7 A	6.00	9	23.30	35.60	2
2681	A0A2R6RTL7	Casein kinase 1-like protein	1.00	1	2.56	2.56	3
2682	A0A2R6RTN1	Heterogeneous nuclear ribonucleoprotein like	1.00	1	2.93	2.93	2
2683	A0A2R6RTN9	Serine/threonine protein phosphatase 2A regulatory subunit	2.00	2	3.42	3.42	2
2684	A0A2R6RTP7	Nucleic acid-binding, OB-fold protein	2.80	4	22.19	32.12	4
2685	A0A2R6RTQ7	ADP-ribosylation factor	10.00	14	58.01	63.54	4
2686	A0A2R6RTR1	Acetyltransferase NATA1-like	1.75	2	8.30	9.61	4
2687	A0A2R6RTR8	Universal stress protein A-like protein	1.50	2	9.22	12.29	2
2688	A0A2R6RTS7	40S ribosomal protein (Fragment)	3.80	5	23.98	26.24	4
2689	A0A2R6RTV7	Nuclear mitotic apparatus protein like	5.25	8	9.81	15.01	4
2690	A0A2R6RTW5	Phosducin-like protein	2.75	3	14.88	16.27	4
2691	A0A2R6RTW7	Chalcone-flavonone isomerase family protein	1.50	2	6.70	8.79	4
2692	A0A2R6RTX9	Non-specific serine/threonine protein kinase	1.00	1	2.22	2.22	1
2693	A0A2R6RTZ2	Tubulin beta chain	28.40	43	61.83	74.05	4
2694	A0A2R6RU24	SWI/SNF-related matrix-associated actin-dependent regulator of chromatin subfamily A member	1.00	1	1.02	1.02	1
2695	A0A2R6RU36	Eukaryotic translation initiation factor 3 subunit E	7.50	10	32.10	41.96	4
2696	A0A2R6RU47	Eukaryotic translation initiation factor 3 subunit E	9.60	16	38.07	60.44	4
2697	A0A2R6RU51	Calcium-transporting ATPase	1.00	1	1.58	1.58	1
2698	A0A2R6RU55	Calcium-transporting ATPase like	1.00	1	2.16	2.16	1
2699	A0A2R6RU58	Eukaryotic translation initiation factor 3 subunit E like	3.00	4	22.98	31.06	3
2700	A0A2R6RU66	Methionyl-tRNA formyltransferase	1.00	1	3.30	3.30	2
2701	A0A2R6RU67	Calcium-transporting ATPase	1.00	1	1.91	1.91	1
2702	A0A2R6RU68	Protease Do-like	8.00	10	8.27	10.40	4
2703	A0A2R6RU70	Calcium-binding protein	1.00	1	4.17	4.17	4
2704	A0A2R6RU71	Annexin	4.67	7	13.50	20.25	3
2705	A0A2R6RU81	Calcium-transporting ATPase	1.00	1	1.09	1.09	1
2706	A0A2R6RU86	40S ribosomal protein S7	5.20	6	39.79	43.98	4
2707	A0A2R6RU96	14-3-3-like protein	13.00	13	62.94	62.94	1
2708	A0A2R6RUA1	Eukaryotic translation initiation factor 5 like	1.00	1	2.22	2.22	4
2709	A0A2R6RUB8	14-3-3-like protein	20.60	25	67.31	71.92	4
2710	A0A2R6RUC0	T-complex protein 1 subunit zeta	15.80	21	42.91	58.32	4
2711	A0A2R6RUD7	Sugar transport protein	1.00	1	1.36	1.36	2
2712	A0A2R6RUF9	Eukaryotic translation initiation factor 3 subunit M	9.40	15	24.26	35.40	4
2713	A0A2R6RUG2	Ubiquitin conjugation factor like	3.50	6	3.20	5.41	4
2714	A0A2R6RUH1	60S ribosomal protein	2.60	3	20.34	22.69	4

2715	A0A2R6RUH7	Thioredoxin-like fold protein	1.67	2	7.80	9.27	3
2716	A0A2R6RUI7	Non-specific serine/threonine protein kinase	3.00	4	6.42	8.56	4
2717	A0A2R6RUI8	Pectate lyase	1.33	2	3.04	4.57	3
2718	A0A2R6RUK2	Vacuolar protein sorting-associated protein 29	1.67	2	8.68	10.94	3
2719	A0A2R6RUL8	Tubulin alpha chain	33.00	49	56.80	59.56	4
2720	A0A2R6RUN4	Protein transport protein SEC13 B like	7.00	9	28.32	38.21	4
2721	A0A2R6RUP1	Nuclear transport factor 2 like	1.00	1	11.38	11.38	4
2722	A0A2R6RUS2	Enoyl-CoA delta isomerase 2, peroxisomal like	2.00	2	8.68	8.68	2
2723	A0A2R6RUT0	Malate dehydrogenase	18.20	23	53.13	59.64	4
2724	A0A2R6RUU7	DNA/RNA-binding protein Alba-like protein	1.50	2	12.34	15.82	4
2725	A0A2R6RUV1	40S ribosomal protein S15-4 (Fragment)	3.00	4	32.33	40.67	4
2726	A0A2R6RUW4	Acylamino-acid-releasing enzyme like	2.50	4	4.29	6.67	4
2727	A0A2R6RUX1	GDP-mannose 3,5-epimerase	18.00	24	49.36	60.64	4
2728	A0A2R6RUX6	Stem-specific protein	6.33	8	29.31	38.55	3
2729	A0A2R6RUY4	40S ribosomal protein like (Fragment)	10.00	13	46.07	53.70	4
2730	A0A2R6RUZ5	Transmembrane emp24 domain-containing protein	1.00	1	5.00	5.00	2
2731	A0A2R6RV19	GPI-anchored protein	2.60	3	14.77	16.41	4
2732	A0A2R6RV20	40S ribosomal protein S16	9.25	11	54.79	57.53	4
2733	A0A2R6RV22	Prefoldin subunit like	1.00	1	6.12	6.12	2
2734	A0A2R6RV33	NEDD8-activating enzyme E1 catalytic subunit	1.33	2	4.80	7.21	3
2735	A0A2R6RV92	1-deoxy-D-xylulose-5-phosphate synthase	1.00	1	1.67	1.67	2
2736	A0A2R6RVC3	Acetyl-coenzyme A synthetase	6.50	8	14.48	17.36	4
2737	A0A2R6RVC6	Serine/threonine-protein phosphatase 2A regulatory subunit B'' subunit like	1.00	1	8.00	8.00	2
2738	A0A2R6RW70	Pyruvate kinase	1.00	1	1.91	1.91	1
2739	A0A2R6RW82	Trafficking protein particle complex subunit	1.33	2	7.49	11.24	3
2740	A0A2R6RW93	Reticulon-like protein	1.00	1	3.18	3.18	2
2741	A0A2R6RWA4	Actin-depolymerizing factor 7 like (Fragment)	13.60	22	58.38	63.24	4
2742	A0A2R6RWB0	60S ribosomal protein L36	3.00	4	22.42	29.09	3
2743	A0A2R6RWB6	Alpha-protein kinase	1.00	1	4.38	4.38	1
2744	A0A2R6RWC5	Sorbitol dehydrogenase	14.60	17	54.07	62.09	4
2745	A0A2R6RWC6	Interleukin-16 like	1.33	2	5.72	8.79	3
2746	A0A2R6RWF3	40S ribosomal protein S13	4.60	6	32.32	40.40	4
2747	A0A2R6RWH0	Fructokinase-7 like	9.50	14	28.16	37.65	4
2748	A0A2R6RWI0	Ras-related protein RABD2a	5.67	6	29.89	31.53	3
2749	A0A2R6RWI1	Ribosomal protein L15	5.60	8	28.14	39.22	4
2750	A0A2R6RWI6	Glutamate dehydrogenase	3.00	3	8.23	8.23	2
2751	A0A2R6RWK1	2-phosphoglycerate kinase	1.33	2	3.28	5.47	3
2752	A0A2R6RWQ4	Eukaryotic translation initiation factor 2 subunit alpha like	8.40	13	27.91	39.83	4
2753	A0A2R6RWQ9	Clathrin heavy chain	94.60	126	54.67	63.52	4
2754	A0A2R6RWT4	GDSL esterase/lipase	1.00	1	3.14	3.14	3
2755	A0A2R6RWV5	Delta-1-pyrroline-5-carboxylate synthase	8.50	13	12.00	17.02	4
2756	A0A2R6RWW4	26S proteasome non-ATPase regulatory subunit 7 A like	8.60	12	32.19	43.87	4

2757	A0A2R6RWY0	Mannose-1-phosphate guanylyltransferase	4.50	6	17.52	24.93	4
2758	A0A2R6RWY1	Actin-97 like	63.00	63	65.26	65.26	1
2759	A0A2R6RWY2	Triosephosphate isomerase	23.20	30	76.14	79.92	4
2760	A0A2R6RWZ7	40S ribosomal protein S15a-1	6.00	8	39.54	50.00	4
2761	A0A2R6RX08	Histone H4	1.00	1	11.65	11.65	2
2762	A0A2R6RX18	60S ribosomal protein L35	1.80	2	15.12	16.26	4
2763	A0A2R6RX20	60S ribosomal protein like	4.60	7	24.21	32.89	4
2764	A0A2R6RX25	Ras-related protein like	3.00	3	16.28	16.28	2
2765	A0A2R6RX30	Aldo-keto reductase	1.80	3	6.12	10.50	4
2766	A0A2R6RX35	Proteasome inhibitor PI31 subunit	1.00	1	4.50	4.50	2
2767	A0A2R6RX40	Macrophage erythroblast attacher like	2.50	4	7.30	11.72	4
2768	A0A2R6RX42	Protein transport protein SEC23	7.00	9	13.75	17.77	4
2769	A0A2R6RX62	Tubulin beta chain	35.00	46	62.34	69.51	2
2770	A0A2R6RX73	60S ribosomal protein L35a-1	2.40	4	24.82	41.96	4
2771	A0A2R6RX86	Protein NRT1/ PTR FAMILY 8.1 like	1.00	1	1.81	1.81	2
2772	A0A2R6RXD6	LIMR family protein	2.00	2	4.13	4.13	2
2773	A0A2R6RXF2	40S ribosomal protein like (Fragment)	9.60	14	33.08	47.91	4
2774	A0A2R6RXH0	ERBB-3 BINDING PROTEIN 1 like	14.25	19	39.77	49.43	4
2775	A0A2R6RXH1	Importin subunit beta-1 like	5.67	7	8.29	10.08	3
2776	A0A2R6RXH3	PRA1 family protein	1.50	2	10.68	14.55	2
2777	A0A2R6RXH5	Uncharacterized protein	1.75	3	11.91	20.59	4
2778	A0A2R6RXL4	Receptor-like protein kinase	1.00	1	1.34	1.34	1
2779	A0A2R6RXL8	V-type proton ATPase subunit E like	6.40	9	34.96	46.90	4
2780	A0A2R6RXM7	Developmental and secondary metabolism regulator veA like	3.00	4	6.72	9.11	4
2781	A0A2R6RXN2	Calcium-binding protein like	1.80	3	9.84	14.29	4
2782	A0A2R6RXN5	26S protease regulatory subunit 6B	18.80	28	52.57	67.38	4
2783	A0A2R6RXN7	Vacuolar-sorting receptor 1 like	3.60	5	11.25	13.74	4
2784	A0A2R6RXP7	Receptor-like kinase	1.00	1	1.51	1.51	2
2785	A0A2R6RXQ0	Ubiquitin-conjugating enzyme E2 protein	3.80	6	28.11	37.84	4
2786	A0A2R6RXR8	Glycine-rich RNA-binding protein	1.00	1	8.73	8.73	2
2787	A0A2R6RXS7	Acyl-[acyl-carrier-protein] desaturase	1.50	2	4.67	6.31	4
2788	A0A2R6RXT3	2-alkenal reductase	3.75	6	13.44	22.25	4
2789	A0A2R6RXT6	Guanosine nucleotide diphosphate dissociation inhibitor	28.67	41	48.12	61.49	3
2790	A0A2R6RXT8	Mitogen-activated protein kinase	8.75	12	25.90	35.81	4
2791	A0A2R6RXU4	Guanosine nucleotide diphosphate dissociation inhibitor	28.40	42	49.10	60.59	4
2792	A0A2R6RXU7	Elongation factor 1-alpha	56.25	84	66.39	75.62	4
2793	A0A2R6RXX5	Ubiquitin carboxyl-terminal hydrolase	6.00	8	16.26	21.20	4
2794	A0A2R6RXY1	26S proteasome non-ATPase regulatory subunit 1 homolog	21.00	27	25.07	31.91	4
2795	A0A2R6RXY6	Tubulin beta chain	26.60	40	58.79	70.25	4
2796	A0A2R6RXZ5	D-cysteine desulfhydrase	1.75	3	4.64	7.92	4
2797	A0A2R6RXZ8	Phosphopyruvate hydratase	47.80	65	77.08	79.78	4
2798	A0A2R6RY09	Non-reducing end alpha-L-arabinofuranosidase	2.80	5	4.40	7.89	4

2799	A0A2R6RY18	Pyruvate kinase	17.60	26	40.46	54.08	4
2800	A0A2R6RY29	Fructokinase-4 like	17.20	23	47.42	51.98	4
2801	A0A2R6RY59	UDP-glucuronate decarboxylase	2.50	3	5.23	6.14	2
2802	A0A2R6RY63	Actin-depolymerizing factor 2 like (Fragment)	2.67	3	15.94	18.84	3
2803	A0A2R6RY64	Aldo-keto reductase family 4 member like	3.00	4	8.92	12.12	4
2804	A0A2R6RY65	60S ribosomal protein L38 (Fragment)	3.40	5	35.00	36.76	4
2805	A0A2R6RY77	5-oxoprolinase	10.60	16	10.04	14.87	4
2806	A0A2R6RY78	Ras-related protein like	7.00	9	31.94	41.20	2
2807	A0A2R6RYB7	Protease Do-like	9.00	10	9.90	10.84	2
2808	A0A2R6RYD3	Eukaryotic translation initiation factor 5 like	1.00	1	2.23	2.23	4
2809	A0A2R6RYE0	40S ribosomal protein S7	4.20	5	26.18	29.32	4
2810	A0A2R6RYE8	T-complex protein 1 subunit zeta 1 like	16.60	22	42.24	55.70	4
2811	A0A2R6RYF6	14-3-3-like protein	20.60	25	67.31	71.92	4
2812	A0A2R6RYL2	Ubiquitin conjugation factor like	4.00	7	3.74	6.49	4
2813	A0A2R6RYL9	Non-specific serine/threonine protein kinase	2.50	3	5.05	5.83	4
2814	A0A2R6RYM7	Uncharacterized protein	16.60	26	38.56	47.61	4
2815	A0A2R6RYP0	60S ribosomal protein	2.60	3	20.34	22.69	4
2816	A0A2R6RYP2	Eukaryotic translation initiation factor 3 subunit M	6.25	10	15.49	25.12	4
2817	A0A2R6RYP5	Tubulin alpha chain	33.40	50	63.52	69.40	4
2818	A0A2R6RYQ4	Cullin-3A like	3.33	5	4.82	7.23	3
2819	A0A2R6RYR1	Plasma membrane ATPase	10.00	10	11.43	11.43	1
2820	A0A2R6RYU5	Protein transport protein SEC13 B like	7.25	9	28.32	35.55	4
2821	A0A2R6RYV3	RING-H2 finger protein	1.00	1	3.34	3.34	4
2822	A0A2R6RYV5	Vacuolar protein sorting-associated protein 29	1.67	2	8.82	11.11	3
2823	A0A2R6RYV9	Nucleic acid-binding, OB-fold protein	2.80	4	22.19	32.12	4
2824	A0A2R6RYW3	Hypersensitive-induced response protein	2.00	2	7.69	7.69	2
2825	A0A2R6RYX0	ADP-ribosylation factor like	10.33	15	53.87	58.08	6
2826	A0A2R6RYY8	Universal stress protein A-like protein	1.50	2	9.22	12.29	2
2827	A0A2R6RYZ3	Heterogeneous nuclear ribonucleoprotein like	1.00	1	2.92	2.92	2
2828	A0A2R6RZ11	Mitogen-activated protein kinase	1.00	1	2.90	2.90	2
2829	A0A2R6RZ18	Serine/threonine protein phosphatase 2A regulatory subunit	3.00	3	5.02	5.02	2
2830	A0A2R6RZ23	Protein TPLATE like	11.75	17	12.62	17.48	4
2831	A0A2R6RZ25	Early nodulin-like protein	4.40	6	22.89	24.53	4
2832	A0A2R6RZ47	Phosducin-like protein	2.75	3	14.88	16.27	4
2833	A0A2R6RZ58	Nuclear transport factor 2 like	1.00	1	11.38	11.38	4
2834	A0A2R6RZ63	60S ribosomal protein L7a	6.80	10	20.86	29.14	4
2835	A0A2R6RZ75	Translocon-associated protein subunit beta like	1.00	1	8.12	8.12	2
2836	A0A2R6RZ85	Transcription factor like	1.00	1	2.80	2.80	1
2837	A0A2R6S034	Heterogeneous nuclear ribonucleoprotein	1.67	2	5.30	6.32	3
2838	A0A2R6S042	Serine hydroxymethyltransferase	42.20	59	72.23	83.01	4
2839	A0A2R6S063	Adenosylhomocysteinase	47.25	62	80.35	86.05	4
2840	A0A2R6S083	Selenium-binding protein	3.50	4	10.88	12.47	2

2841	A0A2R6S0A7	60S ribosomal protein like	5.00	6	24.63	29.61	4
2842	A0A2R6S0C3	Ras-related protein like	2.00	2	10.05	10.05	2
2843	A0A2R6S0C8	Endochitinase	1.00	1	5.47	5.47	3
2844	A0A2R6S0E5	Acyl-[acyl-carrier-protein] desaturase	1.50	2	4.67	6.31	4
2845	A0A2R6S0F2	Desiccation protectant protein like (Fragment)	6.40	9	28.63	38.41	4
2846	A0A2R6S0F5	Phosphoinositide phosphatase	5.00	7	3.70	5.03	3
2847	A0A2R6S0G5	Methylenetetrahydrofolate reductase	42.40	60	64.74	75.96	4
2848	A0A2R6S0G6	La-related protein like	2.50	3	5.14	6.45	4
2849	A0A2R6S0H0	Type I inositol polyphosphate 5-phosphatase	10.40	18	11.81	20.64	4
2850	A0A2R6S0I9	Plasminogen activator inhibitor 1 RNA-binding protein	1.00	1	2.51	2.51	2
2851	A0A2R6S0L4	60S ribosomal protein L38 (Fragment)	3.40	5	35.00	36.76	4
2852	A0A2R6S0L7	COP9 signalosome complex subunit 7 like	3.25	5	15.73	23.94	4
2853	A0A2R6S0N1	Perakine reductase	1.33	2	4.26	6.40	3
2854	A0A2R6S0P5	Transcription factor PosF21 like	1.00	1	2.45	2.45	3
2855	A0A2R6S0P8	Probable tRNA N6-adenosine threonylcarbamoyltransferase	1.00	1	2.63	2.63	1
2856	A0A2R6S0Q5	Isoleucyl-tRNA synthetase	39.40	64	32.85	49.58	4
2857	A0A2R6S0S8	Fructokinase-2 like	29.60	38	74.08	83.49	4
2858	A0A2R6S0S9	Vesicle-associated membrane protein	2.33	4	8.79	15.00	3
2859	A0A2R6S0T3	PTI1-like tyrosine-protein kinase	6.00	9	15.64	20.85	4
2860	A0A2R6S0U0	Voltage-gated potassium channel subunit beta like	4.40	7	16.22	25.00	4
2861	A0A2R6S0W2	Clathrin interactor EPSIN like	1.00	1	1.07	1.07	2
2862	A0A2R6S0X1	Eukaryotic translation initiation factor 3 subunit H	5.80	10	18.02	30.03	4
2863	A0A2R6S0Z0	Ubiquitin-associated and SH3 domain-containing protein	2.00	2	8.15	8.15	2
2864	A0A2R6S0Z5	Malate dehydrogenase	19.20	24	57.11	60.54	4
2865	A0A2R6S133	Organellar oligopeptidase	23.00	33	36.34	50.27	4
2866	A0A2R6S160	Methionine aminopeptidase	1.33	2	4.81	7.21	3
2867	A0A2R6S166	60S ribosomal protein like	3.80	6	23.83	30.82	4
2868	A0A2R6S170	Polcalcin Bet v like	3.00	5	35.29	49.41	4
2869	A0A2R6S172	Calcium-transporting ATPase	1.00	1	1.08	1.08	1
2870	A0A2R6S1A0	Indole-3-acetic acid-amido synthetase	1.00	1	1.25	1.25	1
2871	A0A2R6S1A3	ADP-ribosylation factor like (Fragment)	2.50	3	10.61	10.61	2
2872	A0A2R6S1C6	Nicotinate phosphoribosyltransferase	1.00	1	1.43	1.43	1
2873	A0A2R6S1G9	Transmembrane 9 superfamily member	1.33	2	2.23	3.35	3
2874	A0A2R6S1L3	Transmembrane 9 superfamily member	1.00	1	2.04	2.04	2
2875	A0A2R6S1L5	Leucine aminopeptidase	17.80	23	42.39	53.32	4
2876	A0A2R6S1L8	Tetratricopeptide repeat protein like	1.00	1	3.76	3.76	1
2877	A0A2R6S1M8	Eukaryotic translation initiation factor 4G-1 like	2.00	3	2.38	3.58	3
2878	A0A2R6S1N9	Eukaryotic translation initiation factor 5A	7.00	7	45.63	45.63	2
2879	A0A2R6S1Q2	Expansin	1.00	1	3.64	3.64	1
2880	A0A2R6S1S9	ADP-ribosylation factor	2.00	2	11.54	11.54	2
2881	A0A2R6S1U3	Glutamate dehydrogenase	1.00	1	2.43	2.43	1
2882	A0A2R6S1X3	40S ribosomal protein like	9.20	13	36.51	41.98	4

255

2883	A0A2R6S1X5	Tubulin alpha chain	21.00	26	38.59	42.98	4
2884	A0A2R6S1Z6	Actin	69.50	92	73.74	75.60	4
2885	A0A2R6S1Z9	Protein kinase	1.00	1	2.85	2.85	1
2886	A0A2R6S208	40S ribosomal protein	2.00	2	29.23	29.23	4
2887	A0A2R6S214	TBCC domain-containing protein 1	6.00	9	11.74	17.22	4
2888	A0A2R6S242	Villin-3 like	4.00	4	4.99	4.99	1
2889	A0A2R6S244	Enoyl-[acyl-carrier-protein] reductase	1.00	1	2.05	2.05	2
2890	A0A2R6S260	YTH domain-containing family protein like	2.00	2	3.02	3.02	2
2891	A0A2R6S269	Terpene cyclase/mutase family member	2.50	3	3.90	4.49	2
2892	A0A2R6S277	40S ribosomal protein like	9.00	9	31.16	31.16	2
2893	A0A2R6S280	60S acidic ribosomal protein like	1.60	2	11.36	14.41	4
2894	A0A2R6S282	Proteasome subunit beta	8.00	9	33.42	35.44	4
2895	A0A2R6S288	Calcium-transporting ATPase	1.00	1	0.73	0.73	1
2896	A0A2R6S295	RING-box protein like	1.00	1	11.86	11.86	3
2897	A0A2R6S2A0	Vacuolar protein sorting-associated protein	1.00	1	4.48	4.48	2
2898	A0A2R6S2A5	40S ribosomal protein like	10.67	11	55.27	57.69	3
2899	A0A2R6S2B7	Omega-amidase	1.00	1	5.07	5.07	2
2900	A0A2R6S2D6	Oligouridylate-binding protein like	1.00	1	1.96	1.96	3
2901	A0A2R6S2F7	Casein kinase 1-like protein	1.00	1	2.10	2.10	1
2902	A0A2R6S2G8	Xaa-Pro aminopeptidase	8.80	13	17.08	23.66	4
2903	A0A2R6S2H9	Late embryogenesis abundant protein like	12.60	15	45.04	52.26	4
2904	A0A2R6S2L7	ADP-ribosylation factor-like protein	1.00	1	6.90	6.90	2
2905	A0A2R6S2M0	Purple acid phosphatase	2.00	2	4.54	4.54	2
2906	A0A2R6S2N8	Thioredoxin	3.60	5	43.48	58.26	4
2907	A0A2R6S2Q1	26S proteasome non-ATPase regulatory subunit like	8.80	11	22.60	27.21	4
2908	A0A2R6S2Q3	Cold shock domain-containing protein	0.00	0	0.00	0.00	1
2909	A0A2R6S2Q9	Rac-like GTP-binding protein RHO1	9.20	13	31.57	40.10	4
2910	A0A2R6S2S7	Proteasome subunit alpha type	14.60	19	53.90	56.63	4
2911	A0A2R6S2U6	Trafficking protein particle complex subunit 11	1.33	2	1.18	1.77	3
2912	A0A2R6S2V2	Serine/threonine-protein kinase	1.33	2	3.74	5.60	3
2913	A0A2R6S2W5	Protein-serine/threonine phosphatase	2.75	3	9.01	10.18	4
2914	A0A2R6S2X2	UTP--glucose-1-phosphate uridylyltransferase	26.50	33	43.10	48.63	4
2915	A0A2R6S2Y0	Isocitrate dehydrogenase [NADP]	11.80	17	29.42	40.38	4
2916	A0A2R6S2Y6	60S ribosomal export protein	1.00	1	8.70	8.70	2
2917	A0A2R6S2Z7	Mannitol dehydrogenase	12.80	17	53.06	65.28	4
2918	A0A2R6S306	Ras-related protein RHN1	1.67	2	8.83	10.50	3
2919	A0A2R6S307	Eukaryotic translation initiation factor 3 subunit J	1.00	1	6.76	6.76	2
2920	A0A2R6S331	Kinase-interacting protein	8.33	11	8.21	10.11	3
2921	A0A2R6S332	Ubiquitin carboxyl-terminal hydrolase	1.00	1	2.97	2.97	2
2922	A0A2R6S344	Inositol-3-phosphate synthase	6.20	8	15.10	19.41	4
2923	A0A2R6S361	Ras-related protein RABH1e	7.50	10	34.30	44.93	2
2924	A0A2R6S382	GLABRA2 expression modulator like	2.25	3	7.72	10.61	4

2925	A0A4D6FUC6	ATP synthase subunit alpha	0.00	0	0.00	0.00	1
2926	A7YVW2	Glucose-6-phosphate 1-dehydrogenase	3.75	6	8.65	14.31	4
2927	A7YVW3	Glutamate dehydrogenase	1.00	1	2.43	2.43	1
2928	A7YVW4	Glutamate dehydrogenase	3.00	3	8.27	8.27	2
2929	B1NDI3	Calmodulin	8.00	11	57.26	62.16	4
2930	B7SFB0	Glyceraldehyde 3-phosphate dehydrogenase (Fragment)	8.00	8	61.36	61.36	1
2931	B7SFB7	Glyceraldehyde 3-phosphate dehydrogenase (Fragment)	9.00	9	66.67	66.67	1
2932	B7SFC0	Glyceraldehyde 3-phosphate dehydrogenase (Fragment)	7.00	7	50.76	50.76	1
2933	B8YLW1	Flavanone 3-hydroxylase	2.00	3	7.10	10.38	3
2934	E3T802	ADP-ribosylation factor	9.60	14	55.80	63.54	4
2935	Q5J3N7	Sucrose-phosphatase	12.00	12	32.71	32.71	1
2936	Q5J3N8	Sucrose-phosphatase	10.25	12	26.88	30.35	4
2937	Q8S559	Sucrose-phosphate synthase (Fragment)	3.00	3	4.73	4.73	1
2938	Q8S560	Sucrose-phosphate synthase	10.00	14	7.94	10.21	4
2939	Q8S561	Sucrose-phosphate synthase (Fragment)	6.00	6	7.37	7.37	1
2940	Q9MT59	ATP synthase subunit beta (Fragment)	1.00	1	2.25	2.25	2
2941	S4SKC1	Alkaline/neutral invertase	18.80	24	32.19	38.54	4
2942	S4SKD6	Alpha-amylase	1.00	1	2.42	2.42	1
2943	S4SKE2	Fructokinase	26.60	34	66.87	67.78	4
2944	S4SKP6	Fructokinase	12.80	17	44.22	58.13	4
2945	V5TE41	Inositol-3-phosphate synthase	6.20	8	15.10	19.41	4

Supplementary to chapter 7

Supplementary material 1. Negative controls (secondary antibody only) for confocal fluorescence microscopy (A) and TEM (B). No unspecific signal was detected.
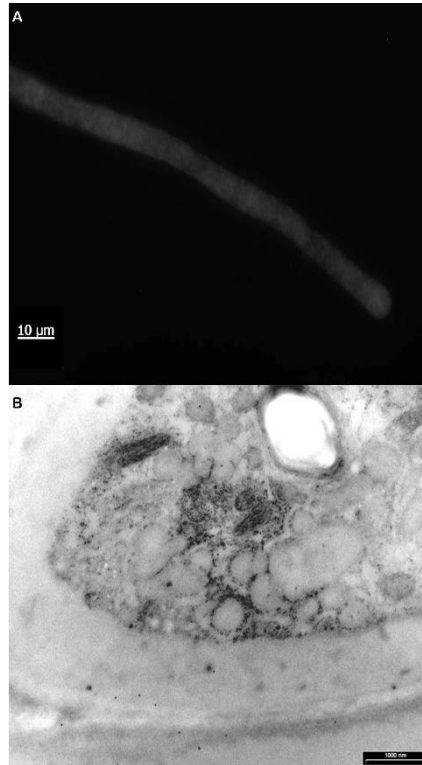
Supplementary material 2. Electrophoresis gel of cell wall (CW), membrane-organelles (MEM-ORG) and cytosol fractions of pollen tubes growth in standard condition (control) and after EGTA supplement (+EGTA).